ONCOTHERMIA JOURNAL

A publication of Oncotherm® ISSN 2191-6438

Volume 33 - May 2023

Imprint

Editorial

Dear Reader, Dear Fellow Researchers, Dear Colleagues,

I recommend the 33rd volume of our Oncothermia Journal to the readers' attention. Essential new results are published and presented in this volume.

I published two basic articles to clarify the role of resonances in modulated electro-hyperthermia (mEHT) applications.

As discussed in the article of Cancer-Specific Resonances a possible stochastic explanation is given on the topic, that the resonant phenomena provide a selection possibility of malignant cells.

The publication of Stimulation and Control of Homeostasis presents another perspective on the topic of the importance of homeostasis in clinical practice and shows its stimuli by vagus-nerve excitation, used by mEHT.

Furthermore, another article focuses on the complementary applications of mEHT with radiotherapies. New results draw attention to critical facts in the relationship between ionizing and non-ionizing radiations applied in radiation oncology. The article comprehensively presents the most recent theoretical results with modern clinical radiology practice.

The heat-shock-proteins (HSPs) challenge the efficacy of hyperthermia due to their ability to develop heat resistance. The article of Dr. Minnaar demonstrates how mEHT goes over this problem and uses HSPs for apoptosis of malignant cells.

In Dr. Marcell Szasz' article, a comprehensive investigation is carried out on the similarities and differences between the mEHT and the TTF methods, pointing out the advantages of the electric field effects.

Prof. Lee's publication validates and provides additional support for the special results of mEHT in cancer of the uterus cervix.
Prof. Wust's article is a new milestone in showing the effect of modulation in mEHT success. The preclinical results prove the basic impacts of modulation on cell killing.

A strong international team of medical professionals leading by Prof. Arrojo wrote comments on Liebl et al. article, which made the incorrect evaluation of hyperthermia and presented false and misunderstood data.

I hope you will enjoy reading these articles and using the provided information in your medical practice.

Dr. Andras Szasz
Professor, Chair, Biotechnics Department of St. Istvan University

Liebe Leserinnen und Leser, liebe Forscherkollegen, liebe Kolleginnen und Kollegen,

Ich empfehle den Lesern den 33. Band unseres Oncothermia Journals zur Kenntnis zu nehmen. In diesem Band werden wesentliche neue Ergebnisse veröffentlicht und vorgestellt.

Prof. Szasz veröffentlichte zwei grundlegende Artikel zur Klärung der Rolle von Resonanzen bei Anwendungen der modulierten Elektrohyperthermie (mEHT).

In dem Artikel Krebsspezifische Resonanzen wird eine mögliche stochastische Erklärung dafür gegeben, dass die Resonanzphänomene eine Selektionsmöglichkeit bösartiger Zellen darstellen.

Die Publikation Stimulation and Control of Homeostasis stellt eine weitere Perspektive zum Thema der Bedeutung der Homöostase in der klinischen Praxis dar und zeigt deren Stimulierung durch Vagusnerv-Erregung, die von mEHT genutzt wird.

Ein weiterer Artikel befasst sich mit den komplementären Anwendungen der mEHT mit Strahlentherapien. Neue Ergebnisse lenken die Aufmerksamkeit auf kritische Fakten in der Beziehung zwischen ionisierenden und nicht-ionisierenden Strahlen, die in der Radioonkologie eingesetzt werden. Der Artikel stellt umfassend die neuesten theoretischen Ergebnisse mit der modernen klinischen Radiologiepraxis dar.

Die Hitzeschock-Proteine (HSP) stellen aufgrund ihrer Fähigkeit, Hitzeresistenz zu entwickeln, die Wirksamkeit der Hyperthermie in Frage. Der Artikel von Dr. Minnaar zeigt, wie die mEHT dieses Problem umgeht und HSPs zur Apoptose bösartiger Zellen nutzt.

Im Artikel von Dr. Marcell Szasz werden die Gemeinsamkeiten und Unterschiede zwischen der mEHT- und der TTF-Methode umfassend untersucht und die Vorteile der elektrischen Feldeffekte herausgestellt.

Die Publikation von Prof. Lee validiert und untermauert zusätzlich die besonderen Ergebnisse der mEHT bei Gebärmutterhalskrebs.

Der Artikel von Prof. Wust ist ein neuer Meilenstein in der Darstellung des Modulationseffekts für den Erfolg der mEHT. Die präklinischen Ergebnisse belegen die grundlegenden Auswirkungen der Modulation auf die Zellabtötung.

Ein starkes internationales Team von Medizinern unter der Leitung von Prof. Arrojo hat Kommentare zum Artikel von Liebl et al. verfasst, der eine falsche Bewertung der Hyperthermie vornimmt und falsche und missverstandene Daten präsentiert.

Ich hoffe, Sie werden diese Artikel mit Vergnügen lesen und die darin enthaltenen Informationen in Ihrer medizinischen Praxis nutzen.

Dr. Andras Szasz
Professor und Vorsitzender der Fakultät für Biotechnik an der St. Istvan Universität

Rules of submission

As the editorial team we are committed to a firm and coherent editorial line and the highest possible printing standards. But it is mainly you, the author, who makes sure that the Oncothermia Journal is an interesting and diversified magazine. We want to thank every one of you who supports us in exchanging professional views and experiences. To help you and to make it easier for both of us, we prepared the following rules and guidelines for abstract submission.

Als redaktionelles Team vertreten wir eine stringente Linie und versuchen, unserer Publikation den höchst möglichen Standard zu verleihen. Es sind aber hauptsächlich Sie als Autor, der dafür Sorge trägt, dass das Oncothermia Journal zu einem interessanten und abwechslungsreichen Magazin wird. Wir möchten allen danken, die uns im Austausch professioneller Betrachtungen und Erfahrungen unterstützen. Um beiden Seiten die Arbeit zu erleichtern, haben wir die folgenden Richtlinien für die Texterstellung entworfen.

1. Aims and Scope

The Oncothermia Journal is an official journal of the Oncotherm Group, devoted to supporting those who would like to publish their results for general use. Additionally, it provides a collection of different publications and results. The Oncothermia Journal is open towards new and different contents but it should particularly contain complete study-papers, case-reports, reviews, hypotheses, opinions and all the informative materials which could be helpful for the international Oncothermia community. Advertisement connected to the topic is also welcome.

- Clinical studies: regional or local or multilocal Oncothermia or electro cancer therapy (ECT) treatments, case-reports, practical considerations in complex therapies, clinical trials, physiological effects, Oncothermia in combination with other modalities and treatment optimization
- Biological studies: mechanisms of Oncothermia, thermal- or non-temperature dependent effects, response to electric fields, bioelectromagnetic applications for tumors, Oncothermia treatment combination with other modalities, effects on normal and malignant cells and tissues, immunological effects, physiological effects, etc.
- Techniques of Oncothermia: technical development, new technical solutions, proposals
- Hypotheses, suggestions and opinions to improve Oncothermia and electro-cancer-therapy methods, intending the development of the treatments

Further information about the journal, including links to the online sample copies and content pages can be found on the website of the journal: www.oncothermia-journal.com

Umfang und Ziele

Das Oncothermia Journal ist das offizielle Magazin der Oncotherm Gruppe und soll diejenigen unterstützen, die ihre Ergebnisse der Allgemeinheit zur Verfügung stellen möchten. Das Oncothermia Journal ist neuen Inhalten gegenüber offen, sollte aber vor allem Studienarbeiten, Fallstudien, Hypothesen, Meinungen und alle weiteren informativen Materialien, die für die internationale Oncothermie-Gemeinschaft hilfreich sein könnten, enthalten. Werbung mit Bezug zum Thema ist ebenfalls willkommen.

- Klinische Studien: regionale, lokale oder multilokale Oncothermie oder Electro Cancer Therapy (ECT) Behandlungen, Fallstudien, praktische Erfahrungen in komplexen Behandlungen, klinische Versuche, physiologische Effekte, Oncothermie in Kombination mit anderen Modalitäten und Behandlungsoptimierungen
- Biologische Studien: Mechanismen der Oncothermie, thermale oder temperaturunabhängige Effekte, Ansprechen auf ein elektrischesFeld, bioelektromagnetische Anwendungen bei Tumoren, Kombination von Oncothermie und anderen Modalitäten, Effekte auf normale und maligne Zellen und Gewebe, immunologische Effekte, physiologische Effekte etc.
- Oncothermie-Techniken: technische Entwicklungen, neue technische Lösungen
- Hypothesen undMeinungen, wie die Oncothermie- und ECT-Methoden verbessert werden können, um die Behandlung zu unterstützen

Weitere Informationen zum Journal sowie Links zu Online-Beispielen und Inhaltsbeschreibung sind auf der Website zu finden: www.oncothermia-journal.com

2. Submission of Manuscripts

All submissions should be made online via email: info@oncotherm.org

Manuskripte einreichen

Manuskripte können online eingereicht werden: info@oncotherm.org

3. Preparation of Manuscripts

Manuscripts must be written in English, but other languages can be accepted for special reasons, if an English abstract is provided.
Texts should be submitted in a format compatible with Microsoft Word for Windows (PC). Charts and tables are considered textual and should also be submitted in a format compatible with Word. All figures (illustrations, diagrams, photographs) should be provided in JPG format.

Manuscripts may be any length, but must include:

- Title Page: title of the paper, authors and their affiliations, 1-5 keywords, at least one corresponding author should be listed, email address and full contact information must be provided
- Abstracts: Abstracts should include the purpose, materials, methods, results and conclusions.
- Test: unlimited volume
- Tables and Figures: Tables and figures should be referred to in the text (numbered figures and tables). Each table and/or figure must have a legend that explains its purpose without a reference to the text. Figure files will ideally be submitted as a jpg-file (300dpi for photos).
- References: Oncothermia Journal uses the Vancouver (Author-Number) system to indicate references in the text, tables and legends, e.g. [1], [1-3]. The full references should be listed numerically in order of appearance and presented following the text of the manuscript.

Manuskripte vorbereiten

Manuskripte müssen in englischer Sprache vorliegen. Andere Sprachen können in Ausnahmefällen akzeptiert werden, wenn ein englisches Abstract vorliegt.
Texte sollten in einem mit Microsoft Word für Windows (PC) kompatiblen Format eingereicht werden. Tabellen sollten in einem Word-kompatiblen Format eingefügt werden. Alle Graphiken (Illustrationen, Diagramme, Photographien) sollten im jpg Format vorliegen.

Manuskripte können jede Länge haben, müssen aber die folgenden Punkte erfüllen:

- Titelseite: Titel der Arbeit, Autor, Klinikzugehörigkeit, 1-5 Schlüsselworte, mindestens ein Autor muss genannt werden, E-Mail-Adresse und Kontaktdetails des Autors
- Abstracts: Abstracts müssen Zielsetzung, Material und Methoden, Ergebnisse und Fazit enthalten.
- Text: beliebige Länge
- Abbildungen und Tabellen: Abbildungen und Tabellen sollten im Text erläutert werden (nummeriert). Jede Abbildung / Tabelle muss eine erklärende Bildunterschrift haben. Bilder sollten als jpg eingereicht werden (300 dpi).
- Zitate: Das Oncothermia Journal verwendet die Vancouver Methode (Autornummer), um Zitate auszuweisen, z.B. [1], [1-3]. Die Bibliographie erfolgt numerisch in Reihenfolge der Erwähnung im Text.

4. Copyright

It is a condition of publication that authors assign copyright or license the publication rights in their articles, including abstracts, to the publisher. The transmitted rights are not exclusive, the author(s) can use the submitted material without limitations, but the Oncothermia Journal also has the right to use it.

Copyright

Es ist eine Publikationsvoraussetzung, dass die Autoren die Erlaubnis zur Publikation ihres eingereichten Artikels und des dazugehörigen Abstracts unterschreiben. Die überschriebenen Rechte sind nicht exklusiv, der Autor kann das eingereichte Material ohne Limitation nutzen.

5. Electronic Proofs

When the proofs are ready, the corresponding authors will receive an e-mail notification. Hard copies of proofs will not be mailed. To avoid delays in the publication, corrections to proofs must be returned within 48 hours, by electronic transmittal or fax.

Elektronische Korrekturfahne

Wenn die Korrekturfahnen fertig gestellt sind, werden die Autoren per E-Mail informiert. Gedruckte Kopien werden nicht per Post versandt. Um Verzögerungen in der Produktion zu verhindern, müssen die korrigierten Texte innerhalb von 48 Stunden per E-Mail oder Fax zurückgesandt werden.

6. Offprints and Reprints

Author(s) will have the opportunity to download the materials in electronic form and use it for their own purposes.
Offprints or reprints of the Oncothermia Journal are not available.

Sonderdrucke und Nachdrucke

Die Autoren haben die Möglichkeit, das Material in elektronischer Form herunterzuladen, Sonderdrucke und Nachdrucke des Oncothermia Journals sind nicht erhältlich.

7. Advertisement

The Oncothermia Journal accepts advertising in any language but prefers advertisements in English or at least partially in English. The advertising must have a connection to the topics in the Oncothermia Journal and must be legally correct, having checked that all information is true.

Werbung

Das Oncothermia Journal akzeptiert Werbeanzeigen in allen Sprachen, bevorzugt, aber die zumindest teilweise Gestaltung in englischer Sprache. Die Werbung muss eine Beziehung zu den Themen des Oncothermia Journals haben und der Wahrheit entsprechende Inhalte aufweisen.

8. **Legal responsibility**

Authors of any publications in the Oncothermia Journal are fully responsible for the material which is published. The Oncothermia Journal has no responsibility for legal conflicts due to any publications. The editorial board has the right to reject any publication if its validity has not been verified enough or the board is not convinced by the authors.

Haftung

Die Autoren aller im Oncothermia Journal veröffentlichten Artikel sind in vollem Umfang für ihre Texte verantwortlich. Das Oncothermia Journal übernimmt keinerlei Haftung für die Artikel der Autoren. Die Redaktion hat das Recht Artikel abzulehnen.

9. **Reviewing**

The Oncothermia Journal has a special peer-reviewing process, represented by the editorial board members and specialists, to whom they are connected. To avoid personal conflicts the opinion of the reviewer will not be released and her/his name will be handled confidentially. Papers which are not connected to the topics of the journal could be rejected without reviewing.

Bewertung

Die Texte für das Oncothermia Journal werden durch die Redaktion kontrolliert. Um Konflikte zu vermeiden, werden die Namen des jeweiligen Korrektors nicht öffentlich genannt. Artikel, die nicht zu den Themen des Journals passen, können abgelehnt werden

Contents

Cancer-Specific Resonances

Andras Szasz

Department of Biotechnics, Hungarian University of Agriculture and Life Sciences, Godollo, Hungary

Cite this article as:
Szasz, A. (2022) Cancer-Specific Resonances. Open Journal of Biophysics , 12, 185-222.
https://doi.org/10.4236/ojbiphy.2022.124009

Oncothermia Journal 33, May 2023: 8 – 36.
www.oncotherm.com/sites/oncotherm/files/2023-05/SzaszA_Cancer_Specific_Resonances.pdf

Abstract
The research of cancer-specific resonances started with Raymond R. Rife's controversial results. The intensive debate began on the topic, and various interpretations of the results deepened after his death. This theme presently sparks desperate debates with extreme opinions, from the dangerous quackery to the brilliant discovery. A part of medical practices applies the resonance principle in various anticancer therapies and uses a variety of devices. Most medical experts refuse such "resonance therapies" due to their confidence in their quackery. I summarized some present problems and proposed a possible solution. My present article aims to discuss some aspects of the biological resonances, trying to clear some vague details of this subject and give a possible stochastic explanation of some resonances in cancer therapy. However, when considering the stochastic explanations of resonance frequencies, there are as many of these as there are enzymatic processes affecting the biological systems.

Keywords:
Rife Frequencies, Pythagorean Mystics, Resonances, Noises, Fluctuations, Stochastic Processes, Enzymatic Resonances

1. Introduction

The resonance embraces a broadcategory of systems, especially reaction on a periodic excitation. Resonance occurs in many interactions: mechanical (e.g. strings, acoustic, tuned vibrations, etc.), electrical (e.g. tuned circuits for selectivity, impedance extremes, etc.), atomic (e.g. Mossbauer effect, nuclear magnetic resonance, electron spin-resonance, etc.) or optical (e.g. laser, spectral lines, etc.) and many of their combined effects. In some cases, the phenomenon of harmony is also related to resonances, for example, musical harmony which is composed of various mechanical resonances, or the homeostatic balance created by a complex set of selected bio-interactions.

The role of bioelectromagnetics in the resonance phenomena has turned into a "battlefield" in science. The medical facts and their interpretations are mixed with quackeries and medically not proven theories [1]. These unsatisfactory proofs make the "healing electro-therapeutics" highly controversial. For example, electro homeopathy (or Mattei cancer cure [2] [3]) proposes different resonant optical "colors" of electricity to treat cancer. Experts described it as "utter idiocy" [4].

Severe medical doubts make this topic an impossible research venture. The broad legal and illegal medical applications draw attention to this attention grabbing topic despite its great challenge with multiple unclear details. Differentiating the quackeries from scientifically approved facts confuses the discussion. Unfortunately, these concepts have been adopted and misinterpreted by the non-scientific community, resulting in the development of pseudoscientific beliefs. A further complication is that almost all unscientific explanations include well-proven facts within their unproven or false statements. Unfortunately, these concepts have been adopted and misinterpreted by the non-scientific community, resulting in the development of pseudoscientific beliefs. This further contributes to the poor acceptance of the topic by professionals. The judgment of a great scientist, Stephen Hawking, summarized it: "The greatest enemy of knowledge is not ignorance , it is an illusion of knowledge " [5]. An example of the misuse of a scientific concept involves mechanical resonance, a condition in which a mechanical system responds with increased amplitude when the frequency of the system's oscillations matches the system's natural vibration frequency. A frequency limit and definite boundary conditions are disregarded when the concept is used to describe pseudoscientific theories. Another frequent "shift" uses the well-proven quantum-mechanical effects in the micro-world atoms and molecules to explain macroscopic bodies. Therefore, the use of resonance in oncological applications requires in-depth investigations to filter out the facts from the pseudoscience. The question is: "Who is the fake one now?" [6]. I try to collect many ideas connected to resonance phenomena, point out the dubious parts, and focus on possible developments.

2. The Pythagorean Harmony

The ancient Greek culture developed the first resonance theory. Centered on the mechanical resonances of a tense string, Pythagoras introduced a set of resonances that explained leading musical harmony in European culture. The Pythagorean school developed mystic numerology by observing the connections between the mechanical resonance of the tense string and its environmental matter (musical sound). Pythagoras created an approach to the vibration of string using ratios of integers. His discovery became the basis of some geometric and musical works, establishing the numerological harmony of musical tuning [7].

When one string is exactly half the length of another string, the notes will have different pitches but will till be in harmony. The interval between the two notes is called an octave. The Pythagorean tuning system, eveloped by Pythagoras, is based on a frequency ratio of musical intervals of 2:3, or the "perfect fifth" (3/2). In musical Pythagorean tuning, the power function of the ratio of "perfect fifth" $\left(\frac{3}{2}\right)^n$.

The structure forms a scale and the 2^{-p} transposes the scale to the fundamental octave [8]. The perfect fifth can be divided further on the same ratio following the 2^n3^m (where n and m are integers) division rates on the string. This way the Pythagorean music makes the sounds based on the length of tense strings in a scale, where the template is the "perfect fifth" which divides the string by 2/3 portion. Hence, the correct set of tense string vibrations has a $\frac{1}{2^p}\left(\frac{3}{2}\right)^n = 3^n 2^{n-p}$ [8] divisions in musical structure.

The subjective human sense enjoys musical harmony, which does not fit properly with the mathematical construction. A dissonance appears in senses, the "Pythagorean comma," or "wolf fifth". A critical feature appears here: the "dissonance" of the wolf-fifth, a fundamentally psychological rather than based on mathematical objectivity.

The "magic" $\frac{3}{2}$ also appears in other ancient science. Aristotle, a significant influencer of the European culture of ancient times and the middle ages, observed the same ratio between the volumes of the cylinder and its inner nesting sphere, which is valid for their surfaces. Kepler also applied the musical ratio in the cosmos' harmony, forming the cosmic monochord of the universe [9]. Kepler's observation of the planets' distances follows a musical harmony (music of spheres). The proof of this theory, of course, considers the limited possibilities of the observations in Kepler's time.

Interestingly this early mysticism has some real roots in nature, mainly due to the standing harmonic waves formed in the tense string with fixed ends showing $n \cdot \frac{\lambda}{2}$, where n is integer and $\frac{\lambda}{2}$ is the half-wavelength of the formed wave. The hypothesis of applying ancient numerical wisdom in modern physics surprisingly supported the other "Pythagorean quantization". The mathematical apparatus of such modern fields as quantum mechanics [10] and the structure of DNA [11] apply the Pythagorean symmetries. The wave quanta with integers appear in the string theory of the standard cosmologic model [12].

The other Pythagorean discovery is the triplets of the right triangle drive obtaining Sommerfeld's fine-structure constant and show similarities with the quantum Hall effect. It could be applied in the time-dependent quantum mechanics connected to the time-dependent complex nonlinear Riccatti equations [13], and the $\frac{e^2}{c}$ $\left[=\frac{e^2}{4\pi\varepsilon_0 c}\right.$ in SI units] least Coulombic action. The generalized Pythagorean theorem appears in many topics in physics [10]. It also appears in the space-time distances in special relativity [14], and could be connected to optical imaging by the reciprocal values [15]. The applied Pythagorean triplets are well described theoretically [16] [17]. The applicability's main origin covers the fundamental distance-like values in the Cartesian coordinate system or the law of cosines in any coordinates. However, the similarities of the Pythagorean triplets and numerical string theory with the quantum effects and differential equations do not mean the quantum-mechanical application or relevance of Pythagorean theorems. These similarities are formal. The simple deterministic mechanical concept has no fundamental connection with the probability-based quantum ideas.

3. Therapies with Bioelectromagnetic Resonant Frequencies

The mechanical behavior of the electromagnetic phenomenon is nonlinear in space distances, causing many complications for the first modern scientific investigators, Coulomb and Ampere. The electric and magnetic fields introduced by Maxwell [18] solved this problem by linearizing the forces depending only on the fields and the resting or moving electric charges. These new constructions could only be detected in specific materials with charges and currents and were otherwise insensible to the human senses. The concept of the electric and magnetic field was therefore perceived as a "miracle" by many laypeople, and many pseudoscientific beliefs targeted it. The main controversial "battlefield" is bioelectromagnetism, the effect of electromagnetic fields on living objects. Heated debates have emerged on the effects of environmental factors on health and on the development of malignancies, for example, induced by the energy transfer

networks (like powerlines) [19] [20] [21] [22] [23]. However, the explanations proved controversial and often found to be inconsistent [24]. Broad approaches are discussed in the topics of "electrosmog" [25] [26], "magnetic field medicine", [27], "new biophysical field", "force-free actions" [28], "scalarwave effects" [29], and "subtle energies" [30]. These topics have created upheaval in the field of bioelectromagnetics, with strong opposing arguments from physical [31] and mathematical points of view [32] [33]. Most of the measured and medically proven but contradictory results in bioelectromagnetism characterize the complex behavior of the biosystems, which has a "Janus face" feature because it inherently depends on internal and external conditions. The same "electrosmog" radiation could be "healthy" or "unhealthy" depending on the conditions [34]. Most of the bioresonance theories involve electromagnetics and/or quantummechanical explanations. Nikola Tesla considered resonances as the most general law of nature [35], which focused attention on this topic. Tesla applied electromagnetic resonance in most of his numerous patents, like the alternative current [36] and wireless communication [37], founding a unique bioelectromagnetic view [38]. Tesla worked out a method for electro-therapeutics, using "ultraviolet rays" [39].

The other influence on the bioresonances has a quantum-mechanical origin. The Aharonov-Bohm effect [40] led to new ideas. This quantum-mechanical in terference phenomenon may be applied in the concept of the "field-free" vectorpotential with possible biological application [41] [42]. The vector potential deals with the influences of the inherent fluctuations that allow the unmeasurable field-effect in a macroscopic spatiotemporal measurement, the vector-potential acts in macro ranges [43].

The "resonance topic" in cancer therapy started with a revolutionary step of optical microscopy, developed by Raymond Royal Rife [44]. The Rifemicroscope had the ultimate resolution at that time [45]. The microscope was able to observe the cellular morphology and changes in cell culture in natural, time-lapse conditions with as high as 31,000 resolution with low aberration, while the standard laboratory microscopes at that time had only 2000 to 2500 [46].

The great advantage of the microscope was its resolution and the possibility of observing the time-lapse dynamics of living microbes [47]. The Rife microscope does not harm the specimens under observation. The microscope's ability allowed researchers to study the processes caused by environmental interactions. The time-lapse facility was an extraordinary chance to study living interacting cells by visualization and registering the dynamics of cells alive over a long time [48] [49] [50]. Recording the time-lapse microscopy movies of microbes excited the researchers of the time. Note, the time-lapsing nowadays remained very popular and used in many microscopic solutions, mostly applying modern, extreme high-resolution live-cell imaging without Rife's microscopy.

Using Tesla's arc lamp idea [51], Rife constructed arc radiation ("beam ray") in an argon-filled glassflask, pumping it with various modulated radiofrequency (RF) power [52], and he used its radiation for microbes under his microscope [53]. He observed "resonant frequencies," where the pathogens will perish [54] [55] [56] [57]. Rife collected these unique frequencies and registered the "mortal oscillatory rate" (MOR) for various pathogenic organisms. The resonance idea spread rapidly among the experts and laypersons, assuming the same "curative effect" in vivo, without proof. The new claim declares the cure of cancer without relevant observations. The rigorous theoretical and clinical studies are nowadays also largely missing. Later Rifemodified the cancer-cure idea, saying that he may devitalize the disease.

After the death of Raymond Rife, a large market developed, using his work to provide false hopes for cancer patients (at this point, the market-related profitmaking substantially impacted the field). The new "Rife-machines" do not use plasma radiation. Instead, they apply only minimal current (milliamperes) of various modulated RF carrier frequencies, which promises to kill the cancer cells in the whole body. Most of the devices were utterly deceptive, and while they directly did not harm the patients, those who used these were isolated from the benefits of proven treatments by their firm belief that the Rifemachine helps. More and more publications were available by elapsing time, showing the problems with the original Rife frequencies and its "theory" behind them. The theoretical part was fragile; the experimental results had no explanations, while the publications did not describe the experimental conditions professionally. The lack of evidence and the presentation of only a selection of favorable cases supposedly treated by Rife resulted in the development of a field of "pseudomedicine" supported by electronics [58] [59]. The fraudulent activities were punished [60] [61]. Such "Rife devices" have figured prominently in several fraud cases in the US, typically centered around the uselessness of the devices contrary to their marketed grandiose claims. In a 1996 case, the marketers of a "Rife device" claiming to cure numerous diseases, including cancer and AIDS, were convicted of felony health fraud [62]. The sentencing judge described them as "target[ing] the most vulnerable people, including those suffering from a terminal disease," and providing false hope [63].

Rife machines have been blamed for the deaths of cancer patients who might have been cured with conventional therapy [64].

Unfortunately, many questionable methods use the "phenomenon" of generating profit from believers without acceptable scientifically and medically approved evidence. Rife devices are currently classified as a subset of radionics devices generally viewed as pseudomedicine by mainstream experts [65]. No evidence was produced [66], and it was declared quackery [67] [68]. The Rife frequency generator is an electronic device purported to cure cancer by transmitting radio waves. Authorities in the UK and the US studied this device: "there is no evidence to show that the Rife machine does what its supporters say it does" [69].

However, the appearance of the bioelectromagnetic resonance needs clarification despite many unsuccessful experiments and sometimes misleading or even falsified data. The mixture of the facts and the hidden false statements using scientific language makes the debate too complicated. Such patented ideas as Lakhovsky's radio-cellular-oscillator [70] [71], Rife'sresonant waves [57] [72], Priore's electromagnetic therapy [73] [74] [75], are unproven in systematic studies, but some positive case reports were published. However, these selected results do not provide enough proof to verify the effect. On the other hand, the missing proofs do not mean directly that the idea is quackery. Future discoveries may find the missing proofs with new research facilities like Gurwitsch's morphogenesis-based mitotic wave in mitosis [76] [77] [78] and some enzymatic reactions [79]. Gurwitsch's pioneering work has a revision integrating the bioelectric interactions [80] [81]. However, presently we have only indirect proofs in this field as well. Not enough sensitive tools exist to measure the supposed effects [82].

The psycho-effects of otherwise safe (maybe ineffective) methods keep many of these therapies alive, providing a placebo for the patient [83]. The placebo treatment does not mean "no treatment" [84]; it could help with belief. This psychological issue is mostly palliative [85]. The missing efficacy becomes harmful because the patient remains without professional medical care, and the disease may become irreversible.

Low-level, non-stationary magnetic fields have been observed [86] and adopted [87] as a nonthermal electromagnetic effect. One of the essential nonthermal processes is the so-called "window" effects [88], which shows significant calcium influx to the cell at the low-frequency modulation of radiofrequency around 16 Hz frequency "window", having an optimum frequency and amplitude to interact with cellular membranes [89]. The window effects have some resonance characteristics. The measured frequency dependence varies based on the experimental conditions and could act in a synergistic way with chemical processes [90]. The "window" was measured in multiple power ranges [91]. These experiments were considered to be nonthermal due to the low energy (max5 uW/g energy). The maximum of the active Na+ flux was observed between 0.1 – 10 MHz [92], which "window" effect could be well explained by the active transport system model in the membrane [93].

4. Controversial "Quantum Resonance" Based on Pythagorean Harmony

The quantum-mechanical resonances attracted the attention of many researchers. For example, the "orchestrated objective reduction of the quantum state" [94] concentrates on microtubules in the cells; the quantum-field approach of the water [95]. Many publications were devoted to living organisms' healthsustaining coherent, decoherent frequencies (detrimental) [96]. The idea has a root in the interference of waves. The interference pattern could be constructive and destructive, giving the biological rationale of the wave harmony [97]. These facts prompted the application of the Pythagorean wave harmony on strings to explain the resonance frequencies, including the Rife frequency spectrum. This resulted in a shift from the integer-based ancient set of wavenumbers to the quantum-mechanical energy eigenvalues starting from a reference frequency (ref 1Hz f = , due to practical reason) set of frequencies, defined by the formula called "GM scale" [98]:

$$E_n = hf_{ref}\, 2^n 3^m \left(2^p\right) = \hbar\omega_{ref}\, 2^{n+p} 3^m \qquad (1)$$

where E^n is the energy values of the discrete coherent electromagnetic waves, h is the Planck constant, and n, m, and p, are selected integers [99]. Analyzing the powerdensity of this generated Pythagorean spectrum, it follows a scaling law of S (f) noise density: $S(f) = f^{-\alpha}$ shown in **Figure 1**. By sorted number sequences of n, m, and p.

This mathematically correct scaling requests in (1) n = 0.5 (wolf sound) too, which is not an integer. The Pythagorean musical structure $\frac{1}{2^p}\left(\frac{3}{2}\right)^n = 3^n 2^{n-p}$ [6] limits the "freedom" of (1), so the spectrum differs from the assumptions of [99].

The consequences of the quantum wave in musical harmonic ratio had induced some doubtful research using the "cosmic musical master-code" [100]. The "mastercode" follows the Pythagorean harmony, with an extended anthropomorphic presentation of the human musical sense of harmony. Dubious research explains some fundamental problems in quantum mechanics with the ancient Pythagorean numerology. The descriptions include Bohm's implicate order [101], quantum coherence in living processes [102] [103], and even attempting to explain the origin of life with mineral interactions [104].

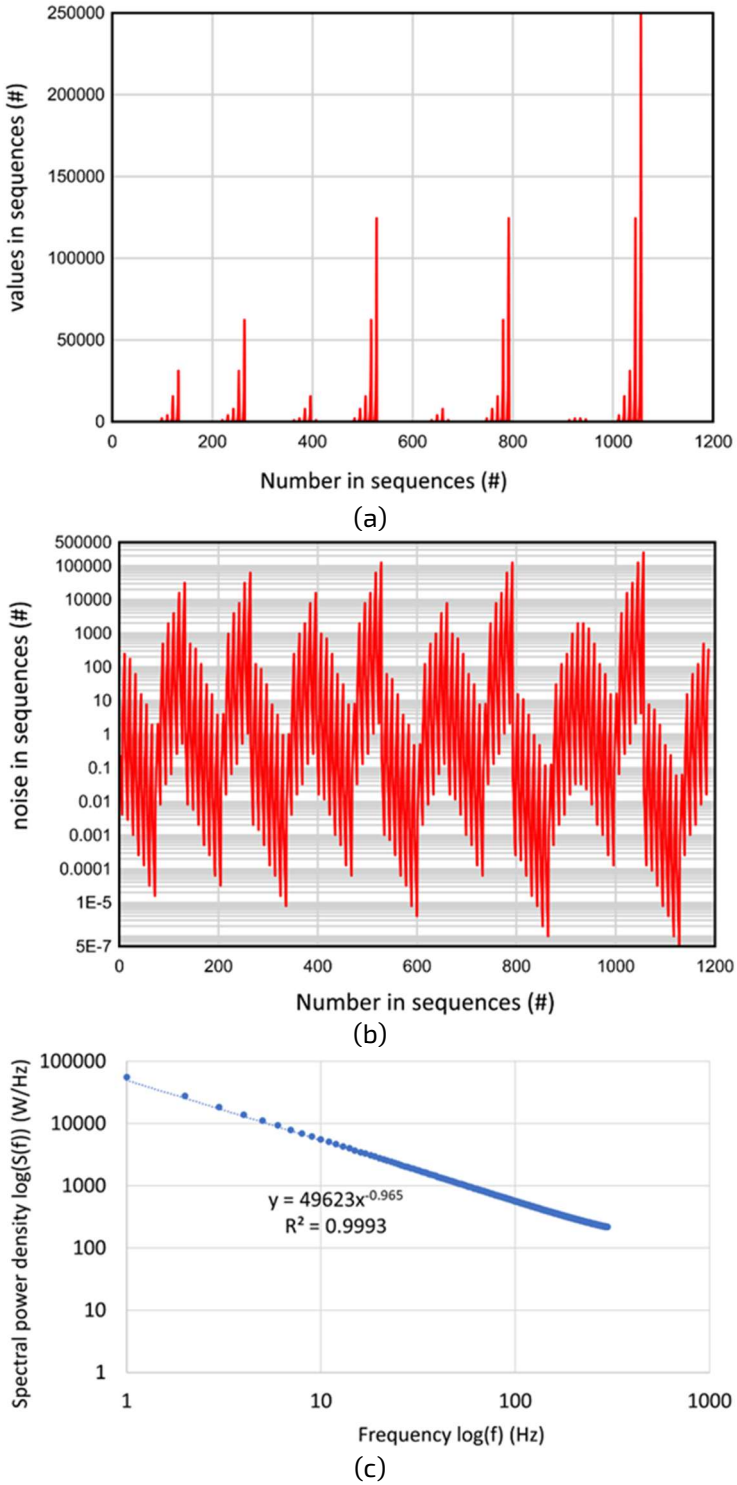

Figure 1. The frequency spectrum of the Geesink-Meijer "GM scale"

(a) The spectrum in frequency;
(b) The noise of the spectrum;
(c) The S(f) fit with Fourier transformation (FT, α = 0.965 , Microsoft excel), which practically approaches the pink-noise spectrum [99].

The consciousness is described with the help of the generalized Pythagorean musical harmony [105]. The theory also supports such mystique as the afterlife [106].

The theory and its presented proofs have serious challenges:

1) The Pythagorean harmony is valid in a tense string. The waves are formed in fixed boundary conditions, and these determine the waves in a system. What are boundary conditions fixed in this harmony concept? Where are these "strings" which resonate with the Pythagorean scale? How could the tense string waves be formed in the macroscopic cells?

2) The h ≅ 6.6×10^{-34} J ·s , which means subtle energy by (1). The quantum energy is enough to act in a quantum-mechanical object (like an electron in the atoms). However, the proteins are macroscopic (the cells are even more on a macro-scale) and immersed in the environment with thermal fluctuation in body temperature, which drastically exceeds the subtle energy transfer: 1 26 meV 4.2 10^{-21} J B k T ≈ ≈ × – [107]. One of the lowest binding energy in biosystems are the hydrogen bonds in various structures, having 6 - 30 kJ/mol (≈2 - 12 kBT) [108] [109] [110]; which are 2 - 12 times more than the thermal fluctuation in the living body. How is the energy of "quantum resonance", which is ≈1013 times less than the energy in hydrogen bonds, expected to alter the cancer cells? A question also arises: which signal pathway is chosen and which molecules are involved?

3) The description of (1) uses the 1D string vibrations and the wave-forming on the plane sheets [111]. However, the plane waves (membrane resonances) depend on the shape and thickness of the vibrating sheet (boundary conditions) [112] [113] and are not as simple to interpret as is proposed by the analogy f the tense string vibrations. A detailed and correct description is necessary to explain the proposed effects.

4) This quantum hypothesis continues the Pythagorean number-mystique as a mathematical algorithm for coherent quantum frequencies, used to support the Rife frequencies [114]; and the nonthermal electromagnetic interactions [96]. The Geesink Meijer "GM" scale appears to use similar divisions as the cents. It ranks from 1.0 to 1.898 for "coherent" ("GM-scale") and from 0.974 to 1.837 for "decoherent" "GM spectra", with the same twelve divisions of the "octave" [115]. The normalized frequency spectrum of the "beneficial" vs. "detrimental" signals [96] shows a continuation of the spectrum in an extensive range of frequencies. The slope of the beneficial vs. detrimental plot shows a ≈3.4% deviation from the equality of the two opposite effects increasing the doubt about the validity of the hypothesis Figure 2.

5) The further dubious consequence of the GM scale is the identical frequency dependence in Hz and GHz regions Figure 2. This contradicts the expectations of different mechanisms in these scales. The low frequency is principally active in the extracellular matrix and the cellular membrane, while the high frequency penetrates the cytosol and changes the molecular processes intracellularly.

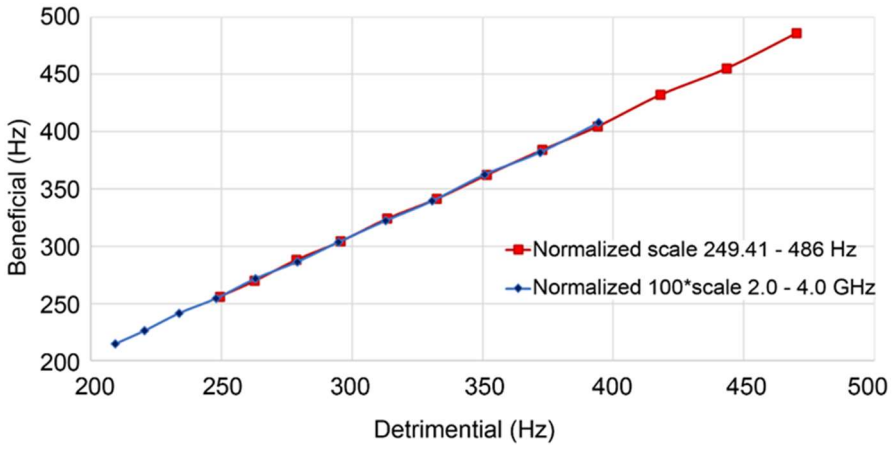

Figure 2. The "beneficial" vs. "detrimental" frequencies of "GM scale" [96]-[101]. A comparison of the GHz and Hz spectra shows complete identical slopes (slope = 1.03, R^2 = 0.998).

6) The fundamental doubt about this hypothesis comes from the harmony itself. The living systems have heterogenic "strings" and "plates" with complex interactions. The existence of these strings and plates resonating in "harmony" is illusory because all the strings and plates have different boundary conditions, so their resonances are far from the same, so their harmony needs much more conditional assumptions than Equation (1) describes. The healthy "harmony" is regulated and controlled by homeostasis, which induces 1/f noise calculated by multiple entropy analyses [116].

7) The data contain 219 and 123 separate biomedical studies for healthy homeostatic and cancerous situations, respectively [117]. The essential request of the statistical evaluation is cohort homogeneity which does not exist in the data for the GM-scale. The vast number of observations collect various experimental setups and use various substances, so these do not fit one unified GM-scale. The data do not belong to the same group of experiments, so their interpretation as a cohort is incorrect. We must have data collection and clinical trials according to international standards to surmount the trap of dubious assumptions.

8) According to the above doubts, the Pythagorean quantum coherence is a proofless continuation of the ancient Pythagorean number mysticism. The Pythagorean vibrating strings concept deals with mechanical conditions in a deterministic way. How does it fit the stochastic probability methodology of quantum mechanics? It is not as universal as quantum mechanics and has no such probability-dependent, stochastic phenomena, which are regarded as the corner point of quantum phenomena [118].

5. Doubts on Cancer-Specific "Resonant Harmony"

The health-supporting and detrimental signals from only a few Hz to THz frequencies are included in the massive set of "resonant" frequencies [119], mostly corresponding with Rife-frequencies results. Decoherence as the hypothetical cause of cancer [120] is also a noteworthy hypothesis. However, there are also numerous open, unanswered questions:

1) Cancer cells are "softer" than their normal host cells, and their membrane tension increases [121]. At the same time, their tumor is "harder" due to the place-demanding proliferation. Cancer elevates the lateral motility of membrane compartments [122], and at the same time, the membrane becomes more rigid in the perpendicular direction [123]. How do these cellular effects act positively or negatively on the resonances of tumor cells?

2) The tumor cells have lower membrane potential than their healthy host cells [124] [125], having shallower potential-well. Consequently, the probability of fixing the wave function inside the well is low (the tunnel effect dominates). How does the strict spectrum form?

3) The extracellular matrix in the cancer cells' microenvironment is highly disordered [126] [127] because the tumor cells break their networking connections (these are primarily individual, "autonomic" cells). How could resonances modify the harmony between them?

4) The minimal change which we need to modify the cellular structure is the transition of the unfolded state of polypeptides to the α-helix, when the entropy changes (decreases) by $\Delta S_{fold} = -1.38 \times \ln\left(6^{20}\right) \times 10^{-23}\ \mathrm{J/K} \cong -4.95 \times 10^{-22}\ \mathrm{J/K}$ which means the change of the internal energy $\Delta U = T\Delta S_{fold} \cong 1.4 \times 10^{-19}\ \mathrm{J}$ [128]. This is considerable energy compared to E_{quant} from (1), where $E_{quant} \cong 10^{-30}\ \mathrm{J}$ up to f is in kHz-region. From where does the energy come? Note, the THz frequency or higher (like optical) would be enough to provide the missing energy, but the RF range can not.

5) Cancer cells differ by size and shape from normal cells [129] and from each other [130] and even vary by metastatic potential [131]. How could the resonances with a single frequency modify these objects with various forms and conditions?

6) The beneficial and detrimental frequencies are linearly connected. The general biological frequencies [117] differ from cancerous frequencies in Figure 3. An explanation is needed, why are they generally "beneficial" frequencies not beneficial for cancer, and the opposite is that the systemic noncancerous "detrimental" frequencies differ from the detrimental resonances of cancer? Does this mean that the cancerous state is not detrimental?

7) Multiple measurements also show the effects of various parts of the cells in low-frequency regions. These changes are chemical and have nothing to do with such energy described by (1). These effects are induced by the electric field interaction in the classical energy exchanges, such as the Drude-model, frequency dispersions, or charge movements. These exchange energies are much higher than the supposed quantum-mechanical effect in (1). According to our current knowledge, the quantum description of the macro-particles and giant molecules like proteins or DNA is missing. Consequently, the wavefunction and the eigenvalues used in (1) do not describe the macro-objects in such small energies as supposed in (1).

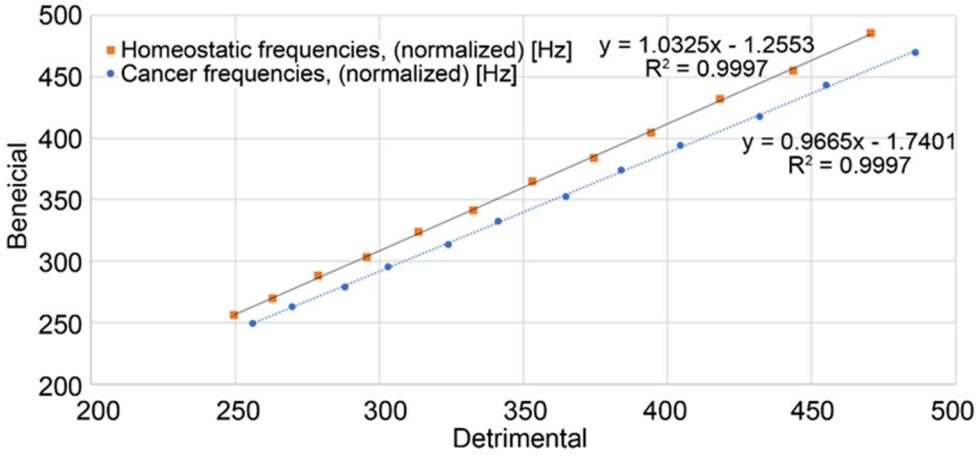

Figure 3. The normalized "beneficial" vs. "detrimental" frequencies (low-frequency spectrum) in cancerous and healthy states. It looks that the "detrimental" frequencies in a healthy state are not parts of the cancerous "detrimental" frequencies, and those frequencies which are "beneficial" in a healthy state are not parts of the beneficial frequencies of the cancer states showing the difference of the "detrimental" categories. A question arises: What do the defined "detrimental" and "beneficial" categories mean?

6. The Clinical Renewal of the Rife Concept

The resonant frequencies' concept was renewed about ten years ago [132]. The "Rife machine", which uses galvanically coupled current through the body from the electrodes in hands or feet, had been modified for under tongue electrode, providing high RF-frequency (27 MHz) as a carrier and delivering the "resonant frequencies by amplitude modulation of this carrier [133]. The in vitro experiments based on the historical roots [134], including Rife, Laskowski, and others, were used to prove the subtle energy application's clinical effect [135]. The method could also influence the effect of the cancer stem cells on chemoresistance [136]. A remarkable effect is shown for brain metastases on mammary carcinoma [137] and applied to one of the great challenges of the current oncology approach to hepatocellular carcinoma [138]. The method looks like a 'shift again' [139] after the long and complicated hectic changes in resonant frequencies" history.

The protocol of the treatment is simple and ultimately differs from GM-scale. The patient receives the electrode intra-orally, and nothing else is necessary for the process. The applied modulation frequencies are mainly in audio, but in some tumors, it goes up to 100 kHz range [140]. According to the protocol [140] I visually show the spectra for different cancer locations (Figure 4).

The patient receives every individual frequency for 3 s and sorts up to the higher values. Spectrum modulation frequencies are provided. The entire therapy session has 1 h duration, where the scan of frequencies is repeated when all the "prescribed" resonances were given [141] (Figure 5).

Together with the questioned, unknown molecular mechanisms of the method, the technical realization of the treatment has many challenges and doubts.

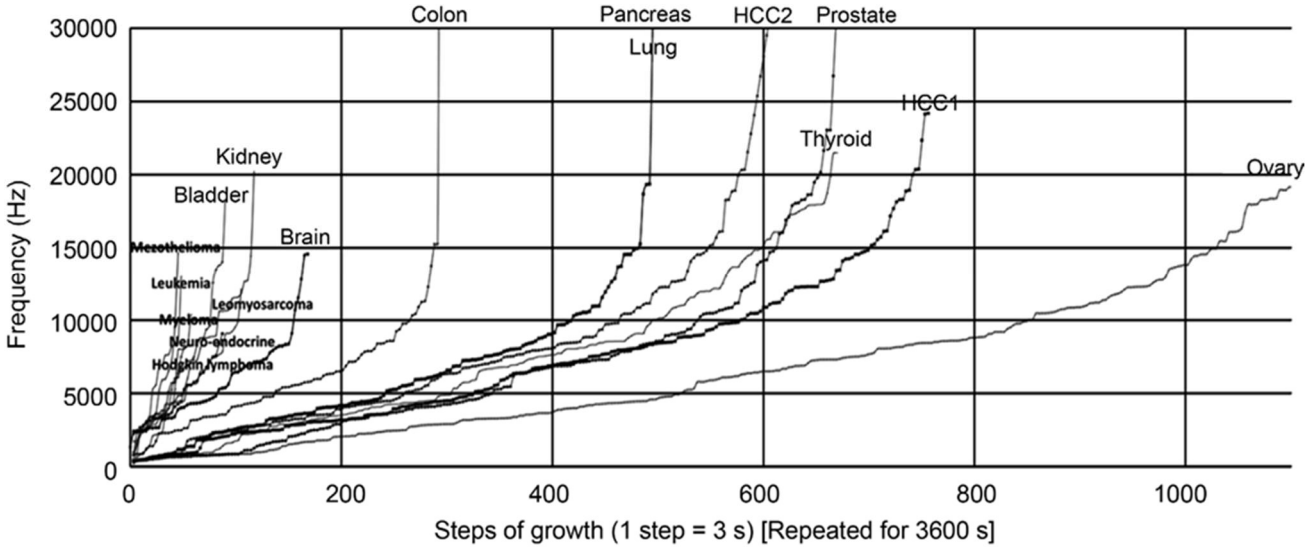

Figure 4. The frequency spectrum vs. time of the treatment in different diseases. The discrete points of the frequencies subsequently increase by 3 s constant state. The 60min duration of the treatment involves repetition of the discrete spectrum until the end of the treatment period.

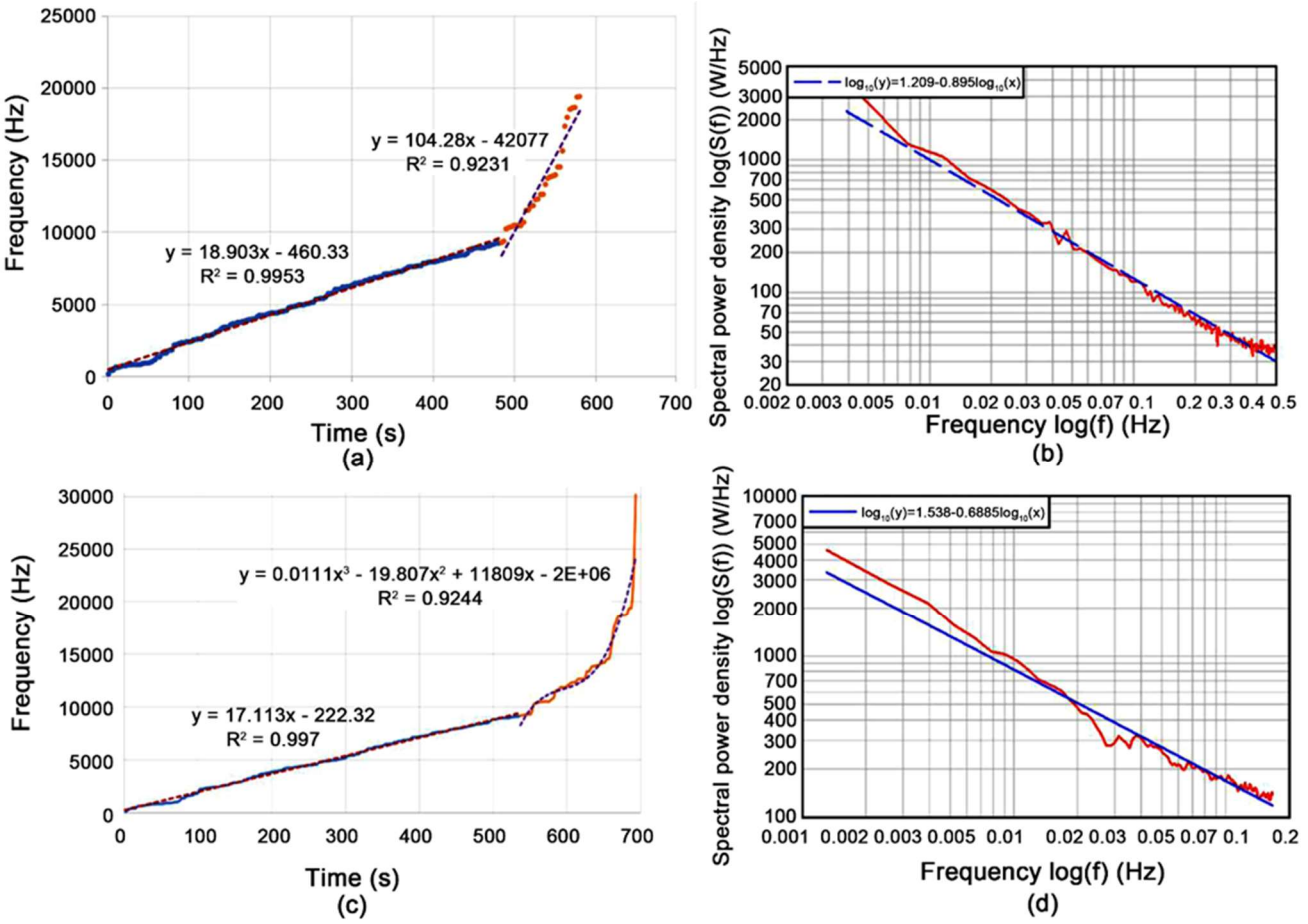

Figure 5. Example of breast treatment frequency applications.
(a) the discrete frequencies by time
(1 step = 3 s) [142]. Treatment repeats it until 60 min;
(b) the spectral power density S(f) fit by FFT (α = 0.895 , Dplot);
(c) Breast treatment in other publication;
(d) its spectral density by FFT
(α = 0.6885 , Dplot).

1) Only a single electrode, the intrabuccal spoon-shaped one, exists immersed in a saline environment. This single electrode does not form a definite RF electric circuit. The missing fixed RF circuit occasionally closes capacitively, coupled to the actual, uncontrolled environment of the patient [143].

2) The patient receives uncontrolled minimal (subtle) current intensity (μA) on an uncontrolled path of the current flow. How does it act selectively on the malignant cells throughout the whole body?

3) Notably, the shown SAR is ≈5 W/kg which is shown in the many independent parts of the body [143], implying the homogeneous SAR in the entire system. In the case of a 60 kg patient, it requests tremendous 300 W power homogeneously distributed into the body. From where this extreme power is coming? It is not possible to introduce such high power intrabucally, and the power supply is via a rechargeable battery.

4) There is no information on how the frequencies were chosen. Was it measured (not published) or is there a principal hypothesis? The frequency's power density has a slope of ≈0.6 - 0.8 on the double logarithmic scale. A publication referring to the treatments of breast cancer, hepatocellular carcinoma (HCC) [142] shows inhibited cancer-cell proliferation by specific modulation frequencies compared to random frequency reference. Frequencies differ by the individuals [140], while the power density fits well to the different diseases: for breast cancer $S_{breast}(f) \cong 1.533 - 0.8797 \log(f)$; HCC: $S_{HCC}(f) \cong 1.554 - 0.8790 \log(f)$ and the random frequencies although the method of randomizing the frequencies was not published) $S_{random}(f) \cong 1.598 - 0.8754 \log(f)$.

5) Technical details are missing about the modulation depth, accuracy of the frequencies, and the applied voltage.

6) The patient's impedance is very personal. No information was given about how it was tuned for personal parameters.

7) The in vitro and in vivo applications have no adequate technical description of the method, and it appears as if these have much higher energies per unit mass than the subtle (nonthermal) energy in human applications (≈1 W/(wholebody)). The cell sizes and shapes differ in vitro, in vivo, and ex vivo conditions [144] and significantly depend on their tumor microenvironment [145] and the signaling processes [146]. How can the resonances be compared?

8) Case reports show the efficacy. However, the reports on the clinical trials which were started 14 years ago [147] [148] are not available on scientific or academic platforms. The design of a new clinical trial is also announced, but no further information is available [149]. Despite the dubious theoretical concepts, the in-vitro and in-vivo experiments and the clinical data support the resonant phenomena. In the following, I am trying to give a possible stochastic explanation of the observed results.

7. Stochastic Processes

The living systems form a complex dynamic equilibrium that allows adaptation to the environmental conditions and internal regulative actions on broad scales in space and time [150]. The dynamic living structures perform random stationary stochastic self-organizing processes. Fractal physiology describes the system with interconnected self-similar spatiotemporal composition by fractal structures in space and time [151] [152] [153]. Moreover, the fractal physiology approach has practical medical applications in diagnoses [154] and therapies [155].

The conventional deterministic descriptions are insufficient to explain he observations, and stochastic processes determine the living objects [156]. The deterministic description is valid only in broad averages in space and time. The averages are macroscopic and could mislead microscopic research, which is necessary for resonance phenomena. Understanding the biological dynamism requires stochastic methodology, using probability "decisions" in all steps, and going over transition states that frequently have enzymatic assistance. The often ignored homeostatic balance governs the living processes in all spatiotemporal scales. Involving homeostasis in explanations is mandatory in order to understand the living complexity [157].

Due to the stochastic phenomena, the signals of the diagnostic parameters of the living processes fluctuate around the average of the band of acceptance signal level. The dynamical changes of microstates of the processes vary the fluctuations, regulated by feedback mechanisms. The negative feedback is the easiest way to regulate the desired values because when it stimulates the suppressor, the promoter limits the changes when it increases. The positive feedback triggers the development of a dynamic step, using the suppressor-promoter actions to reach a new equilibrium state. The overlapping signals and their interconnection create noise. The relatively constant noise time averages $\langle D_i \rangle$ of the microscopic diagnostic states D_i and standard deviation (σD_i) varies according to internal and external conditions. The homeostasis controls the complete spatiotemporal setting, regulates the order of noise structure, and keeps the signal within a tolerance band around the lD_i (Figure 6).

The subject is healthy when the homeostatic control faultlessly keeps the lD_i bands. Fluctuations $f_{D_i} = D_i - \langle D_i \rangle$ carry the details of the microscopic changes. The change of regulative processes drastically varies the f D_i, delivering information about the transformation of the microscopic interactions. The decomposition of the dynamically varying signals to periodic components (Fourier transformation) allows the signals' frequency, amplitude, and phase changes as components of the "noises". The noise varies when the immune system develops new functions by "learning" to fight against pathogens. The variation could be observed in cancer development, too [158]. Healthy dynamism correlates with metabolic circles and other fundamental living processes. The emitted (measured) fluctuation components characterize the time-set of different interactions and energy exchanges, showing a correlation of the signal with its earlier value at time-lag τ. The time delay describes the similarity of the signal parts when the exact microscopic change happens in the repeated molecular signal pathways. The timelag of the autocorrelation function informs the dynamism of the microstates.

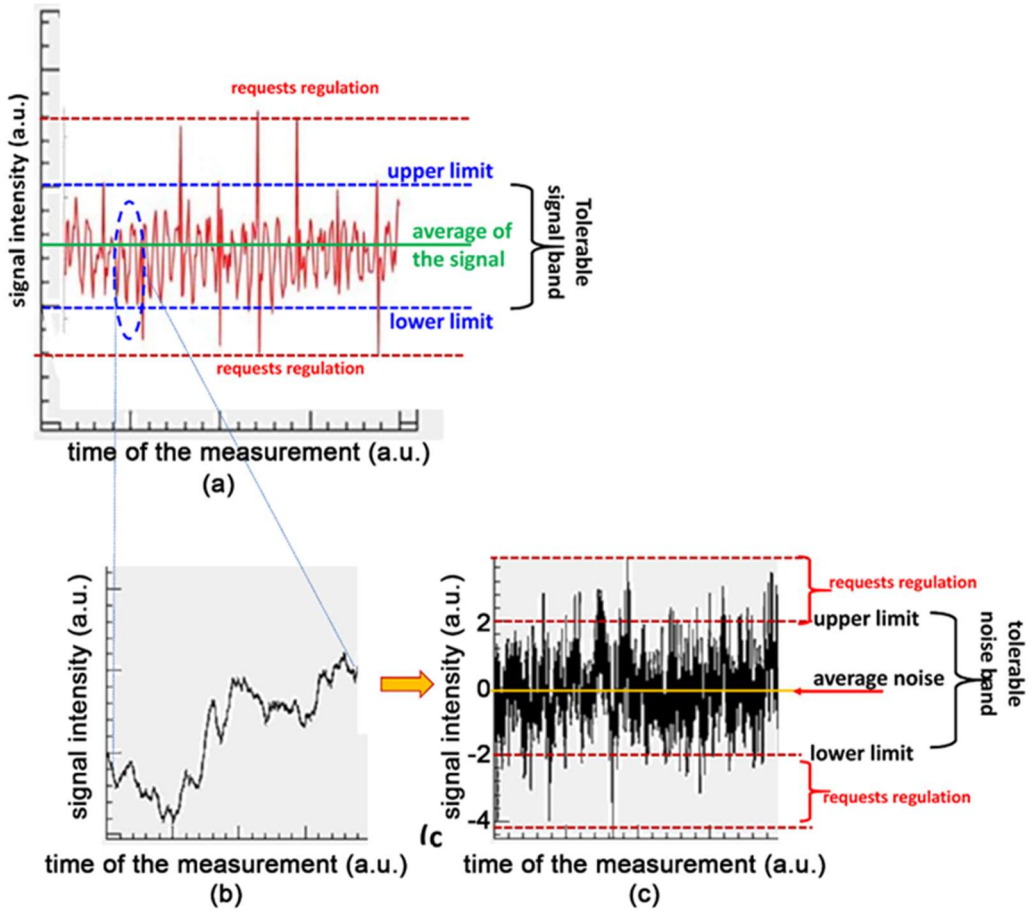

Figure 6. Example of a bio-signal and its noise.
(a) the measured signal
(b) the enlarged part of the signal,
(c) the signal's noise. The usual approach considers the average as the value of a measurement, despite the time dynamics of the signal and the standard deviation being different. The homeostatic control keeps the signal in a tolerable band in equilibrium, and the noise must not exceed the tolerance limit.

The homeostatic balance determines the correlating set of signals involved in the biological changes [159] [160]. The autocorrelation shows the preferences of possible variants of the molecular reactions [161], selection of their timing, and ordering for the desired signal-pathway or enzymatic actions. The frequencydependent power density spectrum S(f) is a fundamental characterization of the stochastic signals. The commonly studied simple noise is Gaussian (the amplitudes have normal distribution). The power function of the Gaussian noise is self-similar through many orders of magnitudes showing a simple power function with α

$$S(f) = \frac{A}{f^{\alpha}} \qquad (2)$$

As a consequence of the self-similar, self-organizing processes, the α = 1 (1/f noise or pink noise) appears in the timing of healthy life's dynamism [162], [163]. Self-organizing happens in structural and time arrangements [164] and dynamically regulates the processes in the living matter [165]. Halving or doubling the frequency carries an equal amount of noise energy in the 1/f noise, which has some similarities with musical harmony indeed. The self-organized symmetry of the healthy living system transforms the white noise into pink [166], forming the most common signal in biological systems [167].

8. Effect of Low-Frequency, Low-Intensity Intrinsic Excitation

The literature on cellular resonances concentrates on the low-frequency electromagnetic field (LFEMF), which appears in most of the technics of cancerspecific resonance considerations. Numerous reviews [168] [169], and articles eport the response of biological matter to LFEMF [170] [171] [172]. The current expectation is that the periodic intrinsic signal of the low-frequency region s biologically active. The earlier model approximations conclude that external excitation with low frequency is not able to make any effects connected to the cellular membrane. The early models assumed that changes in the field strength result from fluctuations of charges on both sides of the cellular membrane, and this fluctuation completely overwhelms the external excitations [173]. The thermal noise fluctuations at the cell membrane exceed any possible LFEMF-induced signals by some orders of magnitudes [173] [174], so thermal noise limits the electromagnetic influences.

Following the method of symmetrical components (zero-mode) of noise [175], a successful model was developed [176]. The noise of electric current mostly follows a directional symmetry between the electrodes. The zero-mode is a noise-sequence of the RF current inducing electrical energy of the cellmembrane capacity and has a uniform potential in spherical symmetry on the membrane, despite the unidirectional current [176]. The low-frequency zero-mode of noise enables the effect of the subtle external excitation in a relatively high thermal noise environment around the cells [177]. The zero-mode noisesequence excitation produced by an external periodic signal is symmetrical around the cell.

The complete symmetry required in order to induce a pure zero-mode field at a single cell using outer field generators is impossible because most applied external fields are unidirectional. However, there are self-induced and non-direct methods of constructing zero-mode noise components by applying external energy. Dynamic changing of the extracellular matrix (ECM) composition induces ionic currents producing zero-mode noise around the cell. The thermodiffusion offers another possibility of zero-mode noise. It could be achieved by capacitively coupled electromagnetic field within a specific frequency range [178] [179] [180] provided the RF current is able to penetrate directly into the cytosol.

Only negligible field penetrates the cell in low-frequency RF current (<10 kHz). The ECM absorbs the vast majority of the energy at these frequencies. The deviation of current flow leads to thermal gradients (thermal currents) from the ECM to the inside of the cell [181]. This thermal current also carries ions through, leading to thermo-diffusion, thus creating the symmetric electric current, which induces a zero-mode noise in the cell membrane. Both methods generate a centrally symmetric effect by the ionic and/or thermal gradient through the cellular membrane (Figure 7); therefore, even small fields with zero-mode components could elicit biological effects. The isotropic membrane appears as a condition of the symmetrical zero-mode noises. However, all cells have anisotropy on their membranes, especially the unhealthy cells (like malignant cells). Here various membrane segments with different electrical properties exists, allowing additional ionic exchanges. The anisotropy increases the non-zero noise mode, having less possibility of direct excitation with signal amplification of the membrane by ion-diffusion. In these conditions, thermal diffusion and its assistance for ionic exchanges remain the option to produce zero-mode noise.

9. Stochastic Resonance

The resonant behavior of stochastic processes is a noise-guided phenomenon [182]. Adding noise to an external deterministic signal of a nonlinear system produces a stochastic resonant (SR) output. The processes in living objects are inherently nonlinear and have bifurcative and probability-determined (stochastic) decisions of the promoter-suppressor actions at all levels of the organism [183]. The anharmonic factor of the potential well of molecules does not allow deterministic decisions. The applied external signal modulation is intended to go over the energy barrier ΔE(x) between the targeted initial substrate material (S) and the final product (P). The amplitude A of periodic external signal is small compared to the internal noises of the system, and so the provided formation does not become compelling enough.

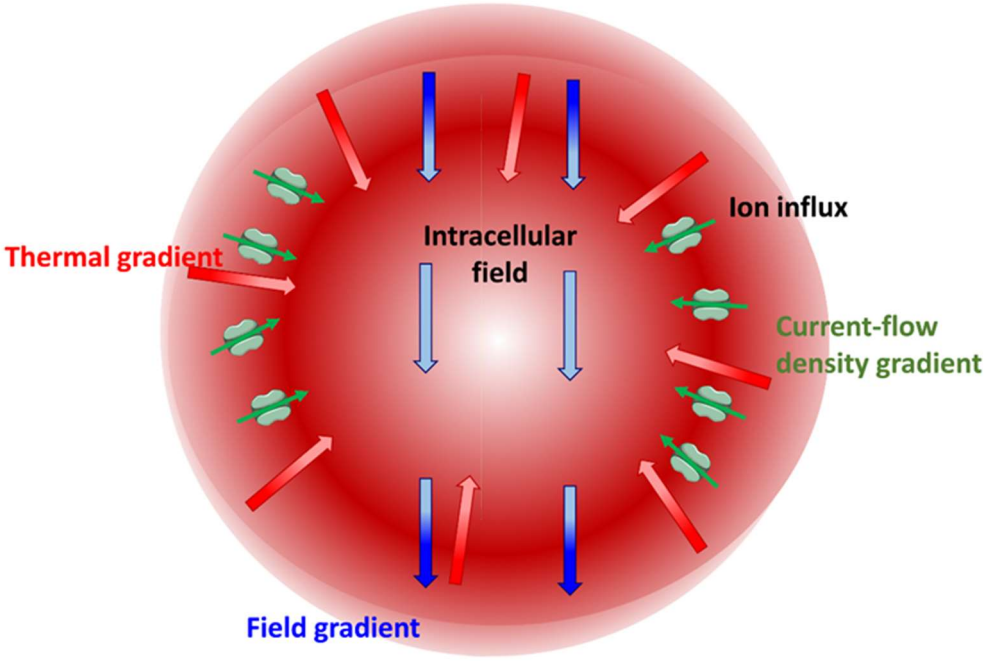

Figure 7. The various gradients at the cell membrane created by the RF-current.

Nevertheless, considerable amplification of the weak periodic signal could be observed by SR, depending on the strength of additional external noise to the intended excitation signal (Figure 8). The SR is only possible in nonlinear systems like living matter when the exciting signal is “noisy”. In the models and also in a majority of the practical situations, external or internal Gaussian white noise [184] [185], pink noise [186], Gaussian colored noises [187], or non- Gaussian noises [186] [188] accompany the specific periodic signal.

The signal-to-noise ratio (SNR) amplification has a broad peak in SR conditions, depending on the noise intensity [189] (Figure 9). The optimal noise intensity appears in the maxima of SNR. When the external noise level or the external periodic signal is kept fixed, the SNR has a saturation of increasing frequency or noise intensity, respectively [190]. However, the residence time intervals between consecutive signal peaks have SR peaks depending on the noise intensity or frequency of the external signal [190]. The SR peak limits the lower and upper levels of SNR, creating a window of the periodic frequency at constant noise. The internal noises adapt to the complex living system by a negative feedback correction of the optimal noise [191] [192]. The optimal noise induces the maximal SNR, dominating all other states. When the noise intensity deviates from the optimal, the signal weakens. The resonant signal obtains its maximum at some noise intensity, which makes the coherence of the multiple resonating units easier, creating feedback driven by the collectivity of the complex system. The optimizing driving force creates collectivity, which surmounts the individual needs of the cells.

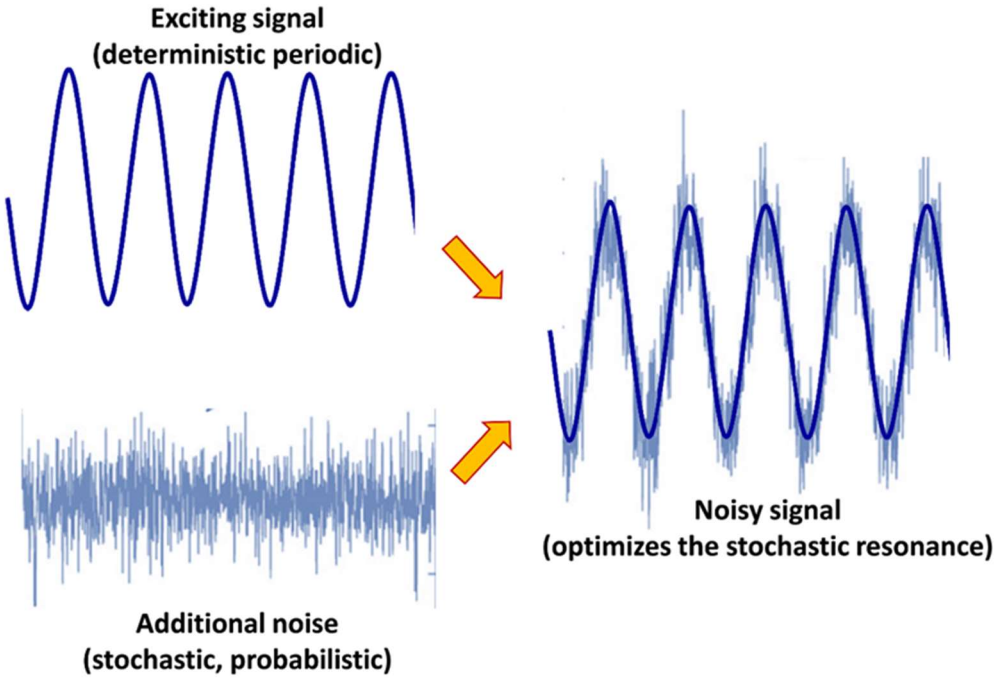

Figure 8. The mixture of the deterministic periodic signal with noise. The resulted "noisy" exciting can induce optimal stochastic resonance.

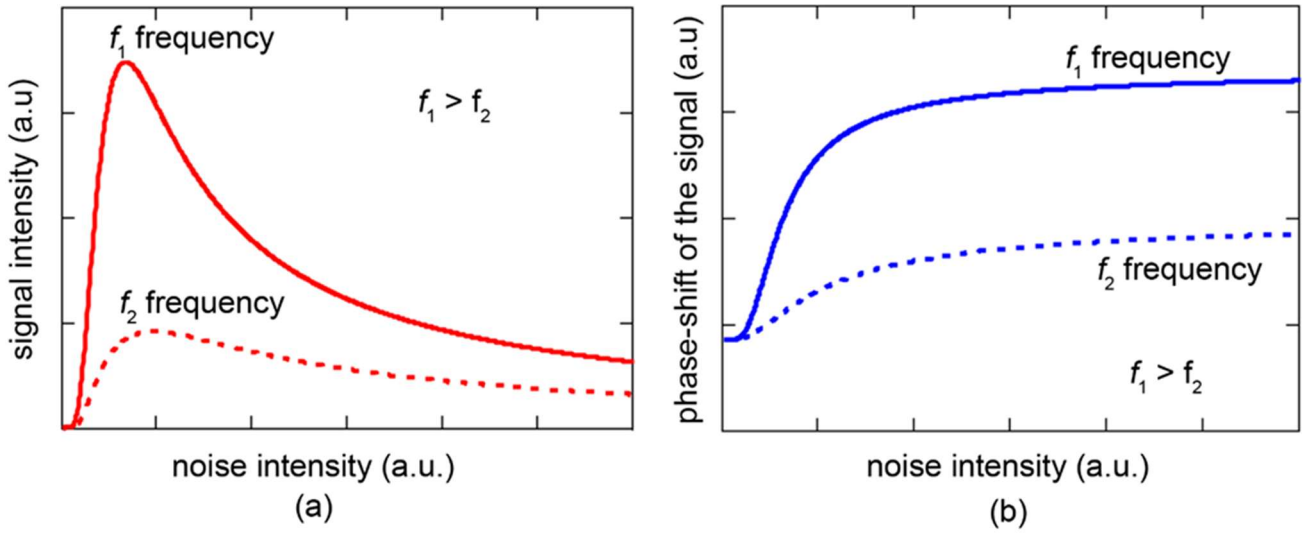

Figure 9. Noise dependence of the parameters of stochastic resonance.
(a) Signal intensity.
(b) Phase shift.

The cell waives a part of its energy for collective utilization in exchange for some shared services and enjoys systemic functions connected to its alimentation, optimal survival with the lowest energy consumption, and overall surveillance against pathogens and other invaders. The collectivity works like some kind of democracy [193] within the tissues. The cell became a part of a network exchanging information and materials as well, and in case of damage, the injured tissue has immediate help from its environment. Cancer follows the opposite way [194]. Its state is a "dismantling of multicellularity" [195], and the cellular collectivity disappears [196]. This development is similar to atavism [197]. In this way, cancer development opposes the collective driving force, its "Achillesheel" [198]. While the collectivity emits pink noise [116], the cancer cells deviate in their nose spectrum.

The applied single, noiseless frequency excitation was declared effective in various tumor-specific resonance studies [132] may use the internal noises for SR. However, the internal noise differs between healthy and cancerous emissions. The SR is sensitive to the noises, allowing its tuning to the optimal conditions.

Different noise spectra develop a variation of the amplitude maxima of resonant frequencies. The original Rife studies [54] [55] [56] [57], used an argongas-filled arc-lamp as the source. It differs from other cancer-specific resonant descriptions because the arc-discharge provides white noise for the carrier frequency and improves a well-formed SR's probability. The enzymes execute the molecular biological changes. Most intra and extracellular molecular reactions have a catalytic boost by enzymes to ease the reactions by transition states and the chemical reactions [199]. A simple, early model, the Michaelis-Menten enzyme model [200] (MME), describes the dynamism of the processes where the quantum mechanical rules govern the transition states [201]. The transition changes the cluster configuration and activates the transitional complex [202].

The MME description involves an enzyme (E) starting the formation of the product (P) from a substrate material (S) through a transition state ($E*$) with different conversion rates from S to $E*$ for progressive and reverse C_p , C_r , rates respectively, and finally from $E*$ to P with C_f .

$$E + S \underset{C_r}{\overset{C_p}{\rightleftarrows}} E^* \xrightarrow[C_f]{} A + P$$

The first step from the substrate to the transition state is reversible, and the conditions drive its balance in a negative feedback loop while getting the final product is an unconditional change, the result of the positive feedback process: The enzymatic processes regenerate the original conformal state of the E enzyme for reuse in a catalytic way. The $E*$ state has two sub-states (E_1* and E_2*) in the reaction: the E_1* = ES complex transforms to P product, via E_2* = EP complex, while the enzyme transforms back to E state at the end of the process. Like all reactions, chemical activity steps are reversible; the progress ↔ reverse interaction rate balances all steps. The production mechanism must have positive feedback to force P product from the S substrate and shift the equilibrium to a definite direction. The driving force is usually the standard environmental living condition that ignites and controls the process. After finishing the production, the enzyme returns to its initial conformal state and may restart the action. This form of a loop ("catalytic wheel" [203], Figure 10), is driven by negative feedback.

The wheel model describes a cyclic catalytic reaction with two conformation states of the process's speed, described by a steady-state technique [204]. The catalytic wheel decreases the energy barrier (activation energy E_a) between the substrate and product. The E_a has thermal (enthalpy factor) and nonthermal (entropy factor) components, and the change of the activation energy (ΔE_a). The subthreshold signal induces SR resonance which causes modification even in single cells [205], controlling the gating membrane channels and selecting ions, and molecules' entry to the cytosol [205]. While experimental general Arrhenius law considers a single step jump over the Ea energy barrier, in real processes, the substrate state never transform into products in a single direct step [206] [207], [208]. In this transition, the thermal and electric effects have similarities, unifying the phenomena in a complex unit [209]. Additionally, a typical quantummechanical phenomenon, the tunneling effect through the barrier, could modify the transition [210].

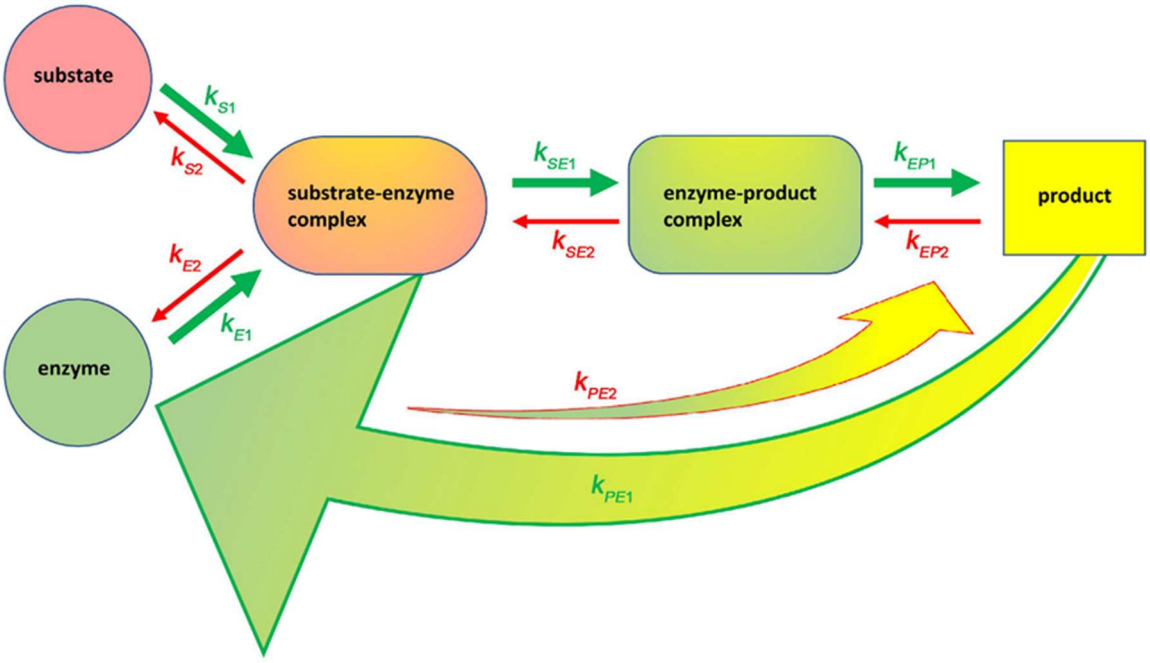

Figure 10. The enzymatic changes during the S → P transformation. The well applied ECC conditions drive the relation $k_{S2} < k_{S1}$, $k_{SE2} < k_{SE1}$, $k_{EP2} < k_{EP1}$ and , $k_{PE2} < k_{PE1}$ so the "wheel" works in one direction, by the Michaelis-Menten process.

The electric field of various electromagnetic signals could actively ignite, modify or block the enzymatic wheels by electro-conformal coupling (ECC, [211] [212]). ECC uses oscillatory SR stimulation to promote the transition of the substrate to the product [213]. The SR controls the probability of the S → P enzymatic process fixing it in the homeostatic dynamic equilibrium [214]. The environmental thermal noise drives the SR providing energy to this process by the Brownian engine [215] [216]. A periodic electric field may convert the accessible energy-producing transports to chemical reactions coupled through enzymatic processes [217]. The ECC rectifies the thermal fluctuations, driving one-directional dynamics [218] [219], representing a "ratchet" like behavior pumping the processes in one direction only, blocking the opposite turn. The thermal fluctuations, together with the electric noises of the incident signal, provide the available free energy [218]. The thermal energy is high: the ATP hydrolysis has ≈10–16 W, while the thermal factor of dynamic molecular scattering provides 10–8 W [220]. The Brownian engine processes work with irreversible thermodynamics with an external periodic perturbation [221]. The thermal components of the micro and macro environment of the tumor cells determine the ECC. When the noise is thermal (white), the ECC has an optimal temperature, but in colored noise (like 1/f noise) conditions, the temperature dependence is weaker.

A considerable number of enzymes and enzymatic reactions exist in human biology. The cancer metabolic pathways alone have many enzymatic processes [222] [223], which is a small part of the complete number of enzymes involved in various homeostatic bioreactions. The complexity makes the huge adaption of the system to environmental changes possible when the homeostatic network substitutes a missing process with others. The enormous number of enzymatic reactions determines the number of SR resonant frequencies. Due to the noise dependence of SR, the actual resonance sharply depends on the reaction's environmental temperature and the excitation signal's noise. Consequently, the same bioreaction may have various exciting signals for effective and optimal SR. Complicates the selection of SR that the excitation could also be effective on other nonlinear bistable structures, like the activation of voltage-gated ion channels. The electrically generated subthreshold stimuli affect the transition state of molecular reactions in various biological processes [224]. One of the explanations of the Rife resonant frequencies could involve the SR phenomena. However, in this case, the resonant frequencies express a dense spectrum. It has as many resonances as enzymatic reactions that exist in the target. However, another request is to drive the cancer cell's cell death when we do not expect prompt necrosis. The SR amplification has to be multiple, with steps of the signal pathway involving different enzymatic processes and resonances. The complexity offers multiple signal variants, which could direct the pathway to the different final results.

Consequently, the stable solution needs a set of SR frequencies in an appropriate time set. The networking has chain reactions through the signal pathways. The subsequent reactions in the chain define the order of the necessary enzymatic action, which can be modified by external signals when their autocorrelation supports the reaction sequences. The optimally chosen exciting signal with properly fitting autocorrelation can drive the ordered chain reaction with subsequent SRs [225].

10. Conclusions

The enzymatic stochastic resonance defines specific resonant frequencies [226] [227] on the molecular level. The stochastic resonance (SR) describes the interaction of a deterministic subthreshold signal and a fluctuation (noise) spectrum. The phenomenon inherently depends on temperature. The resonant frequencies of neuronal-like healthy and cancer cell membrane channels differ and are excitable [228]. The SR may explain the Rife frequencies. The response to weak external electric fields by definite modulation frequencies could remain active far below the thermal noise limit and ignites some molecular processes by the stochastic resonance. The number of resonant frequencies acting in the cellular processes is at least as many as enzymatic activities. Multiple conditional factors modify the resonance and the frequency of the peak, producing a vast number of different resonances.

Additionally, the SR depends on the temperature and pH in the cell's microenvironment. Furthermore, the cellular structure (like size, form), state (like age, stress), and dynamic development (like chemotaxis and cellular division) certainly affect the resonance and shift or even block the resonant frequency. The size of a studied group of molecules offers a typical size dependence of resonances, including harmony between the group members [229]. The intercellular interaction changes the resonances and multiplies the observable resonant peaks. The modulation excitation of membrane rafts [230] [231] considers this possibility with a well-defined spectrum of modulation frequencies [226] [232]. The resonant reaction complexity operates in

a network of interactive intra- and extracellular functions. The interconnection of the intracellular complex multi- pathway feedback loops and the multicellular interactions does not allow for the division of the resonance into two distinct “detrimental” and “beneficial” categories. The biological complexity does not permit the black-and-white categorizing and does not allow to deterministically determine that some resonances are healthy and some are not. The “beneficial” signal pathways may work “detrimentally” among various tumor microenvironment conditions. All the participating molecules of the complex network have a “double-edged sword” quality, having optimal molecular reactions in a narrow range of conditions. The molecular change presents deterministic-like processes only when we form a large average of the considered parameters on the macroscale. The microscale offers only probabilistic considerations. The apparent deterministic Pythagorean harmony of numbers is valid only in macroscopic averages, but the resonance is microscopic. The explanation of molecular resonance processes incorrectly describes the phenomena in a classical deterministic way.

Electromagnetic medicine represents a new modality, using molecular biology for therapy [233], including oncology [234]. The molecular excitation by using resonances [235] has enormous opportunities. Some bioresonances, like cyclotron resonance [236], are well proven and hypothesized for new kinds of vaccination [237]. The antitumoral vaccination forces tumor-specific immune reactions ignited by thermal and nonthermal effects of nonionizing RF radiation. Bioelectromagnetismactivates both the innate and adaptive immune system [238], promoting the abscopal effect [239] [240], and becomes a part of the complementary clinical therapies [241] [242]. However, presently our knowledge about bioelectromagnetic resonances is somewhat limited. Rigorous theoretical and experimental investigations with randomized prospective clinical studies are mandatory for the further clearance of the cancer-specific resonant frequencies.

Acknowledgements
This work was supported by the Hungarian National Research Development and Innovation Office PIACI KFI grant: 2019-1.1.1-PIACI-KFI-2019-00011.

Conflicts of Interest
The author declares no conflicts of interest regarding the publication of this paper.

References

[1] Kempf, E.J. (1906) European Medicine: A Résumé of Medical Progress during the Eighteenth and Nineteenth Centuries. Journal of the Medical Library Association, 3, 231-248.

[2] Mattei, C.C. (1880) Principles of Electrohomoeopathy. A New Science Discovered by Count Cesar Mattei of Bologna. Printing and Stereotype Offices V.-E. Gauthier and Co., Nice.

[3] Baylen, J.O. (1969) The Mattei Cancer Cure: A Victorian Nostrum. Proceedings of the American Philosophical Society , 113, 149-176.

[4] Memorial Sloan-Kettering Cancer Center (2012, May 29) BioResonance Therapy

[5] Suresh, S.K. (2018) The Greatest Enemy of Knowledge Is Not Ignorance, It Is the Illusion of Knowledge. https://medium.com/@somesh.ks/the-greatest-enemy-of-knowledge-is-not-ignorance-it-is-the-illusion-of-knowledge-5c0dd1dcca7e

[6] Hornberger, J. (2019) Who Is the Fake One Now? Questions of Quackery, Worldiness and Legitimacy. Critical Public Health , 29, 484-493. https://doi.org/10.1080/09581596.2019.1602719

[7] Sethares, W.A. (2005) Tuning, Timbre, Spectrum, Scale. Springer, Berlin.

[8] Sikic, Z. (2016) Generalized Pythagorean Comma. CroArtScia 2011, Zagreb, 4-7 May 2011, 169-174.

[9] Livio, M. (2003) The Golden Ratio: The story of Phi, the World’s Most Astonishing Number. Broadway Books, New York City, 145 p.

[10] Cui, H.Y. (2002) To String Together Six Theorems of Physics by Pythagoras Theorem.

[11] Darvas, G., Koblyakov, A.A., Petoukhov, S.V. and Stepanian, I.V. (2012) Symmetries in Molecular-Genetic Systems and Musical Harmony. Symmetry : Culture and Science , 23, 343-375.

[12] Garrett, S.L. (2020) String Theory. In: Understanding Acoustic s, Springer, Berlin, 133-178. https://doi.org/10.1007/978-3-030-44787-8_3

[13] Schuch, D. (2010) Pythagorean Quantization, Action(s) and the Arrow of Time. Journal of Physics : Conference Series , 237, Article ID: 012020. https://doi.org/10.1088/1742-6596/237/1/012020

[14] Overduin, J. and Henry, R.C. (2005) Physics and the Pythagorean Theorem.

[15] Richinick, J. (2008) The Upside-Down Pythagorean Theorem. The Mathematical Gazette , 92, 313-316. https://doi.org/10.1017/S0025557200183275

[16] Kappraff, J. and Adamson, G.W. (2009) Generalized Genomic Matrices. Silver Means , and Pythagorean Triples , Forma , 24, 41-48.

[17] Overmarch, A., Ntogramatzidis, L. and Venkatraman, S. (2019) A New Approach to Generate All Pythagorean Triples. AIMS Mathematics , 4, 242-253. https://doi.org/10.3934/math.2019.2.242

[18] Maxwell, J.C. (1998) A Treatise on Electricity and Magnetism. Clarendon Press, Oxford.

[19] Benett, W.R. (1994) Cancer and Power Lines. Physics Toda y, 47, 23-29. https://doi.org/10.1063/1.881417

[20] Portier, C.J. and Wolfe, M.S. (1998) Assessment of Health Effects from Exposure to Power-Line Frequency Electric and Magnetic Fields. NIH Publication 98-3981. National Institute of Environmental Health Sciences, Research Triangle Park.

[21] Harland, J.D. and Liburdy, R.P. (1997) Environmental Magnetic Fields Inhibit the Antiproliferation Action of Tamoxifen and Melatonin in a Human Breast Cancer Cell Line. Bioelectromagnetics , 18, 555-562. https://doi.org/10.1002/(SICI)1521-186X(1997)18:8<555::AID-BEM4>3.0.CO;2-1

[22] Ahlbom, A., Day, N., Feychting, M., Roman, E., Skinner, J., et al . (2000) A Pooled Analysis of Magnetic Fields and Childhood Leukemia. British Journal of Cancer , 83, 692-698. https://doi.org/10.1054/bjoc.2000.1376

[23] Greenland, S., Sheppard, A.R., Kaune, W.T., et al . (2000) A Pooled Analysis of Magnetic Fields, Wire Codes, and Childhood Leukemia. Epidemiology, 11, 624-634. https://doi.org/10.1097/00001648-200011000-00003

[24] Takebe, H., Shiga, T., Kato, M. and Masada. E. (2001) Biological and Health Effects from Exposure to Power-Line Frequency Electromagnetic Fields. IOS Press, Amsterdam.

[25] Randerson, J. (2007, January 18) Electrosmog in the Clear with Scientists. The Guardian. http://www.guardian.co.uk/technology/2007/jan/18/guardianweeklytechnologysection4

[26] Oschman, J. (2000). Energy Medicine—The Scientific Basis. Churchill Livingstone, Edinburgh.

[27] Loja, T., Stehlikova, O., Palko, L., Vrba, K., Rampl, I. and Klabusay, M. (2014) Influence of Pulsed Electromagnetic and Pulsed Vector Magnetic Potential Field on the Growth of Tumor Cells. Electromagnetic Biology and Medicine , 33, 190-197. https://doi.org/10.3109/15368378.2013.800104

[28] Rein, G. and Tiller, W.A. (1996) Anomalous Information Storage in Water: Spectroscopic Evidence for Non-Quantum Informational Transfer. Proceedings 3rd International Conference New Energy , Denver, 24-28 April 1996, 365.

[29] Meyl, K. (2001) Scalar Waves: Theory and Experiments. Journal of Scientific Exploration, 15, 199-205.

[30] Tiller, W.A. (1999) Subtle Energies. Science & Medicine , 6, 28 p.

[31] Hall, H. (2005) A Review of Energy Medicine: The Scientific Basis. Skeptic Magazine, 11, 89-93.

http://quackfiles.blogspot.com/2006/01/review-of-energy-medicine-scientific.html

[32] Bruhn, G.W. (2000) Commentary on the Chapter “Scalar Waves”, in “Energy Medicine— The Scientific Basis”. http://www.mathematik.tu-darmstadt.de/~bruhn/Commentary-Oschman.htm

[33] Bruhn, G.W. (2001) On the Existence of K. Meyl’s Scalar Waves. Journal of Scientific Exploration, 15, 206-210.

[34] Saliev, T., Begimbetova, D., Masoud, A.R. and Matkarimov (2019) Biological Effects of Non-Ionizing Electromagnetic Fields—Two Sides of a Coin. Progress in Biophysics and Molecular Biology, 141, 25-36. https://doi.org/10.1016/j.pbiomolbio.2018.07.009

[35] Carlson, W.B. (2013) Tesla: Inventor of the Electrical Age. Princeton University Press, Princeton. https://doi.org/10.1515/9781400846559

[36] Tesla, N. (1891) Patent Title: Alternating Electric Current Generator. US447,921.

[37] Tesla, N. (1914) Patent Title: Apparatus for Transmitting Electrical Energy. US1119732 A.

[38] Tesla, N. (1905) Art of Transmitting Electrical Energy through the Natural Medium. United States Patent, No. 787,412.

[39] Tesla, N. (1898) High Frequency Oscillators for ElectroTherapeutic and Other Purposes. The Electrical Engineer , 26, 346-348.

[40] Aharonov, Y. and Bohm, D. (1959) Significance of Electromagnetic Potentials in Quantum Theory. Physical Review, 115, 485-491. https://doi.org/10.1103/PhysRev.115.485

[41] Szasz, A., Vincze, Gy. andocs, G. and Szasz, O. (2009) Do Field-Free Electromagnetic Potentials Play a Role in Biology? Electromagnetic Biology and Medicine, 28, 135-147. https://doi.org/10.1080/15368370802711938

[42] Hegyi, G., Vincze, Gy. and Szasz, A. (2007) Axial Vector Interaction with Bio-Systems. Electromagnetic Biology and Medicine , 26, 107-118. https://doi.org/10.1080/15368370701380835

[43] Andocs, G., Vincze, Gy., Szasz, O., Szendro, P. and Szasz, A. (2009) Effect of Curl-Free Potentials on Water. Electromagnetic Biology and Medicine , 28, 166-181. https://doi.org/10.1080/15368370902724724

[44] A Brief History of Dr. Royal Raymond Rife. https://www.nationallibertyalliance.org/files/NaturalHealing/Rife/History%20of%20Dr%20Rife.pdf

[45] Bird, C. (1976) What Has Become of the Rife Microscope? New Age Journal , March 1976, 41-47.

[46] Seldel, R.E. and Winter, M.E. (1944) The New Microscopes. Journal of the Franklin Institute , 237, 103-130.

[47] Kendall, A.I. and Rife, R.R. (1931) Observations on Bacillus Typhosus in Its Filterable State: A Preliminary Communication. California and Western Medicine , 35, 409-411.

[48] Stylianidou, S., Connor, B., Nissen, S.B., Kuwada, N.J. and Wiggins, P.A. (2016) SuperSegger: Robust Image Segmentation, Analysis and Lineage Tracking of Bacterial Cells. Molecular Microbiology, 102, 690-700. https://doi.org/10.1111/mmi.13486

[49] Merouan, A., Rey, Villamizar, N., Lu, Y.B., Liadi, I., Romain, G., Lu, J., Singh, H., Cooper, L.J.N., Varadarajan, N. and Roysam, B. (2015) Automated Profiling of Individual Cell-Cell Interactions from High-Throughput Time-Lapse Imaging Microscopy in Nanowell Grids (TIMING). Bioinformatics , 31, 3189-3197. https://doi.org/10.1093/bioinformatics/btv355

[50] Young, J.W., Locke, J.C.W., Altinok, A., Rosenfeld, N., Bacarian, T., Swain, P.S., Mjolsness, E. and Elowitz, M.B. (2011) Measuring Single-Cell Gene Expression Dynamics in Bacteria Using Fluorescence Time-Lapse Microscopy. Nature Protocols, 7, 80-88. https://doi.org/10.1038/nprot.2011.432

[51] Tesla, N. (1885) Electric Arc Lamp. US171,416.

[52] Scoon, A. (2001) Special Supplement of Everyday Practical Electronics, April 2001. Wimbore Publishing Ltd., Dorset, and Maxfield & Montrose Interactive Inc., Madison. https://www.rife.de/files/epearticle.pdf

[53] Jones, N. (1938) Dread Disease Germs Destroyed by Rays, Claim of S.D. Scientist: Cancer Blow Seen after 18-Year Toil by Rife. The San Diego Union-Tribune , 1.

[54] Line, B. (2017) Rife's Great Discovery: Why "Resonant Frequency" Therapy Is Kept Hidden from Public Awareness. BioMed Publishing Group, South Lake Tahoe.

[55] Lynes, B. (1997) The Cancer Cure That Worked: 50 Years of Suppression. Marcus Publishing, Canada.

[56] Allegretti, M. (2018) The Frequencies of Rifing—From the First Frequencies Discovered by Royal Rife to Today: Guide to Selection and Use of Spooky2 Frequencies.

[57] Silver, N. (2001) The Handbook of Rife Frequency Healing: Holistic Technology for Cancer and Other Diseases. The Center for Frequency Education Publishing, Stone Ridge.

[58] Energy Medicine—Radionics Rife Machine. http://www.skepdic.com/radionics.html

[59] (1994) Questionable Methods of Cancer Management: Electronic Devices. CA: A Cancer Journal for Clinicians , 44, 115-127. https://doi.org/10.3322/canjclin.44.2.115

[60] Barrett, S. (2010) Device Watch—Rife Device Marketer Sentenced to Prison. https://quackwatch.org/device/reports/rife/folsom

[61] Barrett, S. (2012) Rife Machine Operator Sued. Quackwatch. https://www.quackwatch.org/04ConsumerEducation/News/rife.html

[62] Farley, D.F. (1996) Unproven Medical Clamims Land Men in Prison, Investigators' Reports. FDA Consumer. U.S. Food and Drug Administration. https://web.archive.org/web/20071214170405/https://www.fda.gov/fdac/departs/796_irs.html

[63] Kurtzweil, P. (1996) Investigators' Reports. FDA Consumer. U.S. Food and Drug Administration. https://web.archive.org/web/20071214170405/https://www.fda.gov/fdac/departs/796_irs.html

[64] Willmsen, C. and Berens, M.J. (2007) Pair Indicted on Fraud Charges in Medical-Device Probe. The Seattle Times. https://www.seattletimes.com/seattle-news/pair-indicted-on-fraud-charges-in-medical-device-probe

[65] Barrett, S. (2009) Rife Device Marketers Convicted. Quackwatch.

[66] Johnson, J. (2019) Can the Rife Machine Treat Cancer? https://www.medicalnewstoday.com/articles/325628.php

[67] Hill, B. (2000) Cheating Death. The Sydney Morning Herald. http://www.healthwatcher.net/Quackerywatch/Cancer/Cancer-news/smh001230rife-aus.html

[68] No Authors Listed (1994) Questionable Methods of Cancer Management: Electronic Devices. CA: A Cancer Journal for Clinicians , 44, 115-127. https://doi.org/10.3322/canjclin.44.2.115

[69] (2013) Rife Machines and Cancer. Cancer Research UK.

[70] Lakhovsky, G. (1925) Curing Cancer with Ultra Radio Frequencies. Radio News, February, 1282-1283.

[71] Lakhovsky, G. (1988) Secret of Life: Electricity Radiation & Your Body. 4th Revised Edition, Noontide Press, Newport Beach.

[72] Rife, R.R. (1953) History of the Development of a Successful Treatment for Cancer and Other Virus, Bacteria and Fungi. Rife Virus Microscope Institute, San Diego.

[73] Bearden, T.E. (1995) Vacuum Engines and Priore's Methodology: The True Science of Energy Medicine. Explore , 6, 66-76.

[74] Bateman, J.B. (1978) A Biologically Active Combination of Modulated Magnetic and Microwave Fields: The Prioré Machine. Office of Naval Research, London, Report R-5-78.

[75] Camp, J. (1973) Magic, Myth and Medicine. Priory Press Ltd., Dunstable.

[76] Gurwitsch, A.G. (1944) A Biological Field Theory. Nauka, Moscow. (In Russian)

[77] Beloussov, L.V., Opitz, J.M. and Gilbert, S.F. (1997) Life of Alexander G. Gurwitsch and His Relevant Contribution to the Theory of Morphogenetic Fields. The International Journal of Developmental Biology , 41, 771-777.

[78] Spemann, H. (1938) Embryonic Development and Induction. Yale University Press, New Haven.

[79] Manning, C.A. and Vanrenen, L. (1989) Bioenergetic Medicines East and West. North Atlantic Books, Berkeley.

[80] Levin, M. (2012) Morphogenetic Fields in Embryogenesis, Regeneration, and Cancer: Non-Local Control of Complex Patterning. Biosystems , 109, 243-261. https://doi.org/10.1016/j.biosystems.2012.04.005

[81] Levin, M. (2003) Bioelectromagnetics in Morphogenesis (Review). Bioelectromagnetics , 24, 295-315. https://doi.org/10.1002/bem.10104

[82] Volodiaev, I. and Belousssov, L.V. (2015) Revisiting the Mitogenetic Effect of Ultra- Weak Photon Emission. Frontiers in Physiology , 6, Article No. 241. https://doi.org/10.3389/fphys.2015.00241

[83] Thompson, W.G. (2005) The Placebo Effect and Health, Combining Science and Compassionate Care. Prometheus Books, New York.

[84] Gauler, T.C. and Weihrauch, T.R. (1997) Placebo. Urban & Schwarzenberg, Munich.

[85] Hróbjartsson, A. and Gøtzsche, P.C. (2010) Placebo Interventions for All Clinical Conditions. The Cochrane Database of Systematic Reviews, 106, CD003974. https://doi.org/10.1002/14651858.CD003974.pub3

[86] Lin, J.C. (1989) Electromagnetic Interaction with Biological Systems. Pergamon Press, New York, London. https://doi.org/10.1007/978-1-4684-8059-7

[87] Bersani, F. (1999) Electricity and Magnetism in Biology and Medicine. Kluwer Academic Plenum Publishers, New York, Boston. https://doi.org/10.1007/978-1-4615-4867-6

[88] Marko, M. (2005) “Biological Windows”: A Tribute to WR Adey. The Environmentalist , 25, 67-74. https://doi.org/10.1007/s10669-005-4268-8

[89] Adey, W.R. (1984) Nonlinear, Nonequilibrium Aspects of Electromagnetic Field interactions at Cell Membranes. In: Adey, W.R. and Lawrence, A.F., Eds., Nonlinear Electrodynamics in Biological Systems , Plenum Press, New York, London, 3-22. https://doi.org/10.1007/978-1-4613-2789-9_1

[90] Adey, W.R. (1990) Joint Actions of Environmental Nonionizing Electromagnetic Fields and Chemical Pollution in Cancer Promotion. Environmental Health Perspectives , 86, 297-305. https://doi.org/10.1289/ehp.9086297

[91] Blackman, C.F., Kinney, L.S., House, D.E., et al . (1989) Multiple Power-Density Windows and Their Possible Origin. Bioelectromagnetics , 10, 115-128. https://doi.org/10.1002/bem.2250100202

[92] Liu, D.S., Astumian, R.D. and Tsong, T.Y. (1990) Activation of Na+ and K+ Pumping Modes of (Na,K)-ATPase by an Oscillating Electric Field. The Journal of Biological Chemistry , 265, 7260-7267. https://doi.org/10.1016/S0021-9258(19)39108-2

[93] Markin, V.S. and Tsong, T.Y. (1991) Frequency and Concentration Windows for the Electric Activation of a Membrane Active Transport System. Biophysics Journal , 59, 1308-1316. https://doi.org/10.1016/S0006-3495(91)82345-1

[94] Hameroff, S. and Penrose, R. (2014) Consciousness in the Universe: A Review of the “Orch OR” Theory. Physics of Life Reviews, 11, 39-78. https://doi.org/10.1016/j.plrev.2013.08.002

[95] Del Giudice, E. (2011) The Interplay of Biomolecules and Water at the Origin of the Active Behavior of Living Organisms. Journal of Physics : Conference Series , 329, Article ID: 012001. https://doi.org/10.1088/1742-6596/329/1/012001

[96] Geesink, H.J. and Meijer, D.K.F. (2020) An Integral Predictive Model That Reveals a Causal Relation between Exposures to Non-Thermal Electromagnetic Waves and Healthy or Unhealthy Effects. https://www.researchgate.net/publication/340488204

[97] Bowling, D.L. and Purves, D. (2015) A Biological Rationale for Musical Consonance. PNAS, 112, 11155-11160. https://doi.org/10.1073/pnas.1505768112

[98] Geesink, J.H. and Meijer, D.K.F. (2018) A Semi-Harmonic Electromagnetic Frequency Pattern Organizes Non-Local States and Quantum Entanglement in both EPR Studies and Life Systems. Journal of Modern Physics , 9, 898-924. https://doi.org/10.4236/jmp.2018.95056

[99] Geesink, H.J.H. and Meijer, D.K.F. (2016) Quantum Wave Information of Life Revealed: An Algorithm for Electromagnetic Frequencies That Create Stability of Biological Order, with Implications for Brain Function and Consciousness. Neuro- Quantology, 14, 106-125. https://doi.org/10.14704/nq.2016.14.1.911

[100] Meijer, D.K.F., Jerman, I., Melkikh, A.V. and Sbitnev, V.I. (2019) Consciousness in the Universe Is Tuned by a Musical Master Code: A Hydrodynamic Superfluid Quantum Space Guides a Conformal Mental Attribute of Reality. The Hard Problem in Consciousness Studies Revisited. Project: The Information Universe. On the Missing Link in Concepts on the Architecture of Reality.

[101] Geesink, H.J.H. and Meijer, D.K.F. (2018) Mathematical Structure for Electromagnetic Frequencies That May Reflect Pilot Waves of Bohm’s Implicate Order. Journal of Modern Physics , 9, 851-897. https://doi.org/10.4236/jmp.2018.95055

[102] Geesink, H.J. (2020) Proposed Informational Code of Biomolecules and Its Building Blocks-Quantum Coherence versus Decoherence. Project: Quantum Coherence in Animate and Non-Animate Systems.

[103] Geesink, H.J.H., Jerman, I. and Meijer, D.K.F. (2019) Water: The Cradle of Life in Action, Cellular Architecture Is Guided by Coherent Quantum Frequencies as Revealed in Pure Water. Projects: Existence, Nature and Significance of Biological Field (the Biofield) Quantum Coherence in Animate and Non-Animate Systems.

[104] Geesink, H., Meijer, D. and Jerman, I. (2020) Clay Minerals-Information Network Linking Quantum Coherence and First Life. Projects: The Origin of Organisms (Life, Living Process) Based on Long Range Long Term Dynamic Interfacial Water Structures Quantum Coherence in Animate and Non-Animate Systems.

[105] Brueck, R.L. and Meijer, D.K.F. (2020) A New Premise for Quantum Physics, Consciousness and the Fabric of Reality. Project: The Information Universe. On the Missing Link in Concepts on the Architecture of Reality.

[106] Meijer, D.K.F. (2019) The Anticipation of Afterlife as Based on Current Physics of Information. Project: The Information Universe. On the Missing Link in Concepts on the Architecture of Reality.

[107] Milo, R. and Phillips, R. (2016) Cell Biology by the Numbers. Garland Science, New York. https://doi.org/10.1201/9780429258770

[108] Donald, T.H. (2001) Biological Thermodynamics. Cambridge University Press, Cambridge, 37.

[109] Garrett, G. (1995) Biochemistry. Saunders College Publishing, Philadelphia, 16.

[110] Lodish, et al . (2000) Molecular Cell Biology. 4th Edition, W. H. Freeman, New York.

[111] Geesink, H.J.H. and Meijer, D.K.F. (2020) Electromagnetic Frequency Patterns That Are Crucial for Health and Disease Reveal a Generalized Biophysical Principle: The GM Scale. Quantum Biosystems, 8, 1-16.

[112] Guo, W. and Feng, Q. (2019) Free Vibration Analysis of Arbitrary-Shaped Plates Based on the Improved Rayleigh-Ritz Method. Advances in Civil Engineering, 2019, Article ID: 7041592. https://doi.org/10.1155/2019/7041592

[113] Senjanivic, I., Tomic, M., Vladimir, N. and Cho, D.S. (2013) Analytical Solutions for Free Vibrations of a Moderately Thick Rectangular Plate. Mathematical Problems in Engineering, 2013, Article ID: 207460. https://doi.org/10.1155/2013/207460

[114] Geesink, H.J.H. and Meijer, D.K.F. (2017) Nature Unites First, Second and Third Harmonics to Organize Coherent Electromagnetic Frequency Patterns That Are Crucial for Health and Disease. https://www.researchgate.net/publication/317003066

[115] Sonderkamp, T., Geesink, H.J.H. and Meijer, D.K.F. (2019) Statistical Analysis and Prospective Application of the GM-Scale, a Semi-Harmonic EMF Scale Proposed to Discriminate between “Coherent” and “Decoherent” EM Frequencies on Life Conditions. Quantum Biosystems, 12, 33-51.

[116] Costa, M., Goldberger, A.L. and Peng, C.K. (2002) Multiscale Entropy Analysis of Complex Physiologic Time Series. Physical Review Letters , 89, 1-5. https://doi.org/10.1103/PhysRevLett.89.068102

[117] Meijer, D.K.F. and Geesink, H.J.H. (2018) Favourable und Unfavourable EMF Frequency Patterns in Cancer: Perspectives for Improved Therapy and Prevention. Journal of Cancer Therapy , 9, 188-230. https://doi.org/10.4236/jct.2018.93019

[118] Pauri, M. (2003) Don’t Ask Pythagoras about the Quantum. Science & Education, 12, 467-477. https://doi.org/10.1023/A:1025330129744

[119] Geesink, J.H. and Meijer, D.K.F. (2017) Bio-Soliton Model That Predicts Non-Thermal Electromagnetic Frequency Bands, That either Stabilize or Destabilize Living Cells. Electromagnetic Biology and Medicine, 36, 357-378. https://doi.org/10.1080/15368378.2017.1389752

[120] Geesink, H.J.H. and Meijer, D.K.F. (2017) Cancer Is Promoted by Cellular States of Electromagnetic Decoherence and can Be Corrected by Exposure to Coherent Non-Ionizing Electromagnetic Fields, a Physical Model about Cell-Sustaining and Cell-Decaying Soliton Eigen-Frequencies. https://www.researchgate.net/publication/316058728_Cancer_is_promoted_by_cellular_states_of_electromagnetic_decoherenceandcanbecorrectedbyexposuretocoherentnon-ionizingelectromagneticfields

[121] Tsujita, K., Satow, R., Asada, S., Nakamura, Y., Arnes, L., Sako, K., Fujita, Y., Fukami, K. and Itoh, T. (2021) Homeostatic Membrane Tension Constrains Cancer Cell Dissemination by Counteracting BAR Protein Assembly. Nature Communications , 12, Article No. 5930. https://doi.org/10.1038/s41467-021-26156-4

[122] Csoboz, B., Balogh, G.E., Kusz, E., Gombos, I., Peter, M., Crul, T., Gungor, B., Haracska, L., Bogdanovics, G., Torok, Z., Horvath, I. and Vigh, L. (2013) Membrane Fluidity Matters: Hyperthermia from the Aspects of Lipids and Membranes. International Journal of Hyperthermia , 29, 491-499. https://doi.org/10.3109/02656736.2013.808765

[123] Galeotti, T., Borrello, S., Minotti, G. and Masotti, L. (1986) Membrane Alterations in Cancer Cells: The Role of Oxy Radicals. Annals of the New York Academy of Sciences , 488, 468-480. https://doi.org/10.1111/j.1749-6632.1986.tb46579.x

[124] Yang, M. and Brackenbury, W.J. (2013) Membrane Potential and Cancer Progression. Frontiers in Physiology , 4, Article No. 185. https://doi.org/10.3389/fphys.2013.00185

[125] Kadir, L.A., Stacey, M. and Barrett, J.R. (2018) Emerging Roles of the Membrane Potential: Action beyond the Action Potential. Frontiers in Physiology, 9, Article No. 1661. https://doi.org/10.3389/fphys.2018.01661

[126] Szentgyorgyi, A. (1968) Bioelectronics, a Study on Cellular Regulations, Defence and Cancer. Academic Press, New York, London.

[127] Szentgyorgyi, A. (1998) Electronic Biology and Cancer. Marcel Dekker, New York.

[128] Maroti, P., Berkes, L. and Tolgyesi, F. (1998) Biophysics Problems. AkademiaiKiado, Budapest.

[129]Shashini, B., Ariyasu, S., Takeda, R., Suzuki, T., Shiina, S., Akimoto, K., et al . (2018) Size-Based Differentiation of Cancer and Normal Cells by a Particle Size Analyzer Assisted by a Cell-Recognition PC Software. Biological and Pharmaceutical Bulletin 41, 478-503. https://doi.org/10.1248/bpb.b17-00776

[130] Baba, A.I. and Catoi, C. (2007) Chapter 3. Tumor Cell Morphology. In: Buchares, R.O., Ed., Comparative Oncology , The Publishing House of the Romanian Academy, Bucharest. https://www.ncbi.nlm.nih.gov/books/NBK9553/

[131] Lyons, S.M., Alizadeh, E., Mannheimer, J., Schuamberg, K., Castle, J., Schroder, B., et al . (2016) Changes in Cell Shape Are Correlated with Metastatic Potential in Murine and Human Osteosarcomas. Biology Open, 5, 289-299. https://doi.org/10.1242/bio.013409

[132] Pache, B. (2018) How Tumor-Specific Modulation Frequencies Were Discovered. The Cancer Letter , 44, 24-29.

[133] Barbault, A., Costa, F.P., Bottger, B., Munden, R.F., Bomholt, F., Kuster, N. And Pasche, B. (2009) Amplitude-Modulated Electromagnetic Fields for the Treatment of Cancer: Discovery of Tumor-Specific Frequencies and Assessment of a Novel Therapeutic Approach. Journal of Experimental and Clinical Cancer Research, 28, 51. https://doi.org/10.1186/1756-9966-28-51

[134] Jaminez, H., Blackman, C., Lesser, G., Debinski, W., Chan, M., Sharma, S., et al . (2018) Use of Non-Ionizing Electromagnetic Fields for the Treatment of Cancer. Frontiers in Bioscience , Landmark, 23, 284-297. https://doi.org/10.2741/4591

[135] Zimmerman, J.W., Jimenez, H., Pennison, M.J., Brezovich, I., Morgan, D., Mudry, A., et al . (2013) Targeted Treatment of Cancer with Radiofrequency Electromagnetic Fields Amplitude-Modulated at Tumor-Specific Frequencies. Chinese Journal of Cancer , 32, 573-581. https://doi.org/10.5732/cjc.013.10177

[136] Bose, D., Zimmerman, L.J., Pierobonn, M., Petricoin, E., Tozzi, F., Parikh, A., et al . (2011) Chemoresistant Colorectal Cancer Cells and Cancer Stem Cells Mediate Growth and Survival of Bystander Cells. British Journal of Cancer , 105, 1759-1767. https://doi.org/10.1038/bjc.2011.449

[137] Sharma, S., Wu, S.Y., Jimenez, H., Xing, F., Zhu, D., Liu, Y., et al . (2019) Ca2+ and CACNA1H Mediate Targeted Suppression of Breast Cancer Brain Metastasis by A? RF EMF. EBioMedicine , 44, 194-208. https://doi.org/10.1016/j.ebiom.2019.05.038

[138] Zimmerman, J.W., Pennison, M.J., Brezovich, I., Yi, N., Yang, C.T., Ramaker, R., et al . (2012) Cancer Cell Proliferation Is Inhibited by Specific Modulation Frequencies. British Journal of Cancer , 106, 307-313. https://doi.org/10.1038/bjc.2011.523

[139] Blackman, C.K. (2012) Treating Cancer with Amplitude-Modulated Electromagnetic Fields: A Potential Paradigm Shift, Again? British Journal of Cancer , 106, 241-242. https://doi.org/10.1038/bjc.2011.576

[140] Pasche, B. and Barbault, A. (2010) Electromagnetic System for Influencing Cellular Functions in a Warm-Blooded Mammalian Subject. Patent Nr. EP 2139557 B1. https://patents.google.com/patent/EP2139557B1/en

[141] Costa, F.P., de Oliveira, A.C., Meirelles, R., Machado, M.C.C., Zanesco, T., Surjan, R., et al . (2011) Treatment of Advanced Hepatocellular Carcinoma with Very Low Levels of Amplitude-Modulated Electromagnetic Fields. British Journal of Cancer , 105, 640-648. https://doi.org/10.1038/bjc.2011.292

[142] Zimmermann, J.W., Pennison, M.J., Brezovich, I., Yi, N., Yang, C.T., Ramaker, R., et al . (2011) Cancer Cell Proliferation Is Inhibited by Specific Modulation Frequencies. British Journal of Cancer , 1-7.

[143] Jimenez, H., Wang, M., Zimmerman, J.W., Pennison, M.J., Sharma, S., Surratt, T.,et al . (2019) Tumour-Specific Amplitude-Modulated Radiofrequency Electromagnetic Fields Induce Differentiation of Hepatocellular Carcinoma via Targeting Cav3.2 T-Type Voltage-Gated Calcium Channels and Ca2+ Influx. EBioMedicine , 44, 209-224. https://doi.org/10.1016/j.ebiom.2019.05.034

[144] Hum, N.R., Sebastian, A., Gilmore, S.F., He, W., Martin, K.A., Hinckley, A., et al . (2020) Comparative Molecular Analysis of Cancer Behavior Cultured in Vitro. In Vivo , and Ex Vivo, Cancers , 12, 690. https://doi.org/10.3390/cancers12030690

[145] Fares, J., Fares, M.Y., Khachfe, H.H., et al . (2020) Molecular Principles of Metastasis: A Hallmark of Cancer Revisited. Signal Transduction and Targeted Therapy , 5, Article No. 28. https://doi.org/10.1038/s41392-020-0134-x

[146] de Loof, M., de Jong, S. and Kruyt, F.A.E. (2019) Multiple Interactions between Cancer Cells and the Tumor Microenvironment Modulate TRAIL Signaling: Implications for TRAIL Receptor Targeted Therapy. Frontiers in Immunology, 10, Article No. 1530. https://doi.org/10.3389/fimmu.2019.01530

[147] Pasche, B. and Barbault, A. (2007) A Study of Therapeutic Amplitude-Modulated Electromagnetic Fields in Advanced Tumors (THBC001). ClinicalTrials.gov, Identifier: NCT00440570.

[148] Pasche, B. and Barbault, A. (2007) A Study of Electromagnetic Waves in the Treatment of the Advanced Hepatocarcinoma (THBC002). ClinicalTrials.gov, Identifier: NCT00440934.

[149] Pasche, B. and Grant, S.C. (2014) Non-Small Cell Lung Cancer and Precision Medicine, a Model for the Incorporation of Genomic Features into Clinical Trial Design. JAMA, 311, 1975-1976. https://doi.org/10.1001/jama.2014.3742

[150] Anteneodo, C. and da Luz, M.G.E. (2010) Complex Dynamics of Life at Different Scales: From Genomic to Global Environmental Issues. Philosophical Transactions of the Royal Society A , 368, 5561-5568. https://doi.org/10.1098/rsta.2010.0286

[151] Deering, W. and West, B.J. (1992) Fractal Physiology. IEEE Engineering in Medicine and Biology, 11, 40-46. https://doi.org/10.1109/51.139035

[152] West, B.J. (1990) Fractal Physiology and Chaos in Medicine. World Scientific, Singapore, London. https://doi.org/10.1142/1025

[153] Bassingthwaighte, J.B., Leibovitch, L.S. and West, B.J. (1994) Fractal Physiology. Oxford Univ. Press, New York, Oxford.

[154] Goldberger, A.L., Amaral, L.A., Hausdorff, J.M., et al . (2002) Fractal Dynamics in Physiology: Alterations with Disease and Aging. PNAS Colloquium, 99, 2466-2472. https://doi.org/10.1073/pnas.012579499

[155] Szasz, A., Szasz, N. and Szasz, O. (2010) Oncothermia—Principles and Practices. Springer Science, Heidelberg. https://doi.org/10.1007/978-90-481-9498-8

[156] Eskov, V.M., Filatova, O.E., Eskov, V.V., et al . (2017) The Evolution of the Idea of Homeostasis: Determinism, Stochastics, and Chaos—Self-Organization. Biophysics , 62, 809-820. https://doi.org/10.1134/S0006350917050074

[157] Billman, G.E. (2020) Homeostasis: The Underappreciated and Far Too Often Ignored Central Organizing Principle of Physiology. Frontiers in Physiology, 11, Article No. 200. https://doi.org/10.3389/fphys.2020.00200

[158] Lovelady, D.C., Richmond, T.C., Maggi, A.N., et al . (2007) Distinguishing Cancerous from Noncancerous Cells through Analysis of Electrical Noise. Physical Review E, 76, Article ID: 041908. https://doi.org/10.1103/PhysRevE.76.041908

[159] Potoyan, D.A. and Wolynes, P.G. (2014) On the Dephasing of Genetic Oscillators. PNAS, 111, 2391-2396. https://doi.org/10.1073/pnas.1323433111

[160] Ptitsyn, A.A., Zvonic, S. and Gimble, J.M. (2007) Digital Signal Processing Reveals Circadian Baseline Oscillation in Majority of Mammalian Genes. PLOS Computational Biology, 3, e120. https://doi.org/10.1371/journal.pcbi.0030120

[161] Wang, Y., Wang, X., Wohland, T. and Sampath, K. (2016) Extracellular Interactionsand Ligand Degradation Shape the Nodal Morphogen Gradient. ELife , 5, e13879. https://doi.org/10.7554/eLife.13879

[162] Cramer, F. (1995) Chaos and Order (The Complex Structure of Living Systems). VCH, Weinheim.

[163] Peng, C.K., Buldyrev, S.V., Hausdorff, J.M., et al . (1994) Fractals in Biology and Medicine: From DNA to the Heartbeat. In: Bunde, A. and Havlin, S., Eds., Fractals in Science , Springer-Verlag, Berlin, 49-87. https://doi.org/10.1007/978-3-662-11777-4_3

[164] Bak, P., Tang, C. and Wieserfeld, K. (1988) Self-Organized Criticality. Physical Review A, 38, 364-374. https://doi.org/10.1103/PhysRevA.38.364

[165] Musha, T. and Sawada, Y. (1994) Physics of the Living State. IOS Press, Amsterdam.

[166] Szendro, P., Vincze, G. and Szasz, A. (2001) Bio-Response on White-Noise Excitation. Electromagnetic Biology and Medicine , 20, 215-229. https://doi.org/10.1081/JBC-100104145

[167] Szendro, P., Vincze, G. and Szasz, A. (2001) Pink-Noise Behaviour of Biosystems. European Biophysics Journal , 30, 227-231. https://doi.org/10.1007/s002490100143

[168] Ho, M.W., Popp, F.A. and Warnke, U. (1994) Bioelectrodynamics and Biocommunication. World Scientific, Singapore. https://doi.org/10.1142/2267

[169] Bernardi, P. and D'Inzeo, G. (1989). Physical Mechanisms for Electromagnetic Interaction with Biological Systems. In: Lin, J.C., Ed., Electromagnetic Interaction with Biological Systems , Plenum Press, New York, 179-214. https://doi.org/10.1007/978-1-4684-8059-7_9

[170] Markov, M.S. (1994) Biological Effects of Extremely Low Frequency Magnetic Fields. In: Ueno, S., Ed., Biomagnetic Stimulation, Plenum Press, New York, 91-104. https://doi.org/10.1007/978-1-4757-9507-3_7

[171] Bauerus, Koch, C.L.M., Sommarin, M., Persson, B.R.R., Salford, L.G. and Eberhardt J.L. (2003) Interaction between Weak Low Frequency Magnetic Fields and Cell Membranes. Bioelectriomagnetics , 24, 395-402. https://doi.org/10.1002/bem.10136

[172] Blackman, C.F., Benane, S.G. and House, D.E. (2001) The Influence of 1.2 μT, 60 Hz Magnetic Fields on Melatonin- and Tamoxifeninduced Inhibition of MCF-7 Cell Growth. Bioelectromagnetics , 22, 122-128. https://doi.org/10.1002/1521-186X(200102)22:2<122::AID-BEM1015>3.0.CO;2-V

[173] Weaver, J.C. and Astumian, R.D. (1990) The Response of Living Cells to Very Week Electric Fields: The Thermal Noise Limit. Science , 247, 459-462. https://doi.org/10.1126/science.2300806

[174] Adair, R.K. (1991) Constraints on Biological Effects of Weak Extremely-Low Frequency Electromagnetic Fields. Physical Review A, 43, 1039-1048. https://doi.org/10.1103/PhysRevA.43.1039

[175] White, D.C. and Woodson, H.H. (1959) Electromechanical Energy Conversion. John Wiley & Sons, New York.

[176] Vincze, Gy., Szasz, A. and Szasz, N. (2005) On the Thermal Noise Limit of Cellular Membranes. Bioelectromagnetics , 26, 28-35. https://doi.org/10.1002/bem.20051

[177] Bier, M. (2005) Gauging the Strength of Power Frequency Fields against Membrane Electrical Noise. Bioelectromagnetics , 26, 595-609. https://doi.org/10.1002/bem.20148

[178] Szasz, A. (2019) Thermal and Nonthermal Effects of Radiofrequency on Living State and Applications as an Adjuvant with Radiation Therapy. Journal of Radiation and Cancer Research , 10, 1-17. https://doi.org/10.4103/jrcr.jrcr_25_18

[179] Ferenczy, G.L. and Szasz, A. (2020) Ch. 3. Technical Challenges and Proposals in Oncological Hyperthermia. In: Szasz, A., Ed., Challenges and Solutions of Oncological Hyperthermia , Cambridge Scholars, Newcastle upon Tyne, 72-90.

[180] Lee, S.Y., Fiorentini, G., Szasz, A.M., Szigeti, Gy., Szasz, A. and Minnaar, C.A. (2020) Quo Vadis Oncological Hyperthermia (2020)? Frontiers in Oncology, 10, Article No. 1690. https://doi.org/10.3389/fonc.2020.01690

[181] Szasz, A., Vincze, Gy., Szasz, O. and Szasz, N. (2003) An Energy Analysis of Extracellular Hyperthermia. Magneto- and Electro-Biology, 22, 103-115. https://doi.org/10.1081/JBC-120024620

[182] Anishchenko, V.S., Neiman, A.B., Moss, F. and Schimansky-Geier, L. (1999) Stochastic Resonance: Noise-Enhanced Order. Physics -Uspekhi , 42, 7-36. https://doi.org/10.1070/PU1999v042n01ABEH000444

[183] Szasz, A. (1991) An Electronically Driven Instability: The Living State. PhysiologicalChemistry and Physics and Medical NMR, 23, 43-50.

[184] Gingl, Z., Makra, P. and Vajtai, R. (2001) High Signal-to-Noise Ratio Gain by Stochastic Resonance in a Double Well. Fluctuation and Noise Letters , 1, L181-L188. https://doi.org/10.1142/S0219477501000408

[185] Szendro, P., Vincze, Gy. and Szasz, A. (1999) Response of Bio-Systems on White Noise Excitation. Hungarian Agricultural Engineering, 12, 31-32.

[186] Szendro, P., Vincze, Gy. and Szasz, A. (1998) Origin of Pink-Noise in Bio-Systems. Hungarian Agricultural Engineering, 11, 42-43.

[187] Ma, J., Xiao, T., Hou, Z. and Xin, H. (2008) Coherence Resonance Induced by Colored Noise near Hopf Bifurcation. Chaos , 18, Article ID: 043116. https://doi.org/10.1063/1.3013178

[188] Bybiec, B. and Gudowska-Nowak, E. (2013) Resonant Activation Driven by Strongly Non-Gaussian Noises.

[189] Revelli, J.A., Sanchez, A.D. and Wio, H.S. (2001) Effect of Non Gaussian Noises on the Stochastic Resonance-Like Phenomenon in Gated Traps.

[190] Rosso, O.A. and Masoller, C. (2009) Detecting and Quantifying Stochastic and Coherence Resonances via Information-Theory Complexity Measurements. Physical Review E , 79, 040106(R). https://doi.org/10.1103/PhysRevE.79.040106

[191] Krauss, P., Metzner, C., Schilling, A., Schütz, C., Tziridis, K., Fabry, B. and Schulze,H. (2017) Adaptive Stochastic Resonance for Unknown and Variable Input Signals.Scientific Reports , 7, Article No. 2450. https://doi.org/10.1038/s41598-017-02644-w

[192] Krauss, P., Tziridis, K., Metzner, C., Schilling, A., Hoppe, U. and Schulze, H. (2016) Stochastic Resonance Controlled Upregulation of Internal Noise after Hearing Loss as a Putative Cause of Tinnitus-Related Neuronal Hyperactivity, Hypothesis and Theory. Frontiers in Neuroscience , 10, Article No. 597. https://doi.org/10.3389/fnins.2016.00597

[193] West, G.B. and Brown, J.H. (2005) The Origin of Allometric Scaling Laws in Biology from Genomes to Ecosystems: Towards a Quantitative Unifying Theory of Biological Structure and Organization. Journal of Experimental Biology, 208, 1575-1592. https://doi.org/10.1242/jeb.01589

[194] Trigos, A.S., Pearson, R.B., Paenfuss, A.T., et al . (2018) How the Evolution of Multicellularity Set the Stage for Cancer. British Journal of Cancer , 118, 145-152. https://doi.org/10.1038/bjc.2017.398

[195] Alfarouk, K.O., Shayoub, M.E.A., Muddathir, A.K., Elhassan, G.O. and Bashir, A.H.H. (2011) Evolution of Tumour Metabolism Might Reflect Carcinogenesis as a Reverse Evolution Process (Dismantling of Multicellularity). Cancers , 3, 3002-3017. https://doi.org/10.3390/cancers3033002

[196] Szentgyorgyi, A. (1978) The Living State and Cancer. Marcel Dekker Inc., New York.

[197] Lineweaver, C.H., Bussey, K.J., Blackburn, A.C. and Davies, P.C.W. (2021) Cancer Progression as a Sequence of Atavistic Reversions. BioEssays, 43, Article ID: 2000305. https://doi.org/10.1002/bies.202000305

[198] Lineweaver, C.H., Davies, P.C.W. and Vincent, M.D. (2014) Targeting Cancer's Weaknesses (Not Its Strengths): Therapeutic Strategies Suggested by the Atavistic Model. Bioessays , 36, 827-835. https://doi.org/10.1002/bies.201400070

[199] Eyring, H. (1935) The Activated Complex in Chemical Reactions. The Journal of Chemical Physics , 3, 107-115. https://doi.org/10.1063/1.1749604

[200] Michaelis, L. and Menten, M.L. (1913) Die Kinetik der Invertinwirkung. Biochemische Zeitschrift , 49, 333-369. https://doi.org/10.1021/bi201284u

[201] Hele, T.J.H. (2014) Quantum Transition-State Theory. Dissertation.

[202] Evans, M.G. and Polanyi, M. (1935) Some Applications of the Transition State Method to the Calculation of Reaction Velocities, Especially in Solution. Transactions of the Faraday Society , 31, 875-894. https://doi.org/10.1039/tf9353100875

[203] Tsong, T.Y. and Chang, C.H. (2007) A Markovian Engine for a Biological Energy Transducer: The Catalytic Wheel. BioSystems , 88, 323-333. https://doi.org/10.1016/j.biosystems.2006.08.014

[204] Savageau, M.A. (1998) Development of Fractal Kinetic Theory for Enzyme-Catalysed Reactions and Implications for the Design of Biochemical Pathways. Biosystems , 47 9-36. https://doi.org/10.1016/S0303-2647(98)00020-3

[205] Bezrukov, S.M. and Vodyanoy, I. (1997) Stochastic Resonance at the Single-Cell Level. Nature , 388, 632-633. https://doi.org/10.1038/41684

[206] Pearce, J.A. (2013) Comparative Analysis of Mathematical Models of Cell Death and Thermal Damage Processes. International Journal of Hyperthermia, 29, 262- 280. https://doi.org/10.3109/02656736.2013.786140

[207] Vincze, Gy., Szasz, O. and Szasz, A. (2015) Generalization of the Thermal Dose of Hyperthermia in Oncology. Open Journal of Biophysics , 5, 97-114. https://doi.org/10.4236/ojbiphy.2015.54009

[208] O'Neill, D.P., Peng, T., Stiegler, P., Mayrhauser, U., Koestenbauer, S., Tscheliessnigg, K., et al . (2011) A Three-State Mathematical Model of Hyperthermic Cell Death. Annals of Biomedical Engineering, 39, 570-579. https://doi.org/10.1007/s10439-010-0177-1

[209] Vincze, Gy. and Szasz, A. (2018) Similarities of Modulation by Temperature and by Electric Field. Ojbiphy, 8, 95-103. https://doi.org/10.4236/ojbiphy.2018.83008

[210] Thompson, W.H. (1999) Quantum Mechanical Transition State Theory and Tunneling Corrections. The Journal of Chemical Physics , 110, 4221-4228. https://doi.org/10.1063/1.478304

[211] Tsong, T.Y. and Astumian, R.D. (1988) Electroconformational Coupling: How Membrane- Bound ATPase Transduces Energy from Dynamic Electric Fields. Annual Review of Physiology, 50, 273-290. https://doi.org/10.1146/annurev.ph.50.030188.001421

[212] Astumian, R.D. (1994) Electroconformational Coupling of Membrane Proteins. Annals of the New York Academy of Sciences , 720, 136-140. https://doi.org/10.1111/j.1749-6632.1994.tb30441.x

[213] Markin, V.S., Liu, D., Rosenberg, M.D. et al . (1992) Resonance Transduction of Low Level Periodic Signals by an Enzyme: An Oscillatory Activation Barrier Model. Biophysical Journal , 61, 1045-1049. https://doi.org/10.1016/S0006-3495(92)81913-6

[214] McNamara, B. and Wiesenfeld, K. (1989) Theory of Stochastic Resonance. Physical Review A, 39, 4854-4869. https://doi.org/10.1103/PhysRevA.39.4854

[215] Astumian, R.D. (1997) Thermodynamics and Kinetics of a Brownian Motor. Science ,276, 917-922. https://doi.org/10.1126/science.276.5314.917

[216] Astumian, R.D. and Bier, M. (1994) Fluctuation Driven Ratchets: Molecular Motors. Physical Review Letters , 72, 1766-1769. https://doi.org/10.1103/PhysRevLett.72.1766

[217] Chock, P.B., Tsong, T.Y., et al . (1987) Can Free Energy Be Transduced from Noise? Proceedings of the National Academy of Sciences of the United States of America , 84, 434-438. https://doi.org/10.1073/pnas.84.2.434

[218] Astumian, R.D. and Derényi, I. (1998) Fluctuation Driven Transport and Models of Molecular Motors and Pumps. European Biophysics Journal , 27, 474-489. https://doi.org/10.1007/s002490050158

[219] Linke, H., Downton, M.T. and Zuckermann, M.J. (2005) Performance Characteristic of Brownian Motors. Chaos , 15, Article ID: 026111. https://doi.org/10.1063/1.1871432

[220] Tinoco, I., Sauer, K., Wang, J.C., et al . (2002) Physical Chemistry. Principles and Applications in Biological Sciences. 4th Edition, Prentice-Hall Inc., Hoboken.

[221] Astumian, R.D. and Chock, P.B. (1989) Effects of Oscillations and Energy-Driven Fluctuations on the Dynamics of Enzyme Catalsysis and Free-Energy Transduction.Physical Review A, 39, 6416-6435. https://doi.org/10.1103/PhysRevA.39.6416

[222] Babbi, G., Baldazzi, D., Savojardo, C., Luigi, M.P. and Casadio, R. (2020) Highlighting Human Enzymes Active in Different Metabolic Pathways and Diseases: The Case Study of EC 1.2.3.1 and EC 2.3.1.9. Biomedicines , 8, 250. https://doi.org/10.3390/biomedicines8080250

[223] Romero, P., Wagg, J., Green, M.L., Daiser, D., Krummenacker, M. and Karp, P.D. (2005) Computational Prediction of Human Metabolic Pathways from the Complete Human Genome. Genome Biology, 6, R2. https://doi.org/10.1186/gb-2004-6-1-r2

[224] McDonnell, M. and Abbott, D. (2009) What Is Stochastic Resonance? Definitions, Misconceptions, Debates, and Its Relevance to Biology. PLOS Computational Biology, 5, e1000348. https://doi.org/10.1371/journal.pcbi.1000348

[225] Szasz, A. and Szasz, O. (2020) Ch. 17. Time-Fractal Modulation of Modulated Electro- Hyperthermia (mEHT). In: Szasz, A., Ed., Challenges and Solutions of Oncological Hyperthermia , Cambridge Scholars, Newcastle upon Tyne, 377-415.

[226] Szasz, A. (2021) Therapeutic Basis of Electromagnetic Resonances and Signal Modulation. Open Journal of Biophysics , 11, 314-350. https://doi.org/10.4236/ojbiphy.2021.113011

[227] Szasz, A. (2022) Time-Fractal Modulation—Possible Modulation Effects in Human Therapy. Open Journal of Biophysics , 12, 38-87. https://doi.org/10.4236/ojbiphy.2022.121003

[228] Calabro, E. and Magazu, S. (2020) New Perspectives in the Treatment of Tumor Cells by Electromagnetic Radiation at Resonance Frequencies in Cellular Membrane Channels. The Open Biotechnology Journal , 13, 105-110. https://doi.org/10.2174/1874070701901301O5

[229] Hanggi, P., Schmid, G. and Goychuk, I. (2002) Excitable Membranes: Channel Noise, Synchronization, and Stochastic Resonance. In: Kramer, B., Ed., Advances in Solid State Physics , Vol. 42, Springer-Verlag, Berlin, 359-370. https://doi.org/10.1007/3-540-45618-X_28

[230] Szasz, O., Szasz, A.M. Minnaar, C. and Szasz, A. (2017) Heating Preciosity—Trends in Modern Oncological Hyperthermia. Open Journal of Biophysics , 7, 116-144. https://doi.org/10.4236/ojbiphy.2017.73010

[231] Szasz, O. and Szasz, A. (2014) Oncothermia—Nano-Heating Paradigm. Journal of Cancer Science and Therapy , 6, 117-121. https://doi.org/10.4172/1948-5956.1000259

[232] Szasz, A. (2013) Chapter 4. Electromagnetic Effects in Nanoscale Range. In: Shimizu, T. and Kondo, T., Eds., Cellular Response to Physical Stress and Therapeutic Applications , Nova Science Publishers, Inc., Hauppauge, 55-81.

[233] Foleti, A., Grimaldi, S., Lisi, A., Ledda, M. and Liboff, A.R. (2013) Bioelctromagnetic Medicine: The Role of Resonance Signaling. Electromagnetic Biology and Medicine , 32, 484-499.

[234] Lucia, U., Grisolia, G., Ponzetto, A., Bergandi, L. and Silvagno, F. (2020) Thermomagnetic Resonance Affects Cancer Growth and Motility. Royal Society Open Science , 7, Article ID: 200299. https://doi.org/10.1098/rsos.200299

[235] Sahu, S., Ghosh, S., Fujita, D. and Bandyopadhyay, A. (2014) Live Visualizations of Single Isolated Tubulin Protein Self-Assembly via Tunneling Current: Effect of Electromagnetic Pumping during Spontaneous Growth of Microtubule. Scientific Reports , 4, Article No. 7303. https://doi.org/10.1038/srep07303

[236] Liboff, A.R. (1997) Electric-Field Ion Cyclotron Resonance. Biolectromagnetics , 18, 85-87. https://doi.org/10.1002/(SICI)1521-186X(1997)18:1<85::AID-BEM13>3.0.CO;2-P

[237] Liboff, A.R. (2012) Electromagnetic Vaccination. Medical Hypotheses , 79, 331-333. https://doi.org/10.1016/j.mehy.2012.05.027

[238] Krenacs, T., Meggyeshazi, N., Forika, G., et al. (2020) Modulated Electro-Hyperthermia- Induced Tumor Damage Mechanisms Revealed in Cancer Models. International Journal of Molecular Sciences , 21, Article No. 6270. https://doi.org/10.3390/ijms21176270

[239] Chi, M.S., Mehta, M.P., Yang, K.L., et al . (2020) Putative Abscopal Effect in Three Patients Treated by Combined Radiotherapy and Modulated Electrohyperthermia. Frontiers in Oncology, 10, Article No. 254. https://doi.org/10.3389/fonc.2020.00254

[240] Minnaar, C.A., Kotzen, J.A., Ayeni, O.A., et al . (2020) Potentiation of the Abscopal Effect by Modulated Electro-Hyperthermia in Locally Advanced Cervical Cancer Patients. Frontiers in Oncology , 10, Article No. 376. https://doi.org/10.3389/fonc.2020.00376

[241] Chi, K.H. (2020) Tumour-Directed Immunotherapy: Clinical Results of Radiotherapy with Modulated Electro-Hyperthermia. In: Szasz, A., Ed., Challenges and Solutions of Oncological Hyperthermia , Cambridge Scholars, Newcastle upon Tyne, 206-226.

[242] Schirrmacher, V., Lorenzen, D., Van, Gool, S.W., et al . (2017) A New Strategy of Cancer Immunotherapy Combining Hyperthermia/Oncolytic Virus Pretreatment with Specific Autologous Anti-Tumor Vaccination—A Review. Austin Oncology Case Reports , 2, 1-8. https://doi.org/10.26420/austinoncolcaserep.1006.2017

Stimulation and Control of Homeostasis

Andras Szasz

Department of Biotechnics, Szent Istvan University, Budaors, Hungary

Cite this article as:
Szasz, A. (2022) Stimulation and Control of Homeostasis. Open Journal of Biophysics , 12, 89-131.
https://doi.org/10.4236/ojbiphy.2022.122004

Oncothermia Journal 33, May 2023: 37 – 69.
www.oncotherm.com/sites/oncotherm/files/2023-05/SzaszA_Stimulation_and_Control_Homeostasis.pdf

Abstract:
Healthy homeostasis is a principal driving force of the dynamic equilibrium of living organisms. The dynamical basis of homeostasis is the complex and interconnected feedback mechanisms, which are fundamentally governed by the nervous system, mainly the balance of the sympathetic and parasympathetic controlling actions. The balancing regulation is well presented in the heart's sinus node and can be measured by the time-domain heart-rate variation (HRV) of its frequency domain to analyze the constitutional frequencies of the variation. This last is a fluctuation that shows 1/f time fractal arrangement (f is the composing frequency). The time-fractal arrangement could depend on the structural fractal of the His-Purkinje system of the heart and personally modify the HRV. The cancers gradually destroy the homeostatic harmony, starting locally and finishing systemically. The controlling activity of vagus-nerve changes the HRV or the power density spectrum of the signal fluctuations in malignant development, presenting an appropriate control of the cancerous processes. The modified spectrum by a non-invasive radiofrequency treatment could arrest the tumor growth. An appropriate modulation could support the homeostatic control and force reconstructing of the broken complexity.

Keywords:
Homeostasis, Vagus Stimulation, Heart-Rate Variability, Immune-Stimuli, Cancer, Time-Fractal Modulation, Bifurcations, 1/f Noise, mEHT, Personalized Therapy

1. Introduction

Homeostasis is the vital basis of the dynamic stability of living organisms. The network of negative and positive feedback reactions creates the backbone of complex regulatory processes. The synergy of chemical and physical actors generates homeostasis in a stochastic harmony. The water is a mandatory constituent. The aqueous electrolytes provide the active fundament of various changes in the living systems. The water molecules participate in the harmonization of the complex processes in the separated solutions. The cellular lipid structures (membranes) and some specialized tissues divide the electrolytes, but at the same time, these surfaces regulate most of the chemical reactions for living equilibrium by intensive dynamic processes of various ionic exchanges and electromagnetic forces.

The control of the stochastic regulatory processes has highly self-organized accuracy creating the appropriate products, but some perturbances could disorient the standard mechanisms. The homeostatic system has a variety of tools to correct errors. A significant challenge arose when the collaborative networks were disrupted, and the natural processes could not correct this fault. Such complication happens in the development of malignancy, driven by the unicellular individualism of the involved cells. The malignant structure breaks the multicellular organization (healthy networking). The autonomous cells adapt to the challenges and avoid homeostatic control. These cells hide their erroneous structure, imitate a wound, and force the homeostatic control to heal, support them [1]. This activity changes the micro and macro environment of the malignant cells,disorganizing the network and the harmonic interactions of the multicellular structure. Due to the high individual energy demand, these cells use a primitive transcriptional program [2]. The tumor organizes a unicellular autonomy to safeguard the survival of the "colony" of malignant cells [3]. The healthy host provides active support to cancer, trying to "heal" the abnormality. Neo-angiogenesis, induced injury current, and numerous other boosts appear, guided by misled general homeostatic regulation of the body.

Cancer starts locally but becomes systemic when the structurally and dynamically disordered tissue appears in the body. The dynamic control is not able to repair the local malignant development due to various reasons: genetic aberration [4], mitochondrial dysfunction [5], and other intra [6] and extracellular [7] hallmarks of cancer. Furthermore, the permanent uncontrolled stress [8], the recognition of the lesion as an unhealed wound [9], the permanent inflammation [10], and the missing apoptotic activity [11] worsen the situation.

Cancer is the disease of the multicellular system disrupting the organized network, exchanging the cooperative advantages to the selfish individual demands [12]. One therapeutic help could support multicellular harmonic control, boosting the standard natural homeostatic regulation for effective action. The task is as complex as life itself, so the external actions are limited. We do not expect any changes from the therapy alone. The intention is only backing the natural control to do the job. Our approach is an electromagnetic action [13]. The fundamental tool for this task is the amplitude-modulated radiofrequency (RF) carrier with 1/f spectrum, which supports the homeostatic multicellular harmony, helps to correct the malignant lesion's cellular disorder, and induces apoptosis of the malignant cells. The forcing cooperative harmony may influence the precancerous cells to return to the healthy network. Our objective is to study this possibility considering the personalization of the modulation.

2. Method—The 1/f Spectrum

2.1. Embedded Bifurcation Dynamism

The control of life reaction has stochastic feedbacks [14], which drive all the processes in complex, embedded structures. Positive feedback is a process to generate a specific new product or state, with a point of no return. The positive feedback mechanisms are usually complex and have some intermediate potential wells keeping the process controlled and avoiding the expansive quick unregulated outcome. A characteristic example is the catabolism of humans, where the positive feedback is driven with the never-resting electrons: "Life is nothing but an electron looking for a place to rest" [15]. In the metabolism of the eukaryotic cells, the glucose has a degradation, and finally, the process ends in CO2 + H2O products, while the liberated energy kept the cells living Figure 1.

The positive feedback has no direct general balancing, but the subsequent steps in this have metastable positions, requiring some extra energy to overcome the barriers. The simplest and most common negative feedback regulation processes in a living system have two opposite regulation effects: the promoter and suppressor balance each other. This balancing process compensates for the opposite factors, fluctuating between two possible states Figure 2. When the negative feedback is out from the pre-set limits, the process becomes unbalanced, the negative feedback weakens, and a sign of irregularity appears. The bifurcation potential wells usually have a longer chain of embedded bifurcations as part of the complex process. In this way, the complexity develops a multifurcation system at the level of the entire living organism.

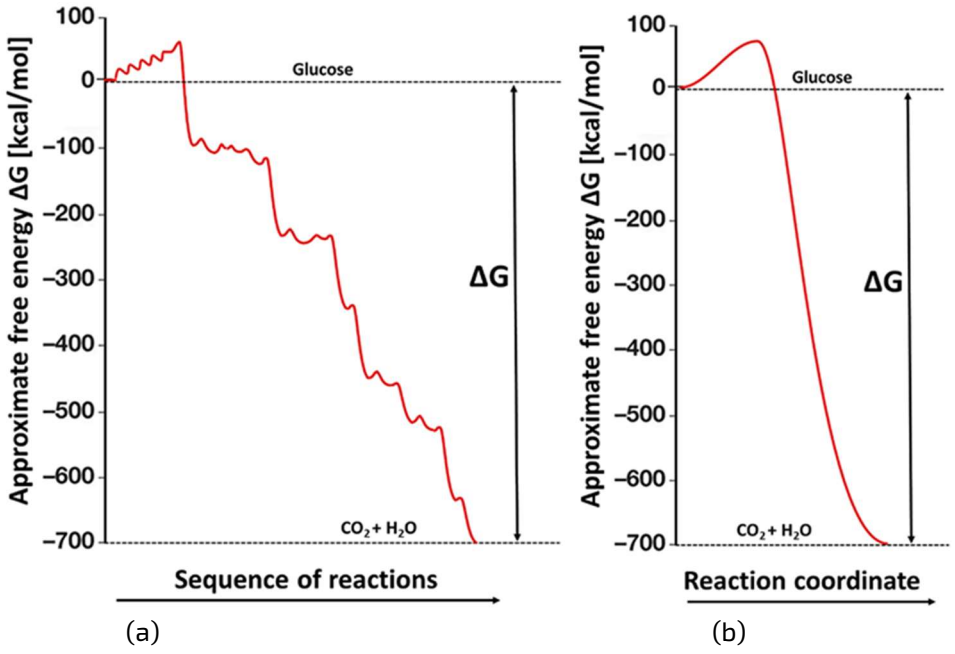

Figure 1. The approximate "degradation" of glucose to the final molecules CO2 + H2O of catabolism. All peaks are transition states assisted by devoted enzymes, and the wells are metastable intermediate states.

The primary step of the embedded multifurcation starts with the water structure. The hydrogen bridges allow a chain transport of H+ ions, creating a fundamental mechanism in living systems [16]. The proton tunneling (jumping) between the water molecules forms low dissipation ionic transport (the proton migrates) [17] [18]. The involved ion multifurcates in the potential wells of the chain connected by the bifurcative hydrogen bridges, connecting the water molecules dynamically. Such construction from bifurcative to multifurcative connection appears in the whole organism following the hydrogen-bridge mechanisms [19] [20] [21]. The bifurcative steps appear in structural connections of the DNA helix connecting the nucleotides, which may cause protein's bending and be involved massively in the stochastic processes of life. Self-organized processes connect the bifurcation steps, which are arranged in fractal structure Figure 3.
The amplitudes of the harmonically oscillated particles of the bifurcative potential wells in the self-organized setting form a Cantor set, which is in mathematical expression:

$$x \to f(x) = \frac{\left[\frac{1}{2} - \left|x - \frac{1}{2}\right|\right]}{r} \tag{1}$$

where r is the section removed from the middle of the Cantor's template. The vibration produced by the k-th bifurcation-set (multifurcation) has the following shape

$$x_k(t) = A_k \sin(2\pi f_k t + \varphi_k) \tag{2}$$

The power spectrum of the vibration superimposed on these in the case where f_k is a multiple of f_1 fundamental frequency. The average of x^2 is:

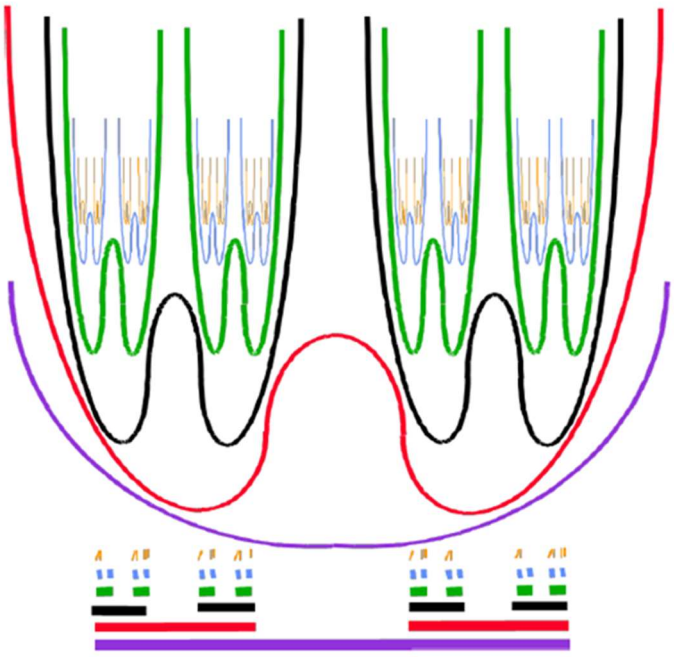

Figure 3. The self-similarity produces the embedded multifunction system. Stochastic resonances promote the bifurcation steps. The probability distribution follows a Cantordust fractal.

$$\langle x^2 \rangle = \sum_k \frac{A_k^2}{2} \tag{3}$$

We suppose the expected $1/f$ spectral behavior, so it is a condition of the spectral density $S(f_k) \propto A_k^2$

$$S(f_k) \propto A_k^2 \propto \frac{1}{f_k} \tag{4}$$

Due to the Cantor-set character, using the assumption of (4) when $r = 3$

$$\frac{A_{k+1}}{A_k} = \sqrt{\frac{f_{k+1}}{f_k}} = 3 \tag{5}$$

So the frequencies form a geometric series

$$\frac{f_{k+1}}{f_k} = 3^2 \tag{6}$$

So the k-th frequency

$$f_k = 3^{2k} f_1 \tag{7}$$

This is a discrete power spectrum, but their amplitudes follow the assumed 1/f pink noise (4). In the above described discrete subsequent embedding, the particles oscillate in one dimension and are independent from each other. However, the reality differs. The oscillation is three-dimensional. All the directions of the space

could be active, and these oscillating dimensions could be dependent. Weak interactions connect the wells, forming networks and dynamical harmony. The net of the weak interactions ensures a stable system with low vulnerability [22]. The natural overlaps create a continuous 1/f spectrum, even in this simple model. Self-similarity and self-organization are the general features of the living system, generalizing pink noise in stationary random stochastic processes [23].

The living systems are far from thermodynamical equilibrium, seeking to realize the lowest available energy with the highest efficacy in dynamic stability (homeostasis), balancing the energy incorporation and the energy combustion. The natural processes seek to minimize their energy consumption, using the least-action principle, which drives the biological processes and the biological evolution.

2.2. The Frequency-Order

The living systems show 1/f noise in homeostasis, a distribution of the stochastic processes keeping the system in dynamic equilibrium. However, this character does not identify the system because the 1/f is a spectrum, a distribution of the frequencies by their power density, without the time series of signals in the organism. The time-dependence vanishes with the Fourier transformation, and the obtained power density gives general information like the status of self-organizing, the scaling, and the dynamic equilibrium of the body; the time-function disappears. Some general info about the interaction chains could be derived from the autocorrelation function, but the actual time-dependent signal remains hidden.

The 1/f frequency spectrum is a distribution, which defines various frequencies, taking no attention to their sequences in the actual signal. For example, most musical pieces have near 1/f distribution, but they are, of course, very different in their musical sounds. The frequency distribution does not inform us about the temporal sequences of the frequencies. However, the temporal signal is used for modulation, so derive this information from the spectral density function to increase the theranostics approach's efficacy and accuracy. Facing this problem, study first the power spectrum of pink noise, assuming a trivial, energetic criterion for self-similarity. When f (t) is a self-similar function on the whole real axis, we know:

$$f(\tau t) = \tau^k f(t) \tag{8}$$

when the function in (8) is chosen as integrally quadratic:

$$0 < \int_{-\infty}^{\infty} |f(t)|^2 \, \mathrm{d}t < \infty \tag{9}$$

The used |f (t)| is the absolute value of the signal allows complex functions. This is physically a possibility to examine self-similar function pairs. The above criterion for physical signals usually means that the energy of the signal is finite. This is true of all physically meaningful signs [24]. Note the integral of the quadratic function with E:

$$E = \int_{-\infty}^{\infty} |f(t)|^2 \, \mathrm{d}t \tag{10}$$

So using (8):

$$\begin{aligned} E &= \tau \int_{-\infty}^{\infty} |f(\tau z)|^2 \, \mathrm{d}z \\ &= \tau \left(\tau^k\right)^2 \int_{-\infty}^{\infty} |f(z)|^2 \, \mathrm{d}z \\ &= \tau^{1+2k} \int_{-\infty}^{\infty} |f(z)|^2 \, \mathrm{d}z \\ &= \tau^{1+2k} E \end{aligned} \tag{11}$$

with substitution of E from (10) to (11):

$$\tau^{1+2k} = 1 \rightarrow k = -\frac{1}{2} \tag{12}$$

Below we prove that Equation (12) leads to the 1/f power spectrum. The quadratic integrity (finite energy signals) has a Fourier transform, which is also self-similar in a frequency domain, so:

$$F\left[f(t)\right]=X(j\omega)=\frac{B}{(j\omega)^{1+k}}=\frac{B}{(j\omega)^{\frac{1}{2}}} \tag{13}$$

Taking advantage of this, the Wiener-Khinchin theorem [25] states that

$$\int_{-\infty}^{\infty}\left|f(t)\right|^2\mathrm{d}x=\int_{-\infty}^{\infty}X(j\omega)X^*(j\omega)\mathrm{d}\omega=\int_{-\infty}^{\infty}\frac{BB^*}{\omega}\mathrm{d}\omega \tag{14}$$

Hence the power spectrum of the self-similar finite energy signal is 1/f . Note that the signal can also be deterministic, and even as we show below, the theorem does not apply to stationary noises in the above form. In the case of the principle of infinitely long stationary self-similar signals, finite energy cannot be guaranteed. In this case, the physically meaningful claim is the finiteness of the average:

$$0<\lim_{T\to\infty}\frac{1}{T}\int_{-T/2}^{T/2}\left|f(t)\right|^2\mathrm{d}t<\infty \tag{15}$$

The repeated above calculation resulting (12), the average power of (15) delivers the same result, namely that the power spectrum of the self-similar signals with finite average power is 1/f . We have to make some theoretical remarks and move on to ergodic signals and correlation functions to discuss the stochastic processes in the above way. In the case of stationary ergodic signals, the correlation functions can be formed from each representation by forming the following limit value:

$$R(\tau):=\lim_{T\to\infty}\frac{1}{T}\int_{-T/2}^{T/2}f(t)f(t-\tau)\mathrm{d}t \tag{16}$$

Because we assumed finite mean performance, this correlation function exists. Introduce the notation for the T-length representation of the signal. This is defined as:

$$f_T(t)=\begin{cases}f(t) & -\frac{T}{2}\le t\le\frac{T}{2}\\ 0 & \text{otherwise}\end{cases} \tag{17}$$

The Fourier transform of the T-length representation:

$$X(j\omega,T)=\frac{1}{2\pi}\int_{-T/2}^{T/2}f(t)\mathrm{e}^{j\omega t}\mathrm{d}t \tag{18}$$

The average power density of T-length representations approaches the Fourier transformation. Based on this, it might be supposed that every single being's autonomic nervous system produces an individually coded 1/f homeostatic noise.

In this sense, we can talk about personalized 1/f noise. Transform of the autocorrelation function [26], so

$$\Phi(\omega)=\lim_{T\to\infty}\pi\frac{X(j\omega,T)X^*(j\omega,T)}{T}=\frac{1}{2\pi}\int_{-\infty}^{\infty}R(\tau)\mathrm{e}^{-j\omega t}\mathrm{d}t \tag{19}$$

Conversely, the inverse Fourier transform of the average power density is the autocorrelation function, so

$$R(\tau)=\frac{1}{2\pi}\int_{-\infty}^{\infty}\Phi(\omega)\mathrm{e}^{j\omega\tau}\mathrm{d}\omega \tag{20}$$

From this, we obtain the average performance of

$$R(0)=\lim_{T\to\infty}\frac{1}{T}\int_{-T/2}^{T/2}\left(f(t)\right)^2\mathrm{d}t=\frac{1}{2\pi}\int_{-\infty}^{\infty}\Phi(\omega)\mathrm{d}\omega \tag{21}$$

expression, which is the Wiener-Khinchin theorem for stochastic signs. As shown above, the Fourier transform of the self-similar signal is a self-similar signal in the frequency domain. With the substitution in (21):

$$
\begin{aligned}
R(0) &= \frac{1}{2\pi}\int_{-\infty}^{\infty}\Phi(\omega)\mathrm{d}\omega \\
&= \tau\frac{1}{2\pi}\int_{-\infty}^{\infty}\Phi(\tau\varpi)\mathrm{d}\varpi \\
&= \tau\tau^{\alpha}\frac{1}{2\pi}\int_{-\infty}^{\infty}\Phi(\varpi)\mathrm{d}\varpi \\
&= \tau^{\alpha+1}R(0)
\end{aligned}
\tag{22}
$$

According to (11), $R(0)$ is self-similar. The power spectrum $S(\omega)$ equal with $\Phi(\omega)$, as it is shown in (19), which is its definition, so

$$
S(\omega) = \Phi(\omega) = \frac{A^2}{\omega} = \frac{A}{\sqrt{\omega}}\frac{A^*}{\sqrt{\omega}} = \frac{|A|\mathrm{e}^{i\varphi(\omega)}}{\sqrt{\omega}}\frac{|A|\mathrm{e}^{-i\varphi(\omega)}}{\sqrt{\omega}} \tag{23}
$$

The power density spectrum is the product of the signal and its conjugate spectrum. Then the temporal representation of the stochastic signal is:

$$
f(t) = inverseFourier\left(\frac{|A|\mathrm{e}^{i\varphi(\omega)}}{\sqrt{\omega}}\right) \tag{24}
$$

where the phase $\varphi(\omega)$ is an arbitrary function that can be deterministic but can also be random, characterized by its distribution functions. When an ergodic function represents the stochastic process, it facilitates the characterization.

Like it is shown in (24) that each 1/f signal differs in the distribution (power spectrum) of a random variable in phase. Since the phase is the carrier of the information, its distribution determines the signal's temporal form, which allows a better understanding of the step-by-step changes of the signal in the biological processes, while the power spectrum gives systemic information.

The scaling of the power density by frequency is a piece of general information about the system. The cancerous lesion is a local disorder that hurts the standard healthy conditions. Consequently, cancer cannot accept harmonic modulation. The signal attacks the cells by absorbing energy, while in the healthy harmonic tissues, these absorptions are much weaker, keeping the harmony in proper rhythm.

It is essential to identify when the system does not work correctly, so have tissues out from the overall self-organized control. The general request of the homeostatic harmony can be forced by a compulsory force by the 1/f signal. The following ways could personalize the general harmonization attempt:

1) Apply a 1/f random spectrum. This spectrum generates the frequency components randomly, but their distribution is strict. This method well shows the general harmony of the homeostasis, but no information about the actual processes in the molecular reactions of the cells. However, with the relatively high frequency (in the audio range up to 20 kHz, which changes 20.000 times in a second) and the vast number of enzymatic reactions, this method satisfactorily approaches reality stochastic meaning. The reactions occur in a randomized fashion in a large target. There are stochastically several proper excitations from the few billion excited molecular reactions. This is presently the best harmonizing approach.

2) Measure one of the personal electric signals (like heart rate, nerve-activity), and apply it as a compulsory modulator. This approach is very personal, but the signal depends on the patient's actual state, stress, mood, or the development of the disease, so it may be that its power density function deviates from the ideal 1/f scaling. In such a case, the modulation is suboptimal.

3) The local physiological signals could detect the target-oriented control signal. This method could compare the harmonic healthy host tissue with the anharmonic malignant tumor. This simple principle, however, has complications:

    a) The non-invasive impedance measurement is inaccurate, depends on many internal and external modifying factors, so it is unsatisfactory. If the impedance measurement is not accurate, then why accurate enough treatment with a non-invasive impedance basis? The treatment uses a high-frequency carrier of the modulation, and the radiofrequency delivers the information to the

target, and the electrical nonlinearity of the cellular membrane applies the info directly to the targeted cells.

b) Choosing the control target is not easy in such a complex disease as malignancy, where we have no precise information about the systemic effect of the tumor. (The present imaging and measuring technique or not cellular accurate.)

c) An electric signal is requested directly from the control target to measure its physiological harmony. This is usually the local arterial blood-flow fluctuation. In most cases, it needs invasive measurements, and even with this, the accuracy to form an appropriate signal is low.

4) The modulation signal may be applied not only for the treated target but also for the central energy supply manifested in the heart rate. The heard delivers the oxygen, nutrients, and electrolyte components (including special cells and compounds) which energize the dynamics all over the body. The heart-rate variation is the result of the parasympathetic and sympathetic controller signal summary in the sinus nodes [27]. The 1/f signal of the vagus nerve could harmonize the overall metabolism by nerves' action and control the oxygen supply by the heart rate, which determines the homeostatic stochastic process.

3. Result—The Personalization

The template will number citations consecutively within brackets [1]. The sentence punctuation follows.

The study of biomarkers evaluates the actual status of the organism with possible indications of the presence of locally systemically derail of homeostasis, forming pathological condition [28]. A particular group of biomarkers is the tumor markers, which refers to an elevated amount of body-identical substance in a tumorous patient, while it has only a low amount or not at all in a non-tumor patient. The tumor markers do not have enough diagnostic value in prevention, so the biomarkers have emerging importance indicating deviation from the healthy homeostatic balance. The deviation of the biomarkers from the healthy standard has three values [29], which are especially important for cancer [30].

1) Diagnostic biomarkers help the accurate analysis [31], and the design of clinical trials [32];

2) The prognostic biomarkers can indicate the possible prognosis of the disease [33];

3) The predictive markers can inform about the efficacy of the applied therapy [34].

The medicine practice needs reliable biomarkers indicating a disease/tumor early, showing its growth, spreading, being effective, or ineffective in therapy. It is extremely important to assess and monitor the general condition of patients during treatment to assess how well they are receiving the therapy they are receiving, but we can also obtain the information needed to maintain an adequate quality of life. The Karnofsky scale (in the range of 0 to 100, the patient's state of health), the ECOG system (scale of 0 to 5) may be helpful. In addition, questionnaires assessing physical, social, emotional, and functional well-being, such as EORTC QLQ-C30 or FACT-G [35].

According to the present practice, sampling is necessary to determine the prognosis of the cancerous patient. The pathologist provides staging and grading based on the standardized categories. The basic guidelines and protocols describe a generalized proposal for treating patients considering the pathological results. However, the prognostic factors used at present lack stable reliability [36]. Although it would be desired to provide personalized prognosis and decision- making, taking into account the patient's individual clinicopathological and psychological status. Any new reliable prognostic factor and connected therapies (theranostic methods) are expected to step towards personalized treatment. According to the principal considerations [13] [14], and the emerging practices [37], the modulation of a carrier signal could be a reliable option of personalized therapy. The application of modulated carrier presently applied mostly on oncology, but its non-oncological applications are also possible [38] [39] [40] [41].

3.1. Systemic Regulation

The homeostatic regulation shows some measurable electric signals for non-invasive detection of its proper functioning. The non-invasive detection of biomarkers has an extra advantage: less burdensome for the patient and more straightforward for the physician. This practical request emerges the various

electromagnetic signal detection, like the Electroencephalogram, (EEG); Electrocardiogram, (ECG); Electromyogram, (EMG); Electrooculogram, (EOG); Electroretinogram, (ERG); Electrogastrogram, (EGG); Galvanic skin response, (GSR); electrodermal activity, (EDA), electrical impedance tomography (EIT), etc. These signals have not only prognostic and diagnostic value but could be active therapeutic option to correct the deviations [42] [43] [44] [45]. In the following, we study two undoubtfully systemic regulatory signals: the heart rate and the nervous activity.

3.1.1. Vagus Nerve Signal

There are several methods for studying the autonomic nervous system. There are studies based on cardiovascular reflexes elicited by provocative maneuvers. Neurotransmitter levels can also be examined. The cholinergic part of the autonomic nervous system can be performed, for example, by examining sudomotor function (the reaction of sweat glands to various stimuli) [46].

The vagus nerve has an important homeostatic role. Its efferent position gives regulation signals for many muscles and various organs. It participates in the cardiovascular, respiratory, gastrointestinal, metabolic, control, and glucose homeostasis (pancreas, liver, kidney) regulation and controls inflammation by the spleen [47]. The afferent activity includes a significant part (>80%) of the nervous structure transmitting information to the central nervous system about the functioning of the organs of the body [48].

Several studies proved the therapeutic effect of vagus nerve stimulation (VNS) [49]. The emerging application of VNS is transcutaneous, primarily focusing on the auricular branch of the vagus nerve [50]. This non-invasive method targets several disorders, like migraine, tinnitus, headache, pain, applied in both cervical and ear sides. Importantly intensive studies started to clear the possible application of the VNS autoimmune and autoinflammatory diseases [51] and immunity [47].

The importance of studying the autonomic nervous system, among other sciences, is already outlined in oncology. Autonomic neuronal dysfunction has been shown to affect 80% of patients with advanced cancer [52]. The vagus nerve controls glucose homeostasis [53], which is particularly important for cancerous processes. Vagus nerve activity affects tumor growth by inhibiting tumor-promoting mechanisms. The significance of its study in a wide variety of tumors is known. The results of several articles show that vagus activity may play a prognostic role in cancer.

Tumor cells can take advantage of the benefits provided by factors secreted by nerve fibers to produce a stimulating microenvironment for the survival and proliferation of their cells. A reciprocal interaction exists between tumor cells and nerves in humans [54]. Tumor cells induce nerve growth in the tumor microenvironment by secreting neurotrophic factors. The nerves show up as essential regulators of tumor progression. Sympathetic nerves drive tumor angiogenesis with noradrenaline release, increases the migration capacity of tumor cells, and determines the direction and development of metastases, while the cholinergic fibers of the parasympathetic nervous system, in turn, infiltrate tumor tissue and affect tumor cell invasion, migration, and distant metastases [55]. The sensory and parasympathetic nerves stimulate tumor stem cells, while at the same time, the parasympathetic nerves tend to inhibit tumor progression. This balance forms the dynamic complexity of the nervous interactions [56].

The vagus has been an essential pathway in the early preclinical stage of tumorigenesis through the information to the brain about preclinical tumors with an immune-nerve information transformation. It partially regulates tumor formation and progression [57].

The tumor microenvironment has a fundamental influence on its features [58]. It contains innate and adaptive immune cells [59], which have Janus-face behavior, could inhibit [60] or support tumorous processes [61]. A clinical trial shows the feasibility of vagal neuroimmunomodulation as the prognostic factor for pancreatic cancer, and so, the method offers a new prognostic biomarker of advanced cancers [62]. Furthermore, active adjuvant therapy of neuromodulation of cancers improves the quality of life in advanced cases [63]. It is clinically shown that the VNS increases the complexity of heart-rate variability, allowing more stable homeostatic control [64], having a higher probability of a better quality of life and more prolonged survival. The experimental and clinical observations indicate that one of the most promising and far more objective methods for studying the autonomic nervous system is to analyze heart rate variability (HRV).

3.1.2. Heart Rate Signal

It was a long time ago realized that the chaos in physiology has special meaning [65]. The "constrained randomness" [66] is usual in physiology, and its study is a valuable tool to understand its mechanisms as well as recognize the deviation from "normal". The analysis of the noise-like profile of hear-beat in the healthy subject shows 1/f power-law distribution was recognized early [67], and this "chaos" was associated with time-fractal processes in the living organisms. The heart frequency components' expected flat or normal distribution became long-tail, self-similar distribution with scaling possibility.

The heart rate variability (HRV) describes the variability in the intervals between heartbeats. The temporal fluctuation of heart rate is due to autonomic nervous system regulation; it is created by interacting the sympathetic and parasympathetic nervous systems contributing to the measured variation of the signals [68]. HRV strongly correlates with vagus activity [69]. The most common area of HRV analysis is the study of cardiological problems [70]. However, it is often used for other diseases, like diabetes [71], renal failure [72], neurological [73], and psychiatric changes [74], but it is also used for sleep disorders [75] and some psychological phenomena [76]. The viability of using HRV measurement is based on non-invasiveness, ease of construction, and reproducibility [77]. Nowadays, the HRV offers a possible prediction of disease onset and prognosis [78], and so, its application has a significant increase in oncology [79].

The change in heart rate from beat to beat (RR [ms] intervals, the most observable peak in QRS complex in ECG signals) results from the balancing interaction of parasympathetic and sympathetic effects on the sinus node [80]. The RR is frequently estimated by heart rate (HR [beat/min]), which is easy to measure in daily practices. The variability is most frequently measured by time-domain analysis. The basic parameters to evaluate its uses the nth RR interval ((RR)n), and the average value $(\langle \mathrm{RR} \rangle = \frac{1}{N}\sum_{n=1}^{N}(\mathrm{RR})_n$ The calculated time-domain evaluation parameters are:

- the standard deviation of $\mathrm{RR}\ (\mathrm{SDNN}[\mathrm{ms}] = \sqrt{\frac{1}{N-1}\sum_{n=1}^{N}\left[(\mathrm{RR})_n - \langle \mathrm{RR} \rangle\right]^2}\ )$
- the square-root differences between the successive RR intervals:
  $(\mathrm{RMSSD}[\mathrm{ms}] = \sqrt{\frac{1}{N-1}\sum_{n=1}^{N-1}\left[(\mathrm{RR})_{n+1} - (\mathrm{RR})_n\right]^2}\ ).$

Some other characterization of the time domain of HRV is used for particular purposes, like

- NNxx [beats], is the number of successive RR interval pairs that differ more than xx [ms];
- pNNxx [%] is the NNxx divided by the total number of RR intervals.

The time-domain of HRV changes is analyzed for its short-range (SD1), which is connected to the RMSSD [81] and long-range (SD2) features [82]. The Poincare plot is an excellent visualization of the short and long-range changes by studying the subsequent RR-intervals; plots each 1 RR_{n+1} as a function of the previous RR_n interval [83].

Poincare plot analysis gives info about long-range by the $RR_{n+1} = RR_n$ line visualizing how continuous the development in stepby- step points, while its perpendicular line in the midpoint (zero points) shows how the short-range deviates from the long trends, compared the beat-to-beat info to the expectation of the longer performance of the heart [84]. The nonlinear homeostatic regulation could be followed by Poincare sections [85], with "stroboscopic flashes" synchronized to the neuron activity. Due to its simplicity and clearness, an emerging quantitative-visual technique categorizes the degree of heart failure by functional classes in patients [86]. The SD1 and SD2 can be calculated with standard time-domain parameters [87]. The calculation needs to introduce the standard deviation of the successive differences of the RR intervals,

denoted by $\mathrm{SDSD} = \sqrt{\left\langle (\Delta \mathrm{RR}_n)^2 \right\rangle - \left\langle \Delta \mathrm{RR}_n \right\rangle^2}$, where the $\langle\ \rangle$ a sign denotes the mean (average) value, and so $\left\langle \Delta \mathrm{RR}_n \right\rangle = \left\langle \mathrm{RR}_n \right\rangle - \left\langle \mathrm{RR}_{n+1} \right\rangle$. The short and long-range characteristic values are: $(\mathrm{SD1})^2 = \frac{1}{2}(\mathrm{SDSD})^2$ and

$(\mathrm{SD2})^2 = 2(\mathrm{SDNN})^2 - \frac{1}{2}(\mathrm{SDSD})^2$. In stationary conditions:

$\left\langle \Delta \mathrm{RR}_n \right\rangle = \left\langle \mathrm{RR}_n \right\rangle - \left\langle \mathrm{RR}_{n+1} \right\rangle = 0$. In this case, we get statistically: RMSSD = SDSD.

In consequence, RMSSD has a role in both the short- and long-range interactions in stationary conditions. Naturally, the HRV results and parameters depend on the time length of the registration [88].

The detrended fluctuation analysis (DFA) method is devoted to the scaling of correlation inside the time-domain of the signal [89]. This particular method scales the slopes (trends) of the linear regression fit to the n-length grouped segments of measured points in various scales. The sum of actual deviation of the points in the group from their average value is: $y(k) = \sum_{j=1}^{k}\left(\mathrm{RR}_j - \langle \mathrm{RR} \rangle\right)$.

Fit a linear regression (least-squares method) to these points. The obtained regression line is $y_n(k)$, and so the detrended series F (n) is scaled by n: $F(n) = \sqrt{\frac{1}{N}\sum_{k=1}^{N}\left[y(k) - y_n(k)\right]^2}$, calculating it with different segments and shown in double logarithmic scale vs. n, [90] Figure 4. The categorization of the noises is similar to the power density, but the DFA slopes differ from the power density slopes.

The relation of the SDNN and the DFA shows a connection to predicting the survival of patients studying in 7 years intervals [91]. When both parameters (SDNN and DFA) are high, all patients survived 7.5 years. When both were low, 50% of the patients involved in the study died within 2 years. In the groups with high DFA and low SDNN 60% died under 2.5 years, while the SDNN was high and, DFA low, 70% died within 3.5 years. Results support the idea that the health status needs high self-organizing in the system. When the self-organized chaos starts to disappear, and a series of subharmonic bifurcations appear, the ventricular fibrillation becomes more likely [92] [93], the bifurcation phenomena are pathological [94]. Note, the bifurcation in this meaning decreases the self-similar time-fractality, which appears again when the bifurcative processes are sequentially inserted into each other (fractal process) and form Cantor-like fractal in the dynamics, shown in Figure 3.

The variation evaluation with time-domain has some problems because the form of the signal could substantially differ while the RR average and the RR standard deviation could be identical [95]. The frequency domain, determining the S (f) power density, gives information about the distribution of the frequency components, so it clears the form of the signal [96]. The spectral analysis is a valuable tool in the analysis of the autonomic function of HRV [97]. The study of the frequency spectra reveals the healthy dynamics of the heart and is related to the overall homeostatic condition.

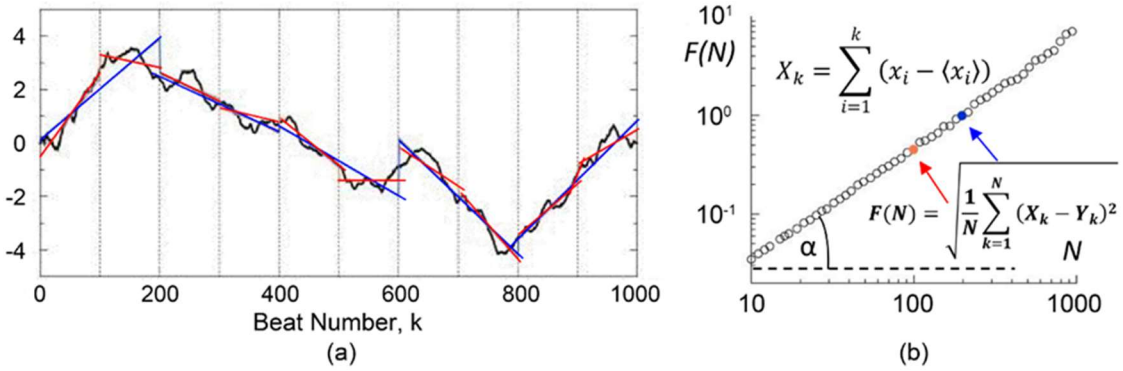

Figure 4. The detrended fluctuation analysis (DFA) method [90]. (a) The process of evaluation of scaled groups of noise parts by the linear regression model. Red lines are the best fit for the subsequent intervals counting 100 beats. The blue fits 200 beats and so on with all possible groups of the beats. (b) The measured slopes from (a). The points for red and blue fits are indicated on the line. The scaling clearly shows linear dependence of grouped slopes.

The frequency domains divided by the physiological ranges [98] like:

- Power (S_{ULF}(f)[ms^2]) ultra-low frequency range (≤0.003 Hz) power density (S_{ULF} (f)[ms^2]), follows the change s of the body's core temperature, the circadian rhythm, the renin-angiotensin controlling system, and the metabolic processes;
- Power (S_{VLF}(f)[ms^2]) of the very-low-frequency range (0.0033 - 0.004 Hz) observes the long-range controlling mechanisms, hormonal processes, heatcontrol;

- Peak frequency (P_{LF}(f)[Hz]) in the low-frequency range (0.004 - 0.15 Hz) is connected to the baroreflex activity and the balancing of sympathetic and parasympathetic nerve actions;
- Power (S_{LF}(f)[ms^2]) in the low-frequency range (0.004 - 0.15 Hz) is connected to the baroreflex activity and breathing;
- Peak frequency (P_{HF}(f)[Hz]) in the high-frequency range related to vagus nerve tone;
    - for adults (0.15 - 0.40 Hz);
    - for babies (and sometimes after sports activity) (0.24 - 1.04 Hz);
- Power (S_{LF}(f)[ms^2]) in the high-frequency range related to vagus nerve tone (0.15 - 0.40 Hz);
- Sometimes the ratio of the power of low (0.004 - 0.15 Hz) and high (0.15 - 0.40 Hz) frequency bands $(\frac{S_{LF}(f)}{S_{HF}(f)}[\%])$ used to study the balance of the vagal and sympathetic activity.

Through the connections of the autonomic nervous system, vegetative, somatic, and psychic effects are integrated into the instantaneous heart rate and variability [99]. Due to the neuro-controlled (sympathovagal) balancing, the HRV is a feasible parameter to quantify homeostasis [100]. In consequence of the homeostatic character, its measurement could be a valuable tool in clinical practices [101].

The vagus-mediated HRV may be associated with higher-level (brain) executive functions. One region, the anterior cingulate cortex, was interestingly found to be associated with both vagus activity and cellular (NK-cell) antitumor immunity [102].

Inflammatory markers and HRV parameters show correlation. The LF-HRV was inversely proportional to CRP, IL-6, fibrinogen, and HF-HRV was inversely proportional to CRP and fibrinogen. These also supported the existence of the vagal anti-inflammatory pathway [102] [103].

Vagus tone (measured by HRV) influences the nervous-immune response to acute stress. This was demonstrated in a study in which people with low and high baseline HRV participated and were presented with a learning task (acute stress factor). With this acute stress, NK-cell and noradrenaline levels in peripheral blood changed only in the high HRV group. Both prefrontal cortex and striatum activity correlated only with values indicative of the immune system only in the high HRV group. It is hypothesized that high vagus tone may mean a more flexible top-down (brain) -down (immune system) regulation [104].

The frequency domain is a helpful tool for analyzing the signal components, but the obtained frequency distribution does not inform us about the signal trends and how the segments correlate. For the personalization, the amplitudephase has to be considered, as shown in (24).

The HRV can be a valuable biomarker to assess disease progression and outcome, and even it could be the future remote, wearable biomarker technology [99], which controls not only the diseases, b but also nutrition and wellness [104].

The HRV contains the homeostatic stage of the patient, so it mirrors the various, not disease-connected parameters (like the age, gender, medications, physical and mental status, and even such simple parameters as the body-position, respiratory rhythm, stress) [105]. This sensitivity of general conditions could influence the medical decisions, which develops a distrust in the method. High practical routine and well-controlled conditions are necessary to obtain the medical value of the results. Furthermore, HRV does not directly measure parasympathetic or sympathetic activity. Its features are indirect, only qualitative information on the autonomic activity, the quantitative measures need independent methods. In addition to methodological errors, there may also be technical pitfalls in data collection, signal processing, and interpretation, leading to inaccurate HRV measurement, l and wrong medical decisions [106] [107]. The mixed information causes that the HRV application as a diagnostic tool does not widely apply in medical practice.

3.2. Local Effects

The modulation is well applied locally in the tumor treatment [108] by forcing the local arrangement order in space-time to fit homeostasis. The local application has similar goals that the systemic VNS, forcing the healthy balance. However, the local application is only in the small part act on the nervous system (mainly on parasympathetic, while the selection is connected to the function of the vagus). The dominant effect forces the healthy local arrangement in space (intercellular bonds) and in time (intracellular signal-

transmissions). The practice of local application is the modulated electrohyperthermia (mEHT, trade name: oncothermia®), which is widely applied in clinical practice [109].

3.2.1. Pattern and Molecular Recognition

The differences between the tumor and healthy host tissue are significant. The tumor cells have a higher metabolic rate than the host because of proliferative energy demand, have no networking connection with the neighboring cells, separate individually, have different membrane structures with more transmembrane lipid rafts, and differ in their overall structure too. This last is used by the pathologist when studying the pattern of the specimens and recognizing the pattern deviation from the expected healthy order. This pattern recognition is one of the factors of the diagnosis, staging, and prognosis too. So, the tumor structure differs, which can be recognized by the homeostatic signal, due to the missing dynamic harmony. In this way, the disordered tumor selectively absorbs energy from the harmonic fluctuation (modulation with 1/f noise), and the various consequences kill the cells. The free genetic information allows recognizing the deviation by the adaptive immune system, which may act against [110] [111].

A part of the modulation effect is the broken cadherin complexes' re-bonding and allowing the intercellular connections again [112] [113]. This reconstruction turns the individual precancerous cells to the network and blocks their movement, decreasing the risk of metastases. The rebuild network allows the intercellular connections, gives the cell a chance to return to normal conditions, or has a signal, and turns to apoptosis.

The physical analysis of temperature-dependent effects of mEHT [114] calculated that the most likely effect is electromagnetic excitation, which develops non-thermal effects of radiofrequency electromagnetic fields [115]. The physical assumptions successfully indicated the possibility that the physical methods may recognize and use the heterogeneity of the target [116]. The vagus nerve assists the body's thermal sensitivity and thermoregulation [117].

3.2.2. Molecular Excitation

Other important local effects of mEHT are the molecular excitations of the cellular receptors and, in general, the transmembrane proteins. The nonthermal membrane's temperature-independent effects of electromagnetic fields had serious debates and controversial opinions. The present research provides some preclinical and clinical data for the nonthermal antiproliferative effects of exposure to mEHT. The excitation promotes membrane vibrations at specific resonance frequencies, which explains some nonthermal membrane effects, and/or resonances causing membrane depolarization, promoting the Ca2+ influx [118], or even form a hole on the membrane. mEHT may be tumor-specific owing to cancer-specific ion channels and because, with increasing malignancy, membrane elasticity parameters may differ from that in normal tissues. The Arrhenius plot fits the thermal properties in mEHT experiments [119], so the treatment is a complex mixture of the thermal and nonthermal processes [120]. The protecting chaperones induced by the heat shock are exhausted [121], so the safeguarding does not suppress the electromagnetic reaction. This mechanism resolves the radiotherapy resistance of pancreas adenocarcinoma cells [122].

The molecular excitation is proven in vitro, showing how different the mEHT complex electromagnetic therapy is from conventional heat-therapies [112]. The recent review of the tumor-damage mechanisms collects the preclinical results [113].

4. Discussion

The modulation of the external bioelectromagnetic signals has well-explained principles [13]. The carrier frequency helps in the selection mechanisms, while its modulation acts. The modulation supports homeostasis by its time fractal (1/f) frequency distribution [108]. The modulation could have multiple effects locally and systematically. The local force for the homeostatic control acts as a further selection factor regarding the lost control of the tumorous cells. Furthermore, the modulation forces the healthy dynamical order providing a compulsory process for apoptosis of the out-of-control cells. HRV may characterize the homeostasis [124], presenting the complexity of the system.

The well applied time-fractal current flow may activate the structural fractals in the living systems, and the personal fractal structure could modify the time-fractal pattern, too [125]. The fundamentally non-linear

physiological system dynamics work on the edge of chaos, a border of order and disorder showing a constant dynamic interplay between these states [126]. The challenge of the homeostatic equilibrium is the apparent chaos. The chaos looks complete randomness which is only ostensible. The chaos in biosystems results from the stochastic self-organizing and the energetically open system, which directly and permanently interacts with the environment. Its structural and temporal structure is fractal, which appears in the fundamental arrangements of the self-similar building and dynamism of the energy exchanges internally and externally. The living processes are complex. They are in self-organized criticality (SOC) [127], which is formulated, as the "life at the edge of chaos" [128]. This chaos is the realization of a well-organized stochastic (probabilistic) system [129]. The disordered chaos is apparent [130].

A simple bifurcation could help to understand this "edge of the chaos" phenomenon. The processes must keep their dynamic energized form. When their energy at the energy breaking point is too low, the process stops and "freeze" in one of the potential wells. However, when the provided energy is too high, the system loses its control, the promoter-suppressor balance can't regulate the processes Figure 5. (Like Einstein formulated: "Life is riding a bicycle. To keep your balance, you must keep moving." [131]) The common idea that bio-systems evolve toward equilibrium is a misperception of reality.

Self-organized chaos was studied in all the living processes like, for example, in immune activities [132], in nerve system [133], in genetic phenomena [134]. The realization of the "edge of chaos" is very personal due to the determining parameters, and their intensity differs from person to person [135]. This character of the living complexity requests personalized treatments.

DFA evaluation of the signal measures the self-similarity scaling of the fluctuations by scaling parameter. This evaluation is similar to the box methods in structural evaluation of the fractals when the scaling is the size of the box like in DFA, the size of the scaling interval. The other time-domain studies focus on the standard deviations of the fluctuations (like the HRV methods the SDNN), which also depends on the length of the investigated interval so also has similarities with boxing evaluations. The standard deviation changes by the s box-sizes in the Ns step-number, and has a scaling behavior:

$$S(s)=\sqrt{\frac{1}{N_s}\sum_{i=1}^{N_s}\left(x_i-\langle x_i\rangle\right)^2}\propto s^H \qquad (25)$$

The exponent is named in honor of HE. Hurst, who first observed this scaling at the water level fluctuations at the Aswan dam in Egypt. The Hurst exponent, H characterizes the scaling exponent of the $S(f)=f^{-\beta}$ power density function (PDF, frequency domain) fitted to the scaling function (calculated for q = 2) in the time domain:

$$\beta=\begin{cases}2H-1 \text{ if } -1<\beta<1 \text{ (PDF)}\\ 2H+1 \text{ if } +1<\beta<3 \text{ (PDF)}\end{cases} \qquad (26)$$
$$\alpha=H+1 \text{ (DFA)}$$

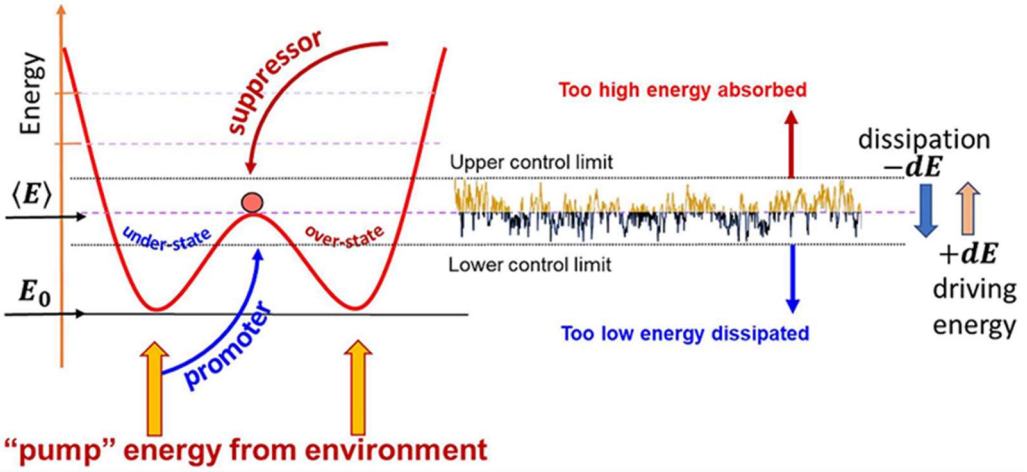

Figure 5. Permanent dynamic changes of the energetically open system cause a never rest situation. The dissipation consumes the energy, while the open, energetic situation drives the process. Promoters and suppressor balance never stop, the dynamism makes life on the "edge of chaos".

In time series: 0 < H < 1. The 0 < H < 0.5 describes anticorrelation, while 0.5 < H < 1 characterizes the correlation, long-memory process. There are two border values: H = 0.5 is the while noise (no correlation), H = 1 is the pink noise [136].

However, most complex systems have no single scaling. The living body contains variants of fractal templates in space-time, and so the exponents of selfsimilarity could change by parts. The multifractal analysis considers the scaling as not a global behavior but local (multifractality). The multifractality appears in the dynamics of the biological processes. The scaling varies in time. The nonlinearity of the processes strongly influences the multifractality.

In the case of multifractality since the scaling property is heterogeneous, H will be different for smaller and larger fluctuations in the process and thus the generalized Hurst exponent, H(q) is obtained as a function of q [137]. It is the scaling of the qth momentum of the fluctuation and called generalized Hurst exponent. The generalized scaling function is:

$$S(q,s)=\left(\frac{1}{N_s}\sum_{i=1}^{N_s}\left(x_i-\langle x_i\rangle\right)_s^q\right)^{1/q}\propto s^{H(q)} \qquad (27)$$

The generalized multi-scaling gives back the mono-scaling Hurst exponent when q = 2 so $S(2,s)\propto s^H$ .In the case of monofractality, the scaling property is homogeneous and thus independent of q. With the growth of the "box-size" by growth of s the different variances (scaling functions by q) approaches each other, and at the largest size (the L size of the entire sample) point on a common focus [138] $S(q,L)=SD(L)\;\forall q$, where SD(L) is the standard deviation character of the entire signal.

The fingerprint of the personalized "chaos" is the self-similar noise of interconnected HRV and VNS in both the time (variation-based evaluations) and frequency (S(f) based evaluation) domains. The characteristic behavior of the frequency-based approach is the 1/f noise. Consequently, forcing the homeostatic control needs 1/f spectrum in the frequency domain. In an ideal case, the frequency domain has a single exponential character. However, it is not the general case; it only approaches a part of the anyway curved double logarithmic plot of the spectral density S(f) , which characterizes a multifractal behavior of the system's dynamics.

The multifractal structure changes the frequency by time, so the Fourier transformation, which produces S (f) power density function (PDF) in the monofractal approach, is not constant in all the observed time. The problem of the multifractal analysis has similarity to the Heisenberg principle: one cannot get the infinite time and frequency resolution beyond Heisenberg's limit: $\Delta t\Delta E\geq\frac{h}{4}$ so $\Delta t\Delta f\geq\frac{1}{4}$. Consequently, one can calculate high-frequency resolution accompanied by an insufficient time resolution or has high resolution in time with a poor frequency resolution. The method of wavelet transformation was developed for space-time multifractal description [139].

For proper multifractal analysis, a local power-law had been developed. This method approaches the function with its Taylor series and observes the scaling in the difference of the real and approached function:

$$\left|f(x)-\sum_{k=0}^{N}b_k\left(x-x_0\right)^k\right|\leq C\left|x-x_0\right|^{h(x_0)} \qquad (28)$$

The $h(x_0)$ value is the Hölder exponent. This is a local power-law, showing local self-similarity in a given discrete t time-point. In the case of any (multi or mono-fractal) approach h(t) is the power of the scale. In monofractals the exponent is constant: h(t) = const . The Hölder exponent forms trajectories when calculated in real-time. The fractal dimension of disjunct sets of the same Hölder exponents in the histogram approach is the multifractal or singularity spectrum, with generalized dimension D(h) , which is mostly used for multifractal characterization. The "size" of the singularity components is $\propto s^{D(h)}$. The monofractal Hurst exponent H (2) tightly connected (but not equivalent) to the maximum (middle) Hölder exponent of the singularity spectra, while the ΔH (n) ,the multifractal character described by ΔH (n) = H (−n) − H (n) is the width of the multifractal spectra. The maximum of D(h) is connected to the autocorrelation and the width of the non-linear character of the processes, introducing the multifractal scale exponent τ (q) from wavelet transformation [140]. This exponent connects all the multifractal characters:

$$\tau(q)=qH(q)-1,\quad h(q)=\frac{\mathrm{d}\tau(q)}{\mathrm{d}q},\quad D(h)=\inf_q qh(q)-\tau(q) \qquad (29)$$

The behavior of τ (q) describes the locally changing dynamic fractals, specifying the details that distinguish these from the global single-exponent character [141], Figure 6.

The well-established, widely applied and approved methods of evidence-based medicine (EBM) work with averages in many respects, as the inclusion criteria, like the sub-grouping of the eligible patients by various aspects. The monofractal application fits this approach, representing an overall average of the homeostatic control of the patients. However, the averaging has multiple pitfalls [135] [142].
The primary challenge is the averaging, despite that no such "average patient" who is supposed in the study exists. More personalization is necessary to avoid the averaging errors.

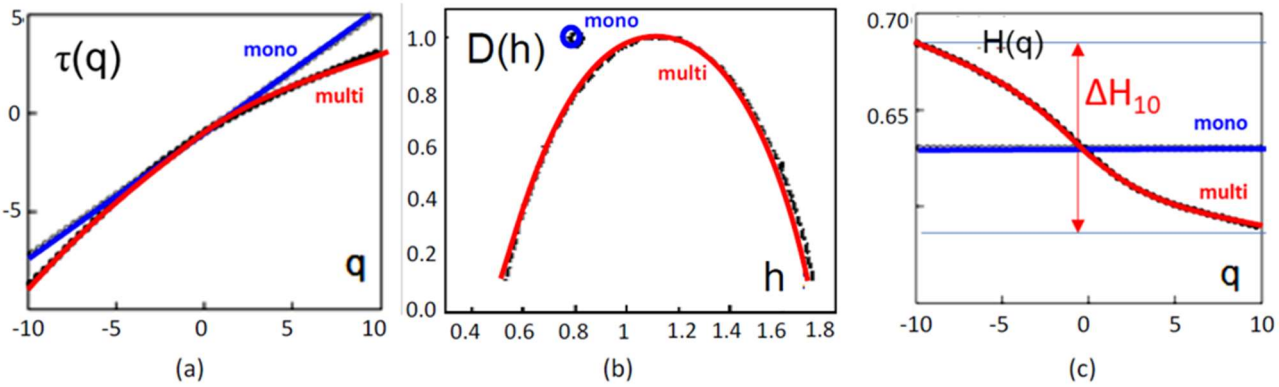

Figure 6. The changes of characteristic scaling exponents in mono-fractal and multifractal stochastic pproaches.
(a) scaling exponent by q^{th} momentum;
(b) multifractal spectrum;
(c) the generalized Hurst exponent does not change by q = H (2) .

The fine-tuning of the information has to consider the time-domain signal analysis. The personalization principle is the inverse transformation of the timeseries from the personally S (f) by the distribution of the amplitude phases (ϕ (ω)) shown in (24). The precise time domain is reconstructed, but it has also averaged in the distribution function of the phase ϕ (ω) . The HRV time-domain has also high averaging due to the form of the signal is not present, only the mean and its standard deviation. However, the HRV and the inverse transformation of the amplitude of S (f) by (24) represent different information about the person, so the combination of the two methods looks the most accurate in our present knowledge. The complex number of the amplitude $A = |A| e^{i\varphi(\omega)} = |A|\left[\cos(\varphi(\omega)) + i \cdot \sin(\varphi(\omega))\right]$ of S (f) in (24) contains the personal frequency order. The geometric representation of the single term of S (f) in the complex sheet is a circle with the radius R = | A | , and a vector with angle of ϕ (ω) . The personal order by geometric description of $\frac{|A| e^{i\varphi(\omega)}}{\sqrt{\omega}}$ from (24) connects these vectors where their size is proportional with $\frac{|A|}{\sqrt{\omega}} = \frac{|A|}{\sqrt{2\pi f}}$ Figure 7.

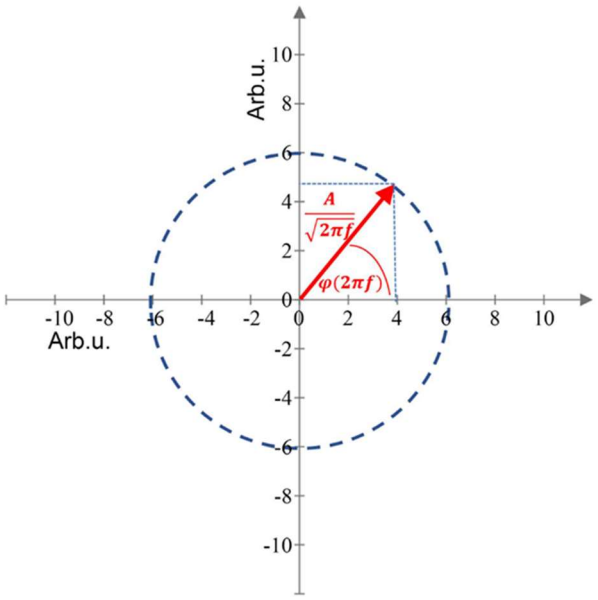

(a)

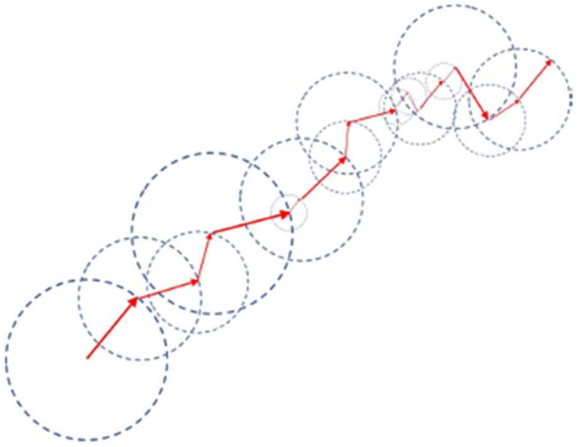

(b)

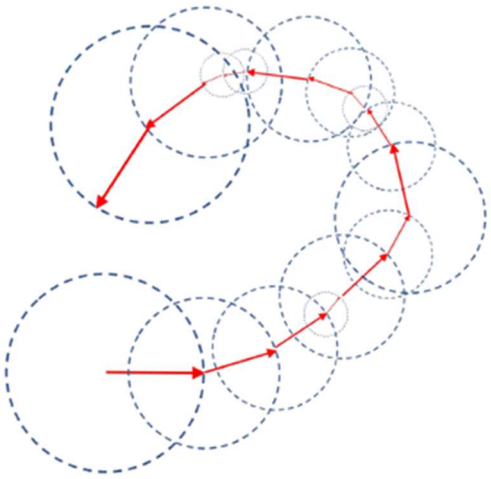

(c)

Figure 7. The series of the $\sqrt{S(f)}$ in personalization.
(a) the vector representation of a single component. The vector rotates as the ϕ (ω) phase angle changes by the changing S(f) .
(b) an example of the series of S(f) s, when the vectors jointly follow each other. The S(f) changes hectically (noisy).
(c) another example of the S(f) series with monotonously growing phase angle ϕ (ω) in a series.

In reality ϕ (f) has a personal distribution, which arranges the frequency order. In a random distribution, we may check the system how we construct the Si (t) time-series of the signal from frequency series with inverse Fourier transformation Figures 8-10. Noteworthy that the S(f) function is identical in all reconstruction processes from the ϕ (f) series, because the phase angle does not change the value of the amplitude, only its direction changes on the complex coordination system.

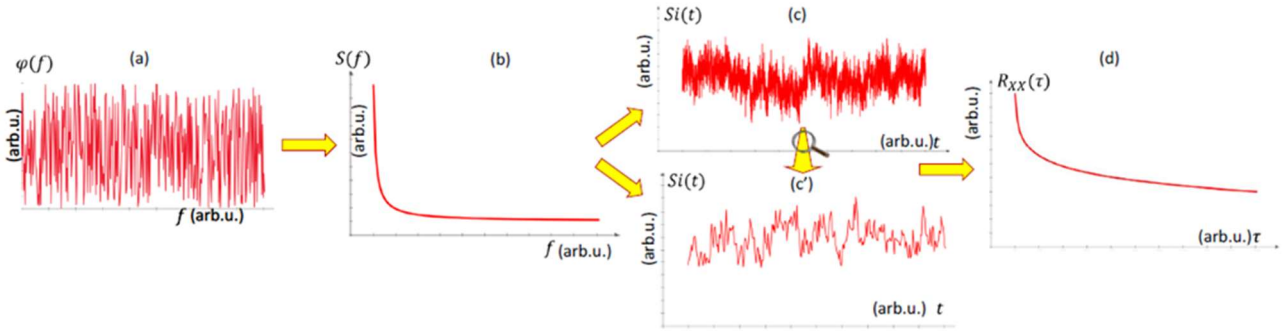

Figure 8. Reconstruction of the time-series from the power density function (PDF)
(a) when the ϕ (ω) phase has a random distribution.
(b) The distribution of phase by frequency from the S (f) phase function on the (a).
(c) The signal function in time (the time series); (c') the enlargement of the signal function in a small time interval;
(d) the correlation function of the Si(t) signal function.

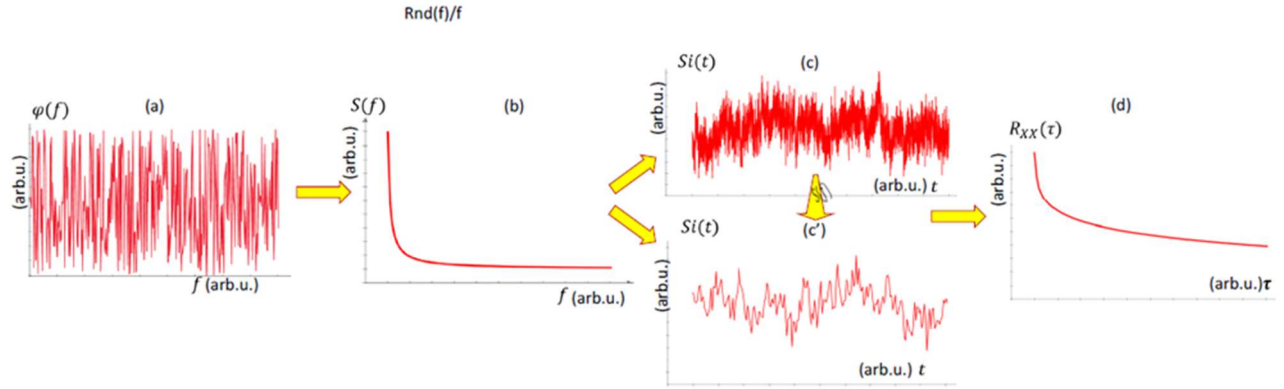

Figure 9. Reconstruction of the time-series from the power density function (PDF) when the ϕ (ω) phase has 1/f distribution. [this figure well follows **Figure 8**; the difference is most obviously seen on the incoming excitation and the Si(t) spectrum]
(a) distribution of phase by 1/f frequency;
(b) the S (f) function from the phase shown in (a) [it is identical with that, repeated only for the control of the calculation];
(c) the signal function in time (the time series); (c') the enlargement of the signal function in a small time-range;
(d) the correlation function.

The strong, definite Weibull distribution causes only minimal and mostly regular time series. Probably this is irrealistic in living systems. The periodicity-like form in correlation length is also the consequence of the well-defined original distribution shown in Figure 10(a).

4.1. Forcing Homeostasis by Modulation

The next step of the personalized idea needs to force healthy homeostasis in the patient, who lost it due to the disease. First, the deviation from the healthy state must be measured, which could be checked with the time-(HRV) or frequency- (S (f)) domain as well. This global information could be the reference for the development of the disease and the chosen treatment's success. Increased risk of progressive disease is connected with the gradual loss of complexity in the decrease of the HRV in patients with cardiovascular diseases [64].

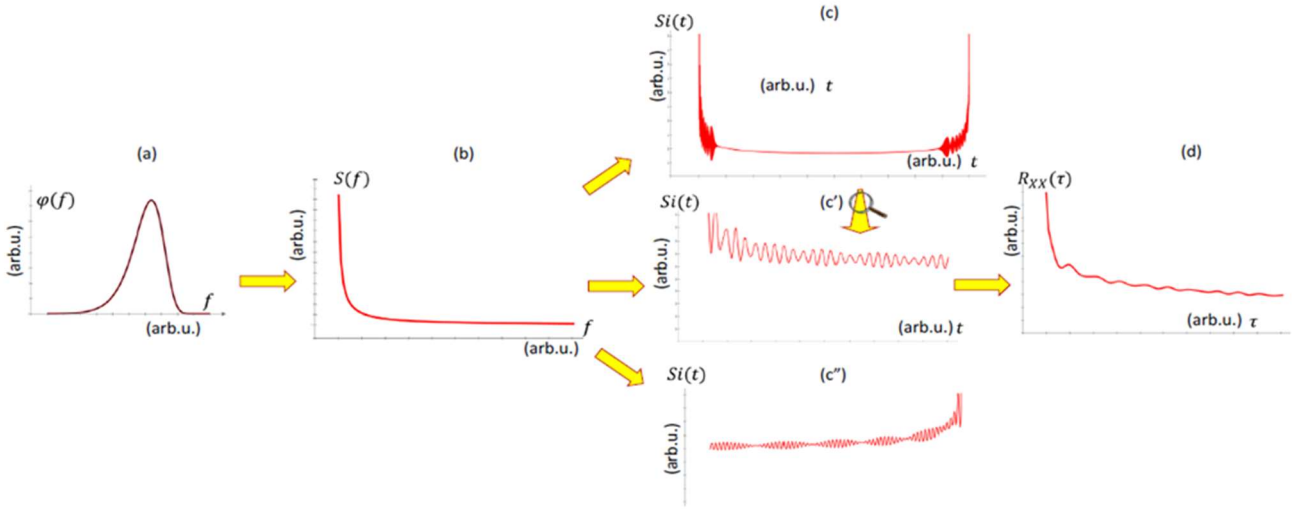

Figure 10. Reconstruction of the time-series from the power density function (PDF) when the ϕ (ω) phase has Weibull distribution.
(a) distribution of phase by frequency;
(b) the S (f) function from the phase shown in (a) [it is identical with that, repeated only for the control of the calculation];
(c) the signal function in time (the time series); (c') the enlargement of the signal function in a small time-range;
(d) the correlation function.

It is observed that the VNS associated to the parasympathetic tone, decreases the heart rate accompanied with increased complexity (increased HRV) especially in sleep [64]. The higher HRV values in various bands were positively correlated with disease regression in the actual band category. Higher HRV meant more advanced coping ability and thus better prognosis.

Together with the dynamic equilibrium's general character, it might be supposed that every person has an individual part of homeostatic control. The overall neuronal surveillance by the autonomic nervous system, the immune system, the transport systems, etc., has a particular path specific for a person and produces an individually coded 1/f homeostatic noise. In this sense, we can talk about personalized 1/f noise. As the (24) shows, the 1/f noise spectrum carries many kinds of information which are hidden in the ϕ (ω) phases of the amplitudes. The phase distribution carries the sequential information of the frequency series.

In the case of one individual subject, the information in the homeostatic noise has the same phase code since these are all results of the work of the same regulatory system. Important perspectives open with the personal homeostatic noise:

- In diagnostics, the measured noise spectrum's irregularities could signal that specific organs do not work correctly.
- In control of the therapy control, the measured changes of the noise spectrum could show the direction of the treatment triggered changes.
- In prognosis, the stored spectrum in individual "noise bank" taken when the patient is healthy could be compared with the actually measured noise prognoses the possible start of the irregularities in the body.
- In therapy, when the healthy fluctuation forces the homeostasis to correct the irregularities and blocks the iatrogenic processes, the healing is actively forced.

The last point is an active function of the noise. We concentrate on this application by personalization forming uniform general 1/f signal it is power spectrum. Like all the homeostatic control, the nervous system also follows 1/f power spectrum. The general regulator of physiological responses to internal and external stimuli is the nervous system. It is based on two large nervous sets like promoter/suppressor pairs: the sympathetic, which mediates catabolic responses, and the parasympathetic, which regulates anabolic responses. The main component of the parasympathetic nervous system is the vagus nerve. The vagus innervates most

tissues dealing with nutrient metabolism, which is crucial for many body functions and cancer development [102] and therapy [58]. The balance of vagus activity with sympathetic regulation needs proper homeostasis [53]. The vagal nerve signals contribute to the care of homeostasis [143] [144].

The homeostatic time-fractal frequency domain (in general, the $1/f^{\alpha}$ noise) is optimal forcing information when no more personal parameters are available This average contains the optimal time-domain fluctuations also when the sole in log-log scale is near to $\alpha \cong 1$. The deviations of $\alpha \gg 1$ mean more step-bystep regulated dynamics (like the brown-movements) while $0 \leq \alpha \ll 1$ goes to the white noise direction, to uncorrelated noise.

A possible constraint of proper homeostasis could be an external electromagnetic compulsory signal. The electromagnetic force is an overall effective influence because electromagnetism represents the biologically active force. Choosing the 1/f signal is a natural selection to induce a forceful corrective action. The penetration of the electric field into the body depends on the frequency of the signal. The penetration of the high frequencies is shallow, while the low frequencies penetrate deep.

On the other hand, the low frequency does not radiate, so the energy-coupling needs excellent contact in safe voltage application; otherwise, no effect exists. This condition complicates the non-invasive applications. Due to the signal having intensive low-frequency components and the broad spectrum of higher frequencies, the penetration will be heterogeneous; the proper frequency distribution cannot be overcome. The solution could be choosing the higher frequency carrier, which delivers its 1/f modulation with approximately proper amplitudes [145]. This modulation solution has a further advantage by its energy delivery, which makes additional mild heating [146], supporting the healthy enzymatic reactions in the body.

A further advantage is that the properly chosen carrier frequency delivers the information to selected regions of the heterogeneous target [147]. Furthermore, the current of the amplitude modulated signal flows through the fractal structures of the living organism, and the necessary frequencies could be selected by the structural dynamism as well. The broad modulation spectrum offers various frequency subgroups, which allows complying with the local demands.

However, it has a disadvantage: demodulation is necessary for the system, which dominantly performs by the cellular membrane nonlinearity [14]. The modulation keeps the system in the regulatory interval, helps the complex living processes correct the faulty regions, and re-establish the healthy control [148] [149].

4.2. Immune Effect of Forcing Homeostasis

One of the effective systemic regulators of homeostatic controls is the immune system. Immune-system terminates many diseases and helps balance the symbiotic life with biotas and broader meaning, as the fundamental cellular reaction, control some inter and extracellular events by molecular chaperone functions [150] [151].

Research on the neural control of the immune response has traditionally focused on the role of the sympathetic nervous system and sensory nerves. However, recent studies have highlighted the role of the efferent parasympathetic system, particularly the vagus nerve, in immunomodulatory actions [58] [152]. The nervous and immune systems communicate in two-way pathways to limit inflammation and maintain homeostasis [58]. The vagus nerve stimulation activates neuroimmune reactions [153].

The vagus nerve is one of the modulating components of innate (like NK-cells) and adaptive (like T-cells) immunity [58]:

- inhibits the TGF-β1, which increases NK
- supports the expression and activity of cytotoxic T-lymphocytes;
- down-regulates the helper T-cells (CD4+ function).

Efferent hepatic vagus activity has anti-inflammatory effects through local IL-1β and IL-6 secretion. This may be an important part of the theory of the beneficial outcome of the relationship between vagus and tumors [154].

The vagal activity reduces the inflammatory response by reducing cytokine release [103]. The B, and C fiber subtypes of the vagal nerve are involved in regulating the heartbeat [103]. This neuroanatomy suggests that the regulation of heart and inflammation by the efferent vagus can be separated. Electrical stimulation (1 V, 5 Hz, 2 ms) was found to be sufficient to elicit an anti-inflammatory effect but did not affect heart rate. Higher striding results decrease in heart rate; consequently, the vagal A fibers are connected to the anti-inflammatory signals. This separation limits the correlation between HRV and vagus-mediated anti-inflammatory effects [103].

The vagal immunomodulatory effect (cholinergic anti-inflammatory pathway) is intertwined with acetylcholine activity. Various immune cells (lymphocytes, macrophages, mast cells, dendritic cells, and bone marrow lymphoid and myeloid cells) express the significant components of cholinergic systems (acetylcholinesterase, choline transporters, AchE, nAChR) and produce acetylcholine. Consequently, the cholinergic system may play a role in regulating the immune response through immune cells [58].

Other systemic effects of vagus nerve stimulation were observed in better outcomes in conditions such as irritable bowel syndrome, metabolic syndrome, diabetes, sepsis, pancreatitis, depression, pain, and epilepsy [102]. Low vagus nerve activity correlates with worse outcomes [102].

An important observation of the modulated treatment is the immunogenic hyperthermic action [155], which can be improved by the independent stimuli of the immune system by dendritic cell therapy [156] [157], or viral therapy [158].

4.3. Cancer and Homeostasis

Tumor cells and the connective tissue surrounding them contain immune cells. However, these cells are double-edged weapons; they can inhibit but also promote tumor growth. The inhibition processes are:

1) activated lymphoid cells can control the tumor growth and malignancy;
2) dense infiltration of T lymphocytes correlates with better prognosis.

While there are promoters:

- tumors often break down the tumor-infiltrating lymphocyte activity;
- supports the differentiation of tumor-associated macrophages (TAMs) and myeloid-derived suppressor cells (MDSCs), promote tumor growth by secretion of growth factors, and inhibition of T lymphocytes.

Mediators and cellular implementers of inflammation are essential components of the local environment of tumors. In some tumor types, inflammatory conditions are already present before malignant transformation occurs. Inflammation promotes proliferation, survival of malignant cells, angiogenesis, metastasis, weakens the adaptive immune response, alters the response to hormones and chemotherapeutic agents. The molecular mechanism of this tumor-associated inflammation may be an important therapeutic and diagnostic target [1]. In some types of tumors, oncogenic transformation induces an inflammatory microenvironment that promotes tumor development [159]. The stimulated vagal activity suppresses the inflammatory developments [58]. Most articles examining the relationship between HRV and tumor prognosis consider vagus activity to be systemic as a positive effect. Analysis of the 12 studies yielded consistent results: HRV has prognostic value in tumors, predictive: for both survival and tumor markers [102]. The analysis also showed that the predictive value of HRV may be strong primarily in the advanced stages, the higher initial vagus activity predicted a better prognosis [102]. However, although the vagus effect systemically slows tumorigenesis, its major neurotransmitter the acetylcholine (Ach), promotes local tumor formation [102]. In other study, anti-inflammatory effects of vagus nerve via ACh - α7nAChR. The α7nAChR is expressed on a number of immune cells, suggesting that the vagus may have an effect on the tumor microenvironment and antitumor immunity [58].

Vagus activity may slow tumor progression in pancreatic tumors because it reduces inflammation. A new vagus index was introduced for pancreatic tumors, the neuroimmunomodulation index: $\mathrm{NIM} = \frac{\mathrm{RMSSD}}{\mathrm{CRP}}$ where CRP is the C-reactive protein. Following more than 200 patients with pancreatic cancer, the NIM index was found to have a protective value (relative risk: (0.688)) [62]. Initial higher vagus activity (characterized by HRV) was significantly correlated with a lower risk of death in pancreatic tumors regardless of age and treatment received [160]. The possible mediating role of C-reactive protein (CRP) was tested in non-small cell

lung cancer (NSCLC) [8], where the CRP was not found to mediate the relationship between HRV and survival time in patients younger than 65 years, but did not predict overall survival. The NIM index was characteristic also in the study NSCLC; where the NIM index indicated also the protective relative risk. Furthermore, a high NIM index correlates with longer survival [62]. However, for advanced NSCLC, HRV should be used to monitor overall patient well-being rather than to judge survival [161].

Another study with meta-analysis (6 studies analyzed, with 1286 patients) also found that HRV has predictive value in cancer patient survival. Also, higher vagus activity may predict longer survival [162]. Similarly, in a study of hospice patients, it was found that HRV (SDNN value) is a prognostic factor in terminal cancer patients [163].

A meta-analysis of 19 high-quality observational studies [164] shows that higher HRV positively correlates with patients' progression of disease and outcome. The individuals with higher HRV and advanced adapting mechanisms seem to have a better prognosis in cancer progression. HRV appears to be a useful aspect to access the general health status of cancer patients.

A study investigating the role of HRV in gastric cancer patients found that HRV decreased in advanced clinical stages (progression) and correlated with tumor size, tumor infiltration, lymph node metastasis, and distant metastasis. Thus, gastric cancer patients had a lower HRV that correlated with the tumor stage. In this research, they also claim that; HRV may serve as a factor in assessing stage and progression in gastric cancer patients [165]. Based on this, HRV can be a promising biomarker, a prognostic factor in gastric cancer patients.

It was also shown that SDNN value significantly predicted the development of CEA levels in colon tumors 1 year after onset. However, when the patient sample was divided into curative and palliative care, it was found that the HRV-CEA relationship could only be demonstrated in palliative care [166].

In the study of liver tumors, it was found that the indices of HRV, including the previously detailed HF, show a significant correlation with the survival time of patients in patients with end-stage hepatocellular tumors [167]. The HRV significantly positively correlated with survival time in HCC patients [154].

Patients with prostate carcinoma (PC) were examined for vagus tone (with HRV measuring the SDNN and RMSSD). HRV shows a significant inverse correlation with PSA levels at follow-up at 6 and 24 months. This correlation was particularly true in metastatic PC patients [168].

Research on breast tumors (metastatic or recurrent) has hypothesized that high-frequency HRV (HF-HRV), a characteristic of parasympathetic nervous system function, may correlate with survival. Vagus activity was found to be strongly associated with survival (well-predicted survival) [169].

One study examined the association between HRV and brain metastases. Low HRV and a low score on the Karnofsky status rating scale were adverse prognostic factors for survival in patients with cerebral metastases. Based on these, it is thought that HRV may also be a prognostic factor in brain metastases [170].

5. Conclusions

The living cellular structures are energetically open. They need transport of the energy sources in and transport of the waste out. The homeostasis drives the complex system to be balanced, structurally, and dynamically tailored to stochastic (probability-based) equilibrium. Without direct cellular communication (no "social signal"), this organized transport would be missing. The malignant transformation breaks this organized transport and seeks to build up new for the new demands. However, there is a fundamental difference that exists: the healthy construction is driven by the collective signal and seeks to optimize the energy use for the highest efficacy. The malignant structure is driven by the topology and biophysical interactions of the competing cells, irrespective of the efficacy of the energy conversion. This collectivism makes a difference in the geometric arrangement, not only in the cell-cell correlations but the autonomic behavior that forms cells individually.

Different pathophysiological mechanisms and risk factors lead to altered signaling of a common homeostatic pathway indicating various diseases. Consequently, its indication has significant biomedical potential. The homeostatic actions are based on self-similarity, leading to structural changes and information flows, which drive the system's dynamics. Many interacting signals in the complex system produce a noise-like summary, which can be measured in variations of the signal in time-domain, and have a definite frequency distribution in noise power, following inverse dependence, called 1/f noise. This noise is meaningful and feasible,

regardless of whether the system's signal is deterministic or stochastic. Forcing the 1/f signal is a possibility to stimulate the homeostatic control of the system. The heart rate variability (HRV) presents a feasible measuring of the individual status of the patient. The activity and effect of the vagus nerve drive numerous pathways of homeostatic control and are well connected to the HRV too.

Some common mechanisms inhibit the vagus activity in the tumorous situation [171], like the local oxidative stress and DNA damage, the inflammatory reactions, and excessive sympathetic activity. Stimuli may correct the inhibitions, either the vagus-nerve directly or by the compulsory spectrum on the local place of the disease.

The active vagus nerve can reduce the risk of cancer and cardiovascular disease, Alzheimer's disease, and metabolic syndrome by influencing their possible common underlying mechanism. The stimulation of the vagus nerve (VNS) could be a helpful tool fighting to re-establish healthy homeostasis. There is growing evidence that vagus activity slows tumorigenesis, primarily by inhibiting inflammation. Recent studies have shown that neuroimmune modulation increases cytotoxic immunity in the tumor microenvironment. Thus, we appear to modulate the tumor microenvironment and antitumor immunity by influencing vagus nerve activity [58]. It is thought that vagus stimulation, in addition to conventional therapeutic methods, may improve tumor prognosis by aiding in antitumor immunity [58]. The vagus activity and the changes by VNS are well measurable by HRV, and vica versa, the changes of HRV could modify the vagal processes.

Based on the interconnection, measuring vagus activity (primarily by HRV determination) can be a huge help to choose therapies in many diseases. The method has multiple benefits from this safe, complex therapeutic option that improves prognosis in various diseases. It is easy to apply and can be used in conjunction with other routine treatments. It can also be suitable for screening and prevention; it is inexpensive, non-invasive [171]. The HRV controlled VNS is a new direction of the physiologic and psychologic applications [172].

The healthy HRV spectrum shows 1/f on average. The averaging is a standard method for investigating diseases, like the evidence-based medicine averages by its various parameters determining the general probability of the studied phenomena. The 1/f spectrum is satisfactory for the VNS and HRV, but for personalization, we need differentiation, which means obtaining personal information about the systemic control. However, the frequency distribution shows only which frequencies produce the noise, but no idea about its sequences in time. We had shown the method to analyze the real-time sequences as a basis of personal treatment and follow-up.

The average 1/f frequency spectrum is a valuable tool to force the homeostatic arrangement. In therapy, this forcing can be safely and non-invasively administered by modulating a well-chosen radiofrequency carrier and using it to improve the patient's status. The improvement may be measured with conventional checks, but also, the HRV analysis gives information about the achievements of the modulated therapy.

Acknowledgements
This work was supported by the Hungarian National Research Development and Innovation Office PIACI KFI grant: 2019-1.1.1-PIACI-KFI-2019-00011.

Conflicts of Interest
The author declares no conflicts of interest regarding the publication of this paper.

References

[1] Dvorak, H.F. (2015) Tumors: Wounds That Do Not Heal—Redux. Cancer Immunology Research , 3, 1-11. https://doi.org/10.1158/2326-6066.CIR-14-0209

[2] Trigos, A.S., Pearson, R.B., Papenfuss, A.T., et al. (2016) Altered Interactions between Unicellular and Multicellular Genes Drive Hallmarks of Transformation in a Diverse Range of Solid Tumors. PNAS, 114, 6406-6411. https://doi.org/10.1073/pnas.1617743114

[3] Davidson, C.D., Wang, W.Y., Zaimi, I., et al. (2019) Cell Force-Mediated Matrix Reorganization Underlies Multicellular Network Assembly. Scientific Reports , 9, Article No. 12. https://doi.org/10.1038/s41598-018-37044-1

[4] Balmain, A., Gray, J. and Ponder, B. (2014) The Genetics and Genomics of Cancer. Nature Genetics , 33, 238-244. https://doi.org/10.1038/ng1107

[5] Szigeti, G.P., Szasz, O. and Hegyi, G. (2017) Connections between Warburg's and Szentgyorgyi's Approach about the Causes of Cancer. Journal of Neoplasm, 1, 1-13.

[6] Hanahan, D. and Weinberg, R.A. (2000) The Hallmarks of Cancer. Cell , 100, 57-70. https://doi.org/10.1016/S0092-8674(00)81683-9

[7] Hanahan, D. and Weinberg, R.A. (2011) Hallmarks of Cancer: The Next Generation. Cell , 144, 646-674. https://doi.org/10.1016/j.cell.2011.02.013

[8] Dyas, F.G. (1928) Chronic Irritation as a Cause of Cancer. JAMA, 90, 457. https://doi.org/10.1001/jama.1928.92690330003008c

[9] Dvorak, H.F. (1986) Tumors: Wounds That Do Not Heal, Similarities between Tumor Stroma Generation and Wound Healing. The New England Journal of Medicine , 315, 1650-1659. https://doi.org/10.1056/NEJM198612253152606

[10] Platz, E.A. and De, Marzo, A.M. (2004) Epidemiology of Inflammation and Prostate Cancer. The Journal of Urology , 171, S36-S40. https://doi.org/10.1097/01.ju.0000108131.43160.77

[11] Punyiczki, M. and Fesus, L. (1998) Heat Shock and Apoptosis: The Two Defense Systems of the Organisms May Have Overlapping Molecular Elements. Annals of the New York Academy of Sciences , 951, 67-74. https://doi.org/10.1111/j.1749-6632.1998.tb08978.x

[12] Aktipis, C.A., Bobby, A.M., Jansen, G., et al. (2015) Cancer across the Tree of Life: Cooperation and Cheating in Multicellularity. Philosophical Transactions of the Royal Society B , 370, Article ID: 20140219. https://doi.org/10.1098/rstb.2014.0219

[13] Szasz, A. (2020) Preface. In: Szasz, A., Ed., Challenges and Solutions of Oncological Hyperthermia , Cambridge Scholars Publishing, Newcastle upon Tyne, 8-13. https://www.cambridgescholars.com/challenges-and-solutions-of-oncological-hyperthermia

[14] Szasz, A. (2021) Time-Fractal Modulation—Possible Modulation Effects in Human Therapy. Open Journal of Biophysics , 12, 38-87. https://doi.org/10.4236/ojbiphy.2022.121003

[15] Conley, B. (2019) Microbial Extracellular Electron Transfer Is a Far-Out Metabolism. The American Society for Microbiology, Washington DC. https://asm.org/Articles/2019/November/Microbial-Extracellular-Electron-Transfer-is-a-Far

[16] Szasz, A., van Noort, D., Scheller, A., et al . (1994) Water States in Living Systems. I. Structural Aspects. Physiological Chemistry and Physics , 26, 299-322.

[17] Agmon, N. (1995) The Grotthuss Mechanism. Chemical Physics Letters, 244, 456-462. https://doi.org/10.1016/0009-2614(95)00905-J

[18] Markovitch, O. and Agmon, N. (2007) Structure and Energetics of the Hydronium Hydration Shells. The Journal of Physical Chemistry A , 111, 2253-2256. https://doi.org/10.1021/jp068960g

[19] Tuckerman, M.E., Laasonen, K., Sprik, M., et al. (1995) Ab Initio Molecular Dynamics Simulation of the Solvation and Transport of Hydronium and Hydroxyl Ions in Water. The Journal of Chemical Physics , 103, 150-161. https://doi.org/10.1063/1.469654

[20] Tuckerman, M.E., Laasonen, K., Sprik, M. and Parrinello, M. (1995) Ab Initio Molecular Dynamics Simulation of the Solvation and Transport of H3O+ and OH− Ions in Water. The Journal of Physical Chemistry , 99, 5749-5752. https://doi.org/10.1021/j100016a003

[21] Marx, D., Tuckerman, M.E., Hutter, J., et al. (1999) The Nature of the Hydrated Excess Proton in Water. Nature , 397, 601-604. https://doi.org/10.1038/17579

22] Csermely, P. (2009) Weak Links: A Universal Key of Network Diversity and Stability. Springer, Berlin. https://doi.org/10.1007/978-3-540-31157-7_3

[23] Szendro, P., Vincze, G. and Szasz, A. (2001) Pink-Noise Behaviour of Biosystems. European Biophysics Journal , 30, 227-231. https://doi.org/10.1007/s002490100143

[24] Lakhtakia, A. (1995) Physical Fractals: Self-Similarity and Square-Integrability. Speculation in Science and Technology, 18, 153-156.

[25] Zbilut, J.P. and Marwan, N. (2008) The Wiener-Khinchin Theorem and Recurrence Quantification. Physics Letters A, 372, 6622-6626. https://doi.org/10.1016/j.physleta.2008.09.027

[26] Lin, Y.K. (1967) Probabilistic Theory of Structural Dynamics. McGraw-Hill, New York.

[27] Aselli, G.B., Porta, A., Montano, N., Gnecchi-Ruscone, T., Lombardi, F. and Cerutti, S. (1992) Linear and Non-Linear Effects in the Beat-by-Beat Variability of Sympathetic Discharge in Decerebrate Cats. 14th Annual International Conference of the IEEE Engineering in Medicine and Biology Society , Vol. 7, 482-483. https://doi.org/10.1109/IEMBS.1992.5761070

[28] Strimbu, K. and Tavel, J.A. (2010) What Are Biomarkers? Current Opinion in HIV and AIDS, 5, 463-466. https://doi.org/10.1097/COH.0b013e32833ed177

[29] Dash, P.K., Zhao, J., Hergenroeder, G. and Noore, A.N. (2010) Biomarkers for the Diagnosis, Prognosis, and Evaluation of Treatment Efficacy for Traumatic Brain Injury. Neurotherapeutics , 7, 100-114. https://doi.org/10.1016/j.nurt.2009.10.019

[30] Henry, N.L. and Hayes, D.F. (2012) Cancer Biomarkers. Molecular Oncology , 6, 140-146. https://doi.org/10.1016/j.molonc.2012.01.010

[31] Byrnes, S.A. and Weigl, B.H. (2018) Selecting Analytical Biomarkers for Diagnostic Applications: A First Principles Approach. Expert Review of Molecular Diagnostics , 18, 19-26. https://doi.org/10.1080/14737159.2018.1412258

[32] Boessen, R., Heerspink, H.J.L., De Zeeuw, D.D., Grobbee, D.E., Groenwold, R.H.H. and Roes, K. (2014) Improving Clinical Trial Efficiency by Biomarker-Guided Patient Selection. Trials , 15, 103. http://www.trialsjournal.com/content/15/1/103 https://doi.org/10.1186/1745-6215-15-103

[33] Ru, Y., Dancik, G.M. and Theodorescu, D. (2011) Biomarkers for Prognosis and Treatment Selection in Advanced Bladder Cancer Patients. Current Opinion in Urology , 21, 420-427. https://doi.org/10.1097/MOU.0b013e32834956d6

[34] Sindo, Y., Hazama, S., Suzuki, N., Iguchi, H., Uesugi, K., et al. (2017) Predictive Biomarkers for the Efficacy of Peptide Vaccine Treatment: Based on the Results of a Phase II Study on Advanced Pancreatic Cancer. Journal of Experimental and Clinical Cancer Research, 36, 36. https://doi.org/10.1186/s13046-017-0509-1

[35] Luckett, T., King, M.T., Butow, P.N., Oguchi, M., et al. (2011) Choosing between the EORTC QLQ-C30 and FACT-G for Measuring Health-Related Quality of Life in Cancer Clinical Research: Issues, Evidence and Recommendations. Annals of Oncology, 22, 2179-2190. https://doi.org/10.1093/annonc/mdq721

[36] Evelyne (2018) Heart Rate Variability as a Prognostic Factor for Cancer Survival—A Systematic Review. Frontiers in Physiology , 9, Article No. 623. https://doi.org/10.3389/fphys.2018.00623

[37] Lee, S.Y., Fiorentini, G., Szasz, A.M., Szigeti, Gy., Szasz, A. and Minnaar, C.A. (2020) Quo Vadis Oncological Hyperthermia (2020)? Frontiers in Oncology, 10, Article No. 1690. https://doi.org/10.3389/fonc.2020.01690

[38] Lu, Y.M., et al . (2013) Deep Regional Hyperthermia Combined with Traditional Chinese Medicine in Treating Benign Diseases in Clifford Hospital. Oncothermia Journal , 7, 157-165.

[39] Casadei, V., Sarti, D., Milandri, C., Dentico, P., Guadagni, S. and Fiorentini, C. (2020) Comparing the Effectiveness of Pain Therapy (PT) and Modulated Electro-Hyperthermia (mEHT) versus Pain Therapy Alone in Treating Patients with Painful Bony Metastases: An Observational Trial. In: Szasz, A., Ed., Challenges and

Solutions of Oncological Hyperthermia , Cambridge Scholars, Washington DC, Ch. 15, 337-345.

[40] Hegyi, G., Molnar, I., Mate, A. and Petrovics, G. (2017) Targeted Radiofrequency Treatment—Oncothermia Application in Non-Oncological Diseases as Special Physiotherapy to Delay the Progressive Development. Clinics and Practice , 14, 73-77. https://doi.org/10.4172/clinical-practice.100098

[41] Zais, O. (2013) Lyme Disease and Oncothermia. Conference Papers in Medicine , 2013, Article ID: 275013. https://doi.org/10.1155/2013/275013

[42] Theodor, W.H. (2003) Transcranial Magnetic Stimulation in Epilepsy. Epylepsy Currents , 3, 191-197. https://doi.org/10.1046/j.1535-7597.2003.03607.x

[43] Nussbaum, E.L., Houghton, P., Anthony, J., Rennie, S., et al. (2017) Neuromuscular Electrical Stimulation for Treatment of Muscle Impairment: Critical Review and Recommendations for Clinical Practice. Physiotherapy Canada , 69, 1-76. https://doi.org/10.3138/ptc.2015-88

[44] Liu, A., Voroslakos, M., Kronberg, G., Henin, S., et al. (2018) Immediate Neurophysiological Effects of Transcranial Electrical Stimulation. Nature Communications , 9, Article No. 2092. https://doi.org/10.1038/s41467-018-07233-7

[45] Gershon, A.A., Dannon, P.N. and Grunhaus, L. (2003) Transcranial Magnetic Stimulation in the Treatment of Depression. American Journal of Psychiatry, 160, 835-845. http://ajp.psychiatryonline.org https://doi.org/10.1176/appi.ajp.160.5.835

[46] Zygmunt, A. and Stanczyk, J. (2010) Methods of Evaluation of Autonomic Nervous System. Archives of Medical Science , 6, 11-18. https://doi.org/10.5114/aoms.2010.13500

[47] Andersson, U. and Tracy, K.J. (2012) Neural Reflexes in Inflammation and Immunity. Journal of Experimental Medicine , 209, 1057-1068. https://doi.org/10.1084/jem.20120571

[48] Berthoud, H.R. and Neuhuber, W.L. (2000) Functional and Chemical Anatomy of the Afferent Vagal System. Autonomic Neuroscience , 85, 1-17. https://doi.org/10.1016/S1566-0702(00)00215-0

[49] Howland, R.H. (2014) Vagus Nerve Stimulation. Current Behavioral Neuroscience Reports , 1, 64-73. https://doi.org/10.1007/s40473-014-0010-5

[50] Yap, J.Y.Y., Keatch, C., Lambert, E., Woods, W., et al. (2020) Critical Review of Transcutaneous Vagus Nerve Stimulation: Challenges for Translation to Clinical Practice. Frontiers in Neuroscience , 14, Article No. 284. https://doi.org/10.3389/fnins.2020.00284

[51] Koopman, F.A., Chavan, S.S., Miljko, S., Grazio, S., et al. (2016) Vagus Nerve Stimulation Inhibits Cytokine Production and Attenuates Disease Severity in Rheumatoid Arthritis. PNAS, 113, 8284-8289. https://doi.org/10.1073/pnas.1605635113

[52] Guo, Y., Koshy, S., Hui, D., Palmer, J.L., Shin, K., Bozkurt, M. and Yusuf, S.W. (2015) Prognostic Value of Heart Rate Variability in Patients with Cancer. Journal of Clinical Neurophysiology , 32, 516-520. https://doi.org/10.1097/WNP.0000000000000210

[53] Teff, K.L. (2008) Visceral Nerves: Vagal and Sympathetic Innervation. Journal of Parenteral and Enteral Nutrition, 32, 569-571. https://doi.org/10.1177/0148607108321705

[54] Mancino, M., Ametler, E., Gascon, P. and Almendro, V. (2011) The Neuronal Influence on Tumor Progression. Biochimica et Biophysica Acta (BBA)—Reviews on Cancer, 1816, 105-118. https://doi.org/10.1016/j.bbcan.2011.04.005

[55] Wang, L., Xu, J., Xiai, Y., Yin, K., Li, Z., Li, B., Wand, W., Xu, H., Yang, L. and Xu,Z. (2018) Muscarinic Acetylcholine Receptor 3 Mediates Vagus Nerve-Induced Gastric Cancer. Oncogenesis , 7, 88. https://doi.org/10.1038/s41389-018-0099-6

[56] Faulkner, S., Jobling, P., March, B. and Jiang, C.C. (2019) Tumor Neurobiology and the War of Nerves in Cancer. Cancer Discovery , 9, 702-710. https://doi.org/10.1158/2159-8290.CD-18-1398

[57] Gidron, Y., Perry, H. and Glennie, M. (2005) Does the Vagus Nerve Inform the Brain about Pre-Clinical Tumours and Modulate Them? The Lancet Oncology , 6, 245-248. https://doi.org/10.1016/S1470-2045(05)70096-6

[58] Reijmen, E., Vannucci, L., De, Couck, M., De, Greve, J. and Gidron, Y. (2018) Therapeutic Potential of the Vagus Nerve in Cancer. Immunology Letters , 202, 38-43. https://doi.org/10.1016/j.imlet.2018.07.006

[59] De, Visser, K.E. and Coussens, L.M. (2006) The Inflammatory Tumor Microenvironment and Its Impact on Cancer Development. Contributions to Microbiology, 13, 118-137. https://doi.org/10.1159/000092969

[60] Pages, F., Galon, J., Dieu, Nosjean, M.C., Tartour, E., Sautes, Fridman, C. and Fridman, W.H. (2010) Immune Infiltration in Human Tumors: A Prognostic Factor That Should Not Be Ignored. Oncogene , 29, 1093-1102. https://doi.org/10.1038/onc.2009.416

[61] Qian, B.Z. and Pollard, J.W. (2010) Macrophage Diversity Enhances Tumor Progression and Metastasis. Cell , 141, 39-51. https://doi.org/10.1016/j.cell.2010.03.014

[62] Gidron, Y., De Couck, M., Schallier, D., De Greve, J., Van Laethem, J.L. and Marechal, R. (2018) The Relationship between a New Biomarker of Vagal Neuroimmunomodulation and Survival in Two Fatal Cancers. Journal of Immunology Research, 2018, Article ID: 4874193. https://doi.org/10.1155/2018/4874193

[63] De Couck, M. and Caers, R. (2018) Why We Should Stimulate the Vagus Nerve in Cancer. Clinical Oncology, 3, 1515. https://doi.org/10.1155/2018/1236787

[64] Balasubramanian, K., Harikumar, K., Nagaraj, N. and Pati, S. (2017) Vagus Nerve Stimulation Modulated Complexity of Heart Rate Variability Differently during Sleep and Wakefulness. Annals of Indian Academy of Neurology , 20, 403-407. https://doi.org/10.4103/aian.AIAN_148_17

[65] Goldberger, A.L. and West, B.J. (1987) Chaos in Physiology: Hearth or Disease? In: Degn, H., et al. , Eds., Chaos in Biological Systems , Springer Science + Business Media, New York, 1-4. https://doi.org/10.1007/978-1-4757-9631-5_1

[66] Mandell, A.J., Knapp, S., Ehlers, C.L. and Russo, P.V. (1983) The Stability of Constrained Randomness: Lithium Prophylaxis at Several Neurobiological Levels. In: Post, R.M. and Ballenger, J.C., Eds., Neurobiology of the Mood Disorders , Williams & Wilkins, Baltimore, 744-776.

[67] Kobayashi, M. and Musha, T. (1982) 1/f Fluctuation of Heartbeat Period. IEEE Transactions on Biomedical Engineering , 29, 456-457. https://doi.org/10.1109/TBME.1982.324972

[68] Trimmel, K., Sacha, J. and Huikuri, H.V. (2015) Heart Rate Variability: Clinical Applications and Interaction between HRV and Heart Rate. Frontiers Media, Lausanne. https://doi.org/10.3389/978-2-88919-652-4

[69] Kleiger, R.E., Stein, D.S. and Bigger, M.D. (2005) Heart Rate Variability: Measurement and Clinical Utility. Annals of Noninvasive Electrocardiology , 10, 88-101. https://doi.org/10.1111/j.1542-474X.2005.10101.x

[70] Malik, M. (1996) Heart Rate Variability. Standards of Measurement, Physiological Interpretation, and Clinical Use. Task Force of the European Society of Cardiology and the North American Society of Pacing and Electrophysiology. European Heart Journal, 17, 354-381. https://doi.org/10.1093/oxfordjournals.eurheartj.a014868

[71] Benichous, T., Pereira, B., Mermillod, M., Tauveron, I., et al. (2018) Heart Rate Variability in Type 2 Diabetes Mellitus: A Systematic Review and Meta-Analysis. PLoS ONE, 13, e0195166. https://doi.org/10.1371/journal.pone.0195166

[72] Chou, Y.H., Huang, W.L., Chang, C.H., Yang, C.C.H., Kuo, T.B.J., et al. (2019) Heart Rate Variability as a Predictor of Rapid Renal Function Deterioration in Chronic Kidney Disease Patients. Nephrology (Carlton), 24, 806-813. https://doi.org/10.1111/nep.13514

[73] Da, Silva, V.P., Oliveira, B.R.R., Mello, R.G.T., Moraes, H., et al. (2018) Heart Rate Variability Indexes in Dementia: A Systematic Review with a Quantitative Analysis. Current Alzheimer Research, 15, 80-88. https://doi.org/10.2174/1567205014666170531082352

[74] Jung, W., Jang, K.I. and Lee, S.H. (2018) Heart and Brain Interaction of Psychiatric Illness: A Review Focused on Heart Rate Variability, Cognitive Function, and Quantitative Electrocephalography. Clinical Psychopharmacology and Neuroscience , 17, 459-474. https://doi.org/10.9758/cpn.2019.17.4.459

[75] Sajjadieh, A., Shahsavari, A., Safaei, A., Penzel, T., Schoebel, C., et al. (2020) The Association of Sleep Duration and Quality with Heart Rate Variability and Blood Pressure. Tanaffos , 19, 135-143.

[76] Kopp, W.J., Synowski, S.J., Newel, M.E., Schmidt, L.A., et al. (2011) Autonomic Nervous System Reactivity to Positive and Negative Mood Induction: The Role of Acute Psychological Responses and Frontal Electrocortical Activity. Biological Psychology, 86, 230-238. https://doi.org/10.1016/j.biopsycho.2010.12.003

[77] Sarlis, N.V., Skordas, E.S. and Varotsos, P.A. (2009) Heart Rate Variability in Natural Time and 1/f "Noise" . EPL, 87, 18003. https://doi.org/10.1209/0295-5075/87/18003

[78] De Couck, M. and Gidron, Y. (2013) Norms of Vagal Nerve Activity, Indexed by Heart Rate Variability in Cancer Patients. Cancer Epidemiology , 37, 737-741. https://doi.org/10.1016/j.canep.2013.04.016

[79] Arab, C., Dias, D.P.M., Barbosa, R.T., de Almeida, de Carvalho, T.D., et al. (2016) Heart Rate Variability Measure in Breast Cancer Patients and Survivors: A Systematic Review. Psychoneuroendocrinology, 68, 57-68. https://doi.org/10.1016/j.psyneuen.2016.02.018

[80] Lombardi, F., Montano, N., Finocchiaro, M.L., Gnecchi, Ruscone, T., Baselli, G., Cerutti, S. and Malliani, A. (1990) Spectral Analysis of Sympathetic Discharge in Decerebrate Cats. Journal of the Autonomic Nervous System, 30, S97-S99. https://doi.org/10.1016/0165-1838(90)90109-V

[81] Task Force of the European Society of Cardiology the North American Society of Pacing Electrophysiology (1996) Heart Rate Variability: Standards of Measurement, Physiological Interpretation, and Clinical Use. Circulation, 93, 1043-1065.

[82] Tulppo, M.P., Makikallio, T.H., Takala, T.E.S., Seppanen, T. and Huikuri, H.V. (1996) Quantitative Beat-to-Beat Analysis of Heart Rate Dynamics during Exercise. American Journal of Physiology, 271, H244-H252. https://doi.org/10.1152/ajpheart.1996.271.1.H244

[83] Acharya, R.U., Sing, O.W., Ping, L.Y. and Chua, T.L. (2004) Heart Rate Analysis in Normal Subjects of Various Age Groups. BioMedical Engineering OnLine , 3, 24. https://doi.org/10.1186/1475-925X-3-24

[84] Kamen, P.W., Krum, H. and Tonkin, A.M. (1996) Poincare Plot of Heart Rate Variability Allows Quantitative Display of Parasympathetic Nervous Activity. Clinical Science, 91, 201-208. https://doi.org/10.1042/cs0910201

[85] Roth, Y. (2018) Homeostasis Processes Expressed as Flashes in a Poincaré Sections. Journal of Modern Physics , 9, 2135-2140. https://doi.org/10.4236/jmp.2018.912134

[86] Woo, M.A., Stevenson, W.G., Moser, D.K., Trelease, R.B. and Harper, R.H. (1992) Patterns of Beat-to-Beat Heart Rate Variability in Advanced Heart Failure. American Heart Journal , 123, 704-707. https://doi.org/10.1016/0002-8703(92)90510-3

[87] Brennan, M., Palaniswami, M. and Kamen, P. (2001) Do Existing Measures of Poincare Plot Geometry Reflect Nonlinear Features of Heart Rate Variability? IEEE Transactions on Biomedical Engineering , 48, 1342-1347. https://doi.org/10.1109/10.959330

[88] Thu, T.N.P., Hernandez, A.I., Costet, N., Patural, H., Pichot, V., et al. (2019) Improving Methodology in Heart Rate Variability Analysis for the Premature Infants: Impact of the Time Length. PLoS ONE, 14, e0220692. https://doi.org/10.1371/journal.pone.0220692

[89] Peng, C.K., Havlin, S., Stanley, H.E. and Goldberger, A.L. (1995) Quantification of Scaling Exponents and Crossover Phenomena in Nonstationary Heartbeat Time Series. Chaos , 5, 82-87. https://doi.org/10.1063/1.166141

[90] Goldberger, A.L., Amaral, L.A.N., Hausdorff, J.M., Ivanov, P.C., Peng, C.K. and Stanley, H.E. (2002) Fractal Dynamics in Physiology: Alterations with Disease and Aging. PNAS, 99, 2466-2472. https://doi.org/10.1073/pnas.012579499

[91] Ho, K.K.L., Moody, G.B., Peng, C.K., et al. (1997) Predicting Survival in Heart Failure Case and Control Subjects by Use of Fully Automated Methods for Deriving Nonlinear and Conventional Indices of Heart Rate Dynamis. Circulation, 96, 842-848. https://doi.org/10.1161/01.CIR.96.3.842

[92] Goldberger, A.L., Bhargava, V., West, B. and Mandell, A.J. (1985) Some Observations on the Question: Is Ventricular Fibrillation "Chaos"? Physica D, 19, 282-289. https://doi.org/10.1016/0167-2789(86)90024-2

[93] Goldberger, A.L., Bhargava, V. and West, B.J. (1985) Nonlinear Dynamics of Heartbeat, II. Subharmonic Bifurcations of the Cardiac Interbeat Interval in Sinus Node Disease. Physica D, 17, 207-214. https://doi.org/10.1016/0167-2789(85)90005-3

[94] Goldberger, A.L. and West, B.J. (1987) Applications of Nonlinear Dynamics to Clinical Cardiology. Annals of the New York Academy of Sciences , 504, 195-213. https://doi.org/10.1111/j.1749-6632.1987.tb48733.x

[95] Goldberger, A.L. (2006) Complex Systems. Proceedings of the American Thoracic Society , 3, 467-472. https://doi.org/10.1513/pats.200603-028MS

[96] Turner, J.D. (1988) Frequency Domain Analysis. In: Instrumentation for Engineers, Palgrave, London, Ch. 7, 159-179. https://doi.org/10.1007/978-1-4684-6300-2_7

[97] Li, K., Rudiger, H. and Ziemssen, T. (2019) Spectral Analysis of Heart Rate Variability: Time Window Matters. Frontiers in Neurology , 10, Article No. 545. https://doi.org/10.3389/fneur.2019.00545

[98] Shaffer, F. and Ginsberg, J.P. (2017) An Overview of Heart Rate Variability Metrics and Norms. Frontiers in Public Health, 5, Article No. 258. https://doi.org/10.3389/fpubh.2017.00258

[99] Owens, A.P. (2020) The Role of Heart Rate Variability in the Future of Remote Digital Diomarkers. Frontiers in Neuroscience , 14, Article ID: 582145. https://doi.org/10.3389/fnins.2020.582145

[100] Fossion, R., Rivera, A.L. and Estanol, B. (2018) A Physicist's View of Homeostasis: How Time Series of Continuous Monitoring Reflect the Function of Physiological Variabilities in Regulatory Mechanisms. Physiological Measurement , 39, Article ID: 084007. https://doi.org/10.1088/1361-6579/aad8db

[101] Riganello, F., Garbarino, S. and Sannita, W.G. (2012) Heart Rate Variability, Homeostasis, and Brain Function: A Tutorial and Review of Application. Journal of Psychophysiology , 26, 178-203. https://doi.org/10.1027/0269-8803/a000080

[102] De Couck, M., Caers, R., Spiegel, D. and Gidron, Y. (2018) The Role of the Vagus Nerve in Cancer Prognosis: A Systematic and a Comprehensive Review. Journal of Oncology, 2018, Article ID: 1236787. https://doi.org/10.1155/2018/1236787

[103] Cooper, T.M., McKinley, P.S., Seeman, T.E., Choo, T.H., Lee, S. and Sloan, R.P. (2015) Heart Rate Variability Predicts Levels of Inflammatory Markers: Evidence for the Vagal Anti-Inflammatory Pathway. Brain, Behavior, and Immunity, 49, 94-100. https://doi.org/10.1016/j.bbi.2014.12.017

[104] Ohira, H., Matsunaga, M., Osumi, T., Fukuyama, S., Shinoda, J., Yamada, J. and Gidron, Y. (2013) Vagal Nerve Activity as a Moderator of Brain-Immune Relationships. Journal of Neuroimmunology , 260, 28-36. https://doi.org/10.1016/j.jneuroim.2013.04.011

[105] Young, H.A. and Benton, D. (2018) Heart-Rate Variabiity: A Biomarker to Study the Influence of Nutrition on Physiological and Psychological Health? Behavioural Pharmacology, 29, 140-151. https://doi.org/10.1097/FBP.0000000000000383

[106] Hayano, J. and Yuda, E. (2019) Pitfalls of Assessment of Autonomic Function by Heart Rate Variability. Journal of Physiological Anthropology, 38, Article No. 3. https://doi.org/10.1186/s40101-019-0193-2

[107] Quintana, D.S. and Heathers, A.J. (2014) Considerations in the Assessment of Heart Rate Variability in Biobehavioral Research. Frontiers in Psychology , 5, Article No. 805. https://doi.org/10.3389/fpsyg.2014.00805

[108] Szasz, A. and Szasz, O. (2020) Time-Fractal Modulation of Modulated Electro-Hyperthermia (mEHT). In: Szasz, A., Ed., Challenges and Solutions of Oncological Hyperthermia , Cambridge Scholars, Washington DC, Ch. 17, 377-415.

[109] Szasz, A.M., Minnaar, C.A., Szentmartoni, Gy., et al . (2019) Review of the Clinical Evidences of Modulated Electro-Hyperthermia (mEHT) Method: An Update for the Practicing Oncologist. Frontiers in Oncology , 9, Article No. 1012. https://doi.org/10.3389/fonc.2019.01012

[110] Szasz, O. (2020) Local Treatment with Systemic Effect: Abscopal Outcome. In: Szasz, A., Ed., Challenges and Solutions of Oncological Hyperthermia , Cambridge Scholars, Washington DC, Ch. 11, 192-205.

[111] Minnaar, C.A., Kotzen, J.A., Ayeni, O.A., et al . (2020) Potentiation of the Abscopal Effect by Modulated Electro-Hyperthermia in Locally Advanced Cervical Cancer Patients. Frontiers in Oncology, 10, Article No. 376. https://doi.org/10.3389/fonc.2020.00376

[112] Andocs, G., Szasz, O. and Szasz, A. (2009) Oncothermia Treatment of Cancer: From the Laboratory to Clinic. Electromagnetic Biology and Medicine , 28, 148-165. https://doi.org/10.1080/15368370902724633

[113] Yang, K.L., Huang, C.C., Chi, M.S., Chiang, H.C., Wang, Y.S. andocs, G., et al. (2016) In Vitro Comparison of Conventional Hyperthermia and Modulated Electro-Hyperthermia. Oncotarget, 7, 84082-84092. https://doi.org/10.18632/oncotarget.11444

[114] Wust, P., Ghadjar, P., Nadobny, J., et al. (2019) Physical Analysis of Temperature-Dependent Effects of Amplitude-Modulated Electromagnetic Hyperthermia. International Journal of Hypertension, 36, 1246-1254. https://doi.org/10.1080/02656736.2019.1692376

[115] Wust, P., Kortum, B., Strauss, U., Nadobny, J., Zschaeck, S., Beck, M., et al. (2020) Non-Thermal Effects of Radiofrequency Electromagnetic Fields. Scientific Reports , 10, Article No. 13488. https://doi.org/10.1038/s41598-020-69561-3

[116] Wust, P., Nadobny, J., Zschaeck, S. and Ghadjar, P. (2020) Physics of Hyperthermia—Is Physics Really against Us? In: Szasz, A., Ed., Challenges and Solutions of Oncological Hyperthermia , Cambridge Scholars, Washington DC, Ch. 16, 346-376.

[117] Chang, R.B. (2019) Body Thermal Responses and the Vagus Nerve. Neuroscience Letters , 698, 209-216. https://doi.org/10.1016/j.neulet.2019.01.013

[118] Andocs, G., Rehman, M.U., Zhao, Q.L., Tabuchi, Y., Kanamori, M. and Kondo, T. (2016) Comparison of Biological Effects of Modulated Electro-Hyperthermia and Conventional Heat Treatment in Human Lymphoma U937 Cell. Cell Death Discovery , 2, 16039. https://doi.org/10.1038/cddiscovery.2016.39

[119] Andocs, G., Rehman, M.U., Zhao, Q.L., Papp, E., Kondo, T. and Szasz, A. (2015) Nanoheating without Artificial Nanoparticles Part II. Experimental Support of the Nanoheating Concept of the Modulated Electro-Hyperthermia Method, Using U937 Cell Suspension Model. Biology and Medicine , 7, 1-9. https://doi.org/10.4172/0974-8369.1000247

[120] Szasz, A. (2019) Thermal and Nonthermal Effects of Radiofrequency on Living State and Applications as an Adjuvant with Radiation Therapy. Journal of Radiation and Cancer Research, 10, 1-17. https://doi.org/10.4103/jrcr.jrcr_25_18

[121] Danics, L., Schvarcz, Cs., Viana, P., et al. (2020) Exhaustion of Protective Heat Shock Response Induces Significant Tumor Damage by Apoptosis after Modulated Electro-Hyperthermia Treatment of Triple Negative Breast Cancer Isografts in Mice. Cancers , 12, 2581. https://doi.org/10.3390/cancers12092581

[122] Forika, G., Balogh, A., Vancsik, T., Zalatnai, A., et al. (2020) Modulated Electro-Hyperthermia Resolves Radioresistance of Panc1 Pancreas Adenocarcinoma and Promotes DNA Damage and Apoptosis in Vitro. International Journal of Molecular Sciences , 21, 5100. https://doi.org/10.3390/ijms21145100

[123] Krenacs, T., Meggyeshazi, N., Forika, G., et al. (2020) Modulated Electro-Hyperthermia-Induced Tumor Damage Mechanisms Revealed in Cancer Models. International Journal of Molecular Sciences , 21, 6270. https://doi.org/10.3390/ijms21176270

[124] Scheff, J.D., Griffel, B., Corbett, S.A., Calvano, S.E., et al. (2014) On Heart Rate Variability and Autonomic Activity in Homeostasis and in Systemic Inflammation. Mathematical Biosciences , 252, 36-44. https://doi.org/10.1016/j.mbs.2014.03.010

[125] Goldberger, A.L., Bhargava, V., West, B.J. and Mandell, A.J. (1985) On a Mechanism of Cardiac Electrical Stability, the Fractal Hypothesis. Biophysics Journal , 48, 525-528. https://doi.org/10.1016/S0006-3495(85)83808-X

[126] Kauffman, S.A. and Johnsen, S. (1991) Coevolution to the Edge of Chaos: Coupled Fitness Landscapes, Poised States, and Coevolutionary Avalanches. Journal of Theoretical Biology, 149, 467-505. https://doi.org/10.1016/S0022-5193(05)80094-3

[127] Bak, P., Tang, C. and Wiesenfeld, K. (1988) Self-Organized Criticality. Physical Review A , 38, 364-374. https://doi.org/10.1103/PhysRevA.38.364

[128] Lewin, R. (1992) Complexity, Life at the Edge of Chaos. University of Chicago Press, Chicago.

[129] Ito, K. and Gunji, Y.P. (1994) Self-Organisation of Living Systems towards Criticality at the Edge of Chaos. Biosystems , 33, 17-24. https://doi.org/10.1016/0303-2647(94)90057-4

[130] Prigogine, I. and Stengers, I. (1985) Order out of Chaos. Flamingo, London. https://doi.org/10.1063/1.2813716

[131] Calaprice A. (2000) The Expanded Quotable Einstein. Princeton University Press, Princeton, 456.

[132] Bernardes, A.T. and dos Santos, R.M. (1997) Immune Network at the Edge of Chaos. Journal of Theoretical Biology, 186, 173-187. https://doi.org/10.1006/jtbi.1996.0316

[133] Bertschinger, N. and Natschlager, T. (2004) Real-Time Computation at the Edge of Chaos in Recurrent Neural Networks. Neural Computation, 16, 1413-1436. https://doi.org/10.1162/089976604323057443

[134] Stokic, D., Hanel, R. and Thurner, S. (2008) Inflation of the Edge of Chaos in a Simple Model of Gene Interaction Networks. Physical Review E, 77, Article ID: 061917. https://doi.org/10.1103/PhysRevE.77.061917

[135] Kauffman, S., Hill, C., Hood, L. and Huang, S. (2014) Transforming Medicine: A Manifesto, Scientific American-World View.
https://web.archive.org/web/20140713110927/http://www.saworldview.com/specialreport-cancer/transforming-medicine-a-manifesto

[136] Eke, A., Hermán, P., Bassingthwaighte, J.B., Raymond, G.M., Percival, D.B., Cannon, M., Balla, I. and Ikrényi, C. (2000) Physiological Time Series: Distinguishing Fractal Noises from Motions. Pflügers Archiv—European Journal of Physiology, 439, 403-415. https://doi.org/10.1007/s004249900135

[137] Barunik, J. and Kristoufek, L. (2010) On Hurst Exponent Estimation under Heavy-Tailed Distributions. Physica A: Statistical Mechanics and Its Applications, 389, 3844-3855. https://doi.org/10.1016/j.physa.2010.05.025

[138] Beran, J. (1994) Statistics for Long-Memory Processes. Taylor & Francis, London.

[139] Arneodo, A., Audit, B., Kestener, P. and Roux, S. (2008) Wavelet-Based Multifractal Analysis. Scholarpedia , 3, 4103. https://doi.org/10.4249/scholarpedia.4103

[140] Ivanov, P.Ch., Amaral, L.A.N., Goldberger, A.L., Havlin, S., Rosenblum, M.G., et al. (2001) From 1/f Noise to Multifractal Cascades in Heartbeat Dynamics. Chaos , 11, 641-652. https://doi.org/10.1063/1.1395631

[141] Ivanov, P.Ch., Amaral, L.A.N., Goldberger, A.L., Havlin, S., Rosenblum, M.G., Struzik, Z.R. and Stanley, H.E. (1999) Multifractality in Human Heartbeat Dynamics. Nature , 399, 461-465. https://doi.org/10.1038/20924

[142] Kravitz, R.L., Duan, N. and Braslow, J. (2004) Evidence-Based Medicine, Heterogeneity, and the Trouble with Averages. The Milbank Quarterly , 82, 661-687. https://doi.org/10.1111/j.0887-378X.2004.00327.x

[143] Imai, J. (2021) Regulation of Adaptive Cell Proliferation by Vagal Nerve Signals for Maintenance of Whole-Body Homeostasis: Potential Therapeutic Target for Insulin-Deficient Diabetes. Tohoku Journal of Experimental Medicine , 254, 245-252. https://doi.org/10.1620/tjem.254.245

[144] Matteoli, G. and Boeckxstaens, G.E. (2013) The Vagal Innervation of the Gut and Immune Homeostasis. Gut , 62, 1214-1222. https://doi.org/10.1136/gutjnl-2012-302550

[145] Szigeti, Gy.P., Szasz, O. and Hegyi, G. (2020) Experiment with Personalised Dosing of Hyperthermia. In: Ito, S., Ed., Current Topics in Medicine and Medical Research, Chapter 15, Vol. 3, Book Publisher International, New York, 140-157.

[146] Szasz, A. (2013) Challenges and Solutions in Oncological Hyperthermia. Thermal Medicine , 29, 1-23. https://doi.org/10.3191/thermalmed.29.1

[147] Ferenczy, G.L. and Szasz, A. (2020) Technical Challenges and Proposals in Oncological Hyperthermia. In: Szasz, A., Ed., Challenges and Solutions of Oncological Hyperthermia , Ch. 3, Cambridge Scholars, Cambridge, 72-90.

[148] Szasz, A. (2014) Oncothermia: Complex Therapy by EM and Fractal Physiology. 31th URSI General Assembly and Scientific Symposium (URSI GASS), Beijing, 20 October 2014, 1-4. https://doi.org/10.1109/URSIGASS.2014.6930100

[149] Szasz, A. (2015) Bioelectromagnetic Paradigm of Cancer Treatment Oncothermia. In: Rosch, P.J., Ed., Bioelectromagnetic and Subtle Energy Medicine , CRC Press, Boca Raton, 323-336.

[150] Zhao, H., Raines, L.N. and Huang, S. (2020) Molecular Chaperones: Molecular Assembly Line Brings Metabolism and Immunity in Shape. Metabolites , 10, 394. https://doi.org/10.3390/metabo10100394

[151] Prohaszka, Z. (2007) Chaperones as Part of Immune Networks. In: Csermely, P. and Vigh, L., Eds., Molecular Aspects of the Stress Response : Chaperones , Membranes and Networks , Landes Bioscience and Springer Science + Business Media, Ch. 14, Berlin, 159-166. https://doi.org/10.1007/978-0-387-39975-1_14

[152] Chavan, S.S., Pavlov, V.A. and Tracey, K.J. (2017) Mechanisms and Therapeutic Relevance of Neuro-Immune Communication. Immunity , 46, 927-942. https://doi.org/10.1016/j.immuni.2017.06.008

[153] Kuwabara, S., Goggins, E. and Tanaka, S. (2021) Neuroimmune Circuits Activated by Vagus Nerve Stimulation. Nephron, 1-5. https://doi.org/10.1159/000518176

[154] Parent, R. (2019) The Potential Implication of the Autonomic Nervous System in Hepatocellular Carcinoma. Cellular and Molecular Gastroenterology and Hepatology, 8, 145-148. https://doi.org/10.1016/j.jcmgh.2019.03.002

[155] Szasz, A. (2020) Towards the Immunogenic Hyperthermic Action: Modulated Electro-Hyperthermia, Clinical Oncology and Research. Science Repository , 3, 5-6. https://doi.org/10.31487/j.COR.2020.09.07

[156] Tsang, Y.W., Huang, C.C., Yang, K.L., Chi, M.S., Chiang, H.C., Wang, Y.S., Andocs, G., Szasz, A., Li, W.T. and Chi, K.H. (2015) Improving Immunological Tumor Microenvironment Using Electro-Hyperthermia Followed by Dendritic Cell Immunotherapy. Oncothermia Journal , 15, 55-66. https://doi.org/10.1186/s12885-015-1690-2

[157] Qin, W., Akutsu, Y., Andocs, G., et al . (2014) Modulated Electro-Hyperthermia Enhances Dendritic Cell Therapy through an Abscopal Effect in Mice. Oncology Reports , 32, 2373-2379. https://doi.org/10.3892/or.2014.3500

[158] Van, Gool, S.W., Makalowski, J., Feyen, O., Prix, L., Schirrmacher, V. and Stuecker, W. (2018) The Induction of Immunogenic Cell Death (ICD) during Maintenance Chemotherapy and Subsequent Multimodal Immunotherapy for Glioblastoma (GBM) . Austin Oncology Case Reports , 3, 1-8.

[159] Mantovani, A., Allavena, P., Sica, A. and Balkwill, F. (2008) Cancer-Related Inflammation. Nature , 454, 436-444. https://doi.org/10.1038/nature07205

[160] De Couck, M., Marechal, R., Moorthamers, S., Van, Laethem, J.L. and Gidron, Y. (2016) Vagal Nerve Activity Predicts Overall Survival in Metastatic Pancreatic Cancer, Mediated by Inflammation. Cancer Epidemiology , 40, 47-51. https://doi.org/10.1016/j.canep.2015.11.007

[161] Kim, K., Chae, J. and Lee, S. (2015) The Role of Heart Rate Variability in Advanced Non-Small-Cell Lung Cancer Patients. Journal of Palliative Care , 31, 103-108. https://doi.org/10.1177/082585971503100206

[162] Zhou, X., Ma, Z., Zhan, L., Zhu, S., Wang, J., Wang, B. and Fu, W. (2016) Heart Rate Variability in the Prediction of Survival in Patients with Cancer: A Systematic Review and Meta-Analysis. Journal of Psychosomatic Research, 89, 20-25. https://doi.org/10.1016/j.jpsychores.2016.08.004

[163] Kim, D.H., Kim, J.A., Choi, Y.S., Kim, S.H., Lee, J.Y. and Kim, Y.E. (2010) Heart Rate Variability and Length of Survival in Hospice Cancer Patients. Journal of Korean Medical Science , 25, 1140-1145. https://doi.org/10.3346/jkms.2010.25.8.1140

[164] Kloter, E., Barrueto, K., Klein, S.D., Scholkmann, F. and Wolf, U. (2018) Heart Rate Variability as a Prognostic Factor for Cancer Survival—A Systematic Review. Frontiers in Physiology , 9, Article No. 623. https://doi.org/10.3389/fphys.2018.00623

[165] Hu, S., Lou, J., Zhang, Y. and Chen, P. (2018) Low Heart Rate Variability Relates to the Progression of Gastric Cancer. World Journal of Surgical Oncology, 16, 49. https://doi.org/10.1186/s12957-018-1348-z

[166] Mouton, C., Ronson, A., Racavi, D., Delhaye, F., Kupper, N., Paesmans, M., Moreau, M., Nogaret, J.M., Hendisz, A. and Gidron, Y. (2012) The Relationship between Heart Rate Variability and Time-Course of Carcinoembryonic Antigen in Colorectal Cancer. Autonomic Neuroscience : Basic and Clinical , 166, 96-99. https://doi.org/10.1016/j.autneu.2011.10.002

[167] Chiang, J.K., Moo, M., Kuo, T.B.J. and Fu, C.H. (2010) Association between Cardiovascular Autonomic Functions and Time to Death in Patients with Terminal Hepatocellular Carcinoma. Journal of Pain and Symptom Management , 39, 673-679. https://doi.org/10.1016/j.jpainsymman.2009.09.014

[168] De Couck, M., Van Brummelen, D., Schallier, D., De Greve, J. and Gidron, Y. (2013) The Relationship between Vagal Nerve Activity and Clinical Outcomes in Prostate and Non-Small Cell Lung Cancer Patients. Oncology Reports , 30, 2435-2441. https://doi.org/10.3892/or.2013.2725

[169] Giese-Davis, J., Wilhelm, F.H., Tamagawa, R., Palesh, O., Neri, E., Taylor, C.B., Kraemer, H.C. and Spiegel, D. (2015) Higher Vagal Activity as Related to Survival in Patients with Advanced Breast Cancer: An Analysis of Autonomic Dysregulation. Psychosomatic Medicine, 77, 346-355. https://doi.org/10.1097/PSY.0000000000000167

[170] Wang, Y.M., Wu, H.T., Huang, E.Y., Kou, Y.R. and H, S.S. (2013) Heart Rate Variability Is Associated with Survival in Patients with Brain Metastasis: A Preliminary Report. BioMedResearch International , 2013, Article ID: 503421. https://doi.org/10.1155/2013/503421

[171] De Couck, M., Mravec, B. and Gidron, Y. (2012) You May Need the Vagus Nerve to Understand Pathophysiology and to Treat Diseases. Clinical Science , 122, 323-328. https://doi.org/10.1042/CS20110299

[172] Kaniuysas, E., Kampusch, S., Tittgemeyer, M., Panetsos, F., Gines, R.F., et al. (2019) Currentdirections in the Auricular Vagus Nerve Stimulation I—A Physiological Perspective. Frontiers in Neuroscinece , 13, Article No. 854. https://doi.org/10.3389/fnins.2019.00854

Heterogeneous Heat Absorption Is Complementary to Radiotherapy

Andras Szasz

Biotechnics Department, Szent Istvan University, H-2040 Budaors, Hungary; Szasz.Andras@gek.szie.hu

Cite this article as:
Szasz, A. (2022) Heterogeneous Heat Absorption Is Complementary to Radiotherapy. Cancers 2022, 14, 901..
https://doi.org/10.3390/cancers14040901

Oncothermia Journal 33, May 2023: 70 – 113.
www.oncotherm.com/sites/oncotherm/files/2023-05/SzaszA_Heterogeneous_Heat.pdf

Simple Summary
This review shows the advantages of heterogeneous heating of selected malignant cells in harmonic synergy with radiotherapy. The main clinical achievement of this complementary therapy is its extreme safety and minimal adverse effects. Combining the two methods opens a bright perspective, transforming the local radiotherapy to the antitumoral impact on the whole body, destroying the distant metastases by "teaching" the immune system about the overall danger of malignancy.

Abstract:

(1) Background:
Hyperthermia in oncology conventionally seeks the homogeneous heating of the tumor mass. The expected isothermal condition is the basis of the dose calculation in clinical practice. My objective is to study and apply a heterogenic temperature pattern during the heating process and show how it supports radiotherapy.

(2) Methods:
The targeted tissue's natural electric and thermal heterogeneity is used for the selective heating of the cancer cells. The amplitude-modulated radiofrequency current focuses the energy absorption on the membrane rafts of the malignant cells. The energy partly "nonthermally" excites and partly heats the absorbing protein complexes.

(3) Results:
The excitation of the transmembrane proteins induces an extrinsic caspase-dependent apoptotic pathway, while the heat stress promotes the intrinsic caspase-dependent and independent apoptotic signals generated by mitochondria. The molecular changes synergize the method with radiotherapy and promote the abscopal effect. The mild average temperature (39–41 C) intensifies the blood flow for promoting oxygenation in combination with radiotherapy. The preclinical experiences verify, and the clinical studies validate the method.

(4) Conclusions:
The heterogenic, molecular targeting has similarities with DNA strand-breaking in radiotherapy. The controlled energy absorption allows using a similar energy dose to radiotherapy (J/kg). The two therapies are synergistically combined.

Keywords:
loco-regional hyperthermia; oncology; modulated electro-hyperthermia; cellular selection; bioelectromagnetics; complexity; immune-effects

6. Introduction

Nowadays, oncology is one of the most complex interdisciplinary experimental and clinical research fields. Clinical success often relies on the sensitive balance between cure and toxicity, providing the most effective but at the same time the safest treatment. Hyperthermia (HT) has promised a simple way to solve the frequent dilemma of complementary treatment choice. Despite its promise and a long history with ancient roots, oncological hyperthermia has had a long and bumpy road to modern medicine, and even today, it has no complete acceptance among oncology professionals. The original ancient idea of hyperthermia is relatively simple: heat the tumor, which forces it to use more resources from the host tissue due to accelerated metabolism, but no extra supply is available. The "starving" tumor destroys itself by acidosis. A deep belief in the curative effect of the feverlike processes, which force self-control of the body, drives the medical concept of "Give me the power to produce fever and I will cure all diseases" [1]. Hippocrates successfully applied radiative heat to treat breast cancer [1]. In vitro measurements have proved this idea [2], measuring a significant impoverishment of Adenosine triphosphate (ATP) and lactate enrichment in treated tumors.

The large group of HT methods contains various therapies using various electromagnetic and mechanical (ultrasound) energy sourses. The attention of hyperthermic oncology presently focuses on local-regional heating (LRHT) methods by electromagnetic effects.

There are two basic categories of LRHT heating; Figure 1.

1. External radiation focused on the target, trying to heat the tumor mass as homogeneously as possible without considerably heating surroundings tissues. The heating intention is isothermal, but due to the heterogeneity of the target and the heat distribution dynamics controlled by blood flow, the temperature is not homogeneous (see later). The intensive heating of a larger volume (regional heating) achieves an approximately controllable condition in the tumor at the central position. The treatment evaluation involves the ratio of the isothermal areas. The specific power density (SAR) ranges from 4.6 to 89 W/kg [3], depending on the location and size of the tumor, determining the heated volume and its blood flow.

2. Heating good energy absorbers in a localized area by electromagnetic effects, which heats these materials extensively, and in the next step, the absorbers heat up their host tissues. The heating intention is heterogeneous, targets only the dedicated particles (like nanoparticles, seeds, rods, etc.). The dose homogeneity characterizes this method because of the dispersed absorbers. The particles heat up their environment by heatconduction, realizing more localized heating in the volume. The SAR in nanoparticle methods is surprisingly large because the absorbers have only a tiny mass compared to the surrounding tissue. The small mass (ranging density of 1 mg/cm3 specifically absorbs extralarge SAR >> 1 W/g = 1 kW/kg or higher [4], because of the absorption on the tiny target. When it heats the neighboring tissues, the average SAR corresponds to the isothermal heating conditions in the range of about a few W/kg. Targeting various chemical bonds uses even higher SAR because the absorbing mass is lighter than the metallic nanoparticle. These methods focus on molecular changes. The temperature is a possible cofactor.

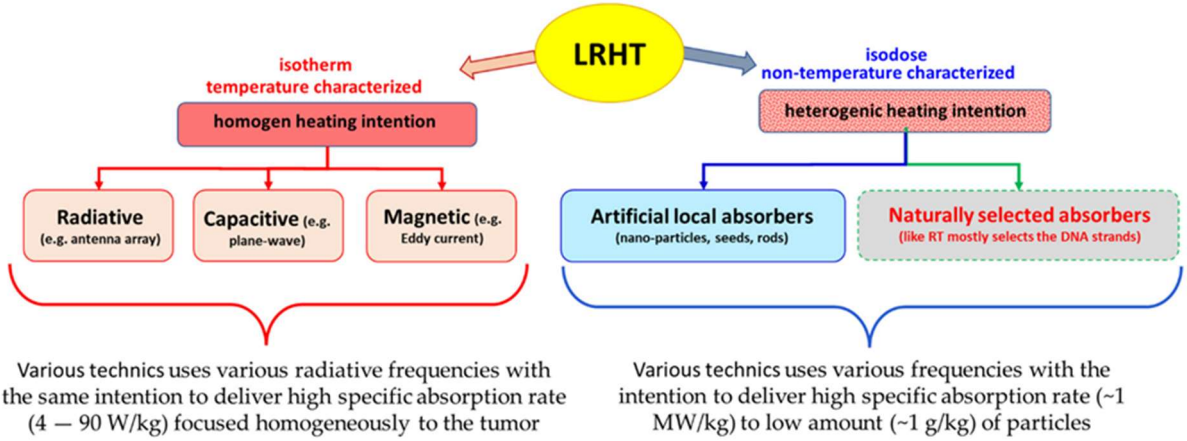

Figure 1. The two essential branches of electromagnetic LRHT methods. The majority of applications use the conventional focusing with isothermal intention. The method requests to measure the temperature as dose characterization. Heterogeneous (non-isothermal) heating is an emerging category of LRHT applications with nanoparticle insertion (mainly magnetic suspension). The heterogenic heating methods do not need direct temperature measurement. The dose measures the absorbed energy (J/kg = Ws/kg), so the tumor's temperature develops by the heat-conduction from the targeted particles. The figure does not show the popular non-electromagnetic LRHT methods (e.g., HIPEC and HiFu).

The success of LRHT is unquestionably conclusive. Results regarding many tumors, including breast [5], head and neck [6], cervix [7], pancreas [8], soft-tissue sarcoma [9], and others [10], provide convincing proof of its place in the field of oncotherapies. In particular, LRHT has had remarkable success, such as in a complementary application with radiation therapy (RT) [11–14], showing a solid synergy [15,16] and being applied successfully in various curative therapies [17–19]. The success of complementary RT + LRHT has a broad spectrum of clinical evidence [20–24], and has been well-reviewed in its details [25–28]. The introduced thermal enhancement ratio (TER) characterizes LRHT's additional gain over RT [29].

Together with the high rate of successes, challenges, of course, also appear. To fulfill our strong motivation to popularize LRHT among oncology professionals, we analyze some of the apparent controversies in LRHT applications, studying these challenges in the search for a solution. The challenges are not limiting but oppositely motivate us to solve the actual difficulties and thereby seize the extreme medical value of hyperthermia in oncology. The challenge guides us to new developments and improvements in the otherwise broad spectrum of hyperthermia facilities in oncology.

6.1. Heating Challenge

The skeptical opinion concerning hyperthermia in oncology was developed in parallel with expectations. A half-century ago, in 1964, a leading German oncosurgeon expressed his doubts [30]: "All of these methods impress the patient very much; they do not impress their cancer at all". His skepticism towards oncological hyperthermia became widespread among medical experts, who eclared hyperthermia to be of no benefit to cancer patients and so did not propose it enter actual therapy protocols. Unfortunately, the method has to fight hard for its well-deserved place among stable routine therapies in oncology. Our task is to show the place of HT as the regular fourth column in the oncology arsenal, together with surgery, chemo, and radiotherapies.

The challenges always concern the complex behavior of living organisms, which balances multiple oppositional regulatory feedbacks. The balance gives a character a "double-edged sword", which determines a window of positive actions. When applied outside this window, the helpful actions act oppositely, the difference between support or degradation being only the dose.

The primary challenge connects hyperthermia to the standard systemic homeostatic thermal control according to the complexity. The body temperature provides fundamental conditions of the proper physiologic and molecular processes, so its stability is essential and ranges in a narrow 7/273 (~2.6%) interval in humans. The homeostatic control regulates the system, keeping it stable and adaptable. Heating locally or systemically attacks the regulatory stability, igniting non-linear physiological reactions to correct the system [31]. The body's homeostatic control monitors thermal conditions and regulates its temperature and parts compared to a set-point in the hypothalamus [32], trying to re-establish the unheated temperature. The feedback regulation non-linearly increases the blood-flow (BF) [33,34], as an effective heat exchanger, as well as the regulation intensifying other physiological mechanisms to control conditions [35]. The reactive BF change causes most of the challenges in LRHT applications.

On the other hand, the reaction to the growing temperature also has a supporting behavior. It induces relatively significant protective heat shock proteins (HSPs) in the targeted cells. The extra stress by heating increases the HSPs only slightly in the otherwise heavily stressed malignant cells but causes a drastic gain (8–10 times) in the healthy ones [36]. The difference makes the malignant cells more vulnerable to the temperature increase than the well adapting healthy cells.

6.2. Complementary Challenge

The correct dose application of LRHT is a critical issue in the future of hyperthermia in oncology [37]. Furthermore, the complementary therapy of LRHT and RT requires the precise dosing of both components to ensure safe and reproducible effectivity. RT has a traditional, well-applicable, accepted dose, which determines the isodose by the equal energy absorption in Gy (= J kg) in the chosen target. The isodose energy absorption is not directly dependent on the size of the tumor. The dose is homogeneously distributed across the entire tumor volume, independently of its size; the same dose is maintained in all volume units. The treatment defines the isodose (e.g., fractional dose for daily application) equally, and the complete sum of fractions composes the final dose, which depends on the tumor conditions (localization, size, stage, conditions, cellular specialties, etc.). It is fixed through the planning process and the focusing adjustments realized.

LRHT uses the temperature as an active part of the treatment, applying it for dose characterization. Contrarily, RT regards it as an adverse effect, causing burns and fibrotic conditions [38,39]. A fundamental difference between RT and LRHT appears in their treatment length, and consequently, the applied energies. RT applies a short shot with only a negligible effect on the physiological regulation, while the LRHT treatment time is long (usually 60 min), so homeostatic control is activated. The radiation focus also shows significant differences: the heating produced with LRHT spreads into non-targeted volumes in conductive and convective ways, while RT remains local, being well focused on the planned volume. The frequency of the standard treatments differs too: while fractional RT treats daily, LRHT, due to the HSP protection that develops, cannot be applied so frequently, requiring at least a 48 h break between applications. Unfortunately, the LRHT-produced HSP could be associated with radioresistance too, but on the other hand, LRHT influences numerous other molecular parameters which could sensitize to the RT [40].

RT and LRHT achieve therapeutic synergy in their complementary application despite the differences. The LRHT supports the RT by the thermosensitizing [41] and oxygenation of the target [42]. The active arrest of the cell cycle can realize an essential synergy in different phases by the RT and LRHT. RT is most active in the

mitosis phase, while moderate heat shock arrests G1/S and G2/M cell-cycle checkpoints [43]. The LRHT predominantly acts in the S phase of the cell cycle [44] in moderately acidic, hypoxic regions, complementing the cell cycle arrest. Various molecular parameters support the RT efficacy [45], e.g., a heat-induced decrease in DNA-dependent protein kinase [46].
The physiological regulation compensates for the heating effect of LRHT, increasing the BF by vasodilatation to maintain thermal homeostasis. The BF counterbalances the increased temperature by intensive heat-interchange, which in exchange delivers an extended oxygen supply for radio-effects, fixing the DNA breaks [47,48].

The possible synergy of RT and LRHT has a contradictory process. The high BF naturally opposes the Hippocratic "thermal starvation" concept. Nevertheless, the higher metabolic rate of the proliferating mass compensates for the missing supply by non-linearly increasing BF [49–51]. The effects of higher radiosensitivity compete with the increased volume of delivered nutrients due to vasodilation and the heat-promoted perfusion through the vessel walls. On the other hand, the neo-angiogenic arteries do not vasodilate in massive tumors, as they lack musculature in their vessel-wall [52].

Consequently, the reaction to heat differs in the healthy and malignant tissues, exhibiting approximately 38 C when the BF in the tumor lags the BF in the healthy host [53]. Additionally, the temperature increase can produce vasoconstriction in certain tumors, which decreases the BF and the decrease in heat exchange offers a relatively higher temperature in these regions [54]. This effective heat trap [55] lowers the available oxygen, affecting the efficacy of RT. Parallel at the same time, vasodilatation in healthy tissues increases the relative BF, presenting more cooling media in the volume [56,57], and increases the RT effect in the healthy host tissue counterproductively to clinical safety.

The BF has a central role in maintaining the overall homeostasis. Besides the temperature, it regulates essential parameters like the acid-alkaline equilibrium, glucose delivery, immune actions, and numerous blood-delivered molecular feedback loops in the body. In the precise interaction of RT with LRHT, these parameters may also have remarkable modifying factors. The vascular response of tissues has a tumor-specific temperature threshold, indicated by the kink in the Arrhenius empirical plot [58,59], in consequence of a structural phase transition in the plasma membrane [60].

The above contradictory processes are natural in complex systems, where the suppressor–promoter pairs have an essential role in the dynamic regulation of the homeostatic balance. As always, the regulative processes balance the progressor and suppressor action, so not surprisingly, the radiotherapy-induced damage could cause the activation of damage-repair mechanisms, and survival signaling adds to other factors of tumor-resistive effects [61]. This complex dynamic behavior otherwise guarantees the robust stability of homeostasis as the regulator of healthy processes. The complementary LRHT and RT synergy also require consideration of the system's complexity. The sum of its distinct parts does not describe the natural cooperating procedures.

The interactions are essentially nonlinear, representing that the whole is more than the sum of the parts. The living structures, in their complexity, have a universal behavior: they are self-organized [62]. The basic synergistic possibilities of LRHT and RT are collected in Table 1.

Table 1. The synergistic possibility shows a broad range of advantages for combined therapy of LRHT and RT.

Tumor Characteristics	Oncological Hyperthermia Including All Technical Solutions	Synergy with Radiotherapy
Cell cycle	Arrests the cycle of cells at the S stage, activates the malignant cell from its dormant (G0) phase making attack possible for chemo- and radio-therapies	Radiotherapy arrests the M/G2 stages of the cell cycle well completes the arrest
pH dependence	Kills cancer cells in an acidic environment (Hippocrates' original idea)	It kills cancer cells in an alkaline environment, completes the cell desertion in all environmental conditions
Oxygenation	Acts in the hypoxic state	Acts in an oxygenated state
Increased temperature	Heated tumor mass increases the oxygen delivery	Makes strand breaks on DNA, the fixing of which means oxygen blocks the reparation

6.3. Dosing Challenge

The present dose of HT measured with cumulative equivalent minutes compared to the 43°C basepoint, (CEM 43 °C) [63,64] fit to the complete necrotic cell killing in vitro [65]. This reference is far from the reality of human medicine. The principal challenge of this dose is that homogenous heating is only an illusion. The approximately isothermal x percent of the heated area at T temperature completes the correct dose. The CEM 43 °C Tx [65], where T_x refers to the x% of the heated mass is approximated with the isothermal conditionat temperature T. The dose is, of course, lowered by the growing x value; Figure 2. The isothermal approach tries macroscopically equalizing the temperature with high SAR. The T_x estimation makes macro characterization and does not consider the tissue-defining microheterogeneity of the target.

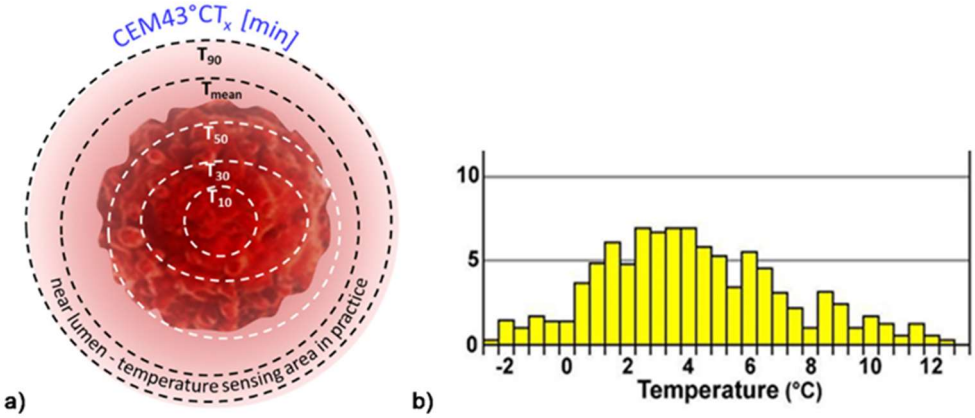

Figure 2. The heated focus rapidly spreads, so the temperature increases in a broader region. (a) The CEM43 dose depends on the isothermal areas, which differ by distance and develop by time. (b) The temperature distribution across the tumor after 64 min of treatment was measured by MRI (Pat.10. relapsed rectum carcinoma) [66].

The dosing of LRHT has serious challenges. It is much less reproducible and controllable than the dosing in RT. LRHT has huge anatomical, physiological, bio-electromagnetic, mechanical, and thermal heterogeneities, limiting the isodose-type approach of LRHT. The associated isothermal heating uses the temperature as a defining factor of the dose. However, the homogeneity and the lengthy treatment time do not maintain the otherwise precise focus. When the temperature stabilizes in a tiny region, the heat spreads from the targeted volume, and in this way, the intended isothermal region represents only a decreasing fraction of the target. The temporarily defined homogeneous volume may dynamically change by elapsed time; the situation is far from equilibrium [67], and the temperature and space distribution vary. The nonlinear BF and other homeostatic regulatory effects, together with the regular heat flow, destroy the homogeneity.

For example, when the measured temperature is actually T_{90} in 90% of the monitored sites (referred to as the thermal isoeffect dose in 90% of the area), considering the average (assumed homogenous) volume, the $T_{90} > T_{80} > \ldots > T_{10}$, and the T_{100} could be achieved only in a WBH situation. This construction certainly contradicts the homogenous idea. Due to technical and safety issues in clinical conditions, achieving the 43 C temperature requires enormous efforts. The challenge is heating the surrounding healthy host by the spread of heat that cannot be avoided with any precise focusing of the radiation beam. Clinical safety requests that the heating not exceed 42 C in the healthy tissue. The blood flow increases more in the healthy host tissues than in the tumor, causing a particular gradient of the flow intensity to heat the tumor's boundary. The tumor periphery contains the most vivid, mostly proliferative malignant cells. The temperature differences at the tumor border develop a certain BF gradient, which could wash out the aggressive malignant cells, increasing the risk of dissemination.

The CEM $43T_x$ dose has numerous principal challenges [68]. It failed to show the local control characterization of clinical results in soft tissue sarcomas [69] and does not correlate with clinical results for superficial tumors [70]. Complete homogeneity in the heating of living objects could be achieved only in the whole-body hyperthermia (WBH) process. It represents an entirely isothermal CEM 43 °C T_{100} situation. Contrary to isothermal heating, the non-isothermal LRHT shows better clinical results [71], and the results of complementary application to chemotherapy also remain behind the chemotherapy alone [72,73]. However, administering a dose of CEM $43T_{90}$ LRHT also did not show a correlation between dose and clinical outcomes (such as local remissions, local disease-free survival, and overall survival) [74].

Measuring the isothermal situation, determining the CEM $43T_x$ dose has practical challenges. Reliable temperature measurement is an unachievable goal; Figure 3.

1. The invasive temperature sensors available are point detectors. When the point is near the arteries of a highly vascularized area, the temperature is less than in the low vascularization part, so many independent sensors are necessary to attain objective results. However, this induces safety and treatment problems.

2. Usually, a near lumen (such as the esophagus, bronchus, colon, or vagina) offers the possibility to approximate the temperature in the distant tumor, but this is again far from the reality in the target.

3. The most effective temperature mapping can be done with MRI measurement, using a phantom for reference, usually unionized water. The MRI measurement depends on the temperature, but also strongly depends on the structure of the measured volume. In the temperature measurement, both factors are included in calculating the result, but the calibration does not consider a final element: the changes in the structure, which is the goal of the LRHT treatment.

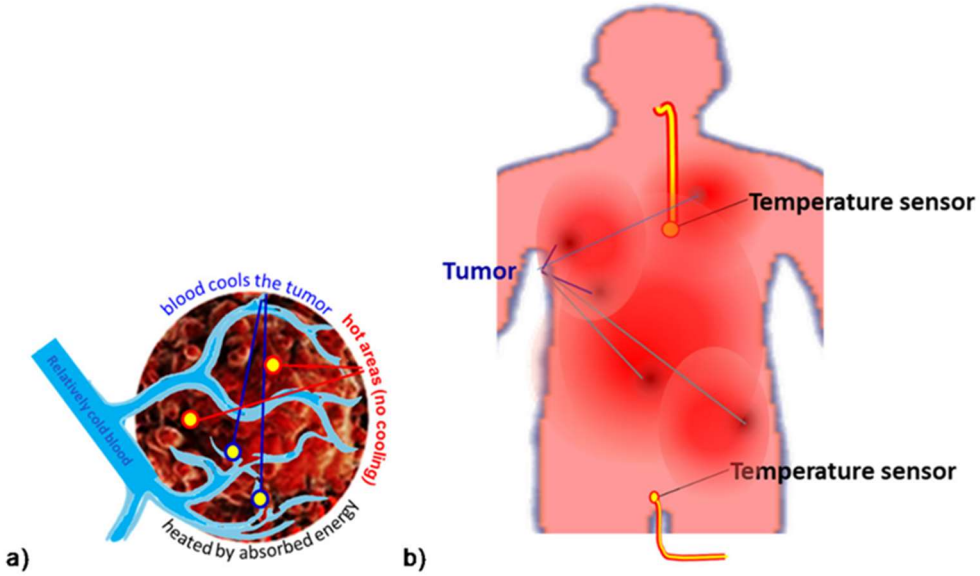

Figure 3. Challenges of temperature measurements:
(a) the invasively inserted point sensors detect the very local temperature and not the average isothermal;
(b) the semi-invasive temperature sensing catheters in lumens measure the temperature in near lumens, which could be far from the actual tumor temperature.

6.4. Challenge of the Heated Body

It looks evident that WBH offers the best heating possibility because of its easy control (measurements in body lumens) and the realized complete isothermal load on all the malignant cells and tissues. Notably, the WBH method does not show such good results in the high-temperature regime (≥41 °C). The prospective double-arm study shows that the overall survival was less in a combined hyperthermia application than in cases when only chemotherapy (ChT) was administered [72]. The same result was obtained in malignant pleural mesothelioma [73] when the toxicity was also higher in the combined treatments. Contrary to the 10+ times higher CEM 43 °C dose of WBH producing isothermal temperature (CEM 43 °C T_{100}), a fourfold development of metastases was measured in canine sarcomas with radiation therapy with or without WBH compared to the local heating [71]. The mild temperature WBH (mWBH < 40 °C and $dose_{mWBH} < \frac{2\ CEM43°CT_{100}}{treatment}$) was effective [75]. (The additional parameter T100 to CEM 43 C denotes that 100% of the tumor received the dose). The mWBH activates the immune reactions, and so it could be a good complementary treatment for other therapies [76-78]. However, the demand for higher temperatures for direct cellular degradation challenges such applications and favors the LRHT application. Contrary to WBH, LRHT does not load the patient's herat, and negligible electrolyte loss happens, and consequently, the inclusion criteria allow more patients.

6.5. Challenge of Homogeneity

The challenge of LRHT differs from that of WBH. While WBH ensured a homogeneous loading of the tumor, achieving homogeneity in LRHT is complicated. The well-focused heated volume spreads by heat-conduction over time, heating larger and larger body regions. The spread of heat triggers BF and so supports the delivery of necessary nutrients (glucose and others) to the tumor. A further challenge is an increasing difference between the BF of the tumor and its healthy host, BF to the host increasing much more quickly than in the tumor. This flow gradient promotes the invasion and dissemination of the cancer cells from the most vivid near-surface region of the proliferating tumor. An early phase III clinical study faced this problem, the straightforward local advances of HT + RT compared to RT alone not appearing in the survival time in breast tumors [79]. Another study obtained the same controversy: local remission success and the opposite in the overall survival [80]. The development of distant metastases was also observed [81]. The same reason led to a debate about LRHT results for the cervix, showing both advantages [17] and disadvantages [82] in survival.

A further study of cervix carcinomas supports the survival benefit [83], but again a critic has questioned this result [84,85]. Another phase III trial of cervical carcinomas with HT plus brachytherapy involving 224 patients noticed the same controversies between survival time and local control [86]. The controversy was observed in a study of locally advanced non-small-cell lung cancer (NSCLC) having a significant response rate improvement, although there was no change in overall survival [87]. A multicenter phase III trial for NSCLC also showed no improvements in overall survival in the hyperthermia cohort [88]. The cause was directly shown: the appearance of distant metastases was five times higher (10/2; p = 0.07) in the HT + RT group than in the RT cohort [88]. The study of the surface tumors had the same contradiction between the local control and survival rate [89].

Most likely, the improved dissemination of malignant cells forming micro- and macrometastases causes contradictory results. We must learn from the contradictions and follow the admonishment of Dr. Storm, a recognized specialist of hyperthermia: “The mistakes made by the hyperthermia community may serve as lessons, not to be repeated by investigators in other novel fields of cancer treatment” [90].

Our task is to improve the controllability of LRHT, ensure the stable, successful applicability of heat therapy combined with RT in oncology, and fulfill the authentic promise that LRHT is an excellent complementary tool for RT [91]. Serious analysis is necessary as has recently been started [92]. I would like to continue this approach and add biophysical aspects. The data showing a highly significant improvement of local control obtained with LRHT and RT represent facts that we must consider as the basis for the further development of oncological hyperthermia and the correction of the problems with overall survival. We must concentrate on blocking invasion and reducing dissemination to overcome the issues. The task is to prevent the formation of metastases caused by heating. Furthermore, we may eliminate the metastases formed earlier, prior to thermal treatment, with the primary tumor’s local hyperthermia.

7. Materials and Methods

The radiation similarity of LRHT and RT induces the proposal to characterize the target volume with the sodose load. The isodose concept ensures reproducibility, safety, and efficacy too. The isodose in RT is simply the energy-dose of ionizing radiation measured in Gy $(= \frac{J}{kg})$ and applied to the tumor volume in daily fractions. The energy dosage may be reached in a session during a short time. The heating conditions limit the provision of the necessary energy. The LRHT needs a significantly longer time for a session than RT needs. Consider power, the applied energy per unit time $(\text{power, } P\ [\ \frac{J}{s} = W])$. The energy dose is the sum of the power P_i during the time t_i when it is applied $(E = \sum_{i=0}^{t} P_i \tau_i)$. The power in the unit of mass is the specific absorption rate (SAR = P/m, where m is the mass of the target) measured in $\frac{W}{kg}$ units. The energy (E/m) is the dose considering the duration of the SAR load in the target, measured in $\frac{J}{kg}$ units, like the dose Gy in RT. In this way, the SAR offers the possibility to unite the doses of LRHT and RT. The energy increases the temperature, so in an ideal case, the SAR could be applied as the isothermal dose of LRHT.

The heating process starts with an approximately linear rate of temperature growth. It is quasi adiabatic. The relatively slow homeostatic feedback does not disturb the heating [93], and the SAR is proportional with this development in time (t): $SAR \cong c\frac{dT}{dt}$ [31].

Physiological regulation and safety issues challenge this concept. The homeostatic regulation increases the BF in the targeted volume, and like a heat exchanger, cools it down. In this way, higher power is necessary than it otherwise would be desired without this physiological control. The systemic control increases rapidly and non-linearly [31] with different speeds as the BF changes. The treatment's safety requires an intensive cooling of the body surface where the heating power penetrates. The cooling takes away a large amount of the applied energy, not contributing to the heating. The cooling and other energy losses (like radiation, heat diffusion, convection, etc.) limit the application of E as the dose because the actual energy absorbed in the body is uncontrolled. Consequently, temperature measurement is mandatory to estimate the amount of the absorbed power (SAR) in the target.

A new paradigm solves the challenge when the heating does not target the whole mass of the tumor, but the individual malignant cells are in focus [94]. This case avoids overly intensive feedback of the homeostatic regulation, and the various other losses also become more easily manageable. The individual cellular heating breaks the homogeneous isothermal requirement. The absorption is heterogeneous and microscopically individual, using the tumor's natural thermal, electromagnetic, mechanical, and physiological heterogeneity [95].

The heterogeneous molecular actions in the selected volume do not contradict the isodose concept. The apparent contradiction originates from the false expectations of the isodose effect. The isodose does not mean that the action in the target involves all molecules and structures. It means that the isodose grants the desired molecular and structural changes in all isodose volumes. Nevertheless, the required molecular actions are individual and heterogenic. This homogenous-heterogenic vision is well observable in medication. When the body takes a dose intravenously, orally, or in other ways homogeneously in the body, the dose is calculated from the body's volumetric parameter (BMI). However, the expected action of the drug is heterogenic, selectively targeting molecular structures. The ionizing radiation-activated DNA damage is the heterogenic goal of RT. LRHT targets other molecular effects, but the expected effect is incidental due to the averaging of the energy by the isothermal conditions.

The crucial point of the new paradigm is to select the malignant cells and concentrate the energy absorption upon them. The new paradigm is electromagnetic heating, as most applied hyperthermia methods use radiofrequency (RF) current. The current delivers energy to depth, its parameters (amplitude, frequency, and phase) being chosen optimally to find the heterogeneities produced by the malignant cells; Figure 4. All three parameters have dynamic changes by time variation, improving the selection mechanisms. The carrier frequency is amplitude modulated, and the modulation frequency is not constant, but follows the demands of the homeostatic control, representing a spectrum suitable for the spatiotemporal distribution of the cancer cells.

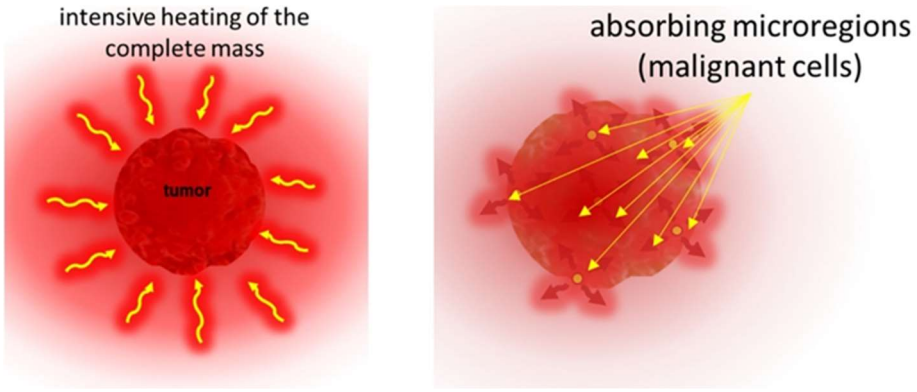

Figure 4. Draft presentation of the heating paradigms:
(a) Homogeneous mass heating trying to achieve isothermal conditions. It intensively heats the surrounding healthy tissues as well.
(b) Selective, heterogeneous (heterothermal) heating. It creates a high temperature in the absorbing points, but mild average temperature (<40 °C) in the surrounding healthy tissue.

The heterogeneous heating has a crucial behavior: it provides a high temperature for the selected malignant cells, but the average temperature of the tumor remains under 40 C. A temperature of over 40 C downregulates the cytotoxicity of innate immune attacks [96,97], including those of the natural killer cells (NKs) [98]. On the other hand, substantial cellular thermal damage has been observed at temperatures above

41–42 C [99]. Modulated electro-hyperthermia's (mEHT's) heterogenic heating could harmonize these two otherwise contradictory demands.

Time-fractal modulated electro-hyperthermia (mEHT) supports the selection and induces programmed cell-killing processes, genuinely breaking the isothermal approach. Instead of homogenous heating of the target, mEHT uses excellent selection to force energy absorption on the malignant cells, heating them locally to the hyperthermia temperature to induce cellular changes in the targeted cells by thermal and nonthermal mechanisms [100]; Figure 5. The thermal component of the absorption heats the selected membrane rafts, which is the source of the temperature of the tumor, as is standard in heterogenic seeds or nanoparticle heating processes. In contrast, the nonthermal component causes molecular excitation for programmed cell death [101]. The excitation by electric field E has similar increase like the temperature increases the molecular reaction rate [102]. The cell-membrane represents decreasing impedance with increasing frequency, so the field penetrates the cell with improved intensity. The membrane practically shortcuts and does not significantly influence the RF current flow over ~25 MHz [103].

Nevertheless, the difference between the energy absorption between the membrane and intra- and extracellular electrolytes remains on high frequencies [104]. The primary energy absorption happens in the transmembrane proteins and their clusters on the rafts [105]. The density of membrane rafts is significantly higher than in the nonmalignant cells [106]. The absorbed energy makes the molecular excitation nonthermal and the temperature an essential joint conditional factor, promoting the reaction rate [107].

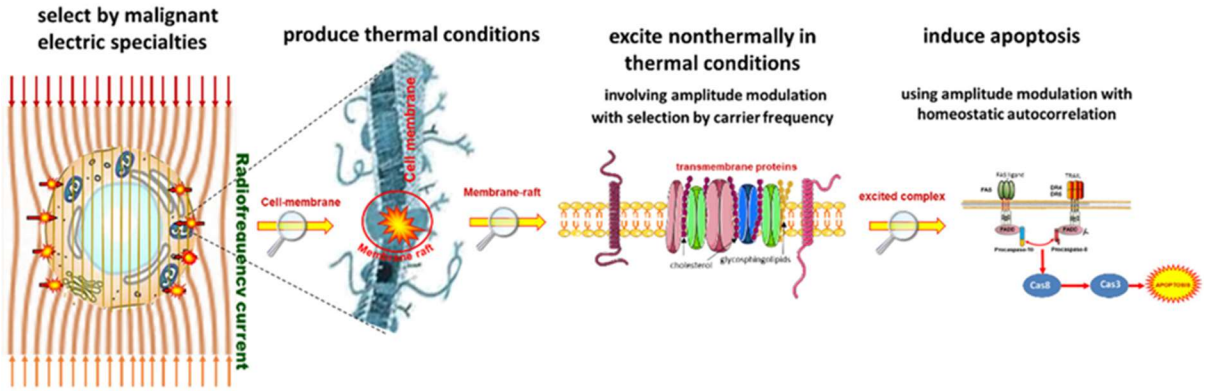

Figure 5. The transmembrane proteins of malignant cells absorb the energy in thermal and nonthermal forms. The amplitude-modulated carrier frequency's nonthermal effect gives the apoptotic signal pathway (see below in results). The carrier frequency delivers the modulated signal and selects the malignant cells, while the modulation with homeostatic autocorrelation (time-fractal) constrains the apoptotic pathway.

The applied selective energy-absorption works like RT and realizes isodose conditions, too, concentrating on very local (nanoscopic) molecular effects, mostly to break the DNA strands in the isodose-defined volume. In this meaning, mEHT and RT have a similar nano targeting philosophy; Figure 6. The target is the natural heterogeneity of the tissues, as RT targets the DNA. The method recognizes the particularities of tumor cells' microenvironment (TME) [108].

Two essential effects are considered for selection: thermal absorption and nonthermal excitation. The thermal component provides the appropriate temperature of the TME by heating the membrane rafts [105]. Another general thermal action affects the extracellular matrix (ECM) and a part thereof, the TME. This acts mechanically and molecularly [109], accompanying the thermal absorption of transmembrane protein clusters.

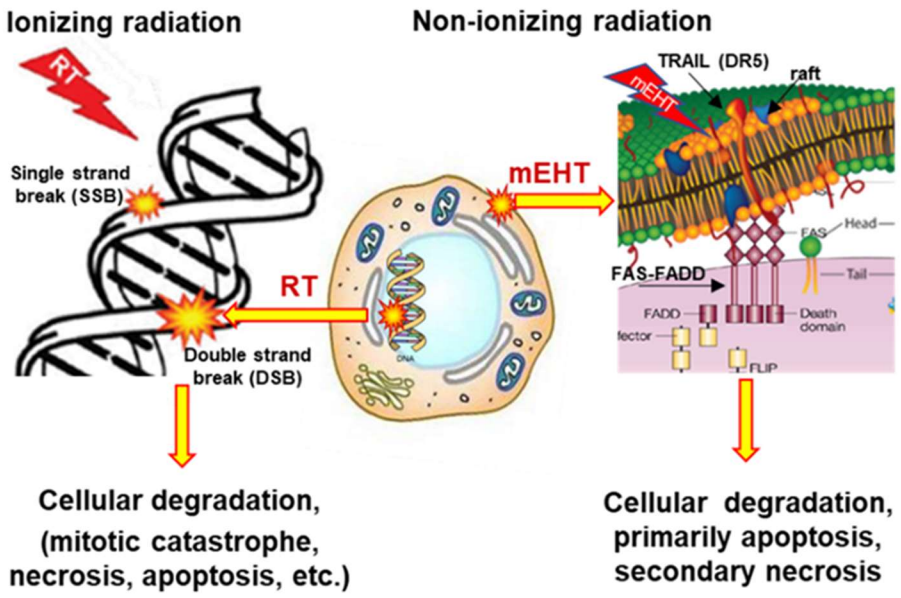

Figure 6. The conceptual similarity of RT and mEHT. Both therapies target molecular bonds, so the primary energy absorption is heterogenic. The result is cellular degradation in various ways.

The nonthermal effect happens when "under the influence of a field, the system changes its properties in a way that cannot be achieved by heating" [110]. The nonthermal component excites the membrane receptors of the cells. The well-chosen electric current an deliver energy for molecular excitations involving various ionic and molecular interactions [31]. The process only has a subtle thermal effect and excites the molecules or structures that fit the applied resonant conditions [111].

The apoptotic signal by the mEHT excited membrane receptors and the apoptosis by the single or double-strand breaking of DNA for cellular degradation are strong similarities of RT and mEHT. Nevertheless, despite conceptional similarities, RT and mEHT have an essential difference: the additional thermal component in HT, which is absent in RT. Thermal absorption is mostly an unwanted side effect in ionizing radiation. The goal is only the molecular effects.

The excitations of transmembrane proteins need low frequency [111], but their neuronal excitation, which may rise to 10 kHz [112], is not safe with the applied power. On the other hand, the frequency for selective heating is in the high RF frequency range. The mEHT solves the challenge of the contradictory simultaneous requirement of high and low frequencies. It uses the appropriate low frequency to modulate the high-frequency carrier; Figure 7 [113]. The membrane rectifies. The carrier frequency in the rectified signal remains active, but mainly at the cellular membrane (b-dispersion, see later). In this way, the original modulation signal makes the excitation process.

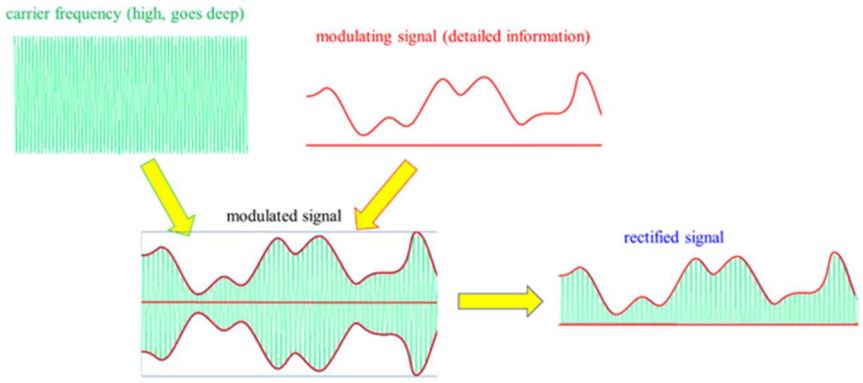

Figure 7. The modulation process compromises between the contradictory high- and low-frequency demands. The unification of the low-frequency modulating signal and the high-frequency carrier forms the modulated signal, a frequency spectrum on the carrier 13.56 MHz. The cell membrane rectifies and works for the excitation of apoptotic pathways. The high-frequency carrier gives the optimal thermal condition for the excitation by the low-frequency info signal in the selected cells.

mEHT is a complex method, which complicates its technical realization. The technical details (Figure 8) need further explanation. I will discuss it in the discussion section of this article.

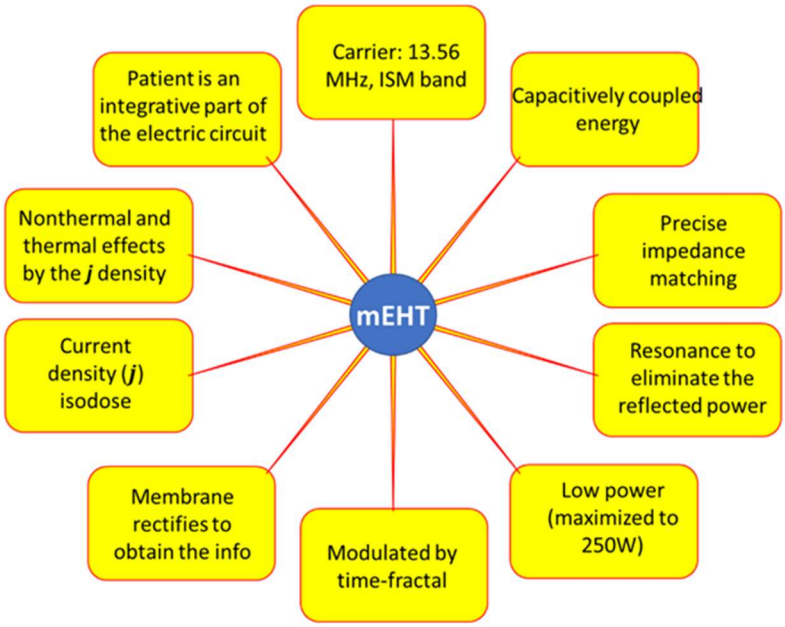

Figure 8. The technical conditions of mEHT. The realization of the method rigorously accommodates and utilizes the complexity of the heterogenic impact of mEHT to arrest the proliferation of cancer and degrade the developed tumor cells.

1) The chosen optimal carrier frequency is 13.56 MHz, which belongs to the freely applicable ISM band [114] and does not need shielding.

2) The energy is capacitively coupled, but it does not use the plane-wave approach. Planewave radiation is devoted to isothermal heating.

3) There is precise impedance matching [108] in the mEHT method. Proper impedance matching produces negligible reflected power (order of 1 W), mimicking the galvanic contact with the skin as much as possible.

4) It has resonant matching with micro-selection ability, which fits the impedance [109]. It eliminates the imaginary part of the impedance. It differs from the usually applied plane-wave matching.

5) The maximum adequate output power of mEHT is limited. The power limit depends on the size of the electrode. In device EHY2000+, the maximal power is 150 W, while in the model of EHY2030, which has optionally larger electrodes too, the limit is 250W. The applied power in therapy depends on the localization and size of the tumor. The power limitation keeps the SAR less than for isothermal heating, but high enough to select and excite the membrane rafts of the malignant cells [100] and sensitizes to the RT [115,116].

6) The modulation spectrum is a low-frequency time-fractal [113], described by fractal physiology [117–120], which agrees with the homeostatic molecular temporal balance [113]. mEHT extensively uses the modulation technique to identify fractal structures in space and time (dynamics) in spatiotemporal identification [113]. The electric parameters (resistance and capacity) depend on the malignant status [121]. The selection between malignant and healthy cells was measured as a characteristic time-fractal [122]. The modulation delivers temporal information executing enzymatic processes at the cell membranes [123], promoting the consequence of the excitation.

7) The membrane rectifies [124,125], and considerably gains the strength of signal intracellularly [103,104]. The rectified signal acts in the low- and high-frequency ranges.

8) The correct impedance matching provides an appropriate electric field that ensures the current density (j). The j is the parameter of the isodose conditions, ensuring the constant current density in the target. A complex value describes the current depending on the phase shift from the applied signal voltage. The dominant dielectric actions (heating and excitation energies) produce thermal and nonthermal effects.

9) Themodulated j-current density actively produces both the thermal and nonthermal effects.

10) The patient is interactively connected to the electric circuit, like a discrete element of the RF-net. This solution allows the real-time control of the patient due to the treated tumor being actively sensed and targeted as part of the tuned electric circuit.

Further technical details can be found elsewhere [108].

8. Results

The mEHT method is the focus of intensive research regarding all attributes. Phantom experiments show the proof of the thermal concept, measuring the temperature development in well-chosen chopped-meat phantoms [126,127], and computed results show the validity of heat selection using tissue heterogeneities, also proven in experimental setups [128].

These macro approaches are well completed with the micro-approach, calculating the nano-range thermal and nonthermal components [105]. In vitro experiments fixed the thermal effects to the reference calibration using the U937 human lymphoma cell line [95], and the HT29 and A431 [94] cell lines. The quantitative dose equivalence of mEHT with RT defines the harmonizing basis of cellular degradation in two different lung cancer cell lines, A549 and NCI-H1299 [129].

mEHT is a mild LRHT in the conventional meaning. The temperature dynamically grows in the mass of the liver when there is no tumor inside because selective targeting does not modify the distribution, as temperature measurement in the liver of an anesthetized pig shows [130]. The thermal component of mEHT heats the target, which may be used for temperature mapping in a preclinical murine model [131] at a mild level. A mild hyperthermia temperature level in humans could be measured in cervical cancer, which increases the peritumoral temperature to 38.5 C, with proper blood flow for the complementary treatments [132].

The comparison of mEHT to wHT and to plane-wave fitted, non-modulated capacitive hyperthermia (cHT) at the same temperature shows a significant improvement of apoptosis with mEHT in the HepG2 cell line [133]. It showed that the wHT and cHT (the homogeneous heating) cause approximately the same low apoptotic rate, which reveals the advantage of the mEHT heterogeneous concept. The breaking of DNA measured with subG1 also significantly improves with mEHT as compared to the conventional homogeneous methods [133]. Radioresistant pancreatic cell lines show extensive DNA fragmentation measured with subG1 after mEHT [134].

The effect has given a possibility to make a reference calibration of mEHT compared to wHT on HepG2 cells shown at ~5 C [133], while in the U937 cell-line [95], it shows a >3 C shift to the advantage of mEHT over wHT (Figure 9), it is supposed that the difference indicates a 3+ C higher temperature of rafts than of the TME. The gain of tumor destruction at 42 C is ~~4.9 fold, which corresponds well with the in vivo experiments (~~4.3) in HT29 colorectal carcinoma [135].

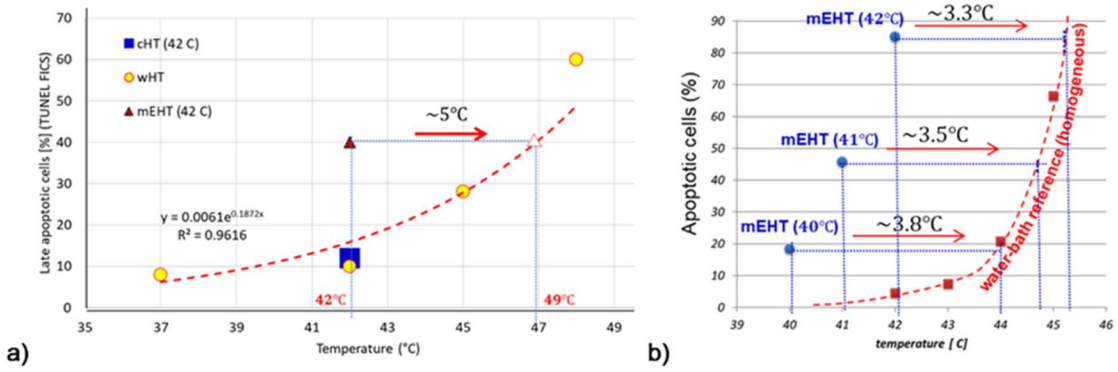

Figure 9. The calibration of the thermal factor of mEHT.
(a) The homogeneous HT (water-bath hyperthermia, wHT) is used to calibrate apoptosis. The mEHT causes effective apoptosis at 42 C, corresponding to the calibration at 5 C higher (HepG2 cell-line) [133]. The mEHT affects the rafts on the cell-membrane with a 5 C higher temperature than the average medium indicates. (b) Another calibration measurement with the U937 cell line [95,136]. The mEHT shows a >3 C temperature difference in apoptotic efficacy at all measured points.

A critical thermal factor is that the possible touching point of two cells has a drastically increased heat-production due to the extensive SAR at that point [105]. The telophase of the cell cycle naturally forms a tight touching of the two just-created daughter-cells, where the increased SAR could block the finalizing of the cycle and cause the daughter to degrade [137]. Like all complex phenomena, the cytoskeleton's effect could also act oppositely. The reorganization of actin filaments and microtubules by an outside modulated electric field can support the proper polymerization of the cytoskeleton when the cell is only pre-malignant [138]. The close independent malignant cells attract each other by the induced dielectrophoretic forces and the vast electric field gradient between the cells [105].

This makes it possible to reconstruct the intercellular E-cadherin connection, allowing the regular networking of the cells [133]. The deformation of the cells by external field depends on the frequency [139]. The carrier of mEHT is high enough that the deformation is negligible due to the higher conductivity in the ECM than in the cytoplasm [104].

The molecular models concentrate on the membrane effects, showing the thermal and nonthermal results. The same heat conditions force the same processes in the cytosol ER and other cellular organelles, and the heat-sensitive transient receptor potential vanilloid receptor (TRPV) also senses the same temperature for action. The excess ionic concentration is caused by mEHT [140], which increases the influx of Ca2+ ions from the ECM to the cytosol. The high iCa2+ promotes apoptosis in the mitochondria-dependent intrinsic signal pathway [141]. The decreased membrane potential of mitochondria [136] well supports the mitochondria-associated apoptotic process. The mEHT induces the Ca2+ influx with the assistance of E2F1 [142], which regulates the HSPs without heat-shock [143], supporting the possible factors of the nonthermal effect of applied electric current.

Research of the nonthermal effects on HT29 and SW480 human colorectal cancer cell lines shows a significant nonthermal impact on the ionic fluxes, and mEHT has doubled the antiproliferative and anticlonogenic effects of conventional water-bath heating (wHT) at 42 C [144].

There are tumor-specific thermal and nonthermal stresses with mEHT related to the metabolic profiles of the targeted malignant cells having elevated glycolysis [145]. The efficacy of mEHT may correlate with the tumor metabolic profile by the targeted selection [146].

The nonthermal activity causes structural changes affecting the intracellular polymerization of filaments [138]. The fluctuations also have an essential role in the electromagnetic interaction, showing thermal and electric noise limitation in the TME connected membrane [147].

mEHT applications focus on induced apoptosis [148,149]. The method may cause caspase-dependent paths through Cas8 (extrinsic way) and Cas9 (mitochondrial, intrinsic way) [133,150] and independent [151,152] apoptosis. A notable factor is the arrest of the XIAP effect to block the main path of caspase-dependent apoptosis by the secretion of SMAC/Diabolo [153] and Septin4 [154].

Experiments show that the aggressively radioresistant cell (L9) could be resensitized by mEHT [155], and also, radio-resistive pancreatic cells (Panc1, Capan1) show extended apoptosis when treated with mEHT [134,156,157]. mEHT also destroys these adenomacarcinoma cell lines [148]. The radiosensitization of mEHT significantly intensifies the autophagy and apoptosis in SCC VII and SAS cell lines compared to RT and wHT [158]. The massive apoptotic activity could be used for thermal dose calibration and energyabsorption-based temperature mapping [159].

Curiously, a notable reduction of apoptosis was measured with the addition of artificial gold suspension nanoparticles (NPS) to the targeted volume [160].

DNA fragmentation drives tumor-cell degradation [152]. The induced stress by mEHT upregulates the tumor suppressor p53 protein, a cell-cycle regulator, one of the key cell-cycle regulation and DNA repair players. mEHT activates DSB production. The phosphorylated form of histone family member X (gH2AX) as a DSB marker can activate p53.

mEHT significantly upregulates the gH2AX producing DSB in treating a B16F10 melanoma murine tumor model [161], in C26 colorectal allografts [101]. The subG1 cell fraction grows significantly in a radioresistant ductal adenocarcinoma cell-line (Panc1) combined with mEHT + RT 24 h posttreatment [134]. In the same study, the cellular viability drastically decreased in these resistant tumors in mono and complementary therapies with mEHT.

As independently expected [162], the thermal component of mEHT acts in synergy with the electric excitation, affecting the repair of DNA. The induced upregulation of cyclindependent kinase inhibitor protein (p21wa f 1) and the reduced Ki67 proliferation marker correlates with gH2AX, showing that the DSB is related to mEHT treatment [101,163]. The suppression of Ki67 and the significant growth inhibition has been shown in breast cancer murine isograft [164].

The heatmap of the gene expression chip shows the gene regulations of the mEHTtreated samples in an HT29 xenograft [165], in various gliomas [142], and also in vitro in the U937 cell line [136]. The gene map shows a distinct difference in the gene regulations between the homogeneous wHT and inhomogeneous mEHT treatments [136] at the same 42 C temperature.

Extended research deals with the possible tumor-specific immune processes of the heterogenic thermal and nonthermal effects and supports the emerging science of immunooncology. This examination's direction is focused on the abscopal effect, an emerging approach in RT research [166], also recognized by the ASCO [167]. The expectation is a tumor-specific immune situation, considering that cancer precludes regular immune attacks. The mEHT being concentrated on the tumor cells provides immunogenic information for the adaptive immune system about the malignant state and simultaneously sensitizes the tumor to the innate immune attack. This situation could extend the RT + mEHT local synergy to be active in the entire system.

The research concentrates on the optimal liberation of the genetic information from the cancer cells during their degradation. We found that the best process to achieve our goals is "soft" killing, not degrading the secreted molecules with too large an energy load. So, we suppressed the necrosis and the observed apoptosis based on the immunogenic efforts. One particular type of apoptosis, immunogenic cell death (ICD), was the aim, which is associated with a damage-associated molecular pattern (DAMP) as expected in the abscopal activity of RT too [168]. The promotion of damage-associated molecular pattern signals in an HT29 xenograft clearly showed a DAMP when treated with mEHT [165]. In parallel research, the innate NK*-cell activation to attack the selected malignant cells was also proven in A2058 melanoma in a murine xenograft model [169].

DAMP productive mEHT has been supported with various immune supports, which otherwise had no impact on cancer alone. The support by dendritic cells (DCs) has shown to be an excellent addition to mEHT, despite its inactivity alone. The combined treatment showed a perfect abscopal effect on the preclinical murine model, using SCC VII malignant cell inoculation to the animal [170], detecting CD3+, CD4+, and CD8+ T-cells resulting from DC maturation create antigen-presenting cells (APCs), increasing the S100 DC marker [171]. The presence of killer-T-cells (CD8+) increased significantly. The mice had two distant tumor lesions (in the femoral and chest region) modeling metastases. The femoral region was treated, and the chest remained untreated. After multiple treatments, an apparent abscopal effect was observed, and the tumor growth was completely blocked in the untreated chest tumor and the treated femoral [170]. Importantly the Treg protumoral activity was blocked as well, measured with Foxp3 suppression.

The abscopal effect of multiple mEHT treatments alone has been shown in B16F10 melanoma pulmonary metastases, where a significant anti-tumor effect, reducing the number of pulmonary metastatic nodules, and high immune cell infiltration was also present [163].

Similar results were obtained in another study, significantly improving the immunological tumor microenvironment with mEHT followed by dendritic cell immunotherapy [172]. This study also showed that no immune-effect happens with wHT at the same 42 C temperature. A remarkable result of this study was that the rechallenge of the cured animals with the same malignant cell-line was rejected, observing the adaptation of the immune system, behaving like "tumor-vaccination".

A natural herbal immune-support, Marsdenia tenacissima (MTE), caused a similar arrest of the tumor development systemically after mEHT, despite it being ineffective alone [173,174].

mEHT's combination with the simple conventional tumor-suppressive drug Doxorubicin (Dox) shows a robust immune activation observed with ICD, DAMP, and APC production and having a solid synergy with mEHT in intensively producing DSB, measured by gH2AX [175].

The starting point of human applications is safety. One of the most sensitive organs, the brain, was tested by dose escalation to measure the safety in human glioma cases, proving the safety of mEHT [176]. Many RT-related clinical therapies combine the heat effects with radio-chemotherapy (ChRT). The reason is to be effective systemically by using the drug when LRHT and RT are only local. The ChRT could be a complete

game-changer because the reaction rate of chemo-agents exponentially rises by reciprocal temperature (Arrhenius law) and makes cell death independent from RT or HT effects.

A Phase III trial comparing randomized cohorts of ChRT mEHT in clinical practice showed an excellent response to the combination with mEHT compared to the ChRT alone [177], and the toxicity was also low [178]. The abscopal effect was directly measured in addition to the Phase III study [179,180], showing a significant increase compared to the otherwise expected systemic effect of the ChRT. RT in combination with mEHT with checkpoint inhibitors also shows the abscopal effect in various tumors [116], supposing the immune-modulator function of mEHT [181]. Tumor-directed immunotherapy in the combination of RT and mEHT is also a possible option [182]. Table 2 lists 25 studies using mEHT complementarily to RT or ChRT, but the complete study list also contains monotherapy and chemotherapy.

Some recent reviews are available for references regarding conceptual [31,111], technical [94,108], preclinical [101,108], and clinical [183–185] aspects of the mEHT method, showing its efficacy in oncology.

Table 2. The table refers only to the clinical results obtained with mEHT complementary to RT or ChRT.

No.	Tumor Site	Number of Patients	Treatment Used	Results	Reference
1	Advanced gliomas	12	mEHT + RT + ChT	CR = 1, PR = 2, RR = 25%. Median duration of response = 10 m. Median survival = 9 m, 25% survival rate at 1 year.	Fiorentini, et al., 2006 [186]
2	Various brain-gliomas	140	mEHT + RT + ChT	OS = 20.4 m. mEHT was safe and well tolerated.	Sahinbas, et al., 2007 [187]
3	High-grade gliomas	179	mEHT + RT + ChT	Longstanding complete and partial remissions after recurrence in both groups.	Hager, et al., 2008 [188]
4	Glioblastoma & Astrocytoma	149	mEHT + RT + ChT (BSC, palliative range)	5y-OS = 83% (AST) in mEHT vs. 5y-OS = 25% by BSC. 5y-OS = 3.5% in mEHT vs. 5y-OS = 1.2% by BSC for GBM. Median OS = 14 m of mEHT for GBM and OS = 16.5 m for AST.	Fiorentini, et al., 2019b [189]
5	Advanced cervical cancer	236	Random. Phase III (RT + ChT ± mEHT [preliminary data]	Preliminary data for the first 100 participants. A positive trend in survival and local disease control by mEHT. There were no significant differences in acute adverse events or quality of life between the groups.	Minnaar, et al., 2016 [190]
6	Advanced cervical cancer	72	mEHT + RT + ChT	CR + PR = 73.5%; SD = 14.7%. The addition of mEHT increased the QoL and OS.	Pesti, et al., 2013 [191]
7	Advanced cervical carcinoma	20	mEHT + RT + ChT	mEHT increases the peri-tumor temperature and blood flow in human cervical tumors, promoting the radiotherapy + chemotherapy	Lee, et al., 2018 [132]
8	Advanced cervical carcinoma	206	Random. Phase III (RT + ChT ± mEHT) [abscopal effect]	The abscopal effect grows significantly with mEHT complementary to ChRT.	Minnaar, et al., 2020 [178]

Table 2. Cont.

No.	Tumor Site	Number of Patients	Treatment Used	Results	Reference
9	Advanced cervical carcinoma	206	Random. Phase III (RT + ChT ± mEHT) [toxicity & Quality of life]	mEHT does not increase the toxicity of ChRT but increases the quality of life	Minnaar, et al., 2020 [178]
10	Advanced cervical carinoma	202	mEHT + RT + ChT	Six-month local disease-free survival (LDFS) = 38.6% for mEHT and LDFS = 19.8% without mEHT ($p = 0.003$). Local disease control (LDC) = 45.5% with mEHT LDC = 24.1% without mEHT; ($p = 0.003$).	Minnaar, et al., 2019 [177]
11	Advanced NSCLC	97	mEHT + RT + ChT	Median OS = 9.4 m with mEHT OS = 5.6 m without mEHT; ($p < 0.0001$). Median PFS = 3 m for mEHT and PFS = 1.85 m without mEHT; $p < 0.0001$.	Ou, et al., 2020 [192]
12	Advanced NSCLC	311 (61 +197 +53)	mEHT + RT + ChT	Two centers PFY (n = 61), HTT (n = 197) control (n = 53). 80% (PFY), 80% (HTT) had distant metastases, conventional therapies failed. Median OS = 16.4 m (PFY), 15.6 m (HTT), 14 m (control); 1st y survival 67.2% (PFY), 64% (HTT), 26.5% (control).	Dani, et al., 2011 + Szasz, 2014 [193]
13	Advanced rectal cancer	76	mEHT + RT + ChT	Downstaging + tumor regression, ypT0, and ypN0 were better with mEHT than without. No statistical significance.	You et al., 2020 [194]
14	Various types of sarcoma	13	mEHT + RT + ChT	Primary, recurrent, and metastatic sarcomas responded to mEHT, the masses regressed.	Jeung, et al., 2015 [195]
15	Advanced pancreas carcinoma	106	mEHT + RT + ChT	After 3 m, PR = 22 (64.7%), SD = 10 (29.4%), PD = 2 (8.3%) with mEHT after 3 m of the therapy. In group without mEHT in the same time: PR = 3 (8.3%), SD = 10 (27.8%), PD = 23 (34.3%). The median OS = 18 m with mEHT and OS = 10.9 m without mEHT.	Fiorentini, et al., 2019 [196]
16	Advanced pancreas carcinoma	133 (26 +73 +34)	mEHT + RT + ChT	Two centers PFY (n = 26), HTT (n = 73) control (n = 34). 59% (PFY), 88% (HTT) had distant metastases, conventional therapies failed. Median OS = 12.0 m (PFY), 12.7 m (HTT), 6.5 m (control); 1st y survival 46.2% (PFY), 52.1% (HTT), 26.5% (control) QoL was improved.	Dani, et al., 2008 [197]
17	Metastatic cancers (colorectal, ovarian, breast)	23	mEHT + RT + ChT	OS and time to progression (TTP) were influenced by the number of chemotherapy cycles ($p < 0.001$) and mEHT sessions ($p < 0.001$). Bevacizumab-based chemotherapy with mEHT has a favorable tumor response, is feasible, and well-tolerated for metastatic cancer patients.	Ranieri, et al., 2017 [198]
18	Rectal cancer	120	mEHT + RT + surgery	In mEHT group, 80.7% showed down-staging compared with 67.2% in non-mEHT group.	Kim et al., 2021 [199]
19	Gliomas	164	mEHT + RT + ChT	CR + PR is 41.4% for mEHT and 33.4% for conventional therapies.	Fiorentini et al., 2020 [200]
20	Ovarian, cervical cancer		mEHT + RT + ChT	The feasibility and success of oncothermia is proven.	Wookyeom, et al., 2018 [201],
21	Various sites	784	mEHT + RT + ChT + surgery	Preliminary results show promising survival trajectories. mEHT is a safe treatment with very few adverse events or side effects, allowing patients to maintain a higher quality of life.	Parmar et al., 2020 [184]
22	Various sites		mEHT + RT + ChT	Planned trial.	Arrojo et al., 2020 [202]
23	Various sites		mEHT + RT + ChT	The feasibility and success of oncothermia are proven.	Szasz AM et al., 2019 [183]
24	Advanced glioblastoma	60	mEHT + RT + ChT	No added toxicity by immunotherapy. Median progression-free survival (PFS) = 13 m. Median follow-up 17 m, median OS was not reached. The estimated OS at 30 m was 58%.	Van Gool, et al., 2018 [203]
25	Different types of metastatic/recurrent cancers	33	mEHT + RT	CR = 2 (6.1%), Very good PR = 5 (15.2%), PR = 13 (39.4%), SD = 9 (27.3%), PD = 4 (12.1%). Three patients (9.1%) developed autoimmune toxicities. All these three patients had long-lasting abscopal responses outside the irradiated area.	Chi, et al., 2020 [116]

9. Discussion

All complex therapies overcome a contradictory process by considering one of the robust behaviors of this complexity: self-organization and the consequent self-similarity [204]. Recent decades have seen the development of various approaches describing the complexity of systems with self-organization [205,206]. The homogenous approach does not consider the natural heterogeneity of complex living systems. mEHT applies the selection of microtargets to distinguish the various parts and functions of the living organism.

9.1. The Electromagnetic Selection

The selection at the macro scale uses the intensive metabolic activity of the malignant cells to produce increased ionic density in the TME of the cells. In this way, the entire tumor has a higher complex conductivity (σ^*) for the electric current than its healthy environment [105,207–210]. The conductivity is proportional with the imaginary part of the complex dielectric function (ε^*), , depending on the ionic density (strength) of the target.

A part of the high conductivity could be followed using positron emission tomography (PET). The PET measures the intensified glucose metabolism, producing enhanced ionic concentration (primarily lactic acid). The PET results could be considered in the planning of RT [211], as it is a good addition for mEHT seeing the tumor activity, which is connected to the selectivity of the method. The electric current will choose the most accessible route (the most conductive one), flowing through the tumor.

Another electromagnetic selection mechanism concentrates on microregions (TMEs) using distinct structural heterogeneity. The individual autonomic development of cancer cells weakens the intercellular connections, breaking the E-cadherin protein connections. The malignant processes' breaking of the networking order also differentiates them in this parameter. In this way, the TME starts becoming gradually disordered by the development of the malignant network-breaking character shown in early observations by NMR measurements [212–214]. The disorder increases the dielectric permittivity (#) of the microregion [215–218]. The high # drives the mainly chosen radiofrequency (RF) current like the high s does. The plasma membrane and the TME absorbs the central part of the energy in the MHz region of the RF current [104]. The microregion of the tumor cells has considerable gradients of the electrolyte constituents of the electrolyte. The TME is in direct contact with tumor cells, containing molecular bonds to the membrane surface, while ECM is wide. Its primary function is connected to the transport processes. The water content of the TME interacts with the membrane [219], having variant bonds [220], and critically alters the membrane effect, showing a low SAR but high voltage drop [221], which can help the signal's excitation of the raft proteins [222]. The electrostatic charge of the membrane attracts the ions from the ECM, whose very different effect is sufficient to establish a transmembrane potential [223].

The rafts operate as a trigger of the cellular processes [224]. The rafts collect dynamic proteins [225], including proteins with high lateral mobility in the membrane [226]. The cataphoretic forces generated by modulated electric fields induce lateral movements and are sensed by the rafts in the membrane [140]. The size of these clusters is in the nano range. It depends on the ratio of protein to lipid content, different ranges of their horizontal diameters have been measured: 10–100 nm [227]; 25–700 nm [228]; 100–200 nm [229]. The width of the membrane is 5 nm [230], but the thickness of rafts, due to their transmembrane proteins, has a larger size. Note that the temperature increase of the nanoparticle (NP) is proportional to the square of its radius [231], which gives an easy comparison of the temperature using the sizes of the particles. The standard applied SAR in nanoparticles, considering their weight heating is 100–1500 MW/kg [4]. The mEHT heats not only the rafts but heats the TME and also the tissues to a lesser extent. Rough approximation of the absorbed power of rafts by mEHT is SAR > 1 MW/kg [105]. However, the role of absorption differs in nanoparticle and raft heating. The absorbed energy in nanoparticles produces only heat, while in the rafts with excitable structures, the energy divides into thermal and nonthermal effects.

The relatively large rafts contain approximately half of the membrane mass because of their relatively large mass compared to the lipids, representing only 2% of the membrane components [104]. The targeting of the rafts induces accurate energy absorption. The incorporation of energy happens at clusters of transmembrane proteins [95,140]. The temperature of the selected rafts is over the thermal averaging of the tissue. On average, the relatively small SAR is high in the rafts, similarly to the nanoparticle selective heating.

The selection of mEHT is demonstrated in an experiment with artificial NPs added from suspension to the targeted volume [160]. The injecting gold NPs or other artificial good energy absorbers produce a higher quantity of energy absorption in the target. The temperature grows by the diffuse heating from these too. Despite the more intensive energy absorption, the observed apoptosis in these cases decreases [160]. Probably, the sharing of the energy between the membrane rafts and the NPs causes this contradictory effect. The phenomenon supports the proofs of the selection by mEHT.

The selection appears in the ECM too. The current which flows in the extracellular electrolyte heats it more in the areas of selected TMEs than in the membrane-isolated cytosol. The energy analysis of the heating differences explains how this effect contributes to cell-killing mechanisms [109].

Well-defined conditions limit the SAR in the target, which limits the average power provided.

1) The thermal effect happens in nanoscopic local "points", the rafts. These NPs are molecular clusters and sensitive to overheating. When the absorbed energy is too large, it destroys the rafts by overheating. The mEHT loses its most significant advantage, the excitation of signal-transports for apoptosis and immunogenic cell death (ICD).

2) The selection mechanisms of mEHT also limit the SAR, which forces temperature development. At high temperatures, the heat spreads extensively, and the microscopic differences vanish on average. A macroscopic average will characterize the target, as in WBH. The limited energy absorption is mandatory for the selection of rafts.

3) The appropriate frequency is selected around 10 MHz [94]. When the frequency is larger (>15 MHz), the membrane impedance becomes too small to select the disordered TME accurately. The current will flow through the entire target tissue almost homogeneously, neglecting the selection heterogenic selection factors of malignant cells. When the carrier frequency does not ensure selection, the modulation also activates the healthy cells. The significantly larger amount of membrane rafts between healthy and malignant cells [106] remain selective factors only.

9.2. Nonthermal Processes

Healthy dynamism realizes a certain and strictly ordered set of molecular signals in space and time to maintain homeostatic control. The functional signals repeatedly correlate with the given functions (for example, the metabolic cycles), causing an autocorrelation of the resultant signal [232,233]. Note that spatial autocorrelation is a valuable tool in studying the microarchitecture of TME [234]. A significant periodic component in a data set has data points in a time series that correlate with the preceding data points in time, consequently measuring the self-similarity of different delay times in the signal. The autocorrelation could be simply visualized in the particular self-overlapping value of the signal (how the signal correlates with its earlier values). Hence, when the signal is shifted with a time lag, it correlates with earlier values.

The autocorrelation makes preferences of bioeffect variants [235], changing chemical reactions, selecting them by their timing, and ordering them by the time required for the desired signal-pathway or enzymatic actions. The biological effects happen on a broad time-scale. An adequately chosen time-fractal modulation promotes the desired autocorrelation of the signal. This modulation noise regulates the biosystems to their normal homeostasis [236], and the spatial autocorrelation also ensures the harmlessness of white-noise excitation [237]. On the other hand, the otherwise healthy support has an opposite impact on malignant processes. It does not harmonize with the malignant processes, is absorbed in an anharmonic way (heating), and does not excite the molecular signals. The modulation signal selectively supports or blocks the cellular membrane's preferred (healthy) or avoidable (malignant) processes. This dynamic effect expands the electrodynamic selection mechanisms, taking effect not only in structural but also in dynamical malignant irregularities in the health system. Both the structure and dynamics of living organisms have a fractal pattern. The spatiotemporal structure and its consequence, the signal character measured by the fluctuations, differentiate malignant tissue from healthy [121] and are measurable by the RF current [122]. The fluctuation difference between malignant and healthy tissues grounds the applied modulation on the RF carrier. The mEHT therapy uses a pattern recognizing and harmonizing fractal modulation [113] to keep the natural homeostatic control as effective as possible. The well-chosen fractal modulation favors the healthy homeostatic control and combats malignancies outside this regulation [113]. The applied modulation in mEHT considers the natural heterogeneity in space and dynamics, including the autocorrelation of living processes.

Depending on the RF frequency, various processes happen in biomaterials, described by frequency dispersions [238]. The a-dispersion covers the low-frequency interactions (~10 Hz–~10 kHz). This dispersion affects the molecules near the cell membrane interacting with the TME, the various membrane components, and the transmembrane proteins. Ionic electrodiffusion affects the dielectric loss of bound water in molecules. Intercellular charging appears as the main change in a-dispersion. This region signifies our excitation activity. However, its direct application is limited by its missing selectivity and the risk of dangerous nerve stimulation. The task was to find a frequency that selects, does not make nerve stimuli safe, and penetrates deeply into the body. The higher frequencies are satisfactory, and the combination of those with low frequency in modulation solves this complex problem by applying 13.56 MHz carrier frequency and modulating it with a spectrum of frequencies in a-dispersion range.

The 13.56 MHz belongs to the b-dispersion. The broad range of b frequency dispersion [111,239] (known as the interfacial polarization effect) allows selective treatment [240]. The chosen 13.56 MHz select the cellular formations [241] interacting with the interface of membrane-electrolyte structures, using Maxwell-Wagner relaxation [239] causing interfacial polarization of the cell membranes [242]. It changes the charge distribution at the cellular or interfacial boundaries [219]. A part of b-dispersion takes effect in the torque of biological macro-molecules (like proteins) and orients these contrary to the thermal background [243].

The range of the d-dispersion [244,245] overlaps with b-dispersion interacts with the dipolar moments of proteins and other large molecules (like cellular organelles, biopolymers) [246], and affects the suspended particles in TME [247]. The d-dispersion is primarily selective for water-bonded lipid-protein complexes in the membrane rafts [219].

Important practical point to choose the carrier frequency in the b/d interval, and internationally approved for industrial, scientific, and medical use. A total of 13.56 MHz was ideal for these requests. The model calculation also shows the importance of the 13.56 MHz [248]. The electrolyte and membrane differences between the malignant and healthy tissue [249,250] are involved in the selection. The membrane lipid targeting has recently come into focus, and it is recognized as having potential for cancer therapy [251]. Note that the rearranging (disordering) of the water structure at the membrane is clearly visible in the absorption spectra and needs energy [252], which could be obtained from the RF current density.

The carrier frequency's RF energy ensures the selection and absorbs on the membrane rafts [105]. The modulation in a-dispersion makes the requested excitation affects their receptors [140], which destructs the malignant cells dominantly in an apoptotic way [253]. Theoretical considerations also prove the nonthermal effect of mEHT, showing that the observed effects could not have a solely thermal origin [254]. The physical origin is also explained [255] and centers on the effect of the modulation.

The bioelectromagnetism determines various features of homeostasis [256]. The modulation is not a single frequency. It is a spectrum of 1/f spectral density in the audio range (<20 kHz), improving the electric field's homeostatic connection by a similar timefractal structure. The autocorrelation of the signal prefers the external apoptotic pathway. The membrane gains the rectified signal [106], so the 10% modulation depth satisfies theexpected signal excitation. The adaptation of this spectrum is in its 1/f ("pink") noise structure [236,237] which depends on the target and automatically modifies the effect of modulation by the noise structure in the TME [147].

This dynamic selection and distortion of malignant cells detect and treat. In this way, the mEHT is a kind of theranostic method.

9.3. Effect of RF Current Density and the Dynamic Heating

Impedance-matched mEHT uses the current density j as an isodose parameter. The current density does not depend on the technical losses outside of the target. It considers only the power which goes into the body. The isodose of j is approximative. It is rigorously true only for homogeneous targets. A large average statistically offers a quasi-homogeneity. This homogeneity expectation is a typical challenge in doses of chemotherapies, which expect the homogeneously transported drug in the body, which selectively destroys the malignancy. In the mEHT method, the same challenge appears in the homogeneity concept.

The j depends on the conductivity (σ) and the electric field strength vector (E): $j = \sigma E \left(\frac{A}{m^2}\right)$. The j vector and the s conductivity are complex numbers, and due to the biomaterial not being a perfect conductor, it is lossy. The electric field drives both the thermal heating and the nonthermal excitation processes, and it is linearly proportional with the complex $j, (E = \frac{1}{\sigma} j)$ so the current density well describes the amount of excitation, so linearly generates a nonthermal effect. In a good approximation, j does not depend on the size of the applied capacitor plates. The size of the plate defines the area $A = r^2 \pi$, of the circular electrode with radius r. The current (I) depends on the electrode voltage (V) and the resistivity (R) between the electrodes: $I = \frac{V}{R}$. The current density $j = \frac{I}{A}$ while $R = \frac{d}{\sigma A}$, where d is the distance between the electrodes. Consequently $j = \frac{V\sigma}{d}$, depends on only the constant parameters and does not depend on the area or radius of the electrode. The j can be kept constant when the electric potential is constant. The volume between the plates has an equal dose, as with the homogeneity principle of systemic chemotherapy.

The power (P) as the absorbed thermal energy depends on the square of the field: $P = \sigma E^2 = \frac{1}{\sigma} j^2 \left(\frac{W}{kg}\right)$. In homeostatic conditions, when the general energy loss is negligible, the measurement of the incident power (correlation with $\mathbf{j}^2$) offers a dose identification. The dose, in this case, is the time summary of the power $(dose = \frac{energy}{mass} = \int P dt = \int \frac{j^2}{\sigma} dt, [\frac{J}{kg}])$. The high efficacy of current matching [257], and the low value of the cooling energy-loss allows this simple dose monitoring [68,258] instead of by the local temperature.

Consequently, mEHT has no compulsory demand to measure the temperature. It has enough accuracy to measure the absorbed energy by the incident, not forced RF current density [68].

When the temperature grows, the heating period demands a higher dose than when keeping the temperature constant [150,159]. The higher power increases the dose by $j \sim \sqrt{P}$.
The heating excites the selected molecular clusters and actively promotes the ICD and the essential immuno-related processes [31]. Maintaining the temperature compensates for the energy losses, so it needs a smaller dose. The unchanged temperature with lower current density produces significantly less apoptosis as the active heating period raises the temperature [259]; Figure 10. The amount of apoptosis increases by the synergy of the temperature dynamics and the electric field, but practically does not change when the temperature stabilizes and remains approximately constant. Stochastic explanation describes this phenomenon [31]. This complexity involves the similarity of the temperature and the electric field to improve the chemical reaction rate [102]. This effect provides a possibility to improve the heterogenic selective cell destruction by mEHT in clinical practices. The therapy needs a protocol that keeps the temperature development's dynamism [31]. Step-up heating considering the blood flow washing time (approximately 6 min) works approximately well.

Contrary to the homeostatic balancing, intensive cooling supports the growth of the incident power. Forced intensive cooling increases the current density because the incident power must increase quadratically, replacing the power taken by the cooling. Due to the applied cooling (energy loose), significantly modifying the incident power does not provide accurate dose measurement. The dose needs other direct registering, like temperature or current density j. The j flows through the patient practically independent from the energy losses, characterizes the absorbed SAR only. Consequently, the direct measurement of the current density appears as the dose in an intensive cooling process instead of the power.

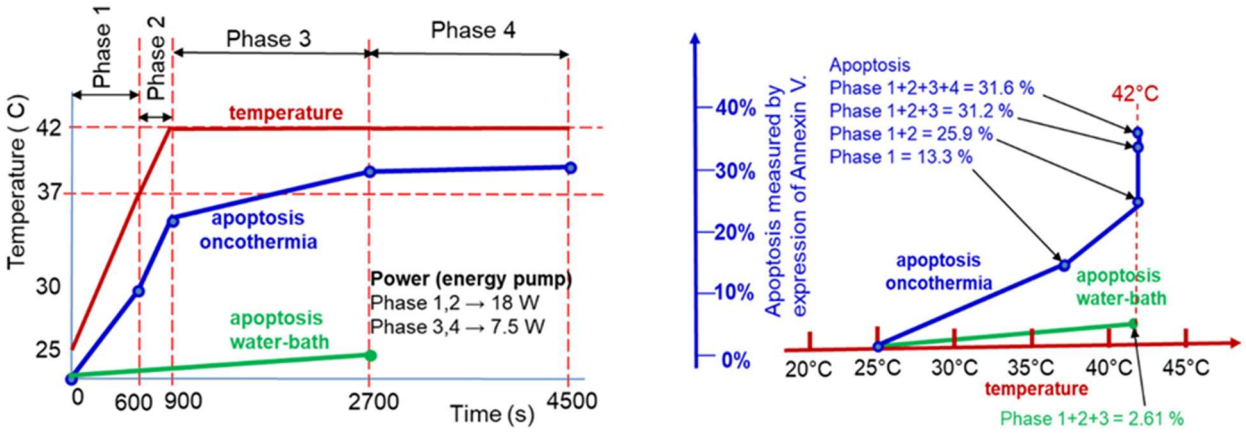

Figure 10. The effect of heating and maintaining the temperature on apoptosis. The mEHT had significantly higher apoptotic cells than the wHT at the same temperature.
(a) The apoptosis saturated when the temperature became constant at the temperature maintenance period of treatment.
(b) The temperature dependence of apoptosis shows a limit at the saturated temperature.

The apoptosis of malignant cells shows the efficacy of mEHT therapy. The apoptotic cellular degradation could be used for dosing in the active heating period [259]; Figure 11. Consequently, the connection of the apoptotic cell degradation and current density appears like an essential task of the new dose when the j is enhanced by cooling.

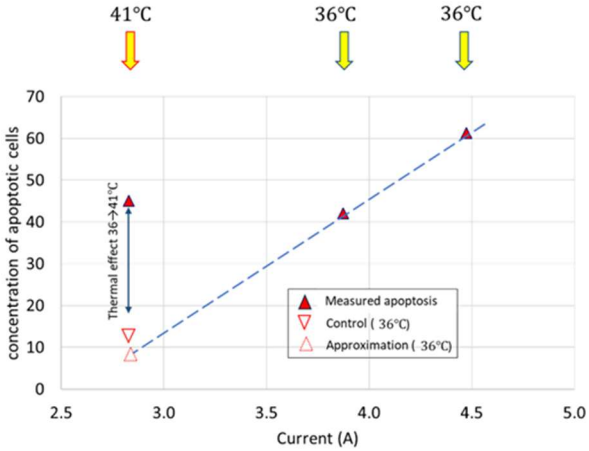

Figure 11. The apoptosis linearly increases by the increase of current density. The higher current density was reached by intensive cooling of the sample, keeping the medium at 36 C, while the standard treatment was at 41 C. The difference in the approximated apoptosis at low current at 36 and at 41 C is produced by the thermal effect.

The current density is proportional to the percentage of apoptosis. Measurements on the U937 cell line well prove this concept [136]. The concentration of apoptotic cells grows linearly with the current density j of mEHT; Figure 11. The standard mEHT treatment was performed at 41 C, with a standard current density. The control is a sham experiment, which fits a linear line. The heat effect of the standard treatment could be approximated from this experiment.

The current density j appears as an optimal dose of mEHT. On the other hand, the j does not offer a dose solution for conventional LRHT methods, where the patient impedance matching is far from the resonance. The measured current density in LRHT does not show the effective targeting of the tumor, having reflected imaginary parts and various other impedance losses. Temperature measurement remains mandatory in the conventional homogeneous mass heating of LRHT.

The percentage of the apoptotic processes induced by mEHT grows by increasing current density, which participates in both fundamental processes of this method: in the thermal and nonthermal action components. The thermal effects ensure the conditions for optimal nonterminal (excitation) processes and the rates of chemical reactions (mostly enzymatic assistances) afterward. We may regard the current density as a treatment dose, having the same role in mEHT as the ionizing isodose in RT.

The j represents an isodose distribution in the target with mEHT, like the beam isodose in the RT method. Note that this dose could happen only when the energy loss is low, and the overall energy intake is not as high as the heterogeneity differences that may appear with massive heating. Hence, the sensing heterogeneity limits the incident power. When the heating forces isothermal conditions, the $SAR \sim j^2$ dominates, and the heterogenic structure becomes thermally homogeneous. The isothermal temperature overshadows the electrical differences in the target. The electromagnetic differences become gradually visible when the incoming energy decreases. The electromagnetic effects distinguish the electrical differences when its average absorption intensity does not exceed the distinct energy levels of the difference between the absorption values of the desired differentiable units, so when the $j \geq j^2$. So, in conditions when $j \leq 1$, the selection of tumor cells is effective.

The proper modulated signal may trigger resonant excitations of the proteins [111], which initiates extrinsic signal pathways for apoptosis [101,253] in a dose-dependent way [259]. Consequently, the thermal factor generating hyperthermia temperatures creates an appropriate condition for the nonthermal electric field effect by optimizing the reaction rates and enzymatic reactions. The direct thermal and nonthermal effects complete each other, creating a complex synergy of mEHT actions; Figure 12.

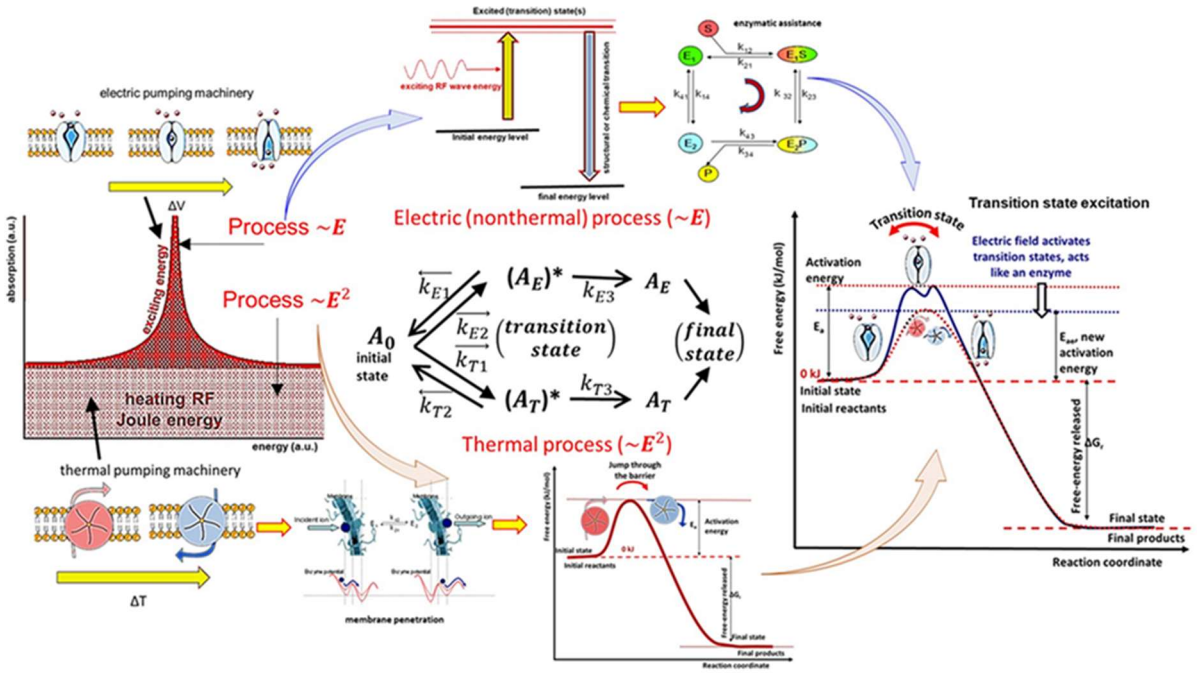

Figure 12. The measured thermal and nonthermal effects of mEHT. The thermal effect has an Arrhenius character, while the nonthermal effects are quantum-mechanical, promoting enzymatic processes, pushing through the transitional state. The nonthermal processes use the thermal conditions for optimal reaction rates. (For details, see in the text.). The * denotes metastable transitional state.

9.4. Complementary to Radiotherapy

The temperature distribution in the hyperthermic process also has complex balancing. The homogeneously high temperatures (>42 C) in LRHT could block the enzyme activity [260] and so arrest the DNA-repairing enzymes and optimize the cellular degradation of malignant cells [261]. However, they produce massive necrosis, which makes the DAMP release unstable, as well as the high temperature (>40 C) blocking the immune-cell activity [96], which would be necessary for APC production to form tumor-specific processes.
The heterogenic heating of mEHT unites the advantages of the high cellular temperature with the mild average. The thermal component of mEHT (T_{mEHT}) produces a mild hyperthermic average $(38\ ^{\circ}\mathrm{C} \leq T_{mEHT} < 40\ ^{\circ}\mathrm{C})$, which is enough for a blood-flow increase [132] to sensitize the RT, but less than the immune-cell inactivation limit [96]. The temperature of the selected cells (T_{cell}) is well over the average $(T_{cell} \gg T_{mEHT})$, at least by 3 C as obtained from the apoptotic rate [95,133] and tumor degradation [135,150] (see Figure 9). Complex balancing appears in various features of the hyperthermia processes. LRHT accelerates the distortions ofmalignant cells, reducing the a/b ratio in the linear-quadraticmodel (LQM) of cell-survival in RT [262]. The LQMneglects the third termof the Taylor expansion of the function of dose (f (D)) in an exponential dependence from the efficacy (RT_{eff}), which is reciprocal with the cellular survival $(S_{cell} = \frac{1}{RT_{eff}})$, supporting $S_{cell} = e^{-f(D)} \cong e^{-\alpha D - \beta D^2}$.

High efficacy means a quick decrease of the Scell by the applied RT dose, so the quadratic term is expected to be high. The hypo- or hyper-fractionating tries to fit the a/b ratio to the survival of cellular variants [263]. It is predicted that LRHT optimizes the a/b ratio [264], which can be used for quantitative reference for an equivalent radiation dose of mEHT [129]. Due to the LRHT effect varying by types of cancer cells, the quantitative dose reference was measured on two different lung cancer cell lines, A549 and NCI-H1299. The dose escalation by mEHT well fits LQM and made it possible to estimate the reference dose determined by equivalence.

The daily RT fractions destabilize the cellular membrane [265], which is a possible general target for cancer therapy [266]. The mEHT attacks the membrane by thermal and electric field load, supporting the membrane destabilization. The double stress of mEHT (heat and field) probably also destabilizes the plasma membrane. The observed intensive apoptosis in many mEHT measurements in various tumors and the synergy with fractional RT concludes that the membrane destabilization helps the apoptosis and does not lead to necrotic cell death. The tripling of the apoptotic bodies in radioresistant pancreas tumors in mono-mEHT and mEHT + RT combined therapies [134] supports the idea that the destabilized membrane helps form apoptotic bodies.

Both the RT and the mEHT induce reactive oxygen species (ROS) as well as damaging subcellular structures and organelles (such as the cytoplasmic membrane, endoplasmic reticulum (ER), ribosome, mitochondria, and lysosome), affecting various biological activities globally altering the living processes of cancer cells, and possibly promoting autophagy too [61]. Results show the intensive promotion of autophagy with mEHT and mEHT + RT to produce apoptosis [158].

The synergy has been proven clinically in the combination of mEHT compared to RT or ChRT alone [116,179]. The frequency of LRHT and the timing with RT are essential considerations in the clinical practice of complementary therapy. The combined application of these methods has synergy, considering the complex regulations connected with both parts. The central focus of the RT makes a single or double break of a DNA strand (SSB or DSB). Inhibiting the DNA repair is the expected primary support from LRHT. RT needs radiosensitive conditions to fulfill its task, while LRHT (as shown with mEHT too [132]) gives oxygenation for the inhibition of the repair and/or arrests the activity of repair enzymes. The gH2AX monitors the repair after RT is connected to the DSB of DNA.

9.5. Sequences and Timing of Treatments in Complementary Therapy

Both therapies, mEHT and RT, could cause cellular destruction in their stand-alone application, inducing necrosis. mEHT in monotherapy produces massive apoptosis [134,142,150], even in radioresistant cases [148]. These distortion mechanisms are mostly independent of the subsequent therapy,while in the application as the second in the sequence, a strong dependence could be formed.

The optimal timing between RT and mEHT has a spatiotemporal complexity, challenging the sequencing and frequency of the combination. The RT defines the application sequence:

- When the oxygenation (blood flow intensity) is high, we expect sensitivity for RT, so apply it first. The maximal frequency of mEHT is every second day.
- When the tumor has hypoxic conditions (low oxygen content), apply the first mEHT to increase it and sensitize the RT. Further considerations can modify the above sequences depending on the tumor and its grade. The temperature effect also modifies the clinical issues, so we list some features in general for HT effects, where mEHT could also be involved.
- When HT is applied first, it sensitizes the RT by oxygenation of the tumor, but there could also be an inhibitory effect when HT induces hypoxic conditions, which may happen at higher temperatures than 43 C, which usually does not happen with mEHT.
- Both HT and RT produce heat shock proteins (HSPs). The RT-induced stress also produces these chaperone proteins in different amounts and types. For example, HSP70 and HSP27 are involved in regulating the base excision repair (BER) enzymes in response to RT stress [267].
- Developing an antiapoptotic HSP70 chaperone defines the minimal time between the repeated HT treatments. Due to the HSP70 back to the baseline 48 h post-treatment. Consequently, every second day is recommended as the most frequent application. The maximal time between the HT treatments is one week when the possible buildup of the adaptive immune system finishes.
- HT has effects that are not dependent on enzyme activity, such as a variety of irreparable DNA mismatches, heat-activated methylation, hydrolysis, mono- or di-adduct damages, etc. The activity of repairing enzymes grows by temperatures, but at high temperatures (generally 43 C) it blocks their activity. The enzyme block could be helpful. The high temperature causes intense hypoxia in the tumor and suppresses the RT efficacy, so mild heating of mEHT is optimal.
- HT at lower temperatures is sufficient to enhance perfusion [70] and the formation of numerous reactive oxygen species (ROS), such as hydrogen peroxide, superoxide anions, nitric oxide, hydroxyl radical, etc. Superoxide dismutase (SOD) forms an essential component in the defense against ROS. Heat stress could cause a decrease in SOD levels, which also leads to cell death [268].
- There is a risk that HT could support the activity of DNA repairing enzymes when it is applied after RT, even also when the end temperature is as high to block the enzymatic activity, because the first part of the heating is a “warming up”, presenting a preheating, which could increase the activity of reparation enzymes [269].

The DSBs are typically repaired within two to six hours following RT. A higher rate of the $\gamma H2AX$ expression was observed at three hours as compared to one hour post-RT treatment, signaling that the DSBs are still

left unrepaired [270] 3 h posttreatment. However, this could depend on the type of malignant cells [271]. By 6 h posttreatment, $\gamma H2AX$ decreases approximately to half the amount [272]. Combining LRHT with 2 Gy radiation, the concentration of $\gamma H2AX$ after 1 h at 42 C is higher than at 39 °C [273], and it is observed that a shorter time between the treatment parts results in a higher number of $\gamma H2AX$.

A 90 min timing between LRHT and RT significantly decreases the treatment efficacy in clinical practice compared to a shorter (60 min) delay [274]. The subsequent in vitro modeling on SiHa and HeLa cell lines [275] did not significantly impact the time interval as in the clinical data, while earlier in vitro studies showed a significant difference preferring the treatments to follow each other quickly [276]. Another in vitro experiment supports quick sequences, observing that the DSB of DNA, measured with $\gamma H2AX$, vanishes after 2 h of RT [274]. Earlier, it was shown that simultaneous application has the highest efficacy [277].

A high number of patients was studied, and a large impact of timing between LRHT and RT of 4 h was not observed [278]. This contradictory result started an intensive debate between the research groups [279,280]. The discussed disagreement of the two clinical studies is confusing indeed. The reasons could have multiple components. The different devices, the sequence order of the treatments, and the frequency of the LRHT application could represent differences between the therapies and lead to a contradictory conclusion.

The first thirty minutes of “warming up” could be considered preheating, which could increase the activity of reparation enzymes, including a risk that LRHT increases the DNArepairing enzyme activity and supports the repair of DNA when LRHT is applied second in the sequence [269]. The warming-up period is mostly technically dependent, but dependson the nonlinear physiologic control of the complex regulation of the patient, which could rely on the bolus cooling and other device-dependent conditions. The warmingup period with the non-homogeneous thermal effect by mEHT behaves oppositely than conventional LRHT. mEHT generates the most significant apoptotic activity in the warmingup period [259]. When the LRHT-induced temperature is high enough (>42.5 C), it could imply the blocking of the repairing enzymes. However, the necrotic cell-killing is also intensive in this high-temperature regime so that the DNA damage could have secondary importance in cellular degradation.

Note, the murine models in vivo (C3H mammary carcinoma) [281] show the thermal enhancement ratio (TER) extensively decreases and at the end vanishes after 4 h in both sequences when the LRHT precedes or follows RT, while the tumor control has a much narrower (30 min) and non-symmetric interval.

The cell-cycle arrest is connected to the electric field activity and is primarily nonthermal [282]. A part of the electric field penetrates the cell through the voltage-sensitive phosphatase (VSP) [283] and modifies the cytoskeletal polymerization [138]. The field controlled phosphorous hydrolysis could have an essential role in cytoskeleton restructuring and resonant-type behavior phenomena. The amplitude-modulated carrier frequency can produce stochastic resonance, selectively inducing biological enzymatic reactions and polymerization [111].

With care about the physiologic complexity, mEHT takes this contradictory situation seriously and defines the clinical guideline for the complementary therapy, considering the BF as the primary factor [284]. When the BF is low, the RT efficacy is suboptimal; the guideline proposes applying mEHT first, increasing the oxygenation, and helping the set of RT reactions be more effective with the higher reaction rate of molecular changes promoting the fixing of the strand break in the DNA. The mild hyperthermic factor of mEHT optimizes the blood-perfusion to support the RT, and the most optimal frequency of mEHT is every two to three days [285], which well correlates with the timing relaxation of the induced protective HSP70 in the heated malignant cells [253]. This frequency of mEHT treatment fits well with the clinical evaluations, which are fixed in the internationally accepted guideline of mEHT therapy [284].

When LRHT or mEHT is the first in the chosen sequence, it provides oxygenation, which sensitizes the RT and produces protecting HSPs. The RT-induced stress also produces repairing chaperone proteins, like HSP70 and HSP27, which regulate the base excision repair (BER) enzymes in response to RT stress [267]. In addition, the heat effect has other enzyme-independent effects such as sensitizing to the RT: it could cause a variety of irreparable DNA mismatches, heat-activated methylation, hydrolysis, etc. Mild heating also produces a sufficient enhancement of blood perfusion [70] and enhances the formation of numerous reactive oxygen species (ROS), such as hydrogen peroxide, superoxide anions, nitric oxide, hydroxyl radicals, etc. The heat stress could decrease the superoxide dismutase (SOD) level, weakening the defense against ROS, leading to cell death [268]. mEHT increases the ROS level more extensively than homogeneous (isothermal) heating [136], supporting the RT. Other physiological effects of heating (such as the increase in the electrolyte transport systems like the blood flow and lymph) could enhance the success of RT, together with the

increased oxygenation. However, there could also be an inhibitory effect when LRHT induces hypoxic conditions, which may happen at higher temperatures, while mEHT reduces the hypoxic level [286], vastly promoting the better efficacy of RT.

9.6. Immunogenetic Effects

The heat and electrical stresses produce HSP chaperone proteins with mEHT to protect the cells from stress damage. The most characteristic protein family of chaperones, HSP70, acts like a "double edge sword" [287,288], exhibiting both inflammatory and anti-inflammatory, protumoral or antitumoral, immune stimulator or immune suppressor, etc. functions. The role of HSPs depends on the conditions of their activity forming "friends or foes" [289–291]. The primary function of intracellular HSPs (iHSPs) is to avoid the cell's apoptosis and protect the cell's living conditions irrespective of its malignant or healthy state. Nevertheless, certain conditions may promote the secretion of HSPs in the transmembrane position (mHSPs) or their escape extracellularly to the TME milieu (eHSPs). mHSPs may signal to make malignant cells recognizable to NK cells [169]. eHSPs could offer even more help in the elimination of malignancies. The mHSP70 carries an "info signal" [292], with the genetic properties for producing antigen-presenting cells (APCs) and creating killer T-cells [293], by the maturation of dendritic cells (DCs) [294]. This process requires that the destruction of the cell is "gentle enough" and does not degrade the DAMP proteins.
When the appropriate molecules have a particular spatiotemporal order (immunogenic cell death, ICD), the set of molecules ensures that the mHSP70 becomes a forceful "friend" losing its "double-edge sword" behavior, and the genetic info well maturates the DCs forming APCs. The process directly applies immune-oncology principles, and so ICD is of tremendous clinical interest [295].

The major achievement of mEHT is activating the innate and adaptive immune system to eliminate tumor cells both locally and systemically in the whole body. The induced mHSPs mark cancer such as to be recognized by the innate immune action with NK cells [169]. The secretion of eHSPs and the correct spatiotemporal set of DAMP may develop tumor-specific adaptive immune processes to attack the cancer cells all over the body.

In such a way, mEHT turns the local treatment systemic (abscopal), as proven preclinically [170,174] and clinically too [116,179,296].

The abscopal effect was discovered in RT more than 60 years ago [297], but its application was hindered because it was observable only in low radiation doses, limiting the expected direct local degradation. The recent rediscovering of the abscopal effect with RT shifts the idea from myth to reality [298] and sees it explained by molecular processes [299]. The synergy of RT with the emerging checkpoint inhibitor and antibody immune-therapies provides new curative possibilities [300–302]. This field could have a new combination: mEHT supported TSI develops immune adaptation by the tumor antigens providing an abscopal addition to local RT.

The synergy of mEHT and RT turns these local treatments systemic, creating tumorspecific immune processes (TSI) that extend the abscopal effect. The immunotherapy strategy optimizes the RT with mEHT for the best efficacy [303] and highest safety [178]. The abscopal effect could renew the complementary applications of RT with this theranostic synergy and well fits to the emerging trend of immuno-oncology too. This function connects mEHT to the emerging trend in the field, to immuno-oncology [304]. The in-situ feedback loop of the immune effects of mEHT is shown in Figure 13.

Finally, we may conclude that the thermal and nonthermal effects represent the nonlinear (~ j2) and linear (~ j) dependence of the current density and in consequence of the electric field, but their functions differ. The thermal effect ensures the general energy background, while the nonthermal is resonant; Figure 14.

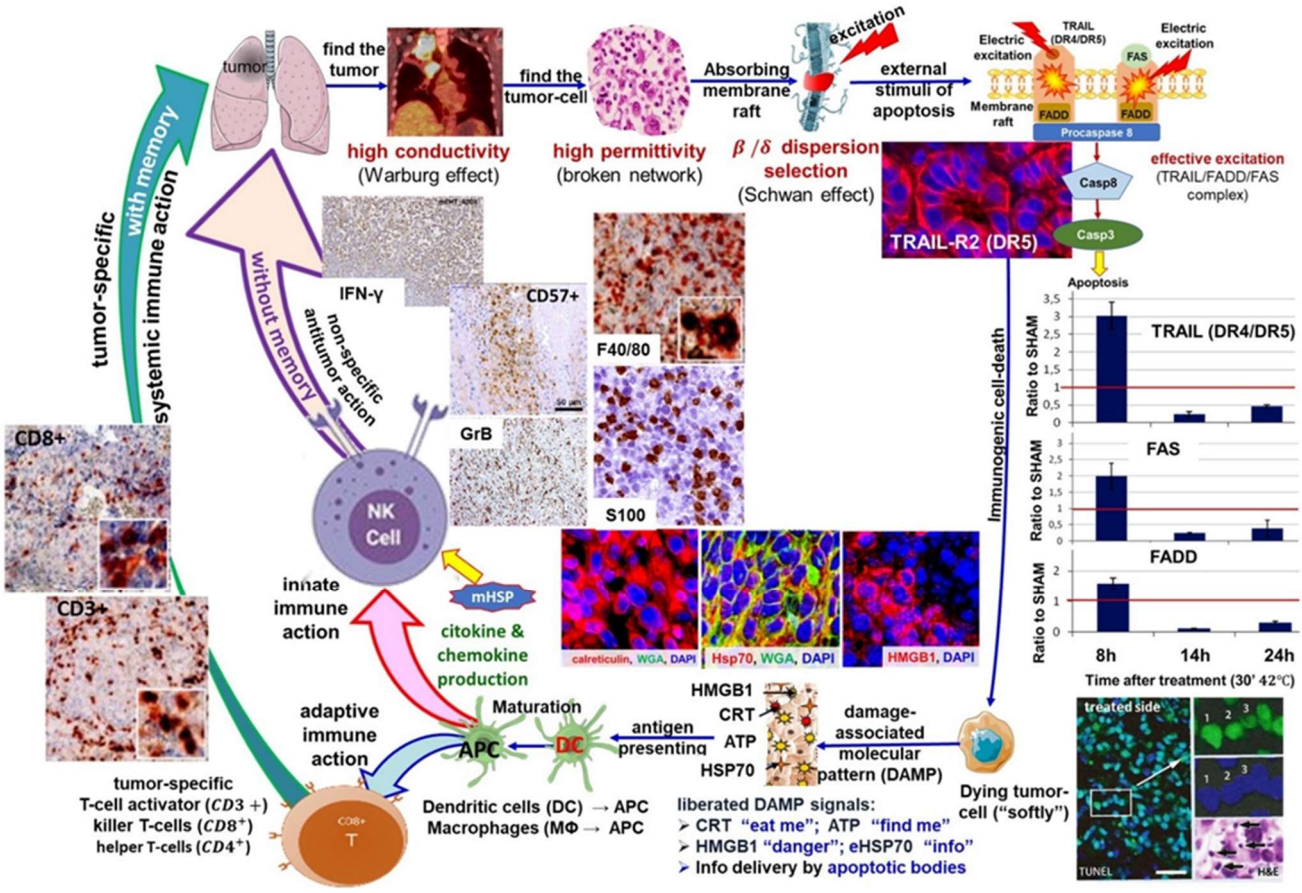

Figure 13. The negative feedback structure of the abscopal effect shows a complex loop from recognizing the antigens to their use in tumor-specific immune processes. The experiments are from various publications. The loop summary only demonstrates how the loop works. The measurements are from the following publications: the selection line reviewed [101], TRAIL-R2-FAS-FADD complex [153]; apoptosis [133,150], ICD [305]; DAMP [174], APC [163] immune [172], NK, Granzyme [169], IFN- g [182], CD3+, CD8+ [163,170].

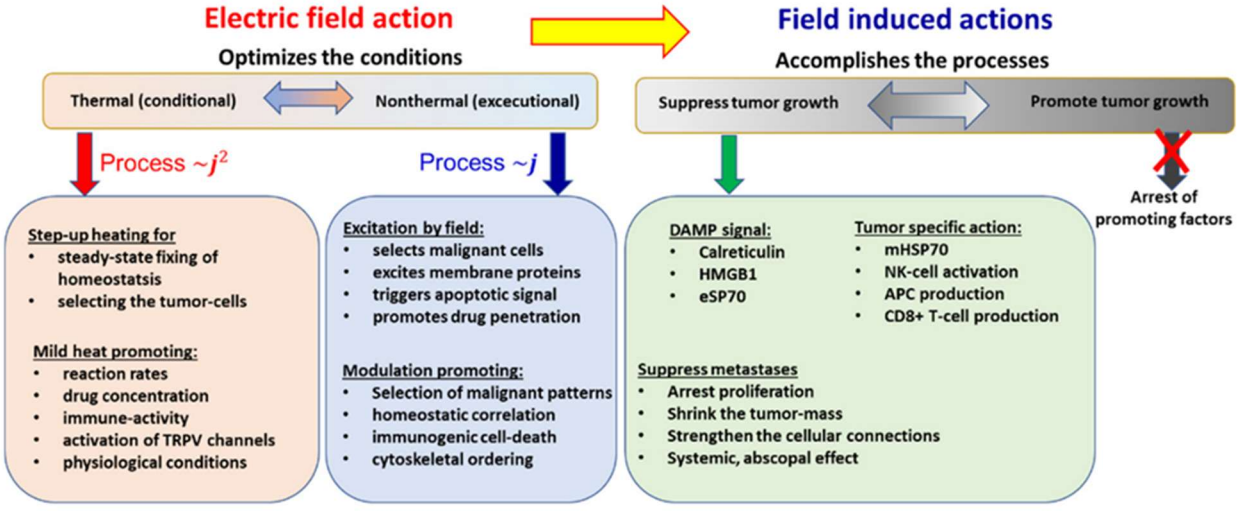

Figure 14. The process of thermal and nonthermal effects of selective, heterogenic heating. The field-induced actions are complex, requiring both the thermal (conditional) and nonthermal (excitation) processes.

The synergy of mEHT with radiotherapy completes the advantages with essential factors additionally to the conventional heating processes; Table 3.

Table 3. The essential addition of mEHT to the synergistic RT-with-hyperthermia methods

Synergistic Addition of Modulated Electrohyperthermia	
Nanoscopic action	Selects malignant cells and nonthermally excites, marginal heating of the healthy cells renders less vulnerable to ionizing radiation
Apoptotic effect	Mostly natural apoptosis, no inflammation, no large cytokine liberation, no extra injury current, no extra pH hypoxia
Immune effect	Immunogenic processes, abscopal effect. Both the innate and adaptive immune system are activated, vaccination facility (patented)
Homeostatic effect	Harmonized with homeostatic controls, the temperature increase in the nuclei is moderate, does not make an additional enzymatic activity for reparation
Side effects	Lower incident power puts less load on the skin, which is anyway irritated by radiotherapy, so the synergy has fewer adverse effects
Quality of life	Improves quality of life by reducing side effects
The broad range of application	Possible to combine with radiotherapy in localizations which were not possible with radiative hyperthermia (like the brain)
Applicable for palliative conditions	Resensitizes to radiotherapy in highly metastatic advanced refractory cases, when conventional therapies are ineffective
Long-time application	mEHT is applicable as a chronic treatment for as long as is necessary with radiotherapy complementation
Applicability	mEHT is applicable with most comorbidities as well as in combination with any other oncotherapies

10. Summary

To solve the challenges of conventional LRHT, mEHT has modified the isothermal concept of oncological hyperthermia, focusing on the cellular distortion of malignant cells. The new paradigm strongly considers the goal of LRHT, concentrates on the malignant cells, and destroys them in the targeted volume. The principal idea is to use the natural heterogeneity of the cancerous tissue, using the particular living conditions of malignant cells, making them different from healthy cells and healthy host tissue. mEHT has an isodose. The RF current density is defined similarly to the ionizing isodose in RT practice. The degradation of the malignant cells and controllable stable dosing guides the efforts in synergy with RT.

Modulated electro-hyperthermia complements radiotherapy with the precise heterogenic cellular selection of malignant cells. The transmembrane protein clusters (rafts) are excited by mEHT and heated in synergy with the double-strand breaking of the DNA by RT. The synergistic harmony of ionizing, thermal, and nonthermal effects allows the immunogenic cell death of the malignant cells and develops tumor-specific immune actions in both the innate and adaptive immune system in situ during the treatment. The recognition characteristic is amalgamated with the curative therapy, so the mEHT + RT synergy is theranostic.

The selection process of mEHT uses the malignant attributes that characterize all malignancies: the metabolic, dynamic, and structural differences. This universality of mEHT does not depend on the mutation variants of cancer. Consequently, mEHT—like RT—independently breaks the DNA strands of various malignant mutants, so the synergy of the two methods may form a forceful cancer therapy. The final result is a systemic abscopal) effect that destroys the malignant cells in the entire body irrespective of the possibility of its visual imaging. The complex integrating effect of mEHT + RT triggers physiologic and cellular changes by thermal and ionizing components. Additionally, the complementary application to RT triggers molecular and immunological changes with resonant and ionizing excitation. All complex balances have progenitors of functioning promoters and suppressors for balancing.

mEHT changes the LRHT paradigm from homogeneous mass heating to a heterogeneous selective one. The difference between the two approaches has been proven in various experiments. Figure 15 shows a rough comparison of mass heating with selective heating.

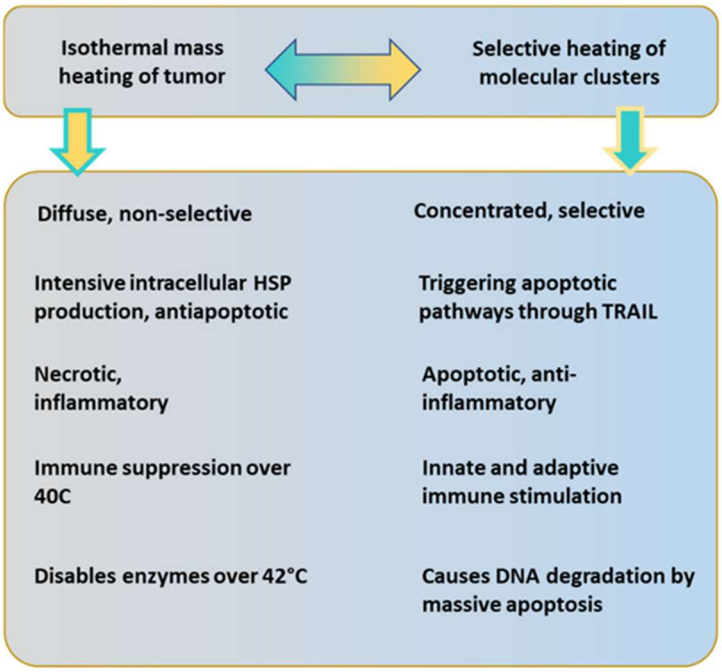

Figure 15. The major differences between isothermal and selective paradigm heating are listed in the columns.

11. Conclusions

mEHT results well prove the nanothermia efficacy and its conceptual success. The synergy with RT delivers effective cell degradation in tumors and develops an abscopal effect, using the homeostatic adaptation of the healthy immune regulation to degrade the malignant cells systemically in the entire body. The synergy is verified by preclinical and validated by clinical results.

Funding: This work was supported by the Hungarian National Research Development and Innovation Office PIACI KFI grant: 2019-1.1.1-PIACI-KFI-2019-00011.

Conflicts of Interest: Andras Szasz is the Chief ScientificOfficer ofOncothermKft. Hungary/Oncotherm GmbH Germany.

References

1. Seegenschmiedt, M.H.; Vernon, C.C. A Historical Perspective on Hyperthermia in Oncology. In Thermoradiotherapy and Thermochemotherapy; Seegenschmiedt, M.H., Fessenden, P., Vernon, C.C., Eds.; Springer: Berlin/Heidelberg, Germany, 1995; Volume 1, pp. 3–44.
2. Vaupel, P.W.; Kelleher, D.K. Metabolic status and reaction to heat of normal and tumor tissue. In Thermoradiotherapy and Thermochemiotherapy; Seegenschmiedt, M.H., Fessenden, P., Vernon, C.C., Eds.; Springer: Berlin/Heidelberg, Germany, 1995; Volume 1, pp. 157–176.
3. Griffiths, H.; Ahmed, A.; Smith, C.W.; Moore, J.L.; Kerby, I.J.; Davies, R.M.E. Specific absorption rate and tissue temperature in local hyperthermia. Int. J. Radiat. Oncol. Biol. Phys. 1986, 12, 1997–2002. [CrossRef]
4. Dutz, S.; Hergt, R. Magnetic nanoparticle heating and heat transfer on a microscale: Basic principles, realities and physical limitations of hyperthermia for tumour therapy. Int. J. Hyperth. 2013, 29, 790–800. [CrossRef] [PubMed]
5. Datta, N.R.; Puric, E.; Klingbiel, D.; Gomez, S.; Bodis, S. Hyperthermia and Radiation Therapy in Locoregional Recurrent Breast Cancers: A Systematic Review and Meta-analysis. Int. J. Radiat. Oncol. 2016, 94, 1073–1087. [CrossRef] [PubMed]
6. Datta, N.R.; Rogers, S.; Ordonez, S.G.; Puric, E.; Bodis, S. Hyperthermia and radiotherapy in the management of head and neck cancers: A systematic review and meta-analysis. Int. J. Hyperth. 2016, 32, 31–40. [CrossRef] [PubMed]

7. Datta, N.R.; Rogers, S.; Klingbiel, D.; Gomez, S.; Puric, E.; Bodis, S. Hyperthermia and radiotherapy with or without chemotherapy in locally advanced cervical cancer: A systematic review with conventional and network meta-analyses. Int. J. Hyperth. 2016, 32, 809–821. [CrossRef]

8. Rogers, S.J.; Datta, N.R.; Puric, E.; Timm, O.; Marder, D.; Khan, S.; Mamot, C.; Knuchel, J.; Siebenhüner, A.; Pestalozzi, B.; et al. The addition of deep hyperthermia to gemcitabine-based chemoradiation may achieve enhanced survival in unresectable locally advanced adenocarcinoma of the pancreas. Clin. Transl. Radiat. Oncol. 2021, 27, 109–113. [CrossRef]

9. Issels, R.D.; Lindner, L.H.; Verweij, J.; Wessalowski, R.; Reichardt, P.; Wust, P.; Ghadjar, P.; Hohenberger, P.; Angele, M.; Salat, C.; et al. Effect of Neoadjuvant Chemotherapy Plus Regional Hyperthermia on Long-term Outcomes Among Patients with Localized High-Risk Soft Tissue Sarcoma. JAMA Oncol. 2018, 4, 483–492. [CrossRef]

10. Falk, M.H.; Issels, R.D. Hyperthermia in oncology: Invited Review. Int. J. Hyperth. 2001, 17, 1–18. [CrossRef]

11. Streffer, C.; van Beuningen, D.; Dietzel, F.; Röttinger, E.; Robinson, J.E.; Scherer, E.; Seeber, S.; Trott, K.R. Cancer Therapy by Hyperthermia and Radiation; Urban and Schwarzenberg: Baltimore, MD, USA; Munich, Germany, 1978.

12. Seegenschmiedt, M.H.; Fessenden, P.; Vernon, C.C. Thermoradiotherapy and Thermochemotherapy, Volume 2: Clinical Applications;Springer: Berlin/Heidelberg, Germany, 1996.

13. Kosaka, M.; Sugahara, T.; Schmidt, K.L.; Simon, E. Thermotherapy for Neoplasia, Inflammation, and Pain; Springer: Tokyo, Japan, 2001.

14. Matsuda, T. Cancer Treatment by Hyperthermia, Radiation and Drugs; Taylor & Francis: London, UK; Bristol, PA, USA, 1993.

15. Urano, M.; Douple, E. Hyperthermia and Oncology: Volume 2, Biology of Thermal Potentiation of Radiotherapy; VSP BV: Utrecht, The Netherlands, 1992.

16. Hehr, T.; Wust, P.; Bamberg, M.; Budach, W. Current and potential role of thermoradiotherapy for solid tumors. Onkologie 2003, 26, 295–302.

17. van der Zee, J.; Gonzalez, D.G.; van Rhoon, G.C.; van Dijk, J.D.; van Putten,W.L.; Hart, A.A.; The Dutch Deep Hyperthermia Group. Comparison of radiotherapy alone with radiotherapy plus hyperthermia in locally advanced pelvic tumors: A prospective, randomised, multicentre trial. Lancet 2000, 355, 1119 1125. [CrossRef]

18. Wust, P.; Hildebrandt, B.; Sreenivasa, G.; Rau, B.; Gellermann, J.; Riess, H.; Felix, R.; Schlag, P.M. Hyperthermia in combined treatment of cancer. Lancet Oncol. 2002, 3, 487–497. [CrossRef]

19. Overgaard, J.; Gonzalez, D.; Hulshof, M.C.; Arcangeli, G.; Dahl, O.; Mella, O.; Bentzen, S.M. Randomised trial of hyperthermia as adjuvant to radiotherapy for recurrent or metastatic malignant melanoma. Lancet 1995, 345, 540–543. [CrossRef]

20. van der Zee, J.; Truemiet-Donker, A.D.; The, S.K.; Helle, P.A.; Seldenrath, J.J.; Meerwaldt, J.H.; Wijnmaalen, A.J.; van den Berg, A.P.; van Rhoon, G.C.; Broekmeyer-Reurink, M.P.; et al. Low-dose reirradiation in combination with hyperthermia: A palliative treatment for patients with breast cancer recurring in previously irradiated areas. Int. J. Radiat. Oncol. Biol. Phys. 1988, 15, 1407–1413. [CrossRef]

21. Vernon, C.C.; Harrison, M. Hyperthermia with low-dose radiotherapy for recurrent breast carcinoma. Lancet 1991, 337, 59. [CrossRef]

22. Bicher, J.I.; Al-Bussam, N.; Wolfstein, R.S. Thermotherapy with curative intent–breast, head, and neck, and prostate tumours. Dtsch. Z. Fur Oncol. 2006, 38, 116–122.

23. Peeken, J.C.; Vaupel, P.; Combs, S.E. Integrating Hyperthermia into Modern Radiation Oncology: What Evidence Is Necessary? Front. Oncol. 2017, 7, 132. [CrossRef]

24. Horsman, M.R.; Overgaard, J. Hyperthermia: A Potent Enhancer of Radiotherapy. Clin. Oncol. 2007, 19, 418–426. [CrossRef]

25. Molls, M. Hyperthermia—The actual role in radiation oncology and future prospects. Strahlenther. Oncol. 1992, 168, 183–190.

26. Seegenschmiedt, M.H.; Feldmann, H.J.; Wust, P. Hyperthermia–Its actual role is radiation oncology. Strahlenther. Oncol. 1995, 171, 560–572.

27. Emami, B.; Scott, C.; Perez, C.A.; Asbell, S.; Swift, P.; Grigsby, P.; Montesano, A.; Rubin, P.; Curran, W.; Delrowe, J.; et al. Phase III study of interstitial thermoradiotherapy compared with interstitial radiotherapy alone in the treatment of recurrent or persistent human tumours: A prospectively

controlled randomized study by radiation therapy oncology group. Int. J. Radiat. Oncol. Biol. Phys. 1996, 34, 1097–1104. [CrossRef]

28. Wust, P.; Rau, B.; Gremmler, M.; Schlag, P.; Jordan, A.; Löffel, J.; Riess, H.; Felix, R. Radio-Thermotherapy in Multimodal Surgical Treatment Concepts. Oncologie 1995, 18, 110–121. [CrossRef]
29. Overgaard, J. The current and potential role of hyperthermia in radiotherapy. Int. J. Radiat. Oncol. Biol. Phys. 1989, 16, 535–549. [CrossRef]
30. Bauer, K.H. Das Krebsproblem; Springer: Berlin/Heidelberg, Germany, 1964.
31. Szasz, O.; Szasz, A. Approaching Complexity: Hyperthermia Dose and Its Possible Measurement in Oncology. Open J. Biophys. 2021, 11, 68–132. [CrossRef]
32. Romanovsky, A.A. Thermoregulation: Some concepts have changed. Functional architecture of the thermoregulatory system. Am. J. Physiol. Integr. Comp. Physiol. 2007, 292, R37–R46. [CrossRef]
33. Vaupel, P.W.; Hammersen, F. Mikrozirkulation in malignen Tumoren. 6. Jahrestagung der Gesellschaft für Mikrozirkulation e.V., München, November 1982; Karger: Basel, Switzerland, 1983; ISBN 978-3-8055-3762-9.
34. Charkoudian, N. Skin Blood Flow in Adult Human Thermoregulation: How ItWorks, When It Does Not, and Why. Mayo Clin. Proc. 2003, 78, 603–612. [CrossRef]
35. Zhao, Z.; Yang, W.Z.; Gao, C.; Fu, X.; Zhang, W.; Zhou, Q.; Chen,W.; Ni, X.; Lin, J.-K.; Yang, J.; et al. A hypothalamic circuit that controls body temperature. Proc. Natl. Acad. Sci. USA 2017, 114, 2042–2047. [CrossRef]
36. Watanabe, M.; Suzuki, K.; Kodama, S.; Sugahara, T. Normal human cells at confluence get heat resistance by efficient accumulation of HSP72 in nucleus. Carcinogenesis 1995, 16, 2373–2380. [CrossRef]
37. Jones, E.; Thrall, D.; Dewhirst, M.W.; Vujaskovic, Z. Prospective thermal dosimetry: The key to hyperthermia's future. Int. J. Hyperth. 2006, 22, 247–253. [CrossRef]
38. di Lalla, V.; Chaput, G.; Williams, T.; Sultanem, K. Radiotherapy Side Effects: Integrating a Survivorship Clinical Lens to Better Serve Patients. Curr. Oncol. 2020, 27, 107–112. [CrossRef]
39. Majeed, H.; Gupta, V. Adverse Effects of Radiation Therapy; StatPearls Publishing: Treasure Island, FL, USA, 2021. Available online: https://pubmed.ncbi.nlm.nih.gov/33085406/ (accessed on 11 December 2021).
40. Kaur, P.; Hurwitz, M.D.; Krishnan, S.; Asea, A. Combined Hyperthermia and Radiotherapy for the Treatment of Cancer. Cancers 2011, 3, 3799–3823. [CrossRef]
41. Rao, W.; Deng, Z.-S.; Liu, J. A Review of Hyperthermia Combined with Radiotherapy/Chemotherapy on Malignant Tumors. Crit. Rev. Biomed. Eng. 2010, 38, 101–116. [CrossRef]
42. Elming, P.B.; Sorensen, B.S.; Oei, A.L.; Franken, N.A.P.; Crezee, J.; Overgaard, J.; Horsman, M.R. Hyperthermia: The optimal treatment to overcome radiation resistant hypoxia. Cancers 2019, 11, 60. [CrossRef] [PubMed]
43. Kühl, N.M.; Rensing, L. Heat shock effects on cell cycle progression. Cell. Mol. Life Sci. CMLS 2000, 57, 450–463. [CrossRef] [PubMed]
44. Roti, J.L.; Laszlo, A. The effects of hyperthermia on cellular macromolecules. In Hyperthermia and Oncology Volume 1, Thermal Effects on Cells and Tissues; Urano, M., Douple, E., Eds.; VSP: Utrecht, The Netherlands, 1988; pp. 13–56.
45. Pandita, T.K.; Pandita, S.; Bhaumik, S.R. Molecular parameters of hyperthermia for radiosensitization. Crit. Rev. Eukaryot. Gene Expr. 2009, 19, 235–251. [CrossRef] [PubMed]
46. Okumura, Y.; Ihara, M.; Shimasaki, T.; Takeshita, S.; Okiachi, K. Heat inactivation of DNA-dependent protein kinase: Possible mechanism of hyperthermic radiosensitization. In Thermotherapy for Neoplasia, Inflammation, and Pain; Kosaka, M., Sugahara, T., Schmidt, K.L., Kosaka, M., Sugahara, T., Simon, E., Eds.; Springer: Tokyo, Japan, 2001; pp. 420–423.
47. Vujaskovic, Z.; Song, C.W. Physiological mechanisms underlying heat-induced radiosensitization. Int. J. Hyperth. 2004, 20, 163–174. [CrossRef]
48. Song, C.W.; Shakil, A.; Osborn, J.L.; Iwata, K. Tumour oxygenation is increased by hyperthermia at mild temperatures. Int. J. Hyperth. 2009, 25, 91–95. [CrossRef] [PubMed]

49. Dudar, T.E.; Jain, R.K. Differential response of normal and tumor microcirculation to hyperthermia. Cancer Res. 1984, 44, 605–612. [PubMed]

50. Song, C.W.; Lokshina, A.; Rhee, J.G.; Patten, M.; Levitt, S.H. Implication of blood-flow in hyperthermic treatment of tumors. IEEE Trans. Biomed. Eng. 1984, 31, 9–16. [CrossRef] [PubMed]

51. Pence, D.M.; Song, C.W. Effect of heat on blood-flow. In Hyperthermia in Cancer Treatment; Anghileri, L.J., Robert, J., Eds.; CRC Press Inc.: Boca Raton, FL, USA, 1986; Volume 2, pp. 1–17.

52. Vaupel, P. Pathophysiological mechanism of hyperthermia in cancer therapy. In Methods of Hyperthermia Control, Clinical Thermology; Gautherie, M., Ed.; Springer: Berlin/Heidelberg, Germany, 1990; pp. 73–134.

53. Erdmann, B.; Lang, J.; Seebass, M. Optimization of temperature distributions for regional hyperthermia based on a nonlinear heat transfer model. Ann. NYAS 1998, 858, 36–46.

54. Vaupel, P.; Kallinowski, F.; Okunieff, P. Blood flow, oxygen and nutrient supply, and metabolic microenvironment of human tumours: A review. Cancer Res. 1989, 49, 6449–6465.

55. Takana, Y. Thermal responses of microcirculation and modification of tumour blood flow in treating the tumours. In Theoretical and Experimental Basis of Hyperthermia. Thermotherapy for Neoplasia, Inflammation, and Pain; Kosaka, M., Sugahara, T., Schmidt, K.L., Simon, E., Eds.; Springer: Tokyo, Japan, 2001; pp. 408–419.

56. Song, C.W.; Choi, I.B.; Nah, B.S.; Sahu, S.K.; Osborn, J.L. Microvasculature and perfusion in normal tissues and tumours. In Thermoradiometry and Thermochemotherapy; Seegenschmiedt, M.H., Fessenden, P., Vernon, C.C., Eds.; Springer: Berlin/Heidelberg, Germany, 1995; Volume 1, pp. 139–156.

57. Song, C.W.; Park, H.; Griffin, R.J. Theoretical and experimental basis of hyperthermia. In Thermotherapy for Neoplasia, Inflammation, and Pain; Kosaka, M., Sugahara, T., Schmidt, K.L., Simon, E., Eds.; Springer: Tokyo, Japan, 2001; pp. 394–407.

58. Lindholm, C.E. Hyperthermia and Radiotherapy. Ph.D. Thesis, Lund University, Malmo, Sweden, 1992.

59. Hafström, L.; Rudenstam, C.M.; Blomquist, E.; Ingvar, C.; Jönsson, P.E.; Lagerlöf, B.; Lindholm, C.; Ringborg, U.;Westman, G.; Ostrup, L. Regional hyperthermic perfusion with melphalan after surgery for recurrent malignant melanoma of the extremities. J. Clin. Oncol. 1991, 9, 2091–2094. [CrossRef] [PubMed]

60. Dewey, W.C.; Hopwood, L.E.; Sapareto, S.A.; Gerweck, L.E. Cellular Responses to Combinations of Hyperthermia and Radiation. Radiology 1977, 123, 463–474. [CrossRef] [PubMed]

61. Kim, W.; Lee, S.; Seo, D.; Kim, D.; Kim, K.; Kim, E.; Kang, J.; Seong, K.M.; Youn, H.; Youn, B. Cellular Stress Responses in Radiotherapy. Cells 2019, 8, 1105. [CrossRef] [PubMed]

62. Walleczek, J. Self-Organized Biological Dynamics & Nonlinear Control; Cambridge University Press: Cambridge, UK, 2000.

63. Dewhirst, M.W.; Viglianti, B.L.; Lora-Michiels, M.; Hanson, M.; Hoopes, P.J. Basic principles of thermal dosimetry and thermal thresholds for tissue damage from hyperthermia. Int. J. Hyperth. 2003, 19, 267–294. [CrossRef] [PubMed]

64. Perez, C.A.; Sapareto, S.A. Thermal dose expression in clinical hyperthermia and correlation with tumor response/control. Cancer Res. 1984, 44, 4818–4825.

65. Dewey,W.C. Arrhenius relationships from the molecule and cell to the clinic. Int. J. Hyperth. 1994, 10, 457–483. [CrossRef]

66. Gellerman, J. Nichtinvasive Thermometrie bei lokoregionaler Tiefenhyperthermie, Noninvasive thermometry in loco-regional deep hyperthermia. In Proceedings of the Oncothermia Symphosia, 2016, Cologne, Germany, 22–23 September 2006.

67. Hegyi, G.; Vincze, G.; Szasz, A. On the Dynamic Equilibrium in Homeostasis. Open J. Biophys. 2012, 2, 60–67. [CrossRef]

68. Lee, S.-Y.; Szigeti, G.P.; Szasz, A.M. Oncological hyperthermia: The correct dosing in clinical applications. Int. J. Oncol. 2018, 54, 627–643. [CrossRef]

69. Maguire, P.D.; Samulski, T.V.; Prosnitz, L.R.; Jones, E.L.; Rosner, G.L.; Powers, B.; Layfield, L.W.; Brizel, D.M.; Scully, S.P.;Herrelson, M.; et al. A phase II trial testing the thermal dose parameter CEM43 T90 as a predictor of response in soft tissue sarcomas treated with pre-operative thermorasiotherapy. Int. J. Hyperth. 2001, 17, 283–290. [CrossRef]

70. Dewhirst, M.W.; Vujaskovic, Z.; Jones, E.; Thrall, D. Re-setting the biologic rationale for thermal therapy. Int. J. Hyperth. 2005, 21, 779–790. [CrossRef]

71. Thrall, D.E.; Prescott, D.M.; Samulski, T.V.; Rosner, G.L.; Denman, D.L.; Legorreta, R.L.; Dodge, R.K.; Page, R.L.; Cline, J.; Lee, J.; et al. Radiation plus local hyperthermia versus radiation plus the combination of local and whole-body hyperthermia in canine sarcomas. Int. J. Radiat. Oncol. 1996, 34, 1087–1096. [CrossRef]

72. Hildebrandt, B.; Dräger, J.; Kerner, T.; Deja, M.; Löffel, J.; Stroszczynski, C.; Ahlers, O.; Felix, R.; Riess, H.;Wust, P. Whole-body hyperthermia in the scope of von Ardenne's systemic cancer multistep therapy (sCMT) combined with chemotherapy in patients with metastatic colorectal cancer: A phase I/II study. Int. J. Hyperth. 2004, 20, 317–333. [CrossRef] [PubMed]

73. Bakhshandeh, A.; Wiedemann, G.; Zabel, P.; Dalhoff, K.; Kohlmann, T.; Penzel, R.Z.; Wagner, T.; Peters, S. Randomized trial with ICE (ifosfamide, carboplatin, etoposide) plus whole body hyperthermia versus ICE chemotherapy for malignant pleural mesothelioma. J. Clin. Oncol. 2004, 22, 7288. [CrossRef]

74. de Bruijne, M.; van der Holt, B.; van Rhoon, G.C.; van der Zee, J. Evaluation of CEM43 CT90 thermal dose in superficial hyperthermia: A retrospective analysis. Strahlenther. Onkol. Radiother. Oncol. 2010, 186, 436–443. [CrossRef] [PubMed]

75. Kraybill, W.G.; Olenki, T.; Evans, S.S.; Ostberg, J.R.; O'Leary, K.A.; Gibbs, J.F.; Repasky, E.A. A phase I study of fever-range whole body hyperthermia (FR-WBH) in patients with advanced solid tumors: Correlation with mouse models. Int. J. Hyperth. 2002, 18, 253–266. [CrossRef] [PubMed]

76. Toyota, N.; Strebel, F.R.; Stephens, L.C.; Matsuda, H.; Bull, J.M.C. Long-duration, mild whole body hyperthermia with cisplatin: Tumour response and kinetics of apoptosis and necrosis in a metastatic rat mammary adenocarcinoma. Int. J. Hyperth. 1997, 13, 497–506. [CrossRef] [PubMed]

77. Sakaguchi, Y.; Makino, M.; Kaneko, T.; Stephens, L.C.; Strebel, F.R.; Danhauser, L.L.; Jenkins, G.N.; Bull, J.M. Therapeutic efficacy of long duration-low temperature whole body hyperthermia when combined with tumor necrosis factor and carboplatin in rats. Cancer Res. 1994, 54, 2223–2227.

78. Ostberg, R.; Repasky, E.A. Use of mild, whole body hyperthermia in cancer therapy. Immunol. Investig. 2000, 29, 139–142. [CrossRef]

79. International Collaborative Hyperthermia Group; Vernon, C.C.; Hand, J.W.; Field, S.B.; Machin, D.; Whaley, J.B.; van der Zee, J.; van Putten,W.L.; van Rhoon, G.C.; van Dijk, J.D.; et al. Radiotherapy with or without hyperthermia in the treatment of superficial localized breast cancer: Results from five randomized controlled trials. Int. J. Radiat. Oncol. Biol. Phys. 1996, 35, 731–744. [CrossRef]

80. Sherar, M.; Liu, F.-F.; Pintilie, M.; Levin,W.; Hunt, J.; Hill, R.; Hand, J.; Vernon, C.; van Rhoon, G.; van der Zee, J.; et al. Relationship between thermal dose and outcome in thermoradiotherapy treatments for superficial recurrences of breast cancer: Data from a phase III trial. Int. J. Radiat. Oncol. 1997, 39, 371–380. [CrossRef]

81. Sharma, S.; Patel, F.D.; Sandhu, A.P.S.; Gupta, B.D.; Yadav, N.S. A prospective randomized study of local hyperthermia as a supplement and radiosensitiser in the treatment of carcinoma of the cervix with radiotherapy. Endocurietherapy/Hyperth. Oncol. 1989, 5, 151–159.

82. Vasanthan, A.; Mitsumori, M.; Park, J.H.; Zhi-Fan, Z.; Yu-Bin, Z.; Oliynychenko, P.; Tatsuzaki, H.; Tanaka, Y.; Hiraoka, M. Regional hyperthermia combined with radiotherapy for uterine cervical cancers: A multi-institutional prospective randomized trial of the international atomic energy agency. Int. J. Radiat. Oncol. 2005, 61, 145–153. [CrossRef]

83. Harima, Y.; Nagata, K.; Harima, K.; Ostapenko, V.V.; Tanaka, Y.; Sawada, S. A randomized clinical trial of radiation therapy versus thermoradiotherapy in stage IIIB cervical carcinoma. Int. J. Hyperth. 2009, 25, 338–343. [CrossRef]

84. Roussakow, S.V. A randomized clinical trial of radiation therapy versus thermoradiotherapy in stage IIIB cervical carcinoma of Yoko Harima et al. (2001): Multiple biases and no advantage of hyperthermia. Int. J. Hyperth. 2018, 34, 1400. [CrossRef]

85. Harima, Y. A randomised clinical trial of radiation therapy versus thermoradiotherapy in stage IIIB cervical carcinoma of Yoko, Harima et al. (2001): A response letter to the editor of comments from Dr. Roussakow. Int. J. Hyperth. 2018, 34, 1401. [CrossRef]

86. Zolciak-Siwinska, A.; Piotrokowicz, N.; Jonska-Gmyrek, J.; Nicke-Psikuta, M.; Michalski, W.; Kawczy´nska, M.; Bijok, M.; Bujko, K. HDR brachytherapy combined with interstitial hyperthermia in locally advanced cervical cancer patients initially treated with concomitant radiochemotherapy–A phase III study. Radiother. Oncol. 2013, 109, 194–199. [CrossRef]

87. Kay, C.S.; Choi, I.B.; Jang, J.Y.; Choi, B.O.; Kim, I.A.; Shinn, K.S. Thermoradiotherapy in the treatment of locally advanced nonsmall cell lung cancer. Radiat. Oncol. J. 1996, 14, 115–122.

88. Mitsumori, M.; Zhi-Fan, Z.; Oliynychenko, P.; Park, J.H.; Choi, I.B.; Tatsuzaki, H.; Tanaka, Y.; Hiraoka, M. Regional hyperthermia combined with radiotherapy for locally advanced non-small cell lung cancers: A multi-institutional prospective randomized trial of the International Atomic Energy Agency. Int. J. Clin. Oncol. 2007, 12, 192–198. [CrossRef]

89. Jones, E.L.; Oleson, J.R.; Prosnith, L.R.; Prosnitz, L.R.; Samulski, T.V.; Vujaskovic, Z.; Yu, D.; Sanders, L.L.; Dewhirst, M.W. Randomized trial of hyperthermia and radiation for superficial tumors. J. Clin. Oncol. 2005, 23, 3079–3085. [CrossRef]

90. Storm, F.K. What happened to hyperthermia and what is its current status in cancer treatment? J. Surg. Oncol. 1993, 53, 141–143. [CrossRef]

91. van der Zee, J. Heating the patient: A promising approach? Ann. Oncol. 2002, 13, 1173–1184. [CrossRef] [PubMed]

92. Datta, N.R.; Kok, H.P.; Crezee, H.; Gaipl, U.S.; Bodis, S. Integrating Loco-Regional Hyperthermia into the Current Oncology Practice: SWOT and TOWS Analyses. Front. Oncol. 2020, 10, 819. [CrossRef] [PubMed]

93. Wildeboer, R.R.; Southern, P.; Pankhurst, Q.A. On the reliable measurement of specific absorption rates and intrinsic loss parameters in magnetic hyperthermia materials. J. Phys. D Appl. Phys. 2014, 47, 495003. [CrossRef]

94. Szasz, A.; Szasz, N.; Szasz, O. Oncothermia: Principles and Practices; Springer Science: Heidelberg, Germany, 2010. [CrossRef]

95. Andocs, G.; Rehman, M.U.; Zhao, Q.L.; Papp, E.; Kondo, T.; Szasz, A. Nanoheating without Artificial Nanoparticles Part II. Experimental support of the nanoheating concept of the modulated electro-hyperthermia method, using U937 cell suspension model. Biol. Med. 2015, 7, 1–9. [CrossRef]

96. Beachy, S.H.; Repasky, E.A. Toward establishment of temperature thresholds for immunological impact of heat exposure in humans. Int. J. Hyperth. 2011, 27, 344–352. [CrossRef]

97. Shen, R.-N.; Lu, L.; Young, P.; Shidnia, H.; Hornback, N.B.; Broxmeyer, H.E. Influence of elevated temperature on natural killer cell activity, lymphokine-activated killer cell activity and lectin-dependent cytotoxicity of human umbilical cord blood and adult blood cells. Int. J. Radiat. Oncol. 1994, 29, 821–826. [CrossRef]

98. Hietanen, T.; Kapanaen, M.; Kellokumpu-Lehtinen, P.-L. Restoring natural killer cell cytotoxicity after hyperthermia alone or combined with radiotherapy. Anticancer. Res. 2016, 36, 555–563.

99. Repasky, E.; Issels, R. Physiological consequences of hyperthermia: Heat, heat shock proteins and the immune response. Int. J. Hyperth. 2002, 18, 486–489. [CrossRef]

100. Szasz, A. Thermal and nonthermal effects of radiofrequency on living state and applications as an adjuvant with radiation therapy. J. Radiat. Cancer Res. 2019, 10, 1–17. [CrossRef]

101. Krenacs, T.; Meggyeshazi, N.; Forika, G.; Kiss, E.; Hamar, P.; Szekely, T.; Vancsik, T. Modulated Electro-Hyperthermia-Induced Tumor Damage Mechanisms Revealed in Cancer Models. Int. J. Mol. Sci. 2020, 21, 6270. [CrossRef]

102. Vincze, G.; Szasz, A. Similarities of modulation by temperature and by electric field. Open J. Biophys. 2018, 8, 95–103. [CrossRef]

103. Gowrishankar, T.R.; Weaver, J.C. An approach to electrical modeling of single and multiple cells. Proc. Natl. Acad. Sci. USA 2003, 100, 3203–3208. [CrossRef] [PubMed]

104. Kotnik, T.; Miklavcic, D. Theoretical evaluation of the distributed power dissipation in biological cells exposed to electric fields. Bioelectromagnetics 2000, 21, 385–394. [CrossRef]

105. Papp, E.; Vancsik, T.; Kiss, E.; Szasz, O. Energy absorption by the membrane rafts in the modulated electro-hyperthermia (mEHT). Open J. Biophys. 2017, 7, 216–229. [CrossRef]

106. The Physical Sciences-Oncology Centers Network; Agus, D.B.; Alexander, J.F.; Arap, W.; Ashili, S.; Aslan, J.; Austin, R.H.; Backman, V.; Bethel, K.; Bonneau, R.; et al. A physical sciences network characterization of non-tumorigenic and metastatic cells. Sci. Rep. 2013, 3, 01449. [CrossRef]

107. Arrhenius, S. On the reaction rate of the inversion of non-refined sugar upon souring. Z Phys. Chem. 1889, 4, 226–248. [CrossRef]

108. Szasz, A. The Capacitive Coupling Modalities for Oncological Hyperthermia. Open J. Biophys. 2021, 11, 252–313. [CrossRef]

109. Szasz, A.; Vincze, G.; Szasz, O.; Szasz, N. An Energy Analysis of Extracellular Hyperthermia. Electromagn. Biol. Med. 2003, 22, 103–115. [CrossRef]

110. Fröhlich, H. What are non-thermal electric biological effects? Bioelectromagnetics 1982, 3, 45–46. [CrossRef]

111. Szasz, A. Therapeutic Basis of Electromagnetic Resonances and Signal-Modulation. Open J. Biophys. 2021, 11, 314–350. [CrossRef]

112. Neudorfer, C.; Chow, C.T.; Boutet, A.; Loh, A.; Germann, J.; Elias, G.J.; Hutchison, W.D.; Lozano, A.M. Kilohertz-frequency stimulation of the nervous system: A review of underlying mechanisms. Brain Stimul. 2021, 14, 513–530. [CrossRef] [PubMed]

113. Szasz, A.; Szasz, O. Time-fractal modulation of modulated electro-hyperthermia (mEHT). In Book Challenges and Solutions of Oncological Hyperthermia; Szasz, A., Ed.; Cambridge Scholars: Newcastle upon Tyne, UK, 2020; pp. 377–415.

114. Rec. ITU-R SM.1056-1. 1 RECOMMENDATION ITU-R SM.1056-1. Limitation of Radiation from Industrial, Scientific and Medical (ISM) Equipment (Question ITU-R 70/1). Available online: https://www.itu.int/dms_pubrec/itu-r/rec/sm/R-REC-SM.1056-1-200704-I!!PDF-E.pdf (accessed on 31 October 2021).

115. Yeo, S.-G. Definitive radiotherapy with concurrent oncothermia for stage IIIB non-small-cell lung cancer: A case report. Exp. Ther. Med. 2015, 10, 769–772. [CrossRef] [PubMed]

116. Chi, M.-S.; Mehta, M.P.; Yang, K.-L.; Lai, H.-C.; Lin, Y.-C.; Ko, H.-L.; Wang, Y.-S.; Liao, K.-W.; Chi, K.-H. Putative Abscopal Effect in Three Patients Treated by Combined Radiotherapy and Modulated Electrohyperthermia. Front. Oncol. 2020, 10, 254. [CrossRef] [PubMed]

117. Deering, W.;West, B.J. Fractal physiology. IEEE Comput. Graph. Appl. 1992, 11, 40–46. [CrossRef]

118. West, B.J. Fractal Physiology and Chaos in Medicine; World Scientific: Singapore; London, UK, 1990.

119. Bassingthwaighte, J.B.; Leibovitch, L.S.; West, B.J. Fractal Physiology; Oxford University Press: New York, NY, USA; Oxford, UK, 1994.

120. Musha, T.; Sawada, Y. Physics of the Living State; IOS Press: Amsterdam, The Netherlands, 1994.

121. Lovelady, D.C.; Friedman, J.; Patel, S.; Rabson, D.A.; Lo, C.-M. Detecting effects of low levels of cytochalasin B in 3T3 fibroblast cultures by analysis of electrical noise obtained from cellular micromotion. Biosens. Bioelectron. 2009, 24, 2250–2254. [CrossRef]

122. Lovelady, D.C.; Richmond, T.C.; Maggi, A.N.; Lo, C.-M.; Rabson, D.A. Distinguishing cancerous from noncancerous cells through analysis of electrical noise. Phys. Rev. E 2007, 76, 041908. [CrossRef]

123. Astumian, R.D.; Chock, P.B.; Tsong, T.Y.; Westerhoff, H.V. Effects of oscillations and energy-driven fluctuations on the dynamics of enzyme catalysis and free-energy transduction. Phys. Rev. A 1989, 39, 6416–6435. [CrossRef]

124. Astumian, R.D.; Weaver, J.C.; Adair, R.K. Rectification and signal averaging of weak electric fields by biological cells. Proc. Natl. Acad. Sci. USA 1995, 92, 3740–3743. [CrossRef]

125. Sabah, N.H. Rectification in Biological Membranes. IEEE Eng. Med. Biol. 2000, 19, 106–113. [CrossRef]

126. Nagy, G.; Meggyeshazi, N.; Szasz, O. Deep temperature measurements in oncothermia processes. In Proceedings of the Conference of the International Clinical Hyperthermia Society 2012, Budapest, Hungary, 12–14 October 2012.

127. Orczy-Timko, B. Phantom measurements with the EHY-2030 device. In Challenges and Solutions of Oncological Hyperthermia; Szasz, A., Ed.; Cambridge Scholars: Newcastle upon Tyne, UK, 2020; pp. 416–428.

128. Hossain, M.T.; Prasad, B.; Park, K.S.; Lee, H.J.; Ha, Y.H.; Lee, S.K.; Kim, J.K. Simulation and experimental evaluation of selective heating characteristics of 13.56 MHz radiofrequency hyperthermia in phantom models. Int. J. Precis. Eng. Manuf. 2016, 17, 253–256. [CrossRef]

129. Prasad, B.; Kim, S.; Cho, W.; Kim, J.K.; Kim, Y.A.; Kim, S.; Wu, H.G. Quantitative estimation of the equivalent radiation dose escalation using radiofrequency hyperthermia in mouse xenograft models of human lung cancer. Sci. Rep. 2019, 9, 3942. [CrossRef] [PubMed]

130. Balogh, L.; Polyák, A.; Pösténvi, Z.; Kovács-Haász, V.; Gyöngy, M.; Thuróczy, J. Temperature increase induced by modulated electrohyperthermia (onco-thermia®) in the anesthetized pig liver. J. Cancer Res. Ther. 2016, 12, 1153–1159. [PubMed]

131. Kim, J.K.; Prasad, B.; Kim, S. Temperature mapping and thermal dose calculation in combined radiation therapy and 13.56 MHz radiofrequency hyperthermia for tumor treatment. In SPIE 10047, Optical Methods for Tumor Treatment and Detection: Mechanisms and Techniques in Photodynamic Therapy XXVI, Proceedings of the SPIE Conferences and Exhibitions, San Francisco, CA, USA, 28 January–2 February 2017; SPIE: Bellingham,WA, USA, 2017.

132. Lee, S.-Y.; Kim, J.-H.; Han, Y.-H.; Cho, D.-H. The effect of modulated electro-hyperthermia on temperature and blood flow in human cervical carcinoma. Int. J. Hyperth. 2018, 34, 953–960. [CrossRef] [PubMed]

133. Yang, K.-L.; Huang, C.-C.; Chi, M.-S.; Chiang, H.-C.; Wang, Y.-S.; Hsia, C.-C.; Andocs, G.; Wang, H.-E.; Chi, K.-H. In vitro comparison of conventional hyperthermia and modulated electro-hyperthermia. Oncotarget 2016, 7, 84082–84092. [CrossRef]

134. Forika, G.; Balogh, A.; Vancsik, T.; Zalatnai, A.; Petovari, G.; Benyo, Z.; Krenacs, T. Modulated Electro-Hyperthermia Resolves Radioresistance of Panc1 Pancreas Adenocarcinoma and Promotes DNA Damage and Apoptosis In Vitro. Int. J. Mol. Sci. 2020, 21, 5100. [CrossRef]

135. Andocs, G.; Renner, H.; Balogh, L.; Fonyad, L.; Jakab, C.; Szasz, A. Strong synergy of heat and modulated electro- magnetic field in tumor cell killing, Study of HT29 xenograft tumors in a nude mice model. Strahlenther. Onkol. 2009, 185, 120–126. [CrossRef]

136. Andocs, G.; Rehman, M.U.; Zhao, Q.-L.; Tabuchi, Y.; Kanamori, M.; Kondo, T. Comparison of biological effects of modulated electro-hyperthermia and conventional heat treatment in human lymphoma U937 cells. Cell Death Discov. 2016, 2, 16039. [CrossRef]

137. Kirson, E.D.; Gurvich, Z.; Schneiderman, R.; Dekel, E.; Itzhaki, A.; Wasserman, Y.; Schatzberger, R.; Palti, Y. Disruption of Cancer Cell Replication by Alternating Electric Fields. Cancer Res. 2004, 64, 3288–3295. [CrossRef]

138. Vincze, G.; Szasz, A. Reorganization of actin filaments and microtubules by outside electric field. J. Adv. Biol. 2015, 8, 1514–1518.

139. Dimova, R.; Bezlyepkina, N.; Jordö, M.D.; Knorr, R.L.; Riske, K.A.; Staykova, M.; Vlahovska, P.M.; Yamamoto, T.; Yang, P.; Lipowsky, R. Vesicles in electric fields: Some novel aspects of membrane behavior. Soft Matter 2009, 5, 3201–3212. [CrossRef]

140. Vincze, G.; Szigeti, G.; Andocs, G.; Szasz, A. Nanoheating without Artificial Nanoparticles. Biol. Med. 2015, 7, 249.

141. Guo, J.; Lao, Y.; Chang, D.C. Calcium and Apoptosis. In Handbook of Neurochemistry and Molecular Neurobiology; Lajtha, A., Mikoshiba, K., Eds.; Springer: Boston, MA, USA, 2009. [CrossRef]

142. Cha, J.; Jeon, T.-W.; Lee, C.G.; Oh, S.T.; Yang, H.-B.; Choi, K.-J.; Seo, D.; Yun, I.; Baik, I.H.; Park, K.R.; et al. Electro-hyperthermia inhibits glioma tumorigenicity through the induction of E2F1-mediated apoptosis. Int. J. Hyperth. 2015, 31, 784–792. [CrossRef] [PubMed]

143. Li, J.; Chauve, L.; Phelps, G.; Brielmann, R.M.; Morimoto, R.I. E2F coregulates an essential HSF developmental program that is distinct from the heat-shock response. Genes Dev. 2016, 30, 2062–2075. [CrossRef] [PubMed]

144. Wust, P.; Kortüm, B.; Strauss, U.; Nadobny, J.; Zschaeck, S.; Beck, M.; Stein, U.; Ghadjar, P. Non-thermal effects of radiofrequency electromagnetic fields. Sci. Rep. 2020, 10, 13488. [CrossRef] [PubMed]

145. Krenacs, T.; Benyo, Z. Tumor specific stress and immune response induced by modulated electrohyperthermia in relation to tumor metabolic profiles. Oncothermia J. 2017, 20, 264–272.

146. Forika, G.; Vancsik, T.; Kiss, E.; Hujber, Z.; Sebestyen, A.; Krencz, I.; Benyo, Z.; Hamar, P.; Krenacs, T. The efficiency of modulated electro-hyperthermia may correlate with the tumor metabolic profiles. Oncothermia J. 2017, 20, 228–235.

147. Vincze, G.; Szasz, N.; Szasz, A. On the thermal noise limit of cellular membranes. Bioelectromagnetics 2004, 26, 28–35. [CrossRef]

148. Forika, G.; Balogh, A.; Vancsik, T. Elevated apoptosis and tumor stem cell destruction in a radioresistant pancreatic adenocarcinoma cell line when radiotherapy is combined with modulated electrohyperthermia. Oncothermia J. 2019, 26, 90–98.

149. Meggyeshazi, N.; Andocs, G.; Krenacs, T. Modulated electro-hyperthermia induced programmed cell death in HT29 colorectal carcinoma xenograft. Virchows Arch. 2012, 461 (Suppl. 1), S131–S132.

150. Danics, L.; Schvarcz, C.A.; Viana, P.; Vancsik, T.; Krenács, T.; Benyó, Z.; Kaucsár, T.; Hamar, P. Exhaustion of Protective Heat Shock Response Induces Significant Tumor Damage by Apoptosis after Modulated Electro-Hyperthermia Treatment of Triple Negative Breast Cancer Isografts in Mice. Cancers 2020, 12, 2581. [CrossRef]

151. Meggyeshazi, N.; Andocs, G.; Spisak, S.; Krenacs, T. Modulated electrohyperthermia causes caspase independent programmed cell death in HT29 colon cancer xenografts. Virchows Arch. 2013, 463, 329.

152. Meggyesházi, N.; Andocs, G.; Balogh, L.; Balla, P.; Kiszner, G.; Teleki, I.; Jeney, A.; Krenács, T. DNA fragmentation and caspaseindependent programmed cell death by modulated electrohyperthermia. Strahlenther. Onkol. 2014, 190, 815–822. [CrossRef] [PubMed]

153. Meggyeshazi, N.; Andocs, G.; Spisak, S.; Krenacs, T. Early changes in mRNA and protein expression related to cancer treatment by modulated electro-hyperthermia. Hindawi Publ. Corp. Conf. Pap. Med. 2013, 2013, 249563.

154. Jeon, T.-W.; Yang, H.; Lee, C.G.; Oh, S.T.; Seo, D.; Baik, I.H.; Lee, E.H.; Yun, I.; Park, K.R.; Lee, Y.-H. Electro-hyperthermia up-regulates tumour suppressor Septin 4 to induce apoptotic cell death in hepatocellular carcinoma. Int. J. Hyperth. 2016, 32, 648–656. [CrossRef] [PubMed]

155. McDonald, M.; Corde, S.; Lerch, M.; Rosenfeld, A.; Jackson, M.; Tehei, M. First in vitro evidence of modulated electrohyperthermia treatment performance in combination with megavoltage radiation by clonogenic assay. Sci. Rep. 2018, 8, 16608. [CrossRef] [PubMed]

156. Forika, G. Radiotherapy and modulated electro-hyperthermia effect on Panc1 and Capan1 pancreas adenocarcinoma cell lines. Oncothermia J. 2018, 24, 455–463.

157. Forika, G.; Balogh, A.; Vancsik, T.; Benyo, Z.; Krenacs, T. Apoptotic response and DNA damage of the radioresistant Panc1 pancreas adenocarcinoma to combined modulated electro hyperthermia and radiotherapy. Oncothermia J. 2020, 29, 103–109.

158. Yoshikata, M.; Junki, H.; Yuta, S. Radiosensitization effect of novel cancer therapy, oncothermia toward overcoming treatment resistance. Oncothermia J. 2019, 25, 68–84.

159. Prasad, B.; Kim, S.; Cho, W.; Kim, S.; Kim, J.K. Effect of tumor properties on energy absorption, temperature mapping, and thermal dose in 13.56-MHz radiofrequency hyperthermia. J. Therm. Biol. 2018, 74, 281–289. [CrossRef]

160. Chen, C.-C.; Chen, C.-L.; Li, J.-J.; Chen, Y.-Y.;Wang, C.-Y.;Wang, Y.-S.; Chi, K.-H.;Wang, H.-E. Presence of Gold Nanoparticles in Cells Associated with the Cell-Killing Effect of Modulated Electro-Hyperthermia. ACS Appl. Bio Mater. 2019, 2, 3573–3581. [CrossRef]

161. Besztercei, B.; Vancsik, T.; Benedek, A.; Major, E.; Thomas, M.J.; Schvarcz, C.A.; Krenács, T.; Benyó, Z.; Balogh, A. Stress-Induced, p53-Mediated Tumor Growth Inhibition of Melanoma by Modulated Electrohyperthermia in Mouse Models without Major Immunogenic Effects. Int. J. Mol. Sci. 2019, 20, 4019. [CrossRef] [PubMed]

162. Oei, A.L.; Vriend, L.E.M.; Crezee, J.; Franken, N.A.P.; Krawczyk, P.M. Effects of hyperthermia on DNA repair pathways: One treatment to inhibit them all. Radiat. Oncol. 2015, 10, 165. [CrossRef] [PubMed]

163. 163. Thomas, M.B.; Major, E.; Benedek, A.; Horváth, I.; Máthé, D.; Bergmann, R.; Szasz, A.M.; Krenacs, T.; Benyo, Z. Suppression of metastatic melanoma growth in lung by modulated electro-hyperthermia monitored by a minimally invasive heat stress testing approach in mice. Cancers 2020, 12, 3872. [CrossRef] [PubMed]

164. Schvarcz, C.; Danics, L.; Krenács, T.; Viana, P.; Béres, R.; Vancsik, T.; Nagy, Á.; Gyenesei, A.; Kun, J.; Fonovi´c, M.; et al. Modulated Electro-Hyperthermia Induces a Prominent Local Stress Response and Growth Inhibition in Mouse Breast Cancer Isografts. Cancers 2021, 13, 1744. [CrossRef]

165. Andocs, G.; Meggyeshazi, N.; Balogh, L.; Spisak, S.; Maros, M.E.; Balla, P.; Kiszner, G.; Teleki, I.; Kovago, C.; Krenacs, T. Upregulation of heat shock proteins and the promotion of damage-associated molecular pattern signals in a colorectal cancer model by modulated electrohyperthermia. Cell Stress Chaperones 2014, 20, 37–46. [CrossRef]

166. Daguenet, E.; Louati, S.; Wozny, A.-S.; Vial, N.; Gras, M.; Guy, J.-B.; Vallard, A.; Rodriguez-Lafrasse, C.; Magné, N. Radiationinduced bystander and abscopal effects: Important lessons from preclinical models. Br. J. Cancer 2020, 123, 339–348. [CrossRef]

167. Piana, R. The Abscopal Effect: A Reemerging Field of Interest. The ASCO Post 2018. Available online: https://ascopost.com/issues/november-25-2018/the-abscopal-effect-a-reemerging-field-of-interest/ (accessed on 12 December 2021).

168. Hu, Z.I.; McArthur, H.L.; Ho, A.Y. The Abscopal Effect of Radiation Therapy: What Is It and How CanWe Use It in Breast Cancer? Curr. Breast Cancer Rep. 2017, 9, 45–51. [CrossRef]

169. Vancsik, T.; Máthé, D.; Horváth, I.; Várallyaly, A.A.; Benedek, A.; Bergmann, R.; Krenács, T.; Benyó, Z.; Balogh, A. Modulated Electro-Hyperthermia Facilitates NK-Cell Infiltration and Growth Arrest of Human A2058 Melanoma in a Xenograft Model. Front. Oncol. 2021, 11, 590764. [CrossRef]

170. Qin, W.; Akutsu, Y.; Andocs, G.; Suganami, A.; Hu, X.; Yusup, G.; Komatsu-Akimoto, A.; Hoshino, I.; Hanari, N.; Mori, M.; et al. Modulated electro-hyperthermia enhances dendritic cell therapy through an abscopal effect in mice. Oncol. Rep. 2014, 32, 2373–2379. [CrossRef]

171. Lee, Y.J.; Kang, S.Y.; Jo, M.S.; Suh, D.S.; Kim, K.H.; Yoon, M.S. S100 expression in dendritic cells is inversely correlated with tumor grade in endometrial carcinoma. Obstet. Gynecol. Sci. 2014, 57, 201–207. [CrossRef]

172. Tsang, Y.W.; Huang, C.C.; Yang, K.L.; Chi, M.-S.; Chiang, H.-C.; Wang, Y.-S.; Andocs, G.; Szasz, A.; Li, W.-T. Improving immunological tumor microenvironment using electro-hyperthermia followed by dendritic cell immunotherapy. BMC Cancer 2015, 15, 708. [CrossRef] [PubMed]

173. Vancsik, T.; Kiss, E.; Kovago, C.; Meggyeshazi, N.; Forika, G.; Krenacs, T. Inhibition of proliferation, induction of apoptotic cell death and immune response by modulated electro-hyperthermia in C26 colorectal cancer allografts, thermometry. Oncothermia J. 2017, 20, 277–292.

174. Vancsik, T.; Kovago, C.; Kiss, E.; Papp, E.; Forika, G.; Benyo, Z.; Meggyeshazi, N.; Krenacs, T. Modulated electro-hyperthermia induced loco-regional and systemic tumor destruction in colorectal cancer allografts. J. Cancer 2018, 9, 41–53. [CrossRef] [PubMed]

175. Vancsik, T.; Forika, G.; Balogh, A.; Kiss, E.; Krenacs, T. Modulated electro-hyperthermia induced p53 driven apoptosis and cell cycle arrest additively support doxorubicin chemotherapy of colorectal cancer in vitro. Cancer Med. 2019, 8, 4292–4303. [CrossRef]

176. Wismeth, C.; Dudel, C.; Pascher, C.; Ramm, P.; Pietsch, T.; Hirschmann, B.; Reinert, C.; Proescholdt, M.A.; Rümmele, P.; Schuierer, G.; et al. Transcranial electro-hyperthermia combined with alkylating chemotherapy in patients with relapsed high-grade gliomas: Phase I clinical results. J. Neuro-Oncol. 2009, 98, 395–405. [CrossRef]

177. Minnaar, C.A.; Kotzen, J.A.; Ayeni, O.A.; Naidoo, T.; Tunmer, M.; Sharma, V.; Vangu, M.-D.-T.; Baeyens, A. The effect of modulated electro-hyperthermia on local disease control in HIV-positive and -negative cervical cancer women in South Africa: Early results from a phase III randomized controlled trial. PLoS ONE 2019, 14, e0217894. [CrossRef]

178. Minnaar, C.A.; Kotzen, J.A.; Naidoo, T.; Tunmer, M.; Sharma, V.; Vangu, M.-D.-T.; Baeyens, A. Analysis of the effects of mEHT n the treatment-related toxicity and quality of life of HIV-positive cervical cancer patients. Int. J. Hyperth. 2020, 37, 263–272. [CrossRef]

179. Minnaar, C.A.; Kotzen, J.A.; Ayeni, O.A.; Vangu, M.-D.-T.; Baeyens, A. Potentiation of the Abscopal Effect by Modulated Electro-Hyperthermia in Locally Advanced Cervical Cancer Patients. Front. Oncol. 2020, 10, 376. [CrossRef]

180. Minnaar, C.A.; Kotzen, J.A.; Baeyens, A. Possible potentiation of the abscopal effect of ionising radiation by modulated electrohyperthermia in locally advanced cervical cancer patients. Oncothermia J. 2018, 24, 122–132.

181. Minnaar, C.; Kotzen, J. Modulated electro hyperthermia as an immune modulator with checkpoint inhibitors and radiotherapy. Eur. J. Cancer 2019, 110, S19–S20. [CrossRef]

182. Chi, K.H. Tumor-directed immunotherapy: Combined radiotherapy and oncothermia. Oncothermia J. 2018, 24, 196–235.

183. Szasz, A.M.; Minnaar, C.A.; Szentmartoni, G.; Szigeti, G.P.; Dank, M. Review of the clinical evidences of modulated electrohyperthermia (mEHT) method: An update for the practicing oncologist. Front. Oncol. 2019, 9, 1012. [CrossRef] [PubMed]

184. Parmar, G.; Rurak, E.; Elderfield, M.; Li, K.; Soles, S.; Rinas, A. 8-year observational study on naturopathic treatment with modulated electro-hyperthermia (mEHT): A single-centre experience. In Challenges and Solutions of Oncological Hyperthermia; Szasz, A., Ed.; Cambridge Scholars: Newcastle upon Tyne, UK, 2020; pp. 227–266.

185. Fiorentini, G.; Sarti, D.; Gadaleta, C.D.; Ballerini, M.; Fiorentini, C.; Garfagno, T.; Ranieri, G.; Guadagni, S. A Narrative Review of Regional Hyperthermia: Updates from 2010 to 2019. Integr. Cancer Ther. 2020, 19, 1–13. [CrossRef] [PubMed]

186. Fiorentini, G.; Giovanis, P.; Rossi, S.; Dentico, P.; Paola, R.; Turrisi, G.; Bernardeschi, P. A phase II clinical study on relapsed malignant gliomas treated with electro-hyperthermia. Vivo 2006, 20, 721–724.

187. Sahinbas, H.; Groenemeyer, D.H.W.; Boecher, E.; Szasz, A. Retrospective clinical study of adjuvant electro-hyperthermia treatment for advanced brain-gliomas. Dtsch. Z. Für Onkol. 2007, 39, 154–160. [CrossRef]

188. Hager, E.D.; Sahinbas, H.; Groenemeyer, D.H.; Migeod, F. Prospective phase II trial for recurrent high-grade gliomas with capacitive coupled low radiofrequency (LRF) hyperthermia. J. Clin. Oncol. 2008, 26, 2047. [CrossRef]

189. Fiorentini, G.; Sarti, D.; Milandri, C.; Dentico, P.; Mambrini, A.; Fiorentini, C.; Mattioli, G.; Casadei, V.; Guadagni, S. Modulated Electrohyperthermia in Integrative Cancer Treatment for Relapsed Malignant Glioblastoma and Astrocytoma: Retrospective Multicenter Controlled Study. Integr. Cancer Ther. 2018, 18, 1–11. [CrossRef]

190. Minnaar, C.; Baeyens, A.; Kotzen, J. O34. Update on phase III randomized clinical trial investigating the effects of the addition of electro-hyperthermia to chemoradiotherapy for cervical cancer patients in South Africa. Phys. Med. 2016, 32, 151–152. [CrossRef]

191. Pesti, L.; Dankovics, Z.; Lorencz, P.; Csejtei, A. Treatment of advanced cervical cancer with complex chemoradio–hyperthermia. Hindawi Publ. Corp. Conf. Pap. Med. 2013, 2013, 192435. [CrossRef]

192. Ou, J.; Zhu, X.; Chen, P.; Du, Y.; Lu, Y.; Peng, X.; Bao, S.;Wang, J.; Zhang, X.; Zhang, T.; et al. A randomized phase II trial of best supportive care with or without hyperthermia and vitamin C for heavily pretreated, advanced, refractory non-small-cell lung cancer. J. Adv. Res. 2020, 24, 175–182. [CrossRef]

193. Szasz, A. Current Status of Oncothermia Therapy for Lung Cancer. Korean J. Thorac. Cardiovasc. Surg. 2014, 47, 77–93. [CrossRef] [PubMed]

194. You, S.H.; Kim, S. Feasibility of modulated electro-hyperthermia in preoperative treatment for locally-advanced rectal cancer: Early phase 2 clinical results. Neoplasma 2019, 67, 677–683. [CrossRef] [PubMed]

195. Jeung, T.S.; Ma, S.Y.; Choi, J.; Yu, J.; Lee, S.Y.; Lim, S. Results of Oncothermia Combined with Operation, Chemotherapy and Radiation Therapy for Primary, Recurrent and Metastatic Sarcoma. Case Rep. Clin. Med. 2015, 04, 157–168. [CrossRef]

196. Fiorentini, G.; Sarti, D.; Casadei, V.; Milandri, C.; Dentico, P.; Mambrini, A.; Nani, R.; Fiorentini, C.; Guadagni, S. Modulated electro-hyperthermia as palliative treatment for pancreas cancer: A retrospective observational study on 106 patients. Integr. Cancer Ther. 2019, 18, 1–8. [CrossRef]

197. Dani, A.; Varkonyi, A.; Magyar, T.; Szasz, A. Clinical study for advanced pancreas cancer treated by oncothermia. Forum Hyperthermie 2008, 1, 13–20.

198. Ranieri, G.; Ferrari, C.; di Palo, A.; Marech, I.; Porcelli, M.; Falagario, G.; Ritrovato, F.; Ramuni, L.; Fanelli, M.; Rubini, G.; et al. Bevacizumab-Based Chemotherapy Combined with, Regional Deep Capacitive Hyperthermia in Metastatic Cancer Patients: A Pilot Study. Int. J. Mol. Sci. 2017, 18, 1458. [CrossRef]

199. Kim, S.; Lee, J.H.; Cha, J.; You, S.H. Beneficial effects of modulated electro-hyperthermia during neoadjuvant treatment for locally advanced rectal cancer. Int. J. Hyperth. 2021, 38, 144–151. [CrossRef]

200. Fiorentini, G.; Sarti, D.; Casadei, V.; Milandri, C.; Dentico, P.; Mambrini, A.; Guadagni, S. Modulated electro-hyperthermia for the treatment of relapsed brain gliomas. In Challenges and Solutions of Oncological Hyperthermia; Szasz, A., Ed.; Cambridge Scholars: Newcastle upon Tyne, UK, 2020; pp. 110–125.

201. Wookyeom, Y.; Han, G.H.; Shin, H.Y.; Lee, E.-J.; Cho, H.; Chay, D.B.; Kim, J.-H. Combined treatment with modulated electrohyperthermia and an autophagy inhibitor effectively inhibit ovarian and cervical cancer growth. Int. J. Hyperth. 2018, 36, 9–20.

202. Arrojo, E.E. The position of modulated electro-hyperthermia (oncothermia) in combination with standard chemo- and radiotherapy in clinical practice–Highlights of upcoming phase III clinical studies in hospital Universitario Marqués de Val-decilla (HUMV). In Challenges and Solutions of Oncological Hyperthermia; Szasz, A., Ed.; Cambridge Scholars: Newcastle upon Tyne, UK, 2020; pp. 91–104.

203. van Gool, S.W.; Makalowski, J.; Feyen, O.; Prix, L.; Schirrmacher, V.; Stuecker, W. The induction of immunogenic cell death (ICD) during maintenance chemotherapy and subsequent multimodal immunotherapy for glioblastoma (GBM). Austin Oncol. Case Rep. 2018, 3, 1–8.

204. Kurakin, A. The self-organizing fractal theory as a universal discovery method: The phenomenon of life. Theor. Biol. Med Model. 2011, 8, 1–66. [CrossRef] [PubMed]

205. Haken, H. Self-Organization and Information. Phys. Scr. 1987, 35, 247–254. [CrossRef]

206. Sornette, D. Chaos, Fractals, Self-Organization and Disorder: Concepts and Tools; Springer: Berlin/Heidelberg, Germany; Los Angeles, CA, USA, 2000.

207. Sha, L.; Ward, E.R.; Stroy, B. A Review of Dielectric Properties of Normal and Malignant Breast Tissue. In Proceedings of the IEEE Southeast Con. 2002, Columbia, SC, USA, 5–7 April 2002; pp. 457–462.

208. Scholz, B.; Anderson, R. On electrical impedance scanning-principles and simulations. Electromedica 2000, 68, 35–44.

209. Haemmerich, D.; Staelin, S.T.; Tsai, J.Z.; Tungjitkusolmun, S.; Mahvi, D.M.; Webster, J.G. In vivo electrical conductivity of hepatic tumors. Physiol. Meas. 2003, 24, 251–260. [CrossRef]

210. Smith, S.R.; Foster, K.R.; Wolf, G.L. Dielectric Properties of VX-2 Carcinoma Versus Normal Liver Tissue. IEEE Trans. Biomed. Eng. 1986, 33, 522–524. [CrossRef]

211. Gregorie, V.; Chiti, A. PET in radiotherapy planning: Particularly exquisite test or pending and experimental tool? Radiother. Oncol. 2010, 96, 275–276. [CrossRef]

212. Cope, F.W. A review of the applications of solid state physics concepts to biological systems. J. Biol. Phys. 1975, 3, 1–41. [CrossRef]

213. Damadian, R. Tumor Detection by Nuclear Magnetic Resonance. Science 1971, 171, 1151–1153. [CrossRef]

214. Hazlewood, C.F.; Nichols, B.L.; Chamberlain, N.F. Evidence for the Existence of a Minimum of Two Phases of OrderedWater in Skeletal Muscle. Nature 1969, 222, 747–750. [CrossRef]

215. Durney, C.H.; Johnson, C.C.; Barber, P.W.; Massoudi, H.; Iskander, M.F.; Allen, S.J.; Mitchell, J.C. Descriptive summary: Radiofrequency radiation dosimetry handbook-Second edition. Radio Sci. 1979, 14, 5–7. [CrossRef]

216. Szent-Györgyi, A. The living state and cancer. Physiol. Chem. Phys. 1980, 12, 99–110. [CrossRef]

217. Szent-Györgyi, A. Electronic Biology and Cancer; Marcel Dekker: New York, NY, USA, 1998.

218. Szent-Györgyi, A. Bioelectronics, a Study on Cellular Regulations, Defense and Cancer; Acadamic Press: New York, NY, USA; London, UK, 1968.

219. Pething, R. Dielectric and Electronic Properties of Biological Materials; John Wiley and Sons: New York, NY, USA, 1979.

220. Volkov, V.V.; Palmer, D.J.; Righini, R. DistinctWater Species Confined at the Interface of a Phospholipid Membrane. Phys. Rev. Lett. 2007, 99, 078302. [CrossRef] [PubMed]

221. Liu, L.M.; Cleary, S.F. Absorbed Energy Distribution from Radiofrequency Electromagnetic Radiation in a Mammalian Cell Model: Effect of Membrane-BoundWater. Bioelectromagnetics 1995, 16, 160–171. [CrossRef] [PubMed]

222. Hendry, B. Membrane Physiology and Membrane Excitation; Croom Helm: London, UK, 1981.

223. Ma, Y.; Poole, K.; Goyette, J.; Gaus, K. Introducing Membrane Charge and Membrane Potential to T Cell Signaling. Front. Immunol. 2017, 8, 1513. [CrossRef] [PubMed]

224. Horváth, I.; Multhoff, G.; Sonnleitner, A.; Vígh, L. Membrane-associated stress proteins: More than simply chaperones. Biochim. Biophys. Acta 2008, 1778, 1653–1664. [CrossRef] [PubMed]

225. Nicolau, D.V.; Burrage, K.; Parton, R.G.; Hancock, J.F. Identifying Optimal Lipid Raft Characteristics Required to Promote Nanoscale Protein-Protein Interactions on the Plasma Membrane. Mol. Cell. Biol. 2006, 26, 313–323. [CrossRef]

226. Nicolson, G.L. The Fluid—Mosaic Model of Membrane Structure: Still relevant to understanding the structure, function and dynamics of biological membranes after more than 40 years. Biochim. Biophys. Acta 2014, 1838, 1451–1466. [CrossRef]

227. Gramse, G.; Dols-Perez, A.; Edwards, M.A.; Fumagalli, L.; and Gomila, G. Nanoscale Measurement of the Dielectric Constant of Supported Lipid Bilayers in Aqueous Solutions with Electrostatic Force Microscopy. J. Biophys. 2013, 104, 1257–1262. [CrossRef]

228. Dharia, S. Spatially and Temporally Resolving Radio-Frequency Changes in Effective Cell Membrane Capacitance. Ph.D. Thesis, University of Utah, Salt Lake City, UT, USA, 2011.

229. Pike, L.J. Lipid rafts: Bringing order to chaos. J. Lipid Res. 2003, 44, 655–667. [CrossRef]

230. Andersen, O.S.; Koeppe, I.I.; and Roger, E. Bilayer Thickness and Membrane Protein Function: An Energetic Perspective. Annu. Rev. Biophys. Biomol. Struct. 2007, 36, 107–130. [CrossRef]

231. Govorov, A.O.; Richardson, H.H. Generating heat with metal nanoparticles. Nano Today 2007, 2, 30–38. [CrossRef]

232. Potoyan, D.A.; Wolynes, P.G. On the dephasing of genetic oscillators. Proc. Natl. Acad. Sci. USA 2014, 111, 2391–2396. [CrossRef] [PubMed]

233. Ptitsyn, A.A.; Zvonic, S.; Gimble, J.M. Digital Signal Processing Reveals Circadian Baseline Oscillation in Majority of Mammalian Genes. PLOS Comput. Biol. 2007, 3, e120. [CrossRef] [PubMed]

234. Carey, S.P.; Kraning-Rush, C.M.; Williams, R.M.; Reinhart-King, C.A. Biophysical control of invasive tumor cell behavior by extracellular matrix microarchitecture. Biomaterials 2012, 33, 4157–4165. [CrossRef]

235. Wang, Y.; Wang, X.; Wohland, T.; Sampath, K. Extracellular interactions and ligand degradation shape the nodal morphogen gradient. Elife 2016, 5, e13879. [CrossRef]

236. Szendro, P.; Vincze, G.; Szasz, A. Pink noise behaviour of the biosystems. Eur. Biophys. J. 2001, 30, 227–231. [CrossRef]

237. Szendro, P.; Vincze, G.; Szasz, A. Bio-response to white noise excitation. Electro- Magn. 2001, 20, 215–229. [CrossRef]

238. Nasir, N.; Al Ahmad, M. Cells Electrical Characterization: Dielectric Properties, Mixture, and Modeling Theories. J. Eng. 2020, 2020, 1–17. [CrossRef]

239. Cole, K.S. Membranes, Ions and Impulses; University of California Press: Berkeley, CA, USA, 1968.

240. Schwan, H.P. Determination of biological impedances. In Physical Techniques in Biological Research; Academic Press: New York, NY, USA, 1963; pp. 323–406.

241. Schwan, H.P.; Takashima, S. Dielectric behavior of biological cells and membranes. Bull. Inst. Chem. Res. 1991, 69, 459–475.

242. Anderson, J.C. Dielectrics; Chapman & Hall: London, UK, 1964.

243. Grant, E.H.; Sheppard, R.J.; South, S.P. Dielectric Behavior of Biological Molecules in Solution; Clarendon Press: Oxford, UK, 1978.[CrossRef]

244. Pennock, B.E.; Schwan, H.P. Further observations on the electrical properties of hemoglobin-bound water. J. Phys. Chem. 1969, 73,2600–2610. [CrossRef]

245. Pethig, R.R. Dielectrophoresis: Theory, Methodology and Biological Applications; John Wiley & Sons: Hoboken, NJ, USA, 2017.

246. Asami, K. Characterization of biological cells by dielectric spectroscopy. J. Non-Cryst. Solids 2002, 305, 268–277. [CrossRef]

247. Pauly, H.; Schwan, H.P. Über die Impedanz einer Suspension von kugelförmigen Teilchen mit einer Schale. Z. Für Nat. B 1959, 14,125–131. [CrossRef]

248. Stubbe, M.; Gimsa, J. Maxwell's Mixing Equation Revisited: Characteristic Impedance Equations for Ellipsoidal Cells. Biophys. J.2015, 109, 194–208. [CrossRef] [PubMed]

249. Pliquett, F.; Pliquett, U. Tissue impedance, measured by pulse deformation. In Proceedings of the 8th International Conference on Electrical Bio-impedance, University of Kuopio, Kuopio, Finland, 28–31 July 1992; pp. 179–181.

250. Loft, S.M.; Conway, J.; Brown, B.H. Bioimpedance and cancer therapy. In Proceedings of the 8th International Conference on Electrical Bio-impedance, University of Kuopio, Kuopio, Finland, 28–31 July 1992; pp. 119–121.

251. Tan, L.T.-H.; Chan, K.-G.; Pusparajah, P.; Lee, W.-L.; Chuah, L.-H.; Khan, T.M.; Lee, L.-H.; Goh, B.-H. Targeting membrane lipid a potential cancer cure? Front. Pharmacol. 2017, 8, 12. [CrossRef] [PubMed]

252. Chidambaram, R.; Ramanadham, M. Hydrogen bonding in biological molecules—An update. Phys. B Condens. Matter 1991, 174, 300–305. [CrossRef]

253. Meggyeshazi, N. Studies on Modulated Electrohyperthermia Induced Tumor Cell Death in a Colorectal Carcinoma Model. Ph.D. Thesis, Pathological Sciences Doctoral School, Semmelweis University, Budapest, Hungary, 2015.

254. Wust, P.; Ghadjar, P.; Nadobny, J.; Beck, M.; Kaul, D.; Winter, L.; Zschaeck, S. Physical analysis of temperature-dependent effects of amplitude-modulated electromagnetic hyperthermia. Int. J. Hyperth. 2019, 36, 1245–1253. [CrossRef] [PubMed]

255. Wust, P.; Nadobny, J.; Zschaeck, S.; Ghadjar, P. Physics of hyperthermia–Is physics really against us? In Challenges and Solutions of Oncological Hyperthermia; Szasz, A., Ed.; Cambridge Scholars: Newcastle upon Tyne, UK, 2020; pp. 346–376.

256. Romanenko, S.; Begley, R.; Harvey, A.R.; Hool, L.; Wallace, V. The interaction between electromagnetic fields at megahertz, gigahertz and terahertz frequencies with cells, tissues and organisms: Risks and potential. J. R. Soc. Interface 2017, 14, 20170585. [CrossRef]

257. Szasz, O.; Szasz, A. Heating, Efficacy and Dose of Local Hyperthermia. Open J. Biophys. 2016, 6, 10–18. [CrossRef]

258. Szasz, O. Bioelectromagnetic Paradigm of Cancer Treatment—Modulated Electro-Hyperthermia (mEHT). Open J. Biophys. 2019, 9, 98–109. [CrossRef]

259. Kao, P.H.J.; Chen, C.H.; Chang, Y.W.; Lin, C.-S.; Chiang, H.-C.; Huang, C.-C.; Chi, M.-S.; Yang, K.-L.; Li, W.-T.; Kao, S.-J.; et al. Relationship between energy dosage and apoptotic cell death by modulated electro-hyperthermia. Sci. Rep. 2020, 10, 8936.[CrossRef]

260. Almeida, V.M.; Marana, S.R. Optimum temperature may be a misleading parameter in enzyme characterization and application. PLoS ONE 2019, 14, e0212977. [CrossRef]

261. Eppink, B.; Krawczyk, P.M.; Stap, J.; Kanaar, R. Hyperthermia induced DNA repair deficiency suggests novel therapeutic anti-cancer strategies. Int. J. Hyperth. 2012, 28, 509–517. [CrossRef] [PubMed]

262. Datta, N.R.; Bodis, S. Hyperthermia with radiotherapy reduces tumor alpha/beta: Insights from trials of thermoradiotherapy vs radiotherapy alone. Radiother. Oncol. 2019, 138, 1–8. [CrossRef] [PubMed]

263. Fowler, J.F. The linear-quadratic formula and progress in fractionated radiotherapy. Br. J. Radiol. 1989, 62, 679–694. [CrossRef][PubMed]

264. Kok, H.P.; Crezee, J.; Franken, N.; Stalpers, L.J.; Barendsen, G.W.; Bel, A. Quantifying the Combined Effect of Radiation Therapy and Hyperthermia in Terms of Equivalent Dose Distributions. Int. J. Radiat. Oncol. 2014, 88, 739–745. [CrossRef] [PubMed]

265. Wang, J.-S.;Wang, H.-J.; Qian, H.-L. Biological effects of radiation on cancer cells. Mil. Med. Res. 2018, 5, 1–10. [CrossRef]

266. Zalba, S.; Ten Hagen, T.L.M. Cell membrane modulation as adjuvant in cancer therapy. Cancer Treat. Rev. 2016, 52, 48–57. [CrossRef]

267. Mendez, F.; Sandigursky, M.; Franklin,W.A.; Kenny, M.K.; Kureekattil, R.; Bases, R. Heat-Shock Proteins Associated with Base Excision Repair Enzymes in HeLa Cells. Radiat. Res. 2000, 153, 186–195. [CrossRef]

268. Gaitanaki, C.; Mastri, M.; Aggeli, I.-K.S.; Beis, I. Differential roles of p38-MAPK and JNKs in mediating early protection or apoptosis in the hyperthermic perfused amphibian heart. J. Exp. Biol. 2008, 211, 2524–2532. [CrossRef]

269. Daniel, R.M.; Danson, M.J. Temperature and the catalytic activity of enzymes: A fresh understanding. FEBS Lett. 2013, 587, 2738–2743. [CrossRef]

270. Vashum, S.; Singh, I.R.R.; Das, S.; Azharuddin, M.; Vasudevan, P. Quantification of DNA double-strand break induced by radiation in cervix cancer cells: In vitro study. J. Radiother. Pract. 2019, 18, 55–62. [CrossRef]

271. Macphail, S.H.; Banáth, J.P.; Chu, E.H.M.; Lambur, H.; Olive, P.L. Expression of phosphorylated histone H2AX in cultured cell lines following exposure to X-rays. Int. J. Radiat. Biol. 2003, 79, 351–359. [CrossRef] [PubMed]

272. Banáth, J.P.; MacPhail, S.H.; Olive, P.L. Radiation sensitivity, H2AX phosphorylation, and kinetics of repair of DNA strand breaks in irradiated cervical cancer cell lines. Cancer Res. 2004, 64, 7144–7149. [CrossRef] [PubMed]

273. Mei, X.; Ten Cate, R.; van Leeuwen, C.M.; Rodermond, H.M.; de Leeuw, L.; Dimitrakopoulou, D.; Stalpers, L.J.A.; Crezee, J.; Kok, H.P.; Franken, N.A.P.; et al. Radiosensitization by hyperthermia: The effects of temperature, sequence, and time interval in cervical cell lines. Cancers 2020, 12, 582. [CrossRef] [PubMed]

274. van Leuwen, C.M.; Oei, A.L.; Chin, K.W.T.K.; Crezee, J.; Bel, A.;Westerman, A.M.; Buist, M.R.; Franken, N.A.P.; Stalpers, L.J.A.; Kok, H.P. A short time interval between radiotherapy and hyperthermia reduces in-filed recurrence and mortality in women with advanced cervical cancer. Radiat. Oncol. 2017, 12, 1–8. [CrossRef]

275. van Leuwen, C.M.; Oei, A.L.; Ten Cate, R.; Franken, N.A.P.; Bel, A.; Stalpers, L.J.A.; Crezee, J.; Kok, H.P. Measurement and analysis of the impact of time interval temperature and radiation dose on tumor cell survival and its application in thermoradiotherapy plan evaluation. Int. J. Hyperth. 2018, 34, 30–38. [CrossRef]

276. Raaphorst, G.P. Thermal radiosensitization in vitro. In Hyperthermia and Oncology; Urano, M., Douple, E., Eds.; VSP: Utrecht, The Netherlands, 1994; Volume 2, pp. 17–51.

277. Overgaard, J. Simultaneous and sequential hyperthermia and radiation treatment of an experimental tumor and its surrounding normal tissue in vivo. Int. J. Radiat. Oncol. 1980, 6, 1507–1517. [CrossRef]

278. Kroesen, M.; Mulder, H.T.; van Holthe, J.M.L.; Aangeenbrug, A.A.; Mens, J.W.M.; van Doorn, H.C.; Paulides, M.M.; Oomen-de Hoop, E.; Vernhout, R.M.; Lutgens, L.C.; et al. The Effect of the Time Interval Between Radiation and Hyperthermia on Clinical Outcome in 400 Locally Advanced Cervical Carcinoma Patients. Front. Oncol. 2019, 9, 134. [CrossRef]

279. Crezee, H.; Kok, H.P.; Oei, A.L.; Franken, N.A.P.; Stalpers, L.J.A. The Impact of the Time Interval Between Radiation and Hyperthermia on Clinical Outcome in Patients with Locally Advanced Cervical Cancer. Front. Oncol. 2019, 9, 412. [CrossRef]

280. Kroesen, M.; Mulder, H.T.; van Rhoon, G.C.; Franckena, M. Commentary: The Impact of the Time Interval Between Radiation and Hyperthermia on Clinical Outcome in Patients with Locally Advanced Cervical Cancer. Front. Oncol. 2019, 9, 1387. [CrossRef]

281. Horsman, M.R.; Overgaard, J. Thermal radiosensitization in animal tumors: The potential for therapeutic gain. In Hyperthermia and Oncology; Urano, M., Douple, E., Eds.; VSP: Utrecht, The Netherlands, 1989; Volume 2, pp. 113–145.

282. Aguilar, A.; Ho, M.; Chang, E.; Carlson, K.; Natarajan, A.; Marciano, T.; Bomzon, Z.; Patel, C. Permeabilizing Cell Membranes with Electric Fields. Cancers 2021, 13, 2283. [CrossRef]

283. Okamura, Y.; Kawanabe, A.; Kawai, T. Voltage-Sensing Phosphatases: Biophysics, Physiology, and Molecular Engineering. Physiol. Rev. 2018, 98, 2097–2131. [CrossRef] [PubMed]

284. Szasz, A.M.; Arkosy, P.; Arrojo, E.E.; Bakacs, T.; Balogh, A.; Barich, A.; Borbenyi, E.; Chi, K.H.; Csoszi, T.; Daniilidis, L.; et al. Guidelines for local hyperthermia treatment in oncology. In Challenges and Solutions of Oncological Hyperthermia; Szasz, A., Ed.; Cambridge Scholars: Newcastle upon Tyne, UK, 2020; pp. 32–71.

285. Griffin, R.J.; Dings, R.P.M.; Jamshidi-Parsian, A.; Song, C.W. Mild temperature hyperthermia and radiation therapy: Role of tumor vascular thermotolerance and relevant physiological factors. Int. J. Hyperth. 2010, 26, 256–263. [CrossRef] [PubMed]

286. Kim, W.; Kim, M.S.; Kim, H.J.; Lee, E.; Jeong, J.-H.; Park, I.; Jeong, Y.K.; Jang, W.I. Role of HIF-1 in response of tumors to a combination of hyperthermia and radiation in vivo. Int. J. Hyperth. 2017, 34, 276–283. [CrossRef]

287. Hance, M.W.; Nolan, K.D.; Isaacs, J.S. The Double-Edged Sword: Conserved Functions of Extracellular Hsp90 in Wound Healing and Cancer. Cancers 2014, 6, 1065–1097. [CrossRef]

288. Tittelmeier, J.; Nachman, E.; Nussbaum-Krammer, C. Molecular Chaperones: A Double-Edged Sword in Neurodegenerative Diseases. Front. Aging Neurosci. 2020, 12, 581374. [CrossRef]

289. Giri, B.; Sethi, V.; Modi, S.; Garg, B.; Banerjee, S.; Saluja, A.; Dudeja, V. Heat shock protein 70 in pancreatic diseases: Friend or foe. J. Surg. Oncol. 2017, 116, 114–122. [CrossRef]

290. Pockley, A.G.; Multhoff, G. Cell Stress Proteins in Extracellular Fluids: Friend or Foe? Ciba Found. Symp. Nat. Sleep 2008, 291, 86–100. [CrossRef]

291. Wu, T.; Tanguay, R. Antibodies against heat shock proteins in environmental stresses and diseases: Frend or foe? Cell Stress Chaper. 2006, 11, 1–12. [CrossRef]

292. Taha, E.A.; Ono, K.; Eguchi, T. Roles of Extracellular HSPs as Biomarkers in Immune Surveillance and Immune Evasion. Int. J. Mol. Sci. 2019, 20, 4588. [CrossRef]

293. Derer, A.; Deloch, L.; Rubner, Y.; Fietkau, R.; Frey, B.; Gaipl, U.S. Radio-Immunotherapy-Induced Immunogenic Cancer Cells as Basis for Induction of Systemic Anti-Tumor Immune Responses–Pre-Clinical Evidence and Ongoing Clinical Applications. Front. Immunol. 2015, 6, 505. [CrossRef]

294. Stagg, A.J.; Knight, S.C. Antigen-Presenting Cells, Nature. 2001. Available online: http://labs.icb.ufmg.br/lbcd/pages2/bernardo/Bernardo/Artigos/Antigen-presenting%20Cells.pdf (accessed on 7 October 2020).

295. Rapoport, B.L.; Anderson, R. Realizing the Clinical Potential of Immunogenic Cell Death in Cancer Chemotherapy and Radiotherapy. Int. J. Mol. Sci. 2019, 20, 959. [CrossRef] [PubMed]

296. Szasz, O. Local treatment with systemic effect: Abscopal outcome. In Challenges and Solutions of Oncological Hyperthermia; Szasz, A., Ed.; Cambridge Scholars: Newcastle upon Tyne, UK, 2020; pp. 192–205.

297. Mole, R.H. Whole body irradiation-radiology or medicine? Br. J. Radiol. 1953, 26, 234–241. [CrossRef] [PubMed]

298. Yilmaz, M.T.; Elmali, A.; Yazici, G. Abscopal Effect, From Myth to Reality: From Radiation Oncologists' Perspective. Cureus 2019, 11, e3860. [CrossRef] [PubMed]

299. Craig, D.J.; Nanavay, N.S.; Devanaboyina, M.; Stanbery, L.; Hamouda, D.; Edelman, G.; Dworkin, L.; Nemunaitis, J.J. The abscopal effect of radiation therapy. Future Oncol. 2021, 17, 1683–1694. [CrossRef] [PubMed]

300. Liu, Y.; Dong, Y.; Kong, L.; Shi, F.; Zhu, H.; Yu, J. Abscopal effect of radiotherapy combined with immune checkpoint inhibitors. J. Hematol. Oncol. 2018, 11, 1–15. [CrossRef]

301. Reynders, K.; Illidge, T.; Siva, S.; Chang, J.Y.; de Ruysscher, D. The abscopal effect of local radiotherapy: Using immunotherapy to make a rare event clinically relevant. Cancer Treat. Rev. 2015, 41, 503–510. [CrossRef]

302. Dewan, M.Z.; Galloway, A.E.; Kawashima, N.; Dewyngaert, J.K.; Babb, J.S.; Formenti, S.C.; Demaria, S. Fractionated but not single dose radiotherapy induces an immune-mediated abscopal effect when combined with anti-CTLA-4 antibody. Clin. Cancer Res. 2009, 15, 5379–5388. [CrossRef]

303. Chi, K.H. Tumour-directed immunotherapy: Clinical results of radiotherapy with modulated electro-hyperthermia. In Challenges and Solutions of Oncological Hyperthermia; Szasz, A., Ed.; Cambridge Scholars: Newcastle upon Tyne, UK, 2020; pp. 206–226.

304. Dank, M.; Meggyeshazi, N.; Szigeti, G.; Andocs, G. Immune effects by selective heating of membrane rafts of cancer-cells. J. Clin. Oncol. 2016, 34, e14571. [CrossRef]

305. Andocs, G.; Meggyeshazi, N.; Okamoto, Y.; Balogh, L.; Kovago, C.; Szasz, O. Oncothermia treatment induced immunogenic cancer cell death. Oncothermia J. 2013, 9, 28–37.

Forcing the Antitumor Effects of HSPs Using a Modulated Electric Field

Carrie Anne Minnaar [1,2] and Andras Szasz [3],*,

[1] Wits Donald Gordon Academic Hospital, Johannesburg 2193, South Africa; carrie@onc-hyperthermia.co.za
[2] Department of Radiation Sciences, University of the Witwatersrand, Johannesburg 2000, South Africa
[3] Biotechnics Department, Hungarian University of Agriculture and Life Sciences, 2100 Godollo, Hungary
* Correspondence: szasz.andras@gek.szie.hu

Cite this article as:
Minnaar, C.A. et al (2022) Forcing the Antitumor Effects of HSPs Using a Modulated Electric Field. Cells 2022, 11, 1838. https://doi.org/10.3390/cells11111838

Oncothermia Journal 33, May 2023: 114 – 145.
www.oncotherm.com/sites/oncotherm/files/2023-05/MinnaarCA_et_al_Forcing_Antitumor_Effects.pdf

Abstract:
The role of Heat Shock Proteins (HSPs) is a "double-edged sword" with regards to tumors. The location and interactions of HSPs determine their pro- or antitumor activity. The present review includes an overview of the relevant functions of HSPs, which could improve their antitumor activity. Promoting the antitumor processes could assist in the local and systemic management of cancer. We explore the possibility of achieving this by manipulating the electromagnetic interactions within the tumor microenvironment. An appropriate electric field may select and affect the cancer cells using the electric heterogeneity of the tumor tissue. This review describes the method proposed to effect such changes: amplitude-modulated radiofrequency (amRF) applied with a 13.56 MHz carrier frequency. We summarize the preclinical investigations of the amRF on the HSPs in malignant cells. The preclinical studies show the promotion of the expression of HSP70 on the plasma membrane, participating in the immunogenic cell death (ICD) pathway. The sequence of guided molecular changes triggers innate and adaptive immune reactions. The amRF promotes the secretion of HSP70 also in the extracellular matrix. The extracellular HSP70 accompanied by free HMGB1 and membraneexpressed calreticulin (CRT) form damage-associated molecular patterns encouraging the dendritic cells' maturing for antigen presentation. The process promotes CD8+ killer T-cells. Clinical results demonstrate the potential of this immune process to trigger a systemic effect. We conclude that the properly applied amRF promotes antitumor HSP activity, and in situ, it could support the tumor-specific immune effects produced locally but acting systemically for disseminated cells and metastatic lesions.

Keywords:
oncology; hyperthermia; modulation; modulated electro-hyperthermia; bio-electromagnetics; transmembrane protein; raft; immunogenic cell-death; abscopal effect; nonthermal field effect

1. Heat Shock Proteins

The stress- or heat shock proteins (HSPs) represent a large family of highly conserved molecules vital in almost every living cell, on their surfaces, and in their extracellular microenvironments, throughout the cells' lifetime regardless of their evolutionary level [1]. Their regulatory roles are complex and diverse, including protection from stresses, regulation of neurodevelopment [2], and modulating immune functions [2]. Some HSPs are present at relatively constant levels, while the large quantities of the expression of others appear only in response to stress [3]. Most HSPs act as molecular chaperones which play a role in protein maturation or degradation and can either reverse or inhibit the denaturation or unfolding of cellular proteins in response to stress. There are many different families of HSP chaperones. Each family acts differently to aid protein folding, as summarized by Horvath and colleagues in their review [4]. Additional functions include blocking aggregation, facilitating protein translocation through intracellular compartments, and the maintenance of steroid receptors and transcription factors [4].

Any change in the dynamic equilibrium of the cell's life, such as environmental stresses [5], pathogenic processes [6], diseases [7], or even psychological stresses [8], activates the synthesis of HSPs. The genetic orchestrator of the HSPs is the master transcription factor, the heat shock factor (HSF) [9], which plays a role in disease and aging [10]. The HSF1 [11], and some other inducers, such as hypoxia-inducible factor 1 (HIF-1) [12], matrix metalloproteinase 3 (MMP-3), and heterochromatin protein 1 [13], trigger the production of the relevant HSPs in a coordinated manner.

The roles and impacts of HSPs are highly complex. The complexity determines their role in immune modulation and in cancer development. For example, increased expressions of the members of the HSP70 family HSPa1a, HSPa1b, and HSPa7 are associated with a poor prognosis in human colorectal cancer observed in the comparison of the pretreatment tumor samples with the clinical data. However, the increased expression of the same family member, HSPa9, in tumors was associated with a favorable prognosis [14]. Heat shock proteins also play a role in many human pathologies. Low levels of HSPs are typically seen in Type II Diabetes and neurodegenerative diseases, while malignant cells have abnormally high levels [15].

While the primary function of most HSPs is the protection of cells against stresses, their function is not limited to protection on a cellular basis. Under certain conditions, they participate in the collective protection of multicellular structures and tissues and may even play a role in systemic processes [16,17].

HSPs are able to transport intracellular antigenic peptides to antigen-presenting cells (APCs), which produce antigen-specific cytotoxic T-lymphocytes (CD8+). During this process, the intracellular HSPs (iHSPs) transfer through the cellular membrane and into the ECM [18]. The secretion of HSPs on the membrane (mHSPs), or release of them into the ECM (eHSPs), appears to be associated with lysosomal endosomes or via the release

of exosomes containing HSPs [19]. The iHSP may be translocated to the cellular membrane via the same transport pathway of secretory lysosomes during this process. A fusion between the lysosome and cell membrane occurs, followed by the insertion of the lysosomal membrane protein LAMP1 into the extracellular portion of the cell membrane and the secretion of the HSPs, along with other lysosomal proteins, into the ECM [20]. All three variants of HSPs concerning their position to the plasma membrane (iHSP, mHSP, eHSP) regulate the complex interactions of the cells with their environment but have different roles. Intracellular HSPs are typically cytoprotective, while membrane-associated and extracellular HSPs are not.

Furthermore, iHSPs have active essential functions in various locations within the cell, including the nucleus, the mitochondria, the endoplasmic reticulum (ER), and the cytosol [21]. The mHSPs and eHSPs have a physiological role in inflammation and pro-, and antitumor activity [22].

Intracellularly, the HSPs as molecular chaperones assist in maintaining the balance between the intracellular proteins, participate in the regulation of apoptosis, and protect the cells from stress [23] caused by various external stressors, such as hypoxia, thermal or oxidative stress, mechanical stressors, or even electromagnetic interactions. Membrane-bound HSPs modulate membrane characteristics such as fluidity, permeability, and secretary routes, while eHSPs are important mediators of intercellular signaling [4].

The different families of HSPs represent the further functional division at numerous locations. Therefore, each has specific activities and functions in a cooperative network of homeostatic control.

HSPs: Friend or Foe in Oncology

The multifunctional behavior of HSPs results in opposing actions. They may either support cellular defense [1] or, in some instances, promote cellular death [24]. This dual function of HSP has led them be classified as a “friend” or “foe” [25–27]. The HSPs participate in the maintenance of the dynamic and complex homeostatic balance. The stochastic mechanisms of the HSPs’ balance their contribution to regulative processes, participating as promoters or suppressors. The decision between the two opposing behaviors depends on their microenvironment’s conditions and interactions. The balancing creates a “double-edged sword” [28,29] exhibiting both sides: inflammatory and anti-inflammatory; protumoral and antitumoral; immune-stimulatory and immune-suppressant, etc. In standard homeostatic conditions, HSPs support cell protection in the case of healthy functioning cells and support cellular death in the case of cellular dysfunction.

The distinction of functions in malignancy is rather complex. The individually wellfunctioning cells with unicellular preference renounce multicellularity, causing fundamental challenges in malignancy decisions [30]. The malignant cells vividly function, immortally proliferating as unicellular units, but their activity is destructive to the system, in part, where they are located. In this meaning, the malignant proliferation and the evolutional unicellular invasion have a lot in common [31]. The phenomenon is similar to atavism [30], considering the self-ruled unicellular activities. The loss of multicellular connections potentiates adaptability. These cells are robustly vivid. The malignant cells do not use the living advantages of collectivism; their individualism is predominant [32]. However, unicellular autonomy requires nutrition-rich environmental conditions for survival [33]. Cancer has a supportive environment provided by their healthy host. Cancer modifies its environmental conditions for support, and the homeostatic control tries to “heal” the abnormality [34]. The cancerous process avoids natural apoptosis [35]. The HSPs protect the malignant cells and appear as a “foe” of the organism in these processes. The curative task is straightforward: favor converting the role of HSPs to support cellular death.

Sensing the immunosurveillance of the system could serve as the reversing factor from a foe to a friend. The effects of the stress proteins were recognized early on in immunology [36] and have become a popular topic in the emerging field of immunooncology [37]. Furthermore, the use of HSPs as biomarkers of environmental analyses [38], prognoses [39], immune surveillance [12], and as therapeutic targets in malignant [40,41] and other diseases [42], is rapidly expanding.

Most oncological treatment methods cause extra stress, which induces HSPs. The increased HSP synthesis is seen after conventional hyperthermia [43], chemotherapy [44], radiotherapy [45], and even phototherapy [46]. The protection of the malignant cells depends on the chaperone functions of iHSPs from the HSP70, HSP27, and HSP90 families [13,47]. Overexpression of specific HSPs provides a selective advantage for malignant cells to inhibit apoptosis, promoting tumor metastasis and influencing immune responses for their benefits [48–50].

Stress also induces the translocation of iHSPs to the malignant cell’s membrane [51], forming mHSPs [23]. The mHSP is dual-action [52] as well, and could support [53] and suppress the survival abilities [54] of the

malignant cells. The signaling of mHSPs may subsequently alert the NK cells to the presence of the malignant cells [55] as the first sign of immune activation. The extracellularly released HSPs could play a crucial role in tumor immunity [56]. In addition to the iHSP → mHSP → eHSP conversion sequences, the iHSP may be liberated directly into ECM from necrotic cells, providing eHSP without intermediate location on the plasma membrane.

2. Electromagnetic Method of Hyperthermia in Oncology

Electromagnetism is one of the active factors in biological processes, and it has a broad therapeutic application in oncology. One of the widely used treatments is the local-regional heating of the tumor and its environment. The absorption of electromagnetic energy heats the tissues in these therapies utilizing radiofrequency (RF) and microwaves [57,58]. It is a complementary oncological treatment applied in combination with the relevant standard protocols to support and enhance the effects of various other oncotherapies.

The heat stress-induced iHSPs present a significant challenge for oncological hyperthermia treatment because these chaperones' elevated level develops treatment resistance and promotes the malignant processes [59]. The HSP27, HSP70, and HSP90 chaperone families reduce the tumor-suppression ability to support angiogenesis and metastases [59,60]. The Cells 2022, 11, 1838 4 of 32 heat shock regulator HSF1 plays a considerable role in tumorigenesis, thus, its knockdown significantly reduces the proliferation of cancer cells [61]. Consequently, developments of HSP inhibitors became a target of tumor research [62]. The disruption of HSP47 shows substantial sensitizing of such chemoresistant cancer as pancreatic ductal adenocarcinoma [63]. The inhibition of lactate dehydrogenase impairs the stress response and increases the radiosensitivity of many aggressive, otherwise radioresistant, tumors [64].

Paradoxically, hyperthermia has shown profound success in inhibiting cancerous growth. Hyperthermia combined with conventional chemo- and radiotherapies, surgery, and the emerging immunotherapies [65] achieved significant tumor destruction in clinical practices. It is an effective radio- and chemosensitizer and cooperates well with the immune system [66]. Multiple high evidence levels of the clinical studies prove the method's success [67]. The strengths, weaknesses, and opportunities of hyperthermia applications in oncology have been analyzed in detail, showing general overall promise for exceptional success in treating tumors [68].

The apparent controversy between supporting or inhibiting tumor growth indicates, again, the complex behavior of heating interventions, which appears in the "double-edged sword" phenomena Cooperation with the natural homeostatic regulations could be a decisional factor to push the balance to the favorite side. One of the overall regulators of the homeostatic control is the immune-surveillance, which may have an excellent partner to win [69].

The bioelectromagnetic interactions potentially manipulate the locations and functions of the HSPs, driving the complex challenge of cooperating with the immune effects and re-establishing the healthy homeostatic balance.

Bioelectromagnetic energy absorption heats the targets. Heating has two fundamental concepts in oncological practice:

- One way is to heat the whole tumor volume isothermally. The applied focusing techniques intend to maximize the temperature of the tumor volume and minimize it in healthy surroundings [70]. The original heating goal is necrosis. The applied dose compares the actual cellular distortion to the necrosis achieved in vitro at 43 C [71];
- Another way heats small selected targets, either artificially or naturally available centers in the tumor volume:
    - The method injects artificial (mostly inorganic metallic nanoparticles) into the tumors. These invasively placed exclusive energy absorbers [72,73] distribute locally throughout the tumor, absorb the energy selectively, and transfer heat to their environment;
    - The tumor's heterogenic structure offers natural targets. The optimally chosen electromagnetic properties such as the frequency, the intensity, the phase, and the delivered time–information (modulation) allow for tuning to select the chosen particle (molecular cluster). For example, the membrane rafts (lipid micro-domains found in the plasma membranes of cells [74]) offer the perfect opportunity. The high electromagnetic contrast

allows selection between the lipid-supported transmembrane proteins (membrane rafts) and their pure double lipid holding membrane material.

All heating methods induce the expression of various HSPs [75]. While homogeneous heating and the heating of artificially injected particles act only with their thermal activity, the natural particles may have additional nonthermal excitation by the field [76,77]. Note that an effect is considered nonthermal "when, under the influence of a field, the system changes its properties in a way that cannot be achieved by heating" [78].

The lipid raft micro-domains respond to electromagnetic fields [79]. Membrane rafts are highly heterogeneous and dynamic sterol- and sphingolipid-enriched domains, which may also involve protein interactions and compartmentalize cellular processes [80]. The rafts operate as a trigger of the intracellular processes [4]. The rafts collect dynamic proteins [74], including proteins with high lateral mobility in the membrane [81]. The raft's size varies within the nano range, depending on the protein content in the cluster. The membrance of the malignant cells presents a significantly higher number of transmembrane proteins and their clusters than their nontumorigentic counterparts. [82].

The heating of the molecular clusters on the tumor cells causes extreme stress on the cells, which can trigger programmed cell death [83]. The electromagnetic field extends the production of active HSPs [84,85]. The absorbed energy results in the heating of the target and resonantly excites the molecules, driving the signaling and the development of HSPs. A great part of the energy absorbed by the natural heterogeneities is nonthermal [86], and if characteristic, the optimally tuned electromagnetic wave could deliver energy for molecular excitations. The excitations focus on signal triggering and transmission and are involved in the various ionic and molecular interactions, focused on re-establishing the missing apoptosis in malignant cells. The process results in a subtle heterogeneously distributed thermal effect with the resonant conditions [87,88]. Research shows that the nonthermal resonant absorption adds to HSP expression [89] and function [90].

This review focuses on hyperthermia driving HSP activity in a "friendly way". Our goal is to convert the HSPs' role from "foe" to "friend", promoting ICD of the tumor cells. This could shift the approach to treating malignancy with hyperthermia from targeting local disease to producing systemic activity.

The heterogenic selection principle proposes a solution to the challenge of tissue selection in hyperthermia [91] by applying non-isothermal heating [92]. We use the principles of modulated electro-hyperthermia (mEHT), which has already demonstrated its clinical benefits, improving outcomes for patients when combined with chemotherapy and radiotherapy [93-95]. The mEHT synergically utilizes mild heating, which improves blood flow and perfusion [96] and the modulated electic field [97]. The heterogenic characteristics guide the mEHT-induced electric current through the target tissue. The unique attributes of malignant cells, such as their high proliferation rates, produce enhanced concentrations of ions in the ECM, resulting in their particular electromagnetic properties. As a result, the tumor microenvironment (TME) is more conductive and drives the flow of current through the target tumor using an appropriate frequency and modulation [87], Figure 1a,b.

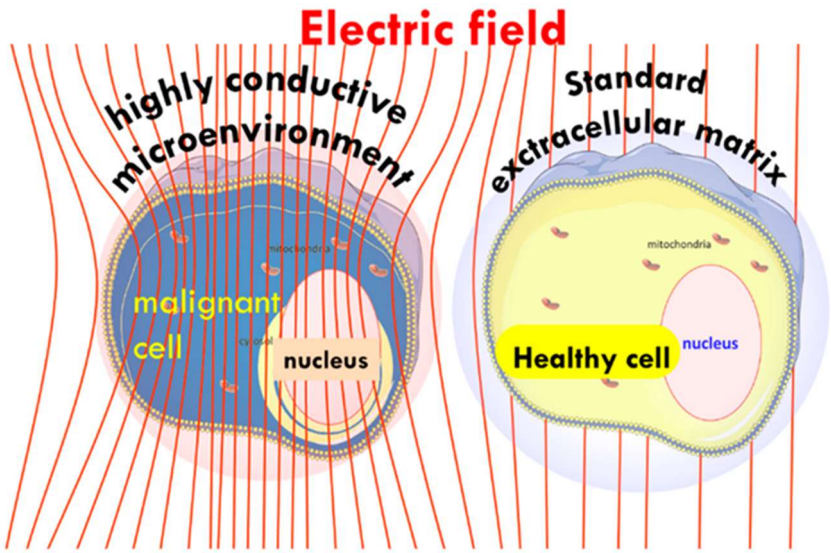

(a)

Figure 1 Cont.

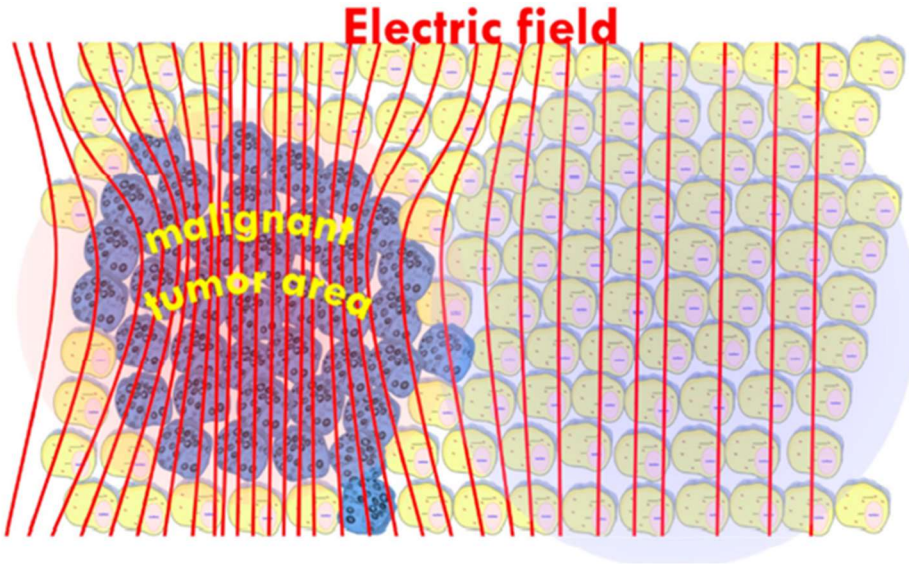

(b)

Figure 1 Schematic illustration of the current focus using impedance selection: (a) the microscopic illusion of an increase in absorbed energy by the malignant cell compared to the healthy cell, and (b) macroscopic illustration of the energy flowing more easily through malignant versus healthy tissue.

The selection uses the relatively high number of membrane rafts on the surface of malignant cells [82], which have a selectively high energy absorption rate of RF current [98] and appear to be the highest energy absorbers in the malignant tissue [98] (Figure 2).

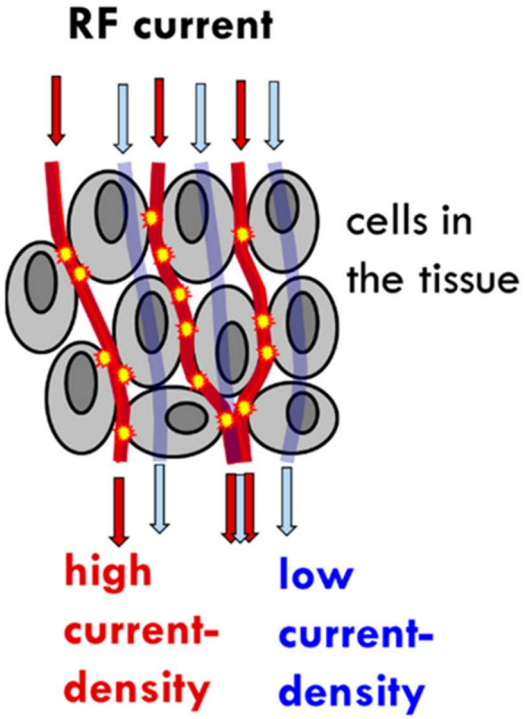

Figure 2. Nano-heating: schematic representation of the flow of current through malignant tissue, between the cells, and the absorption of the energy in the membrane rafts, leading to areas of high current density.

The mEHT technology applies capacitive-coupled energy, using precise impedance matching [99] in order to create an electric field with characteristics that ensure the appropriate current density (j). The j acts thermally (Joule heat) and nonthermally (molecular excitation). The power of the thermal energy production depends on the j^2, while the j excites the molecules linearly. The j has to over-dominate the j^2 otherwise the electrical selection becomes negligible to the increased heating. A low current density (low power) must be applied to prevent the over-powering heat and ensure electrical selection. The mEHT uses a much lower power output than conventional hyperthermia [97]. This solution allows for the real-time control and adaption of the treatment to the patient, as the treated tumor forms a part of the tuned electric circuit [100]

(Figure 3). Cells 2022, 11, 1838 7 of 32 must be applied to prevent the over-powering heat and ensure electrical selection. The mEHT uses a much lower power output than conventional hyperthermia [97]. This solution allows for the real-time control and adaption of the treatment to the patient, as the treated tumor forms a part of the tuned electric circuit [100] (Figure 3).

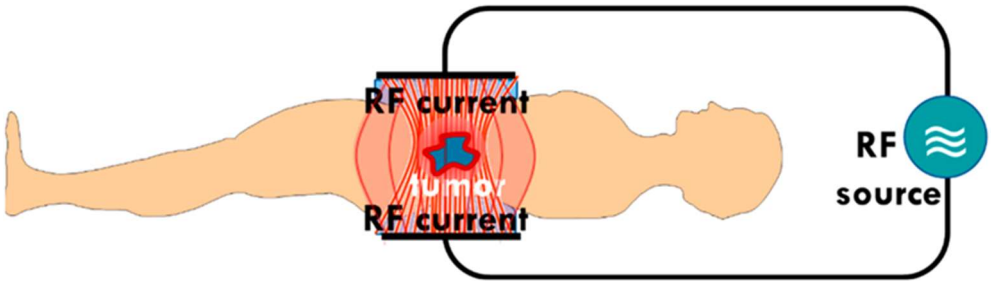

Figure 3. Schematic representation of the patient forming part of the tuned electric circuit. The low impedance of the tumor drives the current to select the malignant cells. There is precise, real-time control of the impedance matching of the patient and the tumor in situ.

3. The Effect of mEHT on HSPs

The mEHT treatment induces up-regulation and increased expression of all major HSPs at an mRNA [101] and protein level [102] in HT29 xenografts. These preclinical studies have demonstrated the effects of mEHT on the up- and down-regulation of specific genes [83].

The heat-map of gene expression showed that mEHT induced significant up- or down-regulation of 48 transcripts of 39 genes compared to controls in the study on HT29 xenografts. The relative mRNA expression of HSP70 reached maximum expression four hours post-treatment [101]. Gene coding for members of the HSP70 family were upregulated, including HSPa1a, HSPa1b, HSPa4, HSPa6, and HSPa8, and their co-chaperones HSP40 (DNAJB1 and DNAJB4) and Bag3. The transcription of HSP90 alpha (HSP90AA1) and HSP60 (HSPD1) was also up-regulated in HT29 xenografts. An increase in a broad spectrum of HSP families at an mRNA level was observed in HT29 xenografts four hours post-treatment [103].

The up-regulation of several genes, including HSPb1, HSPa1a, HSPa1b, and HSPh1, was also seen in triple-negative 4T1 breast cancer isografts treated with mEHT. This observation was noted 24 h post-treatment and was associated with inhibiting tumor growth and proliferation. HSPa1a and HSPa1b are the most common isoforms of the HSP70 family. The RNA sequencing showed significant HSP70-1 (HSP72), HSP70-2, HSPB1, and chaperone HSP105 development 24 h after treatment, along with the up-regulation of the associated genes [104]. An increase in the HSP70 concentrations around the peripheral margin of the tumors 24 h post-treatment was observed.

A gene chip analysis of the U937 (human lymphoma) cell line showed an activation of the cytoprotective gene network in samples heated with water-bath homogeneous heating (wHT). The up-regulation of genes, such as HSP105 and HSP90A, have been shown to block apoptosis by interfering with caspase activation and directly and indirectly inhibit apoptosis. In this study, the HSPs appeared to play an antiapoptotic role as they prevented apoptotic cell death in the cells heated with wHT, but not in the cells heated with mEHT [105]. Here the gene map showed a distinct difference in the gene regulations between the water-bath and mEHT-treated samples at the same temperature. The ingenuity pathway analysis revealed the cell death's specific gene network, including EGR1, JUN, and CDKN1A genes. Despite the same thermal condition, the mEHT treatment does not appear to activate the cytoprotective network while the water-bath treatment activates it. The activation of the ERK-JUN pathway was present only in the mEHT-treated samples. The FAS, c-JUN N-terminal kinases (JNK), and ERK signaling pathways dominate the apoptotic pathway. The ingenuity pathway study uncovered the HSP network (Figure 4a–c), which significantly differs from the wHT at the same temperature. As the temperatures in both heating methods were the same, the difference in pathway activations is most likely due to the electric field effects [105].

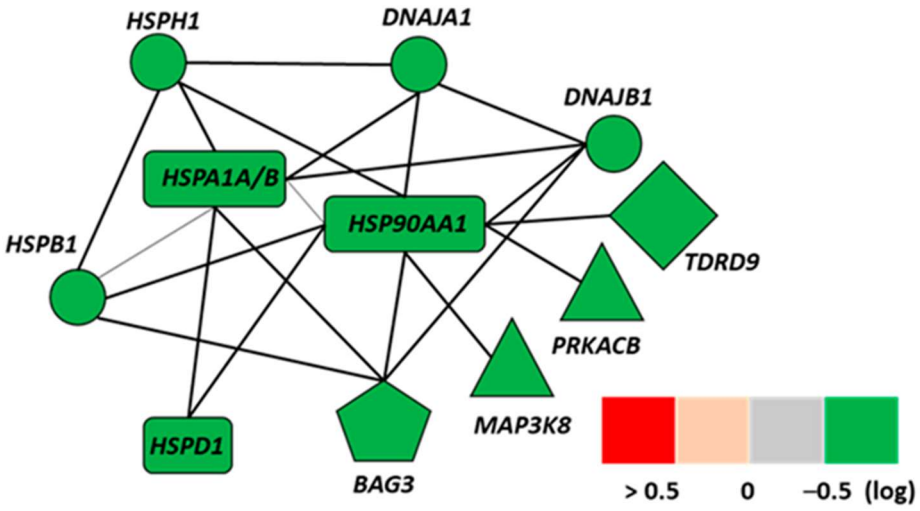

(a)

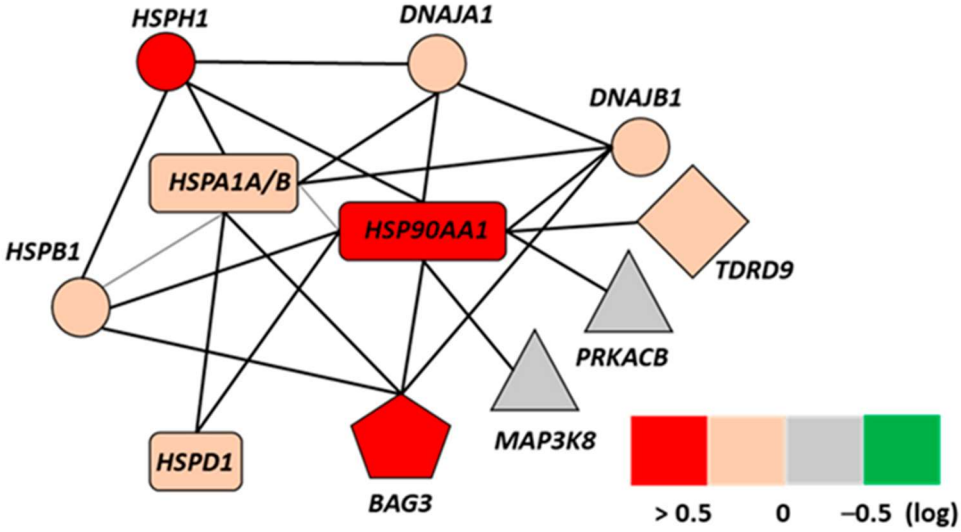

(b)

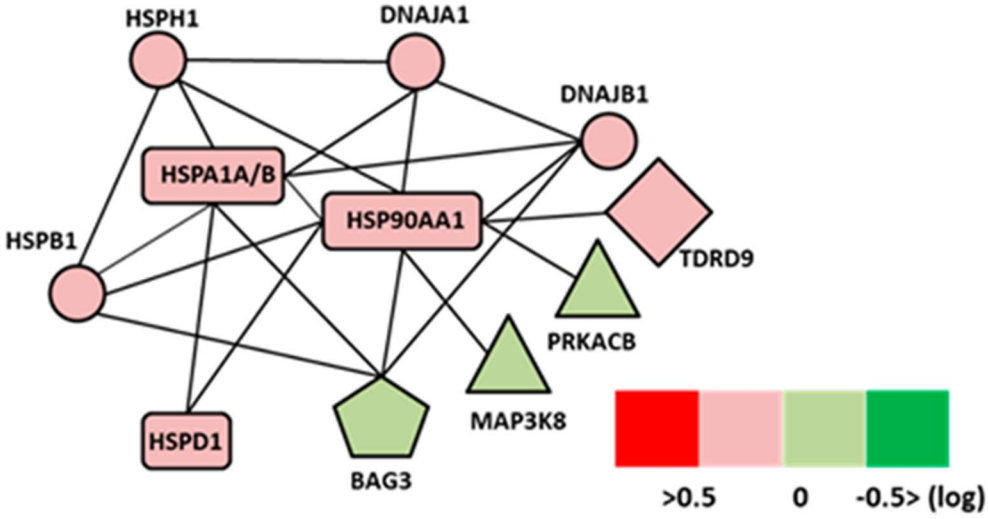

(c)

Figure 4. Ingenuity analysis of the network of HSP-related interactions at a genetic level [105]:
(a) control samples (38 ℃),
(b) wHT-treated samples (42 ℃),

(c) mEHT (42 ℃). Important differences between wHT and mEHT treatments at the same temperature: the less intensive tumor-protective HSP functions in the mEHT sample; the pro-tumor BAG3 remains nonregulated in the mEHT sample.

The level of mRNA-associated iHSP70 peaks at four hours post-treatment in 4T1 isograft models [104], while the HSP protein-associated expression reaches its maximum between 12 and14 h (Figure 5a), and decreases to the baseline concentration after 48 h in the 4T1 isograft [106] and the HT29 xenograft [101] samples (Figure 5b).

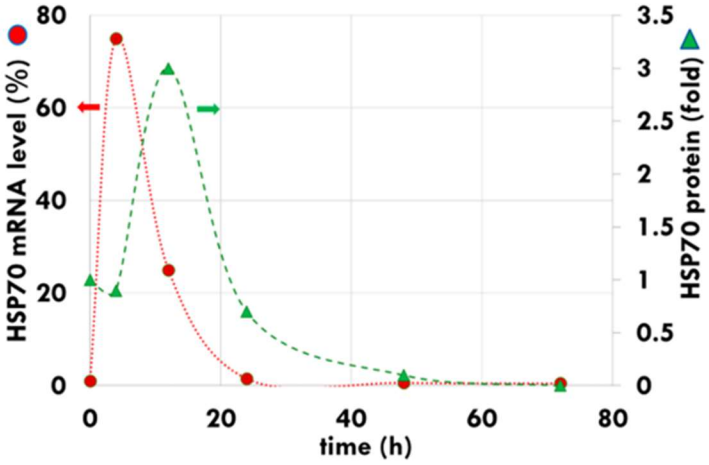

(a)

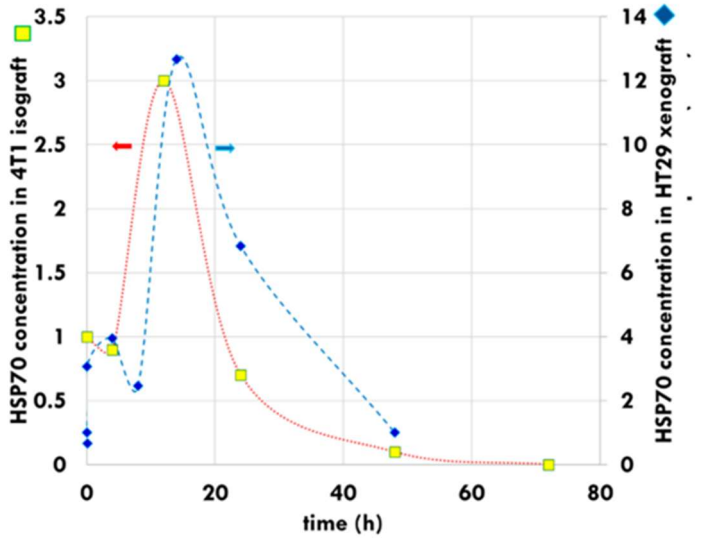

(b)

Figure 5. Development of iHSP by mEHT.
(a) The HSP70 peak is indicated at mRNA level (dots, left axis) approximately eight hours earlier than the measured HSP70 folded protein peak (triangles, right axis).
(b) The HSP peak has similar features in the measurements of the 4T1 isograft (square, left axis) and HT29 xenograft (diamond, right axis). The curves are for guiding the eye.

It is clearly shown that the up-regulation of the HSP70 in the HT29 xenograft model treated with mEHT increases, peaking at 14 h post-treatment, followed by a decline and a return to baseline levels at 48 h. The distribution of HSP70 shows a large increase in iHSPs during this first peak. The second peak in HSP expression occurs between 72 and 120 h posttreatment, followed by a return to baseline levels after 168 to 216 h post-treatment (Figure 6). The second peak is likely a result of the release of mHSPs into the extracellular environment producing eHSPs [101].

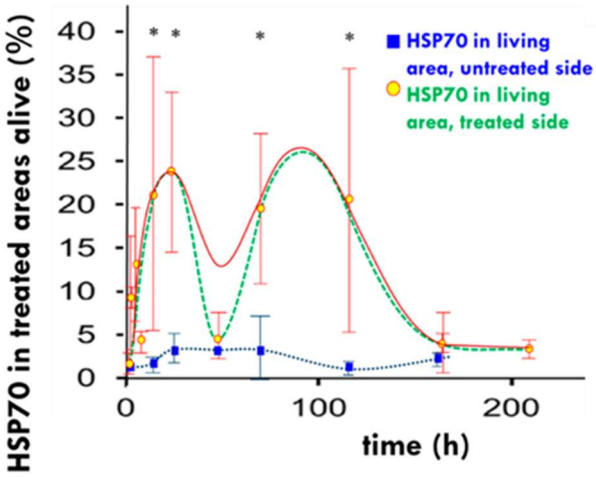

Figure 6 The measured development of HSP70 (dots, solid line). The dual peak pattern represents two types of HSP70. The first is primarily anti-apoptotic connected to the chaperone functions, while th second is pro-apoptotic as a part of the immunogenic cell death. The dashed line approximately represents the two preak separations. The dotted line shows the development of HSP70 in the untreated tumor of the immunocompromised murine HT29 xenograft model. The asterisks on the top indicate significant differences between the HSP70 recorded on the treated side and the untreated side. The curves are for guiding the eye. * $p < 0.05$.

The levels of mHSP70 and eHSP70 also show an increase in B16F10 melanoma allograft models treated with mEHT, compared to the control, at 24 h post-treatment (Figure 7).

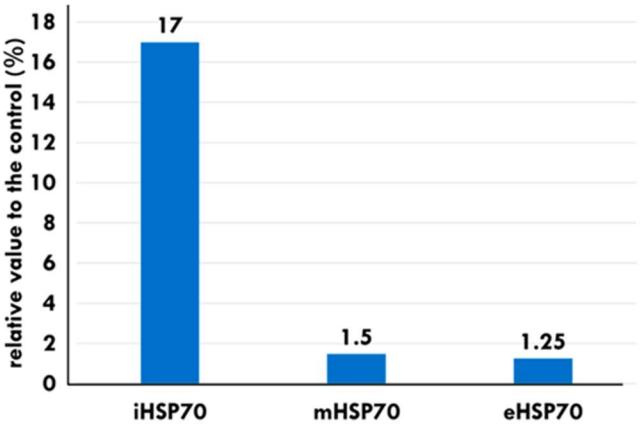

Figure 7. The localization distribution of HSP70s in B16F10 melanoma allografts at 24 h [107]. Massive apoptosis appeared despite increased chaperoning by iHSP70.

Yang et al. Showed that heat stress in the HepG2 cell line produces massive increases in iHSPs following all heating methods. The secretion of eHSP70 also appears post-treatment between 24 and 48 h in all heating methods. However, the levels of eHSPs are significantly higher following mEHT treatments [75] (Figure 8). The data of 24 h post-treatment show an accelerated increase in the eHSP concentration. The increase in the eHSP70 expression was also noted in vivo in B16F10 melanoma allografts [107] and in HT29 colorectal xenografts [105].

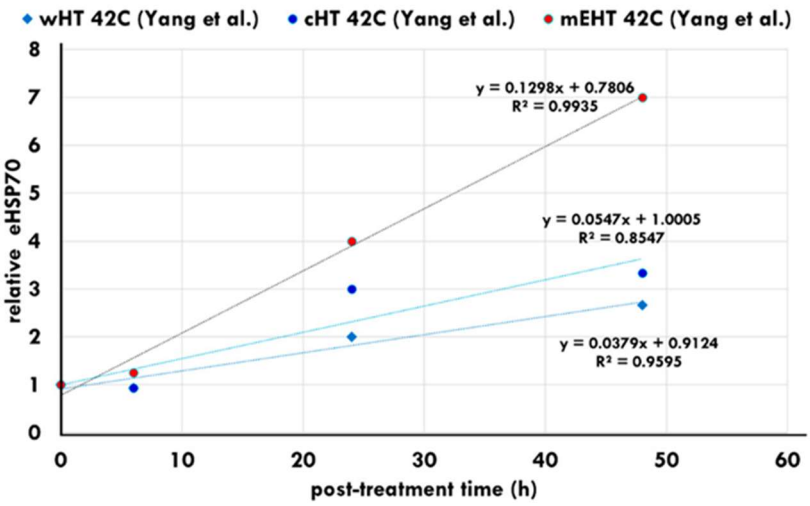

Figure 8 eHSP concentrations following water heating (wHT), capacitive heating (cHT) and heating using mEHT. The increase in eHSPs is significantly higher following mEHT heating compared to the other heating techniques [75].

The inoculation of tumors into two different regions in vivo, e.g., the left and right femoral region [108], or the femoral and thoracic region [109], is a popular method for evaluating tumor responses to treatment as each tumor has its control in the same animal. When both mice's femoral regions were inoculated with xenografted human colorectal cell line (HT29) tumors [108], the right tumor of each mouse had a treatment with 30 min of mEHT, and their left tumor remained untreated. After treatment, resected samples showed an increase in HSP60 and HSP70 concentration in the treated tumors, peaking at eight hours post-treatment [102] (Figure 9a,b).

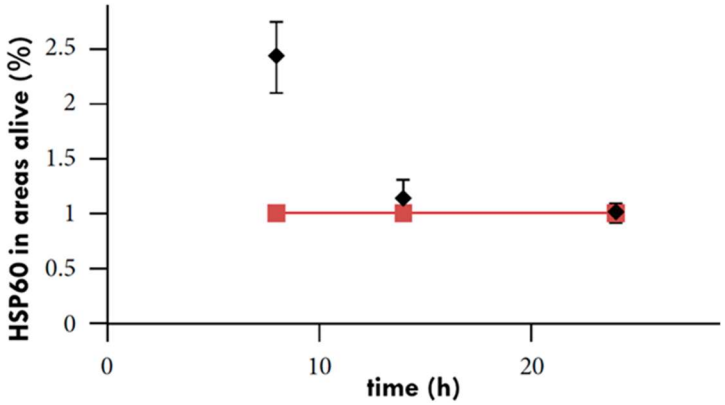

(a)

Figure 9 Cont.

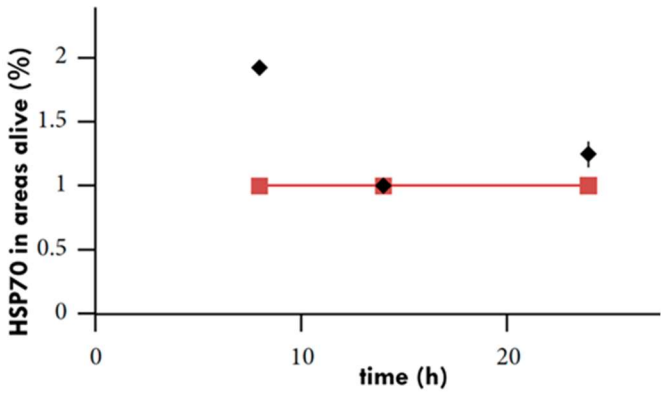

(b)

Figure 9 Relative protein expressions of
(a) HSP60 and
(b) HSP90 in murine models. The diamonds represent HSP levels in treated tumors and the squares represent untreated tumors in the same mouse [102].

In a follow-up study by Andocs et al., mice were inoculated with HT29 xenograft cells in both hind legs. One of the resulting tumors in each model was treated with mEHT and the other was left untreated. A consistent increase in HSP90 was observed in the tumors treated with mEHT. In these tumors, two peaks in the expression of iHSP90 were observed; the first at ~24 h post-treatment and the second between 168 and 216 h post-treatment [101] (Figure 10). An increase in HSP90 expression was also observed in the untreated tumor in each model [101]. In the untreated tumor, the HSP90 expression peaked at ~14 h posttreatment, reaching levels close to those seen in the treated tumor at ~14 h post-treatment, before declining. The observation that the untreated tumor also responds with an increase in the level of HSP90 may suggest the presence of cross-talk between the two tumors, although this is speculative and further investigation is needed to confirm this.

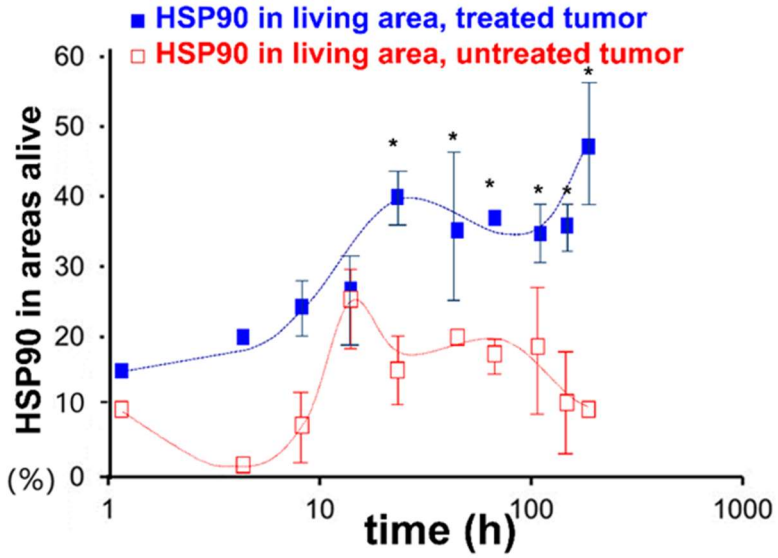

Figure 10. Graph showing the significant increase in HSP90 in the relative mask area (rMA—calculated by dividing the stained area by the whole annotation area), seen between 24 and 216 h posttreatment in the treated tumor cells (solid square markers) compared to the untreated tumor cells (empty square markers) in the morphologically intact areas from excised murine-model tumors (* $p < 0.05$) [101].

4. The Effect of mEHT on Apoptosis

The results of the preclinical apoptosis studies suggest that despite the increased expression of iHSPs, the mEHT has the potential to inhibit tumor growth and support the development of an apoptotic process [110]. When HSP70s reach a peak at approximately 12 h post-treatment, the complex stress on the cells exhausts the HSP response and the subsequent protection capability of the HSPs at 24 h in 4T1 isografts [106]. In the event that the protective mechanisms from the iHSPs are unable to restore normal cell functions after exposure to stress, the stress on the cell results in cell cycle arrest, which is typically by caspase-dependent apoptosis [106]. During caspase-dependent apoptosis, caspase-3 is activated, forming cleaved caspase-3 (cCas3). To understand HSPs and their role post-induction from mEHT treatments, several markers, including cCas-3, have been studied alongside HSPs. The expression of iHSPs were found to peak at approximately 4 h post-treatment with mEHT and returned to normal levels at approximately 24 h post-treatment with mEHT [101,106]. The tumor destruction ratio (TDR,%) also peaked at approximately 24 h after the final mEHT treatment, suggesting that the protective mechanisms from the HSPs had been exhausted by this time. Furthermore, the proportion of the cCas3-positive regions overlapped extensively with the damaged regions of the tumor seen on consecutive sampling [106]. The progress of the development of HSP70 and the tumor destruction ratio alongside cCas3 shows well how the tumor-degradation overthrew the HSP70 protection (Figure 11). The timing suggests that the cCas3-dependent apoptosis plays a major role in destroying the tumor post-mEHT treatment in the 4T1 murine tumor isograft.

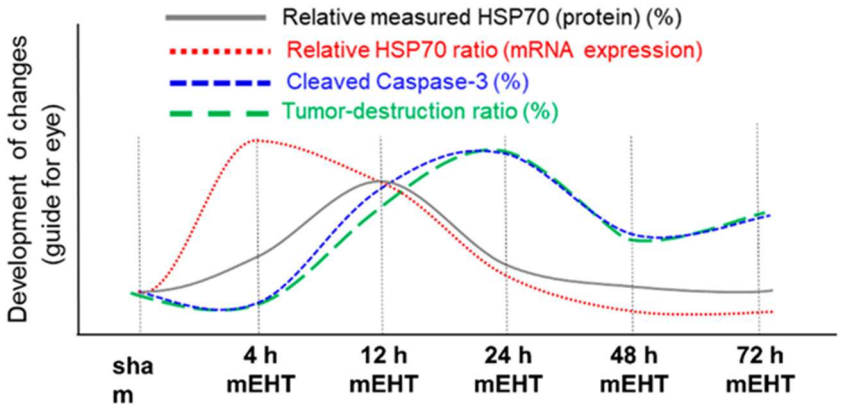

Figure 11. The trend of the development of tumor destruction, HSP expression, and cleaved caspase-3 at discrete time-points in 4T1 murine tumor isograft. The x-axis contains discrete steps, the curves are only to guide the eye.

Apoptosis-inducing factor (AIF), a flavoprotein that resides in the mitochondrial intermembrane space, may also have a role in apoptosis caused by mEHT [111]. Following cellular stress, AIF translocates to the nucleus and triggers chromatin condensation and large-scale DNA degradation, inducing caspase-independent apoptosis [112]. AIF expression provides an additional signal pathway for apoptosis [110,111]. This process has the potential to affect untreated tumors as well [108].

The mEHT may induce other apoptotic pathways detected in vitro [75] (Figure 12). Various studies have shown that the complex apoptotic pathways triggered by mEHT result in higher rates of programmed cell death after cHT and wHT under the same thermal conditions (42 C, 30 min) [75,113]. The multi-path apoptotic processes ensure massive apoptosis despite the various protective mechanisms of HSPs and XIAP.

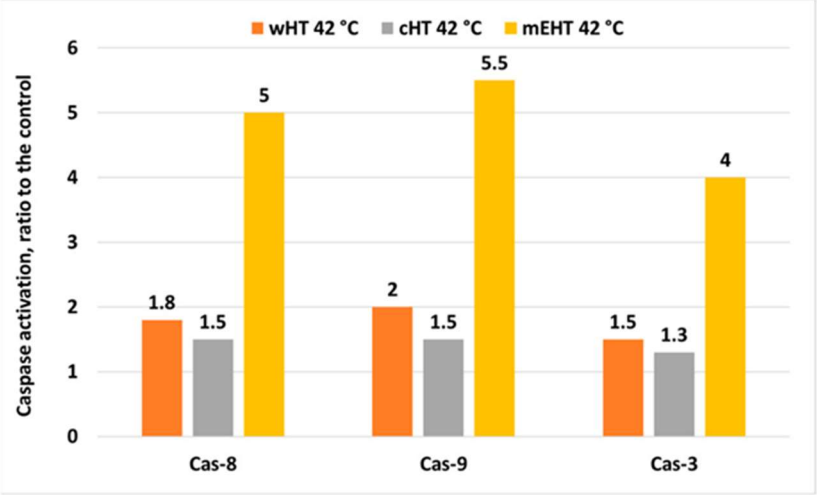

Figure 12. Apoptosis markers: cCas-3, -8, and -9, are increased in samples treated with mEHT compared with samples treated with water heating (wHT) and capacitive heating (cHT) [75].

The comparison of the wHT and mEHT under the same thermal conditions also shows significant differences in the intercellular calcium (iCa^{2+}) concentration [77,105,114]. An overload of Ca^{2+} intracellularly is detrimental to the health of the cell as it may increase their susceptibility to apoptotic cell death. The Ca^{2+} overload also causes the apoptitic destruction of tumor cells following the application of a modulated field [114]. Furthermore, mEHT treatment triggers the up-regulation of the E2F1 protein, which is involved in E2F1-mediated apoptosis [83] in various glioma cell lines. Apoptosis facilitators (such as PUMA and p21^{wafl} (also known as wild-type p53-activated fragment 1:
WAF1) [115]), increased rapidly following the preclinical treatment of melanoma with mEHT and a significant reduction in tumor size was observed following a stress response signaled by iHSP70 and mHSP70 [107].

Another preclinical study on a melanoma model treated with mEHT [116] showed NK-cell infiltration into the tumor. The mHSP facilitates the NK-infiltration [117], which can explain the role of mEHT. Myeloperoxidase (MPO, peroxidase enzyme) positive neutrophil granulocytes (and monocytes) were significantly elevated in xenografts treated with mEHT compared to control tumors from 48 h to approximately 216 h post-treatment

[103] in HT29 xenograft studies. The enrichment of MPO may further enhance cell destruction in mEHT-treated samples, which has support from the peak of the CD3+ T-cells' density at the same peak as MPO at 168 h (Figure 13).

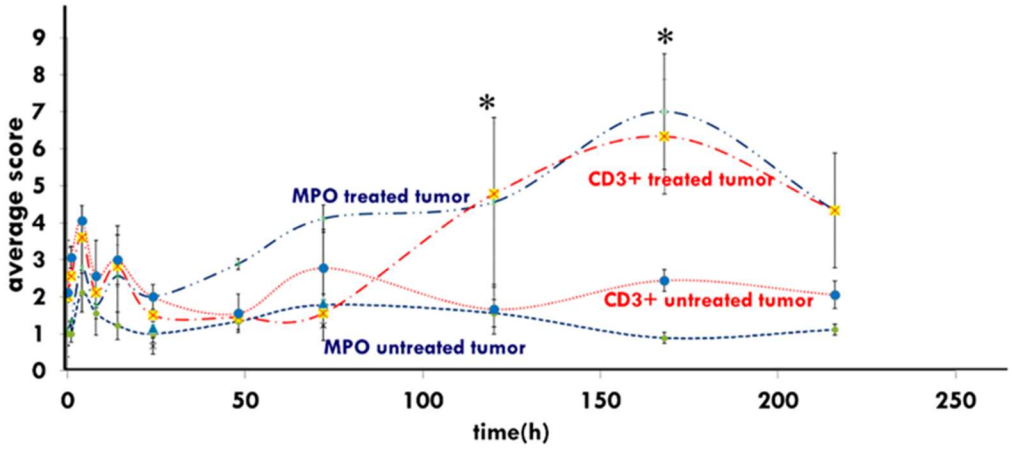

Figure 13. Induced immune reactions appear in both the Myeloperoxidase (MPO) and the $CD3^{+}$-T–cells' peak at one-week post-treatment in the HT29 xenograft [103]. (* means that $p < 0.05$).

Modulated electro-hyperthermia may improve the immunological tumor microenvironment, followed by dendritic cell (DC) immune support [113]. This additional DC therapy is significant for advanced cases accompanied by worsening immune surveillance. The genetic information release delivered by eHSPs results in antigen-presenting and consequently elevated levels of cytotoxic T cells in the region. The increased activity of the CD8+ cytotoxic T-cells by mEHT treatment appeared in a squamous cell carcinoma SCCVII allograft after adding DCs to boost immune activity [109] (Figure 14a,b).

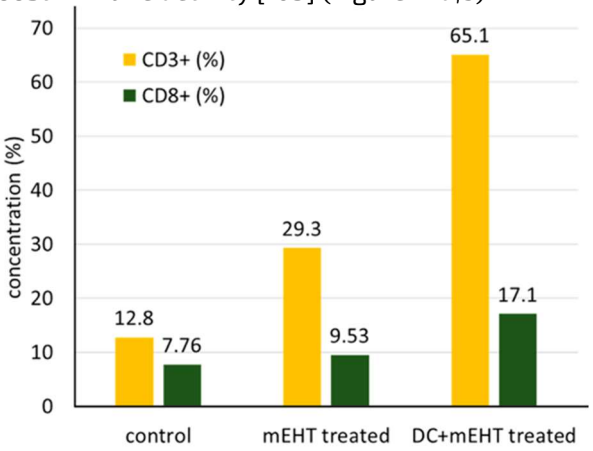

(a)

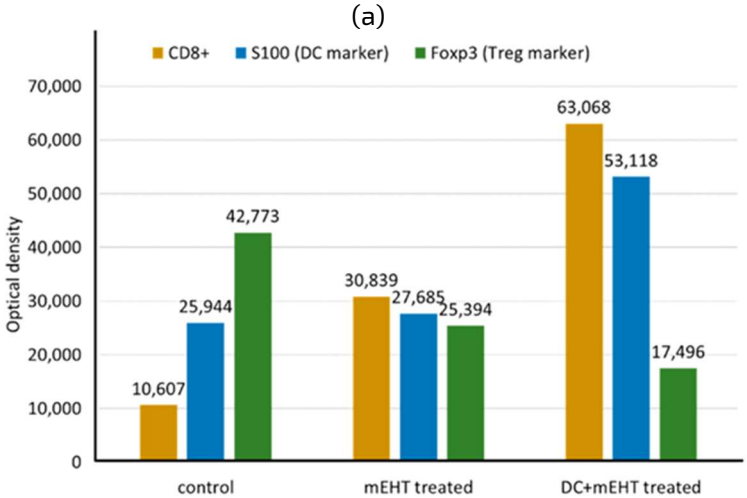

(b)

Figure 14. The mEHT treatment produced increased CD3+ and CS8+ cells, and the addition of immanentizing DC therapy enhanced this. (a) The distribution of CD3+ and CD8+ T-cells shows increased concentration after mEHT. (b) The optical density measurements of S100 DC and Foxp3 Treg markers show the increased antitumor immune activity of mEHT and the addition of DC enhances the effects.

The additional DCs appear to boost the leukocyte invasion of the tumor and support the macrophages and eosinophils (the T-cell organizers) in the CT26 allografts [113] (Figure 15).

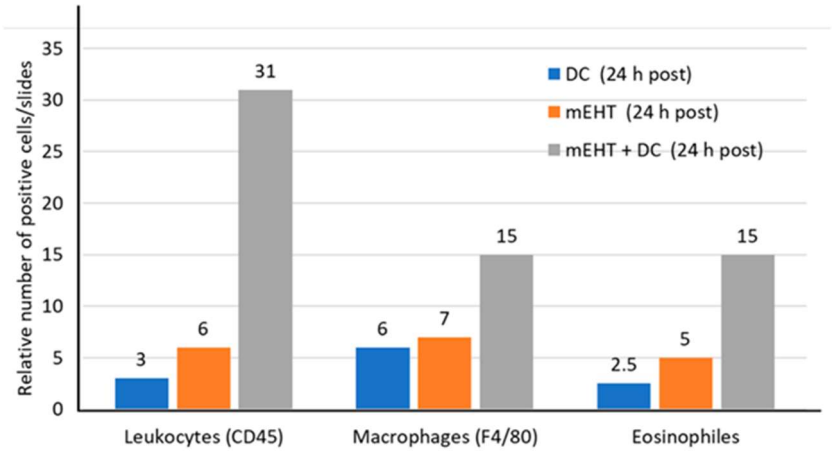

Figure 15. Increased concentration of leukocytes, macrophages, and eosinophils seen after the administration of mEHT combined with DC therapy.

The eHSP70 appears together with a set of other molecules, forming a damageassociated molecular pattern (DAMP), which includes the release of calreticulin (CRT), high-mobility group Box 1 (HMGB1), and adenosine triphosphate (ATP). The cytoplasmic CRT translocates to the plasma membrane during the early stages (four hours) after treatment with mEHT in HT29 xenografts [103]. The DAMP activity measured in C26 allograft is illustrated in Figure 16 [108].

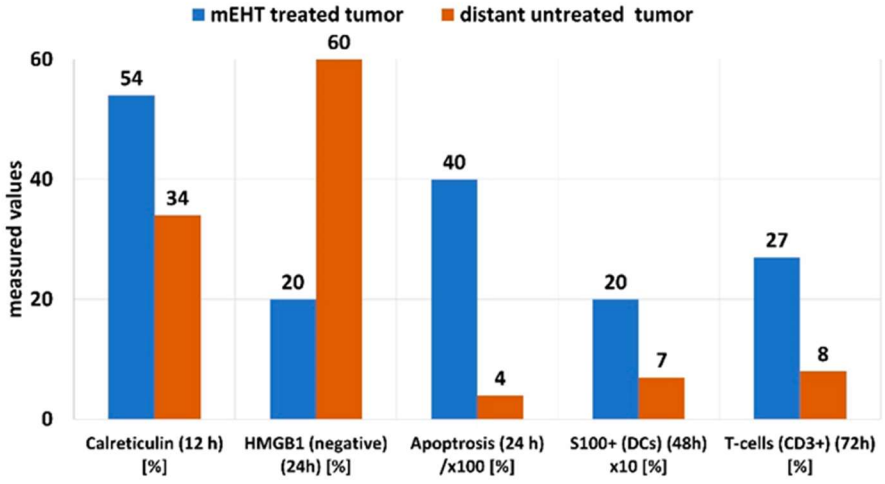

Figure 16. DAMP-related activity in C26 allografts following treatment with mEHT

The addition of other stimuli supporting mEHT has enhanced the success of tumorspecific immune activation. The combination with fluorescently labeled primary NK cells (NK92MI) increased the NK cell penetration to the tumor [116], and the herbal immunestimulator marsdenia tenacissima (MTE) enhanced the DAMP and the DC maturation by genetic information; delivered by eHSP70 [116].

5. Clinical Evidence of a Systemic Immune Effect Induced by mEHT

The radiation-induced abscopal effect does not frequently appear in clinical practice. Radiation therapy demonstrated the first observable abscopal effect [118] as a less common systemic response to ionizing radiation in which non-irradiated lesions respond after irradiation of the primary treatment site [119,120]. Unlike the bystander effect, the abscopal effect describes the response to ionizing radiation in which non-

irradiated lesions respond after irradtiation of the primary treatment site [119, 120]. Unlike the bystander effect, the abscopal effect describes the response of untreated distant metastases to the local treatment of the primary tumor [121]. Activating tumor-specific immune mechanisms is responsible for the abscopal effect [120,122,123]. Only a few case studies deal with the abscopal phenomenon yearly [122,123]. However, the mEHT actively produces clinically observed abscopal phenomena. Following the preclinical studies of abscopal effects [108,109,124,125], case reports [126–129] demonstrated the clinical applicability. Some clinical studies validated the effects for various tumor entities [130–133]. Clinical trials for brain tumors show the combination of mEHT with viral immuno-boosting. The treatments showed significant improvements [134–138]. The combination with viral immune support also works for ovarian cancers [139].

Minnaar et al. (2019), in a Phase III mEHT study, described the possible observation of the abscopal effect in 24% of women with locally advanced cervical cancer and extrapelvic nodal disease [140]. Cisplatin (either one or two doses) was also administered to some patients considering their renal function and hematological toxicity. In the subgroup, the frequency of the visualized abscopal effect (evaluated by 18F-FDG PET/CT scans pre-treatment and at six months post-treatment) was not associated with chemotherapy administration. The administration of mEHT significantly predicted the likelihood of complete metabolic resolution of all pelvic and extra-pelvic malignancies.

6. Discussion

The high biological heterogeneity of the tumor, and its structural and functional differences from the healthy host tissue, are apparent from the electromagnetic and thermal variability of the energy transmission and absorption [141]. These differences allow the targeting of malignant tissue over healthy tissue, using energy deposition and heat. When applied correctly, the energy deposition stimulates the production of HSPs in malignant tissue to act in favor of the host organism, supporting the immunogenic-related cell death of the malignant cells, potentially promoting a systemic immune response.

Immunogenic cell death describes the cellular death pathway triggered by the chronic exposure of DAMPs to the immune system. This immune-stimulatory form of apoptosis promotes an adaptive immune response to the dying cell. In oncology, this process appears to promote the immune recognition of malignant cells and anti-tumor immunity [142].

The electromagnetic interaction resulting from the electric heterogeneities in the tumor tissue offers a selection opportunity for malignant cells, causing stress, which allows for the manipulation of HSP production. Therefore, the applied electric field causes stress via both thermal and nonthermal processes.

The malignant cells have a higher concentration of membrane microdomains (rafts) than the nontumorigenic cells [82]. These rafts are selectively heated and reach a higher temperature than the TME [98,143]. The temperature increase of these nanoclusters is more rapid than the increase in the associated TME [105,144]. Some of these rafts act as stress sensors, operating as a trigger for the apoptotic cellular processes [4]. The cataphoretic forces generated by the modulated electric field induce lateral movements of electrically charged particles sensed by the rafts in the membrane. This results in the activation of the HSF1 and ultimately in the modulation of the actual HSP (mainly HSP70) levels. The heating creates optimal thermal conditions for the nonthermal molecular excitation of the transmembrane proteins in the lipid rafts, exciting the TRAIL death-receptor complexes and triggering the intrinsic apoptotic signals [109].

The initial peak of HSPs between 12 and 24 h post-treatment likely represents a coexistence of iHSPs and mHSPs. The second peak of HSPs seen several days after treatment with mEHT (Figure 6) is likely due to the extracellular expression of HSP70 proteins [101]. The intensive iHSP70 production characteristically follows all thermal shocks, independent of the heating technique [75], followed by the movement of iHSP70 to the cell membrane, forming mHSP70. The liberation of mHSP70 into the ECM appears only in the early stages of apoptosis in the studied preclinical models [106,107].

The gradual temperature increase applied in the step-up heating protocol of mEHT induces more HSPs in healthy cells than in the heavily stressed malignant cells [15]. The difference in the chaperone development results in a moderate increase in the expression of protective, antiapoptotic iHSP70 in the malignant cells compared to its drastic increase in the neighboring healthy cells [15]. This phenomenon provides an additional selective opportunity in the targeting process as the difference makes the malignant cells more vulnerable to stress than healthy cells. Moreover, step-up heating accounts for the blood wash-out time, maintaining the homeostatic equilibrium during the heating periods. Despite the development of the protective iHSP in malignant cells, thermo-resistance does not conflict with the administration of concurrent oncologic

treatments as the natural physiological regulation boosts the blood circulation in the heated volume, which increases drug delivery in the case of chemotherapy, and increases oxygen perfusion necessary for the radio-sensitization of the tumor. During the heating-up period of mEHT treatments, the apoptosis rate is significantly higher than during the stable power output periods [113]. The applied step-up heating procedure could use this difference to improve the apoptotic processes [92]. As the temperature increases, the thermal effect could increase, and the excitation (nonthermal effect) may also increase due to the increased molecular excitation rates. During the periods of stable temperature, the thermal and nonthermal factors are constant, and the absorbed energy replaces the heat loss in the system.

In the pre-clinical studies, temperature measurements were taken during mEHT and classical heating techniques, such as water bath heating and capacitive heating. Most of the studies evaluated the samples from the different heating methods at the same temperature. However, Andocs et al. also compared mEHT heating at 38 degrees Celsius and 42 degrees Celsius to other heating methods at 42 degrees Celsius. This study revealed the nonthermal effects (field effects) as well as the thermal effects of mEHT. During mEHT, the thermal and nonthermal effects occur together, working synergistically [92,145]. The precise electromagnetic impedance tuning optimizes the synergy [146]. The two effects rely on the electromagnetic stimuli's adherence to an intensity limit. A thermal load that is too high may destroy the excited receptor proteins, which could block the major pathways of the nonthermal effects.

Furthermore, high nonthermal doses can stop, or even decrease, the expression of iHSPs [147,148]. The overheating of tissues also cause a significant technical challenge. The forced absorption of high amounts of energy heats up the tissues non-selectively, producing isothermal conditions, marginalizing the selection conditions and overemphasizing the thermal component of the complex treatment effect.

In the case of high nonthermal doses, the strong apoptotic forces overcome the protection facility of the iHSPs, destroying the cellular integrity [106]. The iHSPs may translocate to the plasma membrane [51], forming mHSPs. The membrane expression of the major HSPs (HSP25, HSP60, HSP70, HSP90) has been observed [149], but their function was not readily apparent. They appear to either protect the cell [150] or participate in the immune stimuli [151,152], which act against the cell, resulting in mixed theories regarding the prognostic value of mHSPs on malignant cells [153,154]. The translocation process from iHSP to mHSP is also not yet completely understood. One proposal involves the "flip-flop" transition following the binding of iHSP to phosphatidylserine (PS) in tumor cells, facilitating the transport of HSP70 from inside the cell to the outer leaflet of the cell membrane [155]. This proposal aligns with the vibrational effect of the modulated electric field and the associated electro-osmotic process [156]. However, HSP expression on the cell surface alone does not provide enough signal for immune stimulation. The mHSPs must first form a complex tumor peptide to signal the apoptotic process [157]. Proteotoxic stresses, such as heat and chemical, pathological, and electromagnetic stresses, result in the formation of unfolded, aggregated, and ubiquitinated proteins. Heat shock proteins, such as iHSP70 and mHSP90, stabilize and refold these proteins, preventing their degradation [158]. The mHSP90 may, however, also trigger the DC activation signal required for a cell-to-cell interaction between the dying tumor cell and DCs [159].

The tumor-specific mHSP70 enables the recognition of the malignant cells by NK cells [55,160]. The mHSP70, found mainly in the cholesterol-rich microdomains of the cell membrane [161], activates the NK cells during an immune response [55,117]. ThemEHT process supports the expression of mHSPs and promotes the NK-cell migration to the treated malignant cells (Figure 17) [111]. This extensive ecrishment of NK cells in the tumor was measured in human melanoma (A2058) xenografts. The granzyme B expression increased such that 100% of the population stained positive in flow-cytometry measurements. The dead area of the tumor was measured by staining and fluorescent visualization in vivo. The dead area was also significantly increased following mEHT, and the cleaved Caspase3 was visualized with high intensity, indicating the pathway of the apoptotic cell death (Table 1).

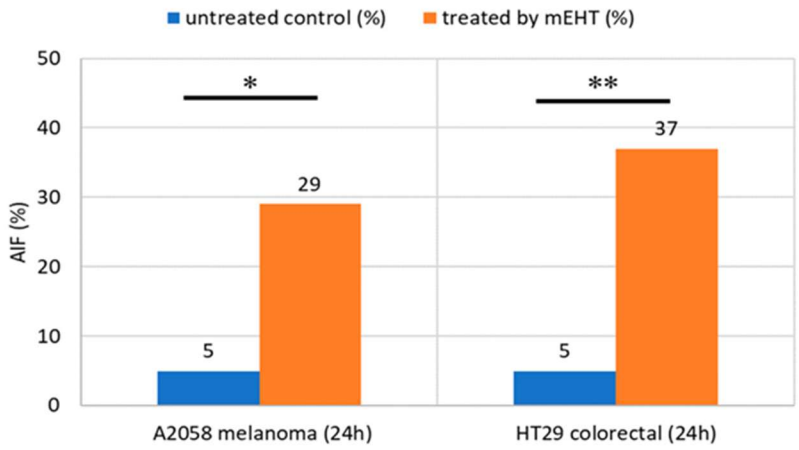

Figure 17. The enrichment of NK cells after 24 h of mEHT treatment in xenograft models for human melanoma and colorectal tumors [116]. * $p < 0.05$, ** $p < 0.01$.

Table 1. NK cell activity and mEHT (** means $p < 0.001$ and *** means $p < 0.0005$).

Tumor (A2058 Melanoma (24 h))	Dead Area (%)			FI Signal Intensity			cCas3 (%)		
	mEHT + Primary NK	mEHT + NK92MI	mEHT Alone	mEHT + Primary NK	mEHT + NK92MI	mEHT Alone	mEHT + Primary NK	mEHT + NK92MI	mEHT Alone
Untreated control (%)	5	9	7	0.9	0.8	0.9	5	6	8.5
Treated by mEHT (%)	63	90	60	1.35	1.39	1.26	26	33	19
Significance		***			**	***	**	***	

The therapeutic goal in the case of mEHT is to both induce the local (treated tumor) and systemic (distant tumors and tumor cells) effect, and the local treatment could produce tumor-specific immune reactions which tackle the systemic targets. We propose using electromagnetically triggered apoptosis to target the local tumor to achieve this. While the local excitation triggers the increased expression of iHSPs, the electric field triggers the transition of iHSPs to the ECM and promotes apoptotic cell death. The overexpression of the iHSPs in the malignant cells is quickly exhausted, paving the way for apoptosis [106]. Additionally, the expressed HSP60 activates cCas3 [162], promoting caspase-dependent apoptosis.

The extrinsic excitationof rafts triggers the cooperationofTRAIL2 (DR5), FAS, and FADD[102]. The elevated expression of the collective group of molecules appears eight hours after treatment with mEHT [110]. The direct extrinsic path follows the Caspase-dependent pathway (Cas8 → Cas3 → apoptosis) [75]. The RF current actively changes various stress factors in the TME [163], potentially resulting in stress, which triggers the intrinsic pathway, starting from the mitochondria and following the Cas9 -> Cas3 -> apoptosis pathway [75]. The Caspase-independent pathway begins with the mitochondrial release of Cytochrome-C, the point of "no return" in the apoptotic process [75], resulting in the expression of apoptosis-inducing factors [102]. Measurements in preclinical studies have confirmed the increase in apoptotic cell death in mEHT-treated samples, resulting from the triggering of various signal pathways by the extrinsic excitation of death receptors in the selected membrane rafts [109]. Eventually, the numerous potential pathways triggered result in cell death via apoptosis (Figure 18). HSP70 impedes mitochondria-related apoptosis. The X-linked inhibitor of apoptosis protein (XIAP) inhibits both extrinsic and intrinsic signal pathways by obstructing cCas3. The mEHT treatment induces the expression of Septin4, impeding XIAP activity [164]. At eight hours post-treatment, SMAC/Diabolo and HtrA2/Omi mitochondrial regulatory proteins are also expressed [102], which also inhibit XIAP and support the caspase-dependent and -independent apoptotic pathways. The HSP60 promotes the (Cas9 → cCas3) signal.

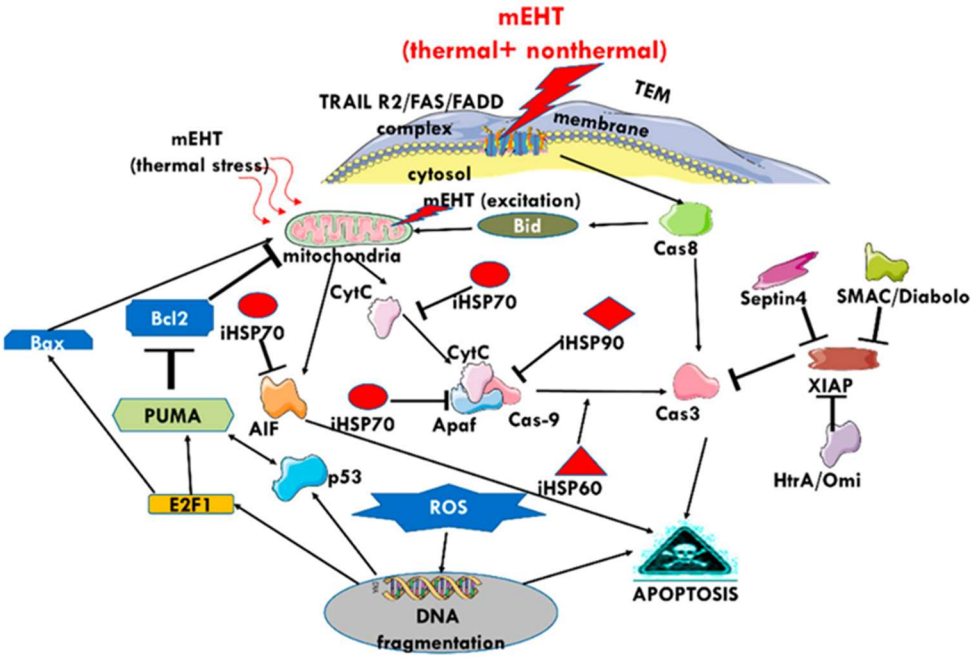

Figure 18. The multiple pathways involved in the apoptotic process of cells after the thermal and nonthermal energy absorption of mEHT. The exhaustion of the protective mechanism and the complex network of pathways ensures apoptosis as a final and-point.

The set of DAMPs triggered by mEHT-induced apoptosis further paves the way toward promoting the immune targeting of systemic disease. DAMPs have variants of molecular sets expressed in response to different stimuli, and these variants are all hallmarks of various types of cell death [165]. The mEHT technique produces thermal and nonthermal mechanisms of electric fields synergistically promoting a specific set of DAMP molecules (Figure 16) as a result of the applied modulation. Multiple mechanisms relate to DAMP release [166]. The various DAMPs contain the HMGB1, eHSP70, and ATP, but numerous other molecules are released together, including some inflammatory molecules.

The key to eliciting systemic immunogenic effects against malignant lesions with mEHT is the promotion of the molecular sequences leading ICD [167]. The membrane rafts absorb the thermal and nonthermal energy, while the applied modulation orchestrates the spatiotemporal order of the exported DAMP-associated molecules to the TME, resulting in the desired ICD [101]. The ICD process releases a DAMP set of HMGB1, ATP, and eHSP70 in a time sequence, starting with membrane secretion of CRT. The mEHT-induced apoptosis delivers eHSPs together with other molecules to the TME, where the eHSP70 has a complex function [22] and acts as an “info signal” [12], which is pivotal in the orchestration of the immune activities.

The extensive heating in conventional homogeneous hyperthermia processes causes necrosis. The heat triggers the expression of iHSPs, which are mostly antiapoptotic. The necrotic cellular rupture also produces eHSP70 as the iHSP70 is released into the extracellular matrix [168,169]. However, the necrosis-induced eHSP does not offer a stable process to produce the desired antitumor immune promotion. Instead, in this instance, the eHSP in the ECM could work against further degeneration of the malignant cells, acting as a pro-tumor agent [170]; it may even regulate the DC capacity inducing immunosuppressive T_{reg} cells [171]. The T_{reg} inhibition presents another example of the opposing actions of the HSPs.

During hyperthermia, the arteries deliver blood, which acts as a cooling media. However, the distribution of the vasculature throughout the tumor is not even, resulting in hot spots in poorly perfused regions. There is a risk that the control of the eHSP action is lost in these overheated micro-regions. Furthermore, the relatively high temperature in these heated regions (>=40 C) inactivates the immune cells [172], whose active participation in the immunogenic processes is essential.

The mEHT method attempts to bypass the necrotic process, avoid inflammation, and suppress immunity [173]. The mEHT treatment promotes optimal DAMP production in a natural molecular cascade, including CRT

expression on the cytoplasmic membrane. In sudden necrosis, the DAMP is released together with tumor-supportive inflammatory factors and mostly bypasses the membrane-secreted CRT.

Preclinical studies confirm that the DAMP-inducing apoptosis dominates in mEHT, and the necrotic cell destruction is relatively low [111,164]. Therefore, the mEHT method can avoid sudden inflammatory reactions and possible local toxicity associated with necrosis [174]. The more "gentle" apoptosis-associated cell death presents the genetic information from the malignant cells in a controlled manner using molecular signal pathways [101]. An advantage of the mEHT method is that the targeted malignant cells achieve a high enough temperature to initialize apoptotic signals [79,144], while the relatively low temperature (<=40 C) in TME promotes the infiltration of the immune cells in the tumor without affecting their functional form.

Furthermore, the apoptosis-inducing stress from mEHT does not degrade the various DAMP molecules, which can deliver the necessary information and sensitizing actions for both the native and adaptive immune processes, offering a way to develop tumor-specific immune effects. The eHSP presents the "info signal" as the carrier [175] of tumor-specific antigens [13]. The peptides delivered by the released eHSP70 during apoptosis can be recognized by the innate and adaptive immune system [176,177] and, with the support of other molecular members of DAMP, can assist in priming the DCs for maturation [178].

Calreticulin acts as the "eat me" signal for phagocytosis [179,180], and its exposure is connected to the ER stress response [181]. It also plays a complex regulatory function in homeostasis [182,183] and carefully controls the intracellular influx of Ca^{2+} [184]. Calreticuli is the first to appear in the set of DAMP molecules. The CRT-controlled strong Ca2+ influx appears to significantly contribute to the electromagnetic stress-induced apoptosis that follows mEHT [105].

The HMGB1, another member of DAMP, represents a "danger signal" [185]. The HMGB1 is usually present in the nucleus; however, following appropriate stress conditions, it translocates to the cytoplasm and is released to the ECM during cell death. The nonoxidized HMGB1 participates in immune activation; however, it supports the inflammatory response in its oxidized form [186]. Furthermore, the oxidized HMGB1 participates in immune tolerance [187] and may boost the immune checkpoint molecule PD-L1 expression, limiting the anticancer immunity [188]. Therefore, the oxidation status of HMGB1 determines the role of HMGB1 in DAMP [189]. The mild thermal process favors conditions that do not support oxidization. The ATP released as a stress response in the apoptotic phase [190] is the "find me" signal [191], and mostly follows an autophagy-dependent pathway [192]. Again, due to the complexity of living conditions, ATP, as an energy source for dynamic changes, could support other functions by supplying energy.

The DAMP, therefore, also has a "double-edged sword" effect [193], acting with or against the tumor by causing apoptosis or promoting tumor progression [194], and the final outcome is the result of the complex effects and interactions of the molecular components of the DAMP [195].

The nonthermal effects of mEHT influence the homeostatic control using the timefractal modulation [196]. The appropriate spatiotemporal order of DAMP molecules is crucial for their action. By applying the appropriate modulation, mEHT may trigger the appropriate timing of the appearance of various DAMP molecules in ECM [101,103] (Figure 19a,b).

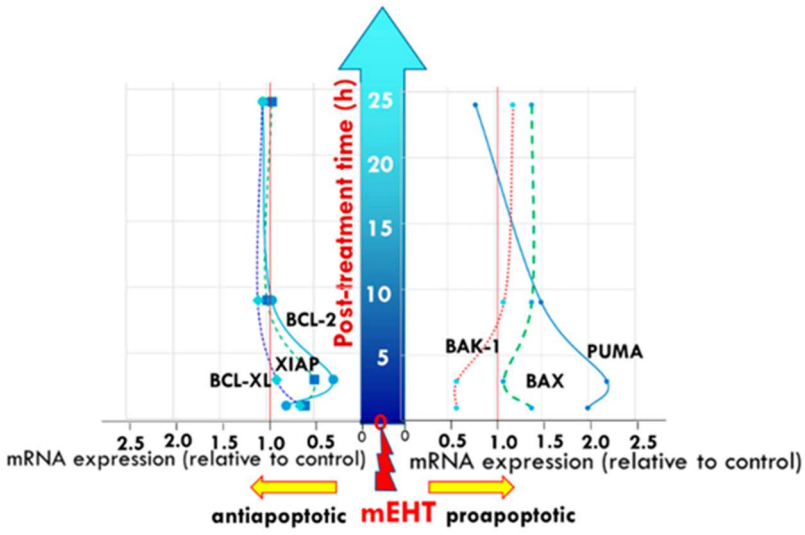

(a)

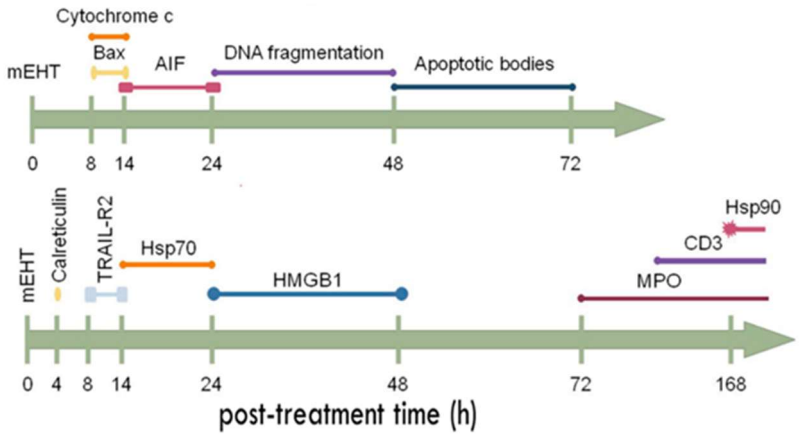

(b)

Figure 19. The time scale of the apoptotic processes:
(a) development of pro- and anti-apoptotic proteins on the first day (24 h) post-treatment;
(b) further developments with cellular reactions visible until the end of the apoptotic process (48 h post-treatment) and the immune reactions that follow three days after treatment.

In this proposal, the electric field effectively participates in limiting the malignant growth [197], harnessing the relatively low membrane potential of malignant cells [198], and creating clusters of cells [144]. The time-ractal modulated electric field in mEHT could potentially force autonomic malignant cells into collective groups [199], and the electromagnetic resonance may provide a reliable basis for molecular changes [87].

The tumor-specific immune activity of mEHT promotes the response of untreated distant metastases to the local irradiation of the primary tumor, known as the abscopal effect.

The DAMPs with the delivered genetic information by eHSP70 activate DCs, generating antigen-presenting cells (APCs) [200]. This process induces the production of T-cells specific to the genetic information of the tumor cells supplied by eHSP70 [122, 123]. The eHSP70 provides the genetic information, with the cooperation of DAMP molecules, to form optimal conditions to maturate the DCs into APCs [201]. The APCs carry specific information about the malignant cell, and this material is used as tumor antigen. The mature APC subsequently provides immunogenic information and produces tumor-specific killers (CD8+) and helper (CD4+) T-cells and activates antitumor T-cell immunity [202,203]. A noteworthy observation in cancer experiments is that mEHT treatment enhances the $\gamma\delta T$ -cell migration towards tumor cells even at temperatures as low as 38 C [204]. The $\gamma\delta T$ -cell cells link the innate and adaptive immune systems [205], participating in the development of immune defenses. The APC induces numerous systemically available molecules (cytokines, chemokines), as well as NK, CD4+ and CD8+ cells and $\gamma\delta T$ -cells to form a complete tumor-specific immune arsenal which can be used against the malignant cells (Figure 20).

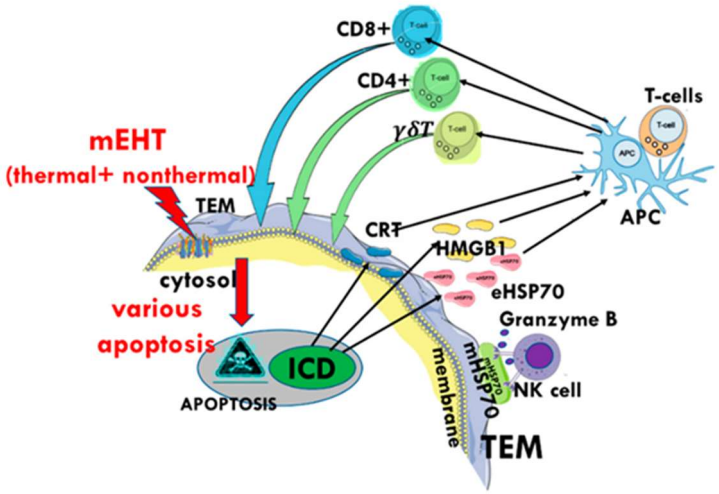

Figure 20. The apoptotic process exhausts the protective functions of iHSPs and secrets the cytoplasmic membrane. The mHSP activates the NK-cells to attack the overstressed and the ICD process presents DAMP which could result in the maturation of the DCs, forming antigen-presenting cells (APCs). The APCs trigger the helper-T, killer-T, and $\gamma\delta T$ -cells, potentially resulting in a tumor-specific immune attack of the tumor cells all over the body (abscopal effect). The adaptive immune response is engaged, and the associated memory could protect the system from malignant relapse.

The various HSPs have crucial roles in forming immune-specific antitumor processes all over the body, including targeting micro- and macro-metastaases (Figure 21). The information delivered by the eHSP develops a tumor-specific adaptive immune response, which may even have the potential to prevent tumor seeding after a tumor re-challenge [113]. Following this, the eHSP, supported by the DAMP cellular collection, may promote antitumor immunity resulting in an anticancer vaccine effect [206].

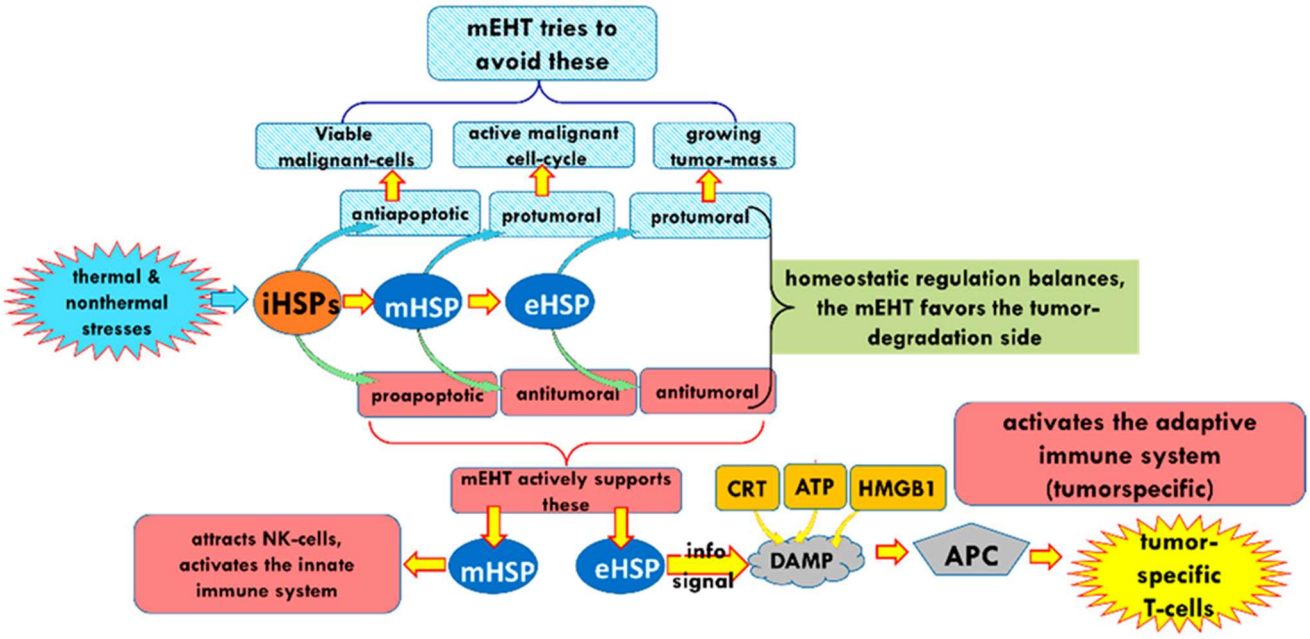

Figure 21. Summary of the role of HSP in the relevant process

7. Conclusion

Heat shock proteins have a complex "double-edged sword" effect, promoting and suppressing the malignant processes. Our goal is to apply an external stimulus, such as an electric field, to induce immune effects and tip the balance towards the side of tumor suppression, promoting the systemic immune recognition of tumor cells. Despite the plethora of literature on heat shock proteins, the precise roles and mechanisms of each HSP in adaptive and innate immunity are still not known. There is still much to learn about these molecules about the precise effects of mEHT and electric fields on the immune modulation of malignant cells. Following a review of the literature, we have proposed a potential mechanism for the outcomes seen in the preclinical and clinical data on mEHT, in which HSPs play a crucial role. The electric field's synergistic action of the thermal and nonthermal effects selectively heats the tumor cells and targets its membrane components [91]. The nonthermal processes following an applied modulated field dominate [114] and effectively excite the voltage-related cellular receptors and channels on the plasma membrane, resulting in a significant reduction in the proliferation and clonogenicity of the malignant cells [76]. The application of mEHT can promote the antitumor HSP activity, and in situ it stimulates the tumor-specific immune effects, which act locally and may also play a role in the systemic management of disseminated cells and metastatic lesions. Enriching of mHSP70 activates the innate (NK-cell) immune attack on the selected malignant cells. The ICD-induced DAMP starts preparing the adaptive immune reactions by forming APCs. The spatiotemporal arrangement of DAMP complexly orchestrates the eHSP70 ("info"), CRT "eat-me", HMGB1 "danger," and ATP "find me" signals. The subsequent maturation of the DCs into APCs creates cytotoxic T-cells and triggers tumor-specific immune processes with a solid potential to act systemically. Therefore, modulated electro-hyperthermia is a potential tool for the manipulation of HSPs to achieve the goal of immunogenic recognition and targeting of the tumor, resulting in the local and systemic control of the disease.

Author Contributions: Conceptualization, data curation, original draft preparation, A.S.; methodology, resources, writing, review and editing C.A.M. All authors have read and agreed to the published version of the manuscript.

Funding: This work was supported by the Hungarian National Research Development and Innovation Office PIACI KFI grant: 2019-1.1.1-PIACI-KFI-2019-00011.

Acknowledgments: The cooperation with the following doctors is highly appreciated: Nora Meggyeshazi, Tamas Vancsik, Lea Danics, Csaba Schvarcz, Thomas Mbuotidem Jeremiah, Gertrud Forika, Tibor Krenacs, Peter Hamar, Samuel Yu-Shan Wang, Kwan-Hwa Chi, Sun Young Lee.

Conflicts of Interest: Andras Szasz is the chief scientific officer of Oncotherm Kft. Hungary and Oncotherm GmbH Germany. Carrie Minnaar does not have any conflict of interest to declare.

References

1. Latchman, D.S. Stress Proteins; Springer: Berlin/Heidelberg, Germany, 1999; ISBN 978-3-642-58259-2. CrossRef]
2. Zügel, U.; Kaufmann, S.H. Role of heat shock proteins in protection from and pathogenesis of infectious diseases. Clin. Microbiol. Rev. 1999, 12, 19–39. [CrossRef]
3. Miller, D.J.; Fort, P.E. Heat Shock Proteins Regulatory Role in Neurodevelopment. Front. Neurosci. 2018, 12, 821. [CrossRef]
4. Horvath, I.; Multhoff, G.; Sonnleitner, A.; Vigh, L. Membrane-associated stress proteins: More than simply chaperones. Biochim. Biophys. Acta 2008, 1778, 1653–1664. [CrossRef] [PubMed]
5. Chen, B.; Feder, M.E.; Kang, L. Evolution of heat-shock protein expression underlying adaptive responses to environmental stress. Mol. Ecol. 2018, 27, 3040–3054. [CrossRef]
6. Chowdhury, R.; Sahu, G.K.; Das, J. Stress response in pathogenic bacteria. J. Biosci. 1996, 21, 149–160. [CrossRef]
7. Kaul, G.; Thippeswami, H. Role of heat shock proteins in diseases and their therapeutic potential. Indian J. Microbiol. 2011, 51, 124–131. [CrossRef]
8. Sriram, K.; Rodriguez-Fernandez, M.; Doyle, F.J. A detailed modular análisis of heat-shock protein dynamics under acute and chronic stress and its implication in anxiety disorders. PLoS ONE 2021, 7, e42958. [CrossRef]
9. Sorger, P.K. Heat shock factor and the heat shock response. Cell 2012, 65, 363–366. [CrossRef]
10. Asea, A.A.A.; Calderwood, S.K. Cellular Trafficking of Cell Stress Proteins in Health and Disease; Springer: Berlin/Heidelberg, Germany, 2012; ISBN -13 978-9400747395.
11. Anckar, J.; Sistonen, L. Regulation of HSF1 function in the heat stress response: Implications in aging and disease. Annu. Rev. Biochem. 2011, 80, 1089–1115. [CrossRef]
12. Taha, E.A.; Ono, K.; Eguchi, T. Roles of extracellular HSPs as biomarkers in immune surveillance and immune evasion. Int. J. Mol. Sci. 2019, 20, 4588. [CrossRef]
13. Piacentivi, L.; Fanti, L.; Berloco, M.; Perrii, B.; Piminelli, S. Heterochromatin protein 1 (HP1) is associated with induced gene expressio in Drosophila euchromatin. J. Cell Biol. 2003, 16, 707–714. [CrossRef]
14. Guan, Y.; Zhu, X.; Liang, J.; Wei, M.; Huang, S.; Pan, X. Upregulation of HSPA1A/HSPA1B/HSPA7 and Downregulation of HSPA9 Were Related to Poor Survival in Colon Cancer. Front. Oncol. 2021, 11, 749673. [CrossRef]
15. Watanabe, M.; Suzuki, K.; Kodama, S.; Sugahara, T. Normal human cells at confluence get heat resistance by efficient accumulation of HSP72 in nucleus. Carcinogenesis 1995, 16, 2373–2380. [CrossRef]
16. Macario, A.J.L.; Conway de Macario, E. Heat Shock Response, Overview. In The Encyclopedia of Stress; Academic Press: San Diego, CA, USA, 2000.
17. Matarredona, L.; Camacho, M.; Zafrilla, B.; Bonete, M.-J.; Esclapez, J. The role of stress proteins in haloarchaea and their adaptive response to environmental shifts. Biomolecules 2020, 10, 1390. [CrossRef] [PubMed]
18. Calderwood, S.K.; Theriault, J.R.; Gong, J. Message in a bottle: Role of th 70-kDa heat shock protein family I anti-tumor immuity. Eur. J. Immunol. 2005, 35, 2518–2527. [CrossRef]

19. Albakova, Z.; Mangasarova, Y. The HSP Immune Network in Cancer. Front. Immunol. 2021, 12, 796493. [CrossRef]
20. Mambula, S.S.; Stevenson, M.A.; Ogawa, K.; Calderwood, S.K. Mechanisms for Hsp70 secretion: Crossing membranes without a leader. Methods 2007, 43, 168–175. [CrossRef]
21. Kregel, K.C. Heat shock proteins: Modifying factors in physiological stress responses and acquired thermotolerance. J. Appl. Physiol. 2002, 92, 2177–2186. [CrossRef]
22. Calderwood, S.K.; Mambula, S.S.; Gay, P.J., Jr.; Theriault, J.R. Extracellular heat shock proteins in cell signaling. FEBS Lett. 2007, 581, 3689–3694. [CrossRef]
23. Shevtsov, M.; Balogi, Z.s.; Khachatryan, W.; Gao, H.; Vigh, L.; Multhoff, G. Membrane-associated heat shock proteins in oncology: From basic research to new theranostic targets. Cells 2020, 9, 1263. [CrossRef]
24. Tang, D.; Kang, R.; Berghe, T.V.; Vandnabele, P.; Kroemer, G. The molecular machinery of regulated cell death. Cell Res. 2019, 29, 347–364. [CrossRef]
25. Giri, B.; Sethi, V.; Modi, S.; Garg, B.; Banerjee, S.; Saluja, A.; Dudeja, V. Heat shock protein 70 in pancreatic diseases: Friend or foe. J. Surg. Oncol. 2017, 116, 114–122. [CrossRef] [PubMed]
26. Pockley, A.G.; Multhoff, G. Cell stress proteins in extracellular fluids: Friend or foe? Novartis Found. Symp. 2008, 291, 86–95. [CrossRef]
27. Wu, T.; Tanguay, R.M. Antibodies against heat shock proteins in environmental stresses and diseases: Friend or foe? Cell Stress Chaperones 2006, 11, 1. [CrossRef]
28. Hance, M.W.; Nolan, K.D.; Isaacs, J.S. The double-edged sword: Conserved functions of extracellular Hsp90 in wound healing and cancer. Cancers 2014, 6, 1065–1097. [CrossRef] [PubMed]
29. Tittelmeier, J.; Nachman, E.; Nussbaum-Krammer, C. Molecular chaperones: A double-sword in neurodegenerative diseases. Front. Aging Neurosci. 2020, 12, 581374. [CrossRef]
30. Trigos, A.S.; Pearson, R.B.; Papenfuss, A.T.; Goode, D.L. How the evolution of multicellularity set the stage for cancer. Br. J. Cancer 2018, 118, 145–152. [CrossRef]
31. Popkin, G. Physics sheds light on cancer and bacteria evolution. APC News 2011, 20, 5.
32. Aktipis, C.A.; Bobby, A.M.; Jansen, G.; Hibner, U.; Hochberg, M.; Maley, C.C.; Wilkinso, G.S. Cancer across the tree of life: Cooperation and cheating in multicellularity. Philos. Trans. R. Soc. B Biol. Sci. 2015, 370, 20140219. [CrossRef] [PubMed]
33. Davidson, C.D.;Wang,W.Y.; Zaimi, I.; Jayco, D.K.P.; Baker, B.M. Cell force-mediated matrix reorganization underlies multicellular network assembly. Sci. Rep. 2019, 9, 12. [CrossRef]
34. Dvorak, H.F. Tumors: Wounds that do not heal, Similarities between tumor stroma generation and wound healing. N. Engl. J. Med. 1986, 315, 1650–1659. [PubMed]
35. Punyiczki, M.; Fesus, L. Heat Shock and Apoptosis: The Two Defense Systems of the Organisms May Have Overlapping Molecular Elements. Ann. N. Y. Acad. Sci. 1998, 951, 67–74. [CrossRef] [PubMed]
36. Young, R.A. Stress Proteins and Immunology. Ann. Rev. Immunol. 1990, 8, 401–420. [CrossRef]
37. Das, J.K.; Xiong, X.; Ren, X.; Yan, J.M.; Song, J. Heat shock proteins in cancer immunotherapy. J. Oncol. 2019, 2019, 3267207. [CrossRef] [PubMed]
38. Moreira-de-Sousa, C.; de Souza, R.B.; Fontanetti, C.S. HSP70 as a biomarker: An excellent tool in environmental contamination analysis—A review. Water Air Soil Pollut. 2018, 229, 264. [CrossRef]
39. Siebert, C.; Ciato, D.; Murakami, M.; Frei-Stuber, L.; Perez-Rivas, L.G.; Moteseri-Garcia, J.L.; Nölting, S.; Maurer, J.; Perez-Rivas, L.G.; Walch, A.K.; et al. Heat shock protein 90 as a prognostic marker and therapeutic target for adrenocortical carcinoma. Front. Endocrinol. 2019, 10, 487. [CrossRef] [PubMed]
40. Carpenter, R.L.; Gokmen-Polar, Y. HSF1 as a cancer biomarker and therapeutic target. Curr. Cancer Drug Targets 2019, 19, 515–524. [CrossRef]
41. Soti, C.; Csermely, P. Molecular Chaperones in the Etiology and Therapy of Cancer. Pathol. Oncol. Res. 1998, 4, 316–321. [CrossRef] [PubMed]
42. Soti, C.; Nagy, E.; Giricz, Z.; Vigh, L.; Csermely, P.; Ferdinady, P. Heat shock proteins as emerging therapeutic targets. Br. J. Pharmacol. 2005, 146, 769–780. [CrossRef]
43. Xu, M.;Wright,W.D.; Higashikubo, R.; Roti, J.L.R. Chronic Thermotolerance with Continued Cell Proliferation. Int. J. Hyperth. 1996, 12, 645–660. [CrossRef]
44. Pirity, M.; Hever-Szabo, A.; Venetianer, A. Overexpression of P-glycoprotein in Heta and/or Drug Resistant Hepatoma Variants. Cytotechnology 1996, 19, 207–214. [CrossRef] [PubMed]

45. Santin, A.D.; Hermonat, P.L.; Ravaggi, A.; Chiriva-Internati, M.; Hiserodt, J.C.; Batchu, R.B.; Pecorelli, S.; Parham, G.P. The Effects of Irradiation on the Expression of a Tumor Rejection Antigen (Heat Shock Protein GP96) in Human Cervical Cancer. Int. Radiat. Biol. 1998, 76, 699–704.

46. Morgan, J.; Whitaker, J.E.; Oseroff, A.R. GRP78 Induction by Calcium Ionophore Potentiates Photodynamic Therapy Using the Mitochondrial Targeting Dye Victoria Blue BO. Photocem. Photobiol. 1998, 67, 155–164. [CrossRef]

47. Calderwood, S.K.; Murshid, A. Molecular chaperone accumulation in cancer and decrease in Alzheimer's disease: The potential roles of HSF1. Front. Neurosci. 2017, 11, 192. [CrossRef]

48. Ciocca, D.R.; Calderwood, S.K. Heat shock proteins in cancer: Diagnostic, prognostic, predictive, and treatment implications. Cell Stress Chaperones 2005, 10, 86–103. [CrossRef]

49. Rothammer, A.; Sage, E.K.; Werner, C.; Combs, S.E.; Multhoff, G. Increased heat shock protein 70 (Hsp70) serum levels and low NK cell counts after radiotherapy-potential markers for predicting breast cancer recurrence? Radiat. Oncol. 2019, 14, 78. [CrossRef] [PubMed]

50. Mosser, D.D.; Caron, A.W.; Bourget, L.; Denis-Larose, C.; Massie, B. Role of the human heat shock protein hsp70 in protection against stress-induced apoptosis. Mol. Cell. Biol. 1997, 17, 5317–5327. [CrossRef]

51. Vega, V.L.; Rodriguez-Silva, M.; Frey, T.; Gehrmann, M.; Diaz, J.C.; Stinem, C.; Multhoff, G.; Arispe, N.; De Maio, A. Hsp70 translocates into the plasma membrane after stress and is released into the extracellular environment in a membrane-associated form that activates macrophages. Immunology 2008, 180, 4299–4307. [CrossRef] [PubMed]

52. Gehrmann, M.; Marinhage, J.; Eichholtz-Wirtz, H.; Fritz, E.; Ellwart, J.; Jaattla, M.; Zilch, T.; Multhoff, D. Dual function of membrane-bound heat shock protein (Hsp70), Bag-4, and Hsp40, protection against radiation-induced effects and target structure for natural killer cells. Cell Death Differ. 2005, 12, 38–51. [CrossRef]

53. Snigireva, A.V.; Vrublevskaya, V.V.; Skarga, Y.Y.; Morenkov, O.S. The role of membrane-bound heat shock Hsp90 proteins in the migration of tumor cells in vitro and the involvement of cell surface heparan sulfate proteoglycans in protein binding to the plasma membrane. Biophysics 2016, 61, 277–283. [CrossRef]

54. Radons, J.; Multhoff, G. Immunostimulatory functions of membrane-bound and exported heat shock protein 70. Exerc. Immunol. Rev. 2005, 11, 17–33.

55. Multhoff, G.; Botzler, C.; Jennen, L.; Schmidt, L.; Ellwart, J.; Issels, R. Heat shock protein 72 on tumor cells: A recognition structure for natural killer cells. J. Immunol. 1997, 158, 4341–4350. [PubMed]

56. Ablakova, Z.; Siam, M.K.S.; Sacitharan, P.K.; Sacitharan, P.K.; Ziganshin, R.H.; Ryazantsev, D.Y.; Sapozhnikov, A.M. Extracellular heat shock proteins and cancer-New perspectives. Transl. Oncol. 2021, 14, 100995. [CrossRef]

57. Gas, P. Essential facts on the history of hyperthermia and their connections with electromedicine. arXiv 2017, arXiv:1710.00652.

58. Paulides, M.M.; Trefna, H.D.; Curto, S.; Rodrigues, D.B. Recent technological advancements in radiofrequency- and microwavemediated hyperthermia for enhancing drug delivery. Adv. Drug Deliv. Rev. 2020, 163–164, 3–18. [CrossRef]

59. Calderwood, S.K.; Gong, J. Heat shock proteins promote cancer: It's a protection racket. Trends Biochem. Sci. 2016, 41, 311–323. [CrossRef] [PubMed]

60. Schilling, D.; Kuhnel, A.; Konrad, S.; Tetzlaff, F.; Bayer, C.; Yaglom, J.; Multhoff, G. Sensitizing tumor cells to radiation by targeting the heat shock response. Cancer Lett. 2015, 360, 294–301. [CrossRef]

61. Desai, S.; Liu, Z.; Yao, J.; Pat, N.; Chen, J.;Wu, Y.; Ah, Y.; Fodstad, O.; Tan, M. Heat Shock Factor 1 (HSF1) Controls Chemoresistance and Autophagy through Transcriptioal Regulation of Autophagy-relatd Protein 7 (ATG7). J. Biol. Chem. 2013, 288, 9165–9176. [CrossRef]

62. Chatterjee, S.; Burns, T.F. Targeting Heat Shock Proteins in Cancer-A Promising Therapeutic Approach. Int. J. Mol. Sci. 2017, 18, 1978. [CrossRef]

63. Yoneda, A.; Miomi, K.; Tamura, Y. Heat shock protein 47 confers chemoresistance on pancreatic cancer cells by interacting with calreticulin and IRE1 . Cancer Sci. 2021, 112, 2803–2820. [CrossRef]

64. Schwab, M.; Thunborg, K.; Azmzadeh, O.; Von Torne, C.;Werner, C.; Shevtsov, M.; De Genio, T.; Zdralevic, M.; Pouyssegur, J.; Renner, K.; et al. Targeting Cancer Metabolism Breaks Radioresistance by Impairing the Stress Response. Cancers 2021, 13, 3762. [CrossRef]

65. Cheng, Y.;Weng, S.; Yu, L.; Zhu, N.; Yang, M.; Yuan, Y. The Role of Hyperthermia in the Multidisciplinary Treatment of Malignant Tumors. Integr. Cancer Ther. 2019, 18, 1534735419876345. [CrossRef]

66. Datta, N.R.; Jain, B.M.; Mathi, Z.; Datta, S.; Johari, S.; Singh, A.R.; Kalbande, P.; Kale, P.; Shivkumar, V.; Bodis, S. Hyperthermia: A potential game-changer in the management of cancers in low-middl-income group countries. Cancers 2022, 14, 315. [CrossRef][PubMed]

67. Fiorentini, G.; Sarti, D.; Gadaleta, C.D.; Ballerini, M.; Fiorentini, C.; Garfango, T.; Ranieri, G.; Guadagni, S. A Narrative Review of Regional Hyperthermia-Updates from 2010 to 2019. Integr. Cancer Ther. 2020, 19, 1534735420932648. [CrossRef] [PubMed]

68. Datta, N.R.; Kok, H.P.; Crezee, H.; Gaipi, U.S.; Bodis, S. Integrating loco-regional hyperthermia into the current oncology practice: SWOT and TOWS analyses. Front. Oncol. 2020, 10, 819. [CrossRef]

69. Hurwitz, M.D. Hyperthermia and immunotherapy: Clinical opportunities. Int. J. Hyperth. 2019, 36, 4–9. [CrossRef]

70. Roussakow, S. The History Of Hyperthermia Rise And Decline. Conf. Pap. Med. 2012, 2013, 428027. [CrossRef]

71. Lee, S.Y.; Szigeti, G.P.; Szasz, A.M. Oncological hyperthermia: The correct dosing in clinical applications. Int. J. Oncol. 2019, 54, 627–643. [CrossRef]

72. Cherukuri, P.; Glazer, E.S.; Curley, S.A. Targeted hyperthermia using metal nanoparticles. Adv. Drug Deliv. Rev. 2010, 62, 339–345. [CrossRef]

73. Sohail, A.; Ahmed, Z.; Beg, O.A.; Arshad, S.; Sherin, L. A Review on hypertermia via nanoparticle-mediated therapy. Bull. Cancer 2017, 104, 452–461. [CrossRef]

74. Nicolau, D.V.; Burrage, K.; Parton, R.G.; Hancock, J.F. Identifying Optimal Lipid Raft Characteristics Required to Promote Nanoscale Protein-Protein Interactions on the Plasma Membrane. J. Mol. Cell Biol. 2006, 26, 313–323. [CrossRef] [PubMed]

75. Yang, K.L.; Huang, C.C.; Chi, M.S.; Chiang, H.C.; Wang, Y.S.; Andocs, G.; Wang, H.-E.; Chi, K.-H. In vitro comparison of conventional hyperthermia and modulated electro-hyperthermia. Oncotarget 2016, 7, 84082–84092. [CrossRef] [PubMed]

76. Wust, P.; Kortum, B.; Strauss, U.; Nadobny, J.; Zschaeck, S.; Beck, M.; Stein, U.; Ghadjar, P. Non-thermal effects of radiofrequency electromagnetic fields. Sci. Rep. 2020, 10, 13488. [CrossRef] [PubMed]

77. Wust, P.; Stein, U.; Ghadjar, P. Non-thermal membrane effects of electromagnetic fields and therapeutic applications in oncology. Int. J. Hyperth. 2021, 38, 715–731. [CrossRef] [PubMed]

78. Frolich, H. What are non-thermal electric biological effects? Bioelectromagnetics 1982, 3, 45–46. [CrossRef]

79. Vincze, G.; Szigeti, G.; Andocs, G.; Szasz, A. Nanoheating without Artificial Nanoparticles. Biol. Med. 2015, 7, 249.

80. Sezgin, E.; Levental, I.; Mayor, S.; Eggelig, C. The mystery of membrane organization: Composition, regulation and roles of lipid rafts. Nat. Rev. Mol. Cell Biol. 2017, 18, 361–374. [CrossRef]

81. Nicolson, G.L. The Fluid—Mosaic Model of Membrane Structure: Still relevant to understanding the structure, function and dynamics of biological membranes after more than 40 years. Biochim. Biophys. Acta 2014, 1838, 1451–1466. [CrossRef]

82. Staunton, J.R.; Agus, D.B.; Alexander, J.F.; Arap,W.; Ashili, S.; Aslan, J.E.; Austin, R.H.; Backman, V.; Bethel, K.J.; Bonneau, R.; et al. The Physical Sciences-Oncology Centers Network; A physical sciences network characterization of non-tumorigenic and metastatic cells. Sci. Rep. 2008, 3, 1449.

83. Cha, J.; Jeon, T.W.; Lee, C.G.; Oh, S.T.; Yang, H.-B.; Choi, K.-J.; Seo, D.; Yun, I.; Bain, I.H.; Park, K.R.; et al. Electro-hyperthermia inhibits glioma tumorigenicity through the induction of E2F1-mediated apoptosis. Int. J. Hyperth. 2015, 31, 784–792. [CrossRef]

84. Blank, M. Evidence for Stress Response (Stress Proteins), Health Risk of Electromagnetic Fields: Research on the Stress Response. 2007. Available online: https://citeseerx.ist.psu.edu/viewdoc/download?doi=10.1.1.534.8023&rep=rep1&type=pdf (accessed on 21 October 2021).

85. Blank, M.; Goodman, R. Electromagnetic fields stress living cells. Pathophysiology 2009, 16T, 71–78. [CrossRef]

86. Schwan, H.P. Nonthermal Cellular Effects of Electromagnetic Fields: AC-Field Induced Ponderomotoric Forces. Br. J. Cancer 1982, 45, 220–224.

87. Szasz, A. Therapeutic basis of electromagnetic resonances and signal-modulation. Open J. Biophys. 2021, 11, 314–350. [CrossRef]

88. Szasz, A.; Iluri, N.; Szasz, O. Local Hyperthermia in Oncology–To Choose or Not to Choose? In Hyperthermia; Huilgol, N., Ed.; InTech: London, UK, 2013; Chapter 1; pp. 1–82. ISBN 980-953-307-019-8.

89. Blank, M. Coupling of AC Electric Fields to Cellular Processes. In Proceedings of the First International Symposium on Nonthermal Medical/Biological Treatments Using Electromagnetic Fields and Ionized Gases, ElectroMed'99, Symposium Record Abstracts, Norfolk, VA, USA, 12–14 April 1999; p. 23.

90. Zeni, O.; Simko, M.; Scarfi, M.R.; Mattsson, M.O. Cellular response to ELF-MF and heat: Evidence for a common involvement of heat shock proteins? Front. Public Health 2017, 5, 280. [CrossRef]

91. Minnaar, C. Challenges Associated with Hyperthermia. In Challenges and Solutions of Oncological Hyperthermia; Szasz, A., Ed.; Cambridge Scholars: Newcastle upon Thyne, UK, 2020; Chapter 1; pp. 1–31.

92. Szasz, O.; Szasz, A. Approaching complexity: Hyperthermia dose and its possible measurement in oncology. Open J. Biophys. 2021, 11, 68–132. [CrossRef]

93. Lee, S.Y.; Lee, N.R.; Cho, D.H.; Kim, J.S. Treatment outcome analysis of chemotherapy combined with modulated electrohyperthermia compared with chemotherapy alone for recurrent cervical cancer, following irradiation. Oncol. Lett. 2017, 14, 73–78. [CrossRef]

94. Minnaar, C.; Kotzen, J.A.; Baeyens, A. Modulated Electro-Hyperthermia Improves Three Year Survival in Cervical Cancer Patients, Presentation number: PH-0551. In Proceedings of the ESTRO Conference, Madrid, Spain, 27–31 October 2021.

95. Minnaar, C.A.; Kotzen, J.A.; Ayeni, O.A.; Naidoo, T.; Tunmer, M.; Sharma, V.; Vangu, M.-D.-V.; Bayes, A. The effect of modulated electro-hyperthermia on local disease control in HIV-positive and -negative cervical cancer women in South Africa: Early results from a phase III randomized controlled trial. PLoS ONE 2019, 14, e0217894. [CrossRef] [PubMed]

96. Lee, S.-Y.; Kim, J.-H.; Han, Y.-H.; Cho, D.-H. The effect of modulated electro-hyperthermia on temperature and blood flow in human cervical carcinoma. Int. J. Hyperth. 2018, 34, 953–960. [CrossRef]

97. Minnaar, C.A.; Kotzen, J.A.; Naidoo, T.; Naidoo, T.; Tunmer, M.; Sharma, V.; Vangu, M.-D.-V.; Bayes, A. Analysis of the effects of mEHT on the treatment- related toxicity and quality of life of HIV-positive cervical cancer patients. Int. J. Hyperth. 2020, 37, 263–272. [CrossRef] [PubMed]

98. Papp, E.; Vancsik, T.; Kiss, E.; Szasz, O. Energy absorption by the membrane rafts in the modulated electro-hyperthermia (mEHT). Open J. Biophys. 2017, 7, 216–229. [CrossRef]

99. Szasz, A. The capacitive coupling modalities for oncological hyperthermia. Open J. Biophys. 2021, 11, 252–313. [CrossRef]

100. Szasz, O.; Szasz, A.; Iluri, N. RF Hyperthermia Device for Personalized Treatment and Diagnosis. U.S. Patent 9,937,357 B2, 10 April 2018.

101. Andocs, G.; Meggyeshazi, N.; Balogh, L.; Spisak, S.; Maros, M.E.; Balla, P.; Kiszner, G.; Teleki, I.; Kovago, C.; Krenacs, T. Upregulation of heat shock proteins and the promotion of damage-associated molecular pattern signals in a colorectal cancer model by modulated electrohyperthermia. Cell Stress Chaperones 2014, 20, 37–46. [CrossRef]

102. Meggyeshazi, N.; Andocs, G.; Spisak, S.; Krenacs, T. Early Changes in mRNA and Protein Expression Related to Cancer Treatment by Modulated Electro-Hyperthermia. In Proceedings of the International Clinical Hyperthermia Society, Budapest, Hungary, 12–14 October 2012; Hindawi Publishing Corporation Conference Papers in Medicine: London, UK, 2013.

103. Meggyeshazi, N. Studies on Modulated Electrohyperthermia Induced Tumor Cell Death in a Colorectal Carcinoma Model. Ph.D. Thesis, Semmelweis University, Budapest, Hungary, 2015.

104. Schvarcz, C.A.; Danics, L.; Krenacs, T.; Viana, P.; Beres, R.; Vancsik, T.; Nagy, A.; Gyenesei, A.; Kun, J.; Fonovic, M.; et al. Modulated electro-hyperthermia induces a prominent local stress response and growth inhibition in mouse breast cancer isografts. Cancers 2021, 13, 1744. [CrossRef]

105. Andocs, G.; Rehman, M.U.; Zhao, Q.L.; Tabuchi, Y.; Kanamori, M.; Kondo, T. Comparison of biological effects of modulated electro-hyperthermia and conventional heat treatment in human lymphoma U937 cell. Cell Death Discov. 2016, 2, 16039. [CrossRef]

106. Danics, L.; Schvarcz, C.A.; Viana, P.; Vancsik, T.; Krenacs, T.; Benyo, Z.; Kaucsar, T.; Hamar, P. Exhaustion of protective heat shock response induces significant tumor damage by apoptosis after modulated

electro-hyperthermia treatment of triple negative breast cancer isografts in mice. Cancers 2020, 12, 2581. [CrossRef]

107. Besztercei, B.; Vancsik, T.; Benedek, A.; Marjor, E.; Thomas, M.J.; Schvarcz, C.A.; Krenacs, T.; Benyo, Z.; Balogh, A. Stressinduced, p53-mediated tumor growth inhibition of melanoma by modulated electrohyperthermia in mouse models without major immunogenic effects. Int. J. Mol. Sci. 2019, 20, 4019. [CrossRef]

108. Vancsik, T.; Kovago, C.; Kiss, E.; Papp, E.; Forika, G.; Benyo, Z.; Meggyeshazi, N.; Krenacs, T. Modulated electro-hyperthermia induced loco-regional and systemic tumor destruction in colorectal cancer allografts. J. Cancer 2018, 9, 41–53. [CrossRef] [PubMed]

109. Qin, W.; Akutsu, Y.; Andocs, G.; Suganami, A.; Hu, X.; Yusup, G.; Komatsu-Akimoto, A.; Hoshino, I.; Hanari, N.; Mori, M.; et al. Modulated electro-hyperthermia enhances dendritic cell therapy through an abscopal effect in mice. Oncol. Rep. 2014, 32, 2373–2379. [CrossRef] [PubMed]

110. Meggyeshazi, N.; Andocs, G.; Krenacs, T. Programmed Cell Death Induced by Modulated Electro-Hyperthermia. In Proceedings of the International Clinical Hyperthermia Society 2012, Budapest, Hungary, 12–14 October 2012; Hindawi Publishing Corporation Conference Papers in Medicine: London, UK, 2013; Volume 2013, p. 187835.

111. Meggyesházi, N.; Andocs, G.; Balogh, L.; Balla, P.; Kiszner, G.; Teleki, I.; Jeney, A.; Krenács, T. DNA fragmentation and caspaseindependent programmed cell death by modulated electrohyperthermia. Strahlenther. Onkol. 2014, 190, 815–822. [CrossRef][PubMed]

112. Sevrioukova, I.F. Apoptosis-inducing factor: Structure, function, and redox regulation. Antioxid. Redox Signal. 2011, 14, 2545–2579. [CrossRef] [PubMed]

113. Tsang, Y.-W.; Huang, C.-C.; Yang, K.-L.; Chi, M.-S.; Chiang, H.-C.; Wang, Y.-S.; Andocs, G.; Szasz, A.; Li, W.-T.; Chi, K.-H. Improving immunological tumor microenvironment using electro-hyperthermia followed by dendritic cell immunotherapy. BMC Cancer 2015, 15, 708. [CrossRef]

114. Wust, P.; Ghadjar, P.; Nadobny, J. Physical analysis of temperature-dependent effects of amplitude-modulated electromagnetic hyperthermia. Int. J. Hyperth. 2019, 36, 1246–1254. [CrossRef] [PubMed]

115. Warfel, N.A.; El-Deiry,W.S. p21WAF1 and tumourigenesis. Curr. Opin. Oncol. 2013, 25, 52–58. [CrossRef] [PubMed]

116. Vancsik, T.; Máthé, D.; Horváth, I.; Várallyaly, A.A.; Benedek, A.; Bergmann, R.; Krenács, T.; Benyó, Z.; Balogh, A. Modulated electro-hyperthermia facilitates NK-cell infiltration and growth arrest of human A2058 melanoma in a xenograft model. Front. Oncol. 2021, 11, 164. [CrossRef]

117. Multhoff, G. Activation of natural killer cells by heat shock protein 70. Int. J. Hyperth. 2002, 18, 576–585. [CrossRef]

118. Yilmaz, M.T.; Elmali, A.; Yazici, G. Abscopal Effect, From Myth to Reality: From Radiation Oncologists' Perspective. Cureus 2019, 11, e3860. [CrossRef]

119. Wahl, R.L.; Jacene, H.; Kasamon, Y.; Lodge, M.A. From RECIST to PERCIST: Evolving Considerations for PET Response Criteria in Solid Tumors. J. Nucl. Med. 2009, 50, 122–151. [CrossRef]

120. Brix, N.; Tiefenthaller, A.; Anders, H.; Belka, C.; Lauber, K. Abscopal, immunological effects of radiotherapy: Narrowing the gap between clinical and preclinical experiences. Immunol. Rev. 2017, 280, 249–279. [CrossRef] [PubMed]

121. Tubin, S.; Casamassima, F.; Menichelli, C. A Case Report on Metastatic Thyroid Carcinoma: Radiation-induced Bystander or Abscopal Effect ? J. Cancer Sci. Ther. 2012, 4, 408–411. [CrossRef]

122. Hlavata, Z.; Solinas, C.; De Silva, P.; Porcu, M.; Saba, L.; Willard-Gallo, K.; Scartozzi, M. The Abscopal Effect in the Era of Cancer Immunotherapy: A Spontaneous Synergism Boosting Anti-tumor Immunity? Target. Oncol. 2018, 13, 113–123. [CrossRef][PubMed]

123. Reynders, K.; Illidge, T.; Siva, S.; Chang, J.Y.; De Ruysscher, D. The abscopal effect of local radiotherapy: Using immunotherapy to make a rare event clinically relevant. Cancer Treat. Rev. 2015, 41, 503–510. [CrossRef]

124. Kao, P.H.-J.; Chen, C.-H.; Tsang, Y.-W.; Lin, C.-S.; Chiang, H.-C.; Huang, C.-C.; Chi, M.-S.; Yang, K.-L.; Li,W.-T.; Kao, S.-J.; et al. Relationship between energy dosage and apoptotic cell death by modulated electro-hyperthermia. Sci. Rep. 2020, 10, 8936. [CrossRef]

125. Krenacs, T.; Benyo, Z. Tumor specific stress and immune response induced by modulated electrohyperthermia in relation to tumor metabolic profiles. Oncothermia J. 2017, 20, 264–272.

126. Yoon, S.-M.; Jung, S.L. Case of Abscopal effect with Metastatic Non-Small-Cell Lung Cancer. Oncothermia J. 2012, 5, 53–57.

127. Fiorentini, G.; Yoon, S.M.; Yan, O.; Andocs, G.; Baronzio, G.F.; Laurent, S.; Balogh, L.; Szasz, A. Abscopal effect: New perspectives in Oncothermia. Oncothermia J. 2013, 7, 279–281.

128. Chi, M.-S.; Wu, J.-H.; Shaw, S.; Wu, C.-J.; Chen, L.-K.; Hsu, H.-C.; Chi, K.-H. Marked local and distant response of heavily treated breast cancer with cardiac metastases treated by combined low dose radiotherapy, low dose immunotherapy and hyperthermia: A case report. Ther. Radiol. Oncol. 2021, 5, 17. [CrossRef]

129. Schirrmacher, V.; Stücker,W.; Lulei, M.; Bihari, A.-S.; Sprenger, T. Long-term survival of a breast cancer patient with extensive liver metastases upon immune and virotherapy: A case report. Immunotherapy 2015, 7, 855–860. [CrossRef]

130. Chi, M.-S.; Mehta, M.P.; Yang, K.-L.; Lai, H.-C.; Lin, Y.-C.; Ko, H.-L.; Wang, Y.-S.; Liao, K.-W.; Chi, K.-H. Putative abscopal effect in three patients treated by combined radiotherapy and modulated electrohyperthermia. Front. Oncol. 2020, 10, 254. [CrossRef]

131. Chi, K.-H. Tumour-Directed Immunotherapy: Clinical Results of Radiotherapy with Modulated Electro-Hyperthermia. In Challenges and Solutions of Oncological Hyperthermia; Szasz, A., Ed.; Cambridge Scholars: London, UK, 2020; Chapter 12; pp. 206–226.

132. Chi, K.H. Tumor-directed immunotherapy: Combined radiotherapy and oncothermia. Oncothermia J. 2018, 24, 196–235.

133. Pang, C.L.K. The Immune Regulating Effect of Hyperthermia in Combination with TCM on Cancer Patients. Oncothermia J. 2016, 18, 170–179.

134. Van Gool, S.W.; Makalowski, J.; Bonner, E.R.; Feyen, O.; Domogalla, M.P.; Prix, L.; Schirrmacher, V.; Nazarian, J.; Stuecker, W. Addition of multimodal immunotherapy to combination treatment strategies for children with DIPG: A single institution experience. Medicines 2020, 7, 29. [CrossRef] [PubMed]

135. Van Gool, S.W.; Makalowski, J.; Fiore, S.; Sprenger, T.; Prix, L.; Schirrmacher, V.; Stuecker,W. Randomized controlled immunotherapy clinical trials for GBM challenged. Cancers 2021, 13, 32. [CrossRef]

136. Van Gool, S.W.; Makalowski, J.; Feyen, O.; Prix, L.; Schirrmacher, V.; Stuecker, W. The induction of immunogenic cell death (ICD) during maintenance chemotherapy and subsequent multimodal immunotherapy for glioblastoma (GBM). Austin Oncol. Case Rep. 2018, 3, 1–8.

137. Van Gool, S.W.; Makalowski, J.; Stuecker, W. Modulated electrohyperthermia (mEHT) as part of multimodal immunotherapy for brain tumors. Oncothermia J. 2018, 248.

138. Van Gool, S.; Makalowski, J.; Marko, M. Hyperthermia as part of multimodal immunotherapy for patients with GBM. Oncothermia J. 2019, 27, 122–137.

139. Van Gool, S.; Makalowski, J.; Marko, M. Multimodal immunotherapy for patients with ovarian cancer. Oncothermia J. 2019, 27, 138–152.

140. Minnaar, C.A.; Kotzen, J.A.; Ayeni, O.A.; Vangu, M.-D.-T.; Baeyens, A. Potentiation of the Abscopal Effect by Modulated Electro-Hyperthermia in Locally Advanced Cervical Cancer Patients. Front. Oncol. 2020, 10, 376. [CrossRef]

141. Blad, B.; Wendel, P.; Jonsson, M.; Lindstrom, K. An electrical impedance index to distinguish between normal and cancerous tissues. J. Med. Eng. Technol. 1999, 23, 57–62. [CrossRef] [PubMed]

142. Zhou, J.;Wang, G.; Chen, Y.;Wang, H.; Hua, Y.; Cai, Z. Immunogenic cell death in cancer therapy: Present and emerging inducers. J. Cell. Mol. Med. 2019, 23, 4854–4865. [CrossRef]

143. Szasz, A. Electromagnetic Effects in Nanoscale Range. In Cellular Response to Physical Stress and Therapeutic Applications; Tadamichi, S., Takashi, K., Eds.; Nova Science Publishers, Inc.: Hauppauge, NY, USA, 2013; Chapter 4.

144. Andocs, G.; Rehman, M.U.; Zhao, Q.L.; Papp, E.; Kondo, T.; Szasz, A. Nanoheating without Artificial Nanoparticles Part II. Experimental support of the nanoheating concept of the modulated electro-hyperthermia method, using U937 cell suspension model. Biol. Med. 2015, 7, 4. [CrossRef]

145. Szasz, A. Thermal and nonthermal effects of radiofrequency on living state and applications as an adjuvant with radiation therapy. J. Radiat. Cancer Res. 2019, 10, 1–17. [CrossRef]

146. Szasz, O.; Szasz AMMinnaar, C.; Szasz, A. Heating preciosity-trends in modern oncological hyperthermia. Open J. Biophys. 2017, 7, 116–144. [CrossRef]

147. Ronchi, R.; Marano, L.; Braidotti, P.; Bianciardi, P.; Calamia, M.; Fiorentini, C.; Samaja, M. Effects of broad band magnetic fields on HSP70 expression and ischemia-reperfusion in rat hearts. Life Sci. 2004, 75, 1925–1936. [CrossRef]

148. Goodman, R.; Blank, M. Insights into electromagnetic interaction mechanisms. J. Cell. Physiol. 2002, 192, 16–22. [CrossRef]

149. Sapozhnikov, A.M.; Ponomarev, E.D.; Tarasenko, T.N.; Telford, W.G. Spontaneous apoptosis and expression of cell-surface heat-shock proteins in cultured EL-4 lymphoma cells. Cell Prolif. 1999, 32, 363–378. [CrossRef]

150. Horvath, I.; Vigh, L. Cell biology: Stability in times of stress. Nature 2010, 463, 436–438. [CrossRef]

151. Hildebrandt, B.; Wust, P.; Ahlers, O.; Dieing, A.; Sreenivasa, G.; Kerner, T.; Felix, R.; Riess, H. The cellular and molecular basis of hyperthermia. Crit. Rev. Oncol. Hematol. 2002, 43, 33–56. [CrossRef]

152. Nishida, T.; Akagi, K.; Tanaka, Y. Correlation between cell killing effect and cell membrane potential after heat treatment: Analysis using fluorescent dye and flow cytometry. Int. J. Hyperth. 1997, 13, 227–234. [CrossRef]

153. Gehrmann, M.; Radons, J.; Molls, M.; Multhoff, G. The therapeutic implications of clinically applied modifiers of heat shock protein 70 (Hsp70) expression by tumor cells. Cell Stress Chaperones 2008, 13, 1–10. [CrossRef]

154. Pfister, K.; Radons, J.; Busch, R.; Tidball, J.G.; Pfeifer, M.; Freitag, L.; Feldmann, H.J.; Milani, V.; Issels, R.; Multhoff, G. Patient survival by Hsp70 membrane phenotype: Association with different routes of metastasis. Cancer 2007, 110, 926–935. [CrossRef]

155. Multhoff, G. Heat shock protein 70 (Hsp70): Membrane location, export and immunological relevance. Methods 2007, 43, 229–237. [CrossRef] [PubMed]

156. Andreev, V.P. Cytoplasmic electric fields and electroosmosis: Possible solution for the paradoxes of the intracellular transport of biomolecules. PLoS ONE 2013, 8, e61884. [CrossRef]

157. Multhoff, G.; Hightower, L.E. Distinguishing integral and receptor-bound heat shock protein 70 (Hsp70) on the cell surface by Hsp70-specific antibodies. Cell Stress Chaperones 2011, 16, 251–255. [CrossRef] [PubMed]

158. Calderwood, S.K. Molecular co-chaperones: Tumor growth and cancer treatment. Scientifica 2013, 2013, 217513. [CrossRef]

159. Spisek, R.; Charalambous, A.; Mazumder, A.; Vesole, D.H.; Jagannath, S.; Dhodapkar, M.V. Bortezomib enhances dendritic cell (DC)-mediated induction of immunity to human myeloma via exposure of cell surface heat shock protein 90 on dying tumor cells: Therapeutic implications. Blood 2007, 109, 4839–4845. [CrossRef]

160. Multhoff, G.; Botzler, C.;Wiesnet, M.; Müller, E.; Meier, T.;Wilmanns,W.; Issels, R.D. A stress-inducible 72-kDa heat-shock protein (HSP72) is expressed on the surface of human tumor cells, but not on normal cells. Int. J. Cancer 1995, 61, 272–279. [CrossRef]

161. Gehrmann, M.; Liebisch, G.; Schmitz, G.; Anderson, R.; Stinem, C.; De Maio, A.; Pockley, G.; Multhoff, G. Tumor-Specific Hsp70 Plasma Membrane Localization Is Enabled by the Glycosphingolipid Gb3. PLoS ONE 2008, 2, e1925–e1933. [CrossRef] [PubMed]

162. Xanthoudakis, S.; Roy, S.; Rasper, D.; Heessey, T.; Aubin, Y.; Cassady, R.; Tawa, P.; Ruel, R.; Rosen, A.; Nicholson, D.W. Hsp60 accelerates the maturation of pro-caspase-3 by upstream activator proteases during apoptosis. EMBO J. 1999, 18, 2049–2056. [CrossRef] [PubMed]

163. Szasz, A.; Vincze, G.; Szasz, O.; Szasz, N. An energy analysis of extracellular hyperthermia. Electromagn. Biol. Med. 2003, 22, 103–115. [CrossRef]

164. Jeon, T.W.; Yang, H.; Lee, C.G.; Oh, S.T.; Seo, D.; Baik, I.H.; Lee, E.H.; Yun, I.; Park, K.R.; Lee, Y.H. Electro-hyperthermia up-regulates tumor suppressor Septin 4 to induce apoptotic cell death in hepatocellular carcinoma. Int. J. Hyperth. 2016, 32, 648–656. [CrossRef]

165. Hou,W.; Zhang, Q.; Yan, Z.; Chen, R.; Zeh, H.J., III; Kang, R.; Lotze, M.T.; Tang, D. Strange attractors: DAMPs and autophagy link tumor cell death and immunity. Cell Death Dis. 2013, 4, e966. [CrossRef]

166. Murao, A.; Aziz, M.; Wang, H.; Brenner, M.; Wang, P. Release mechanisms of major DAMPs. Apoptosis 2021, 26, 152–162. [CrossRef] [PubMed]

167. Garg, A.D.; Nowis, D.; Golab, J.; Vandenabeele, P.; Krysko, D.V.; Agostinis, P. Immunogenic cell death, DAMPs and anticancer therapeutics: An emerging amalgamation. Biochim. Biophys. Acta 2010, 1805, 53–71. [CrossRef] [PubMed]

168. Lin, F.C.; Hsu, C.H. Nano-therapeutic cancer immunotherapy using hyperthermia-induced heat shock proteins: Insights from mathematical modeling. Int. J. Nanomed. 2018, 13, 3529–3539. [CrossRef]

169. Ito, A.; Honda, H.; Kobayashi, T. Cancer immunotherapy based on intracellular hyperthermia using magnetite nanoparticles: A novel concept of “heat-controlled necrosis” with heat shock protein expression. Cancer Immunol. Immunother. 2005, 55, 320–328. [CrossRef]

170. Ablakova, Z.; Armeev, G.A.; Kanevskiy, L.M.; Kovalenko, E.I.; Sapozhikov, A.M. HSP70 multi-funtionality in cancer. Cells 2020, 9, 587. [CrossRef]

171. Stocki, P.; Dickinson, A.M. The immunosuppressive activity of heat shock protein 70. Autoimmune Dis. 2012, 2012, 617213. [CrossRef] [PubMed]

172. Beachy, S.H.; Repasky, E.A. Toward establishment of temperature thresholds for immunological impact of heat exposure in humans. Int. J. Hyperth. 2011, 27, 344–352. [CrossRef]

173. Vakkila, J.; Lotze, M.T. Inflammation and necrosis promote tumour growth. Nat. Rev. Immunol. 2004, 4, 641–648. [CrossRef]

174. Feyerabend, T.;Wiedemann, G.J.; Jager, B.; Vesely, H.; Mahlmann, B.; Richter, E. Local hyperthermia, radiation, and chemotherapy in recurrent breast cancer is feasible and effective except for inflammatory disease. Int. J. Radiat. Oncol. Biol. Phys. 2001, 49, 1317–1325. [CrossRef]

175. Kumar, S.; Deepak, P.; Kumar, S.; Kishore, D.; Acharya, A. Autologous Hsp70 induces antigen specific Th1 immune responses in a murine T-cell lymphoma. Immunol. Investig. 2009, 38, 449–465. [CrossRef] [PubMed]

176. Jolesch, A.; Elmer, K.; Bendz, H.; Issels, R.D.; Nossner, E. Hsp70, a messenger from hyperthermia for the immune system. Eur. J. Cell Biol. 2011, 91, 48–52. [CrossRef]

177. Hicman-Miller, H.D.; Hildbrand, H. The immune response under stress: The role of HSP-derived peptides. Trends Immunol. 2004, 25, 427–433. [CrossRef] [PubMed]

178. Binder, R.J. Functions of heat shock proteins in pathways of the innate and adaptive immune system. J. Immunol. 2014, 193, 5765–5771. [CrossRef]

179. Keep, O.; Galluzzi, L.; Senovilla, L.; Panarkakis, T.; Tesiere, A.; Schlemmer, F.; Madeo, F.; Zitvogel, L.; Kroemer, G. Viral subversion of immunogenic cell death. Cell Cycle 2009, 8, 860–869. [CrossRef]

180. Krysko, D.V.; Ravichandran, K.S.; VAndenabeele, P. Macrophages regulate the clearance of living cells by calreticulin. Nat. Commun. 2018, 9, 4644. [CrossRef] [PubMed]

181. Obeid, M.; Tesniere, A.; Ghiringhelli, F.; Fimia, G.M.; Apetoh, L.; Perfettini, J.-L.; Castedo, M.; Mignot, G.; Panaretakis, T.; Casares, N.; et al. Calreticulin exposure dictates the immunogenicity of cancer cell death. Nat. Med. 2007, 13, 54–61. [CrossRef] [PubMed]

182. Xu, Z.; Yang, Y.; Zhou, J.; Huang, Y.; Wang, Y.; Zhang, Y.; Lan, Y.; Liang, J.; Liu, X.; Zhong, N.; et al. Role of plasma calreticulin in the prediction of severity in septic patients. Dis. Markers 2019, 2019, 8792640. [CrossRef]

183. Gold, L.I.; Eggleton, P.; Sweetwyne, M.T.; Van Duyn, L.B.; Greives, M.R.; Naylor, S.M.; Michalak, M.; Murphy-Ullrich, J.E. Calreticulin: Non-endoplamic reticulum functions in physiology and disease. FASEB J. 2009, 24, 665–683. [CrossRef] [PubMed]

184. Kwon, M.S.; Park, C.S.; Choi, K.r.; Park, C.-S.; Ahnn, J.; Kim, J., II; Eom, S.H.; Kaufman, S.J.; Song, W.K. Calreticulin couples calcium release and calcium influx in integrin-mediatd calcium signaling. Mol. Biol. Cell 2000, 11, 1433–1443. [CrossRef]

185. Klune, J.R.; Dhuper, R.; Cardinal, J.; Billiar, T.R.; Tsung, A. HMGB1, Endogenous Danger Signaling. Mol. Med. 2008, 14, 476–484. [CrossRef]

186. Kang, R.; Chen, R.; Zhag, Q.; Hou,W.;Wu, S.; Cao, L.; Huang, J.; Yu, Y.; Fan, Y.-G.; Yan, Z.; et al. HMGB1 in health and disease. Mol. Aspects Med. 2008, 40, 1–116. [CrossRef] [PubMed]

187. Kazama, H.; Ricci, J.-E.; Herndon, J.M.; Hoppe, G.; Gren, D.R.; Ferguson, T.A. Induction of immunological tolerance by apoptotic cells requires caspase-dependent oxidation of high-mobility group Box-1 protein. Immunity 2008, 29, 21–32. [CrossRef] [PubMed]

188. Li, C.; Zhang, Y.; Cheng, X.; Yuan, H.; Zhu, S.; Liu, J.; Wen, Q.; Xie, Y.; Liu, J.; Kroemer, G.; et al. PINK1 and PARK2 suppress pancreatic tumorigenesis through control of mitochondrial iron-mediated immunometabolism. Dev. Cell. 2018, 46, 441–455.e448. [CrossRef]

189. Yu, Y.; Tang, D.; Kang, R. Oxidative stress-mediated HMGB1 biology. Front. Physiol. 2015, 6, 93. [CrossRef]

190. Galluzzi, L.; Buque, A.; Kepp, O.; Zitvogel, L.; Kroemer, G. Immunogenic cell death in cancer and infectious disease. Nat. Rev. Immunol. 2017, 17, 97–111. [CrossRef]

191. Medina, C.B.; Ravichandran, K.S. Do not let death do us part-'find-me' signals in communication between dying cells and the phygocytes. Cell Death Differ. 2016, 23, 979–989. [CrossRef] [PubMed]

192. Michaud, M.; Martins, I.; Sukkurwala, A.Q.; Adjemian, S.; Ma, Y.; Pellegatti, P.; Shen, S.; Kepp, O.; Scoazec, M.; Mignot, G.; et al. Autophagy-dependent anticancer immune responses induced by chemotherapeutic agents in mice. Science 2011, 334, 1573–1577. [CrossRef]

193. Land, W.G. The role of damage-associated molecular patterns (DAMPs) in human diseases. Sultan Qaboos Univ. Med. J. 2015, 15, e157–e170.

194. Hernandez, C.; Huebener, P.; Schwabe, R.F. Damage-associated molecular patterns in cancer: A double-edged sword. Oncogene 2016, 35, 5931–5941. [CrossRef] [PubMed]

195. Sangiuliano, B.; Perez, N.M.; Moreira, D.F.; Belizario, J.E. Cell death-associated molecular-pattern molecules: Inflammatory signaling and control. Mediat. Inflamm. 2014, 2014, 821043. [CrossRef] [PubMed]

196. Hegyi, G.; Vincze, G.; Szasz, A. On the Dynamic Equilibrium in Homeostasis. Open J. Biophys. 2012, 2, 64–71. [CrossRef]

197. Szigeti, G.P.; Szasz, A.M.; Szasz, A. The growth of healthy and cancerous tissues. Open J. Biophys. 2020, 10, 113–128. [CrossRef]

198. Levin, M. Large-scale biophysics: Ion flows and regeneration. Trends Cell Biol. 2007, 17, 261–269. [CrossRef] [PubMed]

199. Szasz, O.; Szigeti, G.P.; Szasz, A.; Benyo, Z. Role of electrical forces in angiogenesis. Open J. Biophys. 2018, 8, 49–67. [CrossRef]

200. Derer, A.; Deloch, L.; Rubner, Y.; Fietkau, R.; Frey, B.; Gaipl, U.S. Radio-immunotherapy-induced immunogenic cancer cells as basis for induction of systemic anti-tumor immune responses–pre-clinical evidence and ongoing clinical applications. Front. Immunol. 2015, 6, 505. [CrossRef]

201. Stagg, A.J.; Knight, S.C. Antigen-presenting cells. Nature 2001, 1–8. Available online: http://labs.icb.ufmg.br/lbcd/pages2/bernardo/Bernardo/Artigos/Antigen-resenting%20Cells.pdf (accessed on 7 October 2020).

202. Kepp, O.; Galluzzi, L.; Martins, I.; Schlemmer, F.; Adjemian, S.; Michaud, M.; Sukkurwala, A.Q.; Menger, L.; Zitvogel, L.; Kroemer, G. Molecular determinants of immunogenic cell death elicited by anticancer chemotherapy. Cancer Metastasis Rev. 2011, 30, 61–69. [CrossRef] [PubMed]

203. Sachamitr, P.; Fairchild, P.J. Cross presentation of antigen by dendritic cells: Mechanisms and implications for immunotherapy. Expert. Rev. Clin. Immunol. 2012, 8, 547–555. [CrossRef]

204. Chi, K.-W. Tumor-Directed Immunotherapy: Combined Radiotherapy and Oncothermia. In Proceedings of the 36th Conference of the International Clinical Hyperthermia Society, Budapest, Hungary, 28–29 September 2018.

205. Holtmeier,W.; Kabelitz, D. $\gamma\delta$ T-cells link innate and adaptive immune responses. Chem. Immunol. Allergy 2005, 86, 151–183.

206. Andocs, G.; Szasz, A.; Szasz, I.; Szasz, N. Tumor. Vaccination Patent U.S. 2015/0217099, 6 October 2020. Available online: http://www.freepatentsonline.com/20150217099.pdf (accessed on 10 January 2021).

Meta-Analysis of Modulated Electro-Hyperthermia and Tumor Treating Fields in the Treatment of Glioblastomas

Attila Marcell Szasz [1],*, Elisabeth Estefanía Arrojo Alvarez [2,3], Giammaria Fiorentini [4,5], Magdolna Herold [1,6], Zoltan Herold [1], Donatella Sarti [4] and Magdolna Dank [1]

[1] Division of Oncology, Department of Internal Medicine and Oncology, Semmelweis University, 1083 Budapest, Hungary

[2] Oncología Radioterápica, Servicios y Unidades Asistenciales, Hospital Universitario Marqués de Valdecilla, 39008 Santander, Spain

[3] Medical Institute of Advanced Oncology, 28037 Madrid, Spain

[4] Department of Oncology, Azienda Ospedaliera "Ospedali Riuniti Marche Nord", 61121 Pesaro, Italy

[5] IHF Integrative Oncology Outpatient Clinic, 40121 Bologna, Italy

[6] Department of Internal Medicine and Hematology, Semmelweis University, 1088 Budapest, Hungary

* Correspondence: szasz.attila_marcell@med.semmelweis-univ.hu; Tel.: +36-1-459-1500

Cite this article as:
Szasz, A.M. et al. (2023) Meta-Analysis of Modulated Electro-Hyperthermia and Tumor Treating Fields in the Treatment of Glioblastomas. Cancers 2023, 15, 880.
https://www.mdpi.com/2072-6694/15/3/880

Oncothermia Journal 33, May 2023: 146 – 164.
www.oncotherm.com/sites/oncotherm/files/2023-05/SzaszAM_et_al_Meta-Analysis-of-mEHT-Glioblastoma.pdf

Simple Summary:
Glioblastoma is a highly aggressive brain tumor, which has a very poor 5-year survival rate (<5%). In the last decades, the concomitant use of two non-invasive, electromagnetic devices, modulated electro-hyperthermia (mEHT) and Tumor Treating Fields (TTF) has been introduced. Both mEHT and TTF have specific anti-tumor effects, which can help to achieve a more efficient treatment of patients and a higher rate of therapeutic response. In this meta-analysis we investigated how patient survival rates change if either device is used. The significant difference in the 1-year survival rates between the treated (>60%) and untreated groups (historical data: <40%) confirms the observation that the use of both mEHT and TTF in the treatment of glioblastomas benefits patients. In addition, it is important to emphasize that most studies have proven that the mEHT or TTF-treated patients' quality of life is much better than that of the untreated patients.

Abstract:
Background: Glioblastoma is one of the most difficult to treat and most aggressive brain tumors, having a poor survival rate. The use of non-invasive modulated electro-hyperthermia (mEHT) and Tumor Treating Fields (TTF) devices has been introduced in the last few decades, both of which having proven anti-tumor effects. Methods: A meta-analysis of randomized and observational studies about mEHT and TTF was conducted. Results: A total of seven and fourteen studies about mEHT and TTF were included, with a total number of 450 and 1309 cases, respectively. A 42% [95% confidence interval (95% CI): 25–59%] 1-year survival rate was found for mEHT, which was raised to 61% (95% CI: 32–89%) if only the studies conducted after 2008 were investigated. In the case of TTF, 1-year survival was 67% (95% CI: 53–81%). Subgroup analyses revealed that newly diagnosed patients might get extra benefits from the early introduction of the devices (mEHT all studies: 73% vs. 37%, p = 0.0021; mEHT studies after 2008: 73% vs. 54%, p = 0.4214; TTF studies: 83% vs. 52%, p = 0.0083), compared with recurrent glioblastoma. Conclusions: Our meta-analysis showed that both mEHT and TTF can improve glioblastoma survival, and the most benefit may be achieved in newly diagnosed cases.

Keywords: astrocytoma; glioblastoma; modulated electro-hyperthermia; tumor treating fields

1. Introduction

Based on the 2020 GLOBOCAN report, more than 300,000 new central nervous system tumors are confirmed each year, with more than 250,000 deaths [1,2]. Among these, gliomas are the most common [3], which have different origins (e.g., astrocytes and oligodendrocytes) [4,5]. As per the latest WHO classification (2021), depending on the origin and the mutation of isocitrate dehydrogenase (IDH), three major types of diffuse gliomas are known: astrocytomas (IDH mutant), oligodendroglioma (IDH mutant and 1p/19q co-deleted) and glioblastomas (IDH wild type) [6]. Glioblastomas are known to be the most aggressive and the most occurring type [6,7]. Up to 60% of all malignant primary brain tumors in adults are estimated to be glioblastomas [8]. For decades, the only treatment options for astrocytoma/glioblastoma patients were surgery and radiotherapy [9], but with the introduction of concurrent and/or adjuvant temozolomide chemotherapy patient survival significantly improved [10]. Thanks to the combined effect of temozolomide and radiotherapy, 1-year survival has improved to 30–40%, and some studies reported even higher ones (>80%) [11], however, only modest median overall survivals can usually be achieved [12,13].

In the last two decades, semi-invasive and non-invasive electromagnetic devices/ techniques with anti-tumoral effects have been introduced that can be used concomitantly and/or palliatively in the treatment of glioblastomas to supplement chemoradiotherapy. Magnetic hyperthermia, in which the local deposition of magnetic nanoparticles is needed prior the application of an external alternating magnetic field, belongs to the former type [14]. In contrast, modulated electro-hyperthermia (mEHT) and Tumor Treating Fields (TTF) are non-invasive techniques; the devices only have be placed on the skin of the patients. In this article, the latter type is presented in more detail. The most optimal is when the mEHT treatment is done three-times a week, while TTF has to be worn for >18 h daily [15–23]. With an optimal frequency of 200 kHz, TTF focuses on nonthermal effects on the cytokinetic "neck" using capacitive coupling [24,25]. The electric field of TTF reorients the high polarizable microtubules and actin fibers, and it may arrest the cytoskeleton's polymerization process and inhibit the assembling of the mitotic spindle, ultimately blocking the finalization of the last phase of cell division and thus inhibiting further proliferation [26]. TTF also stimulates macrophages, promoting immunogenic cell death via dendritic cell recruitment and maturation, reducing the capacity of cancer cells for migration and invasion, preventing the inhibitory effects of the PI3K/Akt/mTORC1 signaling pathway on autophagy and increasing DNA replication stress and double-strand break formation [27]. Moreover, the electric field generated by TTF increases membrane permeability enhancing the effect of

chemotherapy significantly [28]. It has to be noted though, this latter effect is reversible [28], therefore, it can be expected that the improved chemo-sensitivity will probably reduce when TTF is not in use.

In contrast, mEHT accurately balances both the nonthermal electric processes and the low-power thermal effects. It operates in a precision capacitive coupled impedance matched way, working on a radiofrequency of 13.56 MHz [29]. mEHT exploits various biophysical differences of cancer cells. For example, energy absorption on the membrane rafts is different than those of healthy host cells, and damage-associated molecular patterns (DAMPS) will also occur. All of these eventually lead to programmed or immunogenic tumor cell death [30–32]. It has also been reported that mEHT can enhance DNA fragmentation of tumor cells, increase the fraction of cells with low mitochondrial membrane potential, increase the concentration of intracellular Ca2+, increase the Fas, c-Jun N-terminal kinases and MAPK/ERK signaling pathways, increase the expression of pro-apoptotic Bcl-2 family proteins and can up-regulate the expression of genes associated with the molecular function of cell death (EGR1, JUN, and CDKN1A) and silencing others associated with cytoprotective functions [33,34]. It also has to be mentioned that the use of mEHT is also feasible in tumors of other locations as well [34].

Although both mEHT and TTF have advantageous effects against cancer cells, their use in routine oncology still awaits. The general acceptance of TTF—and perhaps also the awareness about it—is wider than that of the mEHT. One of the latest developments in the widespread application of TTF is that the American Society of Clinical Oncology (ASCO) guidelines recommend TTF therapy for newly diagnosed supratentorial glioblastoma without isocitrate dehydrogenase mutations after the completion of chemoradiation therapy [9]. In contrast, only clinical trial results and development reports are available for mEHT. Therefore, the main purpose of this meta-analysis is to provide comprehensive data and a systematic literature review on the clinical importance of mEHT in glioblastoma. Moreover, presenting the same information about TTF and, last but not least, the direct comparison of the two devices were further goals of this study.

2. Materials and Methods

2.1. Search Strategy

The study was conducted following the Preferred Reporting Items for Systematic Reviews and Meta-Analyses (PRISMA) guidelines [35]. Ethical approval was not required for the study due to the fact that the article presents aggregate data from previously published studies. The meta-analysis was registered in the PROSPERO database with the Registration Number: CRD42022385535. The search for eligible publications was performed in the BioMed Central (BMC), ClinicalTrials.gov, Cochrane Library, European Union Drug Regulating Authorities Clinical Trials Database (EudraCT), Excerpta Medica Database (Embase), PubMed—Medical Literature Analysis and Retrieval System Online (MEDLINE), World Health Organization's International Clinical Trials Registry Platform and in the University hospital Medical Information Network (UMIN) Clinical Trials Registry (for Japan) databases from their inception to 30 June 2022. The following search strings were used. The terms "glioblastoma" and "glioma" were combined with "electrohyperthermia", "electro hyperthermia", "electro-hyperthermia", "hyperthermia", "modulated electrohyperthermia", "oncotherm", "oncothermia", "alternating electric fields", "TTFields", "tumor treating fields" and "tumor-treating fields" using the logical operator AND. Furthermore, individual searches for "EHY-2030", "EHY 2030" and "EHY2030" were also performed. Language restrictions were not used.

Inclusion criteria for the studies were to contain survival data, either in the form of x-year survival rates, the number of deaths in x-year or survival curves from which the proportion of patients alive at the specific timepoints can be read. Concomitant or monotherapeutic use of mEHT/TTF was no limiting factor for inclusion. Exclusion criteria included if the observation period of the study was shorter than 1 year, if the patients treated with one of the two devices could not be separated from the controls (mixed study groups), or if the study contained only median survival and/or hazard rates only.

Type of publications (review, conference abstract, etc.) and species information (human vs. other) were retrieved from databases, where available. Publications belonging to the following categories were excluded without further review: reviews, conference abstracts, in vitro and animal studies and theoretical works. No automation tool was used during the literature search. The literature search was conducted independently by two investigators (A.M.S. and Z.H.), and any discrepancies were resolved by consensus and, if necessary, by the opinion of a third reviewer (M.D.).

2.2. Data Extraction

Collected data included general information about the study: name of author(s) and year of publication. The following study characteristics were recorded from each publication: type of study [prospective

observational study, retrospective observational study or randomized clinical trial (RCT)], sample size of treated and/or control groups, median age of patients, percentage of females, 1-year, 2-year and/or 3-year survival rate if available, and newly diagnosed or recurrent tumor. If the authors did not directly present the x-year survival rate but the corresponding survival curve(s) of the cohort(s) was drawn, the percentage of patients alive at the specific timepoints was read from the survival curve(s). It has to be noted, that grade 4 astrocytomas were previously termed as IDH-mutant glioblastomas, compared with the current WHO classification [6], and most of the articles used for the meta-analysis are older than the current classification, the differences in their nomenclature arise from this.

Statistical analyses were performed within the R forWindows version 4.2.1 environment (R Foundation for Statistical Computing, 2022, Vienna, Austria) using the R package meta (version 6.0-0) [36]. Survival rate at specific timepoints (1-year, 2-year or 3-year, if available) was used for the effect size measure and random-effects models were performed. To estimate the heterogeneity variance measure (τ^2) the restricted maximum-likelihood method [37] was applied with the Q profile method for confidence interval [38]. Betweenstudy heterogeneity was described by the Higgin's and Thompson's I2 statistic [39], and publication bias was tested using the Egger's regression test [40]. The Mantel–Haenszel method was used for group comparisons [41,42], plural models (fixed-effects model between subgroups but studies within the subgroups are pooled using the random-effects model) were used for subgroup analyses [38] and meta-regression methods were used to assess possible confounding/biasing effects (e.g., publication year) over effect size [38]. Forest plots were used to graphically represent study results.

3. Results

3.1. Studies Investigating Modulated Electro-Hyperthermia in Glioblastoma

The electronic database searches for studies about mEHT in glioblastoma patients resulted in a total of 2586 articles. After the removal of duplicates, non-human studies including animal and cellular research reports, reviews and meeting/conference abstracts, 686 articles remained for title and abstract screening. In total, 650 articles were excluded because they either reported results from other tumors, presented results from an animal and/or cellular experiment, were unavailable or had different study interests than the current meta-analysis (e.g., health-economy). Thirty-six studies were considered for full text assessment; however, twenty-seven further studies needed to be excluded. Of the remaining nine studies, two–two articles belonged to the same work ([43–46]), of which only one–one paper ([43,46]) was used for the meta-analysis, resulting in a total of seven available full text articles to be included in the analyses (Figure 1).

Details of the seven mEHT studies [43,46–51] selected for analysis can be read in Table 1. Six [43,46–50] and one [51] studies investigated the effect of mEHT in recurrent/late stage and in newly diagnosed glioblastoma, respectively. A comparison between mEHT-treated and control patients was only present only in one study [46]. The total number of patients included in the meta-analysis was 450, of whom 292 (64.9%) died during the first year after study inclusion. A 42.33% 1-year survival rate [95% confidence interval (CI): 25.17–59.49%] was estimated (Figure 2). Although the heterogeneity between studies was high [91.3% (95% CI: 84.6–95.1%)], no publication bias was present based on the results of the Egger's regression test (p = 0.6449).

Table 1. Details of the selected studies investigating the effect of modulated electro-hyperthermia (mEHT) in glioblastoma.

Author (Year)	Type of Study	Cases (*n*)	mEHT Device	Additional Therapy	Age (Median)	Females
Douwes et al. (2006) [47]	Prospective	19	Oncotherm EHY2000	nimustine	55	– [1]
Fiorentini et al. (2006) [48]	Prospective	12	Oncotherm EHY2000	– [1]	– [1]	– [1]
Sahinbas et al. (2007) [43]	Retrospective	140	Oncotherm EHY2000	temozolomide and/or herbal medicines and/or irradiation	44	35.7%
Hager et al. (2008) [49]	Prospective	179	LRF-DHT	– [1]	– [1]	– [1]
Heo et al. (2017) [50]	Prospective	20	Celsius 42+	re-irradiation	56	60%
Ryabova et al. (2018) [51]	Prospective	30	Celsius 42+	temozolomide + irradiation	56	36.7%
Fiorentini et al. (2019) [46]	Retrospective	50	Oncotherm EHY2000	no	55	– [1]

[1] Not detailed in the original article. LRF-DHT: deep hyperthermia with low radiofrequency capacitive coupled electrodes.

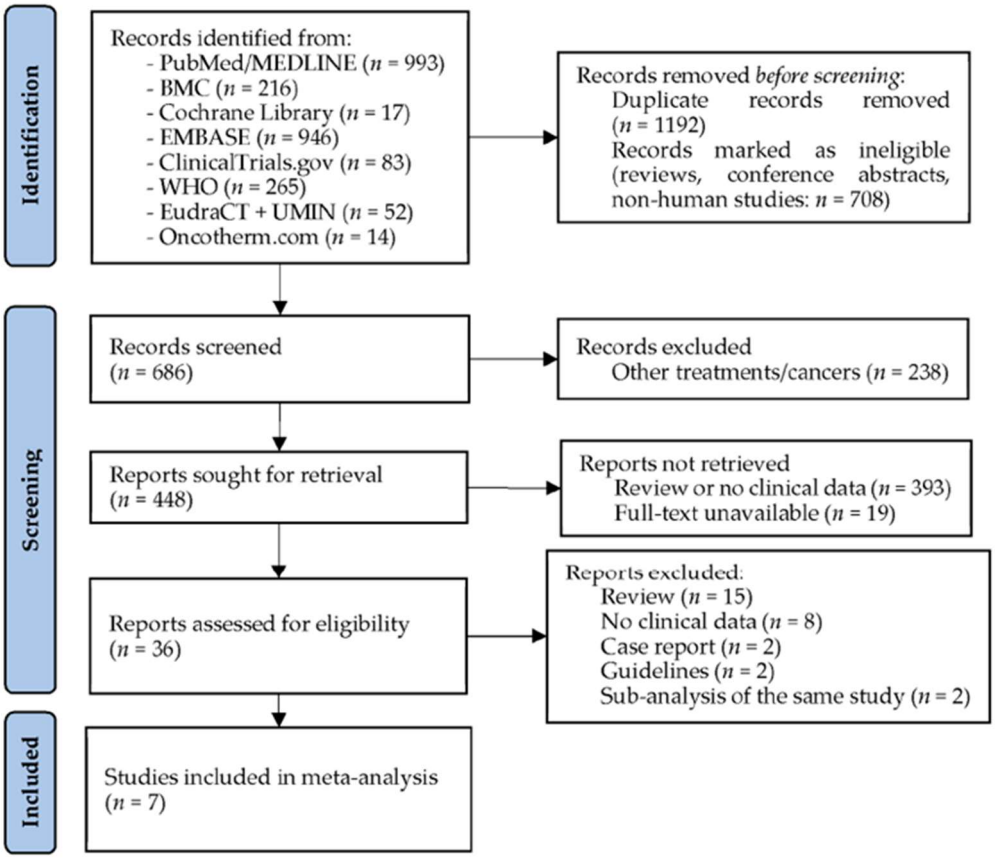

Figure 1. PRISMA flow diagram of studies about modulated electro-hyperthermia. BMC: BioMed Central; EMBASE: Excerpta Medica Database; EudraCT: European Union Drug Regulating Authorities Clinical Trials Database; MEDLINE: Medical Literature Analysis and Retrieval System Online; WHO: World Health Organization's International Clinical Trials Registry Platform; UMIN: University hospital Medical Information Network Clinical Trials Registry (for Japan).

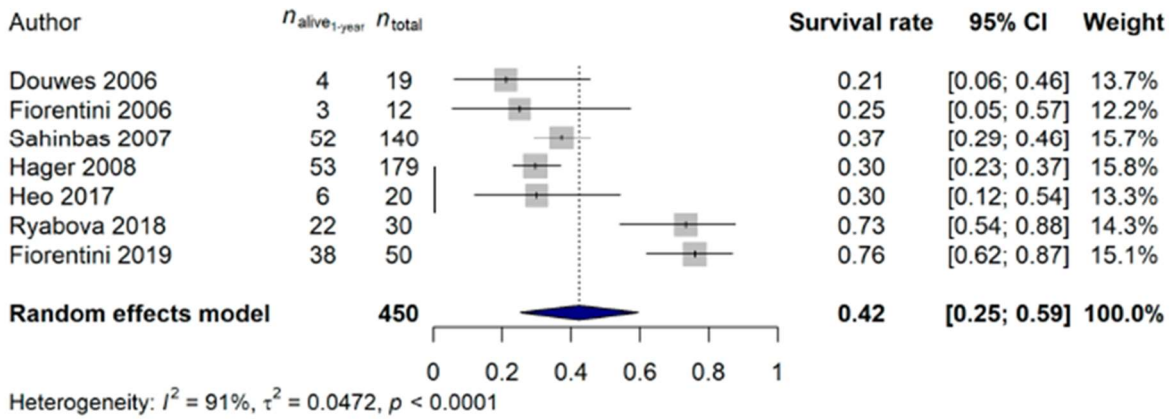

Figure 2. Effect of modulated electro-hyperthermia on 1-year glioblastoma survival rate [43,46–51].

Further analysis was performed to elucidate the confounding effects behind high heterogeneity. In total, 72.26% of the difference in the true effect sizes could be explained by the publication year (p = 0.0008). Comparing the studies published before and after 2008, it was found that in early studies the 1-year survival rate was 31.22% (95% CI: 24.81–37.62%), while in the ones after 2008 it was 60.63% (95% CI: 32.21–89.05%; p = 0.0478; Figure 3). Recurrent glioblastomas had a 37.33% (95% CI: 20.68–53.97%) and a 53.74% (95% CI: 8.69–98.80%) 1-year survival rate for all and for the studies conducted after 2008, respectively, while the single study investigating the effect of mEHT in newly diagnosed tumors [51] reported a 73.33% (95% CI: 57.51–89.16%; vs. all studies: p = 0.0021; vs. studies after 2008: p = 0.4214) 1-year survival rate. Three studies [43,45,47] investigated whether patients under or over 50 years of age have better 1-year survival rate, and

no difference between these patients could be verified (p = 0.1129). No difference was found when the type of study (prospective vs. retrospective; p = 0.3552), the type of device used during the study (p = 0.4273) or the median age of patients (p = 0.6778) was compared.

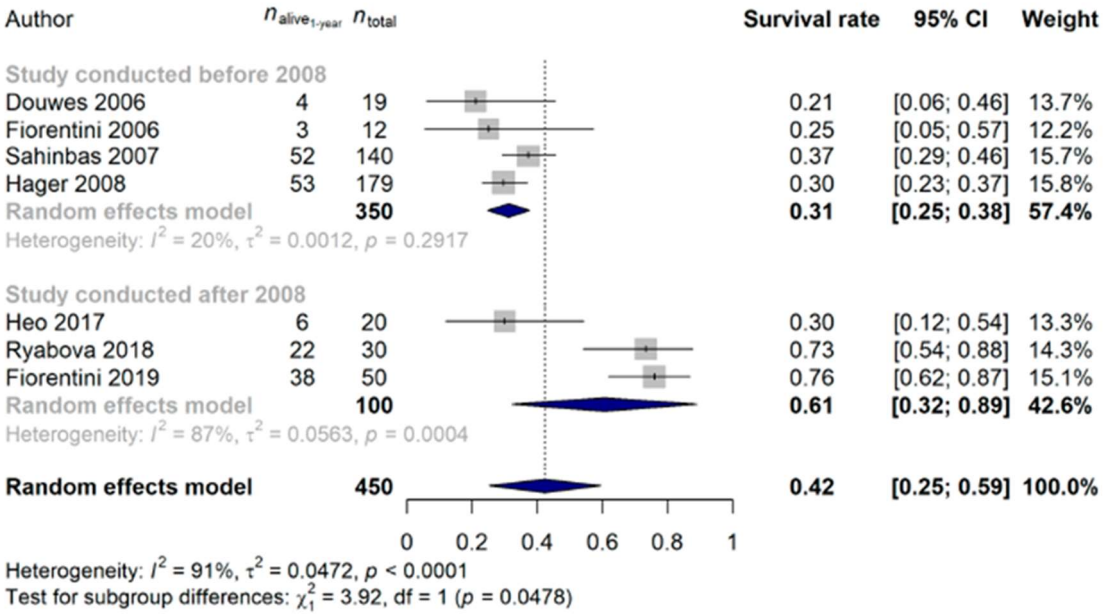

Figure 3. Effect of modulated electro-hyperthermia on 1-year glioblastoma survival rate, grouped by studies published before and after 2008 [43,46–51].

3.2. Studies Investigating Tumor Treating Flields in Glioblastoma

The electronic database searches for studies about TTF in glioblastoma patients resulted in a total of 6036 publications. After the removal of duplicates, non-human studies including animal and cellular research reports, reviews and meeting/conference abstracts, 323 articles remained for title and abstract screening. Then, 278 articles were excluded because they either reported results from other tumors, presented results from an animal and/or cellular experiment, were unavailable or had different study interests than the current meta-analysis (e.g., health-economy). Of the remaining 45 studies considered for full text assessment, 18 further studies were removed because they did not include the target variable of this meta-analysis. Two, five and nine articles reported results about the SPARE [52,53], EF-11 [15,16,54–56] and EF-14 [17–19,57–62] studies, of which only one–one was used for the meta-analysis, resulting in a total of 14 available studies to be included in the analyses (Figure 4).

Details of the fourteen TTF studies [15,21,22,26,53,57,63–70] selected for analysis can be read in Table 2. It has to be noted that the EF-11 study results were gathered from the updated post hoc analysis of Kanner et al. [15] instead of from the original [54], because none of those patients who did not finish at least one cycle of therapy were removed from the original publication, causing a significant change in true survival results. A comparison of TTF treatment to a control group was present in five of eleven studies [15,21,57,69,70].

Table 2. Details of the selected studies investigating the effect of Tumor Treating Fields (TTF) in glioblastoma.

Author (Year)	Type of Study	Cases (*n*)	Controls (*n*)	Additional Therapy	Age (Median)	Females
Kirson et al. (2007) [26]	Prospective	10	–	temozolomide	– [1]	– [1]
Kirson et al. (2009) [63]	Prospective	10	–	temozolomide	– [1]	– [1]
Kanner et al. (2014) [15]	RCT	93	117	no	54	– [1]
Mrugala et al. (2014) [22]	Prospective	457	–	no restriction on any combination therapies, but not detailed	55	32.4%
Wong et al. (2015) [64]	Retrospective	37	–	bevacizumab with or without 6-thioguanine, lomustine, capecitabine, and celecoxib (TCCC)	57	37.8%
Stupp et al. (2017) [57]	RCT	466	229	temozolomide	56	32.2%
Lu et al. (2019) [65]	Retrospective	48	–	temozolomide + bevacizumab + irinotecan or bevacizumab-based chemo regimen	55	33.3%
Bokstein et al. (2020) [66]	Prospective	10	–	temozolomide + irradiation	60	20%
Korshoej et al. (2020) [67]	Prospective	11	–	chemotherapy after skull remodeling surgery	57	18.2%
Lazaridis et al. (2020) [68]	Retrospective	16	–	lomustine + temozolomide	50	43.8%
Liu et al. (2020) [69]	Retrospective	37	67	temozolomide + irradiation	61	37.8%
Dono et al. (2021) [70]	Retrospective	29	120	temozolomide + irradiation	58	34.5%
Miller et al. (2022) [53]	Prospective	30	–	temozolomide + irradiation	58	33.3%
Pandey et al. (2022) [21]	Retrospective	55	57	temozolomide	59	30.9%

[1] Not detailed in the original article. RCT: randomized clinical trial.

The total number of patients investigating the effect of TTF in glioblastoma was 1309, of which 536 patients (40.9%) died during the first year after study inclusion. A 66.65% pooled 1-year survival rate (95% CI: 52.65–80.65%) was observed for the total cohort receiving TTF, regardless of other clinical parameters. Similar to that of the mEHT results, high heterogeneity [96.5% (95% CI: 95.3–97.4%)] and no publication bias (p = 0.6652) was found for the TTF study results. The analysis to identify possible confounding effects revealed 1-year survival rates of 49.01% (95% CI: 1.75–96.27%), 66.29% (95% CI: 48.31–84.27%) and 73.11% (95% CI: 48.89–97.34%) in RCTs, prospective and retrospective studies (p = 0.6680), respectively. The effect of when TTF was introduced during the glioblastoma treatment was also investigated: a significantly better 1-year survival rate was found in those patients with a newly diagnosed tumor [82.61% (95% CI: 73.20–92.02%)], compared with those with recurrent tumors [51.74% (95% CI: 30.84–72.64%); p = 0.0083; Figure 5].

We were also able to compare the survival rates of 2 and 3 years for eleven and eight studies, respectively: 38.87% (95% CI: 21.73–56.01%) and 34.19% (95% CI: 13.33–55.04%) survival rates were estimated. Neither the year of publication (p = 0.9755), the median age (p = 0.2682) nor the study type (p = 0.7085) affected the 2-year survival rates, but the same difference between recurrent and newly diagnosed glioblastoma was observable (newly diagnosed glioblastoma: 59.79%, 95% CI: 34.40–85.17%; recurrent glioblastoma: 20.18%, 95% CI: 8.18–32.18%; p = 0.0057; Figure 6) as described for the 1-year survival rates above. When investigating the 3-year survival rates, patients with newly diagnosed tumors [47.24% (95% CI: 18.31–76.16%)] benefited significantly more from the TTF treatment than those who received TTF for recurrent glioblastoma [11.00% (95% CI: 4.75–17.26%); p = 0.0164; Figure 7]. No difference in 3-year survival rates could be justified for the different study types (p = 0.2075), years of publication (p = 0.4123) or median ages of patients (p = 0.0935).

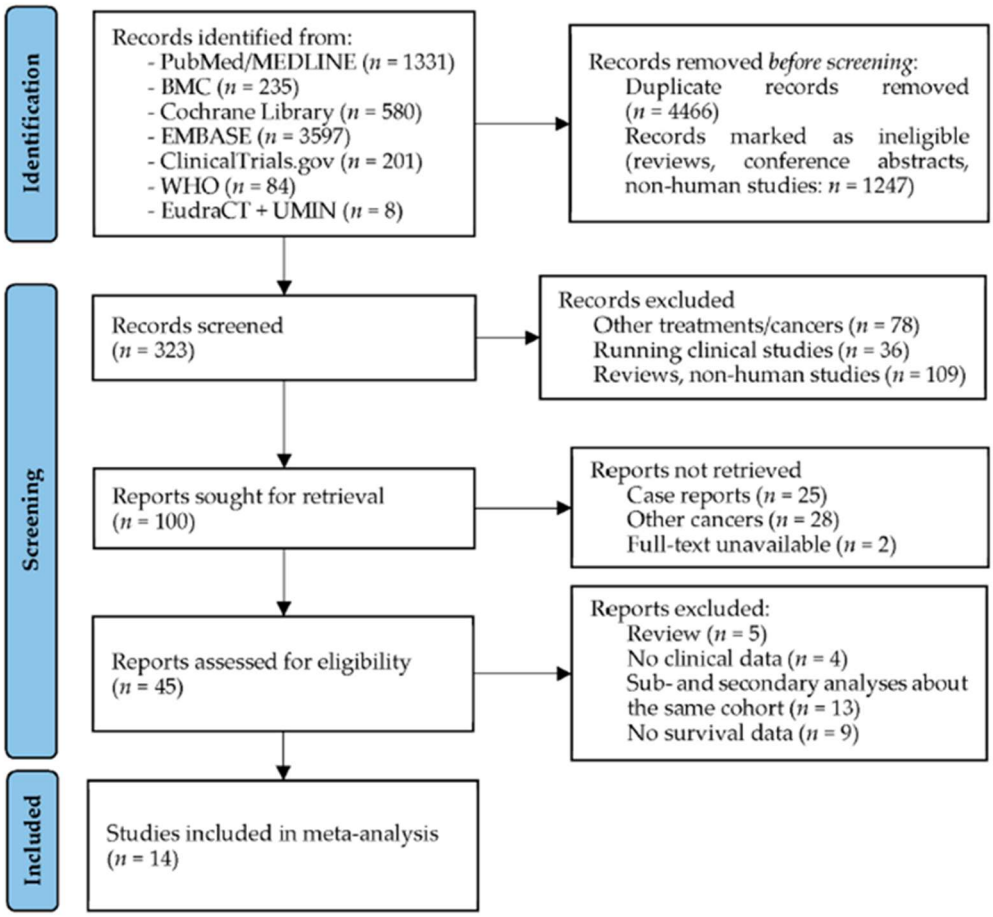

Figure 4. PRISMA flow diagram of studies about Tumor Treating Fields. BMC: BioMed Central; EMBASE: Excerpta Medica Database; EudraCT: European Union Drug Regulating Authorities Clinical Trials Database; MEDLINE: Medical Literature Analysis and Retrieval System Online; WHO: World Health Organization's International Clinical Trials Registry Platform; UMIN: University hospital Medical Information Network Clinical Trials Registry (for Japan).

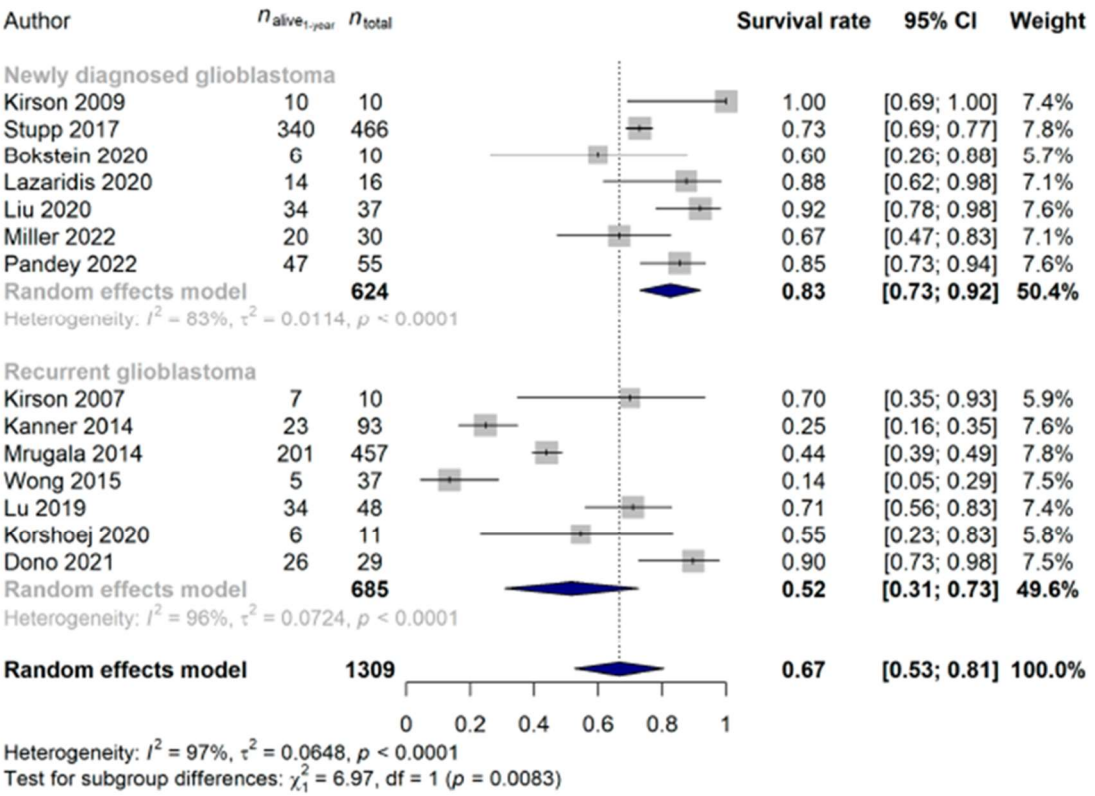

Figure 5. Significantly better 1-ear survival rates were found when Tumor Treating Fields treatment was introduced at an earlier stage of treatment (p = 0.0083) [15,21,22,26,53,57,63–70].

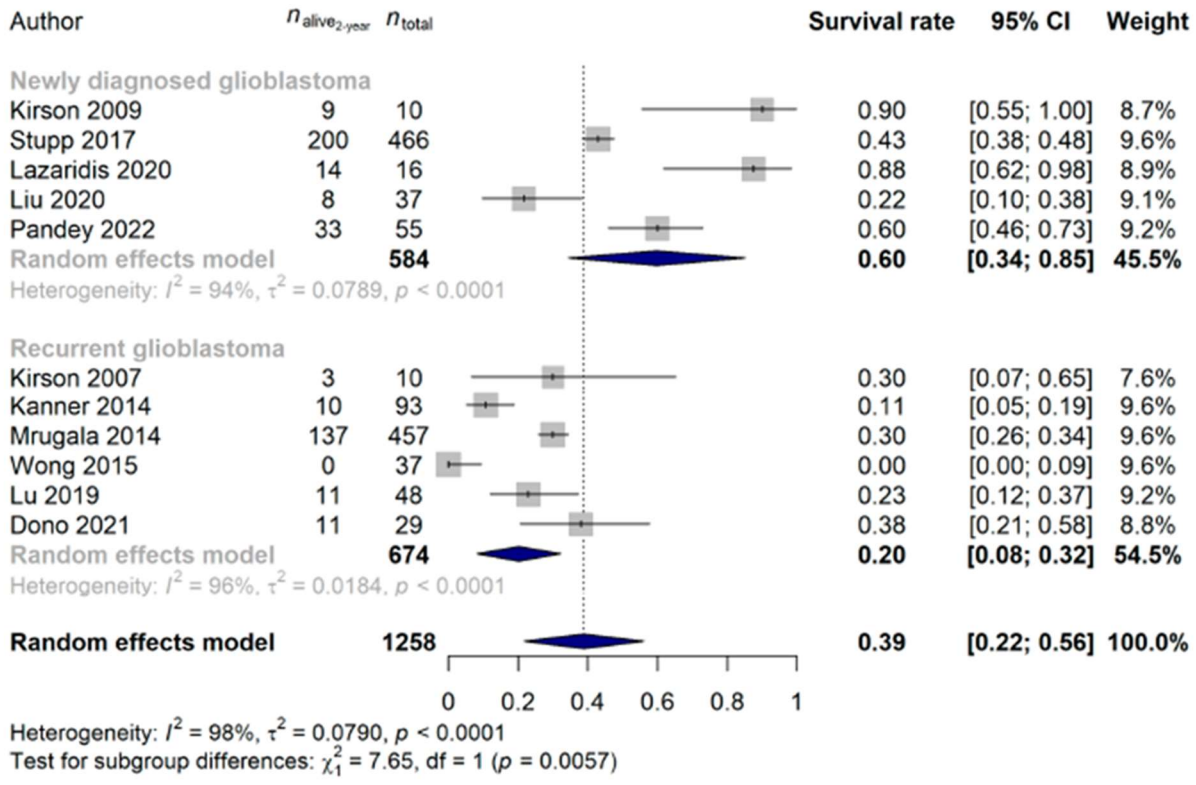

Figure 6. Significantly better 2-year survival rates were found when the Tumor Treating Fields treatment was introduced at an earlier stage of treatment (p = 0.0057) [15,21,22,26,57,63–65,68–70].

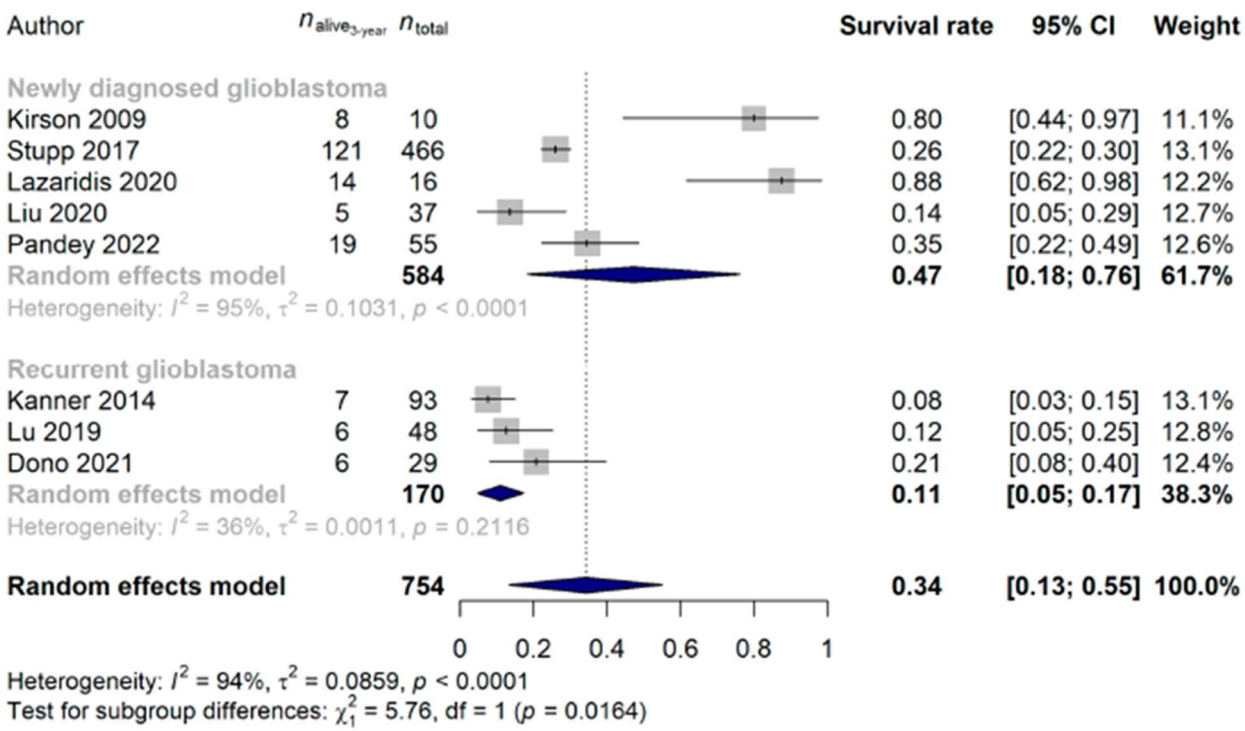

Figure 7. Significantly better 3-year survival rates were found when the Tumor Treating Fields treatment was introduced at an earlier stage of treatment (p = 0.0164) [15,21,57,63,65,68–70].

Only a limited number of the available studies (n = 5) investigated the effect of TTF over a control cohort. It was found that patients on the TTF-treatment arm had significantly better 1-year [risk ratio (RR): 0.6481, 95% CI: 0.4345–0.9668; p = 0.0335; Figure 8A] and 3-year (RR: 0.9215, 95% CI: 0.8819–0.9628; p = 0.0003; Figure 8C) survival rates. However, no difference could be observed in the 2-year survival rates of the patients treated with or without TTF (RR: 0.9032, 95% CI: 0.7713–1.0576; p = 0.2062; Figure 8B).

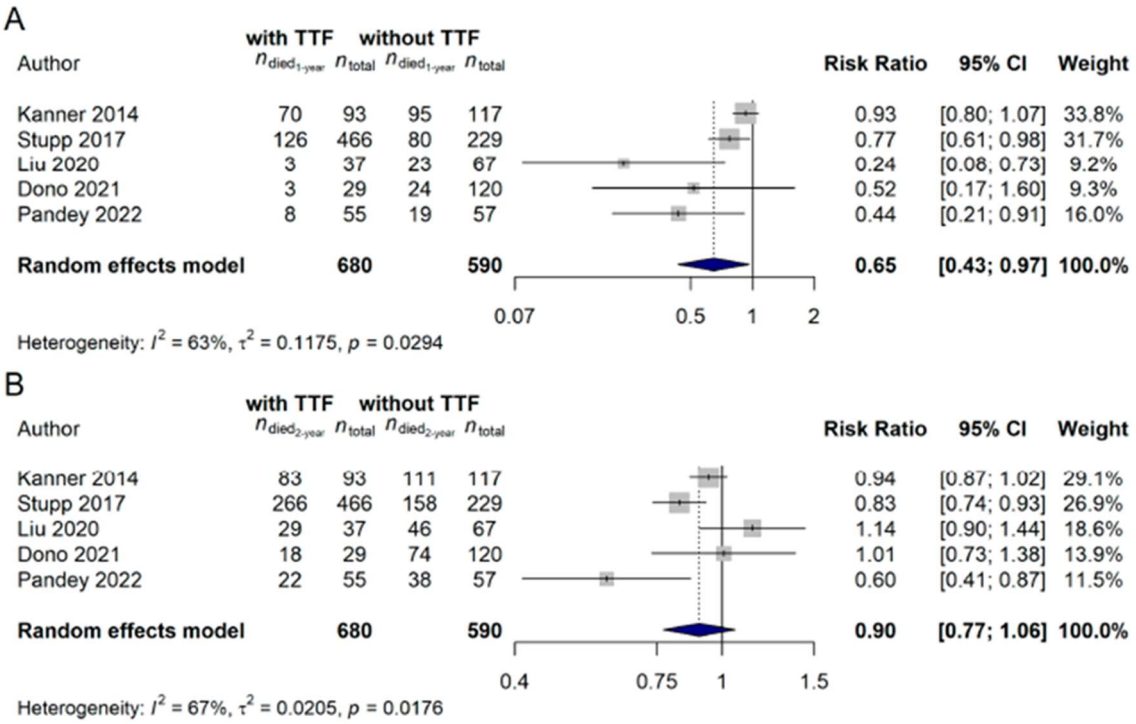

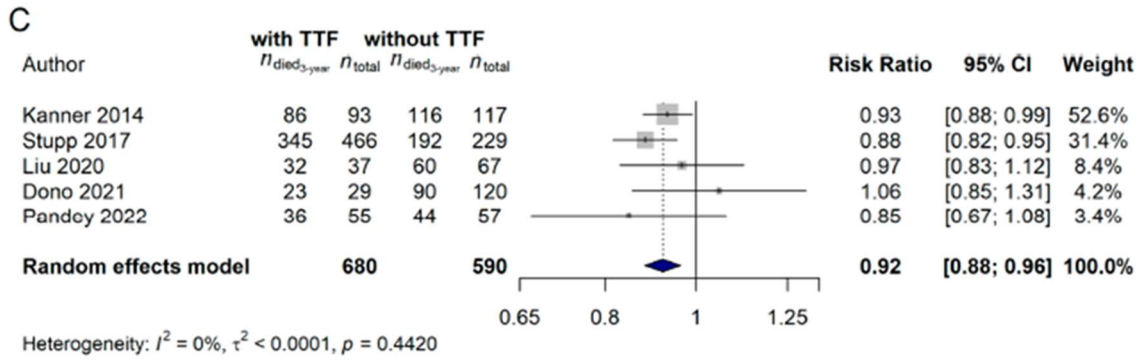

Figure 8. Glioblastoma patients treated with Tumor Treating Fields (TTF) has significantly better (A) 1-year (p=0.0335) and (C) 3-year (p=0.0003) survival rates, while no difference in the (B) 2-year survival rates could be justified (p = 0.2062) compared with those who did not receive TTF during their treatment [15,21,57,69,70].

3.3. The Direct Comparison of Modulated Electro-Hyperthermia and Tumor Treating Fields Studies

We also examined whether there was a difference in the 1-year survival of the patients by directly comparing the mEHT and TTF techniques. It has to be highlighted though that while the majority of the TTF studies were conducted in the last decade, half of the mEHT studies were done prior the general acceptance and use of the Stupp protocol [10,71]. Due to the former and to the fact that glioblastoma survival has significantly improved over the last decade [72], we compared those mEHT studies only with TTF that were performed after 2008. The 1-year survival rate of the 100 and 1289 glioblastoma patients treated with mEHT and TTF was 60.63% (95% CI: 32.21–89.05%) and 63.56% (95% CI: 48.50–78.62%; p = 0.8583), respectively. The same results were obtained if the two devices were compared in newly diagnosed glioblastoma (mEHT: 73.33%, 95% CI: 57.51–89.16%; TTF: 79.81%, 95% CI: 70.97–88.65%; p = 0.4836; Figure 9) and in recurrent glioblastoma (mEHT: 53.74%, 95% CI: 8.69–98.80%; TTF: 49.24%, 95% CI: 25.90–72.57%; p = 0.8618; Figure 10).

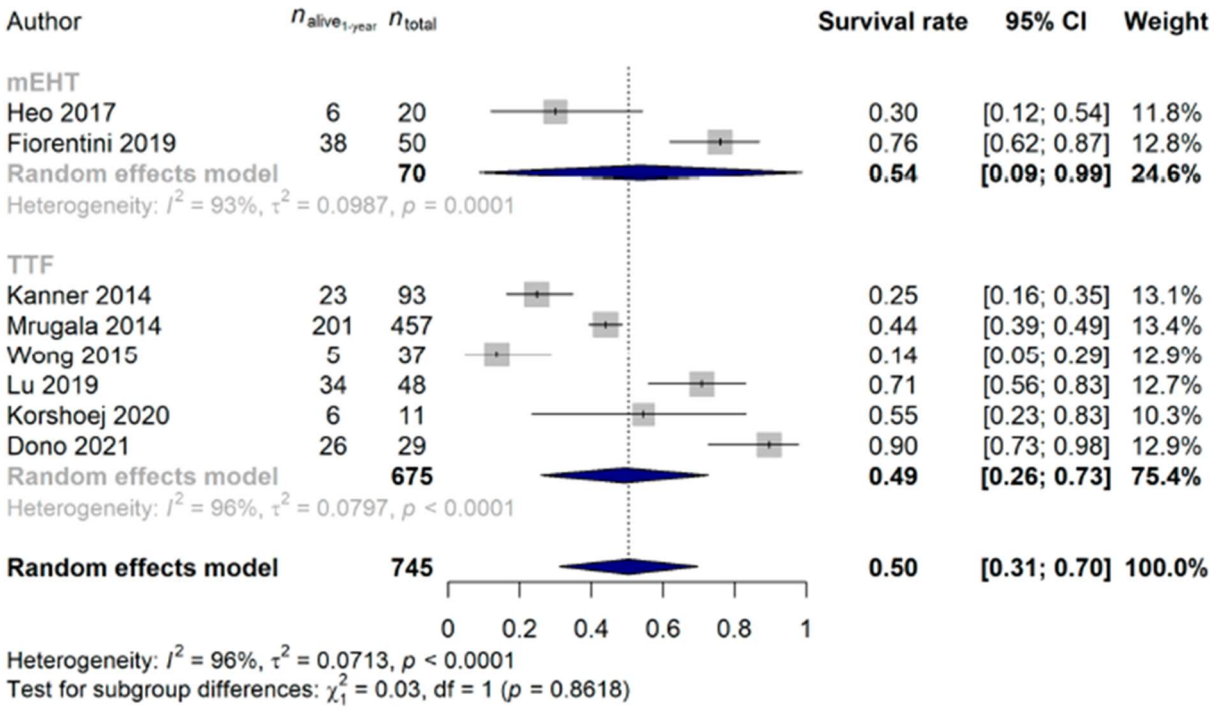

Figure 9. In newly diagnosed glioblastoma, the non-inferiority (p = 0.4836) of modulated electro-hyperthermia (mEHT) could be observed compared with the more widely applied Tumor Treating Fields (TTF). It has to be noted that due to the wider acceptance of the Stupp protocol [10,71] and that patient survival significantly improved in the last decade [72], only the comparison of studies conducted after 2010 were compared [15,22,46,50,64,65,67,70].

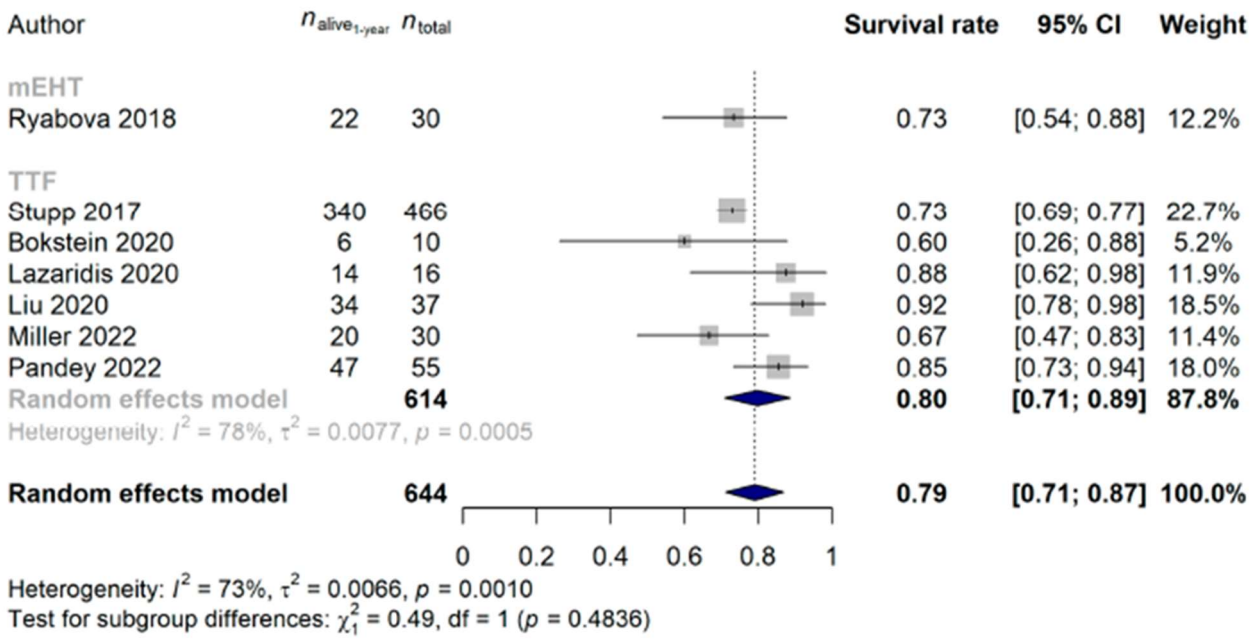

Figure 10. In recurrent glioblastoma, the non-inferiority (p = 0.8618) of modulated electro- hyperthermia (mEHT) could be observed compared with the more widely applied Tumor Treating Fields (TTF). It has to be noted that due to the wider acceptance of the Stupp protocol [10,71] and that patient survival significantly improved in the last decade [72], only the comparison of studies conducted after 2010 were compared [21,51,53,57,66,68,69].

4. Discussion

Glioblastoma is a highly aggressive tumor with a 5-year survival rate of 1–5% [73]. Its standard treatment includes surgery (if feasible) and radiation therapy with concomitant/ adjuvant chemotherapy: procarbazine, lomustine and vincristine (PCV) and temozolomide in the early and late stages, respectively [9,10,74]. Lately, the importance of molecular markers has also emerged [75], e.g., one of the bases of the latest WHO classification of gliomas is the IDH mutation [6]. Additionally, in the last decade an emerging number of reports came to light that the addition of non-invasive, device-based concomitant therapies, mEHT or TTF, might further increase therapy response. Moreover, several studies reported that even if no large differences in patient survivals could be justified, the quality of life of patients was much higher compared with those without the additional treatment options [27,34,76].

A less than 20% 1-year survival rate was reported approximately twenty years ago [77], which has almost doubled today [13,15], moreover, some studies achieved 1-year survival rates over 80% [11], but still, only modest median overall survivals can be achieved [13,15]. If concomitant mEHT or TTF was added to the treatment plan, an average 42% and 64% 1-year survival rate could be achieved, respectively. Similar to the trend reported in the meta-analysis of Poon et al. [72], we observed that the 1-year survival rate significantly improved in those mEHT studies, which were conducted later, than 2008. Taking into account this observation, the adjusted 1-year survival rates were 61% and 67% for the mEHT and TTF studies, respectively, both of which are significantly greater compared with those observed in patients treated without the devices [12]. Survival rates for longer intervals were only available for the TTF studies, and a 39% 2-year and a 34% 3-year survival rate was found. For comparison, by treating glioblastoma patients with either the standard (60 Gy irradiation + 6 cycles of temozolomide) or the extended (temozolomide cycles > 6) Stupp protocol, the reported 2-year and 3-year survival rates are lower [12,71,78], but the opposite was also reported in another study [11].

As a somewhat expected result, further findings of the current meta-analysis included that newly diagnosed glioblastoma patients can benefit more from the early use of TTF: a 83% vs. 52% 1-year survival rate was found for the newly diagnosed and recurrent glioblastoma patients, respectively, although some authors assumed the exact opposite [69]. Similar results could be obtained in the case of mEHT (73% vs. 54%), however, only one study investigated the effect of mEHT in newly diagnosed glioblastoma patients [51], which immediately raises the need for additional studies investigating the effect of mEHT in this setting.

A few studies also investigated whether the use of either of the two devices has a significant advantage compared with conventional treatment. While in the case of TTF we managed to identify five studies that compared patients treated with and without TTF, only one mEHT study made a similar comparison. It has to be noted that the Fiorentini study [46] tested the palliative use of mEHT vs. other palliative options only. For TTF, we found significantly reduced 1- and 3-year mortality rates in the treated with TTF groups, compared with those without TTF. For mEHT, Fiorentini et al. [46] have described significantly longer overall survival times in the mEHT-treated group.

By examining the details of the available clinical trial results, the following can be further confirmed about the two devices. With the introduction of mEHT in the treatment plan, several studies could report improved responses to the treatment [23,44–48], a better quality of life [44,46], increased functional activity of patients measured by the Karnofsky Performance Score scale [51] and complete and/or partial response could be maintained in some cases for longer periods of time as well [45–49,51]. It has to be noted, however, the result on age response is controversial: Fiorentini et al. [46] found no difference between the survival of patients over or under the age of 50 years, while Roussakow [44] and Sahinbas et al. [43] have found the opposite. In this study, we could not justify difference between the younger and older cohorts. Furthermore, in the Phase I study of Wismeth et al. [23] it has been reported that at least three mEHT treatments per week are required for an effective response. As with other treatments options, a few complications of mEHT have been confirmed. Basically, all of the mEHT studies reported only grade I and II side effects: headaches, skin redness and/or mild burning at the treatment site, nausea and vomiting, dizziness, neurological symptoms (aphasia, seizures) and grade I/II anemia and/or leukopenia and/or thrombocytopenia [23,43–48,50,51].

Most results about TTF are known from the EF-11 [15,16,54–56] and EF-14 [17–19,57–62] randomized trials. The first study has investigated 120 chemotherapy-free, only TTFtreated and 117 control patients receiving active chemotherapy, and it could report a marginal difference in survival only [54]. However, by further analyzing the study results [15]—by excluding patients who did not finish at least a single cycle of therapy—the therapeutic advantage of TTF over patient survival became verifiable. In contrast, the concomitant effect of TTF over chemotherapy (first-line: temozolomide) was investigated in the EF-14 study; 466 and 229 patients were treated with and without TTF, respectively [57]. Similar to that of the results of the mEHT studies, a more durable complete and/or partial response to therapy and/or stable disease was more common in the TTF-treated groups [16,26,54,55,62], and TTF-treated patients had a better overall and progression-free survival [18,19,21,22,26,54,57–59,62–64,67,68,70] and stable or improved quality of life status (except for itchy skin [19,60,61,79]) [19,53,54,60,61]. A better compliance to the treatment can improve treatment and prolong survival time [15–22], TTF plus chemotherapy was superior in all age groups compared with chemotherapy alone [19,57], TTF alone is superior to bevacizumab-only chemotherapy [16] and its efficacy might be further improved if 6-thioguanine, lomustine, capecitabine and celecoxib (TCCC) is in combination with bevacizumab [64]. A higher local minimum filed intensity, power density and dose density of the TTF-device is associated with better overall and progression-free survival [17], moreover, no difference has been reported in the cognitive status changes between patients treated with or without TTF [60]. In addition to the EF-11 and EF-14 study result findings, it has been reported that patients with PTEN (phosphatase and tensin homolog) mutations have longer survival compared with those with wild type PTEN (22 months vs. 12 months) [70]. TTF after skull remodeling surgery is safe and a positive correlation between field enhancements and burr hole sizes with a plateau at 15–20 cm^2 has been described [67]. A triple-drug regimen of temozolomide, bevacizumab and irinotecan with TTF is superior to other bevacizumab-based chemotherapies with TTF [65]. Scalp sparing radiation with concurrent temozolomide and TTF is well tolerated by patients, furthermore, a better response for glioblastoma patients with methylated O^6 -methylguanine DNA methyltransferase (MGMT) promoter has been observed [52,53,80]. In contrast, IDH1 and/or IDH2 mutation status has not affected the survival of patients [80]. Mutations in the phosphatidylinositol-4,5-bisphosphate 3-kinase catalytic subunit alpha and epidermal growth factor receptor genes were associated with a decreased or no response to TTF, while the mutated neurofibromatosis type 1 gene has been associated with better overall and progression-free survival, and the tumor protein p53 gene mutations have had no effect on any outcome upon TTF therapy [21]. The following common side effects of TTF have been observed: mild to moderate contact dermatitis (“medical device site reaction beneath the transducer arrays”), headache, fatigue, convulsion or seizure, confusion, mental status changes, mild anemia and/or lymphopenia and/or thrombocytopenia, diarrhea or constipation and neurological decompensation [19,22,26,52–54,57–59,62–67,79]. Further results are expected after the completion of the following TTF clinical trials: NCT05310448, NCT04223999, NCT03642080, NCT04469075, NCT04474353, NCT03477110, NCT04689087, NCT04471844, NCT04397679, NCT04671459, NCT04421378, NCT04492163, ChiCTR2100047049, ChiCTR2100041969, JPRN-UMIN000041745 and ISRCTN14267833.

To our knowledge, this is the first study that systematically reviewed the current knowledge about mEHT in glioblastoma and compared mEHT and TTF directly. In relation to TTF, several reviews and a few meta-analyses have already been published, which in certain aspects are much more detailed than the present work, including but not limited to [27,81–85]. In the meta-analysis of Regev et al. [81], the pooled 1-, 2- and 3-year survival rates were 73%, 45% and 29%, respectively, which are comparable to the ones calculated in the current analysis (67%, 39% and 34%). Similarly, the pooled 1-year survival rate of 47.3% reported by Li et al. [82] for recurrent glioblastoma is not different from the 52% we observed.

Strength and Limitations of the Study

To the best of our knowledge, we are the first to analyze mEHT and TTF study results in a single meta-analysis. However, a few limitations of this analysis should be mentioned, including that only a limited number of trials could be investigated and most of them were non-randomized trials. Although the number of studies analyzed in the meta-analysis could have been slightly increased if median overall/progression-free survivals were used instead of the x-year survival rate, their calculation would have given inaccurate results [86]. Heterogeneity of the included studies was high, which might have also introduced some bias. Another limitation of the current study was that the number of available studies investigating mEHT and TTF were significantly different, which is due to the fact that, up to now, the number of centers adopting mEHT is very limited around the world, as opposed to TTF. This ultimately might have affected the calculated pooled effect sizes.

5. Conclusions

In conclusion, this study investigated the beneficial effects of (concomitant) mEHT and TTF over conventional chemoradiotherapy in glioblastoma. It was found that both mEHT and TTF could significantly increase the survival of glioblastoma patients and the same survival rates can be achieved using both devices in the cohorts of newly diagnosed and recurrent glioblastomas. It has to be emphasized, however, that the small number of centers using mEHT largely limits its application, and there is no data about the combined use of the two devices, therefore, further studies are recommended.

Author Contributions:

Conceptualization, A.M.S., E.E.A.A., G.F., M.H., Z.H., D.S. and M.D.; methodology, A.M.S. and Z.H.; formal analysis, Z.H.; investigation, A.M.S. and Z.H.; resources, A.M.S., D.S. and M.D.; data curation, A.M.S. and Z.H.; writing—original draft preparation, A.M.S. and Z.H.; writing—review and editing, A.M.S., E.E.A.A., G.F., M.H., Z.H., D.S. and M.D.; visualization, M.H. and Z.H.; supervision, A.M.S., E.E.A.A., G.F. and M.D.; project administration, A.M.S. and M.D. All authors have read and agreed to the published version of the manuscript.

Funding: This research received no external funding.

Conflicts of Interest: The authors declare no conflict of interest.

References

1. Sung, H.; Ferlay, J.; Siegel, R.L.; Laversanne, M.; Soerjomataram, I.; Jemal, A.; Bray, F. Global Cancer Statistics 2020: GLOBOCAN Estimates of Incidence and Mortality Worldwide for 36 Cancers in 185 Countries. CA Cancer J. Clin. 2021, 71, 209–249. [CrossRef] [PubMed]
2. Ferlay, J.; Ervik, M.; Lam, F.; Colombet, M.; Mery, L.; Piñeros, M.; Znaor, A.; Soerjomataram, I.; Bray, F. Global Cancer Observatory: Cancer Today. Available online: https://gco.iarc.fr/today (accessed on 22 October 2022).
3. Ostrom, Q.T.; Cioffi, G.; Gittleman, H.; Patil, N.; Waite, K.; Kruchko, C.; Barnholtz-Sloan, J.S. CBTRUS Statistical Report: Primary Brain and Other Central Nervous System Tumors Diagnosed in the United States in 2012–2016. Neuro Oncol. 2019, 21, v1–v100. [CrossRef] [PubMed]
4. Louis, D.N.; Perry, A.; Reifenberger, G.; von Deimling, A.; Figarella-Branger, D.; Cavenee, W.K.; Ohgaki, H.; Wiestler, O.D.; Kleihues, P.; Ellison, D.W. The 2016 World Health Organization Classification of Tumors of the Central Nervous System: A summary. Acta Neuropathol. 2016, 131, 803–820. [CrossRef] [PubMed]
5. Louis, D.N.; Perry, A.; Wesseling, P.; Brat, D.J.; Cree, I.A.; Figarella-Branger, D.; Hawkins, C.; Ng, H.K.; Pfister, S.M.; Reifenberger, G.; et al. The 2021 WHO Classification of Tumors of the Central Nervous System: A summary. Neuro Oncol. 2021, 23, 1231–1251. [CrossRef] [PubMed]
6. Berger, T.R.;Wen, P.Y.; Lang-Orsini, M.; Chukwueke, U.N.World Health Organization 2021 Classification of Central Nervous System Tumors and Implications for Therapy for Adult-Type Gliomas: A Review. JAMA Oncol. 2022, 8, 1493–1501. [CrossRef]

7. Hanif, F.; Muzaffar, K.; Perveen, K.; Malhi, S.M.; Simjee Sh, U. Glioblastoma Multiforme: A Review of its Epidemiology and Pathogenesis through Clinical Presentation and Treatment. Asian Pac. J. Cancer Prev. 2017, 18, 3–9. [CrossRef]
8. Jemal, A.; Siegel, R.; Xu, J.;Ward, E. Cancer statistics, 2010. CA Cancer J. Clin. 2010, 60, 277–300. [CrossRef]
9. Mohile, N.A.; Messersmith, H.; Gatson, N.T.; Hottinger, A.F.; Lassman, A.; Morton, J.; Ney, D.; Nghiemphu, P.L.; Olar, A.; Olson, J.; et al. Therapy for Diffuse Astrocytic and Oligodendroglial Tumors in Adults: ASCO-SNO Guideline. J. Clin. Oncol. 2022, 40, 403–426. [CrossRef]
10. Stupp, R.; Mason,W.P.; van den Bent, M.J.;Weller, M.; Fisher, B.; Taphoorn, M.J.; Belanger, K.; Brandes, A.A.; Marosi, C.; Bogdahn, U.; et al. European Organisation for Research and Treatment of Cancer Brain Tumor and Radiotherapy Groups; National Cancer Institute of Canada Clinical Trials Group. Radiotherapy plus concomitant and adjuvant temozolomide for glioblastoma. N. Engl. J. Med. 2005, 352, 987–996. [CrossRef]
11. Herrlinger, U.; Tzaridis, T.; Mack, F.; Steinbach, J.P.; Schlegel, U.; Sabel, M.; Hau, P.; Kortmann, R.D.; Krex, D.; Grauer, O.; et al. Lomustine-temozolomide combination therapy versus standard temozolomide therapy in patients with newly diagnosed glioblastoma with methylatedMGMT promoter (CeTeG/NOA-09): A randomised, open-label, phase 3 trial. Lancet 2019, 393, 678–688. [CrossRef]
12. Delgado-Lopez, P.D.; Corrales-Garcia, E.M. Survival in glioblastoma: A review on the impact of treatment modalities. Clin. Transl. Oncol. 2016, 18, 1062–1071. [CrossRef] [PubMed]
13. Taylor, O.G.; Brzozowski, J.S.; Skelding, K.A. Glioblastoma Multiforme: An Overview of Emerging Therapeutic Targets. Front. Oncol. 2019, 9, 963. [CrossRef] [PubMed]
14. Mahmoudi, K.; Bouras, A.; Bozec, D.; Ivkov, R.; Hadjipanayis, C. Magnetic hyperthermia therapy for the treatment of glioblastoma: A review of the therapy's history, efficacy and application in humans. Int. J. Hyperth. 2018, 34, 1316–1328. [CrossRef]
15. Kanner, A.A.;Wong, E.T.; Villano, J.L.; Ram, Z.; on behalf of EF-11 Investigators. Post Hoc analyses of intention-to-treat population in phase III comparison of NovoTTF-100A system versus best physician's choice chemotherapy. Semin. Oncol. 2014, 41 (Suppl. S6), S25–S34. [CrossRef]
16. Vymazal, J.;Wong, E.T. Response patterns of recurrent glioblastomas treated with tumor-treating fields. Semin. Oncol. 2014, 41 (Suppl. S6), S14–S24. [CrossRef]
17. Ballo, M.T.; Urman, N.; Lavy-Shahaf, G.; Grewal, J.; Bomzon, Z.; Toms, S. Correlation of Tumor Treating Fields Dosimetry to Survival Outcomes in Newly Diagnosed Glioblastoma: A Large-Scale Numerical Simulation-Based Analysis of Data from the Phase 3 EF-14 Randomized Trial. Int. J. Radiat Oncol. Biol. Phys. 2019, 104, 1106–1113. [CrossRef]
18. Toms, S.A.; Kim, C.Y.; Nicholas, G.; Ram, Z. Increased compliance with tumor treating fields therapy is prognostic for improved survival in the treatment of glioblastoma: A subgroup analysis of the EF-14 phase III trial. J. NeuroOncol. 2019, 141, 467–473. [CrossRef]
19. Ram, Z.; Kim, C.Y.; Hottinger, A.F.; Idbaih, A.; Nicholas, G.; Zhu, J.J. Efficacy and Safety of Tumor Treating Fields (TTFields) in Elderly Patients with Newly Diagnosed Glioblastoma: Subgroup Analysis of the Phase 3 EF-14 Clinical Trial. Front. Oncol. 2021, 11, 671972. [CrossRef] [PubMed]
20. Onken, J.; Staub-Bartelt, F.; Vajkoczy, P.; Misch, M. Acceptance and compliance of TTFields treatment among high grade glioma patients. J. NeuroOncol. 2018, 139, 177–184. [CrossRef]
21. Pandey,M.; Xiu, J.;Mittal, S.; Zeng, J.; Saul,M.; Kesari, S.; Azadi, A.; Newton, H.; Deniz, K.; Ladner, K.; et al. Molecular alterations associatedwith improved outcome in patientswith glioblastoma treatedwith Tumor-Treating Fields. NeuroOncol. Adv. 2022, 4, vdac096. [CrossRef]
22. Mrugala, M.M.; Engelhard, H.H.; Dinh Tran, D.; Kew, Y.; Cavaliere, R.; Villano, J.L.; Annenelie Bota, D.; Rudnick, J.; Love Sumrall, A.; Zhu, J.J.; et al. Clinical practice experience with NovoTTF-100A system for glioblastoma: The Patient Registry Dataset (PRiDe). Semin. Oncol. 2014, 41 (Suppl. S6), S4–S13. [CrossRef] [PubMed]
23. Wismeth, C.; Dudel, C.; Pascher, C.; Ramm, P.; Pietsch, T.; Hirschmann, B.; Reinert, C.; Proescholdt,M.; Rummele, P.; Schuierer, G.; et al. Transcranial electro-hyperthermia combined with alkylating chemotherapy in patients with relapsed high-grade gliomas: Phase I clinical results. J. NeuroOncol. 2010, 98, 395–405. [CrossRef] [PubMed]
24. Kirson, E.D.; Gurvich, Z.; Schneiderman, R.; Dekel, E.; Itzhaki, A.; Wasserman, Y.; Schatzberger, R.; Palti, Y. Disruption of cancer cell replication by alternating electric fields. Cancer Res. 2004, 64, 3288–3295. [CrossRef] [PubMed]
25. Blatt, R.; Davidi, S.; Munster, M.; Shteingauz, A.; Cahal, S.; Zeidan, A.; Marciano, T.; Bomzon, Z.; Haber, A.; Giladi, M.; et al. In Vivo Safety of Tumor Treating Fields (TTFields) Applied to the Torso. Front. Oncol. 2021, 11, 670809. [CrossRef]
26. Kirson, E.D.; Dbaly, V.; Tovarys, F.; Vymazal, J.; Soustiel, J.F.; Itzhaki, A.; Mordechovich, D.; Steinberg-Shapira, S.; Gurvich, Z.; Schneiderman, R.; et al. Alternating electric fields arrest cell proliferation in animal tumor models and human brain tumors. Proc. Natl. Acad. Sci. USA 2007, 104, 10152–10157. [CrossRef]

27. Rominiyi, O.; Vanderlinden, A.; Clenton, S.J.; Bridgewater, C.; Al-Tamimi, Y.; Collis, S.J. Tumour treating fields therapy for glioblastoma: Current advances and future directions. Br. J. Cancer 2021, 124, 697–709. [CrossRef]
28. Chang, E.; Patel, C.B.; Pohling, C.; Young, C.; Song, J.; Flores, T.A.; Zeng, Y.; Joubert, L.M.; Arami, H.; Natarajan, A.; et al. Tumor treating fields increases membrane permeability in glioblastoma cells. Cell Death Discov. 2018, 4, 113. [CrossRef] [PubMed]
29. Szasz, A.; Szasz, N.; Szasz, O. Oncothermia: Principles and Practices; Springer: Dordrecht, The Netherlands, 2011. [CrossRef]
30. Szasz, O.; Szasz, A. Heating, Efficacy and Dose of Local Hyperthermia. Open J. Biophys. 2016, 6, 10–18. [CrossRef]
31. Krenacs, T.; Meggyeshazi, N.; Forika, G.; Kiss, E.; Hamar, P.; Szekely, T.; Vancsik, T. Modulated Electro-Hyperthermia-Induced Tumor Damage Mechanisms Revealed in Cancer Models. Int. J. Mol. Sci. 2020, 21, 6270. [CrossRef] [PubMed]
32. Alshaibi, H.F.; Al-Shehri, B.; Hassan, B.; Al-Zahrani, R.; Assiss, T. Modulated Electrohyperthermia: A New Hope for Cancer Patients. BioMed. Res. Int. 2020, 2020, 8814878. [CrossRef]
33. Andocs, G.; Rehman, M.U.; Zhao, Q.L.; Tabuchi, Y.; Kanamori, M.; Kondo, T. Comparison of biological effects of modulated electro-hyperthermia and conventional heat treatment in human lymphoma U937 cells. Cell Death Discov. 2016, 2, 16039. [CrossRef] [PubMed]
34. Szasz, A.M.; Minnaar, C.A.; Szentmartoni, G.; Szigeti, G.P.; Dank, M. Review of the Clinical Evidences of Modulated Electro-Hyperthermia (mEHT) Method: An Update for the Practicing Oncologist. Front. Oncol. 2019, 9, 1012. [CrossRef]
35. Page, M.J.; McKenzie, J.E.; Bossuyt, P.M.; Boutron, I.; Hoffmann, T.C.; Mulrow, C.D.; Shamseer, L.; Tetzlaff, J.M.; Akl, E.A.; Brennan, S.E.; et al. The PRISMA 2020 statement: An updated guideline for reporting systematic reviews. BMJ 2021, 372, n71. [CrossRef] [PubMed]
36. Balduzzi, S.; Rucker, G.; Schwarzer, G. How to perform a meta-analysis with R: A practical tutorial. Evid Based Ment Health 2019, 22, 153–160. [CrossRef] [PubMed]
37. Viechtbauer, W. Bias and Efficiency of Meta-Analytic Variance Estimators in the Random-Effects Model. J. Educ. Behav. Stat. 2005, 30, 261–293. [CrossRef]
38. Harrer, M.; Cuijpers, P.; Furukawa, T.A.; Ebert, D.D. Doing Meta-Analysis with R: A Hands-On Guide, 1st ed.; Chapman & Hall/CRC Press: Boca Raton, FL, USA; London, UK, 2021.
39. Higgins, J.P.; Thompson, S.G. Quantifying heterogeneity in a meta-analysis. Stat. Med. 2002, 21, 1539–1558. [CrossRef]
40. Egger, M.; Smith, G.D.; Schneider, M.; Minder, C. Bias in meta-analysis detected by a simple, graphical test. BMJ 1997, 315, 629–634. [CrossRef]
41. Mantel, N.; Haenszel, W. Statistical aspects of the analysis of data from retrospective studies of disease. J. Natl. Cancer Inst. 1959, 22, 719–748.
42. Robins, J.; Greenland, S.; Breslow, N.E. A general estimator for the variance of the Mantel-Haenszel odds ratio. Am. J. Epidemiol. 1986, 124, 719–723. [CrossRef]
43. Sahinbas, H.; Grönemeyer, D.H.W.; Böcher, E.; Szasz, A. Retrospective clinical study of adjuvant electro-hyperthermia treatment for advanced brain-gliomas. Dtsch. Z. Für Onkol. 2007, 39, 154–160. [CrossRef]
44. Roussakow, S.V. Clinical and economic evaluation of modulated electrohyperthermia concurrent to dose-dense temozolomide 21/28 days regimen in the treatment of recurrent glioblastoma: A retrospective analysis of a two-centre German cohort trial with systematic comparison and effect-to-treatment analysis. BMJ Open 2017, 7, e017387. [CrossRef] [PubMed]
45. Fiorentini, G.; Sarti, D.; Milandri, C.; Dentico, P.; Mambrini, A.; Guadagni, S. Retrospective observational Clinical Study on Relapsed Malignant Gliomas Treated with Electro-hyperthermia. Oncothermia J. 2018, 22, 32–45.
46. Fiorentini, G.; Sarti, D.; Milandri, C.; Dentico, P.; Mambrini, A.; Fiorentini, C.; Mattioli, G.; Casadei, V.; Guadagni, S. Modulated Electrohyperthermia in Integrative Cancer Treatment for Relapsed Malignant Glioblastoma and Astrocytoma: Retrospective Multicenter Controlled Study. Integr. Cancer 2019, 18, 1534735418812691. [CrossRef]
47. Douwes, F.; Douwes, O.; Migeod, F.; Grote, C.; Bogovic, J. Hyperthermia in Combination with ACNU Chemotherapy in theTreatment of Recurrent Glioblastoma. Available online: https://www.klinik-st-georg.de/wp-content/downloads/Professional-Articles/hyperthermia_in_combination_with_ACNU_chemotherapy_in_the_treatment_of_recurrent_glioblastoma.pdf (accessedon 1 July 2022).
48. Fiorentini, G.; Giovanis, P.; Rossi, S.; Dentico, P.; Paola, R.; Turrisi, G.; Bernardeschi, P. A phase II clinical study on relapsed malignant gliomas treated with electro-hyperthermia. Vivo 2006, 20, 721–724.
49. Hager, E.D.; Sahinbas, H.; Groenemeyer, D.H.; Migeod, F. Prospective phase II trial for recurrent high-grade gliomas with capacitive coupled low radiofrequency (LRF) hyperthermia. J. Clin. Oncol. 2008, 26, 2047. [CrossRef]

50. Heo, J.; Kim, S.H.; Oh, Y.T.; Chun, M.; Noh, O.K. Concurrent hyperthermia and re-irradiation for recurrent high-grade gliomas. Neoplasma 2017, 64, 803–808. [CrossRef]
51. Ryabova, A.I.; Novikov, V.A.; Gribova, O.V.; Choynzonov, E.L.; Startseva, Z.A.; Grigoryev, E.G.; Miloichikova, I.A.; Turgunova, N.D.; Surkova, P.V. Concurrent Thermochemoradiotherapy in Glioblastoma Treatment: Preliminary Results. In Glioma; Ibrahim, O., Kenan, A., Eds.; IntechOpen: Rijeka, Croatia, 2018. [CrossRef]
52. Song, A.; Bar-Ad, V.; Martinez, N.; Glass, J.; Andrews, D.W.; Judy, K.; Evans, J.J.; Farrell, C.J.; Werner-Wasik, M.; Chervoneva, I.; et al. Initial experience with scalp sparing radiation with concurrent temozolomide and tumor treatment fields (SPARE) for patients with newly diagnosed glioblastoma. J. NeuroOncol. 2020, 147, 653–661. [CrossRef]
53. Miller, R.; Song, A.; Ali, A.; Niazi, M.; Bar-Ad, V.; Martinez, N.; Glass, J.; Alnahhas, I.; Andrews, D.; Judy, K.; et al. Scalp-Sparing Radiation With Concurrent Temozolomide and Tumor Treating Fields (SPARE) for Patients With Newly Diagnosed Glioblastoma. Front. Oncol. 2022, 12, 896246. [CrossRef]
54. Stupp, R.; Wong, E.T.; Kanner, A.A.; Steinberg, D.; Engelhard, H.; Heidecke, V.; Kirson, E.D.; Taillibert, S.; Liebermann, F.; Dbaly, V.; et al. NovoTTF-100A versus physician's choice chemotherapy in recurrent glioblastoma: A randomised phase III trial of a novel treatment modality. Eur. J. Cancer 2012, 48, 2192–2202. [CrossRef] [PubMed]
55. Wong, E.T.; Lok, E.; Swanson, K.D.; Gautam, S.; Engelhard, H.H.; Lieberman, F.; Taillibert, S.; Ram, Z.; Villano, J.L. Response assessment of NovoTTF-100A versus best physician's choice chemotherapy in recurrent glioblastoma. Cancer Med. 2014, 3, 592–602. [CrossRef] [PubMed]
56. Wong, E.T.; Lok, E.; Gautam, S.; Swanson, K.D. Dexamethasone exerts profound immunologic interference on treatment efficacy for recurrent glioblastoma. Br. J. Cancer 2015, 113, 232–241. [CrossRef] [PubMed]
57. Stupp, R.; Taillibert, S.; Kanner, A.; Read,W.; Steinberg, D.; Lhermitte, B.; Toms, S.; Idbaih, A.; Ahluwalia, M.S.; Fink, K.; et al. Effect of Tumor-Treating Fields Plus Maintenance Temozolomide vs Maintenance Temozolomide Alone on Survival in Patients With Glioblastoma: A Randomized Clinical Trial. JAMA 2017, 318, 2306–2316. [CrossRef] [PubMed]
58. Stupp, R.; Taillibert, S.; Kanner, A.A.; Kesari, S.; Steinberg, D.M.; Toms, S.A.; Taylor, L.P.; Lieberman, F.; Silvani, A.; Fink, K.L.; et al. Maintenance Therapy With Tumor-Treating Fields Plus Temozolomide vs Temozolomide Alone for Glioblastoma: A Randomized Clinical Trial. JAMA 2015, 314, 2535–2543. [CrossRef] [PubMed]
59. Kesari, S.; Ram, Z.; on behalf of EF-14 Trial Investigators. Tumor-treating fields plus chemotherapy versus chemotherapy alone for glioblastoma at first recurrence: A post hoc analysis of the EF-14 trial. CNS Oncol. 2017, 6, 185–193. [CrossRef] [PubMed]
60. Zhu, J.J.; Demireva, P.; Kanner, A.A.; Pannullo, S.; Mehdorn, M.; Avgeropoulos, N.; Salmaggi, A.; Silvani, A.; David, C.; et al.; on behalf of the EF-14 Trial Investigators. Health-related quality of life, cognitive screening, and functional status in a randomized phase III trial (EF-14) of tumor treating fields with temozolomide compared to temozolomide alone in newly diagnosed glioblastoma. J. NeuroOncol. 2017, 135, 545–552. [CrossRef] [PubMed]
61. Taphoorn, M.J.B.; Dirven, L.; Kanner, A.A.; Lavy-Shahaf, G.; Weinberg, U.; Taillibert, S.; Toms, S.A.; Honnorat, J.; Chen, T.C.; Sroubek, J.; et al. Influence of TreatmentWith Tumor-Treating Fields on Health-Related Quality of Life of PatientsWith Newly Diagnosed Glioblastoma: A Secondary Analysis of a Randomized Clinical Trial. JAMA Oncol. 2018, 4, 495–504. [CrossRef]
62. Kim, C.Y.; Paek, S.H.; Nam, D.H.; Chang, J.H.; Hong, Y.K.; Kim, J.H.; Kim, O.L.; Kim, S.H. Tumor treating fields plus temozolomide for newly diagnosed glioblastoma: A sub-group analysis of Korean patients in the EF-14 phase 3 trial. J. NeuroOncol. 2020, 146, 399–406. [CrossRef]
63. Kirson, E.D.; Schneiderman, R.S.; Dbaly, V.; Tovarys, F.; Vymazal, J.; Itzhaki, A.; Mordechovich, D.; Gurvich, Z.; Shmueli, E.; Goldsher, D.; et al. Chemotherapeutic treatment efficacy and sensitivity are increased by adjuvant alternating electric fields (TTFields). BMC Med. Phys. 2009, 9, 1. [CrossRef]
64. Wong, E.T.; Lok, E.; Swanson, K.D. Clinical benefit in recurrent glioblastoma from adjuvant NovoTTF-100A and TCCC after temozolomide and bevacizumab failure: A preliminary observation. Cancer Med. 2015, 4, 383–391. [CrossRef]
65. Lu, G.; Rao, M.; Zhu, P.; Liang, B.; El-Nazer, R.T.; Fonkem, E.; Bhattacharjee, M.B.; Zhu, J.J. Triple-drug TherapyWith Bevacizumab, Irinotecan, and Temozolomide Plus Tumor Treating Fields for Recurrent Glioblastoma: A Retrospective Study. Front. Neurol. 2019, 10, 42. [CrossRef]
66. Bokstein, F.; Blumenthal, D.; Limon, D.; Harosh, C.B.; Ram, Z.; Grossman, R. Concurrent Tumor Treating Fields (TTFields) and Radiation Therapy for Newly Diagnosed Glioblastoma: A Prospective Safety and Feasibility Study. Front. Oncol. 2020, 10, 411. [CrossRef]
67. Korshoej, A.R.; Lukacova, S.; Lassen-Ramshad, Y.; Rahbek, C.; Severinsen, K.E.; Guldberg, T.L.; Mikic, N.; Jensen, M.H.; Cortnum, S.O.S.; von Oettingen, G.; et al. OptimalTTF-1: Enhancing tumor treating fields therapy with skull remodeling surgery. A clinical phase I trial in adult recurrent glioblastoma. NeuroOncol. Adv. 2020, 2, vdaa121. [CrossRef] [PubMed]

68. Lazaridis, L.; Schafer, N.; Teuber-Hanselmann, S.; Blau, T.; Schmidt, T.; Oster, C.;Weller, J.; Tzaridis, T.; Pierscianek, D.; Keyvani, K.; et al. Tumour Treating Fields (TTFields) in combination with lomustine and temozolomide in patients with newly diagnosed glioblastoma. J. Cancer Res. Clin. Oncol. 2020, 146, 787–792. [CrossRef] [PubMed]
69. Liu, Y.; Strawderman, M.S.; Warren, K.T.; Richardson, M.; Serventi, J.N.; Mohile, N.A.; Milano, M.T.; Walter, K.A. Clinical Efficacy of Tumor Treating Fields for Newly Diagnosed Glioblastoma. Anticancer Res. 2020, 40, 5801–5806. [CrossRef]
70. Dono, A.; Mitra, S.; Shah, M.; Takayasu, T.; Zhu, J.J.; Tandon, N.; Patel, C.B.; Esquenazi, Y.; Ballester, L.Y. PTEN mutations predict benefit from tumor treating fields (TTFields) therapy in patients with recurrent glioblastoma. J. NeuroOncol. 2021, 153, 153–160. [CrossRef] [PubMed]
71. Stupp, R.; Hegi, M.E.; Mason,W.P.; van den Bent, M.J.; Taphoorn, M.J.; Janzer, R.C.; Ludwin, S.K.; Allgeier, A.; Fisher, B.; Belanger, K.; et al. European Organisation for Research and Treatment of Cancer Brain Tumour and Radiation Oncology Groups; National Cancer Institute of Canada Clinical Trials Group. Effects of radiotherapy with concomitant and adjuvant temozolomide versus radiotherapy alone on survival in glioblastoma in a randomised phase III study: 5-year analysis of the EORTC-NCIC trial. Lancet Oncol. 2009, 10, 459–466. [CrossRef]
72. Poon, M.T.C.; Sudlow, C.L.M.; Figueroa, J.D.; Brennan, P.M. Longer-term (>/= 2 years) survival in patients with glioblastoma in population-based studies pre- and post-2005: A systematic review and meta-analysis. Sci. Rep. 2020, 10, 11622. [CrossRef][PubMed]
73. Oronsky, B.; Reid, T.R.; Oronsky, A.; Sandhu, N.; Knox, S.J. A Review of Newly Diagnosed Glioblastoma. Front. Oncol. 2020, 10, 574012. [CrossRef]
74. Stupp, R.; Brada, M.; van den Bent, M.J.; Tonn, J.C.; Pentheroudakis, G. ESMO GuidelinesWorking Group. High-grade glioma: ESMO Clinical Practice Guidelines for diagnosis, treatment and follow-up. Ann. Oncol. 2014, 25 (Suppl. S3), iii93–iii101. [CrossRef]
75. Raposo, C.; Vitorino-Araujo, J.L.; Barreto, N. Molecular Markers of Gliomas to Predict Treatment and Prognosis: Current State and Future Directions. In Gliomas; Debinski, W., Ed.; Exon Publications: Brisbane, Australia, 2021. [CrossRef]
76. 76. Lee, S.Y.; Fiorentini, G.; Szasz, A.M.; Szigeti, G.; Szasz, A.; Minnaar, C.A. Quo Vadis Oncological Hyperthermia (2020)? Front. Oncol. 2020, 10, 1690. [CrossRef]
77. Ohgaki, H.; Kleihues, P. Population-based studies on incidence, survival rates, and genetic alterations in astrocytic and oligodendroglial gliomas. J. Neuropathol. Exp. Neurol. 2005, 64, 479–489. [CrossRef] [PubMed]
78. Gupta, T.; Talukdar, R.; Kannan, S.; Dasgupta, A.; Chatterjee, A.; Patil, V. Efficacy and safety of extended adjuvant temozolomide compared to standard adjuvant temozolomide in glioblastoma: Updated systematic review and meta-analysis. NeuroOncol. Pr. 2022, 9, 354–363. [CrossRef]
79. Lacouture, M.E.; Davis, M.E.; Elzinga, G.; Butowski, N.; Tran, D.; Villano, J.L.; DiMeglio, L.; Davies, A.M.; Wong, E.T. Characterization and management of dermatologic adverse events with the NovoTTF-100A System, a novel anti-mitotic electric field device for the treatment of recurrent glioblastoma. Semin. Oncol. 2014, 41 (Suppl. S4), S1–S14. [CrossRef]
80. Krigers, A.; Pinggera, D.; Demetz, M.; Kornberger, L.M.; Kerschbaumer, J.; Thome, C.; Freyschlag, C.F. The Routine Application of Tumor-Treating Fields in the Treatment of Glioblastoma WHO degrees IV. Front. Neurol. 2022, 13, 900377. [CrossRef]
81. Regev, O.; Merkin, V.; Blumenthal, D.T.; Melamed, I.; Kaisman-Elbaz, T. Tumor-Treating Fields for the treatment of glioblastoma: A systematic review and meta-analysis. NeuroOncol. Pr. 2021, 8, 426–440. [CrossRef]
82. Li, X.; Jia, Z.; Yan, Y. Efficacy and safety of tumor-treating fields in recurrent glioblastoma: A systematic review and meta-analysis. Acta Neurochir. 2022, 164, 1985–1993. [CrossRef] [PubMed]
83. Dongpo, S.; Zhengyao, Z.; Xiaozhuo, L.; Qing, W.; Mingming, F.; Fengqun, M.; Mei, L.; Qian, H.; Tong, C. Efficacy and Safety of Bevacizumab Combined with Other Therapeutic Regimens for Treatment of Recurrent Glioblastoma: A Network Meta-analysis. World Neurosurg. 2022, 160, e61–e79. [CrossRef] [PubMed]
84. Guo, X.; Yang, X.;Wu, J.; Yang, H.; Li, Y.; Li, J.; Liu, Q.;Wu, C.; Xing, H.; Liu, P.; et al. Tumor-Treating Fields in Glioblastomas: Past, Present, and Future. Cancers 2022, 14, 3669. [CrossRef]
85. Jin, L.; Guo, S.; Zhang, X.; Mo, Y.; Ke, S.; Duan, C. Optimal treatment strategy for adult patients with newly diagnosed glioblastoma: A systematic review and network meta-analysis. Neurosurg. Rev. 2021, 44, 1943–1955. [CrossRef]
86. Michiels, S.; Piedbois, P.; Burdett, S.; Syz, N.; Stewart, L.; Pignon, J.P. Meta-analysis when only the median survival times are known: A comparison with individual patient data results. Int. J. Technol. Assess Health Care 2005, 21, 119–125. [CrossRef]

Modulated electrohyperthermia in locally advanced cervical cancer
Results of an observational study of 95 patients

Sun Young Lee, MD, PhD [a,b], Dong Hyun Lee, MD, PhD[c], Dong-Hyu Cho, MD, PhD[b,c,*]

[a] Department of Radiation Oncology, Jeonbuk National University Hospital, Jeonju, Republic of Korea,

[b] Research Institute of Clinical Medicine of Jeonbuk National University-Biomedical Research Institute of Jeonbuk National University Hospital, Jeonju, Republic of Korea,

[c] Department of Obstetrics and Gynecology, Jeonbuk National University Hospital, Jeonju, Republic of Korea.

* Correspondence: Dong-Hyu Cho, Department of Obstetrics and Gynecology, Jeonbuk National University Hospital, Jeonju 54907, Republic of Korea (e-mail: obgyn2001@jbnu.ac.kr).

Cite this article as:
Lee, S.Y. et al. (2023) Modulated electrohyperthermia in locally advanced cervical cancer: Results of an observational study of 95 patients. Medicine 2023;102:3(e32727)
http://dx.doi.org/10.1097/MD.0000000000032727

Oncothermia Journal 33, May 2023: 165 – 173.
www.oncotherm.com/sites/oncotherm/files/2023-05/LeeSY_et_al_mEHT_in_cervical_cancer_study_of_95_patients.pdf

Abstract
Most federation of gynecology and obstetrics stage II or higher locally advanced cervical cancer (LACC) patients are treated with concurrent chemoradiotherapy (CCRT); however, recurrence is high, and the prognosis is poor. In this observational retrospective study, data from LACC patients treated with CCRT alone or combined with modulated electrohyperthermia (mEHT) were collected from 2011 to 2018. Ninety-five LACC patients, including 53 (%) treated with CCRT alone and 42 (%) treated with CCRT + mEHT, were enrolled. The complete remission rate significantly increased with CCRT + mEHT compared with CCRT alone among LACC cases with lymph node metastasis (45% vs 71%, P = .0377). Additionally, at the last follow-up point, the no-evidence-of-disease rate significantly improved with CCRT + mEHT compared with CCRT (58% vs 82%, P = .0315). Disease-free survival increased in the CCRT + mEHT group with lymph node metastasis (P = .04). The addition of mEHT to CCRT led to a better therapeutic response in LACC with regional lymph node metastasis without severe complications.

Abbreviations:
AEs = adverse events, CCRT = concurrent chemoradiotherapy, CR = complete remission, DFS = disease-free survival, HIF-1a = hypoxia-inducible factor-1a, LACC = locally advanced cervical cancer, mEHT = modulated electrohyperthermia, NED = no-evidence-of-disease, OS = overall survival, RF = radio frequency, VEGF = vascular endothelial growth factor.

1. Introduction

Cervical cancer is the fourth most common cancer in women, with 5,70,000 patients being diagnosed and 3,11,000 deaths occurring in 2018 worldwide.[1] In particular, some developing countries, including Africa, have the highest cancer incidence and mortality rates among women.[1,2] Treatment of cervical cancer includes surgery, radiotherapy, and chemotherapy. For locally advanced cervical cancer (LACC), cisplatin-based concurrent chemoradiation therapy (CCRT) is commonly accepted as the primary treatment, and this treatment has been proven to lead to better outcomes than radiation alone.[3–6] Surgical treatment for LACC usually requires adjuvant radiation and has a similar survival rate but is accompanied by various complications.[7] Although the incidence of cervical cancer is decreasing due to the development of screening tests and vaccines for human papillomavirus (HPV), patients diagnosed with LACC still have a high recurrence rate and a poor prognosis even if they are treated with the standard therapy, namely, CCRT.[8] Modulated electrohyperthermia (mEHT), which was used in the present study, is a type of hyperthermia used in oncological treatments that avoids the drawbacks of conventional electromagnetic heating.[9,10] This treatment device is designed to selectively heat malignant tumors and tumor cells by modularly delivering 13.56 MHz radio frequency (RF).[11–14] This method works by heating malignant cells, selectively and effectively acting on the cell membrane,[15] and inducing apoptotic cell death.[9] This advanced treatment produces damage-associated cellular patterns and promotes immunogenic cell death accompanied by the release of damage-associated molecular signal patterns, such as ATP, HMGB1 and hsp70, which have the cytokine-like effects of attracting immune cells.[16,17] The heat-induced increase in the tumor response to radiotherapy is due, at least in part, to an increase in the oxygen supply via increased blood circulation in tumors. The enhanced response of tumors to chemotherapy may be due to various factors. First, mild heating increases the delivery of chemotherapeutic drugs to the tumors by increasing blood flow to and within the tumor. Second, mild heating increases the cellular uptake of drugs by increasing cell membrane permeability. Third, heating facilitates the reaction rate of drugs, which potentiates their cytotoxicity.[11,16].

This method uses a modulated RF for energy delivery and achieves selective thermal action in nonhomogeneous tissue.[18]

It is also notably gentle, and its use on brain malignancies has been successful,[19–21] even at increased doses for advanced cases.[12] In the present study, we analyzed whether there was a better treatment by analyzing the treatment results and recurrence rates of the 2 treatment groups that underwent CCRT alone or CCRT + mEHT for locally advanced cervical cancer.

2. Methods

2.1. Patient selection
All patients with LACC who were treated from January 2011 to December 2018 with CCRT and mEHT at Jeonbuk National University Hospital were included, and patients who underwent follow-up for more than 3 years were analyzed. Data were collected retrospectively, and patients were selected according

to the following inclusion criteria: > 18 years of age, stage II, III, or IV cervical cancer, treatment with CCRT alone or in combination with mEHT, and signed informed consent.

Routine pretreatment work-up consisted of gynecological examination, CT, and MRI scan. Lymph node enlargement on CT or MRI scan is considered clinically positive. A total of 95 patients were enrolled. Fifty-three (%) patients were treated with CCRT alone, and 42 (%) patients were treated with CCRT and mEHT. The patient group was classified using the cancer stage process presented in the 2008 federation of gynecology and obstetrics guideline (Table 1).

2.2. CCRT

Most patients underwent chemotherapy with cisplatin alone, and a few were treated with cisplatin + 5-FU, cisplatin + etoposide and oral 5-FU.

Chemotherapy was started at the same time as radiation therapy, and in the hyperthermia combination group, treatment was carried out on the same day as chemoradiation therapy. Chemotherapy was performed more than 5 times in most patients.

Chemotherapy-associated adverse events (AEs) were pancytopenia, nausea, vomiting, anorexia and gastric discomfort. AEs were determined by investigator inquiry and by spontaneous patient reports. The AEs were recorded with regard to the symptoms, signs, duration and severity (mild, moderate, and severe). Clinical safety parameters, including blood glucose levels, vital signs, 12-lead ECG results and clinical laboratory tests, were observed during the regular chemotherapy cycles. For radiation therapy, after all patients received external radiation therapy with a mean total radiation dose of 54 Gy, an additional boost was administered according to the patient's condition, brachytherapy (6 times, 24 Gy) or external radiation therapy (mean 7 times, 12.4 Gy). Side effects related to radiation therapy included abdominal discomfort and frequent urination, and no serious life-threatening side effects occurred (Table 2).

Table 1

Characteristics of patients with cervical cancer who had previously undergone chemoradiotherapy, who were subsequently subjected to CCRT alone or who received CCRT combined with mEHT.

Parameter	CCRT alone (n = 53, 56%)	CCRT + mEHT (n = 42, 44%)	*P* value
Age, yr	58.7 (28–81)	51.8 (26–78)	.25
mean			
FIGO stage	2 (4%)	1 (2%)	
IIA	44 (83%)	32 (77%)	
IIB	2 (4%)	1 (2%)	
IIIA	5 (9%)	8 (19%)	
IIIB			
Pathology			
squamous cell	45 (85%)	37 (88%)	.157
carcinoma	6 (11%)	4 (10%)	
adenocarcinoma	2 (4%)	1 (2%)	
other			
Pelvic lymph	31 (58%)	34 (81%)	
node status	22 (42%)	8 (19%)	
positive			
negative			

CCRT = concurrent chemoradiotherapy, FIGO = federation of gynecology and obstetrics, mEHT = modulated electrohyperthermia.

Table 2

Chemotherapy treatment characteristics of CCRT alone and CCRT combined with mEHT.

	CCRT alone (n = 53)	CCRT + mEHT (n = 42)
Chemotherapy regimen		
Cisplatin	52 (98%)	35 (84%)
6 cycles	45	31
5 cycles	3	2
4 cycles	4	1
3 cycles	0	1
Cisplatin + 5-FU	0	6 (14%)
(3–7 cycles)		
Cisplatin + etoposide	0	1 (8 cycles, 2%)
5-FU	1 (oral) (2%)	0

CCRT = concurrent chemoradiotherapy, mEHT = modulated electrohyperthermia.

Table 3

Clinical response of CCRT alone and CCRT-combined with mEHT following completion of treatment.

	CCRT alone (n = 53)	CCRT + mEHT (n = 42)	*p* value
response after 1st Tx			
CR	28 (53%)	30 (71%)	.0649
Non-CR	25 (47%)	12 (29%)	
response after last F/U			
NED	36 (68%)	35 (83%)	.0861
Non-NED	17 (32%)	7 (17%)	

CCRT = concurrent chemoradiotherapy, CR = complete remission, mEHT = modulated electrohyperthermia, NED = no-evidence-of-disease.

2.3. mEHT protocol and device

Modulated electrohyperthermia treatment was applied using an EHY2000 clinical heating device (Oncotherm GmbH, Troisdorf, Germany) set at a 13.56 MHz carrier frequency, and the amplitude was modulated according to a time fractal pattern. Modulated electrohyperthermia was performed for 60 minutes. The patients were placed in the supine position on a water mattress electrode. A circular upper electrode (30 cm diameter) was coupled over the pelvic area. Prior to mEHT, all patients underwent a 2-dimensional simulation. The treatment field encompassed the mass with a 3-cm margin in the X, Y directions. Modulated electrohyperthermia was performed 3 times per week beginning at the initiation of CCRT, and patients underwent 24 to 36 sessions (mean 28.6 times).

The power output was 80 W for the first 10 minutes, 120 W for the next 10 minutes, and 150 W for the remaining treatment time. Self-calibration of the device was performed prior to each treatment. The body temperature, blood pressure and pulse rate of each patient were measured prior to, during and following treatment. Body temperature was measured using an infrared ear thermometer (Infrared Thermometer IRT 4020; Braun GmbH, Kronberg, Germany), and the temperature of the abdominal skin surface below the circular upper electrode probe was measured using a non-contact infrared thermometer transmitter (Thermo Checker DT-060; Easytem Co., Ltd., Siheung, Korea). AEs associated with hyperthermia and chemotherapy were monitored throughout the present study. Hyperthermiaassociated AEs were warm sensation, skin burn and gastric discomfort.

2.4. Statistical analysis

The end points of the present study were tumor response with complete remission (CR) or partial remission, stable disease or progressive disease, overall survival, final follow-up status and toxicity. Student's t-test was used for treatment response analysis.

The time to an event variable was estimated using Kaplan– Meier analysis. The statistical analysis was performed using SAS software (version 9.3; SAS Institute, Inc., Cary, NC). A P value < .05 was considered statistically significant.

2.5. Ethics statement

The present study was approved by the Institutional Review Board of Jeonbuk National University Hospital (Jeonju, Republic of Korea, JBNU IRB NO. 2018-06-009-002) and was conducted according to the Declaration of Helsinki regarding biomedical research involving human subjects and the Guidelines for Good Clinical Practice and written the informed consent was obtained from all patients legal guardian.

3. Results

3.1. Patient characteristics

The study included 95 consecutive patients, 53 (56%) of whom received CCRT alone and 42 (44%) of whom received CCRT and mEHT. The patient characteristics are summarized in Table 1.

The mean age, cancer stage, pathology type, and lymph node metastasis were not significantly different between the 2 groups. The mean ages were 58.7 and 51.8 years, and all patients were diagnosed with stage IIA-IIIB disease. Most patients were diagnosed with squamous cell carcinoma (P = .157) based on cervical biopsy using the vaginal approach. The frequency of lymph node metastasis was higher in the CCRT + mEHT group, but the difference was not significant.

3.2. Outcome

Most patients were treated with cisplatin-based CCRT for 6 cycles. A small number of patients were treated with other chemotherapies, but the number was not significant (Table 2).

The CR rates of the 2 groups were 53% and 71%, respectively (P = .0649), and the no-evidence-of-disease (NED) rates at the last follow-up were 68% in the CCRT-alone group and 83% in the CCRT + mEHT group (P = .0861); however, the differences were not significant (Table 3). There was also no significant difference in disease-free survival (DFS) or overall survival (OS) (P = .166 and 0.079, respectively) (Fig. 1).

However, in the separate analysis of patients with pelvic lymph node metastasis, significant variation in the results was observed. More patients showed CR with CCRT + mEHT treatment (45% vs 71%, P = .0377) and more NED (58% vs 82%, P = .0315) (Table 4). There was no difference in OS (P = .10), but a significant difference in DFS was observed (P = .04) (Fig. 2).

3.3. AEs associated with hyperthermia and chemotherapy

Hyperthermia-associated AEs were warm sensation, skin burn and gastric discomfort. The 18 patients (42.8%) complained of warm sensation in treatment area, 4 patients (9.5%) complained of first-degree burns on treatment areas, and 6 patients (14.2%) complained of mild gastric discomfort. All patients' AEs disappeared immediately after treatment without any additional treatment.

4. Discussion

The basic treatment principle of cervical cancer is to remove the primary cancer lesion and remove the potential spread site. The primary treatment is to perform surgery or radiotherapy after setting the clinical stage. Surgical treatment can be performed for cancers up to stage IIA that are limited to the cervix and upper vagina. Radiation therapy can be used to treat all stages and has similar treatment results to those of surgical treatment.

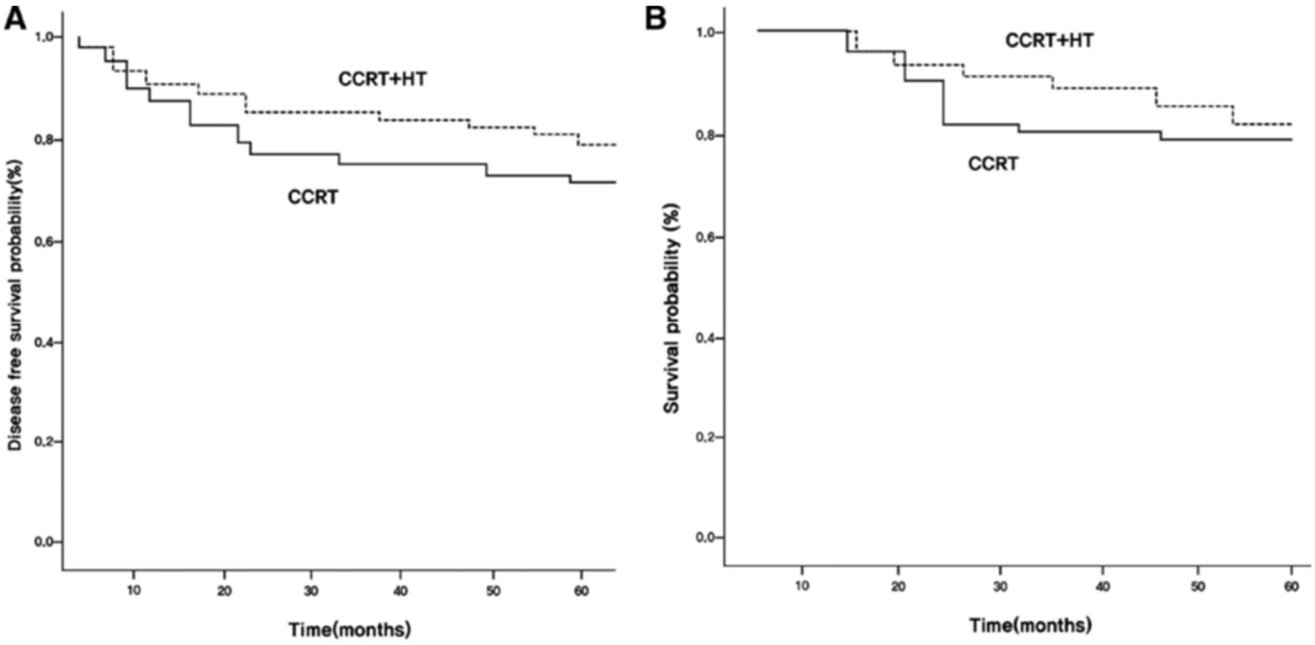

Figure 1. (A,B): Disease-free survival and overall survival of patients treated with CCRT alone compared with those treated with CCRT combined with mEHT. CCRT combined with mEHT did not significantly increase the disease-free survival rate or overall survival rate (P = .166 for DFS, P = .079 for OS). CCRT = concurrent chemoradiotherapy, DFS = disease-free survival, mEHT = modulated electrohyperthermia, OS = overall survival.

Table 4

Clinical response of CCRT alone and CCRT-combined with mEHT following completion of treatment in patients with pelvic lymph node metastasis.

LN metastasis	CCRT alone (n = 31)	CCRT + mEHT (n = 34)	*p* value
Response after 1st Tx	14 (45%)	24 (71%)	.0377
CR	17 (56%)	10 (29%)	
Non-CR			
Response after last F/U	18 (58%)	28 (82%)	.0315
NED	13 (42%)	6 (18%)	
Non-NED			

CCRT = concurrent chemoradiotherapy, CR = complete remission, mEHT = modulated electrohyperthermia, NED = no-evidence-of-disease.

Several studies have shown that CCRT improves the therapeutic outcomes of LACC patients, whose therapeutic outcomes would otherwise be poor with radiation therapy alone.[3,4,22] However, despite treatment with CCRT, patients with LACC still have locoregional recurrence and distant metastasis at a frequency of 27% to 35% and a high mortality rate and poor prognosis in cases of recurrence.[23] Hyperthermia can directly kill cancer cells through heat and increase blood flow to the warmed area and tumor oxygenation. In addition, the effect of chemotherapy can be improved by increasing the intracellular drug concentration through an increase in permeability with membrane damage, an increase in drug uptake, and a change in pH. By increasing the possibility of cell damage and preventing damage recovery, the effect of radiation can be increased.[9] Conventional hyperthermia, at > 43°C or higher, has several limitations. As normal tissue and malignant tissue receive homogeneous heat, the focus of temperature does not match the focus of energy; therefore, temperature does not simply correlate with energy to damage the cancer cell. The energy transfer to the tumor is indirect and difficult to measure. In addition, this homogeneous heating of normal tissues surrounding tumors can increase blood flow and the supply of nutrients to the tumor and can lead to an increase in invasion, dissemination, and metastasis.[16]

Oncothermia is a modular electrohyperthermia based on energy dose control instead of a single parameter of temperature, and this method accurately selects only tumor cells and heats them to transfer a definite energy dose to more effectively lead to apoptotic cell death without unwanted physiologic consequences.[11] Using anesthetized living pigs, Balogh et al[19] reported that 13.56 MHzmodulated RF can increase the temperature by 3 to 5°C in deep tissue. Kim et al[24] reported that mild temperature hyperthermia suppresses hypoxia-inducible factor-1a (HIF-1a) and vascular endothelial growth factor (VEGF), which are upregulated under hypoxic conditions. When only 15 Gy (60 Co) irradiation was performed in FSa fibrosarcoma allograte in C3H mice, blood perfusion was decreased, hypoxia increased, and HIF-1a and VEGF were upregulated, but when mild temperature hyperthermia treatment was performed after irradiation, blood perfusion and tumor oxygenation were increased, and HIF-1a and VEGF were suppressed.[25] Lee et al[20] reported increased blood perfusion to the tumor and increased peritumor temperature from 36.7 ± 0.2°C to 38.5 ± 0.8°C through mEHT in patients with cervical cancer. Vancsik et al[17] reported that mEHT promotes doxorubicin uptake and potentiates doxorubicin-induced cytotoxic effects in the case of a combination of doxorubicin and mEHT in C26 mouse colorectal adenocarcinoma culture.

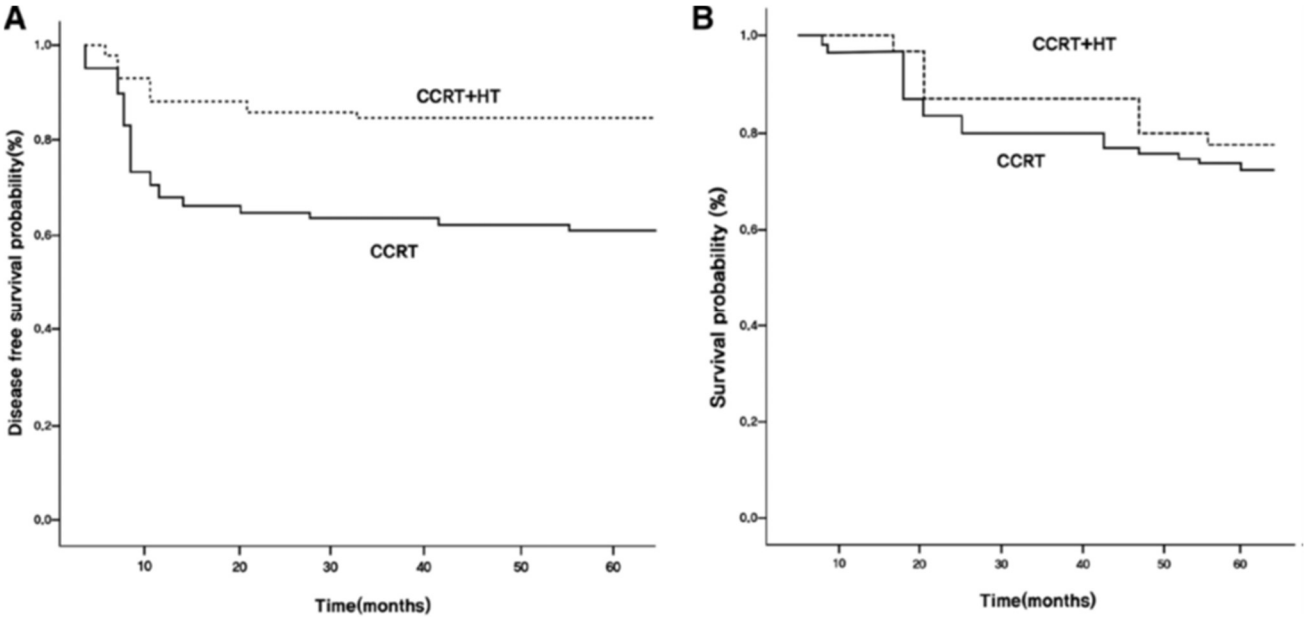

Figure 2. (A,B): Disease-free survival and overall survival of patients with lymph node metastasis compared to patients without lymph node metastasis treated with CCRT alone and CCRT combined with mEHT. DFS, but not OS, was significantly different between the two groups (P = .04 for DFS, P = .104 for OS). CCRT = concurrent chemoradiotherapy, DFS = disease-free survival, mEHT = modulated electrohyperthermia, OS = overall survival.

Recently, several studies on the clinical effectiveness and stability of the combination of conventional therapy and mEHT have been reported. Fiorentini et al[21] reported that when chemotherapy, radiotherapy, and mEHT were combined in patients with stage III-IV pancreatic cancer, the tumor response was improved, and the median overall survival increased from 10.9 months to 18.0 months. A study comparing the effects of supportive care and mEHT in relapsed malignant astrocytoma and glioblastoma reported that the 5-year survival rate of astrocytoma was increased from 25% to 83% in the mEHT group.[20] Gadaleta-Caldarola et al[26] reported that sorafenib plus mEHT combination therapy in advanced hepatocellular carcinoma was feasible and well tolerated without major complications. Grade 4 treatment-related toxicities were not observed, and grade 3 toxicities were related to only sorafenib, not mEHT.[7] In our study, we compared the treatment response of the CCRT treatment group and CCRT + mEHT treatment group for LACC. There was no difference in response rate (CR and NED) between the 2 groups, and DFS and OS also showed no significant difference. However, the CR rate was significantly increased in the CCRT + mEHT group compared to the CCRT alone group in the case of locally advanced cancer (stage IIIC) in women with lymph node metastasis (P = .0377). Additionally, at the last F/U point, the NED rate also showed a significant improvement compared to the CCRT alone group (P = .0315).

DFS also improved in the CCRT + mEHT group with lymph node metastasis (P = .04). In 1 study about recurrent cervical cancer in women who were previously irradiated with chemotherapy combined with mEHT compared with chemotherapy alone, the authors concluded that hyperthermia may be slightly more effective for the treatment of abdominal lymph node metastasis.[27] In the 2018 International Federation of Gynecology and Obstetrics staging system for uterine cervical cancer, pelvic or para-aortic lymph node metastasis was classified as stage IIIC.[28] However, there is no change in therapeutic modality, namely, CCRT. In our study, mEHT combined with CCRT led to a better therapeutic response in patients with LACC with regional lymph node metastasis without severe complications. However, there is a limitation in that this study is a single-center study, has a small number of participants, and cannot explain the pathogenesis, namely, why better results were found in patients with lymph node metastasis. In conclusion, to obtain better treatment results, further discussion or research regarding combined hyperthermia therapy should be conducted. Additional cell-level studies and laboratory studies are also needed to determine why mEHT is more effective in lymph nodes, and large-scale prospective studies are needed in patients with federation of gynecology and obstetrics stage IIIc disease.

Acknowledgements
The authors would like to thank the reviewers for their valuable comments on this manuscript.

Author contributions
Conceptualization: Sun Young Lee, Dong Hyun Lee, Dong-Hyu Cho.
Data curation: Sun Young Lee, Dong Hyun Lee.
Formal analysis: Sun Young Lee, Dong Hyun Lee.
Investigation: Sun Young Lee, Dong Hyun Lee, Dong-Hyu Cho.
Methodology: Sun Young Lee, Dong Hyun Lee.
Supervision: Dong Hyun Lee, Dong-Hyu Cho.
Validation: Sun Young Lee, Dong Hyun Lee.
Visualization: Sun Young Lee, Dong Hyun Lee.
Writing – original draft: Sun Young Lee, Dong Hyun Lee.
Writing – review & editing: Sun Young Lee, Dong Hyun Lee, Dong-Hyu Cho.

References

[1] Arbyn M, Weiderpass E, Bruni L, et al. Estimates of incidence and mortality of cervical cancer in 2018: a worldwide analysis. Lancet Glob Health. 2020;8:e191–203.

[2] Bray F, Ferlay J, Soerjomataram I, et al. Global cancer statistics 2018: GLOBOCAN estimates of incidence and mortality worldwide for 36 cancers in 185 countries. CA Cancer J Clin. 2018;68:394–424.

[3] Rose PG, Bundy BN, Watkins EB, et al. Concurrent cisplatin-based radiotherapy and chemotherapy for locally advanced cervical cancer. N Engl J Med. 1999;340:1144–53.

[4] Morris M, Eifel PJ, Lu J, et al. Pelvic radiation with concurrent chemotherapy compared with pelvic and para-aortic radiation for high-risk cervical cancer. N Engl J Med. 1999;340:1137–43.

[5] Keys HM, Bundy BN, Stehman FB, et al. Cisplatin, radiation, and adjuvant hysterectomy compared with radiation and adjuvant hysterectomy for bulky stage IB cervical carcinoma. N Engl J Med. 1999;340:1154–61.

[6] Green JA, Kirwan JM, Tierney JF, et al. Survival and recurrence after concomitant chemotherapy and radiotherapy for cancer of the uterine cervix: a systematic review and meta-analysis. Lancet. 2001;358:781–6.

[7] Yamashita H, Okuma K, Kawana K, et al. Comparison between conventional surgery plus postoperative adjuvant radiotherapy and concurrent chemoradiation for FIGO stage IIB cervical carcinoma: a retrospective study. Am J Clin Oncol. 2010;33:583–6.

[8] Lukka H, Hirte H, Fyles A, et al. Concurrent cisplatin-based chemotherapy plus radiotherapy for cervical cancer--a meta-analysis. Clin Oncol (R Coll Radiol). 2002;14:203–12.

[9] Hildebrandt B, Wust P, Ahlers O, et al. The cellular and molecular basis of hyperthermia. Crit Rev Oncol Hematol. 2002;43:33–56.

[10] Dewhirst MW, Vujaskovic Z, Jones E, et al. Re-setting the biologic rationale for thermal therapy. Int J Hyperthermia. 2005;21:779–90.

[11] Hegyi G, Szigeti GP, Szasz A. Hyperthermia versus oncothermia: cellular effects in complementary cancer therapy. Evid Based Complement Alternat Med. 2013;2013:672873.

[12] Overgaard J, Bentzen SM, Overgaard J, et al. Randomised trial of hyperthermia as adjuvant to radiotherapy for recurrent or metastatic malignant melanoma. Lancet. 1995;345:540–3.

[13] Wust P, Hildebrandt B, Sreenivasa G, et al. Hyperthermia in combined treatment of cancer. Lancet Oncol. 2002;3:487–97.

[14] Fotopoulou C, Cho CH, Kraetschell R, et al. Regional abdominal hyperthermia combined with systemic chemotherapy for the treatment of patients with ovarian cancer relapse: results of a pilot study. Int J Hyperthermia. 2010;26:118–26.

[15] Datta NR, Rogers S, Klingbiel D, et al. Hyperthermia and radiotherapy with or without chemotherapy in locally advanced cervical cancer: a systematic review with conventional and network meta-analyses. Int J Hyperthermia. 2016;32:809–21.

[16] Szasz A. "Quo vadis" oncologic hyperthermia? Conf Pap Med. 2013;2013:201671.

[17] Vancsik T, Mathe D, Horvath I, et al. Modulated electro-hyperthermia facilitates NK-cell infiltration and growth arrest of human A2058 melanoma in a Xenograft model. Front Oncol. 2021;11:590764.

[18] Andocs G, Meggyeshazi N, Balogh L, et al. Upregulation of heat shock proteins and the promotion of damage-associated molecular pattern signals in a colorectal cancer model by modulated electrohyperthermia. Cell Stress Chaperones. 2015;20:37–46.

[19] Balogh L, Polyak A, Postenyi Z, et al. Temperature increase induced by modulated electrohyperthermia (oncothermia(R)) in the anesthetized pig liver. J Cancer Res Ther. 2016;12:1153–9.

[20] Lee SY, Kim JH, Han YH, et al. The effect of modulated electro-hyperthermia on temperature and blood flow in human cervical carcinoma. Int J Hyperthermia. 2018;34:953–60.

[21] Fiorentini G, Sarti D, Milandri C, et al. Modulated Electrohyperthermia in integrative cancer treatment for relapsed malignant glioblastoma and astrocytoma: retrospective multicenter controlled study. Integr Cancer Ther. 2019;18:1534735418812691.

[22] Fiorentini G, Sarti D, Casadei V, et al. Modulated electro-hyperthermia as palliative treatment for pancreatic cancer: a retrospective observational study on 106 patients. Integr Cancer Ther. 2019;18:1534735419878501534735419878505.

[23] Whitney CW, Sause W, Bundy BN, et al. Randomized comparison of fluorouracil plus cisplatin versus hydroxyurea as an adjunct to radiation therapy in stage IIB-IVA carcinoma of the cervix with negative para-aortic lymph nodes: a gynecologic oncology group and southwest oncology group study. J Clin Oncol. 1999;17:1339–1339.

[24] Kim W, Kim MS, Kim HJ, et al. Role of HIF-1alpha in response of tumors to a combination of hyperthermia and radiation in vivo. Int J Hyperthermia. 2018;34:276–83.

[25] Chemoradiotherapy for Cervical Cancer Meta-analysis Collaboration. Reducing uncertainties about the effects of chemoradiotherapy for cervical cancer: individual patient data meta-analysis. Cochrane Database Syst Rev. 2010;2010:CD008285.

[26] Gadaleta-Caldarola G, Infusino S, Galise I, et al. Sorafenib and locoregional deep electro-hyperthermia in advanced hepatocellular carcinoma: a phase II study. Oncol Lett. 2014;8:1783–7.

[27] Vancsik T, Forika G, Balogh A, et al. Modulated electro-hyperthermia induced p53 driven apoptosis and cell cycle arrest additively support doxorubicin chemotherapy of colorectal cancer in vitro. Cancer Med.2019;8:4292–303.

[28] Bhatla N, Berek JS, Fredes MC, et al. Revised FIGO staging for carcinoma of the cervix uteri. Int J Gynaecol Obstet. 2019;145:129–35.

Radiofrequency Electromagnetic Fields Cause Non-Temperature-Induced Physical and Biological Effects in Cancer Cells

PeterWust [1], Paraskevi D. Veltsista [1], Eva Oberacker [1], Prabhusrinivas Yavvari [2], Wolfgang Walther [3,4,5], Olof Bengtsson [6], Anja Sterner-Kock [7], MarieWeinhart [2,8], Florian Heyd [9], Patricia Grabowski [10], Sebastian Stintzing [10], Wolfgang Heinrich [6], Ulrike Stein [3,4,5], and Pirus Ghadjar [1],*

[1] Department of Radiation Oncology, Charité—Universitätsmedizin Berlin, Corporate Member of Freie Universität Berlin and Humboldt-Universität zu Berlin, Augustenburger Platz 1, 13353 Berlin, Germany,

[2] Institute of Chemistry and Biochemistry, Freie Universität Berlin, Takustr. 3, 14195 Berlin, Germany

[3] Experimental and Clinical Research Center, Charité—Universitätsmedizin Berlin and Max-Delbrück-Center for Molecular Medicine, Germany and Experimental Pharmacology & Oncology (EPO), Robert-Rössle-Str. 10, 13125 Berlin, Germany

[4] Max-Delbrück-Center for Molecular Medicine in the Helmholtz Association, AG Translational Oncology of Solid Tumors, Robert-Rössle-Str. 10, 13125 Berlin, Germany

[5] German Cancer Consortium (DKTK), Im Neuenheimer Feld 280, 69120 Heidelberg, Germany

[6] Ferdinand-Braun-Institut gGmbH, Leibniz-Institut Für Höchstfrequenztechnik, Gustav-Kirchhoff-Str. 4, 12489 Berlin, Germany

[7] Experimental Pharmacology & Oncology GmbH Berlin-Buch, Robert-Rössle-Str. 10, 13125 Berlin, Germany

[8] Institute of Physical Chemistry and Electrochemistry, Leibniz Universität Hannover, Callinstr. 3A, 30167 Hannover, Germany

[9] Laboratory of RNA Biochemistry, Institute of Chemistry and Biochemistry, Freie Universität Berlin, Takustr. 6, 14195 Berlin, Germany

[10] Department of Hematology, Oncology and Cancer Immunology (CCM), Charité—Universitätsmedizin Berlin, Corporate Member of Freie Universität Berlin and Humboldt-Universität zu Berlin, Charitéplatz 1, 10117 Berlin, Germany

* Correspondence: pirus.ghadjar@charite.de

Cite this article as:
Wust, P. et al. (2022) Radiofrequency Electromagnetic Fields Cause Non-Temperature-Induced Physical and Biological Effects in Cancer Cells, Cancers 2022, 14, 5349.
https://www.mdpi.com/2072-6694/14/21/5349

Oncothermia Journal 33, May 2023: 174 – 194.
https://www.oncotherm.com/sites/oncotherm/files/2023-05/WustP_et_al_Radiofrequency_Electromagnetic_Fields.pdf

Simple Summary:
Radiofrequency electromagnetic fields are used for tumor heating as adjunct therapy, but it appears that sufficient temperatures can sometimes not be reached. We therefore aimed to study potential non-temperature-induced anticancer effects when adding amplitude modulation to the radiofrequency waves. We could demonstrate in a colorectal cancer model that radiofrequency electromagnetic fields do have anticancer effects when not being induced by increased temperature that can be further increased by amplitude modulation. Therefore, this treatment could potentially serve as a more effective tumor therapy.

Abstract
Non-temperature-induced effects of radiofrequency electromagnetic fields (RF) have been controversial for decades. Here, we established measurement techniques to prove their existence by investigating energy deposition in tumor cells under RF exposure and upon adding amplitude modulation (AM) (AMRF). Using a preclinical device LabEHY-200 with a novel in vitro applicator, we analyzed the power deposition and system parameters for five human colorectal cancer cell lines and measured the apoptosis rates in vitro and tumor growth inhibition in vivo in comparison to water bath heating. We showed enhanced anticancer effects of RF and AMRF in vitro and in vivo and verified the non-temperature-induced origin of the effects. Furthermore, apoptotic enhancement by AM was correlated with cell membrane stiffness. Our findings not only provide a strategy to significantly enhance non-temperature-induced anticancer cell effects in vitro and in vivo but also provide a perspective for a potentially more effective tumor therapy.

Keywords: radiofrequency; amplitude modulation; hyperthermia; colorectal cancer; anticancer effects

1. Introduction

Non-temperature-induced effects of radiofrequency electromagnetic fields (EMF) have been controversial for decades. Electromagnetic fields can be applied either as continuous waves (RF) or modified with additional amplitude modulation (AM), denoted as AMRF. In the literature, these effects are also, somewhat imprecisely, referred to as “nonthermal” effects. However, non-temperature-induced effects is a more suitable term, and it denotes the effects associated with the deposition of either thermal or nonthermal/isothermal energy. In the context of this work, we introduce the term of isothermal energy to denote energy absorption of a sample/tissue without resulting in a measurable temperature increase. We follow the thermodynamic term of an isothermal process, where a change in internal energy occurs without a concurrent temperature change. This is typically the case in slow processes where the rate of heat exchange is fast enough to prevent a temperature increase, for example, in cases in which the sample is in contact with a cooling reservoir. A non-temperature-induced effect is considered proven if RF or AMRF exposure leads to an increased physical or biological effect under otherwise identical conditions—in particular, identical temperature in the treated sample/region. However, the characteristics of the effects might change with the temperature.

RFs have been used in cancer therapy for decades under the label hyperthermia [1] to improve the effectiveness of chemotherapy [2] or radiation therapy [3,4]. According to the prevailing opinion, the therapeutic effect of RF was attributed only to the temperature increase induced by RF [1]. Due to the technical demands and limitations in achieving the required temperatures of >41 C for tumor therapy [5,6], this therapeutic approach was only established for a few oncological indications.

Recently, non-temperature-induced antitumoral effects have been observed clinically. AMRF either at 13.56 MHz [7–9] or 27.12 MHz [10,11] were applied at rather low specific absorption rates (SAR) of 1 W/kg (or E-fields of 45 V/m) up to an estimated 15–20 W/kg (or E-fields up to 200 V/m) and temperatures below 40–41C or even at a normal body temperature. These AMRF techniques based on capacitive coupling of the EM field could be used with much less effort than the current clinical techniques centering around radiative EMF exposure and for significantly more indications in oncology.

Furthermore, preclinical studies showed various non-temperature-induced anticancer effects in vitro and in vivo applying AMRF at 13.56 MHz [12]. However, to the best of our knowledge, the precise contribution of AM was not investigated until now. This is considered a key question for our current study, because RF at 13.56 MHz (without AM) also showed non-temperature-induced antitumor effects when compared with water bath (WB) heating, both of which were carried out at 42 C [13].

Calcium fluxes, which were observed in response to AMRF at 147 MHz, with low modulation frequencies around 16 Hz, were considered a key effect [14–16]. The various biological endpoints of electromagnetic radiation in the microwave range from mobile phones have also been investigated [17–19]. However, these investigations were mainly made on older cellular systems with pure phase-modulated signals and constant amplitude.

We believe that the long-standing apparent lack of clarification on the non-temperatureinduced effects of harmonic RF or AMRF has two major reasons:

1) So far, no reproducible measurement method has been established that can clearly detect differences in the power deposition in cells exposed either to RF or AMRF.
2) There is a lack of irrefutable in vitro and in vivo experiments that compare WB heating with RF or AMRF and document additional RF and/or AMRF-induced anticancer effects. A typical knockout argument is the assertion of hidden thermal effects (local temperature rises, so-called hot spots). Therefore, such confounders must be methodically excluded using a thorough analysis of the experimental setup.

Using a series of physical measurements and in vitro and in vivo experiments, we addressed the above limitations and substantiated the non-temperature-induced anticancer effects of RF and AMRF. We also aimed to decipher the biophysical mechanisms underlying the antitumoral effects and to open up an innovative field for clinical application, particularly for treating cancer.

2. Materials and Methods

In this study we investigated the behavior of tumor cells in vitro and in vivo when exposed to RF and AMRF versus temperature alone (WB). We analyzed the physical parameters of the sample directly (measurement) or indirectly (system parameters), as well as the biological effectiveness of all treatments. A thorough investigation of the temperature distribution in a heterogeneous in vivo scenario was deciphered using EMF and temperature simulations.

2.1. Experimental System, Applicators, and Physical Parameters

We used the commercially available device LabEHY-200 (Oncotherm Kft., Budapest, Hungary) [20], as described in Figure 1, for RF and AMRF treatment with dedicated applicators for preclinical in vitro experiments with cell suspensions and in vivo experiments with mice tumors. The system consists of a signal generator with a fixed carrier frequency of 13.56 MHz (Figure 1A) and optional AM with a selectable pink noise spectrum with a noise density proportional to f_0/f (for $f \geq f_0$ with $f_0 = 1, 10, 100$ Hz, or 1 kHz). Modulation is applied with a selectable modulation index m (10–100%), where m defines the amplitude of the modulation wave with respect to the amplitude of the carrier wave (A_c). In the frequency spectrum, the (A_M) wave is no longer represented by a single peak at the carrier frequency (f_c) but also exhibits two side peaks at the modulation frequency $(f_c \pm f_M)$.

Each of these peaks contributes to the total power carried by the EM wave:

$$E = A_c \cos(\omega_c t) + m\frac{A_c}{2}\cos((\omega_c - \omega_m)t) + m\frac{A_c}{2}\cos((\omega_c + \omega_m)t)$$

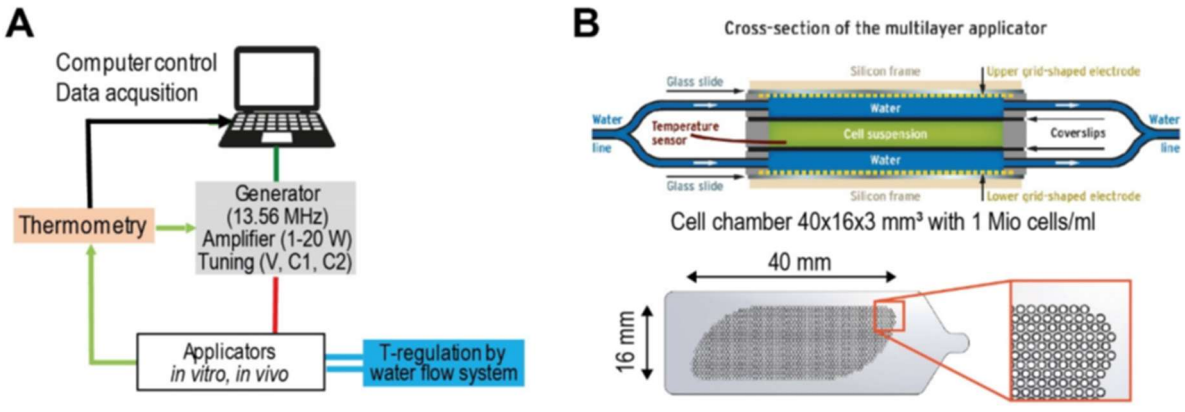

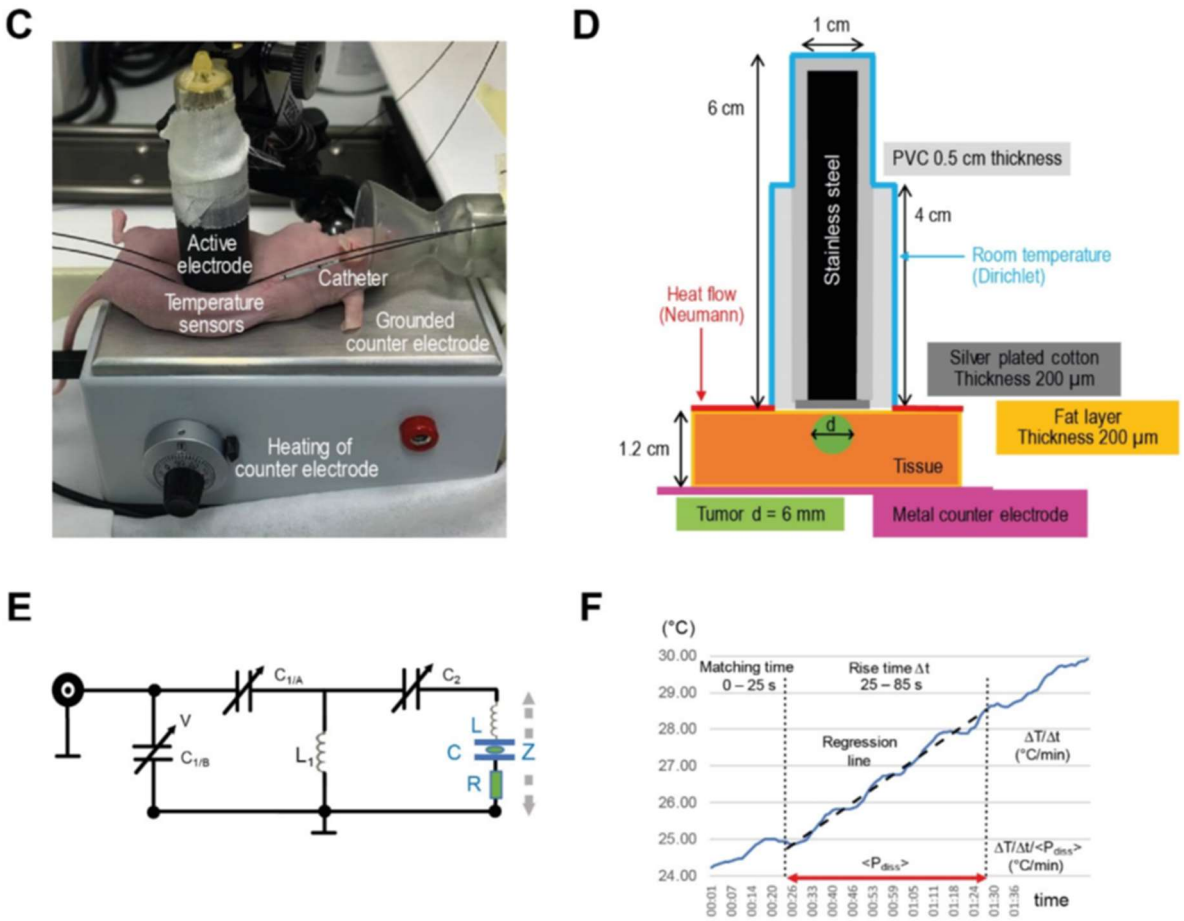

Figure 1.
(A) Experimental system. Schematic of LabEHY-200 system for preclinical in vitro and in vivo studies. With reference to the clinical system EHY-2000+ [8], we initially set the AM-spectrum to $100/f\ (f \geq 100\ \text{Hz})$.

B) In vitro applicator. Schematic cross-section of the in vitro applicator, which is suitable to adjust the power density (via P_{adj}) and temperature (via water flow system) separately. The grid-shaped electrodes (below) enabled enlargement of the cell chamber volume (green) up to ~2mL.

(C) In vivo applicator. Components of the in vivo applicator in situ as positioned upon an implanted HT29 tumor in a nude mouse.

(D) Model of in vivo applicator. The exposed volume is much smaller than for the in vitro applicator, resulting in a Padj = 1 W. Particularly, calculating temperature distributions is a nontrivial task because of this complicated geometry.

(E) Tuning circuit. Tuning circuit for the in vitro applicator with adjustable capacitances C_1/C_2, which are controlled by the voltage V. The complex impedance Z is specified by the fixed inductance L (air coil) in a pre-tuning unit, the capacitance C and a variable lossy resistance R, depending on the load and operation mode. (F) Evaluation procedure for the temperature gradient after the power is turned on. Standardized evaluation of $\Delta T/\Delta t\ (°C/min)$ in the in vitro applicator after switching on the power (P_{adj} = 10 W) under flow conditions in three steps (1–3): (1): Fixed tuning time of 25 s to achieve $<P_{diss}> = P_{adj}$ with a reflected power of <5%. (2): Determination of the slope $\Delta T/\Delta t$ of the regression line in the time interval 25–85 s (red line). (3): Correction of the temperature gradient with respect to the mean P_{diss} during this time interval.

From this, the proportion of the AM side band power of the total signal power can be calculated as: $\frac{m^2}{(2+m^2)}$, yielding 11% for m = 0.5 and 24% for m = 0.8

We used a novel in vitro applicator (Figure 1B) that allowed temperature regulation via temperature control loop operating a water flow cooling system, which was not possible using the previous applicator [13,21]. The in vivo applicator was used for small animal studies (Figure 1C) [22].

Each applicator can be interpreted as a series connection of capacitances (interfaces, deionized water, cell culture growth medium (Gibco Roswell Park Memorial Institute (RPMI) 1640 Medium, Thermo Fisher Scientific, Waltham, MA, USA), and tissues), the electrical parameters of which are listed in Table 1A. A capacitance of $C = \varepsilon_0 \times \varepsilon_r \times A/d$ was calculated for each single component (A: electrode/interface area, d: distance between electrodes/interfaces, ε_0 = vacuum permittivity, and ε_r = = relative permittivity of medium). A basic network analysis shows that the applicators have a total capacitance $C \cong 14\ pF$ in the series, with an inductance $L \text{ of } \cong 10\ \mu H$ forming a series resonant circuit, which, in the lossless case, has the resonance frequency f:

$$f = \frac{1}{2\pi\sqrt{LC}} = 13.56\ MHz$$

Table 1. (A) Electrical parameters (electrode size A, relative permittivity ε_r, and electric conductivity σ required to calculate the capacitances C in vitro and in vivo and to simulate E-field distributions. (B) List of thermal parameters required to calculate the temperature distributions for the in vivo applicator, which is applied for nude mice.

(A)		
Electrical Parameters	**In Vitro Applicator**	**In Vivo Applicator**
electrodes upper electrode counter electrode	grid-shaped electrodes (steel) $4 \times 1.6 \times 0.75\ cm^2$ electrode area reduced by 0.75	stainless steel $ø_1 = 1$ cm, h = 6 cm $ø_2 = (ø_1^2 + d^2)^{1/2}$
distance d (cm) between electrodes	1.3	1.2 (mouse)
RPMI-Medium between electrodes	$\varepsilon_r = 72.5$, $\sigma = 1.2$ S/m	$\varepsilon_r = 100$ (2/3 medium) $\varepsilon_r = 79$ (phantom)
additional interfaces	coverslips, polyolefin 2×0.2 mm, $\varepsilon_r = 2$	silver plated cotton 0.2 mm, $\varepsilon_r = 2$

Table 1. *Cont.*

(B)	
Thermal Parameters	**In Vivo Applicator**
Thermal conductivity λ (W/m/°C)	Electrode (steel): 20 Cover (silver plated cotton): 90 Tissue (mixture muscle/fat): 0.5
Heat capacitance c (Ws/kg/°C)	Electrode (steel): 420 Tissue: 3600
Heat transfer HTC ($W/m^2/°C$)	Mouse body: 6
Perfusion (mL/100 g/min)	Tissue: 100
Heat generation (W/kg)	Tissue: 10

Changes of the absorbed power in the sample represented by a loss resistance R in series with the lossless applicator (Figure 1E) change the resonance frequency. Any change of this absorbed power in the sample adds a slight frequency shift, resulting in detuning of the resonant circuit. A tuning circuit operated by a control voltage V and mechanically adjustable capacitors C_1 and C_2 (Figure 1E) compensates for a change in the absorbed power in order to achieve impedance matching and thereby maximum power transfer to the resonator, i.e., the applicator for the fixed carrier frequency 13.56 MHz.

Practically, the control voltage V is tuned until the internally measured dissipated power P_{diss} (W) approaches the value of the adjusted power P_{adj} chosen for the treatment/experiment [22,23]. Typically, small differences <5% between P_{adj} and P_{diss} are achieved. The complex impedance Z of the applicator unit depends on L, C, and R and is given by the equation $Z = R + j\left(\omega L - \frac{1}{\omega C}\right) = Z \cdot e^{-j\theta}$ with $\omega = \sqrt{\frac{1}{LC} - \frac{R^2}{4L^2}}$, $Z = \sqrt{R^2 + \left(\omega L - \frac{1}{\omega C}\right)^2}$, $\theta = \operatorname{arccot}\left(\frac{\omega L - \frac{1}{\omega C}}{R}\right)$, showing the influence of R on the resonance frequency $\omega = 2\pi f$ of the circuit.

During measurements, Lab-EHY200 software automatically logs the internally measured values for the tuning capacitances C_1 and C_2, power measurements (forward power $P_{forward}$, reflected power P_{refl}, and dissipated power P_{diss}) and temperatures every second and saves to an output file. We analyzed the differences of the mean C_1 and C_2 between different cell lines and non-modulated RF versus AMRF, assuming that they are indicative of changes in the sample's impedance, resulting in changes in the deposited power ΔP.

Determining the dissipated power quantified by the specific absorption rate (SAR in W/kg) in the sample is of particular interest and carried out as follows. At this point, it is important to note that the term of dissipated energy in the physical sense directly refers to energy absorption leading to a change in temperature, whereas the total absorbed power can contain isothermal energy in addition to dissipated energy. If the power is switched on at the initial thermal equilibrium, the SAR can be derived from the temperature gradient $\Delta T/\Delta t$ (in °C/min) quantifying the temperature increase ΔT during a given evaluated rising time Δt. The relationship between SAR and $\Delta T/\Delta t$ is derived from the bioheat transfer equation that is analytically solved for $\nabla^2 T = 0$ (thermal equilibrium) [24,25]. The simple relationship:

$$\mathrm{SAR\ [W/kg]} = 60 \times \Delta T/\Delta t\ [^\circ\mathrm{C/min}] \quad (1)$$

is sufficient if the perfusions w (ml/100 g/min) and time intervals Dt are small enough (1st-order term). In our in vitro experiments, however, a high perfusion w must be assumed if the water flow is running in the in vitro applicator (Figure 1B). Then, the 2nd-order term is non-negligible, yielding:

$$\mathrm{SAR\ [W/kg]} = 60 \times (1 + w\rho\Delta t/2) \times \Delta T/\Delta t\ [^\circ\mathrm{C/min}] \quad (2)$$

If we apply our evaluation interval of Δt = 60 s and a high w = 200 mL/100 g/min, this doubles SAR with Equation (2) (compared to Equation (1)). This has previously been confirmed by temperature–time measurements without the running water flow system at the same P_{adj} = 10 W that delivered about twice as high $\Delta T/\Delta t$ compared to water flow cooling ([26]). If we perform experiments with RF and AMRF under identical settings, a direct comparison of $\Delta T/\Delta t$ is possible after normalization to P_{diss} in order to compensate for slight inaccuracies in tuning < P_{diss} > to P_{adj}: ($\Delta T/\Delta t$)corr. For each experiment, we determined and recorded changes of temperature gradients ($\Delta T/\Delta t$)corr, as we compared AMRF to unmodulated RF.

For the in vitro studies, we applied a standard procedure to determine ($\Delta T/\Delta t$)corr from the respective datasets. We selected a reasonable fixed ramp-up time after the power is on for Pdiss to approach P_{adj} (25 s). During the evaluation time Dt (60 s), we determined the slope of the regression line of the temperature–time curve. The length of Dt is a carefully considered tradeoff between statistics and linearity (Figure 1F). We considered typical fluctuations of the temperature–time curves with cycle times of 10–15 s to be related to the regulatory processes of the LabEHY-200 system.

For the in vivo studies, we had to carry out a graphically supported evaluation process (determination of the tangent) due to the variable settings and adjustments.

2.2. Applicator Models, Simulation Studies, and Isothermal Energy

In the case of the in vitro applicator, the temperatures in the cell suspension are assumed to be sufficiently homogeneous if the water flow is running, given the small sample size and thickness and the large contact area between the sample and the flowing water. The temperature is directly monitored in the cell chamber and further analyzed (Figure 1B).

On the contrary, we expect nonhomogeneous SAR and temperature distributions for the in vivo applicator (Figure 1C,D); therefore, we performed simulation studies for further clarification.

To determine the electric (E-) field, SAR, and temperature distributions, and particularly to exclude undesired thermal effects in the larger and temperature-destabilized volume of the mice treated in the in vivo applicator (Figure 1D), a realistic model of the applicator and a simplified model of a mouse were implemented in Sim4Life V6.0 (ZurichMedTech, Zurich, Switzerland).

For the E-field simulation using the quasistatic solver (13.56MHz) of the FDTD (Finite Difference Time Domain) algorithm, we implemented the electrodes with the dimensions measured at the in vivo applicator (top electrode: ø = 1 cm, bottom electrode: 5.5 x 10.5 cm2). The top electrode was implemented as a solid structure due to the high conductivity of all the components, neglecting its composition of multiple thin rods held in place by a conductive textile to accommodate irregular surfaces. The voltage was directly applied to the top electrode, while the bottom electrode was considered grounded (Dirichlet boundary condition). After an initial simulation with U = 100 V, the voltage was adjusted until the absorbed power matched the adjusted power P_{adj} = 1Wchosen for the in vivo experiments. It is important to note that this power level refers to the continuous RF wave with constant amplitude, since implementing amplitude modulation is not supported in our simulation software. Given the power distribution between the carrier wave and the side bands of the modulation signal, this makes our simulation an upper bound approach to the problem. The mouse was approximated by a rectangle of 6 x 3 x 1.2 cm3, consisting of a $200\ \mu m$ layer of fat enclosing homogeneous muscle tissue. The dimensions were both estimated from pictures taken during the in vivo experiments and adjusted to match the approximate weight of the mouse (here: m = 23 g) for a matching power balance. The overall resolution was set to 0.5 mm isotropic, with a high-resolution box (0.1 mm isotropic) centered underneath the electrode. For model A, a representation of the small tumor shortly after induction, a plane surface of the phantom was implemented. For model B, a sphere with a diameter of 8 mm placed at a depth of 3 mm of the rectangle (representing tumor growth) was used to bulge the surface of the phantom outwards by 1 mm. The superficial fat layer was maintained.

Note that, for in vivo experiments, a mixed tissue of muscle, fat, and intestine yields a mean heat capacitance $c = 3600\ Ws/kg/°C,$ and the relationship SAR (W/kg) = $60 \times \Delta T/\Delta t\ (°C/min)$ holds if the time interval Dt is sufficiently small (Equation (1)) [27]. If high SAR of >1000 W/kg are calculated in a small volume (approximated by a sphere with radius r (mm)), we can apply an analytical solution of the bioheat-transfer equation to quickly estimate the temperature increase [25]:

$$\Delta T_{max}\ [°C] = 4.2 \times 10^{-4} \times 4r^2 \times SAR, \text{ at the center} \quad (3)$$

According to this equation, even an excessive SAR of 10,000 W/kg focused to a sphere of 1 mm would result in a temperature increase of only 2 C, which is not sufficient for any relevant thermal effect. However, accurate numerical calculations of temperature distributions are performed to confirm these estimations.

For the steady-state temperature simulation, the electric loss density result of the EMF simulation with P_{diss} = 1Wwas used as the input. For this simulation, the full geometry, as shown in Figure 1D, was implemented to include the heat sink of the metal electrode rod. The initial body temperature and background temperature were set to 36 C and 22 C, respectively. All electrical and thermal properties are listed in Table 1. Temperature simulations were performed for model A. As a worst-case approximation, the perfusion in the tumor volume was set to zero. The temperature distributions depend considerably on the thermal conductivities λ of the electrode material and mouse tissue (W/m/C), the heat transfer coefficient HTC (W/m^2/C), and the perfusion w (mL/100 g/min), according to previous studies [28,29]. The HTC for nude mice (6–10 W/m^2/C) was doubled in comparison to hirsute mice (Mus musculus, 3–5 W/m^2/C).We generated SAR volume histograms, 2D distributions, and cross-profiles of calculated SAR and temperature datasets. Finally, a comparison of the calculated and measured SAR (via a gradient of temperature increase $\Delta T/\Delta t$) and the temperatures was performed.

If we measure different ($\Delta T/\Delta t$)corr(AMRF) < ($\Delta T/\Delta t$)corr(RF) after correction for P_{diss} (according to Figure 1F), such a difference suggests that isothermal power is deposited in the sample, which is caused by AM. Isothermal energy can primarily be stored electrostatically and chemically as quantified on a microscopic level by the equations in Figure 2 (left panel). A long-term macroscopic correlate for isothermal energy depositions are phase transitions (Figure 2, right panel), which we would expect particularly in cell membranes that can exhibit a transition from a solid to a fluid state at a certain temperature.

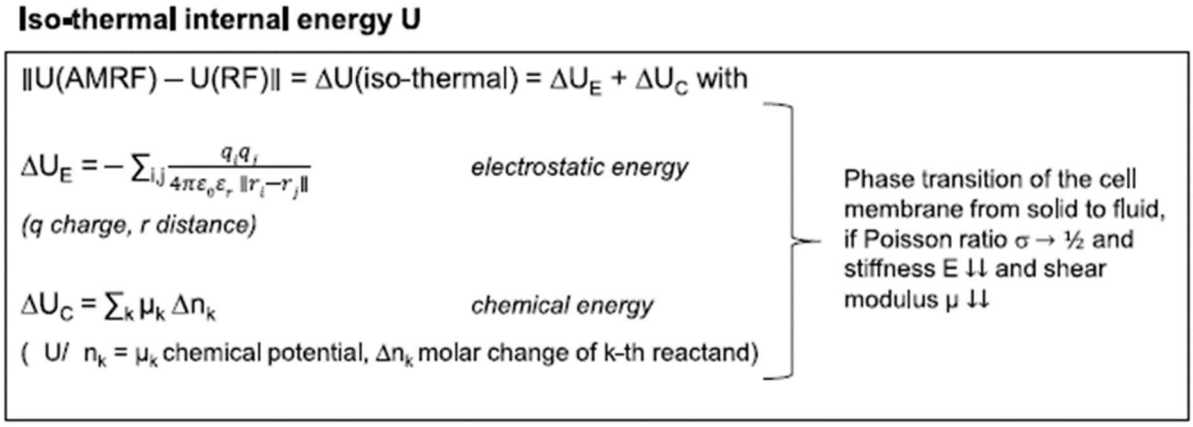

Figure 2. Isothermal energy. Isothermal contributions to the internal energy of tumor cells. These energy depositions do not cause a temperature increase, especially during the heat-up phase. In particular, phase transitions substantially consume isothermal energy. Such phase transitions might occur at the cell membrane under certain circumstances.

Under these conditions, an important aim of the present study was to evaluate the different physical parameters (($\Delta T/\Delta t$)corr, system parameters) for in vitro and in vivo studies, if either RF or AMRF is applied.

2.3. In Vitro Studies

We used five human colorectal cancer cell lines: HT29 (obtained froma primary tumor), SW480 (primary, Duke's B), LoVo (left supraclavicular metastasis), SW620 (lymph node metastasis), and HCT116, which were originally purchased from the American Type Culture Collection (Manassas, VA, USA). The frozen cells were grown in RPMI 1640 medium and maintained at 37 C in a humidified incubator with 5% CO_2. We prepared cell suspensions with approximately one million cells per milliliter.

For the in vitro experiments, two milliliters of cell suspension were injected into the cell chamber of the in vitro applicator (Figure 1B). After careful venting, a fluorooptic temperature sensor (FLUOROPTIC® THERMOMETER m3300 Biomedical Lab Kit by Luxtron, ø = 0.5 mm) was positioned in the center via a provided channel under visual control. We always selected 42 C as the target temperature for the flow system and an adjusted power Padj of 10 W. In the case of AMRF, we selected 100/f (f 100 Hz) and a modulation index of 50%. This particular AM is also used in clinical systems, e.g., EHY- 2000+ (Oncotherm Kft., Budapest, Hungary) and was utilized in two clinical studies [7,9]. The flow system runs a few minutes ahead of the power onset for thermal equilibration at room temperature.

For each of the five cell lines and the RPMI medium, 6 short experiments, i.e., 2 triplicates, were performed per arm (RF versus AMRF) to screen the physical data (($\Delta T/\Delta t$)corr, C_1, C_2, t_{meas} = 10 min). Four cell lines (HT29, SW480, LoVo, and HCT116) were selected for further analysis that showed the highest differences in physical parameters between the medium and cell suspensions and between RF and AMRF exposition.

We hypothesized that AM with modulation frequencies of Hz to kHz (audio frequencies) can deposit energy in membranes by the excitation of mechanical vibrations [12]. The stiffness E (or Young's

modulus) (Pa) is a decisive parameter to estimate the fundamental (or ground) natural (or eigen) frequency fM (Hz) of a membrane sheet with dimensions a x b (μm^2) according to an equation derived in [30] (Vol. VI, §25):

$$f_M = 120 \times E^{1/2} \times \left(1/a^2 + 1/b^2\right) \quad (4)$$

Therefore, we determined the stiffness E of normal cells (represented by hepatocytes and fibroblasts) in comparison to our selected tumor cell lines (HT29, SW480, LoVo, and HCT116) at different temperatures (37 C and 41 C) by indentation measurements using atomic force microscopy. The cells were probed using Bruker (Newark, DE, USA) MLCTBIO- DC cantilevers with a spring constant of 0.01 N/m that were calibrated using a contact-based method on a JPK-NanoWizard® 4 atomic force microscopy system. The cell culture dishes with the adherent cells were equilibrated at respective temperatures in HEPES buffer for 30 min prior to the experimentation, using the JPK PetriDishHeaterTM provided with the instrument. The actual temperature on the sample surface was checked with an IR thermometer on the sample surface prior to the measurements. The indentation experiments were performed at a setpoint of 1 nN and a relative setpoint of 0.8 nN to achieve an indentation depth of 500 nm, ensuring indentation at a larger surface area. A Z length of 4 μm with an extension speed of 1 μm/s and sample rate of 2046 Hz were used for collecting the data. For singularized, nonconfluent cells, three cells per sample were analyzed where five to six force curves were recorded for each cell in a 5 x 5 μm^2 region. Each sample was analyzed in experimental triplicates. The analysis of the force curves was performed using JPK data processing software, and the Young's modulus was calculated using the Hertz-Sneddon model for a triangular pyramid cantilever of 17 half-angle.

The three cell lines with the lowest stiffness E were selected for further in vitro analysis (HT29, SW480, and LoVo). We performed 4 triplicates per cell line and arm for the biological endpoint apoptosis (tmeas = 65 min: t_{heat} = 5 min + t_{treat} = 60 min). In parallel, controls were run in a water bath at 37 C and 42 C for the same time. Apoptosis rates were determined using FACS (fluorescence-activated cell sorting) by measuring the percentage of annexin V-positive cells. A direct comparison was performed by dividing the percentages of RF or AMRF by the mean percentage of the 42 C water bath.

2.4. In Vivo Study

We used HT29 tumor s.c. xenografts for the in vivo study, because for HT29 cells, the largest differences between RF and AMRF had been observed in the in vitro experiments. The animal study with 6–8-week-old female NMRI nu/nu mice was performed at the Experimental Pharmacology & Oncology (EPO) GmbH Berlin-Buch (Berlin, Germany). All animals were maintained in a sterile environment with a daily 12-h light/12-h dark cycle, and sterilized food and water were provided ad libitum. Animals at 6–8 weeks old with a body weight of 22–25 g were used for xenografting. All experiments were carried out in accordance with the 3R (replace, reduce, and refine) and animal welfare (LAGESO Nummer 001/019), in accordance with the German law and Directive 2010/63/EU.

Subcutaneous injection at the femoral region with 1 x 10^7 HT29 cells in 0.1 mL of phosphate-buffered solution (PBS) was performed to form tumor xenografts. Forty mice were randomly assigned to 4 groups of n = 10 animals. We compared the control group and whole body water bath hyperthermia group (WB) at 40 C for 35 min with the RF group and AMRF group, for both adjusting a total power of P_{adj} = 1 W and a measurement time of 35 min (t_{meas} = 35 min: t_{heat} = 5 min + t_{treat} = 30 min). Direct temperature measurements were performed in the tumor center (as precisely as possible), at the skin in contact with the tumor, and in the rectum with the same temperature probes as used for the in vitro experiments. We determined the SAR after the onset of P_{adj} by applying tangents to the temperature time curves using a graphical method and registered P_{diss}, C_1, and C_2 similar to the in vitro studies.

During the induction time of approximately 16 days (series 1), we started with the respective treatments on post-tumor inoculation days 7, 9, and 13. For this, the mice were anesthetized with isoflurane gas and received an injection of 150 mg/kg D-luciferin (Biosynth, Staad, Switzerland). We monitored the luciferase-expressing tumor xenograft activity by bioluminescence imaging using the NightOWL LB 981 imaging system (Berthold Technologies, Bad Wildbad, Germany). Images were analyzed by WinLight software (Berthold Technologies) and quantified using ImageJ 1.48v. In addition, tolerability and feasibility of the application were documented, i.e., potential skin irritations, treatment discontinuations, and the number of regular sessions. We measured the tumor volume (TV) by a digital caliper on study days 6 (baseline), 16, and 20.

On day 20 during the tumor growth period, we started a comparison of RF and AMRF in the so-far-untreated control group. We randomized 5 mice in each group and performed the three treatments on days 20 (after baseline measurements), 23, and 27. Here, we measured the TV on days 20, 23, 30, and 34 and again conducted bioluminescence imaging on days 20, 29, and 34 as the endpoints.

The anesthetized mice in the WB, RF, and AMRF groups were sacrificed on day 13 and in the control group on day 34 after the last TV measurement. The tumor samples were prepared for immunohistochemistry (IHC) by staining and evaluation for Ki67, because Ki67 protein (pKi67) expression is associated with the proliferative activity of intrinsic cell populations in tissues, including tumors. In evaluating the IHC results, the relative percentage of the immunopositive cells was assessed in relation to the total number of target cells. We defined a numerical Ki67 tumor score from 0 to 3.0 as follows: 0 (negative no stain), 0.5 (up to 12.5% of the cells show positive immunoreactivity), 1.0 (12.5–25%), 1.5 (25–37.5%), 2.0 (37.5–50%), 2.5 (50–75%), and 3.0 (75–100%).

2.5. Statistics

We used the software package GraphPad Prism v.6 for the statistics. Variance analyses between several series of measurements of two groups were performed by multiple t-tests and presented either as standard boxplots or dot plots additionally showing mean and mean error bars. Significance was defined as $p < 0.05$ and marked with * (<0.005 with **, etc.).

3. Results

3.1. Physical Parameters (In Vitro Applicator)

We compared RF at 13.56 MHz with AMRF, selecting the pink noise modulation frequency spectrum with a noise density $\propto 100/f \text{ with } f \geq 100 \text{ Hz}$ and modulation index $m \cong 50\%$.

We evaluated and compared three physical parameters in five colorectal cancer cell lines prior to the in vitro and in vivo studies (Figure 3): temperature gradients ($\Delta T/\Delta t$)corr (C/min) after power onset and system parameters C_1 and C_2.

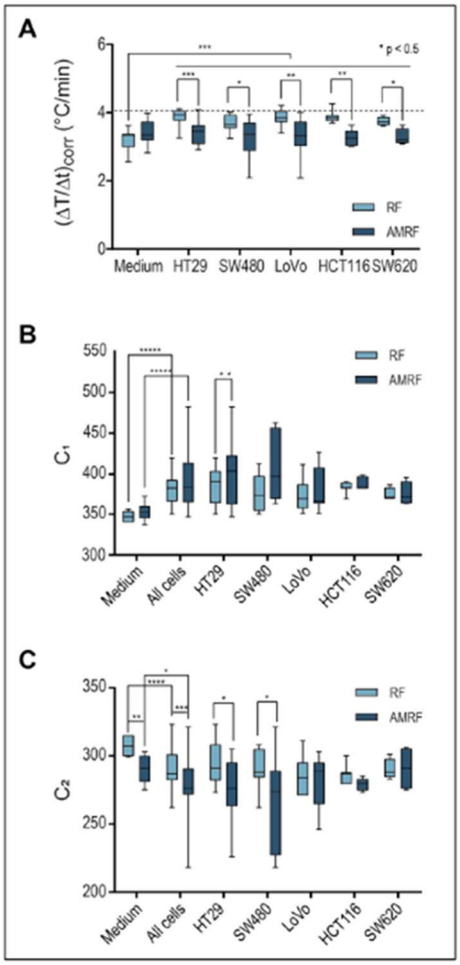

Figure 3.

(A) Power deposition; Detected temperature gradients after radiation onset in the in vitro applicator (10 W with flow, $\pm$ AM with $\geq$ 100 Hz), which are significantly higher for RF in all cell suspensions than in the medium. For RPMI medium, a slight nonsignificant increase is observed for AMRF versus RF. In contrast, for each cell line, a significantly lower value is observed (significance level is shown above the bars: $p < 0.05$ and marked with *, < 0.005 with **, etc.). The dashed line marks the medium level for RF.

(B) Tuning capacitance C_1; C_1 of the in vitro applicator for medium and five cell lines exposed to RF or AMRF radiation. Differences are evident between medium and cell suspensions and between RF and AMRF—in particular, after pooling the cells. Individual cell lines appear to follow a trend. C_1 is higher when using AMRF instead of RF. The difference is lowest for the cell lines (LoVo, SW620, and HCT116).

(C) Tuning capacitance C_2; C_2 of the in vitro applicator for medium and five cell lines exposed to RF or AMRF radiation. Differences occur similar to C_1, but C_2 values are lower for AMRF than for RF. Again, this difference is lowest for the cell lines (LoVo, SW620, and HCT116).

Figure 3A shows that ($\Delta T/\Delta t$)corr under RF exposure were significantly higher by 15–20% for all cancer cell lines (HT29, SW480, LoVo, SW620, and HCT116) in comparison to the RPMI medium. When using AMRF, ($\Delta T/\Delta t$)corr in the medium was slightly (but non-significantly) higher (Figure 3A). If we, however, exposed cell suspensions to AMRF, ($\Delta T/\Delta t$)corr were significantly lower, close to the level found for RPMI medium. Given the normalization to the same power, these measurements suggest that cancer cells were subjected to isothermal energy if AM is added to RF, since the same amount of energy was absorbed, but a smaller fraction was dissipated as thermal energy.

The system parameters C_1 and C_2 (Figure 3B,C) also significantly differed between the medium and cell suspensions for both RF and AMRF exposure. C_1 is significantly higher for SW480 cell suspensions when using AMRF compared to RF. C_2 is more sensitive to a switch from RF to AMRF and is significantly lower for HT29 and SW480 cell suspensions.

3.2. Biological Effectiveness of RF and AMRF Versus WB In Vitro

We measured apoptosis, comparing exposure with RF and AMRF at a targeted temperature of 42 C (measured mean of 41.8 C) in the novel in vitro applicator to conventional water bath (WB) heating at the targeted 42 C (measured mean of 42.3 C) for the three selected colorectal cancer cell lines HT29, SW480, and LoVo. The measured temperature excess of 0.5 C in the WB versus cell chamber (Figure 4A) confirms that additional apoptotic effects induced by RF or AMRF exposure cannot be caused by a higher temperature in the cell chamber and must be of non-temperature-induced origin.

For HT29 cells (Figure 4B), we found no relevant increase of apoptosis for RF versus WB (<10%) but significantly higher apoptosis for AMRF in comparison to either WB or RF (34% versus WB).

Contrarily, for SW480 cells (Figure 4C), we measured a significant increase of apoptosis for RF (45% versus WB); the apoptosis rates were enhanced at similar rates in both RF and AMRF. A similarly high anticancer effect of RF exposure on SW480 cells was previously reported [13]. For the cancer cell line LoVo (Figure 4D), we measured a slightly lower, but still significant, increase of apoptosis for RF (30% versus WB) and no further increase for AMRF. While ($\Delta T/\Delta t$)corr under RF/AMRF behaves similarly for all three cell lines (Figure 3A), the lower sensitivity of LoVo to AM correlates with smaller differences in C_1 and C_2 when AM is used (Figure 3B,C).

To further decipher the reason behind these varied responses of the cell lines to AM with f_0 = 100 Hz, we measured the stiffness E (or Young's modulus) of hepatocytes and fibroblasts (representative for normal tissue cells) and the selected cancer cells as a function of the temperature (Figure 4E, left panel) using atomic force microscopy. The stiffness of normal cells at 37 C ranges at 10–25 kPa, while the stiffness of cancer cells is much lower but still in the range of 2–3 kPa. However, a dramatic drop of E is observed in the cells when the temperature is increased to 41 C. In the cancer cells, E declines to 200–600 Pa, which corresponds to lower mechanical resonance frequencies f_M, which now fall into the audio frequency range (explained in Methods, Equation (4)).

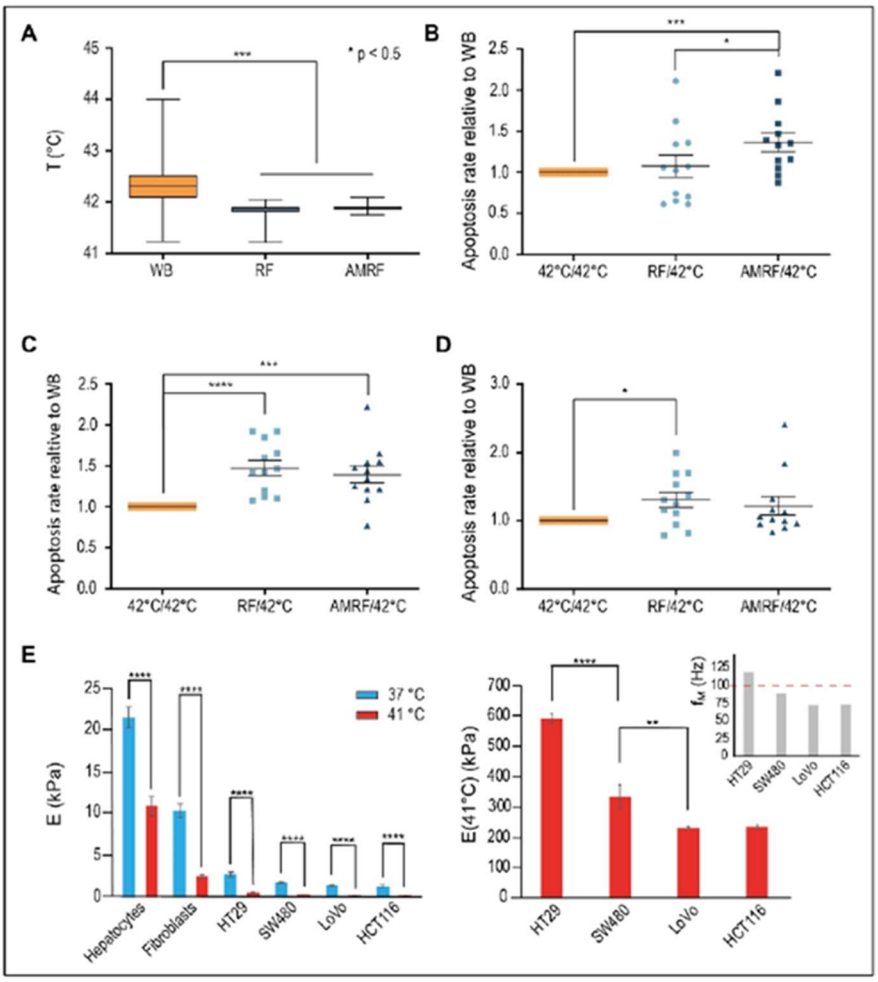

Figure 4.
(A) Measured temperatures in vitro. Mean temperatures during the 60-min treatment time measured in the cell chamber for RF or AMRF in comparison to the water bath (WB). A sample of 26 biological experiments enclosing all cell lines was evaluated.

(B) Normalized apoptosis rate in vitro for HT29 cells. Evaluation of apoptosis rates (annexin V+) for HT29 cells in suspension in the in vitro applicator comparing RF and AMRF versus those of cells in a water bath adjusted to 42 C by normalizing to the mean apoptosis rate of the WB experiments. Significantly higher apoptosis rates are detected in the AMRF arm. Estimated ground natural frequency of the membrane f_M is covered by the AM spectrum (see (E)).

(C) Normalized apoptosis rate in vitro for SW480 cells. Apoptosis rates are equally enhanced in the RF and AMRF arms. Estimated ground natural frequency of the membrane f_M is slightly below the AM spectrum (see (E)).

(D) Normalized apoptosis rate in vitro for LoVo cells. Apoptosis rates are equally enhanced in the RF and AMRF arms. Estimated ground natural frequency of the membrane f_M is clearly below the AM spectrum (see (E)).

(E) Young´s moduli E for different cell lines and temperatures, as determined by atomic force microscopy indentation. The overview (left panel) shows that normal issue cells (hepatocytes and fibroblasts) have higher E than cancer cells. A significant drop of E occurs for each cell type as the temperature increases from 37 C to 41 C. The more detailed representation (right panel) shows that the moduli at 41 C significantly differ between cancer cells and lead to different resonance frequencies fM, which are below or above 100 Hz, according to Equation (4) (Section 2 Methods): $f_M = 120 \times E^{1/2} \times (1/a^2 + 1/b^2)$. Significance was defined as $p < 0.05$ and marked with * (< 0.005 with **, etc.)

A more detailed analysis of the cancer cells at 41 C revealed significant differences of E between the cells and the derived membrane resonances (Figure 4E, right panel). The metastatic, i.e., aggressive

cancer cells LoVo/HCT116 have the lowest E of approximately 200 Pa, as opposed to 600 Pa for HT29 cells. If we assume a spherical segment with an extension of 7 m as the largest possible vibrating membrane section of a spherical cell with a 10 $^{\mu m}$ diameter, we obtain the fundamental characteristic resonance frequencies fM of each cell according to Equation (4). A membrane resonance frequency above 100 Hz is predicted for the HT29 cells, which is thus covered by the applied AM spectrum 100/f $^{(f \geq 100\ Hz).}$ For the other cell lines, we obtain fundamental membrane frequencies below 100 Hz. Thus, a stimulation of fundamental membrane resonances using this AM spectrum, which might cause membrane damages, is only expected in HT29 cells (and not in LoVo and SW480 cells). This is in agreement with our in vitro data (Figure 4B,D).

3.3. Biological Effectiveness of RF and AMRF Versus WB In Vivo

The in vitro data prompted us to perform an in vivo study with the luciferase reporter gene stably expressing HT29 s.c. xenografts using the same AM spectrum.

In series 1, we assessed 4 groups of n = 10 mice each, comparing the relative bioluminescence signal at the start of treatment on day 1 and after 3 treatments (running until day 5) on day 12 (Figure 5A).We measured a slight but nonsignificant increase in the control group and WB group (heating at 40 C, t = 30 min) and a slight nonsignificant decrease in the experimental RF group (RF, P_{adj} = 1 W, t = 35 min, T_{max} < 40 C); however, the experimental AMRF group showed a significant drop (same settings as the RF group). Note that the in vivo treatments were distinctly less intensive compared to the in vitro studies (treatment times 35 min in vivo versus 65 min in vitro and T_{max} < 40 C versus $T_{mean} \cong$ 41.8 C in vitro (Figure 4A)). Nevertheless, the effects in the in vivo AMRF group were significant regarding the antitumoral efficacy.

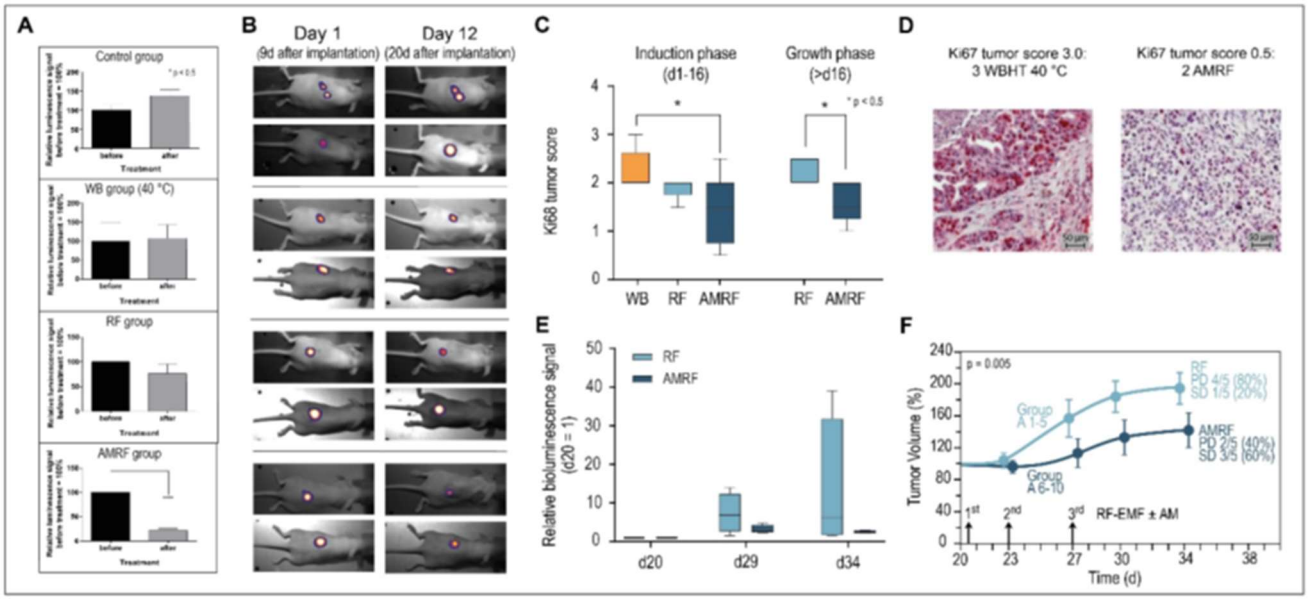

Figure 5.
(A) Relative bioluminescence signals (series 1). Response after three treatments (measured on day 12 after treatment) for all groups, showing the significant drop for the AMRF group.

(B) Bioluminescence images. Demonstration of progression (control group), stable course (WB and RF groups), and response (AMRF group).

(C) Immunohistochemistry. Expression of Ki67 antigen after 3 WBHT or RF/AMRF treatments on day 13 (series 1, left panel) or after 3 RF/AMRF on day 34 (series 2, right panel). The decline of Ki67 after 3 AMRF is significant.

(D) Immunohistochemical staining. Representative images of Ki67 immunohistochemical staining, with the highest score 3.0 (top) and a low score 0.5. (bottom).

(E) Relative bioluminescence signals (series 2). Response after three treatments on d20, d23, and d27 in the RF and AMRF groups as randomized in the control group, normalized to the signal on d20. Due to the large scatter in the RF group, no statistical significance was achieved.

(F) Tumor growth curves (series 2). Significantly different tumor growth curves for the RF group versus AMRF group after three treatments on days 21, 23, and 27. Progressive disease (PD) is halved in the AMRF group (40% versus 80%) and stable disease (SD) tripled (60% versus 20%). PD: tumor volume > 150% on d34. SD: tumor volume 50–150% on d34. Significance was defined as $p < 0.05$ and marked with *(<0.005 with **, ect.)

Figure 5B shows bioluminescence images with typical examples of progression (control group), stable disease/minor response (WB and RF group), and significant antitumoral response, reflected by tumor reduction (AMRF group).

The scores for proliferation marker Ki67 also showed a significant decrease for the AMRF group compared to the WB group (Figure 5C, left panel), while the RF group showed at least a tendency to be more effective than WB heating. Figure 5D shows the highest Ki67 tumor score 3.0 and a rather low Ki67 score 0.5 for illustration (for scoring, see Methods). Additional AM clearly causes a significant improvement of anticancer effectiveness.

Since series 1 (up to 20 days after implantation, Figure 5B) fell mainly in the induction phase (up to 16 days after implantation), tumor volume measurements were not performed on the small tumors (with measured diameter

For the untreated control group of series 1 (n = 10 mice), we conducted a second treatment series during the tumor growth period, with larger tumors (diameter 8 mm) starting on day 20 after implantation. We randomized the mice into an RF and AMRF group of n = 5 mice each treated on days 20, 23, and 27 either with RF or AMRF at the same settings as used for series 1. We again found significantly lower Ki67 scores (Figure 5C, right panel) and a tendency to lower the relative luminescence signals (Figure 5E) in the AMRF group. In particular, the tumor growth curve of the AMRF-group was significantly flattened compared to the RF group (Figure 5F), showing the higher effectiveness of the AMRF treatments. Furthermore, we found less progressive disease (40% versus 80%) and more stable disease (60% versus 20%) in the AMRF arm (Figure 5F).

Pathological examination of the tumor tissues revealed no indication for treatmentrelated tissue damage or necrosis in the surrounding healthy tissues.

3.4. Physical Parameters (In Vivo Applicator)

We evaluated C_1, C_2, ($\Delta T/\Delta t$)corr for HT29 xenografts treated with the in vivo applicator and found the same significant differences between RF and AMRF as for the in vitro applicator comparing all RF and AMRF measurements (Figure 6A,B).

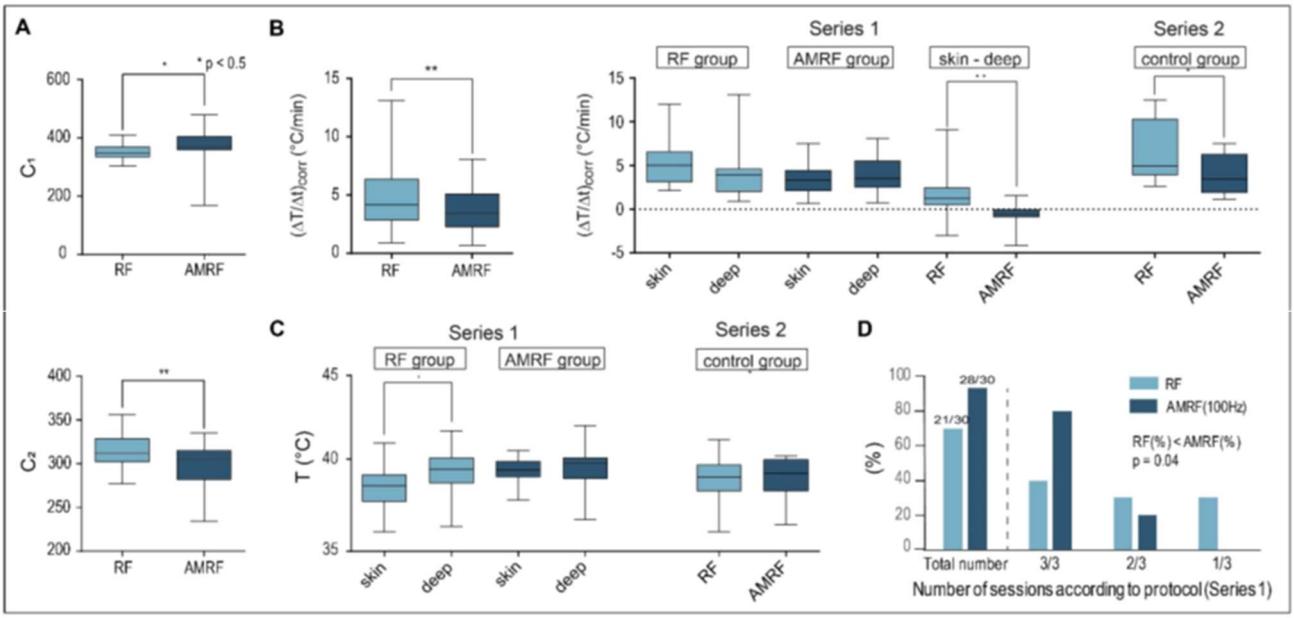

Figure 6.

(A) Tuning capacitances in vivo. Values obtained for C_1 and C_2 in vivo show the same qualitative behavior as those achieved in vitro (Figure 1B,C), with even higher statistical significance. We included all completed RF and AMRF treatments in this analysis.

(B) Corrected power deposition in vivo. The initial temperature gradients $(\Delta T/\Delta t)$corr (corrected for the dissipated power) in vivo behave similar to the in vitro measurements (Figure 3A) if all RF and AMRF measurement points were compared. The temperature gradients as a function of the locations (superficial versus deep in the tumor center) and techniques (RF versus AMRF) suggest that the thermally relevant power density is higher and more nonhomogeneous for RF in comparison to AMRF.

(C) Locationdependent temperatures in vivo. Mean Tmax in tumor-related superficial and intratumoral deep measurement points broken down by RF (light) and AMRF (dark) for series 1 (left panel) and series 2 (right panel). Even though the thermal power is less for AMRF, the measured temperatures are comparable and more homogeneous.

(D) Feasibility and tolerance. Three sessions per mouse were intended in series 1 (RF group versus AMRF group with 2 × 10 mice). The number of successfully completed sessions is significantly higher in the AMRF group. Significance was defined as $p < 0.05$ and marked with *(<0.005 with **, etc.)

We also analyzed $(\Delta T/\Delta t)$corr as a function of the measurement location (either superficial in tumor contact or in the implanted intratumoral catheter) (Figure 6B, right panel) and determined the mean maximum temperatures in the same measurement points (Figure 6C). For the first in vivo study (Series 1: RF versus AMRF group, small tumors of 6 mm in diameter), the thermally relevant $(\Delta T/\Delta t)$corr values (after power onset) tend to be higher at the surface for the RF group, but the opposite was observed for the AMRF group (Figure 6B, middle). The values of the difference $(\Delta T/\Delta t)_{skin}$ - $(\Delta T/\Delta t)_{deep}$ were significantly different when comparing RF to AMRF. Such nonhomogeneous temperature distributions (i.e., big differences between superficial and deep measurement points) are considered unfavorable indicators both in terms of toxicity and effectiveness.

For the second in vivo study (Series 2: RF versus AMRF in the former control group) with larger tumors of 8 mm in diameter in the growth phase, we again found significantly lower values of $(\Delta T/\Delta t)$corr in the AMRF group, which were consistent with our findings in the in vitro applicator.

Although we measured lower thermally relevant dissipated power for AMRF exposure (e.g., 40% reduction for Series 2), the final mean temperatures $<T_{max}>$ in the steady state were not reduced and, in particular, were more homogeneously distributed, i.e., showed a smaller difference $(\Delta T/\Delta t)_{skin}$ - $(\Delta T/\Delta t)_{deep}$ (compare the RF and AMRF groups, Figure 6C, left panel).

Figure 6D shows that the feasibility and tolerance of the AMRF treatments were significantly greater compared to the RF treatments, with 33% more treatments being completed according to protocol (i.e., without complications such as skin irritations) under the same conditions for AMRF. This could be explained by the lower thermal power densities (Figure 6A,B) and more homogeneous temperature distributions of AMRF (Figure 6C).

Both the in vitro and in vivo data consistently show that, for the same applied power, the thermally relevant dissipated power is lower for AMRF, indicating that portions of the absorbed power are transformed into isothermal energy. The in vivo data show, in addition, that this transformation increases the tolerance and is associated with more homogeneous temperature distributions.

In summary, the in vivo study confirmed the in vitro data both physically and biologically. Moreover, the AM-related effects were even more prominent in vivo.

3.5. Measured and Simulated Temperatures for the Applicators

The temperatures measured in the in vitro applicator are representative for the entire cell chamber, because this small volume of 2 mL with a 3 mm thickness is entirely in close contact with a highly effective water flow system for temperature regulation.

The conditions are more complicated for the in vivo applicator and prompted us to carry out SAR and temperature simulations. Our calculations yielded strongly nonhomogeneous SAR distributions for two models; A and B (Figure 7A,B upper/middle row), corresponding to the two tumor growth stages of Series 1 and 2. Outside the tumors, applicator edge effects generated SAR maxima (see profiles at depth

d = 0.05 mm) that might cause skin irritations at these locations (Figure 6B). However, the SAR volume histograms of the tumors (of either 6 or 8 mm in diameter) revealed that the volumes in the tumors with excessive SAR (up to 6500 W/kg) are too small (<0.1 mL) to induce a significant localized temperature increase, as estimated by the 42 C curves (see Methods, Equation (3)), resulting in intratumoral temperatures far below 42 C (Figure 7A,B bottom). Even when considering the temporal peak power levels of the modulated wave (up to 150% for m = 0.5), the peak SAR values will not induce a temperature increase of 2 C or more (see Methods, Equation (3)). The calculated SAR50 in the tumors are consistent with the mean values of our measurements (see inlay, Figure 7A,B, third row).

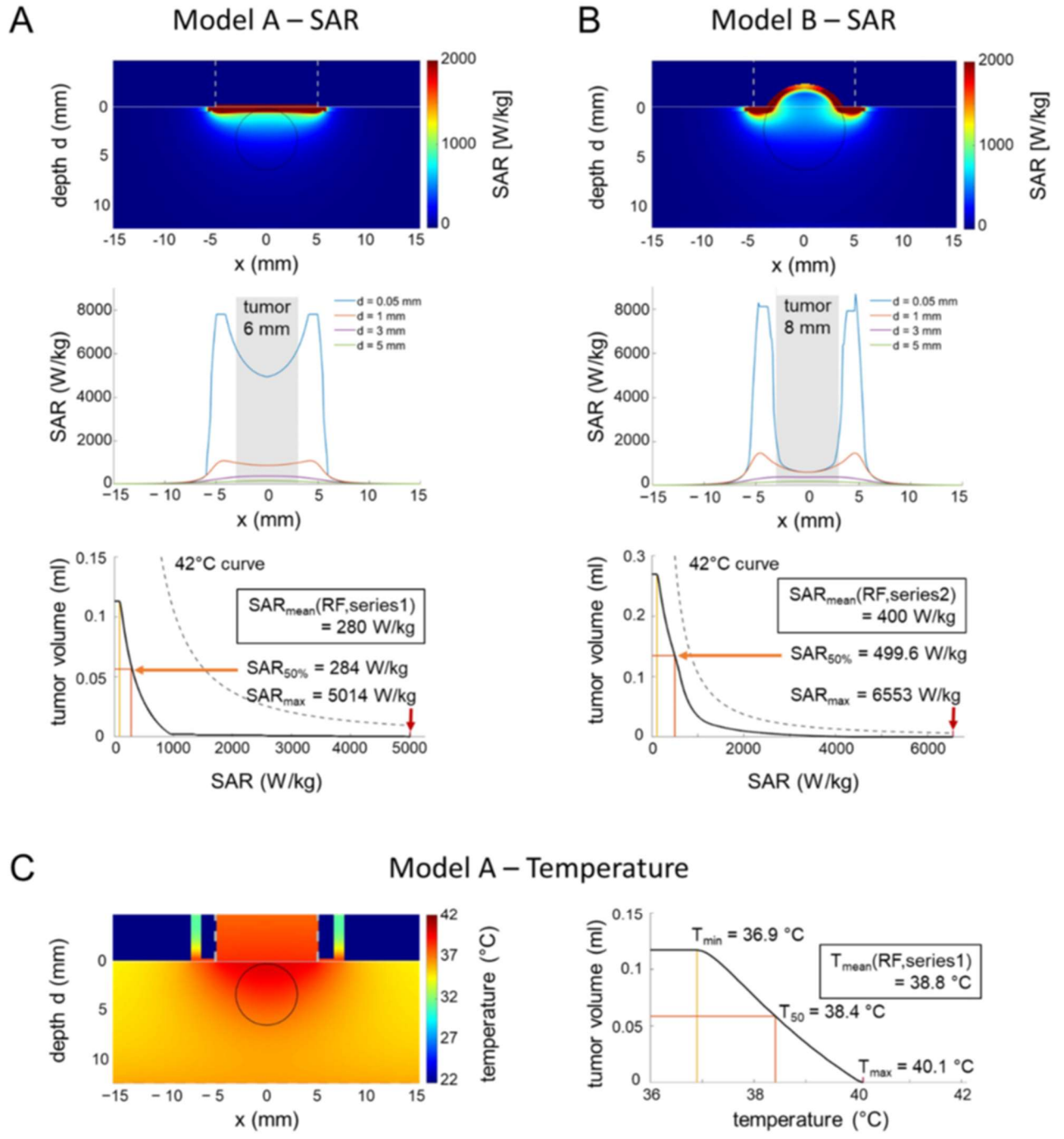

Figure 7.
(A) SAR simulations in an in vivo applicator (small tumor). Two-dimensional SAR distribution (top), depth profiles near the surface (middle), and SAR volume histogram of the tumor for model A representing series 1 with small tumors (6 mm in diameter) during the induction phase. The SAR volume histogram of the tumor is far below the 42 °C curve. SAR_{min}, $SAR_{50\%}$ and SAR_{max} are marked with yellow, orange and red markers respectively. However, overheating might be possible outside the tumor at the applicator edge under unfavorable conditions (see profile at depth d = 0.05 mm).

(B) SAR simulations in an in vivo applicator (large tumor). For model B with larger tumors (8 mm in diameter), the SAR volume histogram yields higher SAR than for model A but is still below the 42 °C curve (please note the adapted scale of the y-axis). Similar to model A, overheating might be possible outside the tumor at the applicator edge with similar SAR peaks (see the profile at depth d = 0.05 mm).

(C) Simulation of temperature distributions. The temperature distribution for model A with the applicator model of Figure 7B and the thermal parameters of Table 1B confirm the estimations of the SAR analysis. The temperature volume histogram of the tumor shows a maximum temperature of 40.1 C.

The simulated temperature distributions (Figure 7C) confirmed that the intratumoral temperatures barely reach 40 C, in agreement with the direct tumor-related temperature measurements, but indicate the possibility of overheating at the applicator edge outside the tumor.

Our careful theoretical analysis of the in vivo applicator could rule out hot spots (temperatures > 40 C) in the implanted tumors.

4. Discussion

We identified non-temperature-induced anticancer effects due to RF in three colorectal cancer cell lines in vitro, which were increased by AMRF in one of the cell lines in vitro, using a frequency spectrum for modulation $(f \geq 100\ \mathrm{Hz},\ 100/f\ \mathrm{spectrum})$. This could be confirmed in vivo, bearing the potential for rapid clinical translation.

Our measurements of the physical parameters revealed that colorectal cancer cells absorb up to 20% additional thermal power from a harmonic RF at 13.56 MHz compared to WB heating. This might be explained by the change of the tissue interactions with EM waves in the investigated frequency range. The delta dispersion on the tail of a beta dispersion [31] around 10 MHz is characterized by a change from membrane-dominated interactions in the β region to dipolar interactions of bound water or side chains of molecules. Owing to the interaction of RF with proteins and protein-bound water, the delta dispersion increases the value of the dielectric constant ε_r up to several hundred, which can result in increased interaction of the RF with the cancer cells [32]. Moreover, others have previously described the mitochondria as a possible specific target of RF at 13 MHz [33,34]. Wust et al. [13] described that a slight DC voltage at ion channels, generated from the RF by rectification and smoothing, can lead to ion disequilibrium of cells—in particular, for Ca^{2+} ions.

If we use AMRF, this excess of dissipated power from RF is decreasing and presumably converted into isothermal energy during the heating-up phase. Particularly, phase transitions—for example, the transition of the cell membrane from a solid-like to a liquidlike state, eventually leading to cell damage—consume substantial isothermal energy.

A demodulation of the AMRF results in the low modulation frequency acting upon the cell membrane and the ion channels thereon [12]. This can trigger a mechanical vibration of membrane parts with a frequency covered by the modulation frequency spectrum, leading to, for instance, a decrease of the membrane potential, opening of voltage-gated channels, or triggering of other processes [12]. Such processes consume isothermal energy but are not necessarily cytotoxic.

A mechanically induced cytotoxicity is expected if a mechanical ground resonance of the whole cell is excited, which we considered as the vibration of a spherical segment as large as possible (estimated as 7 μm diameter for a cell of 10 μm in diameter). We measured the cell membrane stiffness E of the used cell lines by atomic force microscopy and used the results to calculate the potential resonance frequencies of the cells. Our results show that, only for the cell line in which AMRF outperformed the anticancer effects of RF in vitro, the calculated resonance frequency was above 100 Hz, thus being included in the frequency spectrum used for modulation. As this explains the differences between the cell lines, it supports our hypothesis.

Since the interactions at the cell membranes are considered as pure E-field effects [12], the product of E-field (V/m) x time (min) can reasonably be considered as a dose to predict non-temperature-induced antitumoral effects in clinical applications. For our experiments, we estimate a dose of 60,000 V*min/m

per in vitro experiment (of 60 min), while the mean dose per in vivo treatment (of 30 min) was half this value. Since we performed three treatments per arm (see Methods), we achieved a total dose of 90,000 V*min/m for each in vivo experiment.

These preclinical dosages can be compared with clinically achievable doses. An SAR of 20 W/kg (E = 200 V/m) is realistic in the pelvis and abdomen with capacitive systems [35]. Therefore, a dose of 12,000 V*min/m can be estimated for a clinical treatment of 60 min. If we consider a typical scheme of 10 treatments (2 treatments per week), we achieve even higher doses of 120,000 V*min/m for a full course (24,000 V*min/m per week). Thus, a clinical translation of our preclinical results appears feasible.

Even treatments with comparatively low levels of 1 W/kg (E = 45 V/m) for 3 h (on 3 days per week) deliver similar doses of 24,300 V*min/m per week [36,37].

The existence of extraordinary modulation frequencies has been proposed by others in the past [10,11,14,15,36–38] and might be the subject of future studies. In addition, further studies are required regarding the required number, duration, and interval of treatments to optimize the non-temperature-dependent anticancer effects.

5. Conclusions

Our study verified the existence of non-temperature-induced anticancer effects of RF in three tested cell lines in vitro. Moreover, we could demonstrate a further increase of the non-temperature-dependent anticancer effects due to AMRF in one tested cell line in vitro and in vivo. RF/AMRF promises a locoregional oncological therapy using both temperature effects (hyperthermia) and non-temperature-induced anticancer effects with the potential to serve as a more effective tumor therapy. More research in terms of the choice of amplitude modulation frequency and choice of carrier frequency among other variables is required.

Author Contributions:
P.W. designed and directed the project, developed the theory and performed the calculations, planned the experiments, aided in interpreting the results, wrote the manuscript, and approved the manuscript. P.D.V. performed the experiments, aided in preparing the figures and interpreting the results, edited the manuscript, and approved the manuscript. E.O. performed the calculations, aided in preparing the figures and interpreting the results, edited the manuscript, and approved the manuscript. P.Y. performed the experiments and approved the manuscript. W.W. was involved in planning and supervising the experiments, aided in interpreting the results, edited the manuscript, and approved the manuscript. O.B. aided in interpreting the results, edited the manuscript, and approved the manuscript. A.S.-K. performed the experiments and approved the manuscript. M.W. was involved in planning and supervising the experiments, aided in interpreting the results, edited the manuscript, and approved the manuscript. F.H. edited the manuscript and approved the manuscript. P.G. (Patricia Grabowski) edited the manuscript and approved the manuscript. S.S. edited the manuscript and approved the manuscript. W.H. aided in interpreting the results, edited the manuscript, and approved the manuscript. U.S. was involved in planning and supervising the experiments, aided in interpreting the results, edited the manuscript, and approved the manuscript. P.G. (Pirus Ghadjar) designed and directed the project, planned the experiments, aided in interpreting the results, wrote the manuscript, and approved the manuscript. All authors have read and agreed to the published version of the manuscript.

Funding:
This research was funded by the Berliner Krebsgesellschaft e.V., grant number GHFF202006, www.berliner-krebsgesellschaft.de. This project was supported by the H2020 Marie Sklodowska– Curie program—HYPERBOOST (project number 955625).

Institutional Review Board Statement:
All in vivo experiments were carried out in accordance with the 3R (replace, reduce, and refine) and animal welfare (LAGESO Nummer 001/019), in accordance with the German law and Directive 2010/63/EU.

Informed Consent Statement:
Not applicable.

Data Availability Statement:

The data can be shared up on request.

Acknowledgments:
The authors are grateful for the support and helpful discussions with Andras Szasz (Oncotherm Kft., Budapest, Hungary). This work is dedicated to Roland Felix for his invaluable contributions to the advancement of hyperthermia.

Conflicts of Interest:
There are no competing interest of any author in relation to this publication.

References

1. Wust, P.; Hildebrandt, B.; Sreenivasa, G.; Rau, B.; Gellermann, J.; Riess, H.; Felix, R.; Schlag, P.M. Hyperthermia in combined reatment of cancer. Lancet. Oncol. 2002, 3, 487–497. [CrossRef]
2. Issels, R.D.; Lindner, L.H.; Verweij, J.; Wessalowski, R.; Reichardt, P.; Wust, P.; Ghadjar, P.; Hohenberger, P.; Angele, M.; Salat, C.; et al. European Organization for the Research and Treatment of Cancer-Soft Tissue and Bone Sarcoma Group and the European Society for Hyperthermic Oncology Effect of neoadjuvant chemotherapy plus regional hyperthermia on long-term outcomes among patients with localized high-risk soft tissue sarcoma: The EORTC 62961-ESHO 95 randomized clinical trial. JAMA Oncology 2018, 4, 483–492. [PubMed]
3. Van Der Zee, J.; González González, D.; Van Rhoon, G.C.; van Dijk, J.D.; van Putten,W.L.; Hart, A.A. Comparison of radiotherapy alone with radiotherapy plus hyperthermia in locally advanced pelvic tumours: A prospective, randomised, multicentre trial. Dutch Deep Hyperthermia Group. Lancet 2000, 355, 1119–1125. [CrossRef]
4. Harima, Y.; Nagata, K.; Harima, K.; Ostapenko, V.V.; Tanaka, Y.; Sawada, S. A randomized clinical trial of radiation therapy versus thermoradiotherapy in stage IIIB cervical carcinoma. Int. J. Hyperth. 2001, 17, 97–105. [CrossRef]
5. Ademaj, A.; Veltsista, D.P.; Ghadjar, P.; Marder, D.; Oberacker, E.; Ott, O.J.; Wust, P.; Puric, E.; Hälg, R.A.; Rogers, S.; et al. Clinical evidence for thermometric parameters to guide hyperthermia treatment. Cancers 2022, 14, 625. [CrossRef]
6. Mei, X.; Ten Cate, R.; van Leeuwen, C.M.; Rodermond, H.M.; de Leeuw, L.; Dimitrakopoulou, D.; Stalpers, L.J.A.; Crezee, J.; Kok, H.P.; Franken, N.A.P.; et al. Radiosensitization by hyperthermia: The effects of temperature, sequence, and time interval in cervical cell lines. Cancers 2020, 12, 582. [CrossRef]
7. Kim, S.; Lee, J.H.; Cha, J.; You, S.H. Beneficial effects of modulated electro-hyperthermia during neoadjuvant treatment for locally advanced rectal cancer. Int. J. Hyperth. 2021, 38, 144–151. [CrossRef]
8. Minnaar, C.A.; Kotzen, J.A.; Ayeni, O.A.; Naidoo, T.; Tunmer, M.; Sharma, V.; Vangu, M.D.; Baeyens, A. The effect of modulated electro-hyperthermia on local disease control in HIV-positive and -negative cervical cancer women in South Africa: Early results from a phase III randomised controlled trial. PLoS ONE 2019, 14, e0217894. [CrossRef]
9. Minnaar, C.A.; Maposa, I.; Kotzen, J.A.; Baeyens, A. Effects of modulated electro-hyperthermia (mEHT) on two and three year survival of locally advanced cervical cancer patients. Cancers 2022, 14, 656. [CrossRef]
10. Barbault, A.; Costa, F.P.; Bottger, B.; Munden, R.F.; Bomholt, F.; Kuster, N.; Pasche, B. Amplitude-modulated electromagnetic fields for the treatment of cancer: Discovery of tumor-specific frequencies and assessment of a novel therapeutic approach. J. Of Exp. Clin. Cancer Res. 2009, 28, 51. [CrossRef]
11. Costa, F.P.; De Oliveira, A.C.; Meirelles, R.; Machado, M.C.; Zanesco, T.; Surjan, R.; Chammas, M.C.; de Souza Rocha, M.; Morgan, D.; Cantor, A.; et al. Treatment of advanced hepatocellular carcinoma with very low levels of amplitude-modulated electromagnetic fields. Br. J. Cancer 2011, 105, 640–648. [CrossRef] [PubMed]
12. Wust, P.; Stein, U.; Ghadjar, P. Non-thermal membrane effects of electromagnetic fields and therapeutic applications in oncology. Int. J. Hyperth. 2021, 38, 715–731. [CrossRef] [PubMed]
13. Wust, P.; Kortüm, B.; Strauss, U.; Nadobny, J.; Zschaeck, S.; Beck, M.; Stein, U.; Ghadjar, P. Non-thermal effects of radiofrequency electromagnetic fields. Sci. Rep. Sci. Rep. 2020, 10, 13488. [CrossRef] [PubMed]
14. Bawin, S.M.; Kaczmarek, L.K.; Adey,W.R. Effects of modulated VHF fields on the central nervous system. Ann. N. Y. Acad. Sci. 1975, 247, 74–81. [CrossRef] [PubMed]

15. Blackman, C.F.; Elder, J.A.;Weil, C.M.; Benane, S.G.; Eichinger, D.C.; House, D.E. Induction of calcium-ion efflux from brain tissue by radio-frequency radiation: Effects of modulation frequency and field strength. Radio Sci. 1979, 14, 93–98. [CrossRef]
16. Blackman, C.F.; Benane, S.G.; Elder, J.A.; House, D.E.; Lampe, J.A.; Faulk, J.M. Induction of calcium-ion efflux from brain tissue by radiofrequency radiation: Effect of sample number and modulation frequency on the power-density window. Bioelectromagnetics 1980, 1, 35–43. [CrossRef]
17. Diem, E.; Schwarz, C.; Adlkofer, F.; Jahn, O.; Rüdiger, H. Non-thermal DNA breakage by mobile-phone radiation (1800 MHz) in human fibroblasts and in transformed GFSH-R17 rat granulosa cells in vitro. Mutat. Res. 2005, 583, 178–183. [CrossRef]
18. Panagopoulos, D.J.; Chavdoula, E.D.; Karabarbounis, A.; Margaritis, L.H. Comparison of bioactivity between GSM 900 MHz and DCS 1800 MHz mobile telephony radiation. Electromagn. Biol. Med. 2007, 26, 33–44. [CrossRef]
19. Franzellitti, S.; Valbonesi, P.; Ciancaglini, N.; Biondi, C.; Contin, A.; Bersani, F.; Fabbri, E. Transient DNA damage induced by high-frequency electromagnetic fields (GSM 1.8GHz) in the human trophoblast HTR-8/SVneo cell line evaluated with the alkaline comet assay. Mutat. Res. 2010, 683, 35–42. [CrossRef]
20. Szasz, A.; Szasz, O.; Iluri, N. Radiofrequency hyperthermia device with targeted feedback signal modulation. United States Patent US 9(320), 911 B2 (2016).
21. Yang, K.L.; Huang, C.C.; Chi, M.S.; Chiang, H.C.;Wang, Y.S.; Hsia, C.C.; Andocs, G.;Wang, H.E.; Chi, K.H. In vitro comparison of conventional hyperthermia and modulated electro-hyperthermia. Oncotarget 2016, 7, 84082–84092. [CrossRef]
22. Danics, L.; Schvarcz, C.A.; Viana, P.; Vancsik, T.; Krenács, T.; Benyó, Z.; Kaucsár, T.; Hamar, P. Exhaustion of protective heat shock response 2 induces significant tumor damage by apoptosis after modulated electro-hyperthermia treatment of triple negative breast cancer isografts in mice. Cancers 2020, 12, 2581. [CrossRef] [PubMed]
23. Andocs, G.; Renner, H.; Balogh, L.; Fonyad, L.; Jakab, C.; Szasz, A. Strong synergy of heat and modulated electromagnetic field in tumor cell killing. Strahlenther. Onkol. Organ Der Deutsch. Rontgenges. 2009, 185, 120–126. [CrossRef]
24. Wust, P.; Stahl, H.; Löffel, J.; Seebass, M.; Riess, H.; Felix, R. Clinical, physiological and anatomical determinants for radiofrequency hyperthermia. Int. J. Hyperther. 1995, 11, 151–167. [CrossRef] [PubMed]
25. Wust, P.; Ghadjar, P.; Nadobny, J.; Beck, M.; Kaul, D.; Winter, L.; Zschaeck, S. Physical analysis of temperature-dependent effects of amplitude-modulated electromagnetic hyperthermia. Int. J. Hyperther. 2019, 36, 1246–1254. [CrossRef] [PubMed]
26. Wust, P.; Veltsista, P.D.; Oberacker, E.; Ghadjar, P.; Department of Radiation Oncology, Charité—Universitätsmedizin Berlin, Augustenburger Platz 1, 13353 Berlin, Germany. Personal Observation, 2021.
27. Wust, P.; Cho, C.H.; Hildebrandt, B.; Gellermann, J. Thermal monitoring: Invasive, minimal-invasive and non-invasive approaches. Int. J. Hyperther. 2006, 22, 255–262. [CrossRef] [PubMed]
28. Gordon, C.J. The mouse thermoregulatory system: Its impact on translating biomedical data to humans. Physiol. Behav. 2017, 179, 55–66. [CrossRef]
29. Streif, J.U.; Hiller, K.H.; Waller, C.; Nahrendorf, M.; Wiesmann, F.; Bauer, W.R.; Rommel, E.; Haase, A. In vivo assessment of absolute perfusion in the murine skeletal muscle with spin labeling MRI. Magnetic resonance imaging. J. Magn. Resonance Imaging 2003, 17, 147–152. [CrossRef]
30. Landau, L.D.; Lifshitz, E.M. Theory of Elasticity; Pergamon Press: Oxford, UK, 1986.
31. Schwan, H.P. Electrical properties of tissue and cell suspensions. Adv. Biol. Med. Phys. 1957, 5, 147–209.
32. Martinsen, O.G.; Grimnes, S.; Schwan, H.P. Interface phenomena and dielectric properties of biological tissue. Encycl. Surf. Colloid Sci. 2002, 20, 2643–2653.
33. Stoy, R.D.; Foster, K.R.; Schwan, H.P. Dielectric properties of mammalian tissues from 0.1 to 100 MHz: A summary of recent data. Phys. Med. Biol. 1982, 27, 501–513. [CrossRef]
34. Weibel, E.R.; Stäubli, W.; Gnägi, H.R.; Hess, F.A. Correlated morphometric and biochemical studies on the liver cell. I. Morphometric model, stereologic methods, and normal morphometric data for rat liver. J. Cell Biol. 1969, 42, 68–91. [CrossRef] [PubMed]
35. Beck, M.; Wust, P.; Oberacker, E.; Rattunde, A.; Päßler, T.; Chrzon, B.; Veltsista, P.D.; Nadobny, J.; Pellicer, R.; Herz, E.; et al. Experimental and computational evaluation of capacitive hyperthermia. Int. J. Hyperther. 2022, 39, 504–516. [CrossRef] [PubMed]
36. Jimenez, H.; Wang, M.; Zimmerman, J.W.; Pennison, M.J.; Sharma, S.; Surratt, T.; Xu, Z.X.; Brezovich, I.; Absher, D.; Myers, R.M.; et al. Tumour-specific amplitude-modulated radiofrequency electromagnetic fields induce differentiation of hepatocellular carcinoma via targeting Cav3.2 T-

type voltage-gated calcium channels and Ca2+ influx. EBiomedicine 2019, 44, 209–224. [CrossRef] [PubMed]
37. Sharma, S.;Wu, S.Y.; Jimenez, H.; Xing, F.; Zhu, D.; Liu, Y.;Wu, K.; Tyagi, A.; Zhao, D.; Lo, H.; et al. Ca2+ and CACNA1H mediatetargeted suppression of breast cancer brain metastasis by AM RF EMF. EBioMedicine 2019, 44, 194–208. [CrossRef]
38. Zimmerman, J.W.; Pennison, M.J.; Brezovich, I.; Yi, N.; Yang, C.T.; Ramaker, R.; Absher, D.; Myers, R.M.; Kuster, N.; Costa, F.P.; et al. Cancer cell proliferation is inhibited by specific modulation frequencies. Br. J. Cancer 2012, 106, 307–313. [CrossRef]

Commentary on "Systematic review about complementary medical hyperthermia in oncology" by Liebl et al.

Elisabeth Arrojo[1,2], Giammaria Fiorentini[3], Pirus Ghadjar[4], Carrie Minnaar[5,6], A. Marcell Szasz[7], Andras Szasz[8]

[1] University Hospital Marques de Valdecilla, Santender, Cantabria, Spain

[2] Medical Institute of Advanced Oncology (INMOA), Madrid, Spain

[3] Former Director Medical Oncology Unit and Hyperthermia Service, Onco-Hematology Department, Azienda Ospedaliera Marche Nord, Pesaro, Italy

[4] Department of Radiation Oncology, Charité – Universitätsmedizin Berlin, Freie Universität Berlin and Humboldt-Universität Zu Berlin, Berlin, Germany

[5] Department of Radiation Sciences, University of the Witwatersrand, Johannesburg, South Africa

[6] Wits Donald Gordon Academic Hospital, Johannesburg, South Africa

[7] Division of Oncology, Department of Internal Medicine and Oncology, Semmelweis University, Budapest, Hungary

[8] Biotechnics Department, Hungarian University of Agriculture and Life Sciences, Godollo, Hungary

Cite this article as:
Arrojo E. et al. (2022) Commentary on "Systematic review about complementary medical hyperthermia in oncology" by Liebl et al., Clinical and Experimental Medicine, 22(4):667-672.
https://doi.org/10.1007/s10238-022-00902-4

Oncothermia Journal 33, May 2023: 195 – 201.
https://www.oncotherm.com/sites/oncotherm/files/2023-05/arrojoe_etal_commentary_on_liebl_etal.pdf

We read the recent article by Liebl et al. [1]. Unfortunately, several important critical points should be brought to the readers' attention. A variety of hyperthermia methods exist and each has fundamental differences in actions and effects. The authors discuss "complementary hyperthermia" and discriminately include only electrohyperthermia and whole-body hyperthermia (WBH) in this category. This is despite the appropriate definitions for methods of heating used in the field of oncologic hyperthermia having been described [2]. The selection of articles is not inclusive leading to a biased interpretation of the results. There are several positive phase III trials for capacitive hyperthermia (see Table 1), underscoring the authors' incorrect assessment of hyperthermia techniques.

Our major points are:

A) The methodologies and techniques are not correctly described, leading to inaccurate definitions that are not used in the field, and are therefore not useful for the readers.

B) B. The authors have missed essential articles, which may be related to their crude methodology, definitions, and the discriminate selection method.

C) The article Liebl et al. [1] contains several errors and biases:

1. The article only evaluates WBH and capacitive coupled hyperthermia, and this selection does not meet the criteria for a "systematic review." Many applications (such as phased-array, RF radiative heating, nano-heating, and Japanese capacitive hyperthermia) are also techniques employed in the field of complimentary hyperthermia but have been systematically neglected.

2. Contrary to the title of the text of the article;

   a) The selection method described in the text is misleading for the readers: "… we have included in this review only hyperthermia methods that do not belong to conventional medicine and titled these alternative methods." Hyperthermia methods are mostly applied when other treatments alone do not provide satisfactory results. Hyperthermia is a complementary treatment, employed to compliment or enhance the efficacy of conventional therapies. Hyperthermia is not an alternative treatment.

Malignancy	*n*	Intervention	Arms	References	Remark
Uterus cervix	40	RT ± cHT	2	[1]	RR + ST
Uterus cervix	110	RT ± cHT	2	[2]	RR + ST
Uterus cervix	271	RT + ChT ± mEHT	2[a]	[3]	RR + ST
Non-small-cell lung cancer	80	RT ± cHT	2	[4]	RR + ST
Non-small-cell lung cancer	97	ChT ± mEHT ± IVC	2	[5][d]	ST + QoL
Head and neck cancer	65	RT ± cHT	2	[6]	RR
Head and neck cancer	56	RT ± cHT	2	[7]	RR + ST
Esophagus cancer	66	RT + ChT ± cHT	2	[8]	RR + ST
Esophagus cancer	40	ChT ± cHT	2	[9]	RR
Bone metastases	57	RT ± cHT	2	[10]	RR
Uterus cancer	38	ChT ± mEHT	2	[11]	RR + ST
Urinary bladder cancer	49	RT ± cHT	2	[12]	RR + ST
Peritoneal carcinomatosis	260	IPCh ± mEHT ± TCM	2	[13][d]	RR
Nefopam pharmacokinetics	12[c]	ChT ± mEHT	2	[14]	PhK
Fentanyl pharmacokinetics	12[c]	ChT ± mEHT	2	[15]	PhK
Non-small-cell lung cancer	19	RT + cHT	1 + [b]	[16]	RR + ST
Non-small-cell lung cancer	35	RT + cHT	1	[17]	ST
Gastric cancer	21	RT + cHT	1	[18]	RR + ST
Rectal cancer	81	RT + ChT + cHT	1	[19]	RR
Rectal cancer	76	RT + ChT + mEHT	1	[20]	RR + AE
Rectal cancer	120	RT + ChT + mEHT	1	[21]	RR + ST
Pediatric brain tumors	41	IT + mEHT	1	[22]	ST
Soft tissue sarcoma	27	RT + cHT	1	[23]	RR
Recurrent breast cancer	26	RT + cHT	1	[24]	RR
Brain malignancies	140	ChT ± mEHT	1	[25][d]	RR + ST
Non-small-cell lung cancer	15	ChT ± mEHT	1	[26][d]	DE
Glioblastoma	24	ChT ± mEHT	1	[27][d]	DE

ChT chemotherapy, RT radiotherapy, cHT capacitively coupled hyperthermia, mEHT modulated electrohyperthermia, RR response rate, ST survival time, PhK pharmacokinetics, AE adverse effects, IPCh intraperitoneal chemotherapy, TCM Traditional Chinese Medication, QoL the quality of life, IVC intravenous vitamin C, DE dose escalation

[a] Additional sub-arm for HIV patients
[b] Historical reference arm;
[c] Healthy, voluntary participants;
[d] Falsely interpreted

b) The referred methods have medically accepted and significant Phase III trial results, yet the authors claim that these "do not belong to conventional medicine." What is the definition of conventional medicine, according to the authors, and on what basis can they make such a claim when these results have been accepted in peerreviewed journals?

3. The authors do not define electrohyperthermia (EH). It is likely that the authors mean "capacitive coupling," and however, the authors have also included inductive heating results and discussed them in detail (Loboda et al. cite ref. {54}). Inductive heating refers to the use of electromagnetism and magnetic fields and does not include capacitive heating.

4. Authors have further particularities in their selection of studies to include in the systemic review. It is not clear how the selection excludes the following:
   a) "…125 studies did not use alternative hyperthermia". But all selected hyperthermia applications in the article are complementary to “conventional” (chemotherapy/radiotherapy) medicine and are not an alternative to “conventional” medicine.
   b) "…43 studies, multiple interventions were administered simultaneously." But almost all hyperthermia techniques, including those in the article, are applied complementary to other treatments and are therefore applied simultaneously with other therapies (mostly with chemotherapy).
   c) "…assessment of hyperthermia was not possible." Authors do not define how they measured the criteria of "assessment" in the selection.
5. The tables in the article combine the WBH and the local EH results. However, these techniques are fundamentally different, in their methods, indications, safety limits, and physiological actions, and can therefore not be compared directly or be discussed using the same criteria for evaluation.
6. Some statements lack the full information from the article that is referenced and this provides a negative or biased view. For example, when referring to the study on brain tumors by Fiorentini et al., the following statement is made: “Adverse events caused by EH in the RCT by Fiorentini et al. {56} included headache, scalp burn and seizures. More than an hour after treatment, seizures occurred in 4 additional patients.” The authors fail to mention that the study is on brain tumors, and that indeed tumors themselves cause seizures and headaches and that it is not possible to confirm that the adverse events are from the hyperthermia treatments and not from the advanced stage of disease or the concurrent treatments.
7. The authors claim that only the adverse effects of the studies with multiple interventions are reported due to the difficulty in confirming the benefit of the hyperthermia when multiple interventions are administered. The same should therefore be true of the adverse events and toxicity. This is selective reporting of the negative effects of 43 trials without considering the benefits.
8. The article ignored numerous phase II and phase III clinical trials investigating capacitive coupling (electrohyperthermia) which reported significant improvement in the local response and survival times (Table 1.) Many of the ignored studies fall into the “first level category" of evidence.
9. The entire evaluation does not correctly categorize the clinical phases of the trials. It mixes the phase 1 (safety trial), phase 2 (efficacy trial), phase 3 (clinical benefits approval), and phase 4 (market surveillance) methods, where the goals of the studies are obviously different, and so their evaluation has to differ as well.
10. The category of the first level evidence {Fig. 2.} uses category "2b-," which does not exist in the Oxford evidence rank. Furthermore, Fig. 2 evaluates the phase III study as 2b evidence. According

to the Oxford evidence scale, the prospective randomized phase III study is 1b. 2b is a retrospective study, which has entirely different conditions.

11. Authors use different and unclear categories which have no conventional meaning and no explanations. Some points:
    a) What is the difference between the "single-arm" and the "cohort study"? The single-arm study must also use a cohort; otherwise, it is only a case series.
    b) Authors should provide a better explanation for the difference between the "multiple intervention" category (Table 7) and the other categories (for example, the radio-chemo-thermo categories), in previous tables.
    c) The scoring system in Table 3 is undefined (What is the Berlin scoring system?).
    d) The article misinterprets the aim of the clinical results in the article by Kim et. al. {58}. The clinical study used ~ 20% less radiotherapy in the active arm and had similar results to the larger radiation dose in the control group. It is an important and clinically positive result, however, its interpretation in the article is negative.
    e) The research papers by Minnaar et al. {52} and {53} are shown as published in 2019, while these were in 2020. The explanation of outcomes uses study arms A and B, but it is not identified which arm is the active and passive.
    f) The trials of Douwes et al. {79}, Gadaleta- Caldarola et al. {80}, Yoo et al. {82} are phase 2 retrospective trials, with evidence level 2b, so these are in the wrong place and belong to Fig. 2. and Table 3.
    g) The evaluation of Yoo et al. {82} has the expression "time to death," the meaning of which is not clear. Is it overall survival (time from the first diagnosis), or survival from the first hyperthermia treatment, or other? This study had a successful safety (dose escalation) phase but was not registered in Table 4.
    h) The studies by Ko et al. {115} and Qiao et al. {124} was identified as a "cohort study" but were applied to "different entities of cancer." How may we understand the category "cohort"?
    i) The phase 2 randomized prospective clinical trials of Ou et al. {122} (1b evidence), Pang et al. {123} (1b evidence) and Fiorentini et al. {102} are retrospective double-arm studies (2b evidence) in Table 6., despite the fact that the others listed here (40 studies) are single-arm studies or case reports. These trials are missing from Table 3. efficacy studies.
    j) The application of some heating techniques in a palliative setting where there is no cure possible and patients have failed all other treatments is not discussed. In these studies, the heating technique is applied without any chemotherapy or radiotherapy (for example, Fiorentini et al. {102}).

When considering the criticisms of individual studies, it is clear that the authors have either not understood the methodology of the studies. Unfortunately, this comes across as an attempt to discredit some studies by using only selective information. The interpretation and discussion should be reviewed and reassessed in order to prevent what could be perceived to be a biased interpretation of the results. For example, regarding the phase 3 clinical studies by Minnaar et al., the following statements are made, and when reviewing the articles, the answers to all of these questions can be found:

1. “No data on the target temperature in the tumor field are reported.” The reason for the lack of temperature measurement and the dosing methods is discussed in detail {52}.
2. “In these studies, many calculations are performed. However, in the exact comparison of the intervention and control group regarding the therapy, these data are missing. Therefore, it is not possible to accurately compare the treatments between the two arms with and without hyperthermia.” There are numerous exact comparisons between the active (hyperthermia) and control arms. In fact, the objective of all three papers is to compare the hyperthermia arm to the non-hyperthermia arm, and therefore, all of the calculations are direct comparisons, including frequency tables with chi-squared and Fischer exact tests, multivariate regression analyses, and paired and unpaired t-tests evaluating local disease control, disease-free survival, toxicity, and quality of life

between the two groups. All calculations are described in the methodology, reported in results and discussed in the discussion.

3. "In addition, information about prior treatments is not specified and a description of possible additional co-interventions is missing." Prior treatment to cervical cancer is an exclusion, and the investigation is into the primary management of locally advanced cervical cancer, there are therefore no related prior treatments to specify. Additionally, there are no co-interventions, and the prescribed treatments are described in detail and include only radiotherapy, brachytherapy and cisplatin — the standard of care recognized internationally. There are no other standard/accepted interventions for locally advanced cervical cancer. This statement is therefore redundant.
4. "For the endpoints tumor response and local disease control, reasons for the drop-out of part of the participants are not given. Therefore, it cannot be excluded that for these endpoints only suitable patients were considered… The reasons for the missing data of part of the participants are not stated; therefore, selective reporting cannot be excluded. Additionally, with such a high drop-out rate and without any reasons given, the comparability of the groups cannot further be assumed. It is therefore possible that healthier or more motivated patients remained in the study. Those patients then may achieve a better result and do not constitute a representative sample." In all three papers, the CONSORT diagrams give the reasons for the drop-outs. The dropout rate was not considered to be abnormally high (4.7% in the control group and 2.9% in the intervention group).

The systemic review and the conclusions derived by the authors are flawed due to (a) methodological errors in selection and interpretation of papers (b) incorrect interpretation of the technology for hyperthermia delivery and (c) excluding key articles from their systematic review as detailed above. These could result in the erroneous view of hyperthermia to the readers, thereby depriving patients of a multifaceted therapeutic modality that has been shown to be effective when used with radiotherapy and/or chemotherapy for a wide range of malignancies.

Acknowledgments
Critical reading and remarks of our consultation partners, Prof. Stephan Bodis (Department Radiation Oncology, University Hospital Zurich, Medical Faculty University Zurich; ITIS Foundation Board Member, Switzerland) and Prof. Niloy Datta (Department of Radiotherapy, Mahatma Gandhi Institute of Medical Sciences, Sevagram, India), are highly appreciated. These researchers have recognition awards from the European Society of Hyperthermic Oncology. Their broad expertise in hyperthermia substantially helped our work.

Authors contribution
The consensus of the authors followed intensive discussions and all authors participated equally in the formulation and drafting of this letter. The authors are renowned experts in hyperthermia research (The sequence of their names is in alphabetic order): Prof. E.A is a Radiation oncologist; awarded internationally for her acknowledgments in radiation oncology; Hyperthermia Professor at University San Antonio of Murcia in Spain; responsible of hyperthermia's department of University Hospital Marqués de Valdecilla in Spain. Dr. G.F is an expert in locoregional treatments such as intra-arterial chemotherapy and clinical hyperthermia; Active clinical research on hyperthermia for more than 25 years. Prof. P.G is a Radiation oncologist, head of Charité hyperthermia center, clinical scientist. Dr. C.M is an expert in the use of modulated electro-hyperthermia, principle investigator of a phase III randomized controlled trial on mEHT, with international recognition and awards. Dr. A.M.S is a Head of science at cancer center of Semmelweis University, translational and clinical scientist with an expertise in modulated electro-hyperthermic treatments and responsible for the ongoing randomized, prospective, open-label clinical trial in breast cancer. Author of 120 + publications including deep analyses of efficiency of medical approaches utilized in a concomitant manner. Prof. A.S is a developer of modulated electrohyperthermia, scientific director of Oncotherm Kft/GmbH, Hungary/Germany.

References

1. Harima Y, Nagata K, Harima K, Ostapenko VV, Tanaka Y, Sawada S. A randomized clinical trial of radiation therapy versus thermoradiotherapy in stage IIIB cervical carcinoma. Int J Hyperthermia. 2001;17:97–105.
2. Vasanthan A, Mitsumori M, Part JH, et al. Regional hyperthermia combined with radiotherapy for uterine cervical cancers: a multiinstitutional prospective randomized trial of the international atomic energy agency. Int J Rad Oncol Biol Phys. 2005;61:145–53.
3. Minnaar CA, Kotzen JA, Ayeni OA, et al. The effect of modulated electro-hyperthermia on local disease control in HIV-positive and -negative cervical cancer women in South Africa: Early results from a phase III randomized controlled trial. PLoS ONE. 2019;14(6):e0217894.
4. Mitsumori M, Zhi-Fan Z, Oliynychenko P, et al. Regional hyperthermia combined with radiotherapy for locally advanced nonsmall cell lung cancers: a multi-institutional prospective randomized trial of the International Atomic Energy Agency. Int J Clin Oncol. 2007;12:192–8.
5. Ou J, Zhu X, Chen P, et al. A randomized phase II trial of best supportive care with or without yperthermia and vitamin C for heavily pretreated, advanced, refractory non-small-cell lung cancer. J Adv Res. 2020;24:175–82.
6. Datta NR, Bose AK, Kapoor HK, Gupta S. Head and neck cancers: results of thermoradiotherapy versus radiotherapy. Int J Hyperth. 1990;6(3):479–86.
7. Huilgol NG, Gupta S, Sridhar CR. Hyperthermia with radiation in the treatment of locally advanced head and neck cancer: a report of randomized trial. J Cancer Res Ther. 2010;6(4):492–6.
8. Kitamura K, Kuwano H, Watanabe M, et al. Prospective randomized stidy of hyperthermia combined with chemoradiotherapy for esophageal carcinoma. J Surg Oncol. 1995;60:55–8.
9. Sugimachi K, Hl K, Ide H, et al. Chemotherapy combined with or without hyperthermia for patients with oesophageal carcinoma: a prospective randomized trial. Int J Hyperth. 1994;10(4):485–93.
10. Chi M-S, Yang K-L, Chang Y-C, et al. Comparing the effectiveness of combined external beam radiation and hyperthermia versus external beam radiation alone in treating patients with painful bony metastases: A phase 3 prospective, randomized, controlled trial. Int J Radiat Oncol Biol Phys. 2018;100(1):78–87.
11. Lee S-Y, Lee N-R, Cho D-H, et al. Treatment outcome analysis of chemotherapy combined with modulated electro-hyperthermia compared with chemotherapy alone for recurrent cervical cancer, following irradiation. Oncol Lett. 2017;14:73–8.
12. Masunaga SI, Hiraoka M, Akuta K, et al. Phase I-II trial of preoperative thermoradiotherapy in the treatment of urinary bladder cancer. Int J Hyperth. 1994;10(1):31–40.
13. Pang CLK, Zhang X, Wang Z, et al. Local modulated electrohyperthermia in combination with traditional Chinese medicine vs. intraperitoneal chemoinfusion for the treatment of peritoneal carcinomatosis with malignant ascites: a phase II randomized trial. Mol Clin Oncol. 2017;6:723–32.
14. Lee SY, Kim M-G. The effect of modulated electro-hyperthermia on the pharmacokinetic properties of nefopam in healthy volunteers: a randomised, single-dose, crossover open-label study. Int J Hyp. 2015;28:1–6.
15. Lee SY, Kim M-G. Effect of modulated electrohyperthermia on the pharmacokinetics of oral transmucosal fentanyl citrate in healthy volunteers. Clin Ther. 2016;38(12):2548–54.
16. Karasawa K, Muta N, Nakagawa K, et al. Thermoradiotherapy in the treatment of locally advanced nonsmall cell lung cancer. Int J Radiat Biol Phys. 1994;30(5):1171–7.
17. Ohguri T, Imada H, Yahara K, et al. Radiotherapy with 8-MHz radiofrequency-capacitive regional hypethermia for stage III nonsmall-cell lung cancer: the radiofrequency-output power correlates with the intraesophageal temperature and clinical outcomes. Int J Radiat Oncol Biol Phys. 009;73(1):128–35.
18. Nagata Y, Hiraoka M, Nishimura Y, et al. Clinical experiences in the thermoradiotherapy for advanced gastric cancer. Int J Hyperther. 1995;11(4):501–10.

19. Shoji H, Motegi M, Takakusagi Y, et al. Chemoradiotherapy and concurrent radiofrequency thermal therapy to treat primary rectal cancer and prediction of treatment responses. Oncol Rep. 2017;37:695–704.

20. You SH, Kim S. Feasibility of modulated electro-hyperthermia in preoperative treatment for locally-advanced rectal cancer: Early phase 2 clinical results. Neoplasma. 2019;67(3):677–83.

21. Kim S, Lee JH, Cha J, You SH. Beneficial effects of modulated electro-hyperthermia during neoadjuvant treatment for locally advanced rectal cancer. Int J Hyperth. 2021;38(1):144–51.

22. Van Gool SW, Makalowski J, Bonner ER, et al. Addition of multimodal immunotherapy to combination treatment strategies for children with DIPG: a single institution experience. Medicines. 2020;7:29. https:// doi. org/ 10. 3390/ medic ines7 050029.

23. Hiraoka M, Nishimura Y, Nagata Y, et al. Clinical results of thermoradiotherapy for soft tissue tumours. Int J Hyperth. 1995;11(5):365–77.

24. Masunaga S, Hiraoka M, Takahashi M, et al. Clinical results of thermoradiotherapy for locally advanced and-or recurrent breast cancer-comparison of results with radiotherapy alone. Int J Hyperth. 1990;6(3):487–97.

25. Sahinbas H, Groenemeyer DHW, Boecher E, Szasz A. Retrospective clinical study of adjuvant electro-hyperthermia treatment for advanced brain-gliomas. Deutsche Zeitschrift fuer Onkologie. 2007;39:154–60.

26. Ou J, Zhu X, Lu Y, et al. The safety and pharmacokinetics of high dose intravenous ascorbic acid synergy with modulated electrohyperthermia in Chinese patients with stage III-IV nonsmall cell lung cancer. Eur J Pharm Sci. 2017;109:412–8.

27. Wismeth C, Dudel C, Pascher C, et al. Transcranial electro-hyperthermia combined with alkylating chemotherapy in patients with relapsed high-grade gliomas-Phase I clinical results. J Neurooncol. 2010;98(3):395–405.

This work was supported by the

Hungarian National Research Development and Innovation Office

KFI grant: 2019-1.1.1-PIACI-KFI-2019-00011

EHY-2030

A revolutionary new concept

- **Automatic controlled step motor tuning system for rapid impedance matching to achieve faster tuning times**
- **Developed RF generator with modified power**
- **Electronically controlled electrode arm to easily and accurately horizontally position the smart electrode**
- **User friendly touch screen display with full system control**
- **New shape and design to ease patient anxiety**
- **Changeable strechy textile electrode fort he smart electrode system and bed**
- **Hand-held emergency stop switch fort he patients**
- **Integrated PMS-100 Patient Management System**

MANUFACTURER

HUNGARY
Oncotherm Kft.
Gyár utca 2.
2040 Budaörs, Hungary

Phone (+36) 23-555-510
Fax (+36) 23-555-515

info@oncotherm.org
www.oncotherm.com

GERMANY
Oncotherm GmbH
Belgische Allee 9
53842 Troisdorf, Germany

Phone (+49) 2241-319920
Fax (+49) 2241-3199211

info@oncotherm.de
www.oncotherm.de